Elucidating the role and function of Sensitive to Freezing6 (SFR6) and its interacting proteins in the control of stress tolerance

EWON KALIYADASA PANGUKARAGE

Elucidating the role and function of Sensitive to Freezing6 (SFR6) and its interacting proteins in the control of stress tolerance

Ewon Kaliyadasa Pangukarage

Department of Biology

School of Biological and Biomedical Sciences

Elucidating the role and function of Sensitive to Freezing6 (SFR6) and its interacting proteins in the control of stress tolerance

Ewon Kaliyadasa Pangukarage

Submitted for the Degree of Doctor of Philosophy by Research

School of Biological and Biomedical Sciences

February 2016

Statement of Authorship

I certify that all work described in this thesis is my own original research unless acknowledged in the text or by references, and has not been subtitled for a degree in this or any other university.

Declaration of Copyright

Dedication

This thesis is dedicated to my loving family

for their love and encouragement throughout this study and all my teachers who helped to sharpen my academic career.

Abstract

The plant mediator transcriptional co-activator complex consists of in the region of 34 protein subunits that collectively link promoter-bound transcription factors with the activity of RNA polymerase II. Among them, Mediator subunit 16 (MED16; also known as SENSITIVE TO FREEZING6, SFR6) plays a major role in regulating the expression of specific genes in response to a variety of stresses including cold, drought, UV and pathogen infection. The structure of plant mediator has been hypothesised to be similar to that of yeast mediator but has not yet been proven.

Considering the structure of the yeast mediator complex, in which MED14, MED16 and MED2 occupy positions in the so-called “tail”, we would predict a close physical interaction between MED14, MED2 and MED16 in the plant complex. Therefore, this study investigated whether MED2 and MED14 control the same regulons as controlled by MED16. Results showed the necessity of these two proteins, like MED16, in gene regulation under cold, drought, and UV stresses and revealed a clear correlation between reduced levels of tolerance and impaired gene expression under cold and UV but not drought.

To investigate whether particular domains within MED16 might be responsible for the activation of specific genes under different stresses, complementation experiments were used to test the ability of three different truncated MED16 versions to restore cold-, dark- and UV-inducible expression. Some truncated versions were able to complement the mutant but the degree of complementation varied amongst transgenic lines.

Experiments were conducted to study the function of KIN10, an interacting protein of MED16 that appears to play a role similar to MED16 in regulation of stress genes and tolerance. The necessity of KIN10 in the control of a subset of the stress-inducible genes controlled by MED16 was demonstrated. Co-immunoprecipitation experiments revealed that regions within the N-terminal part of MED16 are essential for interaction with KIN10.

Key words: Mediator Complex, SFR6/MED16, MED2. MED14, KIN10, cold, UV, dark/starvation, drought/desiccation

Acknowledgement

This work was funded by the Commonwealth Scholarship Commission, UK, in 2011 and work was carried out at the Plant Cell Signalling laboratory in the School of Biological and Biomedical Sciences, Durham University, Durham, United Kingdom. I am very much grateful to my supervisor Dr. Heather Knight, who guided me since 2010 while I was applying for the scholarship and throughout my study period at Durham. Her role as supervisor as well a mentor with continuous guidance and encouragement helped me to achieve this success. I am also indebted to Professor Marc Knight who encourages us by giving all suggestions and invaluable ideas especially when we were at troublesome situations.

I am grateful for the support that I have received from all past and present expertise of Plant Cell Signalling Lab, Dr. Mark Skipsey, Dr. Ahmed Mohamed, Dr. Piers Hemsley, Dr. Susana Pollastri and all other colleagues Beccy Manning, Alex Sargeant, Rachael Oakenfull, Stephanie Johnson, Charlotte Hurst, Alice Rowland and Gioia Lenzoni those who made nice working environment in the Lab19.

Special thanks are due to my thesis committee members Dr. Adam Benham and Dr. Gary Sharples for their guidance, encouragement and all other advices during my study period at Durham.

I am grateful to present and former Vice Chancellors of Uva Wellassa University University, Dr. G. Chandrasena and Dr. Chandra Embuldeniya for their enormous support given throughout my academic carrier.

My Special thanks go to Dr. Kanthi Senanayake and her family, Ayesha Siddique and her daughter Kiswah, Mr and Mrs. Kwon family and Mr and Mrs. Meheraths family for being good friends to me and my daughter as well as for their support.

Most of all, I owe a debt of thanks to my loving family for their irresistible support, love and courage all the time. I am sincerely grateful to my little daughter who was with me all the time by sharing all happiness and sorrows during our stay at Durham and Senaka for his great support.

Ewon Kaliyadasa Pangukarage

Table of Contents

Abbreviations

Standard abbreviations for length (mm, cm), weight (ng, µg, mg, g), volume (µl, ml, l), temperature (^{o}C), amount (µmol), molarity (µM, mM, M), time (s, min, h) energy (KJ) and pressure (pa, psi) are used.
Standard chemical element symbols, amino acid and protein codes are also used.
Standard convention for gene and protein naming is used: genes are italicised and proteins are not, wild type genes and proteins are capitalised.

All other abbreviations used in this thesis are defined below.

ABA- Abscisic acid
ABF- Abscisic acid binding factor
ABRE- Abscisic acid responsive element
ADH- Alcohol dehydrogenase
AP2/EREBP- Apetala2/ethylene-responsive element binding proteins
bHLH- basic helix–loop–helix
bZIP- basic-domain leucine zipper
CBF- C-repeat binding factor
CDK- Cyclin dependent Kinase
COR- Cold regulated
CRT- C-repeat
DIN- Dark induced
DRE- Drought responsive element
DREB- Drought responsive element binding factor
EMS- ethane methyl sulfonate
ERF- Ethylene responsive factor
GFP- Green florescence protein
GTF- General transcription factor
HOS- High expression of osmotically sensitive
ICE- Inducer of CBF expression
KIN- Cold induced
LB- Luria bertani
LEA- Late embryogenesis abundance

LTI- Low temperature induced

MED- mediator

MS- Murashing and Skoog

NPR- Non-expressor of PR1

OBF- *ocs*- Element binding factor

OD- Optical displacement

ORF- Open reading frame

P5CS- Δ_1-pyrolline-5-carboxilase synthetase

PFT- Phytochrome and flowering time

PR- Pathogenesis responsive

RD- responsive to desiccation

RNAPol II- RNA polymerase II enzyme

ROS- Reactive oxygen species

SA- Salicylic acid

SDS- Sodium dodecyl sulphate

SFR- Sensitive for freezing

STET- Sucrose-Tris-EDTA-Triton

SWP- Struwwelpeter

T-DNA- transfer DNA

UTR- Un-translated region

UV- Ultra violet

WT- Wild type

ZAT- C2H2-EAR zinc finger protein

Chapter 1

Introduction

Crop yields are limited by environmental stresses that prevent them from realising their full yield potentials. Environmental stresses can be caused by one or several factors primarily the extremes of temperature, drought, salinity and radiation, which all have detrimental effects on plant growth and development that affect yield. As plants are sessile in nature, they are always challenged with various stresses in their immediate environment. Extended exposure to different varying environmental stresses results in altered metabolism, growth and development in plants (Claeys and Inzé, 2013). In order to tolerate and survive these extreme conditions plants have evolved defence mechanisms particularly those involving sensing various stress conditions and triggering appropriate biochemical pathways (Lawlor, 2013). The sensing of biotic or abiotic stress conditions induces signalling cascades that activate ion channels, kinase cascades, and accumulation of hormones such as salicylic acid, ethylene, jasmonic acid, and abscisic acid (Verslues et al., 2006). These signals ultimately induce expression of specific subsets of defence genes that lead to the accomplishment of tolerance and survival (Milla et al., 2003).

Enhanced stress tolerance in crop plants is vital to cope with changing environmental conditions to secure food supplies for the increasing world population (Godfray et al., 2010). This is far more challenging with the limited availability of arable lands that is further known as land areas with optimum conditions that accounts for only 10% of total arable lands (Tuteja et al., 2012). Engineering altered expression of genes vital under different stress conditions frequently leads to improvements in

stress tolerance (Yamaguchi-shinozaki and Shinozaki, 1994, Collins et al., 2008) and consequently plant performance.

Sensitive to Freezing 6 (SFR6) was identified as an essential protein for gaining freezing tolerance through cold acclimation and this was demonstrated using the *sfr6* mutant of Arabidopsis, which is unable to acclimate to freezing temperatures (McKown et al., 1996, Warren et al., 1996). This study aimed to investigate the role and function of SFR6 and its interacting proteins in regulating abiotic stress-responsive gene expression and tolerance in Arabidopsis. This chapter reviews major topics related to the present study covering plant stress, the plant mediator complex and Snf1-related protein kinase1 (SnRK1).

1.1 Plant abiotic stress

Any factor exerted by the environment that opposes the optimal functioning of organisms is known as an abiotic stress. Abiotic stresses like heat, cold, freezing, drought, salinity, flooding or ozone damage cellular structures and adversely affect processes that play a major role in determining productivity of crop yields and also the differential distribution of the plant species across different geographical locations (Araus et al., 2002, Verslues et al., 2006). Plants have complex and dynamic systems of response to stress stimuli which are much more intricate than found in animals despite the absence of an immune system in plants. The vital reason for this is that plants do not possess the ability to simply move away from the region of stressful stimuli (Jenks and Hasegawa, 2008).

1.1.1 Low temperature stresses

Low temperature stress is one major environmental factor that limits the agricultural productivity of plants and leads to substantial crop losses. It has a huge impact on the

survival and geographical distribution of plants. Plants differ in their tolerance to chilling (0–15 ^{0}C) and freezing (<0 ^{0}C) temperatures (Knight and Knight, 2012).

Plants from temperate regions are chilling tolerant, although possess varying degrees of tolerance to freezing but can increase their freezing tolerance by being exposed to chilling temperatures, a process known as cold acclimation (Levitt, 1980, Thomashow, 1999, Struhl, 1998). By contrast, plants of tropical and subtropical origins, including many crops such as rice, maize and tomato, are sensitive to freezing stress and lack the capacity for cold acclimation. Most molecular studies on plant responses to cold stress are focused on the mechanism of cold acclimation rather than on chilling tolerance (Katterman, 1990, Mahajan and Tuteja, 2005).

Numerous physiological, biochemical and molecular changes occur during cold acclimation, including up regulation of antioxidative mechanisms, synthesis and accumulation of cryo-protectant solutes and proteins, and changes that protect and stabilize cellular membranes (Chinnusamy et al., 2007, Thomashow, 1999) . To achieve these changes, the transcriptional activation and repression of genes by low temperature are of central importance (Thomashow, 1999). The reprogramming of gene expression results in the accumulation not only of protective proteins but also of hundreds of metabolites, some of which are known to have protective effects (Chinnusamy et al., 2007, Fowler and Thomashow, 2002, Thomashow, 2001).

Chilling stress results from cold temperatures that are enough to produce injury without forming ice crystals in plant tissues, whereas freezing stress results in ice formation within plant tissues (Thomashow, 1999). Unlike in chilling, freezing injuries triggers cell death by cytoplasmic dehydration and ice formation in the cell wall. The exposure of plants to temperatures below freezing results in water loss and cellular dehydration in addition to the formation of extracellular ice (Thomashow,

1999). Therefore, freezing tolerance is correlated with tolerance to dehydration which is caused by drought or salinity. Freezing induced dehydration can cause various disturbances in membrane structure (Steponkus and Webb, 1992). The cellular dehydration induced by freezing is the central cause of the damage, however, additional factors can also contribute to freezing damage. The growth of ice crystals can cause mechanical damage to cells and tissues and low temperatures can cause dehydration, protein denaturation and disruption of macromolecular complexes (Guy et al., 1998, Thomashow, 1999). Freeze-induced dehydration can cause different forms of membrane lesions, relatively high freezing temperatures (between -2^{o}C and -4^{o}C) cause expansion–induced lysis due to osmotic contraction and expansion that occurs with freezing and thawing (Steponkus et al., 1993, Uemura and Steponkus, 1997). Temperatures between -4^{o}C and -10^{o}C cause freeze-induced lamellar-to-hexagonal II phase transitions, an inter-bilayer event involving the fusion of cellular membranes. Temperature beyond -10^{o}C other forms of sever membrane damages occur including fracture jump lesions (Thomashow, 1998, Steponkus et al., 1993, Uemura and Steponkus, 1997). The production of Reactive Oxygen Species (ROS) is one of the responses common to different types of stress that cause damage to various macromolecules in cells. Low temperatures can cause excessive production of ROS and therefore tolerance to cold also correlates with effective systems for elimination of ROS in response to oxidative stress (Hirt and Shinozaki, 2004, Cook et al., 2004).

Despite clear role in protection against the desiccation imposed by freezing, nevertheless, recent evidence indicates that some of the molecular changes that occur during cold acclimation are also important for chilling tolerance (Dong et al., 2006, Gong et al., 2002, Lyons, 2012). In other words, it appears that chilling tolerance is

exhibited by temperate plants is not entirely constitutive, and at least part of it is developed during exposure to chilling temperatures.

1.1.2 Drought stress

Drought is the one of the most unfavourable environmental factors that affects plant productivity. The severity of drought is unpredictable as it depends on many factors such as occurrence and distribution of rainfall, evaporative demands and moisture storing capacity of soil (Wery et al., 1993, Aroca, 2012, Zhu, 2002, Yordanov et al., 2000). Plants have developed specific acclimation and adaptation mechanisms to survive under soil water deficit either by completing the life cycle before severe stress or imposing resistance mechanisms (Yordanov et al., 2000). Resistance mechanisms include drought avoidance and drought tolerance, the latter of which depends on the maintenance of cell turgor by accumulating osmolytes and soluble sugars (Umezawa et al., 2004, Thomashow, 1999, Shinozaki et al., 2003). Low molecular weight osmolytes including glycinebetaine, proline and other amino acids, organic acids and polyols are crucial to sustain cellular functions through maintaining an osmotic balance under dehydration conditions (Shinozaki et al., 2003, Thomashow, 1999, Umezawa et al., 2004). The avoidance mechanism is achievable by the maintenance of high water potential in plant tissue despite soil water deficit. This is achieved by improved water uptake under stress, the ability to hold water within the plant, reduction of water loss through reductions in leaf area and stomatal and cuticular conductance (Mahajan and Tuteja, 2005, Newton et al., 2006, Jarvis, 1976). Under drought conditions plant growth regulators including auxin, gibberrellic acid, abscisic acid, cytokinin and salicylic acid modulate plant stress responses and polyamines, citrullines and antioxidants lead to the reduction of the

adverse effects caused by water deficit (Farooq et al., 2009). At the molecular level several drought responsive transcription factors and genes have been identified such as dehydration responsive element binding proteins, aquaporin and dehydrins.

1.1.3 UV stress

Living organisms are highly vulnerable to some of the wavelengths in the light spectrum, particularly to the 280-320 nm range, and thus greatly affected by the depletion of the ozone layer. Damage occurs in the ozone layer leads many harmful rays reaching on earth and among them ultraviolet (UV) spectrum has gained importance over other spectrum (Hollósy, 2002, Robberecht, 1989). The UV spectrum is divided into three major regions UV-C (220-280 nm), UV-B (280-320 nm) and UV-A (320-400 nm) hence UV-B radiation is the most energetic component of sunlight to reach the earth's surface and various anthropogenic activities lead to accelerate the depletion of ozone layer. UV-B radiation is known to be harmful to living organisms that damage DNA, proteins, lipids and other cell membranes. DNA is one of the most important targets of both UV-B and UV-C irradiation that results in multitude of DNA photoproducts (Sancar and Sancar, 1988) which may cause mutations during replication (Jiang and Taylor, 1993). DNA-protein cross-links, DNA strands break and either deletion or insertion of base pairs can also be induced by UV exposure (Smith, 1992). Proteins have a high capacity to absorb UV-B radiation due to the presence of aromatic amino acids such as phenylalanine, tryptophan, tyrosine and histidine. UV-induced damage to amino acids has been observed in free amino acids and in proteins (Khoroshilova et al., 1990) owing to photooxidation, transfer of energy from one amino acid to another neighbouring one or UV-induced photolysis (Creed, 1984). These photochemical changes results not

only the modifications in amino acid residues but also the inactivation of whole protein and enzymes (Grossweiner, 1984, Prinsze et al., 1990). Lipids can also be photochemically modified by UV absorbance especially phospho and glycolipids, which are the main components of plant cell membranes and are destroyed by UV radiation in the presence of oxygen (Kramer et al., 1991, Panagopoulos et al., 1990).

1.1.4 Starvation stress

Photosynthesis is the only process in plants that converts solar energy to chemical energy, and drives the synthesis of sugars from carbon dioxide and water. Sugars provide the main respiratory substrate for the generation of primary energy and metabolic intermediates that are used for the synthesis of macromolecules. In addition, proper functioning of many proteins and lipids is required to bind to sugars (Lee, 1992) and carbohydrates are important as physiological signals that repress or activate many plant genes that are important in metabolic reactions (Morkunas et al., 2012).

Sugar starvation initiates substantial physiological and biochemical changes in order to sustain metabolic processes and respiration in plants and therefore it is important to study on conditions that leads sugar depletions. The sugar signalling network has the ability to regulate gene expression as well as other signalling pathways (Rolland et al., 2002, Baena-Gonzalez, 2010, Jang and Sheen, 1994, Koch, 2004, Gibson, 2005, Gonzali et al., 2006). Many studies related to sugar sensing and signalling in plants have shown that glucose, fructose, sucrose and trehalose play roles as signalling molecules (Koch, 1996, Müller et al., 1999, Rolland et al., 2006, Cho and Yoo, 2011, Morkunas et al., 2012). In addition to the involvement in signalling of cell wall invertases, sucrose and glucose transporters (and specific sugar receptors),

and hexokinase (an enzyme phosphorylates hexoses) (Sheen et al., 1999, Smeekens, 2000, Loreti et al., 2001, Harrington and Bush, 2003, Moore et al., 2003, Rolland et al., 2002, Rolland et al., 2006, Koch, 2004, Ramon et al., 2008, Smeekens et al., 2010, Hanson and Smeekens, 2009, Cho et al., 2009), evidence has been provided to show the involvement of a variety of protein kinases, including Snf1-related kinases (SnRKs) (Rolland et al., 2006, Smeekens et al., 2010) calcium-dependent protein kinases (CDPKs), mitogen-activated protein kinases, and protein phosphatases in sugar signal transduction (Rolland et al., 2002, Sinha et al., 2002).

Dark conditions lead to a significant decrease in the efficiency of photosynthesis in leaves that synthesise and export carbohydrates, thereby reducing the supply of carbohydrates to non-photosynthetic tissues that import carbohydrates for respiration, growth, and development (Yu, 1999). Therefore sugar starvation in plants initiates changes in substantial physiological and biochemical processes by limiting respiration and other essential metabolic processes in plants (Yu, 1999). Furthermore, plants under sugar starvation initiate changes in cellular processes to recycle cellular constituents and in order to achieve this, dramatically change their patterns of gene expression (Yu, 1999, Buchanan-Wollaston et al., 2005).

1.1.5 Oxidative stress

Oxidative stress arises through diverse metabolic routes in plants subjected to different abiotic stress conditions (Apel and Hirt, 2004). It occurs particularly under extreme temperature conditions, where the production of free radicals or Reactive Oxygen Species (ROS) is noticeably increased (Hasanuzzaman et al., 2011a, Hasanuzzaman et al., 2011b, Mirza Hasanuzzaman et al., 2013). High levels of ROS lead to problematic damage in plants while at low levels, ROS can act as signalling

molecules by acting as friend or foe concept. Recent studies have indicated that under temperature stress, generation of ROS including singlet oxygen (O_2), superoxide radical ($O_2^{\bullet-}$), hydrogen peroxide (H_2O_2) and hydroxyl radicals ($OH^{\bullet}$), is accelerated, thus inducing oxidative stress (Mittler, 2002, Potters et al., 2007). In plant cells, ROS are constantly produced as a result of aerobic metabolism in the chloroplast, mitochondria and peroxisomes (Apel and Hirt, 2004, Sharma et al., 2012), however, the chloroplast is considered as the main source of ROS . Under optimal environmental conditions, the antioxidant system in plant cells effectively protects them from possible deleterious effects of ROS, however, under stress conditions ROS generation is enhanced, thus the cellular antioxidant capacity can be overwhelmed and oxidative stress occurs (Hippeli and Elstner, 1996, Noctor and Foyer, 1998). Recent studies have shown that ROS could also play a main role in mediating important signal transduction events that leading to a central role in stress perception and protection (Suzuki and Mittler, 2006).

Singlet oxygen (O_2) is formed in the chloroplast during photoinhibition, a light-induced reduction of photosynthetic capacity of a plant and PS II electron transfer reactions, and this radical directly oxidises proteins, polyunsaturated fatty acids and DNA (Karuppanapandian et al., 2011b, Karuppanapandian et al., 2011a). Superoxide radicals ($O_2^{\bullet-}$) are formed in photooxidation reactions and photorespiration, various oxidase reactions taking place in chloroplasts, mitochondria and plasma membranes. Hydroxyl radicals ($OH^{\bullet}$) are produced as a consequence of the reaction between H_2O_2 and $O_2^{\bullet-}$, reactions of H_2O_2 with Fe^{2+} and decomposition of O_3 in the apoplastic space (Moller et al., 2007, Halliwell, 2006). Hydroxyl radicals can potentially react with all constituents of cells particularly biomolecules like proteins, lipids, DNA and pigments. Hydroxyl radicals are not considered to have any signalling function

although the products of their reactions can elicit signalling responses (Moller et al., 2007, Halliwell, 2006). All the above effects of ROS result in the autocatalytic peroxidation of membrane lipids and pigments, modification of membrane permeability and its functions (Xu et al., 2006).

During temperature stress, ROS levels can increase, which can result in significant damage to cell structure (Mittler et al., 2004). During heat stress it may disturb the homeostatic balance of the cell and promote lipid peroxidation, either by increasing the production of reactive oxygen species or by decreasing the O_2 radical scavenging ability in the cell (Bowler et al., 1992). In extreme cold conditions, which are beyond the plant tolerance level, the activities of antioxidant enzymes are reduced and the accumulation of ROS occurs in higher amounts. Production of ROS rigorously affects electron transfer and biochemical reactions (Suzuki and Mittler, 2006, Solanke and Sharma, 2008). Low temperature-induced oxidative stress (Prasad, 1996) decreases phospholipid content, increases lipid peroxidation and free and saturated fatty acid content (Sato et al., 2011), leading to damage to lipids, proteins, carbohydrates and DNA (Gill and Tuteja, 2010). Furthermore in extreme cases of ROS-induced oxidative stress, alterations in these enzyme activities and other biochemical reactions ultimately affects plant physiological processes including photosynthesis, respiration, nutrient movement and transpiration, which negatively affects plants survival or causes ultimate death (Apel and Hirt, 2004).

Like environmental stresses, some herbicides have the ability to induce oxidative stress (Camp et al., 1994) in plants. The modes of action of herbicides are different according to the active compound and they may act by inhibiting cell division, photosynthesis, or amino acid production or by mimicking natural auxin hormones, which regulate plant growth, causing deformities in new growth (Ashton, 1981,

Devine et al., 1992). However, nearly half of the commercially important herbicides act by interrupting photosynthetic electron flow (Ashton, 1981, Devine et al., 1992), where the specific sites of action of many of these agents have been found to lie either at the reducing side of photosystem I (eg: paraquat/methyl viologen) or in the quinone acceptor complex in the electron transport chain between the two photosystems (eg: diuron/dichlorophenyl dimethyl urea/DCMU). DCMU only blocks electron flow from photosystem II, and has no effect on photosystem I or other reactions in photosynthesis, such as light absorption or carbon fixation (Lavergne, 1982).

1.2 Gene expression to combat stresses

Under adverse or limiting growth conditions, plants respond by activating tolerance mechanisms at the molecular, tissue, anatomical, and morphological level. This is by adjusting the membrane structure and the cell wall architecture, by altering the cell cycle and rate of cell division, and by the regulation of metabolic processes (Atkinson and Urwin, 2012). At a molecular level expression of many genes is induced or repressed by abiotic stress, involving a precise regulation of extensive stress-gene networks (Grativol et al., 2012, Shinozaki and Yamaguchi-Shinozaki, 2007) in the cells. Products of those genes may function in stress responses and tolerance at the cellular level. Proteins involved in biosynthesis of osmoprotectant compounds, detoxification enzyme systems, proteases, transporters, and chaperones are among the many proteins encoded by such genes and which have roles in direct protection against stress. Microarray studies provide a powerful source to identify gene expression profiles of plants exposed to abiotic stresses such as cold, drought,

high salinity or ABA treatment (Kreps et al., 2002, Seki et al., 2002a, Seki et al., 2001, Seki et al., 2002b).

Transcription factors play key roles in gene expression by regulating expression of downstream genes as *trans*-acting factors via specific binding to *cis*-acting elements in the promoters of target genes. Analysis of stress-responsive gene promoters has identified many *cis*- and *trans*-acting elements involved in the transcriptional responses of stress-responsive genes (Furihata et al., 2006, Lindemose et al., 2013). Approximately 7% of the Arabidopsis genome is comprised of coding sequences that correspond to transcription factors (TFs) (Udvardi et al., 2007). These TFs are divided into seven major TF families, namely basic leucine zipper (bZIP), APETALA 2/ethylene-responsive element binding factor (AP2/ERF), NAM/ATAF1/CUC2 (NAC), WRKY, MYB, Cys2(C2)His2(H2)-type zinc fingers (ZFs), and basic helix-loop-helix (bHLH). At present most of the research studies on TFs that regulate abiotic stress responses has mainly focused on single TFs and their specific functions. However, many of the protein studies indicated that TFs also function as hubs, which involve many interacting proteins, by networking different pathways (Lindemose et al., 2013).

1.2.1 Gene expression in response to cold and drought stresses

In response to cold the initial signalling includes changes in the membrane and cytoskeleton of cells (Örvar et al., 2000), which are accompanied by transiently increased levels of intracellular Ca^{2+} (Knight et al., 1996, Knight et al., 1991) and activation of protein kinase cascades, leading to the activation of TFs ultimately activating the expression of target genes in response to cold (Knight and Knight, 2012, Rehem et al., 2011). Shinozaki and Yamaguchi-Shinozaki (2007) reviewed

that more than half of drought-inducible genes were also induced by high salinity and/or ABA treatments in Arabidopsis. Interestingly, only 10% of the drought-inducible genes were induced by cold stress, despite the fact that dehydration is considered to be a major part of freezing stress. In another study, a cDNA microarray was constructed using ~1700 independent rice cDNAs isolated from three cDNA libraries prepared from rice exposed to drought, cold, or high salinity stresses (Rabbani et al., 2003, Venu et al., 2013). The microarray was used to identify putative genes that respond to these stresses in rice; stress-inducibility was confirmed using RNA gel-blot analysis. This comparison confirmed that 73 of these genes were truly stressed inducible (Rabbani et al., 2003). Around 40% of drought- or high salinity-inducible genes were also induced by cold stress. However, the expression of >98% of the high salinity and 100% of ABA inducible genes were induced by drought stress. All these data suggest that in drought and salt stress signalling they use many of the same pathways. The promoters of many cold and dehydration responsive genes in Arabidopsis have been shown to contain a DNA regulatory element, the CRT (C-repeat)/DRE (dehydration-responsive element) (Baker et al., 1994), which confers both cold and dehydration responsive gene expression (Yamaguchi-shinozaki and Shinozaki, 1994).

Shinozaki et al. (2003) classified the products of the drought-inducible genes that were identified through the microarray analyses in Arabidopsis into two major groups; functional proteins and regulatory proteins. The functional proteins comprised molecules such as chaperones, late embryogenesis abundant (LEA) proteins, osmotin, antifreeze proteins mRNA-binding proteins, key enzymes for osmolyte biosynthesis, water channel proteins, sugar and proline transporters, detoxification enzymes, and various proteases that are essential in function in abiotic

stress tolerance. The regulatory proteins are important in regulation of signal transduction and stress-responsive gene expression and included various transcription factors, protein kinases, protein phosphatases, enzymes involved in phospholipid metabolism, and other signalling molecules such as calmodulin-binding protein. The transcription factors could control the expression of stress-inducible genes in either a dependent or independent manner in many gene networks in Arabidopsis. Rabbani et al. (2003) reported the products of stress inducible genes identified in rice can also be classified as functional and regulatory proteins as similar to Arabidopsis.

Various studies have led to the identification cold-regulated plant genes, especially in model plant Arabidopsis, known as *COR* (cold on-regulated), *KIN* (cold induced), *LTI* (low-temperature induced) or *RD* (responsive to dehydration) genes (Thomashow, 1999). More recently, microarray data have shown that several hundreds of genes are up regulated when plants are transferred from warm to cold conditions (Fowler and Thomashow, 2002, Kilian et al., 2007, Robinson and Parkin, 2008). C-Repeat (CRT)-binding factors (CBFs) (Stockinger et al., 1997), also known as dehydration responsive element binding protein1 (DREB1s) (Baker et al., 1994, Shinozaki and Yamaguchi-Shinozaki, 2000, Thomashow, 1998, Llorente et al., 2002), are upstream transcription factors that bind to the CRT/DRE (drought-responsive element) (Tran et al., 2004) promoter *cis* element and activate the expression of these cold-responsive genes (Jaglo-Ottosen et al., 1998, Thomashow, 1999, Liu et al., 1998).

Three genes encoding members of the CBF/DREB1 family, *CBF1*, *CBF2* and *CBF3* (or *DREB1b*, *DREB1c*, and *DREB1a*, respectively), are transcriptionally induced within 15 min of transferring plants to cold temperatures, followed at ~2 h by

expression of the CBF regulon of target genes, which are those genes whose promoters contain the CRT/DRE regulatory element (Liu et al., 1998, Shinwari et al., 1998, Gilmour et al., 1998). Several *cis*-elements in the CBF2 promoter have been found to be involved in the cold induction of CBF2 (Zarka et al., 2003). Inducer of CBF Expression1 (ICE1), abHLH (basic helix–loop–helix) protein, is an upstream transcription factor that binds to the CBF3 promoter and is required to activate CBF3 expression upon cold stress (Chinnusamy et al., 2003) and an R2R3-type MYB transcription factor, AtMYB15, was found to interact with ICE1 and to play a negative role in regulating the expression of *CBF* genes under cold stress (Agarwal et al., 2006). It appears that cold induction of the three CBF genes (Gilmour et al., 1998, Liu et al., 1998) is controlled by a set of redundant and interacting bHLHs (ICE1 and other related bHLHs) and MYB transcription factors. Some of these transcription factors cross regulate each other (Chinnusamy et al., 2007). In addition, ZAT12 negatively regulates the expression of the *CBF* genes (Vogel et al., 2005). *CBF 2* is a negative regulator of *CBF1* and *CBF3* (Novillo et al., 2004, Novillo et al., 2007) and in contrast to CBF2, CBF1 and CBF3 are not involve in regulating other *CBF* genes and positively regulate cold acclimation.

Ectopic expression of the CBFs in Arabidopsis results in constitutive expression of downstream cold-inducible genes, even at warm temperatures, and in increased freezing tolerance (Jaglo-Ottosen et al., 1998). The CBF regulon includes genes that act in concert to improve freezing tolerance. Overexpression of the CBF/DREB1 transcription factors in transgenic Arabidopsis plants results in the accumulation of compatible solutes that have cryoprotective activities, including proline, sugar, and raffinose (Cook et al., 2004, Gilmour et al., 2000). Overexpression of the CBF/DREB1 proteins in Arabidopsis results in an increase in freezing tolerance at

the whole plant level in both non acclimated and cold acclimated plants (Gilmour et al., 2000, Jaglo-Ottosen et al., 1998, Kasuga et al., 1999, Liu et al., 1998) and enhances the tolerance of plants to dehydration caused by either imposed water deficit or exposure to high salinity (Kasuga et al., 1999, Liu et al., 1998). Studies indicate that the CBF cold-response pathway is conserved in *Brassica napus* (Jaglo et al., 2001) and that components of the pathway are present in wheat and rye (Pellegrineschi et al., 2004), which cold acclimate, as well as in tomato (Chinnusamy et al., 2007, Zhang et al., 2004b). Genome sequence analysis in rice identified ten CBF/DREB1 homologues and four DREB2 homologues (Shinozaki and Yamaguchi-Shinozaki, 2007) and overexpression of OsDREB1A in Arabidopsis shown the similar responses in gene expression and stress tolerance as in rice (Dubouzet et al., 2003). Ito et al. (2006) revealed that overexpression of either OsDREB1 or AtDREB1 could improve both drought and chilling tolerance (Ito et al., 2006) in rice which suggests that the functionally similar transcription factors in dicotyledonous and monocotyledonous plants in abiotic stress tolerance.

Drought stress responses are regulated via both ABA dependent and independent signal transduction pathways. Two *cis*-acting elements ABRE (ABA-responsive element) and DRE (dehydration responsive element)/CRT(C Repeat; described above) elements are present in the promoters of many drought-, high salinity-, and cold-inducible genes; for instance *RD29A* (also known as *COR78* or *LTI78*) (Yamaguchi-shinozaki and Shinozaki, 1994, Yamaguchi-Shinozaki and Shinozaki, 2005) and the ABRE element functions in ABA-dependent expression whilst the DRE/CRT element acts to effect ABA-independent gene expression (Fig. 1.1).

The CBF/DREB1 and DREB2 (Yamaguchi-Shinozaki and Shinozaki, 2005) are the two transcription factors belonging to the ERF/AP2 family, bind to DRE/CRT

elements having, A/GCCGAC as their conserved DNA-binding motif. The CRT/DRE is the common transduction path way (Figure 1.1) which activate in both cold and drought and rapidly induced by cold stress, the products of which activate the expression of target cold stress-inducible genes (Jaglo-Ottosen et al., 1998, Kasuga et al., 1999, Liu et al., 1998).

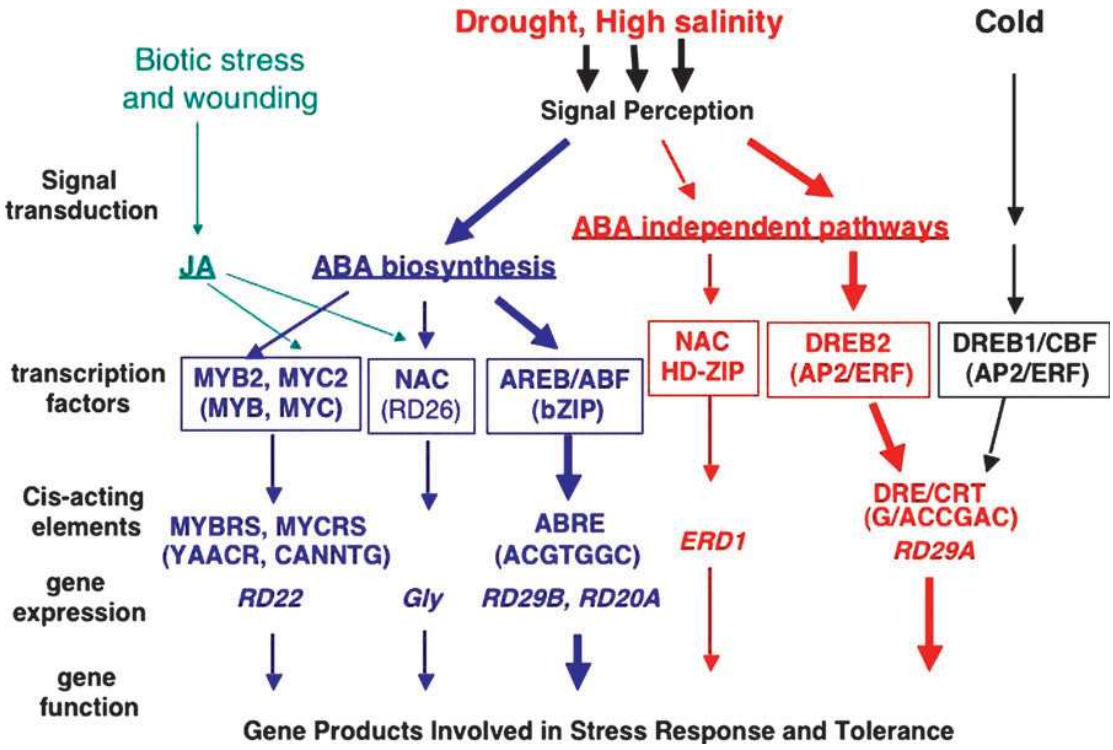

Figure1.1: Transcriptional regulatory networks of abiotic stress signals and gene expression. (From Shinozaki and Yamaguchi-Shinozaki (2007)

In the ABA-dependent pathway, ABRE functions as the major ABA-responsive cis-acting element. AREB/ABFs are AP2 transcription factors involved in this process that regulate the expression of *RD29B* and *RD20A* under drought. MYB2 and MYC2 are two important transcriptional factors regulate in ABA-inducible expression of the RD22 gene in drought. MYC2 is important in JA-inducible gene expression under biotic stress and wounding conditions. The NAC transcription factor (RD26) is involved in ABA- and JA-responsive gene expression, acting in similar manner to MYC2 TFs.

In ABA-independent pathway, DRE is mainly involved in the regulation of genes not only by drought and salt but also by cold stress as explained above in this section. DREB1/CBFs are involved in cold-responsive gene expression whilst DREB2s are important transcription factors in dehydration and high salinity stress-responsive gene expression. The other ABA-independent pathway is controlled only by drought and salt through the NAC and HD-ZIP transcription factors are involved in ERD1 gene expression.

genes involved in drought stress tolerance (Liu et al., 1998). Liu et al. (1998) reported that overexpression of DREB2 in transgenic plants, unlike overexpression of DREB1 (CBF) did not improve stress tolerance, suggesting post translational modification of DREB2 proteins must be necessary for their function. Subsequent findings revealed that, an active form of DREB2 was able to transactivate the target stress inducible genes and improve drought tolerance in Arabidopsis (Sakuma et al., 2006). Though the DREB2 protein is expressed under normal growth conditions, it can be activated by osmotic stress through the post-translational modifications (Shinozaki and Yamaguchi-Shinozaki, 2007).

The existence of another ABA-independent pathway regulating dehydration responses was suggested due to the lack of responsiveness of several drought-inducible genes to either cold or ABA treatment (Shinozaki and Yamaguchi-Shinozaki, 2007) (Figure 1.1) These genes were termed *ERD* genes, and they were induced not only by dehydration but also upregulated during natural senescence and dark-induced senescence (Nakashima et al., 2007). The *ERD1* promoter contains cis-acting element(s) involved both in ABA-independent stress gene expression as well as in senescence-activated gene expression. Simpson et al. (2003) reported that two different novel *cis* acting elements in the *ERD1* promoter were identified that involved under dehydration stress induction and in dark-induced senescence. Further Apel and Hirt (2004) identified the DNA-binding proteins interacting with these cis elements as NAC transcription factors.

The core *cis* acting element in ABA-dependent drought-inducible gene expression is the ABRE (Fig. 1.1) and members of basic leucine zipper (bZIP) transcription factors, AREB/ABF, can bind to ABRE element, thereby activating ABA-dependent drought-responsive gene expression (Choi et al., 2000, Uno et al., 2000). To regulate

the expression of one such gene, *RD29B,* ABA-mediated phosphorylation of the AREB/ABF protein is essential and overexpression of ABF3 or AREB2/ABF4 resulted ABA hypersensitivity (Kang et al., 2002). Fujita et al. (2005) and Furihata et al. (2006) reported that transgenic plants expressing a phosphorylated form of AREB1 with multisite mutations demonstrated the induction of many ABA responsive genes without exogenous application of ABA.

The transcription factors MYB2 and MYC2 (RD22BP1) were shown to bind *cis*-elements and co-operatively activate expression of *RD22*, another drought- and ABA-responsive gene (Abe et al., 2003, Abe et al., 1997) (Fig. 1.1). Accumulation of endogenous ABA is required for both MYB and MYC proteins to be synthesized for the up-regulation (Abe et al., 2003, Abe et al., 1997). The Overexpression of MYB2 and MYC2 resulted in an ABA-hypersensitive phenotype as well as improved osmotic stress tolerance in transgenic Arabidoposis plants (Abe et al., 1997).

Apart from AREB/ABF, MYB2 and MYC2 transcription factors, a NAC TF, RD26, was identified, that is transcriptionally induced under drought, high salinity, ABA and JA treatments (Fujita et al. (2004). It was observed that ABA-responsive and other stress-inducible genes were upregulated in RD26-overexpressing lines and repressed in RD26 repressor/mutant lines suggesting that RD26 overexpressors were hypersensitive to ABA, and RD26 dominant repressor transgenic were insensitive to ABA. Fujita et al. (2004) also reported that common ABA-inducible genes such as *LEA, RD, ERD, COR,* and *KIN* are not target genes of RD26, whereas many JA-inducible genes are target genes of RD26. This suggests that the role of RD26 is in mediating cross talk between ABA signalling and JA signalling during drought and wounding stress responses.

1.2.2 Gene expression in response to UV stress

High levels of UV radiation cause a wide range of morphological and physiological effects on plants that affect plant growth and development through the damage that occurs in plant cells, DNA and proteins (see section 1.1.3). However low levels of UV-B are important to initiate regulatory responses in plants that can be considered as photomorphogenic in nature (Jenkins, 2009). Therefore UV-B leads to the induction of two distinct signalling pathways, depending on the wavelength, duration of exposure and fluence rate that can be categorised as photomorphogenic signalling and nonspecific signalling pathways leading to induction of target specific genes and downstream responses (Jenkins, 2009, Wade et al., 2001). Signalling and responses will be determined by the degree of plant adaptation and acclimation to UV-B and interactions with other stimuli; each pathway initiates specific responses, although there are some overlaps between pathways. So far, the relative importance of different UV-B signalling pathways under natural growing environments has not been well-studied, however, there is evidence for the interactions between short and long wavelength of UV-B pathways (Shinkle et al., 2004), interactions between photomorphogenic UV-B and other light signalling pathways (Wade et al., 2001, Ulm and Nagy, 2005), negative regulation of photomorphogenic UV-B signalling by defence signalling pathways (Logemann and Hahlbrock, 2002) and interactions between UV-B and other environmental stimuli (Caldwell et al., Caldwell et al., 2007).

Non specific UV-B signalling pathways are activated by non-physiological and highly varying environmental signals that alter the levels of CPDs (cyclobutane pyrimidine dimmers), ROS, and wound/defence signalling molecules. Hidema and

Kumagai (2006) reported that some plants maintain low level of DNA damage which could activate signalling through maintaining low levels of ROS.

Above ambient levels of UV, plants are subjected to stress and therefore have evolved UV-induced mechanisms of protection and repair such as synthesis and accumulation of UV absorbing pigments, mainly anthocyanins (Stapleton and Walbot, 1994, Bieza and Lois, 2001, Mazza et al., 2000) and use of UV-A photons to repair most of UV-B induced DNA damage (Britt, 1996). In plants, UV stress elicits changes in gene expression by both up regulation and down regulation, especially of genes involved in the general phenylpropanoid and flavonoid biosynthesis pathways (Jordan et al., 1998). The phenylpropanoid pathway in plants is important for biosynthesis of UV-B protecting pigments and genes that encode the enzymes of this biosynthesis pathway have been shown to be up regulated at the transcript level (Jordan, 1996). In addition to pathogenesis related (*PR1*) genes, the defensin (*PDF1.2*) genes are also up regulated under UV-B stress. Many genes associated with photosynthetic proteins such as D1 protein (psbA) of photosystem II proteins, chlorophyll a/b binding proteins (Lhcb) and RuBisco (Jordan, 1996, Mackerness et al., 1997) are down regulated, however, this may due to direct damage caused by UV-B to these genes and more likely to be specific (Jordan, 1996).

Some UV-B-activated signalling components and signal transduction pathways have been identified (Mackerness et al., 1999, Mackerness and Jordan, 1999, Stratmann, 2003), however, some are not yet well defined. UV-B stimulates the production of Reactive Oxygen Species (ROS) (Dai et al., 1997) and it has been proposed that ROS not only acts as a destructive free radical but also as a signalling molecules during UV-B responses (Green and Fluhr, 1995, Mackerness et al., 1999) (see section

1.1.3). Mackerness et al. (1999) have reported that ROS increases in response to UV-B and are important in regulation of both up and down regulated genes.

The up-regulation of genes for both flavonoid biosynthesis and pathogensis-related genes under UV-B stress conditions suggest that it could be due to the production of ROS by both stress (Lamb and Dixon, 1997, Mackerness et al., 1997, Mackerness, 2000). The functions of ROS in UV-B induced signalling pathways have been studied in Arabidopsis (Mackerness et al., 1999, Mackerness, 2000), however, the origin of ROS remains unclear. The increased ROS levels lead to increases in levels of salicylic acid (SA), jasmonic acid (JA) and ethylene (Figure 1.2), which are important for the acquisition of subsequent tolerance against UV-B exposure and pathogen infections through the regulation of gene expression (Mackerness, 2000, Reymond and Farmer, 1998). Different sources of ROS during plant pathogen infections have been proposed (Wojtaszek, 1997), however, much evidence indicates that NADPH oxidase, a plasma membrane bound multi-component enzyme, analogous to mammalian phagocyte oxidase, is the most likely source in plants (Lamb and Dixon, 1997). Mackerness et al. (2001) reported that UV-B exposure leads to the production of superoxide ($O_2^{\bullet-}$) which directly mediates the up regulation of *PDF1.2* and H_2O_2 derived from $O_2^{\bullet-}$ mediates the up regulation of *PR-1* and down regulation of *Lhcb*.

The source of $O_2^{\bullet-}$ involved in *PR-1* induction is NADPH oxidase while it is peroxidise that generates the $O_2^{\bullet-}$ responsible in up-regulation of *PDF1.2* (figure 1.2)

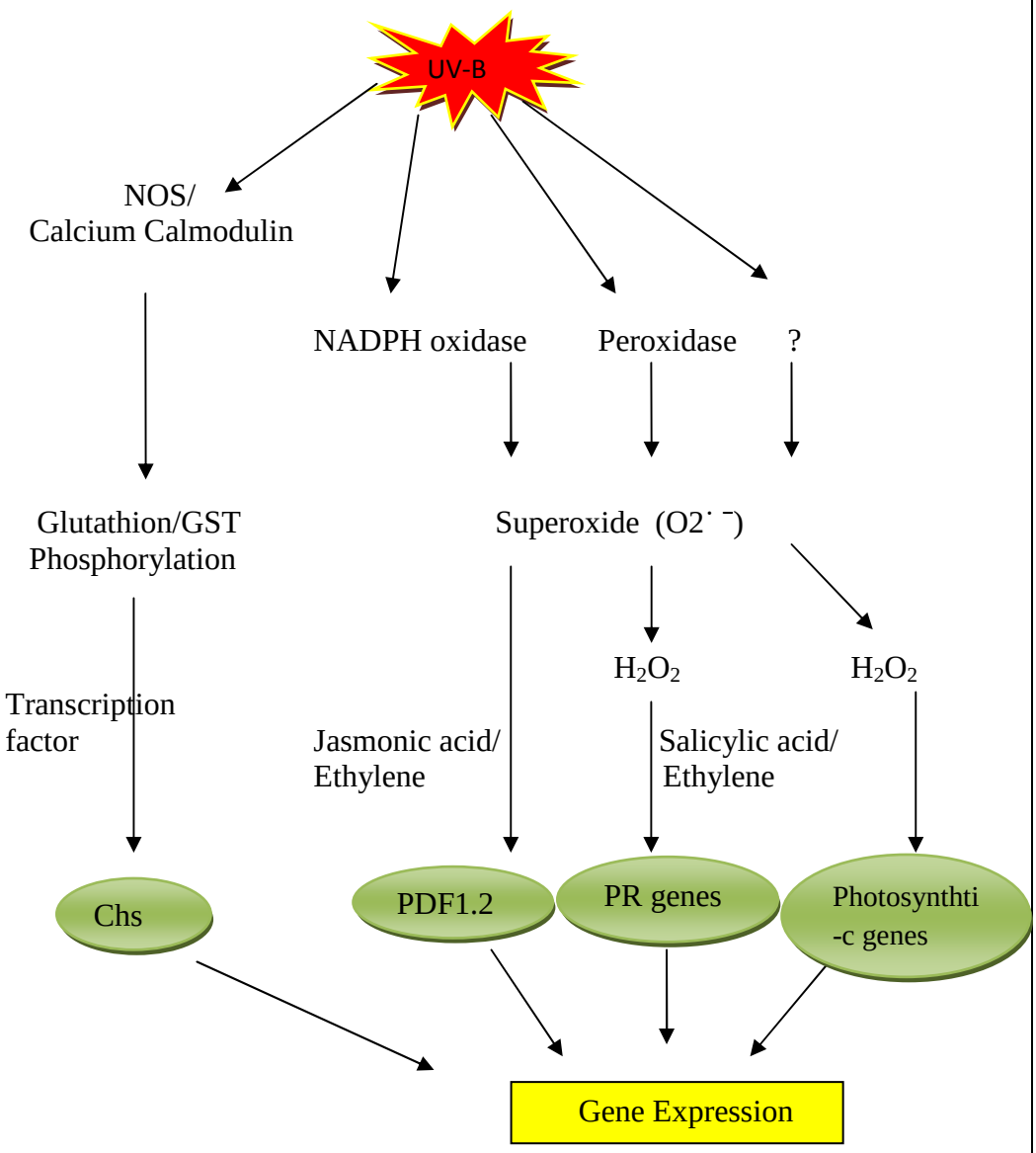

Figure 1.2: Model for the biochemical origin of ROS and signal transduction in UV-B mediated stress in plants. The model is modified from Frohnmeyer and Staiger (2003) and Mackerness et al. (2001).

NOS, nitric oxide synthase; GST: Glutathione *S*-transferase H_2O_2, hydrogen peroxide; PDF1.2, defencin; PR, pathogenesis-related; Chs, chalcone synthase;

(Frohnmeyer and Staiger, 2003). The origin of ROS involved in photosynthetic gene regulation is totally different to the above two sources (Mackerness et al., 2001). Up regulation of CHS (Chalcone synthase) in response to UV-B exposure has been

studied and it has been suggested that NO (Nitric oxide) is the signalling component. Mackerness et al. (2001) reported that source of NO in response to UV-B is most likely to be (Nitric oxide synthase) NOS. Long and Jenkins (1998) and SchÄFer et al. (1997) reported that regulation of *Chs* by UV-B radiation is mediated by calcium- and calmodulin-dependent pathway (Figure 1.2)

1.2.3 Gene expression in response to darkness, nutrient starvation and other related stresses

Depletion of carbon source in living cells induces the expression of genes involved in remobilization of alternative sources of energy, metabolites and nutrients and inhibits other biosynthetic processes and growth (Baena-Gonzalez et al., 2007, Baena-Gonzalez and Sheen, 2008, Thimm et al., 2004, Contento et al., 2004, Wang et al., 2003). However, the application of metabolisable sugars has the opposite effect on gene expression (Palenchar et al., 2004, Li et al., 2006, Price et al., 2004, Osuna et al., 2007) and these observations are supported by the fact that a similar transcriptional pattern is associated with different endogenous sugar levels that result from different rates of photosynthesis (Baena-Gonzalez and Sheen, 2008, Bläsing et al., 2005).

Many early studies focused on individual genes that respond upon dark starvation or removal of sugar from the culture medium (Koch, 1996, Fujiki et al., 2001). However, recent studies using transcriptome profiling have revealed the effect of sugar deprivation or extended darkness is not limited to activation of several genes but it impacts on more than thousands of gene targets (Baena-Gonzalez et al., 2007, Contento et al., 2004, Palenchar et al., 2004, Thimm et al., 2004, Usadel et al., 2008, Bläsing et al., 2005, Li et al., 2006, Osuna et al., 2007, Price et al., 2004, Wang et al.,

2003, Buchanan-Wollaston et al., 2005). Early sugar responses were studied in Arabidopsis by investigating global gene expression changes within 30 minutes of adding 15 mM sucrose to seedlings that had been starved for two days (Osuna et al., 2007).

This study led to identify a set of 165 early responsive genes with marked transcriptional changes in the expression of transcription factors, redox regulators, components of the proteasome and trehalose metabolism (Baena-Gonzalez et al., 2007, Osuna et al., 2007). Many of these genes, including trehalose phosphate synthase-like proteins (TPS8, TPS9, TPS10 and TPS11) and an autophagy-related gene *ATG8e* (AUTOPHAGY 8E), which are repressed by sucrose after 30min and early on in the light period are rapidly expressed during extended dark (night), suggesting that even a small drop in energy (carbon) status is enough to trigger changes in gene expression (Usadel et al., 2008). Further 2-4 hour extension of dark (night) period can results energy deprivation that leads to similar responses under prolonged starvation that affects not only transcription but also translation rate and cell proliferation.

The existence of a set of genes that is similarly induced or repressed by several different adverse conditions was revealed by expression profiling in which a wide range of stress conditions were used to distinguish between ubiquitous and specific stress responses (Baena-Gonzalez et al., 2007, Kilian et al., 2007, Ma and Bohnert, 2007, Swindell, 2006). In addition, the promoters of genes that were affected similarly by a variety of environmental stress conditions have been shown to be enriched in several *cis*-motifs (Geisler et al., 2006, Ma and Bohnert, 2007), however, the transcription factors (TFs) that recognize these *cis* elements particularly their

upstream regulators and common signal responsible for convergent regulation of these genes are still unknown or have not been investigated (Baena-Gonzalez et al., 2007).

1.3 SNF1/AMPK/SnRK1 kinase complexes in energy regulation and in stress signalling

Adaptation to stress is acquired through both defence mechanisms and stress acclimation as well as through the reprogramming of metabolism and gene expression to shunt energy sources from growth-related biosynthetic processes (Baena-Gonzalez, 2010, Wang et al., 2003). Under stress conditions resources are diverted from reproductive processes to metabolic processes that lead to increased stress tolerance, thereby managing energy sources not only at the cellular level but also at the whole plant level through manipulating biosynthetic processes. Initial stress signalling events determine the ability of plants to coordinate a successful response. However, failure to cope with these initial stress responses may lead to nutrient deprivation, irreversible senescence and ultimately death of cells (Baena-Gonzalez, 2010). Protein kinases and phosphatases are key components that recognise stress signals and transmit these signals to different cellular compartments through specialized signalling pathways (Kulik et al., 2011). SNF1-related kinases are known as important elements of transcriptional, metabolic and developmental regulation in response to stress which initiated by the different signalling cascades that helps to make specific metabolic adjustments through energy balance (Baena-Gonzalez et al., 2007, Baena-Gonzalez and Sheen, 2008).

1.3.1 Major functions of SNF1/AMPK/SnRK1 complexes

The crucial role of the highly conserved protein kinases across the kingdoms, SNF1/AMPK/SnRK1 complex is the integration of information relating to nutrient availability and regulation of energy outflow with stress signalling to acquire the adaptations necessary to maintain the internal energy equilibrium. In yeast, SNF1 is essential for the adaptation to glucose limitations where it allows cells to utilise alternative carbon sources such as sucrose or ethanol (Celenza and Carlson, 1984, Celenza and Carlson, 1986) *i.e* to make the transition from a fermentative to an oxidative metabolism to produce ATP (Hardie et al., 1998) The importance of SNF1 in yeast during energy shift has been demonstrated using *snf1* mutants that are unable to grow without glucose, even in the presence of alternative energy sources such as glycerol, saccharose or ethanol (Carlson et al., 1981, Schuller, 2003).

Mammalian AMPK is involved in regulating the cellular energy level and is activated by increased levels of AMP/ATP ratio under conditions such as glucose deprivation, hypoxia and oxidative stress (Ghillebert et al., 2011, Polge and Thomas, 2007). After activation, AMPK causes the upregulation of catabolic pathways (energy producing) such as glycolysis and fatty acid oxidation and downregulates anabolic processes (energy consuming) such as synthesis of proteins, sterols and fatty acids (Hardie, 2004, Hardie, 2007, Steinberg and Kemp, 2009). AMPK also play a major role in regulating the energy metabolism in whole body by controlling energy intake through integrating hormonal and nutritional signals in the hypothalamus (Minokoshi et al., 2008a). The control of food intake takes place by altering the activity of AMPK, which is inhibited by glycose, leptin (hormone regulate energy balance by inhibiting starvation) and insulin, leading to repress food intake. Food intake is stimulated by activating AMPK via the action of a hormone

called ghrelin (Andersson et al., 2004, Minokoshi et al., 2008b). AMPK is important in glucose homeostasis by inhibiting insulin production via secreting islet β cells (da Silva Xavier et al., 2000, da Silva Xavier et al., 2003) when blood glucose level is low and causing the absorption of 70% of the glucose available in blood into skeletal muscles to maintain constant blood glucose level (DeFronzo et al., 1992). Impairment of human AMPK is associated with many disorders such as insulin resistance, obesity, cancer, cardiovascular diseases, stroke and dementia (da Silva Xavier et al., 2003, Minokoshi et al., 2008a, Steinberg and Kemp, 2009) showing the vital impact of this enzyme on survival, growth and development at organismal level. Although much information is available on energy regulation and the metabolic functions of SNF and AMPK protein kinases in yeast and mammalian cells, less is known about the physiological functions of SnRK1 in plants. However, findings suggest that SnRK1 is involved in the global regulation of metabolism, similarly to SNF and AMPK. In addition to the above role, SnRK1 also regulates plant developmental processes during germination, reproduction and senescence and the development of resistance under salt stress and response to infections caused by different pathogens (Baena-Gonzalez et al., 2007, Halford et al., 2003, Rolland et al., 2002) (Figure 1.3).

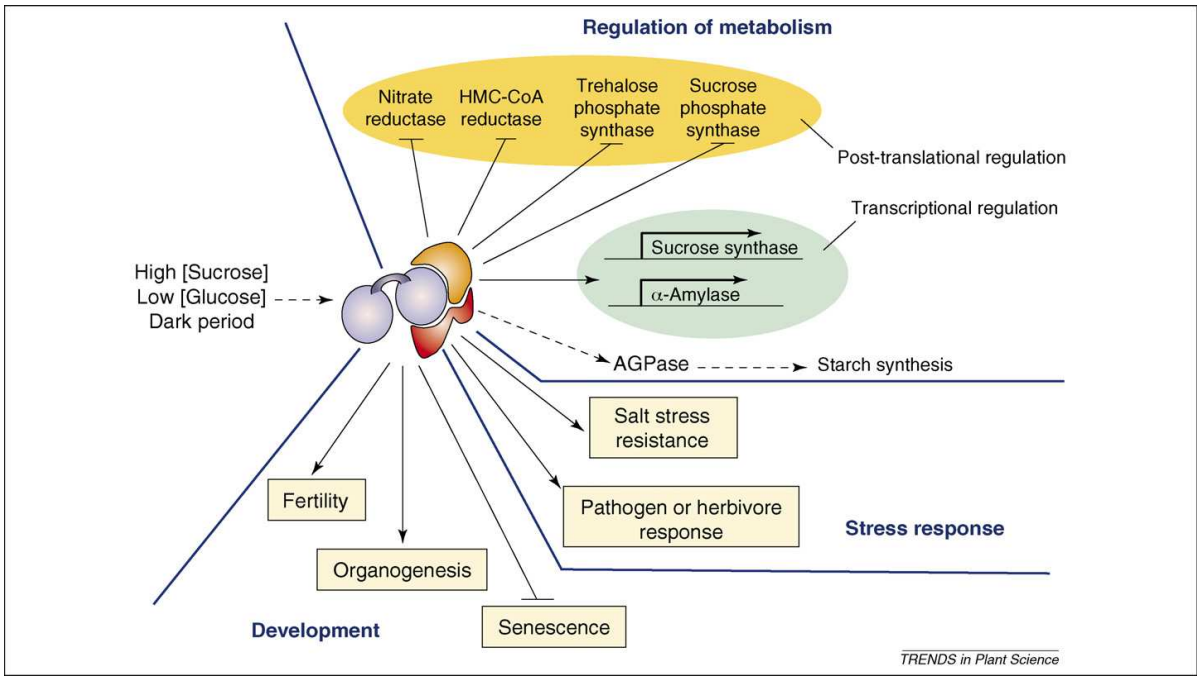

Figure 1.3 Summary of the metabolic and transcriptional reulation of SnRK1 in plants from Polge and Thomas (2007)

High cellular sucrose and/or low glucose or a dark period activates SnRK1. Upon activation, SnRK1 phosphorylates and inactivates four main plant metabolic enzymes namely nitrate reductase (NR), which catalyses the first step of nitrogen assimilation into amino acids, 3-hydroxymethyl-3-methylglutaryl-CoA reductase (HMGR), sucrose phosphate synthase (SPS) which catalyses sucrose biosynthesis and trehalose phosphate synthase 5 (TPS5) a key enzyme in the synthesis of trehalose-6-phosphate, a signalling sugar that regulates plant metabolism and development. Phosphorylation of SnRK1 activates the transcription of sucrose synthase and α –amylase and also indirectly stimulates AGPase activity, the key enzyme of starch synthesis. Altered expression of SnRK1 complex influence on early growth and development of seeds, pollen growth and development and advanced senescence which affects plant developmental processes. SnRK1-regulated stress responses have been recorded in salt hypersensitivity, plant pathogen interactions and in nematode resistance.

1.3.2 SNF1-related protein kinases are conserved in eukaryotes

The protein kinase complexes of sucrose non fermenting 1 (SNF1), AMP–activated protein kinases (AMPK) and Snf1-related protein kinase1 (SnRK1) are a family of highly conserved heterotrimeric serine/threonine kinases in all eukaryotes (Halford and Hey, 2009, Hardie, 2007, Polge and Thomas, 2007). Serine/threonine enzymes are kinases that phosphorylate the -OH group of serine or threonine amino acids, which have similar side chains. The structure of these kinase complexes was first studied in yeast (Jiang and Carlson, 1997) and it was found that this complex consisted of a α (catalytic) subunits and β and γ regulatory subunits. The structural similarities were found in mammalian AMPK complexes, which also exist as a heterotrimer (Davies et al., 1994, Mitchelhill et al., 1994). These catalytic and regulatory units are essential for protein stability and kinase activity. Isolation of β and γ type non-catalytic subunits in Arabidopsis (Bouly et al., 1999) further confirmed the existence of these complexes throughout the evolution process. In the three kingdoms that yeast, mammals and plants belong to nearly 48% of identity across the entire sequence of SNF1-related protein kinases is observed; this value increases up to 60-65% in kinase domains (Halford et al., 2000, Polge and Thomas, 2007). In plants another two types of SNF1 related kinases known SnRK2 and SnRK3 have been found but the sequence similarity that they share with SNF1 is less compared to that of SnRK1 (Polge and Thomas, 2007). Furthermore, they not appear to have a role in energy stress responses. Evolutionary conservation of these protein kinases extends to the two non-catalytic β and γ subunits (Polge and Thomas, 2007). The other two subfamilies, SnRK2 and SnRK3 are known to as plant specific with sequence similarity to yeast and mammalian catalytic subunits however clearly more diverged (Kulik et al., 2011).

1.3.3 Structure of the SNF1/AMPK/SnRK1 kinase complexes

The number of different SNF1/AMPK/SnRK1 kinase complexes that can be formed in each organism is varies hugely and depends on the number of isoforms that exist for each of the catalytic (α) and regulatory (β and γ) sub units, In yeast one catalytic subunit (SNF1) is encoded, whilst two α isoforms exist in mammals (AMPKα1 and AMPKα2) and three in plants (KIN10, KIN11 and KIN12) (see Figure 1.4) (Polge and Thomas, 2007). The SnRK1 subfamily shows similarity to SNF1 and AMPKα and it has three catalytic isoforms KIN10, KIN11 and KIN12.

The catalytic subunit is a highly conserved subunit in SNF1/ AMPK/SnRK1 complexes across three kingdoms particularly at the kinase domain in the N-terminal of the protein (Halford et al., 2003, Carling et al., 1994). To confer the kinase activity, phosphorylation by upstream kinases in the threonine residue in the activation loop of the kinase domain is required (Hedbacker and Carlson, 2008, Polge and Thomas, 2007, Steinberg and Kemp, 2009, Halford and Hey, 2009). Next to the kinase domain an auto inhibitory regulatory sequence (AIS) is present and this makes additional interactions with γ-subunits (Ghillebert et al., 2011, Jiang and Carlson, 1997). the end part of the C terminus of the protein consists of a conserved leptomycin-sensitive nuclear export sequence (NES) (Kazgan et al., 2010).

The classical β-type regulatory subunit was studied in yeast and consists of characteristic and distinct two domains, ASC (ASsociation with SNF1 complex) (Jiang and Carlson, 1997) and a KIS (kinase-interacting terminus) (Jiang and Carlson, 1997) with more variable N-termini (Hedbacker and Carlson, 2008) The KIS domain (largely but not completely overlaps with GBD (Glycogen-binding domain) (Hudson et al., 2003, Polekhina et al., 2003). Three β-type subunits in yeast

have been described as SIP1, SIP2 and GAL83 (Jiang and Carlson, 1997) and later two AMPKβ1 and AMPKβ2 were found in mammals (Halford et al., 2000). In Arabidopsis three β-type subunits have been studied and these have been categorized in to two classes; one has all the characteristics of yeast and mammalian β subunits (AKINβ1 and AKINβ2) (Bouly et al., 1999) and the other class is composed of structurally atypical subunits (AKINβ3), which it has been suggested are plant specific subunits (Gissot et al., 2004). AKINβ3 type proteins are truncated versions of β subunits and lack the entire GDB as well as the N-terminal region (Polge and Thomas, 2007). However AKINβ3 still complements a yeast mutant lacking all β subunits (Gissot et al., 2004) suggesting that some of the basic functions have been conserved.

The ASC domain is found at C-terminus of amino acids (Jiang and Carlson, 1997) and arbitrates the interaction with the γ-subunit of yeast SNF1 and plant SnRK1 (Jiang and Carlson, 1997) and both the α and γ subunits in mammalian AMPK (Iseli et al., 2005). However, plants expressing AKINβ3, an atypical plant specific β subunit which lacks the entire GDB/KIS domain shows the same interaction with both α and γ subunits as in C-terminal ASC domain does in mammalian AMPK. The GDB/KIS domain is located in the middle of the protein and mediates the interaction with the regulatory domain of the catalytic α-subunits of yeast SNF1 and plant SnRK1, but it is not essential in mammalian AMPK to form a stable heterotrimeric complex (Hedbacker and Carlson, 2008). The N-termini of β subunits are important for membrane targeting and binding (Hedbacker and Carlson, 2008, Steinberg and Kemp, 2009) through controlling subcellular localization of the kinase complexes that are sequence specific for nucleo-cytoplasamic translocation (Hedbacker and Carlson, 2006) or N-myristoylation (Hedbacker and Carlson, 2008, Steinberg and

Kemp, 2009). For example under high glucose conditions all β subunits (Sip1, Sip2 and Gal83) in yeast cells are in the cytoplasm while under low glucose conditions Gal83 is translocated to the nucleus whereas Sip1 relocalises to the vacuole and Sip2 remains in the cytoplasm (Vincent et al., 2001). Hedbacker and Carlson (2006) showed that the N terminus of Gal83, is necessary and sufficient for the SNF1-independent regulation of nuclear localization while C terminus of Gal83 is involved in the regulation of localization through its interaction with Snf1. Fragoso et al. (2009) reported that AKIN10 and AKIN11 are targeted to both the cytoplasm and chloroplast, while AKINβ1 is mainly located in the nucleus and AKINβ2 is targeted to both nucleus the and chloroplast. It was predicted that interaction of catalytic subunits with regulatory subunits might localise the complex in different locations within the cell in Arabidopsis (Fragoso et al., 2009).

The γ subunits are characterized by divergent N-termini and two pairs of cyatathionine-beta-synthase (CBS) repeats that known as Bateman domains which bind to adenosine derivatives (Hedbacker and Carlson, 2008, Minokoshi et al., 2008b). The yeast γ subunit is known as SNF4 whereas mammals and plants have three γ subunits (AMPKγ1, AMPKγ2 and AMPKγ3) and two γ subunits (AKINγ and AMPKβγ) respectively. In plants, in addition, to expressing an atypical γ subunit, AKINβγ-type plant-specific proteins resulting from the fusion between a GBD-related domain of β subunits and γ type proteins are present(Lumbreras et al., 2001). This fused GBD related domain mediates the interaction with proteins unrelated to SnRK1complexes (Gissot et al., 2006). This AKINβγ is competent to complement the yeast *snf4* mutant phenotype (Gissot et al., 2006, Kleinow et al., 2000, Lumbreras et al., 2001). However the classical AKINγ is unable to complement the yeast *snf4* mutant phenotype (Bouly et al., 1999, Slocombe et al., 2002).

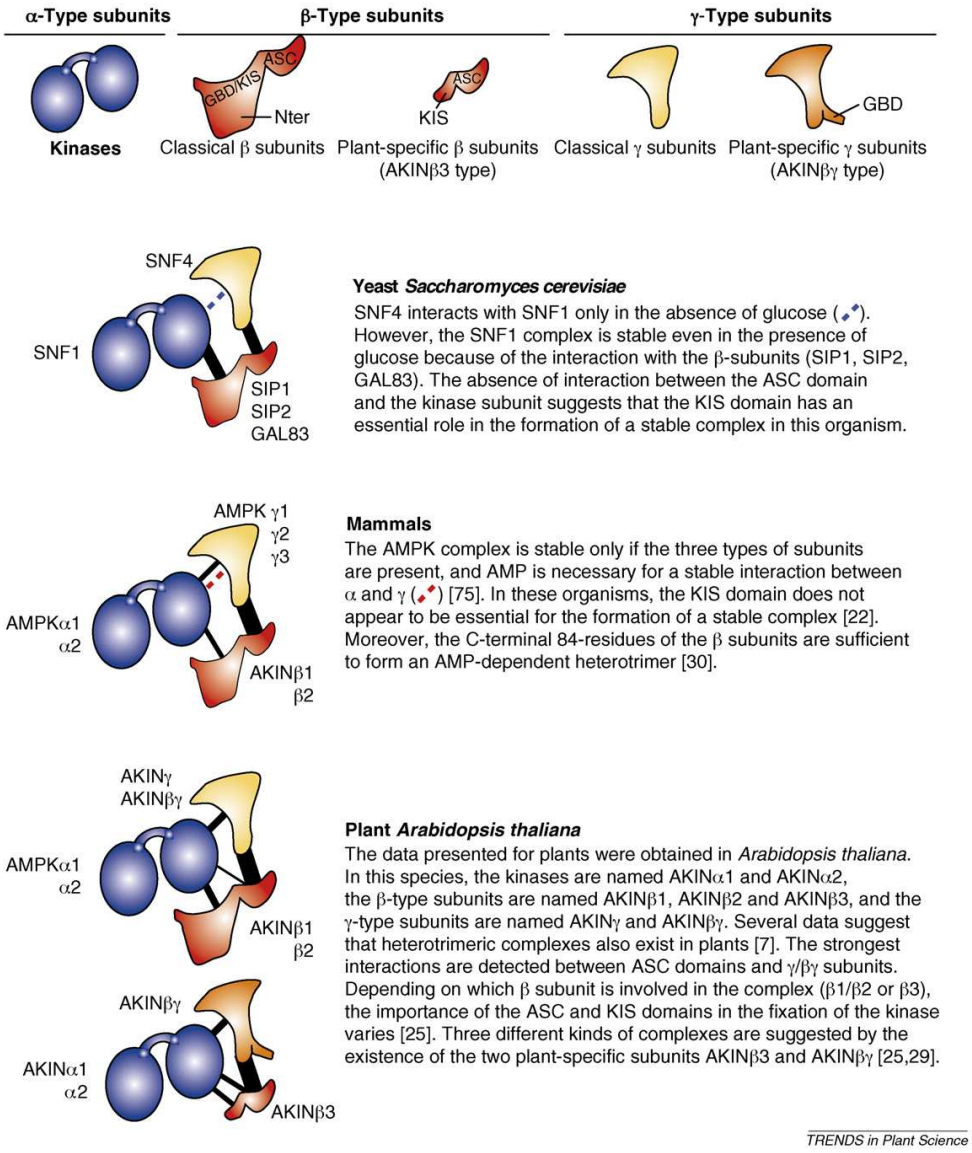

Figure 1.4 Structure of the SNF1/AMPK/SnRK1 kinase complexes. From Polge and Thomas (2007)

The structural composition of SNF1/AMPK/SnRK1 kinase complexes among yeast, mammals and plants is shown in the figure. These heterotrimers consist of a catalytic α subunit and regulatory β and γ sub units and the number of complexes that can be formed in each organism is highly variable and this number is determined by the number of different isoforms in each major sub unit. In yeast alternative 3 SNF1 complexes (one α subunit, 3 β subunits and one γ sub unit), 12 different AMPK complexes (two α subunits, 3 β subunits and 3 γ subunits) in human. In plants this number may greatly varying as it consisted with plant specific β subunits and γ subunits apart from classical two α subunits, 2 β subunits and one γ subunit.

Considering these facts, plants appear to express plant-specific alternative complexes that interact with catalytic subunits to form complexes other than the classical heterotrimeric complexes. These may lead to plant-specific functional features such as autotrophic and sessile lifestyles and cope with more harsh nutritional and environmental stress through stable energy homeostasis.

1.3.4 Regulation of SNF1/AMPK/SnRK1 kinase complexes

SNF1/AMPK/SnRK1 kinase complexes are known to be regulated by two major cascades, phosphorylation and allosteric regulation. However only mammalian AMPKs are subjected to allosteric regulation mediated by AMP/ATP ratio, the most sensitive indicator of energy status in cells (Hong et al., 2003, Nath et al., 2003, Sutherland et al., 2003, Suter et al., 2006, Ghillebert et al., 2011). Phosphorylation , a biochemical process is highly conserved for protein kinases, as demonstrated by well characterize cyclin-dependent kinase and mitogen-activated protein kinase cascades (Shen et al., 2009). The phosphorylation induces changes in the structural confirmation of the protein that move the activation loop and allow access to the kinase active site (Shen and Hanley-Bowdoin, 2006). In yeast, SNF1 has been shown to be activated by three partially redundant kinases PAK1, ELM1 and TOS3 (Hardie, 2007, Hong et al., 2003, Nath et al., 2003, Shen et al., 2009, Sutherland et al., 2003). AMPK in mammals is activated by two kinases (Hawley et al., 2003, Hawley et al., 2005, Hurley et al., 2005, Woods et al., 2005, Woods et al., 2003a, Woods et al., 2003b), of which one, LKB1, is constitutively active (Lizcano et al., 2004) and the other one CaMKK, is activated by Ca^{2+} (Hardie, 2007, Steinberg and Kemp, 2009, Ghillebert et al., 2011). Either LKB1 or CaMKK could complement the

function of mutants lacking PAK1, ELM1 and TOS3 in yeast suggesting that these two upstream AMPK kinases are functionally conserved (Hong et al., 2003).

In Arabidopsis, GRIK1 and GRIK2 (geminivirus Rep interacting kinases) are amongst the upstream activating kinases of SnRK1, of which there are homologues ranging from one to three in other plant species (Kong and Hanley-Bowdoin, 2002, Shen and Hanley-Bowdoin, 2006). GRIK proteins can mainly be found in young tissues such as apical meristems, floral buds and immature siliques where cell division takes place extensively (Shen and Hanley-Bowdoin, 2006, Shen et al., 2009). Each of the Arabidopsis GRIK proteins could complement a yeast *pak1*, *elm1* and *tos3* triple mutant, suggesting GRIKs are upstream activators of SnRK1 and (Shen et al., 2009) reported that GRIK1 and GRIK2 specifically phosphorylate the SnRK1 kinase domain of the α-subunit in *in vitro* kinase assays. Furthermore they revealed that GRIK1 and GRIK2 phosphorylates the conserved Thr residue in the SnRK1 activation loop.

1.3.5 The role of SnRK1 and its catalytic subunits KIN10 and KIN11 in plant stress gene regulation in response to energy stress

Recent work has shown that the evolutionarily conserved Arabidopsis protein kinases KIN10 and KIN11 the two isoforms that exists in plant the catalytic α-subunit control the reprogramming of transcription related to several unrelated stress responses such as darkness, sugar and other stress (Baena-Gonzalez et al., 2007, Baena-Gonzalez and Sheen, 2008). That is because the expression of large number of genes encoding putative TFs and histones and histone deacetylases are highly activated or repressed by KIN10 (Baena-Gonzalez et al., 2007, Buchanan-Wollaston et al., 2005, Contento et al., 2004, Thimm et al., 2004). Moreover, KIN10 has an

effect on the expression of several hormone-responsive genes, genes involved in hormone metabolism as well as many genes that encode other signal transduction components including protein kinases, protein phosphatases and calcium modulators (Baena-Gonzalez et al., 2007).

The evolutionarily conserved structure and functional characteristics of SnRK1 subunits KIN10 and KIN11 have been discussed in detail in the section 1.3.3.

In comparison to yeast and mammals few components of SnRK1 signalling cascade have been studied so far (Baena-Gonzalez, 2010). Under energy deficient stress conditions SnRK1, activates an energy-saving program at the cellular level, including vast transcriptional reprogramming. This includes the Arabidopsis S-group of bZIP TFs, bZIP1, bZIP2/GBF5, bZIP11, bZIP44 and bZIP53 that all are downstream effectors which positively affect the expression of a subset of KIN10 target genes (Baena-Gonzalez et al., 2007, Hanson et al., 2008) (Figure 1.5). S-group bZIPs appear to function as heterodimers with the members of the C-group. In addition, members of these two groups are differentially expressed in response to several stresses, which results a wide range of possible dimer combinations (Weltmeier et al., 2009). Therefore the regulation of SnRK1s through the bZIP network is more complex (Ehlert et al., 2006, Weltmeier et al., 2009). Evidently the S-group bZIP TFs are translationally repressed by sucrose (Rahmani et al., 2009, Wiese et al., 2005), providing the support for opposed regulation by energy deficiency and abundance.

Yeast–two-hybrid studies have uncovered other transcriptional regulators that interact with SnRK1 and possibly play a role in the SnRK1 signalling cascade (Baena-Gonzalez, 2010). A possible interactor of SnRK1 (Baena-Gonzalez, 2010) a recently identified plant specific TF, ATAF1, a member of the NAC family in

Arabidopsis which showed that *ATAF1* is induced by a wide array of stress conditions while plants overexpressing ATAF1 are more tolerant to drought (Wu et al., 2009). Lu et al. (2007) reported that SnRK1 acts upstream of the MYBS1 TF to induce the α-amylase gene *αAmy3* during the early stages of germination to guarantee the energy supply to the developing embryos through the degradation of starchy endosperm using rice embryos (Lu et al., 2007). The importance of this phenomenon is further evident by another study that showed the ability of certain rice varieties to tolerate under flooding even during early development stages, which might be partly accounted for by its ability to remobilise nutrients from embryos (Lee et al., 2009, Lu et al., 2007). Some transcription factors like AZF2 (Arabidopsis zinc finger [C2H2 type] protein 2) and ZAT10 are well known to be involved in stress responses (Mittler et al., 2006, Sakamoto et al., 2004), however, their direct connection to SnRK1 has not been well studied.

Young-Hee Cho et al. (2012) reported that SnRK1 induced stress responsive gene expression through direct association with target gene chromatin and enhance the stress tolerance in plants under submerge conditions specifically submergence induced *ADH1* and *PDC1*, which are involved in establishing stress tolerance in plants. Furthermore they found that this induction was correlated with the direct association of SnRK1s with target gene chromatins. Baena-Gonzalez et al. (2007) identified seven highly correlated gene expression patterns of KIN10 target genes using Arabidopsis ATH1 GeneChips (Palenchar et al., 2004, Buchanan-Wollaston et al., 2005, Thimm et al., 2004) and reported the positive correlation with KIN10 target genes under various sugar and energy starvation conditions where as strong negative correlation with the gene expression profiles obtained from glucose or

sucrose treated seedlings and differential CO_2 fixing adult leaves in intact plants (Palenchar et al., 2004, Price et al., 2004). As previous work reported (Baena-Gonzalez et al., 2007) that KIN10 participates in response to an energy-depleting hypoxic condition which affected the level *DIN6* expression in Arabidopsis, similarly Young-Hee Cho et al. (2012), applied the same condition in the presence of rice SnRK1, hypoxia-inducible *DIN6-LUC* reporter and found activity was further enhanced in a manner similar to that of KIN10. But the inactive form of OsSnRK1 suppressed the hypoxia-induced *DIN6-LUC* activity, confirming the protein kinase activity of OsSnRK1 is essential in activating specific stress *i.e* hypoxia-responsive gene expression similar to that in Arabidopsis thereby confirming rice OsSnRK1 share the sequence and structure similarities with Arabidopsis KIN10.

As in other organisms SnRK1 kinases in Arabidopsis do not seem to response to energy signals (Shen et al., 2009) and this is supported by early findings in spinach (Sugden et al., 1999). However sugars, in the form of trehalose-6-phosphate (T6P), glucose-6-phosphate (G6P), or other forms, have a repressive effect on activity (Figure 1.5) and in addition the specific effect of sugars on the SnRK1 cascade may differ among tissues and developmental stages. As an example sucrose has a specific effect on the SnRK1 signalling cascade by repressing translation of the S-group bZIP TFs. SnRK1 regulation may differ between autotrophic and heterotrophic tissues (Baena-Gonzalez, 2010). When evaluating the effects of sugar on SnRK1, the sugar concentrations used are most important, and determine whether stress and defence responses are triggered (Wingler and Roitsch, 2008). Therefore a particular level of sugar supplied in combination with stress may either not be metabolised or not trigger the following events the same response as the same amount of sugar supplied

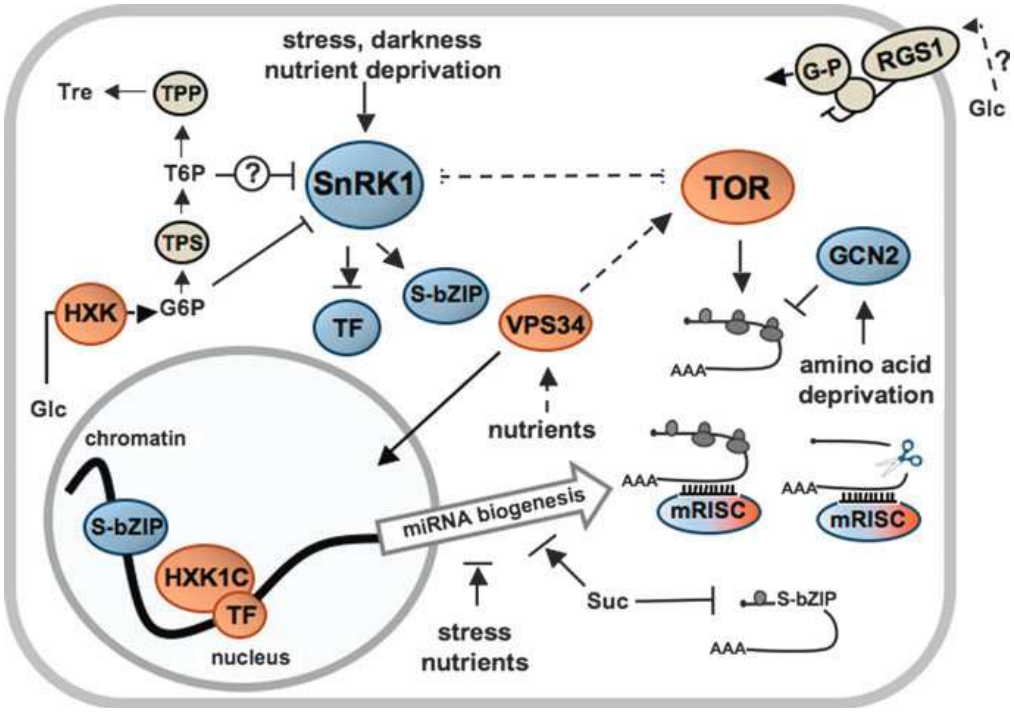

Figure 1.5: Energy and nutrient sensing in regulation of gene expression in response to stress, from Baena-Gonzalez (2010)

Three different colours used to represent three hypothesised network machineries in energy and nutrient sensing. The blue apparatus are hypothesized to constitute a network that, upon sensing nutrient and/or energy deficiency, down regulates growth-related energy-consuming processes and promotes nutrient remobilization and tolerance to stress. The network formed by the orange components is proposed to operate in an antagonistic manner to couple nutrient/energy availability with growth. Components displaying both colours may function in both networks. HXK1C, Hexokinase 1 nuclear complex; Glc, glucose; Tre; trehalose; Suc, sucrose; TPS, trehalose-6-phosphate synthase: TPP, trehalose-6-phosphate phosphatase; RISC, miRNA-induced silencing complex; TOR, target of Rapamycin. Solid lines designate proven connections, whereas dotted lines represent hypothetical ones.

under non stresses conditions (Baena-Gonzalez, 2010). Recent studies by Zhang et al. (2009) have shown that trehalose-6-phosphate (T6P) potentially inhibits SnRK1 activity through unidentified regulatory factor (Figure 1.5).

Rolland et al. (2006) reported that plants are able to sense the presence of sugars through various pathways which recognize directly or indirectly the sucrose, glucose, fructose or trehalose though most of the fundamental molecular mechanisms are still not known. However, Arabidopsis HXK1 (AtHXK1) was identified as a core component in plant sugar sensing and signalling (Figure 1.5) with distinct metabolic and signalling functions (Cho et al., 2006, Moore et al., 2003). AtHXK1 mediates repression by sugars, in the presence of glucose by regulating the photosynthesis-related CAB (chlorophyll a/b binding proteins) (Chen et al., 2006) of other proteins in the nuclear AtHXK1 complex (Cho et al., 2006). Metabolism of glucose through HXK1 independent signalling pathway induces, the expression of the defence and pathogenesis related *PR* genes (Xiao et al., 2000). Tobacco plants overexpressing HXK1 and HXK2 are more resistant to H_2O_2 induced programmed cell death (Kim et al., 2006) and connection between glucose metabolism and defence was described by Wingler and Roitsch (2008). The glycose-6-phosphate (G6P), the product of glucose phosphorylation by HXK, represses SnRK1 activity (Figure 1.5) in spinach leaf extracts (Toroser et al., 2000).

Trehalose is a disaccharide that commonly serves as a storage carbohydrate and stress protectant (Baena-Gonzalez, 2010). Trehaloses are synthesized in two steps, where glucose is converted to trehalose-6-phosphate synthase (TPS) via G6P and T6P is converted to trehalose by trehalose-6-phosphate phosphatise (TPP) (Figure 1.3). Recent research showed that trehaloses accumulate in trace amounts in most plants, and are important in metabolism, development and stress responses (Paul et al., 2008, Ramon and Rolland, 2007). Arabidopsis overexpressing AtTPS1 are more resistant to drought and T6P levels are correlated with improved levels of stress gene

expression under many stresses as well as those involving KIN11(Avonce et al., 2004, Schluepmann et al., 2004).

Sugars has a major role in regulation of gene expression than other major nutrients such as nitrogen and many of the sugar regulated genes are strongly affected by nitrogen and therefore extensive interaction exists between sugar and nitrogen nutrients (Palenchar et al., 2004, Price et al., 2004). It is more likely that energy and glucose dependent metabolic sensors such as SNF1/AMPK/SnRK1 are also important in nitrogen sensing. The TOR (Targets of Rapamycin) a central protein kinase that promotes cell growth and proliferation in response to amino acids and insulin (Avruch et al., 2006). Recent studies suggests that the TOR pathway plays an important role in stress adaptation via responding to a wide range of stimuli, including amino acids, ATP, mitogens, low oxygen, and phosphatidic acid (Baena-Gonzalez, 2010). Decreased TOR activity has been correlated with enhanced resistance to several types of stress (Reiling and Sabatini, 2006). Arabidopsis TOR (AtTOR) is a highly conserved protein, with all of its key domains found in other organisms. As in other organisms, AtTOR is also essential for embryogenesis and endosperm development and knockout mutants of TOR leads to impaired developmental at the globular stage (Menand et al., 2004). Deprost et al. (2007) reported that varying degrees of AtTOR overexpression or knockouts demonstrate that AtTOR is essential also for postembryonic growth which affects root and shoot growth, cell size and seed yield. Arabidopsis VPS34 (AtVPS34) shares a 40% identity with yeast and when AtVPS34 fused to the yeast regulatory domain, its C-terminal catalytic domain is able to complement a yeast Dvps34 mutant (Welters et al., 1994). Transgenic plants with reduced AtVPS34 levels are severely impaired in growth and development (Welters et al., 1994) and are unable to trigger normal

endocytosis and ROS production, resulting in a salt-oversensitive phenotype (Leshem et al., 2007). Moreover, VPS34 and other components of the autophagy machinery play an essential role in plant defence and are required for tolerance to drought and salt stress (Bassham, 2009, Liu et al., 2005).

1.3.6 Effects of SnRK1 regulation in plants

KIN11 targets many regulatory factors and signalling pathways (like ABA like upstream signals) that ultimately affects growth and development of plants (Baena-Gonzalez, 2010, Baena-Gonzalez et al., 2007, Lovas et al., 2003, Lu et al., 2007, Thelander et al., 2004, Zhang et al., 2001) besides its mere impact on metabolic-related functions. In potato, antisense-StubGAL83 (a regulatory β subunit of SnRK1) lines showed not only in delayed in tuberisation, reduction in tuber size and an increase in tuber number per plant but increased sensitivity in salt stress (Lovas et al., 2003). SnRK1 activity in young rice seedlings showed enhanced tolerance against flooding (hypoxia) (Lee et al., 2009) and similarly in Arabidopsis it demonstrated the improved tolerance to stress in plants under submergence (Young-Hee Cho et al., 2012) that expressed rice SnRK1. Apart from several known abiotic stress responses, number of studies links direct involvement of SnRK1 in response to the biotic stresses. Hao et al. (2003) reported that geminivirus AL2 and L2 proteins interact and inactivate SNF1 (in plants it is SnRK1) and demonstrated that geminiviruses are capable of manipulating host metabolism for their own benefits and showed increased resistant to geminivirus infection in tobacco plants overexpressing SnRK1. Gissot et al. (2006) revealed that plant specific AKINβγ subunits interact with proteins involved in resistance to nematodes in Arabidopsis.

1.4 The SFR6 of Arabidopsis

1.4.1 Identification of the *sfr* mutations

Characterising genes and proteins expressed during cold acclimation was of interest during the early 1990s and many research groups were trying to learn how plants respond to freezing tolerance through gene regulation (Houde et al., 1992; Neven et al., 1993; Nordin et al., 1993; Wilhelm and Thomashow, 1993; Castonguay et al., 1994; Dunn et al., 1994; Jarillo et al., 1994). Warren et al (1996) were able to screen an EMS-mutagenised population of Arabidopsis and isolate mutants that were impaired in freezing tolerance by monitoring visible health and re-growth of intact plants after freezing. In this screening process they selected 13 mutant lines that demonstrated strong phenotypes and they tested these lines to identify whether this freezing sensitivity was the result of damage incurred during the cold acclimation process. Therefore, the selected 13 lines were cold acclimated and examined for chilling injury based on two criteria, visible damage during cold acclimation and stunted growth upon a return to normal temperature. Thereby they found five mutant lines showed injury during acclimation (chilling injury) but not upon freezing, and eliminated those five lines from further consideration. The remaining 8 lines confirmed the absence of injury prior to freezing and suggested that they were affected specifically in the development of freezing tolerance (Warren et al., 1996).

To test for dominance, backcrossing was performed and they reported that in each of the 7 mutant lines tested (FS68 and FS79 were co-dominant; FS79 was omitted), freezing sensitivity was caused by mutation in a single nuclear gene. Then they crossed eight mutant lines together in all pair wise combinations and performed complementation studies upon freezing. F_1 progeny were less freezing-sensitive than

either of the parents in each case, confirming that the 8 lines contained mutations in 7 different genes. F_1 progeny from the cross FS68 x FS79 showed freezing sensitivity that was similar to either parent and clearly different from wild type, indicating the mutations in the FS68 and FS79 lines were allelic. This was further confirmed using F_2 progeny. As a result of these studies, seven genes that were important for freezing tolerance after cold acclimation were identified and named as *Sensitive to Freezing* (*SFR1-7*) (Warren et al., 1996).

The visible phenotype of each mutant line used by Warren et al. (1996) is presented in Figure1.6. Comparing 7 different lines after acclimation Warren et al. (1996) reported that degree of freezing sensitivity varied between mutants, however, all lines showed significant damage upon freezing (Figure 1.6). They observed significant visual differences in leaves after freezing particularly in *sfr1* where only young leaves were damaged while all were affected in other mutant lines, though the degree of damage varied (Warren et al., 1996). Furthermore, they conducted electrolyte leakage assays, a well-known method to quantify freezing-induced damage by measuring the effects of damage to the plasmalemma in leaf tissues. They observed significantly higher electrolyte leakage in all mutant lines compared to wild type controls and this difference was greatest in FS67(*sfr4*) and FS69 (*sfr6*). This was consistent with whole plant freezing assay as these two lines were the severely affected mutants (Figure 1.6). Conversely they found FS61 (*sfr2*) obtained similar level of electrolyte leakage as in wild type although it showed severely affected freezing sensitive phenotype (Warren et al., 1996).

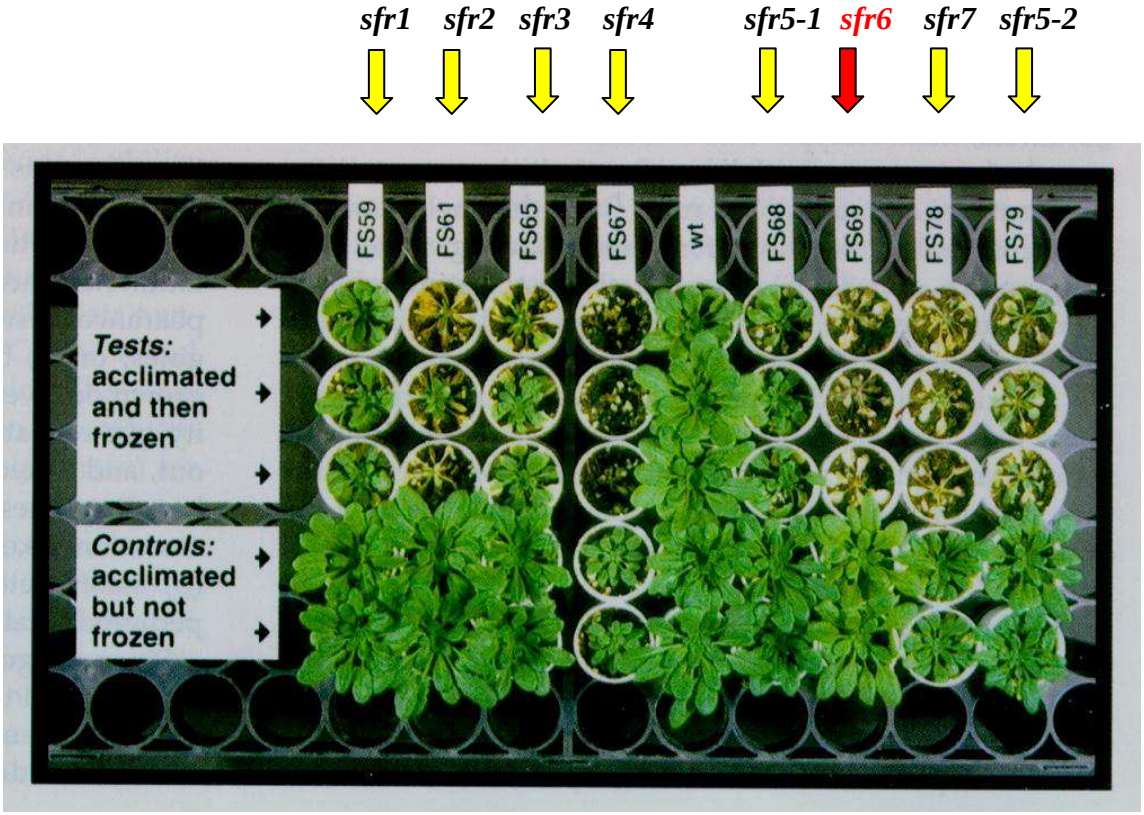

Figure 1.6: Freezing sensitivity of *sfr* mutant lines after cold acclimation and freezing from Warren et al. (1996)

Phenotypes of *sfr* mutant lines are in comparison to wild type (wt). Three plants of each line were frozen at -6.0°C for 24 h after cold acclimation (*tests*) and here are shown 9 d after freezing under standard growth conditions. Two plants of each line were cold acclimated but not frozen, are shown as controls for any injurious following cold acclimation period.

1.4.2 Compositional changes of *sfr* mutants during freezing

McKown et al. (1996) analysed these *sfr* mutant lines further for the expression of different cold-inducible proteins, sucrose, glucose, fatty acid composition of lipids and the accumulation of anthocyanin in foliar tissues, changes that were expected to occur during cold acclimation. They reported that *sfr1*, *sfr2* and *sfr5* did not show significant differences compared to wild type in any of the parameters tested above.

This suggested that these genes have highly specific effects on low temperature-induced responses. Conversely, the other four mutations (*sfr3, sfr4, sfr6,* and *sfr7*) showed significantly low levels of anthocyanin accumulation during cold acclimation process. *sfr4* and *sfr7* exhibited disturbed availability of some fatty acids after cold acclimation and *sfr4* accumulated only low levels of glucose and sucrose during the cold acclimation period. The role of sucrose is vital as a cryopotectant (Crowe et al., 1988, Uemura et al., 2003) and this provide insight reason for the freezing sensitivity of *sfr4* mutant (Uemura et al., 2003).

sfr2, sfr4, sfr6 and *sfr7* mutants showed the most severe freezing sensitive phenotypes (Warren et al., 1996). Comparing the all properties of these mutants (McKown et al., 1996) suggested that lack of anthocyanin accumulation is not the sole cause but that some commonality between anthocyanin biosynthesis and freezing tolerance, either in synthetic or regulatory pathways or both might lead to the cause. Further they reported that all of the *sfr* mutations showed the same boiling-soluble protein profile as in wild type and suggested that no mutant is completely defective in cold-induced gene expression. Lin et al. (1990) reported that limited number of cellular proteins is soluble after boiling and several cold-induced proteins are included in that category of proteins. Therefore studying the profile of boiling-soluble proteins in freezing-sensitive mutants provided a convenient approach to finding any misregulation of cold regulated gene expression even though it is not representative of the entire cold-induced proteome.

The question of whether cold-inducible gene expression is altered in the *sfr* mutants was returned to at a later date, with direct measurement of cold-inducible transcript levels in the mutants (Knight et al. (1999). Expression of three different *COR* genes (*KIN1, LTI78* and *COR15a*) in six *sfr* mutants (*sfr2-sfr7*) lines under cold conditions

(5^{o}C) showed that all mutants except *sfr6* showed similar levels to wild type. Levels of these transcripts in the *sfr6* mutant were almost undetectable, suggesting that for this particular mutant, the mutation was likely to be exerting its effect on freezing tolerance via alterations in gene expression during cold acclimation.

1.4.3 Early evidence on *COR* gene regulation in *sfr6* mutants

Although *COR* gene expression was barely detectable in *sfr6* mutants after a short exposure to cold temperatures, transcripts were detectable after much longer exposures although these were still significantly lower than the levels detected in wild type plants (Knight et al., 1999); *KIN1* expression was detected at very low levels after 6h at 4^{o}C and transcript levels increased thereafter, reaching a maximum between 24 and 48 h, as in wild type. Furthermore, the studies conducted to test co-segregation of expression deficiency with freezing sensitivity by Knight et al. (1999) confirmed that the *COR* gene expression deficient phenotype was linked to the *sfr6* mutation.

COR genes *i.e KIN1, LTI78* and *COR15a* contain CRT/DRE *cis*-acting elements (Baker et al., 1994) in their promoters and are targeted by the CBF1/DREB1B transcription factors (Stockinger et al., 1997), which activate cold-inducible gene expression (see above section). Like CBF1, CBF2 (DREB1C) and CBF3 (DREB1A) (Liu et al., 1998), also bind to the CRT/DRE element and CBF2 and CBF3 genes are themselves expressed in response to cold (Gilmour et al., 1998). Knight et al. (1999) reported that expression of *CBF1, CBF2,* and *CBF3* transcripts was strongly induced after 3 h at 5^{o}C in both wild type and *sfr6* mutants to similar levels, suggesting either that the CBF signalling pathway was not affected in *sfr6* mutants or that SFR6 does affect the CBF pathway but does so downstream of CBF transcription. Promoters of

CBF1, *CBF2* and *CBF3* genes lack CRT/DRE elements (Gilmour et al., 1998) consistent with the hypothesis that the *sfr6* mutation affects the cold-inducible expression only of genes containing CRT/DRE elements and controlled by the CBF transcription factors (Knight et al., 1999). *AtP5CS1* and *AtP5CS2* are two genes encode for D1-pyrroline-5-carboxylate synthetase (Strizhov et al., 1997), the key regulating enzyme in the proline production pathway and known be expressed in response to water stress and low temperature (Savouré et al., 1997). *AtP5CS2* (*P5CSB*) contains a CRT/DRE element in its promoter, whereas the *AtP5CS1* (*P5CSA*) gene does not contain this element. Therefore cold inducibility of *AtP5CS1* in *sfr6* and wild type plants was investigated using RT-PCR. Cold treatment at 5^{o}C for 3h showed similar levels of *P5CS1* transcripts in both wild type and *sfr6* mutants. Therefore these gene expression data (both *CBF* and *P5CS1*) both supported the conclusion that failure to express the *COR* genes *KIN1, LTI78* and *COR15a* related to the presence of CRT/DRE elements in gene promoters (Knight et al., 1999). Knight et al. (2009) revealed that unlike in wild type plants (Jaglo-Ottosen et al., 1998), overexpression of CBF1 and CBF2 did not induce ectopic expression of *COR* genes in *sfr6* mutant in the absence of cold (Knight et al., 2009). This result indicated that SFR6 acts in the CBF pathways downstream of CBF transcript (Knight et al., 2009).

By considering results from their own experiments and analysing the Genevestigator database Knight et al. (2009) concluded that *SFR6* transcript levels did not alter significantly in response to cold. Whilst it was possible that levels of SFR6 protein are controlled by low temperature, it also was equally likely that SFR6 protein is present constitutively in the cell. This latter hypothesis was consistent with previous findings that SFR6 is required for other processes unrelated to low temperature

tolerance, including developmental processes such as flowering (Knight et al., 2008) and chlorophyll biosynthesis/degradation (the mutant exhibited a pale leaf colour), SFR6 regulate groups of genes other than the CBF regulon (Knight et al., 2009).

1.4.4 Mapping and cloning *SFR6*

Classical mapping identified a region on chromosome 4 that contained the SFR6 gene, however, this region was close to the centromere and thus lack of recombination in this region made it impossible to reduce this mapping interval further. Therefore an alternative approach was taken, T-DNA mutant databases were searched for mutants in any gene within the defined mapping interval. Four hundred and twenty nine T-DNA insertion lines were identified as having the potential to be insertions in *SFR6*. Rather than performing a laborious screen for freezing tolerance or cold-inducible gene expression, these lines were subjected to simple screening the visible phenotype associated with *sfr6*; that comprised of larger and paler cotyledons (Figure 1.7) and paler true leaves in seedlings (Knight et al., 2009). This extensive screening approach led to two insertion lines demonstrating the visible phenotype (Knight et al., 2009). These two lines both corresponded to T-DNA insertions in At4g04920. DNA sequencing confirmed that original EMS mutation i.e *sfr6-1,* is a point mutation in At4g04920 that changes a nucleotide from “G” to “A”, changing a UGG tryptophan encoding codon to UGA premature stop codon thereby resulting a truncated protein (Figure 1.8) (Knight et al., 2009). The two insertion lines (T-DNA insertion positions are shown in Figure 1.8) were thus conformed as additional mutant alleles *sfr6-2* and *sfr6-3* and shown to exhibit reduced *COR* gene expression and failure to gain freezing tolerance (Knight et al., 2009).

The *SFR6* coding sequence was deduced by using full-length SFR6 cDNA which was synthesised from cold-treated wild type Arabidopsis tissues. The open reading frame was then sequenced. The predicted SFR6 protein consists of 1268 amino acids, with molecular mass of 137 kDa (Knight et al., 2009).

As initial bioinformatic comparisons failed to establish a likely function for SFR6 subcellular localization studies were conducted in order to help elucidate its possible mode of action. Transient expression of GFP fused to SFR6 in leek cells using particle bombardment showed clear nuclear localisation; a finding confirmed in stably transformed plants (Knight 2009). Nuclear localisation of the protein was consistent with a function in the control of COR gene expression. It was also observed that in the protein was present in the nuclei of unstressed cells, consistent with the observation that the *sfr6* mutation affects both basal and induced levels of *COR* gene expression (Knight et al. (1999) and suggesting that SFR6 is constitutively active and not only under particular stress conditions.

The same visible phenotype was evident in all three mutant alleles and examination of this visible phenotype in F_2 populations of crosses confirmed that *sfr6-1, sfr6-2* and *sfr6-3* are allelic. Moreover, analysis of the visible phenotype of progeny from crosses between *sfr6-2* and *sfr6-3* and wild type (Col-0) confirmed both were recessive, as previously identified *sfr6-1* mutation (Warren et al., 1996).

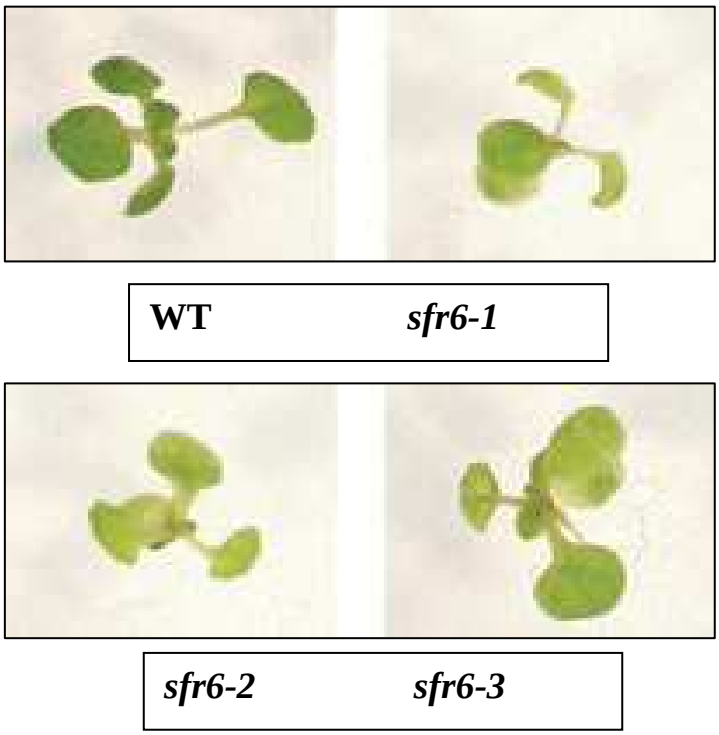

Figure 1.7: Physical appearance of *sfr6* mutants comparing to wild type. From Knight et al., (2009)

Twelve-day old Col-0 (WT) and three *sfr6* mutants are shown in the above. s*fr6* mutants demonstrate paler colouring and larger cotyledons compared to WT. *sfr6-1* is the original EMS mutant, *sfr6-2* is SALK_048091 and *sfr6-3* is WiscDsLox504A08.

Three mutant alleles are the result of interruptions in the At4g04920 coding sequence. The original allele *sfr6-1* is a EMS point mutation at 1452 bp (484 amino acids) resulting in a premature stop codon. *sfr6-2* is an insertion into the 4th intron, and *sfr6-3* is an insertion into the 8th exon. These three mutations occur in approximately the first third of the protein and *sfr6-1* and sfr6-3 are very close to each other (Figure 1.8). At4g04920 consists of 16 exons with a coding region of 3807 bp.

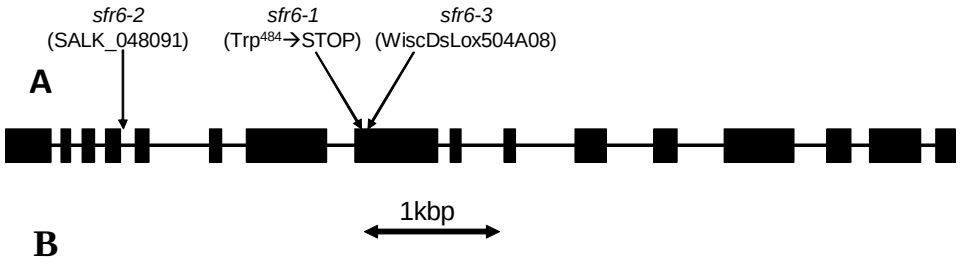


```
   1  MNQQNPEEEVSLVNNSGGGGIIEAPAIVEEKEEEGLQQKQEETIESTDPILVVVEEKLLEKSVDGEKEDDNSSSSNMEIDPVSPATVFCV
  91  KLKQPNSNLLHKMSVPELCRNFSAVAWCGKLNAIACASETCARIPSSKANTPFWIPIHILIPERPTECAVFNVVADSPRDSVQFIEWSPT
 181  SCPRALLIANFHGRITIWTQPTQGSANLVHDATSWQCEHEWRQDIAVVTKWLTGASPYRWLSSKPSSGTNAKSTFEEKFLSQSSESSARW
                          sfr6-2
 271  PNFLCVCSVFSSGSVQIHWSQWPSNQGSTAPKWFSTKKGLLGAGPSGIMAADAIITDSGAMHVAGVPIVNPSTIVVWEVTPGPGNGLQAT
 361  PKISTGSRVPPSLSSSSWTGFAPLAAYLFSWQEYLISEIKQGKKPSDQDSSDAISLSCSPVSNFSAYVSPEAAAQSAATTTWGSGVTAVA
                                 *
 451  FDPTRGGSVIAVVIVEGQYMSPYDPDEGPSITGWRVQRWESSVQPVVLHQIFGNPTSNFGGQVPTQTVWVSRVDMSIPPTKDFKNHQVAA
                                  sfr6-1                                  sfr6-3
 541  AGPSVDAPKEPDSGDEKANKVVFDPFDLPSDIRTLARIVYSAHGGEIAIAFLRGGVHIFSGPTFSPVENYQINVGSAIAAPAFSPTSCCS
 631  ASVWHDAAKDCAMLKIIRVLPPALPRNQSKVDQSTWERAIAERFWWSLLVGVDWWDAVGCTQSAAEDGIVSLNSVIAVMDADFHSLPSTQ
 721  HRQQYGPNLDRIKCRLLEGTNAQEVRAMVLDMQARLLLDMLGKGIESALVNPSALVFEPWRVDGETITGINPEAMAVDPALVSSIQAYVD
 811  AVLDLASHFITRLRRYASFCRTLASHAASAGTGSNRNNVTSPTQNASSPATPQVGQPTTTTTTTATTNSSGSSHVQAWMQGAIAKISSSN
 901  DGSNSTASPISGSPTFMPISINTGTFPGTPAVRLIGDCHFLHRLCQLLLFCFLQRSSRFPQRNADVSSQKLQTGATSKLEEVNSAKPTPA
 991  LNRIEDAQGFRGAQLGTGVKGIDENSARTTKMGSGNAGQGYTYEEVRVLFHILMDLCKRTSGLAHPLPGSQVGSGNIQVRLHYIDGNYTV
1081  LPEVVEAALGPHMQNMPRPRGADAAGLLLRELELHPPSEEWHRRNLFGGPGSEPEDMILTDDVSKLSNSLDLPDTNFSGICDGYNRVHSL
1171  WPRKRRMSERDAAFGSNTSVGLGAYLGIMGSRRDVVTATWKTGLEGVWYKCIRCLRQTSAFASPGATKQPNPNERETWWTSRWVYCCPMC
1261  GGTWVRVV*
```

Figure 1.8: Map of At4g04920 (SFRF6) showing the original EMS point mutation and two T-DNA insertion sites. From Knight et al., (2009)

(a) Representation of the SFR6 (At4g04920) genomic coding sequence in which black blocks represent exons and thin lines represent introns. The *sfr6-1* EMS mutation is caused by a premature stop codon in exon 8. The insertion sites of T-DNA causing the mutations in *sfr6-2* (exon 4) and *sfr6-3* in exon 8 are shown. (b) Predicted protein sequence with sites of T-DNA insertions (*sfr6-2* and *sfr6-3*) and the premature stop codon (*sfr6-1*) are indicated.

1.4.5 *SFR6* encodes a subunit of the Mediator Complex

SFR6 was discovered as a protein required for acquisition of freezing tolerance (Knight et al., 1999, Warren et al., 1996) and later identified as MED16 one of the

tail subunit of plant mediator complex (Bäckström et al., 2007). Protein coding genes are transcribed by RNA Polymerase II (Pol II), Activities of RNA polymerases are modulated either negatively or positively by transcriptional regulatory proteins/cofactors (Conaway and Conaway, 2011) that recognise and bind to promoters to initiate the transcription process (Kornberg, 1999, White, 2004, Russell and Zomerdijk, 2006). General transcription factors are a small set of evolutionary conserved transcriptional regulatory proteins that maintain the hub of transcriptional machinery together with Pol II that is vital for transcription of most of the protein coding genes (Conaway and Conaway, 2011, Guglielmi et al., 2004). The general transcription factors comprise five general initiation factors/ TATA-binding protein (TBP), TFIIB, TFIID, TFIIE, TFIIF, and TFIIH; the minimum set of proteins compulsory for initiation of transcription by Pol II (Conaway and Conaway, 2011, Guglielmi et al., 2004, Carlsten et al., 2013). However *in vitro* transcription assays with RNA polymerase II and the five general transcription factors could not activate transcription in a cell-free system, demonstrating that these components were not sufficient to recapitulate activation (Kim et al., 1994, Thompson et al., 1993), however, transcriptional activity was restored by the addition of a crude cell culture. Subsequent studies on the isolation of the complex that was required to restore the transcriptional activity were carried out and a protein complex, which was termed "the Mediator complex", was purified from yeast (*Saccharomyces cerevisiae*) and shown to be required for coupling Pol II activity with gene-specific activators (Kim et al., 1994).

1.4.5.1 The yeast Mediator complex

The Mediator complex is a multi-subunit protein complex that conserved in all eukaryotes from yeast to human (Elfving et al., 2011, Boube et al., 2002a). The yeast mediator complex was the first to be purified, by Kim et al. (1994) and they reported that the complex consisted of 20 protein subunits. Using genetic screening (Thompson et al., 1993) identified four more subunits referred to as Srb8-11 and together all these 24 subunits form the yeast mediator complex. Yeast-two-hybrid analysis together with co-immuno precipitation studies revealed the presence of an additional subunit, MED31 (Soh1), associated with yeast Mediator and bringing the total number of subunits identified to 25.

Subsequently, Mediator was shown to be highly conserved among eukaryotes, however, in metazoans additional number of mediator subunits was reported that not found in yeast (Bourbon, 2008). Biochemical and morphological studies on yeast mediator suggested that 25 subunits has been grouped in to four modules, named as the head, middle, tail and kinase modules (Guglielmi et al., 2004, Dotson et al., 2000). Studies based on electron microscopy and reconstitution experiments led to identify different subunits in each mediator module/domain (Guglielmi et al., 2004).

The first protein interaction map of the yeast head and middle domains was suggested using pull-down experiments from (Kang et al., 2001, Lee et al., 1998). However it did not include the organization of the tail and kinase domain. The detailed interaction map of all four mediator domains (Figure 1.9) was first produced by (Guglielmi et al., 2004) using two different two-hybrid approaches combined with the pulldown experiments and proteome-wide two-hybrid screens (Ito et al., 2001, Uetz et al., 2000) as well as genetic data.

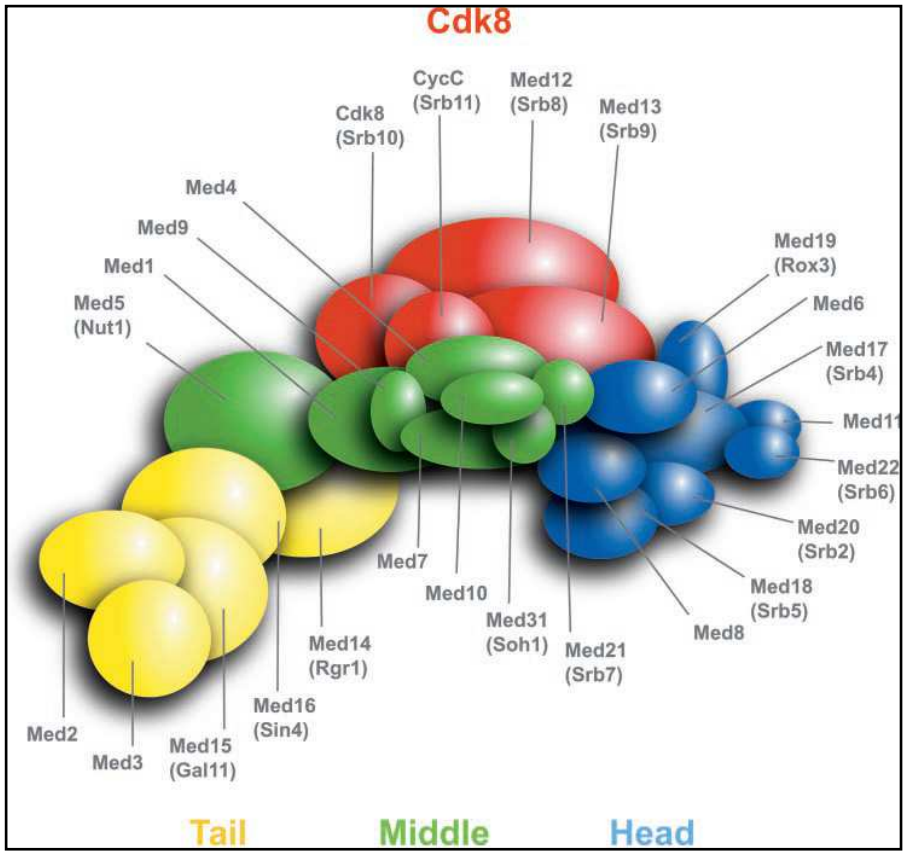

Figure 1.9: Topological organization of yeast Mediator from Guglielmi et al. (2004)

This model was developed by considering the direct interactions between mediator subunits and the relative size of the subunits investigated by several researchers and the novel work done by Guglielmi et al. (2004).

In yeast the head module consists of MED6, MED8, MED11, MED17 (Srb4), MED18 (Srb5), MED19 (Rox3), MED20 (Srb2) and MED22 (Srb6). The head module can directly bind with Pol II (Davis et al., 2002) and general initiation factors thereby stimulate the basal transcription (Takagi et al., 2006, Kang et al., 2001). The middle module includes MED1, MED4, MED7, MED9, MED10, MED21 (Srb7),MED5 (Nut1) and MED31 (Soh1) (Davis et al., 2002, Guglielmi et al., 2004). The middle domain shows interactions with chromatin remodelling

complexes, elongation complexes, as well as histone deacetylases that are important in repression (Zhu et al., 2011). Further it was revealed that histone tail modifications may affect Mediator interaction with chromatin via the middle domain (Zhu et al., 2011).

Several reports strongly suggested that the tail domain, consisting of MED2, MED3, MED14 (Rgr1), MED15 (Gal11) and MED16 (Sin4), is the main target for the transcriptional activators (Han et al., 1999, Park et al., 2000). Much research work in yeast revealed that tail subunits directly interact with DNA binding regulators and thus believed to recruit Mediator to different genes (Lee et al., 1999, Park et al., 2000, Zhang et al., 2004a). The tail domain is known to be the least conserved domain of the Mediator complex, likely reflecting the variation in transcription factors among different organisms (Conaway and Conaway, 2011). MED14 is at the interface of the middle and tail modules and possibly contributes to the overall organization of Mediator (Lee 1999). Med2p, Med3p and Med15p have been termed the tail subunit triad in yeast and are linked to the rest of the mediator complex via Sin4 (Med16) (Kang et al., 2001, Li et al., 1995). The triad can function independently when released from the mediator complex by the deletion of Med16 but less effectively (Galdieri et al., 2012).

Mediator was biochemically identified in fungi like *S. cerevisiae* (Kim et al., 1994, Thompson et al., 1993), metazoans including mammals (Fondell et al., 1996, Sato et al., 2003, Malik and Roeder, 2000), in insects, *Drosophila melanogaster* (Park et al., 2001) and in worms, *Caenorhabditis elegans* (Kwon et al., 1999). Homologues of Mediator complex subunits have been identified in all eukaryotes and the presence of the complex in plants was suggested based on these sequence homologies (Autran et

al., 2002, Clay and Nelson, 2005, Gonzalez et al., 2007) and later confirmed by bioinformatic analysis (Bourbon, 2008).

1.4.5.2 The plant Mediator complex

In 2007, thirteen years after the discovery of Mediator complex in *S. cerevisiae*, the plant Mediator complex was successfully purified by Bäckström et al. (2007) in the model plant Arabidopsis. Twenty-one Mediator subunits were identified in the isolated Arabidopsis Mediator complex that showed homology to Mediator subunit proteins from other eukaryotes. However, there were several subunits apparently missing from the plant complex compared to yeast mediator, including MED1, MED2, MED3, MED5, MED24, MED26, MED27, MED29 and MED30 but later found they were not all missing but some of them were not recognised by that work including MED2, MED3 and MED5. The detachable kinase module did not co-purify with the Arabidopsis complex (Bäckström et al. (2007). However homologs to MED12, MED13 and CDK8 have been identified in Arabidopsis through sequence comparison (Wang and Chen, 2004, Ito et al., 2011, Gillmor et al., 2010) and these subunits have now been identified. Wang and Chen (2004) reported that at least 30 cyclins are known to be present in Arabidopsis and cyclin(s) interacts with CDK8 therefore suggesting potential interaction with Mediator in Arabidopsis (Kidd et al., 2011).

1.4.5.3 Role of the plant Mediator complex

The plant Mediator complex has been identified as a key regulator for diverse range of functions including plant development (Xu and Li, 2011, Autran et al., 2002, Gillmor et al., 2010, Ito et al., 2011, Wang and Chen, 2004, Yang et al., 2014), abiotic stress responses (Cerdán and Chory, 2003, Boyce et al., 2003, Knight et al.,

1999, Hemsley et al., 2014, Elfving et al., 2011), biotic stress responses (Kidd et al., 2009, Wathugala et al., 2012, Lai et al., 2014) and non-coding RNA production (Kim et al., 2011). Prior to the purification of the Arabidopsis Mediator complex, several subunits had been identified genetically in studies related to a wide range of developmental processes and stress responses.

PHYTOCHROME and FLOWERING TIME1 (PFT1), was identified as a regulator of phytochrome B signalling pathway that promotes flowering in response to different levels of light (Cerdán and Chory, 2003). Biochemical purification of the Arabidopsis Mediator confirmed that PFT1 is homologous to the MED25 subunit of the metazoan Mediator complex (Bäckström et al., 2007). Since then much work has been published covering the wide array of functions associated with MED25 in plants, including development, hormone signalling, and stress responses. MED25 has been shown to play roles in plant defence against various biotic (Kidd et al., 2009), and abiotic stresses Elfving et al. (2011) and involvement in plant development by controlling the final organ size has been reported (Xu and Li, 2011). It was reported recently that MED25 positively regulates JA signalling during biotic stress and negative regulation of ABA signalling pathway through the regulation of hormone specific transcription factors (Chen et al., 2012a). As similar role in flowering and development, MED25 is a negative regulator in drought resistance in Arabidopsis.

STRUWWELPETER (SWP) was first identified as a nuclear protein vital in controlling the duration of cell proliferation and dwarfism with an abnormal architecture such with abnormal vegetative and floral structures (Autran et al., 2002). Krichevsky et al. (2009) suggested that MED14 is involved in the regulation of root elongation by repressing the root-specific gene *Lateral Root Primordium1* via histone deacetylation. Later SWP was identified as MED14 (Bäckström et al., 2007)

and later shown to be a key regulator of the salicylic acid (SA) and SAR (system acquired resistance) signalling pathway (Zhang et al., 2014) and *COR* gene expression (Hemsley et al., 2014).

Mutations in genes encoding three of the subunits in the kinase module of the Mediator complex (MED12, MED13 and CDK8) were reported to be associated developmental phenotypes due to altered cell differentiation (Gillmor et al., 2010, Ito et al., 2011, Wang and Chen, 2004) and *med12* and *med13* mutants were affected in the transition during the early stage of embryo development from globular to heart (Gillmor et al., 2010). *med13* was reported to show a defective response to auxin in regulating cell differentiation (Ito et al., 2011) and the *cdk8 /hen3* mutant showed altered development of floral organs as a result of defective cell differentiation (Wang and Chen, 2004). Ding et al. (2008) reported that MED12 promotes the epigenetic silencing via recruiting a histone methyltransferase and methylating chromatin of target genes. Moreover, Imura et al. (2012) and Ito et al. (2011) reported that the MED12 and MED13 act as regulators in flowering and cotyledon organogenesis respectively. Kim et al. (2011) revealed that *med17*, *med18* and *med20a* displayed reduced levels of plant miRNAs and in miRNA promoters in the *med20a* mutant, they observed the low level of RNA Pol II occupancy. This suggested that a functional Mediator complex is required for recruitment of RNA Pol II to the promoter regions of miRNA genes as well (Kim et al., 2011).

The MED34 subunit is important in stabilizing DNA structure as a DNA helicase and MED35 and MED36 subunits have been associated with mRNA and rRNA processing (Kang et al., 2009). The other subunit, MED37 has identified as HEAT SHOCK PROTEIN70 (HSP70) encoding family member, a role outside of the nucleus and shown to localize to the endoplasmic reticulum (Bäckström et al., 2007,

Kidd et al., 2011). The Arabidopsis MED36 shown to encode a fibrillarin which is involved in processing rRNA (Kang et al., 2009), particularly during the early cleavage steps of the large rRNA precursor as well as appropriate ribosome assembly (Tollervey et al., 1993). Mathur et al. (2011) revealed that MED34, MED35, MED36, and MED37 homologs demonstrated the higher expression in reproductive stage as compared with the vegetative stage.

Dhawan et al. (2009) reported that MED21 is important in embryo development thereby controlling the seed development. Further they reported that MED21 activated by microbial infections thereby in stress signalling. However Mathur et al. (2011) suggested that Med21 might be involved in stress signalling during reproductive stages but not in younger vegetative tissues. MED8 is known to regulate jasmonic acid dependent defence responses, salicylic acid mediate defence demonstrated by the reduced resistance of *med8* mutants to leaf infecting necrotrophic pathogens and susceptibility to the root infecting hemibiotrophic fungal pathogen (Kidd et al., 2009, Thatcher et al., 2009). Recent findings indicated that MED18 is vital in multiple plant functions through interaction with a variety of transcription factors including ABI4, YY1 and SUF4 to regulate plant responses to ABA, infection and flowering time respectively (Lai et al., 2014).

It was prior to the purification of the plant mediator complex (Bäckström et al., 2007), SFR6 was known (as described above) as a protein required for the acquisition of freezing tolerance through cold acclimation (Warren et al., 1996, Knight et al., 1999) and later it was indeed identified as MED16 a predicted tail subunit of the plant mediator complex (Bäckström et al., 2007). Altered low temperature signalling in *sfr6* leading to freezing sensitivity particularly due to impaired regulation of *COR* gene expression (Knight et al., 2009, Knight et al.,

1999). Apart from its role in cold-inducible gene expression, SFR6/MED16 is important in gene expression in response to drought (Knight et al., 1999), and in the control of genes associated with the photoperiodic regulatory pathway by the circadian clock (Knight et al., 2008). The regulatory effects of SFR6/MED16 in plant defence systems were investigated by Wathugala et al. (2012) and Zhang et al. (2012) who found altered expression of pathogen associated genes activated by both salicylic acid and jasmonic acid pathways. More recently, MED16/SFR6 was shown to play a role in the transcriptional regulation of iron homeostasis of (Yang et al., 2014, Zhang et al., 2014) and Yang et al. (2014) reported that this regulation occurs in association with MED25.

Together these studies indicate that SFR6/MED16, one subunit of the multi-subunit mediator transcriptional co-activator complex, plays roles in the regulation of numerous different gene regulons in response to a diverse range of stress and developmental conditions. The aim of this thesis was to attempt to understand how SFR6/MED16 can confer specific responses to these different conditions (addressed in chapter 4) and to investigate the importance of other proteins (mediator subunits; chapter 3 and KIN10; chapter 5) in regulating these responses. Moreover to study whether impaired gene expression under cold-, drought-, UV- and starvation-induced stresses correlate with altered tolerance in all different loss-of-function mutant backgrounds that used in this study.

Chapter 2

Materials and Methods

2.1 Plant materials and growth conditions

2.1.1 Plant materials

Arabidopsis thaliana (L.) Heynh. (*A. thaliana*) ecotype Columbia (Col-0) were available as lab stocks propagated from seed obtained from Lehle Seeds (Round Rock, Texas, USA). Lab stocks of *sfr6-1* (Knight et al., 2009, Knight et al., 1999) seeds and three lines of *sfr6-1* mutant complemented with AtSFR6 genomic DNA (*sfr6-1*+35S::gSFR6) (Wathugala et al., 2011) were used. T-DNA insertion lines in Mediator subunits were obtained from the Nottingham Arabidopsis Stock Centre, *med2-1* (SALK_023845) (Hemsley et al., 2014) and *med14-2* (SAIL_373-C07) (Hemsley et al., 2014, Zhang et al., 2013) . *Akin10-1* (SALK_ 127939).(Fragoso et al., 2009) seeds were obtained from Nottingham Arabidopsis Stock Centre and *kin10-2* (GABI-Kat line 579E09) were donated by Dr. Markus Teige, University of Vienna, Department of Biochemistry, Austria) as a gift.

2.1.2 Seed sterilisation

2.1.2.1 Ethanol surface sterilisation

Seeds were sterilised with 70% (v/v) ethanol by shaking on Labnet vortex mixture (Labnet international Inc., Woodbridge) in 1.5ml-microtubes for 5-10 min. Then seeds were pipetted on to filter paper (Whatman International Ltd, Maidstone, Kent UK) and air dried in a laminar flow workstation (M50549, BioQUELL UK Ltd, Hampshire) before being sprinkled on to solid agar medium (see section 2.1.3).

2.1.2.2 Bleach surface sterilisation

Seeds obtained from plants dipped in *Agrobacterium tumefaciens* (see section 2.10.1) were first surface sterilised with 70% (v/v) ethanol by shaking on a vortex mixture (Lab net VX-100) in 15-50ml falcon tubes for 5-10 min. Then seeds were shaken in a solution of 10% (v/v) sodium hypochlorite (NaOCl) and 0.25% (w/v) sodium dodecyl sulphate (SDS) for 10 min on a roller mixer (SRT6, Stuart). Thereafter the seeds were washed 6 times in sterile water, spread directly on to agar plates (see section 2.1.3) and left to dry in a laminar flow cabinet before sowing.

2.1.3 Plant growth media

Sterilised *A. thaliana* seeds were grown on MS medium (Murashing and Skoog) agar plates (Murashige and Skoog, 1962), which contained 0.8% (w/v) plant tissue culture grade agar (Sigma Aldrich) and either 1x or 0.5x Murishige and Skoog salts (Duchefa Biochemie BV, Haarlem, Netherlands) depending on the seed type. The pH of the medium was adjusted to 5.8 before autoclaving. All growth media were sterilised by autoclaving (BOXER, Laboratory Equipment Ltd.) at 121^{o}C for 20 min at 10^5 Pa. If required, appropriate antibiotics were added to the liquid medium when it had cooled to approximately 50^{o}C after autoclaving. For all experiments 9 cm diameter disposable petri dishes (VWR Internationals) were used.

Seeds collected from *Agrobacterium* dipped plants (see section 2.10.1) were sown on full strength MS medium prepared as stated above, supplemented with appropriate antibiotics. Seeds collected from *Agrobacterium* dipped plants expressing vectors using Basta (Glufosinate ammonium) as a selectable marker were directly sown on soil in a mixture of compost and sand in 1:1 ratio.

When soil-grown plants were required, seven-day-old seedlings from agar plates were transferred on to re-hydrated peat discs (Jiffy products Internationals, Norway). Individual plants were gown on small (38mm in diameter) peat discs for drought experiments, crossing and bulking up seeds whilst large (42 mm in diameter) discs were used to grow up to 3 plants per disc for *Agrobacterium* dipping and cold acclimation experiments.

2.1.4 Plant growth conditions

Arabidopsis seeds sprinkled onto germination medium (MS agar plates) as described in section 2.1.3, were cold stratified at 4^{o}C for 2-3 days to synchronize germination. Seed plates were later transferred to a Percival growth chamber (CLF PlantClimatics, Model CU-36L5D, Germany) at 20±1^{o}C set for long day (16 h light/8 h dark) photoperiod with a light level of 150 µE m^{-2} s^{-1} approximately.

Seven-day-old seedlings transferred to peat plugs in trays were covered with cling film and moved to a growth room that maintained approximately 20±1^{o}C temperature with 16 h light/8 h dark (long day photoperiod) and light level at about 150-200 µmol m^{-2} s^{-1}. The cling film was removed after two days. Individual plants grown for seed collection were maintained in the Aracon system (Beta Tech, Ghent, Belgium) that consisted of a transparent cup-shaped base and tube which separated the flowering parts from adjacent plants. Plants were well watered every two days and trays were transferred to a seed drying room after plants and pods were turning to yellow for further drying prior to seed collection.

Tobacco plants grown on soil were maintained up to 5-6 weeks until ready for infiltration (see section 2.11.2), approximately at 24^{o}C temperature with 16h light/8 h dark cycle and light level at approximately 200 µmol m^{-2} s^{-1}.

2.2 Antibiotic, bacterial strains and growth conditions

2.2.1 Antibiotics

Antibiotics purchased from Melford Laboratories Ltd (Ipswich, Suffolk, UK) were used in this study and concentrations were used as in the following Table 2.1. Stock solutions of each antibiotic were sterilised using micro filters (0.22 µm) (Millipore Corporation, Bedford, USA) attached to syringes (VWR International Ltd, Magna Park, Lutterworth, UK).

Table 2.1 Concentrations of antibiotics used the study

Antibiotic	Stock concentration (mg/ml)	Working concentration (µg/ml)
Kanamycin	100	for plants: 50 for bacteria: 100
Spectinomycin	50	50
Rifampicin	200	200
Gentamicin	10	40-10
Timentin (Ticarcillin and Clavulanate)	200	200

2.2.2 Bacterial growth medium

Escherichia coli (*E. coli*) and *Agrobacterium tumefaciens* were grown on Luria-Bertani broth (LB; Tryptone 10g/l, NaCl 5g/l and yeast extract 5g/l) (Melford Laboratories Ltd, Ipswich, Suffolk, UK) with 15g/l micro agar (Melford Laboratories Ltd) or in liquid media of LB as above. All growth media were sterilised by autoclaving at 121^{o}C for 20 min at 10^5 Pa and appropriate antibiotics were added to the pre cooled medium at 50^{o}C after autoclaving.

2.2.3 Bacterial strains

E. coli chemically competent cells Mach1^{TM} (transformation efficiency >10^9 cfu/µg) and silver cells (DH5α strain of *E. coli*, ≥10^8 cfu/µg) were purchased from Invitrogen (Renfrewshire, UK) and Bioline (London, UK) respectively, and were used for entry vector/primary transformations and chemically competent *E. coli* (strain DH5α) made in-house were used in destination vector/secondary transformations. Competent *Agrobacterium* (strain C58C1; (Holsters et al., 1978) and GV3101 (Holsters et al., 1980) were made in-house and used for stable and transient expression in plants respectively.

2.2.4 Bacterial growth conditions

Bacteria were grown overnight either on solid LB or liquid LB media where continuous agitation (150-200 rpm) was given in an incubator (NB-205, N-Biotek) for liquid cultures. *E. coli* cultures were incubated at 37^{o}C overnight and *Agrobacteria* at 29^{o}C for 2-3 days.

2.3 Chemicals

All chemicals and media used in this study were purchased from one of the following companies, where not otherwise stated.

BDH Laboratory supplies Ltd., Lutterworth, Leicestershire, UK.

Bioline, London, UK.

Fisher Scientific UK Limited, Loughborough, Leicestershire, UK.

Melford Laboratories Ltd, Ipswich, Suffolk, UK.

MERCK Chemicals Limited, Padge road, Beeston Nottingham, UK.

Invitrogen, Renfrewshire, UK.

Sigma-Aldrich Company Ltd., Gillingham, Dorset, UK.

2.4 Synthesis, analysis and quantification of DNA fragments

2.4.1 PCR amplification

Polymerase Chain Reaction (PCR) was performed using a 96-well Px2 Thermal Cycler (Thermo Electron Corporation) or Px0.5 Thermal Cycler (Thermo Electron Corporation). Either genomic DNA or cDNA (complementary DNA) (see section 2.8.1 or 2.13.3.1) was used as templates in amplifications.

2.4.1.1 Oligonucleotide primers and reaction mixtures

Primers were designed to anneal to specific regions within the gene of interest either manually or using Primer3 software. Primers were designed to consist of at least 20-25 base pairs (bp), minimum 40-45 % of guanine (G) and cytosine (C) bases and similar melting temperature (T_m) and all primers were purchased from Fisher Scientific UK Ltd (Meadow Road, Leicestershire). The sequences of all the primers used in this study are listed in Appendix 2.1 The reaction mixtures were prepared using buffers supplied with the relevant enzyme (polymerase) and prepared according to the manufacturer's instructions.

2.4.1.2 DNA polymerase

Amplification of targeted fragments for cloning work was performed by using Phusion DNA polymerase (Finnzymes, Keilaranta, Finland), which is a proofreading

polymerase with exonuclease activity. Biotaq, Biotaq red or MY Taq DNA polymerase (Bioline) was used for all other PCR amplification purposes.

2.4.1.3 PCR conditions

Optimum annealing temperatures were selected according to the melting temperature of the primers used in each amplification; these were generally 5^0C lower than the melting temperature of the primer with the lower melting temperature from each pair. The annealing temperature was optimised each time where new DNA templates and primer pairs were used. PCR conditions for different DNA polymerases are listed in Table 2.2.

Table 2.2 PCR conditions for different DNA Polymerases

Cycle and step number	Description	Temperature and time		No. of cycles
		Taq/Bio Taq/MyTaq	Phusion	
1-0	Initial denaturation	95°C - 5 min	98°C - 2 min	1
2-1	Denaturation	95°C – 30 sec	98°C – 30 sec	35
2-2	Annealing	55-60°C- 1min/1Kbp	58°C- 30 sec	
2-3	Extension	72°C – 45 sec	72°C-30 sec/1Kbp	
3-0	Final extension	72°C – 5 min	72°C – 5 min	1
4-0	Holding	4°C	4°C	

2.4.2 Agarose gel electrophoresis of DNA

Agarose gel electrophoresis was used to separate DNA fragments according to their sizes. One percent (w/v) gels were prepared using electrophoresis grade agarose in

0.5x TBE buffer (see Appendix A1.1) in a microwave oven. After cooling to approximately 50°C, ethidium bromide (10mg/ml) or Midori green advance DNA stain, a non-toxic fluorescent DNA binding dye (Geneflow, Lichfield, Staffs),) was added to a final concentration of 5 µg/ml. The molten gel was poured into the gel tank and allowed to set at room temperature using the correct size of gel combs.

DNA samples were loaded in to wells by mixing with 6x DNA loading buffer (see Appendix A1.2) and 0.5x TBE was used as the running buffer. Gels were run at 35 mA (constant current) until satisfactory resolution of band sizes was attained (usually approximately for 1 h). DNA bands were visualised on a UV-trans-illuminator (UVitec Limited, Avebury House, Cambridge, UK) at a wavelength of 254 nm. Fragment size was approximated by comparing the positions with 1 Kb hyperladder (Bioline), a molecular size standard run on the same gel. DNA concentrations were roughly estimated by comparing the intensity of UV fluorescence of ethidium bromide or Midori green-stained DNA, to bands of a known volume of molecular marker.

2.4.3 Gel Extraction and quantification of DNA

Following agarose gel electrophoresis (see section 2.4.2), DNA bands were excised from the agarose gel using a scalpel blade by visualizing on a UV trans-illuminator (at 312 nm) (Ultra-Violet Products Ltd, Cambridge, Cambridgeshire, UK). DNA fragments were purified using QIAquick gel extraction kit (Qiagen, Germany) according to the manufacturer's instructions. In this method, the agarose gel slices were first dissolved in the QG buffer consists with guanidine thiocynate and pH indicator provided (in a volume of three times the gel volume) at 50^0C for 10 min and then mixed with one gel volume of isopropanol. Using QIAquick spin columns

DNA was bound to columns by centrifuging (Progen, GenFuge 24D) at 11,000*g* for 1 min. Columns were washed with given PE buffer at maximum speed (16,300*g*) for a 1 min. Finally, DNA was eluted in EB buffer (10mM Tris-Cl, pH 8.5).

DNA concentration was estimated by comparing the intensity of the correctly sized band with molecular size markers on a 1% (w/v) agarose gel as described in section 2.4.2 or directly quantified using a Nanodrop ND-1000 Spectrophotometer (NanoDrop Technologies, Wilmington, Delaware, USA). With the Nanodrop the concentration was determined by reading the optical density of the sample (approximately 1.6µl) at a wavelength of 260nm (according to the Beer-Lambert equation $E\mathrm{o} = E\mathrm{i}\exp(-\mu a d)$). The buffer used to elute the DNA was used as zero reference in each time.

2.5 Cloning techniques

Details of the vectors used in this study are presented in Appendix A3 including sequence and vector diagrams annotated with specific features.

2.5.1 Primary/entry cloning

A TOPO cloning kit (Promega) was used to insert freshly extracted DNA fragments into the Gateway ™entry vector (pENTR D-TOPO) and the manufacturer's protocol was used to perform the cloning reactions. TOPO® Cloning is a highly efficient, five minute, one-step cloning method ("TOPO® Cloning") for the direct insertion of *Taq* polymerase-amplified PCR products into a plasmid vector. *Taq* polymerase has a non-template-dependent terminal transferase activity that adds a single deoxyadenosine (A) to the 3´ ends of PCR products. The linearised vector supplied in this kit has single, overhanging 3´ deoxythymidine (T) residues. This allows PCR

inserts to ligate efficiently with the vector. Topoisomerase I from *Vaccinia* virus in this kit binds to duplex DNA at specific sites and cleaves the phosphodiester backbone after 5′-CCCTT in one strand. The energy from the broken phosphodiester backbone is conserved by formation of a covalent bond between the 3′ phosphate of the cleaved μbond between the DNA and enzyme can subsequently be attacked by the 5′ hydroxyl of the original cleaved strand, reversing the reaction and releasing topoisomerase (http://tools.lifetechnologies.com/content/sfs/manuals/).

The cloning reaction was set up using 0.5:1 to 2:1 molar ratio of PCR product: TOPO vector in the salt medium supplied (1.2M NaCl; 0.06M $MgCl_2$) and incubated for 5 min at room temperature (22-23^{o}C). Then 2μl of the above reaction mixture was added to chemically competent *E. coli*, which were then incubated for 30 min on ice and followed by 30s heat shock at 42^{o}C without shaking. Thereafter, 250μl of LB/SOC medium was added to the cells and tubes shaken for 1 h at 37^{o}C while shaking at 200rpm. The resultant culture was spread on kanamycin selection plates incubated overnight 37^{o}C. The following day selected colonies were analysed for the presence of the recombined vector with insert using primers designed for the vector and beginning of each insert by colony PCR. Positive colonies from colony PCR were used in restriction digestion (see section 2.6) to further confirm the correct size of insert and then sequenced (see section 2.7).

2.5.2 Gateway cloning: cloning to the destination vector

The Gateway® cloning technology is based on the bacteriophage lambda site-specific recombination system which facilitates the integration of lambda into the *E. coli* chromosome and the switch between the lytic and lysogenic pathways. Lambda recombination occurs between site-specific *att* achment (*att*) sites: *att*B on the *E. coli*

chromosome and *att*P on the lambda chromosome. The *att* sites serve as the binding site for recombination proteins and upon lambda integration, recombination occurs between *att*B and *att*P sites to give rise to *att*L and *att*R sites. (https://www.lifetechnologies.com/us/en/home/life-science/cloning/gateway-cloning.html/). After identifying the correct DNA clone in the entry vector, a gateway LR reaction (lytic reaction; *att*L x *att*R in to *att*B X *att*P) was performed to transfer the insert into the destination vector. This was performed using Gateway® LR Clonase ™ II enzyme mix (Invitrogen) as described in the manufacturer's protocol. The LR reaction mixture consisted of 2 µl of entry clone (50-150ng/ µl), 1µl of destination vector (150ng/ µl), 1 µl of TE buffer (pH 8.0) (see Appendix A1.3) and 1 µl of LR clonase II enzyme. This reaction mix was incubated overnight at 25°C. Then 0.5µl of proteinase K solution (1 µg/µl) was added to stop the reaction followed by incubation at 37°C for 10 min to break down the clonase. Silver competent cells (*E.coli* strain DH5α, Bioline, $\geq 10^8$ cfu/ µg) were transformed using 2.5 µl of reaction mixture by incubating for 30 min on ice followed by 30 sec heat shock at 42°C without shaking. Afterwards 250 µl of LB/SOC medium was added before shaking at 37°C for 1 h at 200rpm. The culture was spread on spectinomycin selection plates and incubated overnight at 37°C. The next day selected colonies were analysed for the presence of the construct. In this cloning method the destination vector was selected according to the desired application. Therefore pB7WG2 for stable constitutive overexpression in Arabidopsis and pK7WGF2 (contain GFP) for transient expression in tobacco were used (Karimi et al., 2002).

2.5.3 DNA ligation

DNA ligation was performed to form recombinant DNA fragments using dsDNA fragments with cohesive (sticky) ends when TOPO cloning failed. T4 DNA ligase (Promega) was used to ligate DNA fragments into a linearised vector backbone by catalysing the formation of a phosphodiester bond between the 3' hydroxyl and 5' phosphate of adjacent DNA residues.

Required DNA fragments were isolated after restriction digestion using specific restriction enzymes (see section 2.6) and the fragment was further purified either using DNA purification kit or using phenol/chloroform (see section 2.8.3). Five microlitres of each purified DNA product was run on a gel to confirm the correct size and stoichiometric quantities were used in a ligation with 1/10 volume of 10X ligase buffer (Promega) and 1µl of T4 DNA ligase in 10 µl of final volume. This mixture was kept in room temperature for 2 h to ligate and 5 µl (half) of the above ligation mixture was transformed either in to Gateway ™entry vector (pENTR D-TOPO) or to *E. coli* chemically competent cells Mach1^{TM} (see section 2.5.1) depending on the original DNA used to obtain the ligated product using standard transformation protocol. The resultant transformed cells were grown on selection plates with the correct antibiotics and incubated overnight 37^{o}C. The following day selected colonies were analysed for the presence of the recombined vector with insert using primers designed for the vector and beginning of each insert in colony PCR. Positive colonies from colony PCR were used in restriction digestion (see section 2.6) to further confirm the correct size of insert and then sequenced (see section 2.7).

2.6 Restriction digests

Restriction enzymes were used to separate fragments of DNA from plasmids to prepare PCR products for cohesive termini ligation and for diagnostic purposes. Restriction digests were performed according to the manufacturer's instructions, using the recommended buffers supplied with relevant enzyme at 37^{o}C for 2-4h except where the enzyme required lower temperatures for optimal activity. Double digests were performed using a buffer in which both the enzymes could function at their highest efficiency. If both enzymes required different buffers, sequential digestion was performed. In all digestions the enzyme volume was 10% of the total volume. NEBCutter was the software (http://www.tools.neb.com/NEBcutter2/index.php) used to work out the restriction sites.

2.7 Sequencing

Plasmid DNA was isolated and purified using Wizard® Plus SV Minipreps DNA purification system (see section 2.8.2.2) or PCR products amplified from plant genomic DNA (gDNA) were used for sequencing (see Appendix 2 for primers). All sequencing reactions were conducted by the in-house Sequencing Laboratory, School of Biological and Biomedical Sciences, Durham University (DBS, Durham University). DNA sequence data was analysed using Sequencher DNA sequence analysis software (http://www.genecodes.com) Database similarity searches were carried out using the BLAST search tool available at the Arabidopsis Information Resource database (TAIR; *http://http//:www.arabidopsis.org/Blast/index.jspfor*

nucleotide) to search for homology. DNA sequence data were analysed using the BLAST 2 sequencing tool (www.ncbi.nlm.nih.gov/blast/bl2seq) and Vector NTI software (Invitrogen).

2.8 Plant and bacterial DNA extraction

2.8.1 Plant genomic DNA extraction

Edwards' DNA extraction (Edwards et al., 1991) method was followed. Approximately 5-10 seedlings of 7-day old plants or 1-2 leaves from 3-weeks-old plants were collected in 1.5-ml microtubes and flash frozen in liquid nitrogen. The tissue was ground with a micro pestle for about 10 sec. Then 400 µl of Edwards' extraction buffer (see Appendix A1.4) was added and tissue ground for another 30 sec. The micro tubes were briefly vortexed for 5 sec and left at room temperature until all preps were ready for the next stage. The tubes were then spun at 16,300*g* for 1 min, and 300 µl of the resulting supernatant was transferred to a new tube. After that 300 µl of 100% (v/v) isoproanol was added to the above tube, and gently mixed by inversion. The microtubes were left at room temperature for 2 min to allow the DNA to precipitate, and then spun at 16,300*g* for 10 min. The resulting supernatant was removed and the pellet was further spun for 1min and the residual supernatant was aspirated. The pellet was left to air-dry for 10 min or dried by spinning 5 min in a concentrator (Eppendorf concentrator 5301, VWR International Ltd, Leicestershire, England), and finally re-suspended in 50 µl of TE buffer overnight at 4°C (see Appendix A1.3).

2.8.2 Bacterial plasmid DNA extraction

A single colony was inoculated (using sterile tip) in to 5 ml of liquid LB with relevant antibiotics. The culture was incubated overnight at 37^{o}C with continuous shaking and the next day 1.5 ml was spun down at 10,000*g* for 1 min (Eppendorf centrifuge 5415D, VWR International Ltd, Leicestershire, England). The supernatant was used for the extraction of plasmid as described below depends on the purpose.

2.8.2.1 STET mini-prep method

The STET (Sucrose-Tris-EDTA-Triton) prep is a cost-effective modified alkaline lysis method (Maniatis et al., 1982) for isolating plasmid DNA from many samples, e.g. when screening bacterial colonies for the presence of construct in a plasmid vector having an antibiotic resistance marker.

The supernatant was discarded and the cell pellet was resuspended in 250µl of pre-chilled STET buffer (see Appendix A1.5). Then 20 µl of lysozyme (10 mg/ml in STET buffer) was added to digest the cell wall and gently mixed by flicking the tube. Then the microtube was incubated at 100^{o}C for 1 min on digital dry-block (D1100, Labnet International, Inc). Next 270 µl of pre-chilled 5 M LiCl was added, mixed by inversion and incubated on ice for 30 min. The microtube was then spun at 4^{o}C) using the Beckman coulter centrifuge (Allegra™ X-22R, VWR international Ltd, Leicestershire, England) at 16,000*g* for 15 min, and the resulting pellet removed with a sterile cocktail stick (at this point, plasmid DNA is enriched in the supernatant, and the pellet consists mostly of proteins, polysaccharides and genomic DNA). One ml of 100% (v/v) ethanol (pre-chilled to -20^{o}C) was added to the remaining supernatant to precipitate plasmid DNA and incubated at -80^{o}C for 30 min or at -20^{o}C overnight.

The microtube was then centrifuged at 16,000*g* for 10 min at 4°C to pellet the plasmid DNA and the supernatant was discarded immediately. The pellet was then washed with 80% (v/v) ethanol by gentle inversion prior to another 10 min 16,000*g* centrifugation step at 4°C. Finally, the supernatant was discarded and the DNA pellet was left to air-dry for 10 min to volatilise any remaining ethanol) before resuspension in 50 µl of buffer TER (see Appendix A1.6).

2.8.2.2 Column purification Mini prep method

For salt-sensitive applications such as DNA sequencing high purity, small scale bacterial plasmid DNA extraction was performed using the Wizard® Plus SV Minipreps DNA purification system (Promega) according to the manufacturer's instructions particularly. In this method, overnight cultures were spun down, resuspended and lysed in the presence of alkaline protease. The supernatant was separated from the flocculated pellet by centrifugation, and plasmid DNA bound to the supplied columns, which were washed in an ethanol-based buffer and eluted in EB buffer.

2.8.2.3 Maxi prep method

High purity, large scale bacterial plasmid DNA extraction was performed using the Qiagen plasmid Maxi Kit (www.qiagen.com) according to the manufacturer's instructions. This method is similar to Wizard mini prep method.

2.8.3 Purification of PCR products/ extracted plant DNA

2.8.3.1 Using purification kit

PCR products directly after amplification were purified using column based Plant DNA Extraction Kits from Roche (http://lifescience.roche.com) or Omega Bio-tek extraction kit (https://us.vwr.com) according to the manufacturer's instructions.

2.8.3.2. Using phenol/chloroform extraction

Extracted DNA samples were made up to 100 µl in TE pH 8.0 and mixed with an equal volume (100µl) of phenol: chloroform: isoamyl alcohol in a ratio of 25:24:1. After vortexing for 30 sec and spinning for 1 min in a bench top at maximum speed the clear upper phase was transferred to a clean tube without disturbing the interphase. Again one volume (100 µl) of chloroform was added and the same procedure repeated and the upper phase transferred to a new tube. Subsequently 1/10 volume of (10 µl) of 3M sodium acetate pH 5.3 was added, vortexed briefly and 2.5 volumes (250 µl) of 100% ethanol added. After briefly vortexing the samples were held at -80^{o}C for 30 min and then spun down at 15^{o}C for 30 min at maximum speed. The supernatant was discarded and dab dried on a tissue. Next 500 µl of 70% ethanol was added without disturbing the pellet and the tube turned gently to make sure that it was coated in ethanol to remove salts from sides of the tubes and spun at 15^{o}C for 10 min at maximum speed. The supernatant was removed and dried the pellet in the concentrator (Eppendorf concentrator 5301, VWR Internationals) for 5 min and finally resuspended in 25 µl of TE buffer (see Appendix A1.3).

2.8.3.3 Use of Exonuclease I and Shrimp/Antarctic Phosphatase (ExoSAP method)

This method was practiced to clean up PCR reactions that had been confirmed as producing only a strong single band on a gel. Two enzymes, Exonuclease I (Exo) and Shrimp/Antarctic Phosphatase (SAP) were used to remove excess dNTPs and primers from the PCR product before use in sequencing. ExoSAP reaction mix was prepared using 0.025 µl of Exonuclease I, 0.250 µlof Shrimp/Antarctic Phosphatase and 9.725 µl of distilled water to a final volum10µl. Ten µl of above 1x ExoSAP mix was added to 15 µl of each PCR sample and incubated at 37^{o}C for 45 min and then 80^{o}C for 15 min in a PCR thermo-cycler. Samples were stored at -20^{o}C until use.

2.9 Bacterial competent cell production and transformation

2.9.1 *E.coli* competent cell production (DH5*α*)

Five-ml overnight cultures (including spectinomycin) were set up by inoculating a single colony from an *E. coli* plate. The following day 1 ml from the above culture was added to 100 ml LB in a 250-ml flask and grown in a shaker at 37°C for about 1.5 h. Then OD value was checked and cells were harvested at 4^{o}C by spinning down at 3500 *g* for 5 min when OD was between 0.2 and 0.3. Each step was performed on ice and then the supernatant was discarded and cells were resuspended in half volume ice cold 100 mM $CaCl_2$ (50 ml). The resuspended solution was left on ice for 20 min and cells harvested by spinning at 3500*g* for 5 min at 4^{0}C. Supernatant was discarded and resuspended again in 1/10 volume of ice-cold 100 mM $CaCl_2$ (10 ml) and added 2 ml ice-cold glycerol to give a final concentration of 17% glycerol.

Empty eppendorfs were kept on ice to chill and 200 µl of competent cells were aliquoted to each tube. Aliquots were immediately frozen in liquid nitrogen and stored in -80 ^{0}C for further use.

2.9.2 Transformation of competent *E.coli* cells

Twenty-five-µl aliquots of either chemically competent *E.coli* cells Mach 1(>10^9 cfu/ µg) for high transformation efficiency or DH5α (≥10^8 cfu/µg) for routine cloning, were thawed on ice before transformation. Ligation mixtures were warmed to 70^{o}C for 10min to inactivate the enzyme, and then transferred onto ice for 1 min. Two and a half µl of ligation reaction mixture was added to the competent cells and cells were incubated on ice for 30 min followed by 1 min heat shock at 42^{o}C in a water bath and immediately transferred back onto the ice for 2 min. Then 1 ml of LB/SOC medium was added to the reaction tube and shaken gently at 150 rpm at 37^{o}C for 1 h. This recovery time allows the cells to initiate replication under optimal conditions. Aliquots of each culture were then spread onto LB agar plates containing the appropriate antibiotics for selection of the plasmid (see table 2.1 for concentrations). Plates were incubated at 37^{o}C overnight to develop colonies, and kept at 4^{o}C for 2-3 weeks storage.

2.9.3 *Agrobacteria* competent cell production

Agrobacterium tumefaciens strains were streaked onto a fresh LB plate with appropriate antibiotic (rifampicin) incubated for 2 days at 28°C. A single colony from the above plate was picked and inoculated in a 5-ml overnight culture of LB with the same combination of antibiotics as above. Cultures were grown overnight at 28°C in a shaking incubator. The next day 5 ml of overnight culture were added to 100 ml of LB in a sterile 500-ml flask and shaken vigorously 250 rpm) at 28°C until

the culture reached an optical density (OD) 600 of 0.5-1 (takes 4-8h). Cultures were chilled on ice and centrifuged at 3000*g* for 5 min at 4°C to pellet the cells. The supernatant was discarded and the cells resuspended in 2 ml of ice cold 20mM $CaCl_2$ solution. Finally cells were dispensed in 0.1-ml aliquots into pre chilled 1.5-ml eppendorf tubes, flash frozen in liquid nitrogen, and stored at -80^{o}C for future use.

2.9.4 Transformation of competent *Agrobacteria* with construct

Agrobacterium strain C58C1 competent cells were used for constitute expression in Arabidopsis using floral dipping (see section 2.10.1) method. Frozen aliquots of 100 µl of strain C58C1 competent cells were placed on ice and allowed to thaw. One µg of plasmid DNA was mixed with the cells by inverting gently. The cells were then heat shocked at 37^{o}C for 5 min using a water bath. After that 1 ml LB medium was added and tubes were shaken at 150 rpm for 2-4 h at 29^{o}C to allow cells to grow. Then the content was transferred to an eppendorf tube and spun down for 30 sec to pellet the cells and most of the supernatant was removed. The pellet was resuspended in about 200 µl of the remaining supernatant. Aliquots were spread on LB agar plates containing rifampicin, spectinomycin and gentamicin (see table 2.1 for the concentrations) for the selection. Plates were incubated in a 29^{o}C incubator for 2-3 days for colonies to develop.

Agrobacterium strain GV3101 (pRM90) competent cells were used for transient expression in tobacco and leek and followed the same transformation procedure as above.

2.9.5 Long term storage of bacterial cultures using glycerol stocks

E.coli and *Agrobacterium* strains carrying the constructs were streaked onto a fresh LB plate with appropriate antibiotics and incubated overnight at 37°C or for 2 days at

28°C respectively. A single colony from the above plates was picked and inoculated in a 5 ml overnight culture of LB with the same combination of antibiotics as in the plate. Cultures were grown overnight at correct temperature as above in a shaking incubator. 850 µl of LB cultures were taken into a new 1.5-µl tube and 150 µl of 100% (v/v) glycerol was added, mixed by pipetting up and down followed by brief vortexing. Cultures were kept at -80^{o}C for future use.

2.10 Plant transformation and crossing

2.10.1 *Arabidopsis* floral dip method for transformation

2.10.1.1 Preparation of plants for floral dip

Seven day old seedlings grown on MS plates were transferred to large hydrated peat plugs (42 mm diameter) with 3 plants per plug, and grown in long day growth room as described in section 2.1.4. When plants reached the initial flowering stage, bolts were clipped to encourage the formation of more floral buds from the axillaries. Plants were clipped 2-3 times prior to dipping, which resulted in a large number of young floral shoots. The bolted plants were supplemented with fertilizer to maintain vigorous growth. The final clipping was done 7 days before transformation, to encourage lateral shoots that actively produced flowers.

2.10.1.2 Preparation of *Agrobacteria* for floral dip transformation

A single colony of *Agrobacterium* having a binary vector construct (as described in section 2.9.4 with pB7WG2) grown on LB agar plate (with appropriate antibiotics) was used to inoculate a 5-ml overnight culture. The next day the above 2 ml of above overnight culture were added to 200 ml of LB In a 1-litre flask (with the same

antibiotics) and grown for a further 24 h at 29^{o}C. Next day, for the transformation, cells were spun down (15 min at 3500*g*) and re-suspended in 5 % sucrose solution in the same volume as original culture. Silwet L-77 surfactant (250 µl per 500 ml) was added immediately prior to use for dipping.

2.10.1.3 Dipping of Arabidopsis plants

The small volume of resuspension was poured into a beaker and flowers were dipped into this suspension for 30-60 seconds. The plants (grown in peat plugs) were then placed on their sides on a tray lined with tissues. Finally the tray was covered with cling film and returned to the growth room and the following day plants were uncovered and the peat plugs returned to a vertical position in a new tray and watering continued as before, but ensuring that the *Agrobacterium* was not washed off.

2.10.1.4 Selection of transformants

The T_1 seeds collected from *Agrobacterium* dipped plants transformed with a vector containing a selectable marker other than Basta resistance (kanamycin), were bleach sterilised as described in section 2.1.2.2 before germinating on MS agar plates with timentin to inhibit growth of *Agrobacterium* (see table 2.1 for concentrations) and appropriate antibiotics to select for the binary vector. Primary transformants (T1 plants) surviving on the selection plates with green cotyledons and developing roots were transferred to peat plugs to obtain their seeds (T2 generation) and harvested separately.

Seeds from plants carrying Basta resistance constructs as the plant selectable marker were sown directly onto soil (see 2.1.3 for the growth conditions) and allowed to germinate. After 7-8 days, Basta herbicide (250 mg/l) was sprayed onto the young

seedlings until visibly wet and treatment was repeated 3-4 times at three-day intervals. The surviving primary transformants were transferred to peat plugs and T2 seeds were collected from each plant separately.

2.10.2 Crossing of *Arabidopsis* plants

Seven-day-old seedlings of *sfr6-1* and other donor plants were transferred to peat plugs (one seedling/plug) in trays and moved to a growth room that maintained long day photoperiod (see section 2.1.4). *sfr6-1* mutant plants were maintained as recipient plants in crossing in this research study and other plants such as *kin10-1* and wild type plants overexpressing KIN10 were used as donor plants and also maintained under long day photoperiod as described in section 2.1.4. Once *sfr6-1* plants reached the flowering stage, elongated and stout but unopened flower buds were selected to continue crossing with pollen taken from donor plants. The green colour outer whorl sepals was first removed using sharp-end forceps and then inner whorl of white petals was removed. Finally immature stamens of *sfr6-1* were removed without damaging the pistil. Mature pollen taken from donor plants was gently deposited on stigma of the above opened pistil of *sfr6-1*. Crossed plants were labelled and allowed to continue growth until successful siliques turned to yellow colour. Those dried seeds were planted on MS plates (see section 2.1.3) and taken forward to selection.

2.10.3 Selection of homozygous segregants using allelic discrimination assay (AD assay)

An allelic discrimination assay was performed using Applied Biosystems 7300 machine. (Applied Biosystems, Foster city, USA) to identify the *sfr6* genotype as the *sfr6-1* EMS mutant has a single nucleotide polymorphism (SNP). This test detects

single nucleotide variants of a nucleic acid sequence. TaqMan SNP probe (Applied Biosystems) was used to distinguish homozygous segregants in different crosses performed in this study using the allelic discrimination assay. Six ng of genomic DNA (see section 2.8.1) at a concentration of 10 ng/µl and 9 µl of master mix that consisted of 0.375 µl of Taqman SNP assay (for SFR6), 7.5 µl of 2xAccu Start genotyping tough mix ROX and 1.125 µl of nuclease-free water were mixed in a 15-µl total reaction in optical 96-well reaction plates (semi-skirted with raised rim qPCR, Star Lab, USA). Three technical replicates were used for each sample. A TaqMan probe for genotyping *SFR6* (see Appendix 2 for probe details) was purchased from Applied Biosystems.

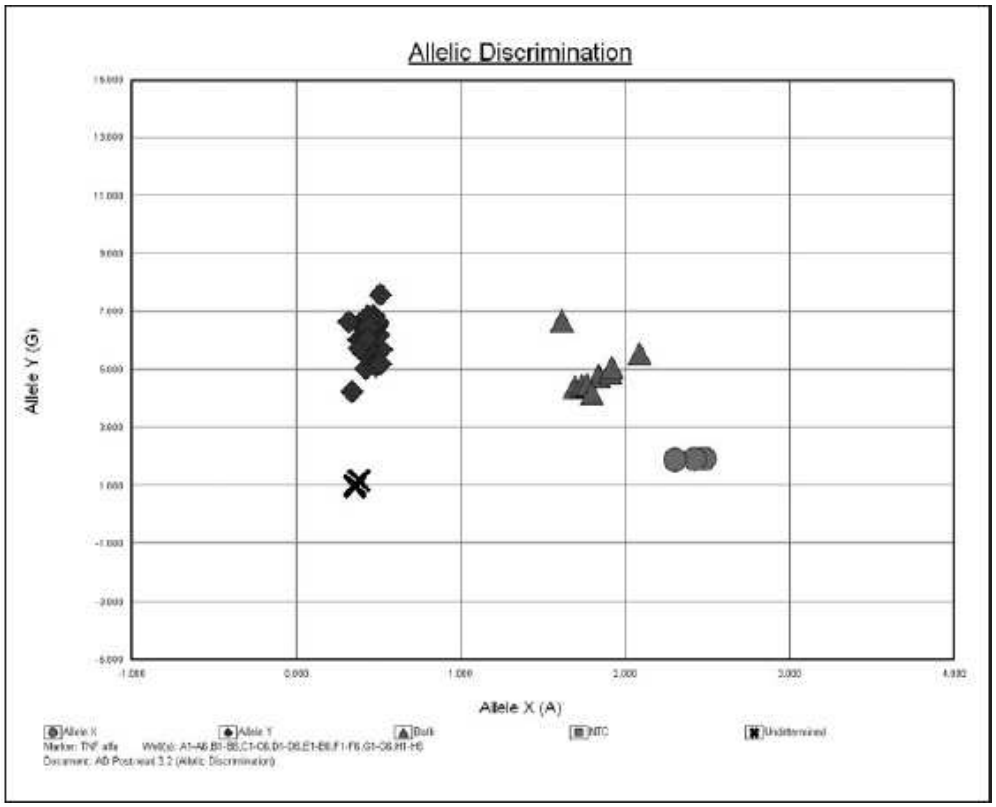

Figure 2.1: Model graph supplied by Applied Biosystems 7300 to illustrate the assay used to identify homozygous segregants of *sfr6* genotype as the *sfr6-1* with the single nucleotide polymorphism (SNP) characteristic of *sfr6-1* using the TaqMan SNP probe. The chart plots the detection of Allele X (wild type, circles) and Y (mutant, diamonds) in each sample.

Positions of unknown samples on the chart are referenced to known genotypes in order to determine whether they are homozygous for either allele or heterozygous.

2.11 Transient expression in plants

2.11.1 Preparation of *Agrobacterium* strains expressing GFP constructs

Constructs were cloned into the entry vector as described in section 2.5.1 and then into the gateway destination vector (see section 2.5.2), pK7WGF2 that allows the cloning of an in-frame fusion of the gene of interest with an N-terminal GFP tag. *Agrobacterium* strain GV3101 competent cells (prepared as described in section 2.9.3) were transformed with a destination vector construct to be used in transient expression in tobacco or leek. One hundred-microlitre aliquots of transformed GV3101 agrobacteria cells (see section 2.9.4) were spread on LB agar plates containing rifampicin, spectinomycin and gentamicin (see table 2.1 for the concentrations) for the selection. Plates were incubated in a 29^{o}C incubator for 2-3 days for colonies to develop. Colonies were re-streaked in fresh plate (containing same antibiotics) and colonies were checked for the presence of the construct.

2.11.2 Transient expression in *Nicotiana benthamiana* (tobacco) using infiltration

A single colony selected from the above plates or freshly streaked out plates using glycerol stocks was harvested in to a 5-ml overnight bottle consists of the same antibiotic combination and grown overnight in a 29^{o}C incubator. Next day a 5-ml culture was transferred to a 15-ml falcon tube and spun down for 5 min at 3000*g* at room temperature. The resulting supernatant was discarded and the pellet was resuspended in 1 ml of 10 mM $MgCl_2$ solution. The absorbance of the solution was measured using 20 µl of the above suspension after mixing with 980 µl of water

using a spectophotometer (BOECO S-20, Germany) at 600 nm wave length. Finally, the rest of the resuspension (980 µl) was diluted in 10 mM $MgCl_2$ solution to obtain correct concentration for infiltration. This dilution was calculated based on optical density to be in final solution *i.e* 0.3 for one construct and 0.6 if two constructs used to infiltrate in the experiment. When two constructs were expressed in a single plant, equal volumes of each construct having 0.6 O.D (optical density) were mixed to obtained final O.D value of 0.3. Tobacco plants were grown for six weeks in a growth room (24^oC temperature with 16 h light/8 h dark cycle, see section 2.1.4) and these plants were used for infiltration. The 5 ml of *Agrobacterium* resuspension described above was applied with pressure through the underside of the tobacco leaves using a 5-ml syringe (without a needle) to a single leaf. Suspension was entering the leaf through the stomata and that visible area was marked using a pen. Then plants were transferred back to the same growth conditions (see section 2.1.4) and incubated for 48h. Later, the plant specimens were observed under a Confocal microscope (Leica SP5 CLSM FLIM FCCS) as described in section 2.11.5.

2.11.3 Biolistic transformation of leek tissue (*Allium porrum*)

Biolistic transformation (particle/microprojectile bombardment) is a process of delivering DNA into plant cells by coated with gold or tungsten particles (Sanford, 1988)

2.11.3.1 Preparation of plant materials

Leek slices (colourless) were taken from the separated inner whorls of the lower part of the stem. The 1×1 cm squares were placed on MS plates as concaved side on top in the centre of the plate into a circle (about 3 cm diameter) covering about most of the area of the circle.

2.11.3.2 Preparation of the gold particles

Sixty mg of 1.6-µm gold micro-carriers were transferred to an eppendorf tube and 1 ml of ethanol was added and the contents vortexed for 1 min. The tube was then spun in a micro-centrifuge for 10 sec to pellet the gold particles and remove the supernatant. Three repeated washes were performed in the same way and after the last wash the tube was spun for 1 min. One ml of sterilised double distilled water was added and the gold particles completely resuspended by vortexing for 1 min. The supernatant and all debris were removed by subsequent spinning for 1 min. Lastly, gold particles were completely resuspended in 1 ml of water by vortexing and the top of the eppendorf tube sealed with parafilm and stored at 4^{o}C until use.

2.11.3.3 Preparation of DNA-coated particles

Large macro-carrier discs were placed into the macro-carrier rings using tweezers and flattened. Gold particles were vortexed hard for 1 min. and 50 µl quickly transferred into an eppendorf tube and 5µg plasmid DNA added before vortexing hard for 30 sec. Then 50 µl 2.5 M $CaCl_2$ was added to each sample and vortexed hard for 30 sec. Subsequently, 20 µl of 0.1 M spermidine free base was added and vortexed hard for 3 min. The tube was spun at 10,000*g* to pellet particles and the supernatant removed as quickly as possible. After that 250 µl of absolute ethanol was added to the particles, vortexed hard to fully resuspend and the supernatant quickly removed after spinning down. Then the pellet was completely resuspended again in 125 µl of ethanol by vortexing. The suspension was then pipetted up and down and 20 µl aliquots of suspension dispensed onto each macro-carrier disc and allowed to dry.

2.11.3.4 Delivering gold coated DNA to explants

Plant bombardment with DNA-coated gold particles was performed using a Bio-Red PDS-1000/He particle delivery system. The vacuum applied to the chamber was 25 mm Hg/in using a vacuum pump. 1100-psi rupture discs were used in the chamber to deliver DNA coated gold particles to plant materials (square pieces of leek lower epidermis approximately 8mm x 8mm). Bombarded Leeks tissue (on MS plates) was incubated for 48 h in the Percival growth chamber.

2.11.4 Visualisation of GFP florescence

After 48 h incubation (as described in section 2.11.3.4) tobacco leaf samples or the lower epidermal peels of leek explants were placed on glass microscope slides (0.8-1.0 mm thick, VWR International) and covered with a cover slip (22 x 22 mm, VWR International) with drop of water. These specimens were observed on a confocal laser scanning microscope (Leica SP CLSM FLIM FCCS) with 40× oil immersion objective. The excitation wavelength for GFP visualisation was 488nm (Argon laser), with emission measured using a 505 nm long pass filter. All images were taken under the same pinhole aperture.

2.12 Stress treatments for gene expression studies

2.12.1 Cold treatment

Seven-day-old seedlings grown on MS agar plates (see section 2.1.4) were transferred to $5^{o}C$ for 6 h (beginning 2-3 h into the light cycle) in a growth chamber (SANYO MLR-351) set for short days 10:14 h light:dark, with a light level of approximately 150 $\mu Em^{-2}s^{-1}$ while control plates were kept at $20^{o}C$ in the Percival

growth chamber. Whole seedlings were collected after cold treatment and quickly frozen in liquid nitrogen. Samples were kept at -80^{o}C prior to RNA extraction. The sample processing time between harvesting and freezing was kept to the minimum; tissue was frozen within less than 1 minute of tissue harvest.

2.12.2 UV stress

Seeds were sown evenly (about 50) on MS agar plates and seven-day-old seedlings were irradiated with 5 or 10 kJm^{-2} of UV-C (254 nm wavelength) (depending on the experiment), in a UV cross linker (Uvitec Ltd, Cambridge, UK). During the UV treatments, the lids were removed from the petri plates and control plates were also exposed to the air for the time taken for the UV exposure. After the treatments, all plates were resealed and returned to the Percival growth chamber. Twenty four hours after the treatments samples were collected; each sample comprised 15-20 seedlings in a microfuge tube and was snap frozen in liquid nitrogen prior to RNA extraction.

2.12.3 Dark/ starvation stress

Seven-day-old seedlings grown on 0.5×MS agar plates were covered in two layers of Aluminium foil to provide dark conditions whilst keeping control samples without foil and all plates were transferred to a Percival growth chamber t at 20±1^{o}C set for long days (16:8 h light:dark photoperiod with light level of approximately 150-200 µE m^{-2} s^{-1}). After 6 h (beginning 2-3 h into the light cycle) seedlings were harvested quickly and frozen in liquid nitrogen. Samples were kept at -80^{o}C prior to RNA extraction.

2.12.4 Desiccation/drought stress

Seeds were sown evenly on MS agar plates and seven-day-old seedlings were used for the treatment. Drought stress was given in terms of desiccation by opening the lids while exposing the seedlings to normal growth conditions in the Percival growth chamber at conditions described above. Plates to be treated were open to the above conditions for 6 h while keeping the control plates closed under same conditions. After 6 h (beginning 2-3 h into the light cycle), 15-20 seedlings were collected in a microfuge tube and quickly frozen in liquid nitrogen prior to RNA extraction.

2.12.5 DCMU (3-(3,4-dichlorophenyl)-1,1-dimethyl urea) treatment

Seven-day-old seedlings grown on MS agar plates were floated (15-20 seedlings per treatment) in 5 ml of sterile water or 20 μM DCMU (3-(3,4-dichlorophenyl)-1,1-dimethyl urea) contained in transparent six-well culture dishes (SARSTEDT Nümbrecht, Germany) for 6 h (beginning 2-3 h into the light cycle) and kept in the in the Percival growth chamber at the conditions described above. After 6 h of the treatment, seedlings were quickly harvested in a microfuge tube by blotting seedlings on tissue paper to remove excess solution. Samples were then quickly snap-frozen in liquid nitrogen.

2.12.6 ABA treatment

Seven-day-old seedlings grown on MS agar plates were floated (15-20 seedlings per treatment) in 5ml of 0.1% ethanol as control and 100 μM ABA (abscisic acid) contained in transparent six-well plates for 6 h and kept in the in the Percival growth chamber at the conditions described above. After 6 h (beginning 2-3 h into the light cycle) of the treatment, seedlings were blotted on tissue paper and quickly placed in a microfuge tube. Samples were then quickly frozen in liquid nitrogen.

2.13 Extraction, quantification and analysis of RNA

2.13.1 RNA extraction

The RNeasy Plant Total RNA Kit (Qiagen), was used to extract RNA from plant materials using the given protocol. Plant samples were frozen in liquid nitrogen and quickly ground using micropestles by hand for few seconds. Four hundred and fifty microliters of pre-chilled RLT lysis buffer (after the addition of 500µl β-mercaptoethanol to every 50 ml) was added, ground again until a relatively homogeneous sample was produced and left on ice whilst processing the other samples. RLT buffer contains guanidine thiocyanate that disrupts the cell structure and has denaturing properties and β-mercaptoethanol acts as a reducing agent. The samples were vortexed and transferred to a pre-heated heat block at 56^0C for three minutes followed by five or more minutes on ice. After samples had cooled down, the lysate was transferred to a QIAshredder spin column (held in a 2-ml collecting tube) and spun down for 2 min at 16300*g*. The flow-through was removed (without disturbing the pellet in the bottom of the tube) to a new tube containing 225 µl of 100% ethanol, mixed by pipetting up and down and transferred to an RNeasy spin column. Ethanol promotes selective binding of RNA to the RNeasy membrane. The content was spun down at 11600*g* for 30 sec, allowing RNA to bind to the column, the supernatant removed and the column washed again as described above with 350µl of buffer RW1 (consisting of guanidium salts), and the flow-through discarded. DNase digestion was performed with RNase-free DNase (10 µl of DNase and 70 µl of RDD buffer per sample) (Qiagen, Hildon, Germany; http:// www. qiagen. com) in order to remove genomic DNA from the RNA and incubated for 20 min, after which the column was washed again with 350 µl of buffer RW1 for 30 sec

at 11600*g*. Two last washes were performed using 500 µl of buffer RPE (which contained 80% ethanol) for 30 sec at 11600*g* followed by a 2-min spin at 16300*g*. Finally, the isolated RNA was eluted from the column in 30µl RNase-free water by spinning down at 11600*g* for 1 min.

2.13.2 RNA quantification

The concentration of RNA was determined by measuring the optical density of samples at a wavelength of 260nm using a Nanodrop ND-1000 Spectrophotometer (NanoDrop Technologies, Wilmington, Delaware, USA). An undiluted sample of 1.6 µl of RNA was applied onto the pedestal of the machine to make a measurement. RNase-free water was used as a zero reference in the measurements. The following equation was used to quantify the concentration.

$$c = A/(E * b)$$

Where c is the nucleic acid concentration in ng/µl, A is the absorbance in AU, E is the wavelength-dependent extinction coefficient in ng-cm/µl,and b is the path length in cm. The generally accepted extinction coefficients for double stranded DNA, single stranded DNA and RNA are 50, 33 and 40 respectively.

2.13.3 Quantification of transcript levels

cDNA was synthesised from total RNA and used for gene expression studies using quantitative Reverse Transcription-Polymerase Chain Reaction (qRT-PCR), a technique used for relative quantification of transcripts levels (see section 2.14).

2.13.3.1 cDNA synthesis with long RNA templates

cDNA was also used to amplify specific gene fragments for cloning. In this case, following the extraction of RNA (see section 2.13.1) Moloney Murine Leukemia

Virus Reverse Transcriptase (M-MLV RT; Promega) was used for cDNA synthesis from long messenger RNA templates. Two microgrammes of RNA was diluted in 10 µl of water and heated at 65^{o}C for 10 min to melt secondary structure within the RNA template and immediately cooled rapdily on ice to avoid reforming of the secondary structure. Then synthesis of the first strand of cDNA was performed by the addition of a master mix (10 µl) consisting of 4µl of M-MLV 5X reaction buffer (250mM Tris-HCl pH 8.3, 375mM KCl, 15mM $MgCl_2$ and 50mM DTT), 2µl of 10mM dNTP, 0.5µl recombinant RNasin® ribonuclease inhibitor, 1µl of M-MLV RT and 2.5µl of nuclease-free water. Then 10µl of the above master mix and 10µl of RNA template were mixed and heated at 37^{o}C for 90 min on a heat block. Then second-strand synthesis was performed either using Taq polymerase (see section 2.4.1) to confirm the correct size of DNA on agarose gel (see section 2.4.2) or to detect the level of transcripts in qRT-PCR (see section 2.14).

2.13.3.2 cDNA synthesis for use in qRT-PCR

A high capacity cDNA synthesis kit (Applied Biosystems, Foster city, USA) was used to reverse transcribe cDNA from 2 µg of total RNA (in a total volume of 10 µl), combined with 10 µl of reverse transcriptase reaction mixture (2 µl of 10×RT buffer, 0.8 µl of 25×dNTP mix, 2 µl of 10×RT Random primers, 1 µl of Reverse transcriptase and 4.2 µl of nuclease-free water. The samples were run in the thermal cycler at 25^{o}C for 10 min (primer annealing) followed by 37^{o}C for 120 min (cDNA synthesis) and then 85^{o}C for 5 sec (reaction termination step to inactivate any remaining active reverse transcriptase that could inhibit qPCR). The resultant cDNA was diluted in nuclease-free water 1:50 prior to use in quantitative realtime (qRT) PCR to study gene expression.

2.14 Measurement of gene expression using qRT- PCR

The relative transcript levels of genes of interest were quantified with reference to the expression of an endogenous control gene by quantitative real-time PCR (qRT-PCR) using an Applied Biosystems 7300 machine. Five microlitres of cDNA (1:50 diluted cDNA as described in section 2.13.3.2) was used with Gotaq® qPCR Master mix (Promega) in a 10-µl reaction in optical 96 well reaction plates (semi-skirted with raised rim, Star Lab UK Ltd, Milton Keynes, UK). Three technical replicates were used for each sample in a single plate and three biological replicates were done for each experiment. Relative gene expression was analysed using the ΔΔ*C*t method (Livak and Schmittgen, 2001) and technical variability calculated for each samples as stated in the Applied Biosystems user manual, 2007 for singleplex data (external control method).

2.15 Stress treatments for plant stress tolerance assays

2.15.1 Freezing tolerance assays

Seedlings were grown on MS agar plates (as in section 2.1.4) for 7 days, then transferred to peat plugs and grown thereafter in the growth room under short day conditions (12:12 h light: dark) at 20^{o}C, and 150-200 µ$Em^{-2}s^{-1}$ light level for four weeks. Afterwards plants were transferred to 5^{o}C for cold acclimation for 14 days in a growth chamber (SANYO chamber set for short day; 10:14 h light: dark cycle), with a light level as described above. The plants used as controls were kept at 20^{o}C in short day conditions (12:12 h light: dark, 60 % humidity and at same light level) for a further 14 days whilst the other plants were kept under acclimation conditions.

Then both acclimated and non-acclimated plants were frozen at -7.5^{o}C for 24 h. Plants were returned to the original growth conditions and monitored for 10 days after freezing, photographed, and their survival recorded.

Photosynthetic efficiency of the plants was measured using the Fv/Fm ratio based on chlorophyll fluorescence using FluorCam (700MF, Photon Systems Instruments, Czech Republic) before acclimation, after acclimation and after the plants had been frozen.

2.15.2. Electrolyte leakage assay

Plants were grown for seven days on MS agar plates and transferred to soil for 27 days under short days to promote rosette growth. After this, were transferred to cold acclimating conditions: 5°C in 10:14h light: dark cycles, 150-200 $\mu E^{-1}m^{-2}s^{-1}$ for 14 days. Rosette leaves of a comparable size in all mutants and wild-type plants were excised and washed in milli-Q water in a clean weigh boat. Leaves were blotted gently on tissue paper to remove excess water and a blunt spatula was used to add leaves to the bottom of the tubes without damaging leaves. Three replicate tubes were prepared for each treatment, with each tube containing three leaves. Test tubes were held on ice until all samples had been prepared. After that, one set of tubes was retained on ice, while the others were transferred in a completely randomized order to a Clifton freezing bath filled with anti-freeze/ heat transfer fluid and cooled by an immersion dip cooler (Nickel-Electro) set at -2°C. Tubes were allowed to equilibrate for 1 h before the addition to each tube of 2-3 ice chips made with milli-Q water. Tubes were plugged with a foam bung and kept at -2°C for a further 2 h. Three tubes from each plant type (as three replicates /each treatment) were removed and placed on ice and then the temperature was reduced to -4^{o}C in the bath. After 30 min at this

temperature another set of tubes was removed and kept in ice. This procedure was continued until the last set of tubes was taken out at -12^{o}C. All tubes were placed in a test tube rack on ice and thawed overnight in the cold room (5^{o}C) to equilibrate.

The following day 5 ml of distilled water was added to each tube and tubes shaken gently for 3 h at room temperature. The resultant liquid was decanted into a labelled set of 6-well plates and electrical conductivity was measured using a hand-held conductivity meter (Hannah Instruments). Then the test tubes containing leaves were transferred to a -80°C freezer for 1 h, allowing complete release of the remaining solutes from the plant tissue. After an hour, the contents in the tubes were allowed to thaw on ice for 30 min, after which the previously decanted fluid was returned back to each tube and the tubes shaken again for 3h before the conductivity was re-measured. Percentage of electrolyte leakage was calculated by expressing the conductivity before freezing as a percentage of the conductivity after freezing.

2.15.3 UV tolerance assay

Seedlings were grown on MS agar plates (see section 2.1.4) up to seven days and 7 day-old-seedlings were irradiated with 5 and 10 kJm^{-2} of UV, in a UV cross linker (Uvitec Ltd, Cambridge, UK) with the plate lids off while control plates were exposed to air for same duration (as in UV treatments). Immediately after treatments, all plates were resealed and returned to the Percival growth chamber (see section 2.1.4) after being wrapped in foil to inhibit the blue light-mediated repair pathway. The number of surviving seedlings with green meristems was recorded 10 days after treatments.

2.15.4 Drought tolerance assay - Water withdrawal

Individual seedlings were grown on 38-mm (diameter) peat plugs and grown in short day conditions (12:12h light: dark cycles) at 150-200$\mu E^{-1}m^{-2}s^{-1}$ at 20°C with constant watering (at two-day intervals) up to 25 days post-germination. Water was withheld for 14 days (after which approximately 50% of wild type plants showed a wilting appearance) and then re-watered. The number of plants surviving and exhibiting re-growth was assessed after a further 10 days and photographed.

2.15.5 Starvation tolerance assay

Seven-day-old seedlings grown on 0.5×MS agar plates were covered in two layers of foil for 14 days to provide dark conditions whilst keeping control samples without foil. All plates were transferred to a Percival growth chamber (see section 2.1.4). After 14 days seedlings were return back under normal conditions in Percival growth chamber and 3 days later the number of plants surviving and exhibiting re-growth was assessed and photographed.

2.16 Protein Expression Assays in Arabidopsis

2.16.1 Protein Extraction for quantitative analysis

Seedlings were grown on MS agar plates (see section 2.1.4) for seven days in the Percival growth chamber. About 20-30 seedlings were collected and quickly frozen in liquid nitrogen in an eppendorf tubes. Samples were ground using micropestles by hand for several seconds and 400 µl of extraction buffer (equivalent to approximately 2 ml/g fresh weight of tissue, see Appendix A1.7 for general extraction buffer and 2 mM DTT; 0.5% (w/v) PVPP; 1% (v/v) protease inhibitor cocktail (Sigma); 1% (v/v)

NP-40, 1mM sodium molybdate and 1mM NaF were freshly added) and further ground the samples. Samples were kept on ice until all the samples had been processed and centrifuged at 13,000*g* for 15 min at 4^{o}C. The supernatant was collected and 200 µl kept in a new tube, before being frozen in liquid nitrogen and stored at-20^{o}C until use. The remaining 20-30 µl of supernatant was used for protein quantification.

2.16.2 Protein quantification

A working solution of Copper tartrate (reagent A) was prepared according to instructions provided in the BioRad DC Protein assay (BioRAD, Hercules, CA, USA) kit. Standard protein dilution series were made using BSA (Sigma, USA) in the range of 0-2 mg/ml and the standard curve was prepared each time the assay was performed. Extraction buffer (see section 2.16.1) was used to prepare the standards each time. Twenty µl of standards (the rest of the samples were frozen and kept at -20°C and samples were transferred into clean, dry test tubes and 100 µl of working reagent was added to each tube and vortexed. Then 800 µl of Folin (reagent B) was added into each tube and left 15-20 min After that absorbance was measured at 650 nm using a spectrophotometer (S-20, BOECO, Germany) based on the reaction of protein with alkaline copper tartrate solution and folin reagent. Using a standard curve, protein concentrations of the samples were calculated. Further dilutions were performed to obtain 2mg/ml of each sample to be used in western blotting using extraction buffer without freshly added additives. Then the required amount of the above samples was mixed with 2X SDS buffer (see Appendix A1.8) and either directly used for loading after being heated at 95^{o}C for 5 min in a heat block or stored at -20^{o}C until use.

2.16.3 SDS gel preparation and electrophoresis

Ten percent acrylamide resolving/separating gel was prepared using resolving buffer (see Appendix A1.9) as described in Appendix A1.10 and 6 ml of the above solution was used to make a single gel. One ml of water saturated iso-butanol was poured on top of the resolving gel to smoothen the gel surface. Once the gel was settled with stacking buffer (see Appendix A1.11), 5% acrylamide stacking gel (see Appendix A1.12) was prepared and 1.5 ml of stacking gel was poured on resolving gel and an appropriate comb was used. The gel apparatus was filled with 1x SDS running buffer (see Appendix A1.13) and predetermined volumes of sample (to obtain a concentration of 2mg/ml) were loaded in to wells after heating at 95^{o}C for 5 min. Five µl of standard protein marker (Precision Plus^{TM} Dual colour standard, Sigma) was added in the first lane of the gel. The gel was run at 120V for the first 30 min and then adjusted to 180V for another 1 h.

2.16.4 Staining and membrane transferring

Following gel electrophoresis, one gel was used to study the quality of the preparation of proteins in the samples using Coomassie staining. The gel was carefully removed from the glass plates and transferred to a box in which it was washed 2-3 times with ultrapure water to remove adhering SDS from the gel. Then 2ml of Imperial ^{Tm} protein stain (blue) was added and left in the shaker for an hour (NB-205, N-BIOTEK, Korea). After that the gel was washed with ultrapure water several times until all the unbound blue dye had been removed, leaving Coumasssie blue-stained proteins. The second gel was used for membrane transfer.

PVDF (polyvinylidene difluoride) (Immun-Blot® PVDF, BioRad) membrane was cut to the same size as the gel and rehydrated in 100% methanol solution for 1-2 min and

then transferred to cold transfer buffer (see Appendix A1.14) for 15-20 min. Wet blotting apparatus was used for transfer and the gel and membrane loaded between two layers of Whatman No.1 filter paper, which were soaked in the same cold transfer buffer. The wet blotter was filled with the same cold transfer buffer and run at low voltage (30V) overnight in a cold room with gentle stirring of the buffer. Alternatively, the membrane transfer was performed for 1h using 20% methanol based transfer buffer (see Appendix A1.15) at high voltage (100V) in a cold room. After complete transfer the membrane was washed 3 times in TBS-T (see Appendix A1.17) with each wash lasting 5 min.

After this the membrane was kept in 50 ml of 5% milk (w/v) (Marvel, UK.) made in TBS-T and shaken (200 rpm) in an incubator for an hour at room temperature to block non-specific protein attachment to the membrane, in order to obtain less background signal in immunoblotting.

2.16.5 Immunoblot analysis (Western blotting)

After blocking, the membrane was washed in TBS-T, with each wash lasting 5 minutes before proceeding to the primary antibody binding stage after trimming the membrane to remove any excess area. Ten millilitres of 5% powdered milk (w/v) suspension made using TBS-T was added to a 50-ml falcon tube and the required amount of primary antibody was added according to the dilution factor given by the manufacturer (in the range of 2-5 μl). Then the membrane was rolled and inserted into the falcon tube and placed on a roller (SRT6, Stuart) in the cold room overnight. Again the membrane was washed in TBS-T with each wash last 5 min before proceeding to the secondary antibody binding stage using a secondary antibody specific for the primary antibodies used. The membrane was transferred to a clean

dish containing 10 ml of 5% milk solution with the required amount of secondary antibody according to the dilution factor and placed on roller (SRT6, Stuart) for 1-2 h at room temperature. Again, the membrane was rinsed three times with TBS-T, each wash lasting 5 min and finally two washes with TBS (see Appendix A1.16) for 5 min.

2.16.6 Visualising the protein using chemiluminescent detection

The membrane was incubated with a substrate that luminesces when exposed to the reporter on the secondary antibody. Antibody-bound proteins were detected on the membrane using a Photon counting camera (Photek, East Sussex, UK). ECL (enhanced chemiluminescent) solution 1 (see Appendix A1.18) was made with Luminol (3-Aminophthal hydrazide) and coumaric acid and ECL solution 2 (see Appendix A1.19) made with hydrogen peroxide were mixed (5 ml of each) and the membrane soaked for 3-5 min before detecting the luminescence emitted from the membrane. Luminescence was detected either digitally using the Photek camera with Photek Image32 software or using CL-X posure ^{TM} film (Thermo scientific) with an X-ray film processor (Xograph Imaging System, Compact X4), with luminescence integrated over a period of between 5 min and 1 h was used to visualise the proteins.

2.16.7 Stripping the membrane

After using the membrane to detect proteins using specific primary and secondary antibodies, the same membrane was used to study different proteins using different primary and secondary antibody combinations after stripping. Pre-prepared stripping solution (see Appendix A1.20) was warmed at 37^{o}C for few minutes and the membrane was washed twice; each wash lasting 5 min. The blot was then washed in TBS-T (see Appendix A1.17) 3 times, each for 5 min and subsequently transferred to

blocking solution, (5% w/v milk) overnight in a cold room before proceeding to the primary antibody binding stage.

2.17 Co-immunoprecipitation assays in tobacco

2.17.1 Infiltration of plants

Tobacco plants (*N. benthamiana*) were infiltrated (as described in section 2.11.2) with *Agrobacterium tumefaciens* expressing GFP-tagged proteins and other proteins under study. Two days post-infiltration, infiltrated leaves were harvested and stored at -20^{o}C until use or protein extraction was performed immediately.

2.17.2 Protein extraction and pull down

Frozen leaf samples (2-3 leaves) were ground using a mortar and pestle (kept cold using liquid nitrogen) using a small amount of sand (Sigma) until a fine powder was produced, which was then transferred to pre-cooled 50-ml falcon tube. Then 10 ml of protein extraction buffer (2 ml/g) was added [see Appendix A1.7 and 10 mM DTT; 0.5% (w/v) PVPP; 1% (v/v) protease inhibitor cocktail (Sigma); 1% (v/v) NP-40 were freshly added before use] and the whole lysate described above was transferred to an Oakridge centrifuge tube (Nalgene Nunc International) on ice. The tube was then centrifuged at 4°C at 13000*g* for 15 min and the supernatant was passed through two layers of miracloth (CalBiochem, UK) before passing through a 0.2-µm filter sterilisation unit (Corning Incorporated, Corning Germany). Protein determination was performed as described in section 2.16.2 with 1:20 diluted samples using BioRad DC Protein assay. After this, samples were diluted to 5 mg/ml of protein and 2 ml transferred to an eppendorf tube. Then 30 µl of GFP-Trap-A beads (50% slurry)

(Chromotek, Planneg-Martinsried, Germany) were added to each sample and the tubes incubated on a roller mixer for 4 h at 4°C in the cold room. Thereafter, tubes were centrifuged at 500 *g* to pellet beads at 4°C and the supernatant discarded. One ml of wash buffer (TBS + 0.5% NP40) was added and inverted several times to rinse the beads. The above step was repeated four times and supernatant was removed carefully at each time. Beads were gently pipetted up and down to collect them and 30 µl of 2x SDS buffer (see Appendix A1.8) containing 10% β-mercaptoethanol (as a reducing agent) was added to each sample. Samples were stored at -20^{o}C until use or used immediately for western blot analysis as described in section 2.16.2 to 2.16.5 after spinning the heated samples at 95°C for 5 min.

2.17.2.1 Silver staining of SDS gel

After the electrophoresis was complete the gel was transferred to a box and fixed in fixative solution consisting of methanol and acetic acid (see Appendix A1.21) for an hour or overnight at room temperature with gentle shaking (175 rpm). The gel was then washed in miliQ water for at least 30 min. Overnight washing with several changes of water helps to remove all acetic acid from fixing solution and reduce the background (resulting in increased sensitivity). Subsequently the gel was transferred to a hypo solution with sodium thiosulphate and sodium acetate (see Appendix A1.22) and incubated for 30 min at room temperature with gentle shaking (175 rpm) followed by three water washes, each lasting for 10 min. After this stage, silver staining (see Appendix A1.23) was performed for 20 min and then the gel was washed twice in water, each wash lasting for 1 min. Afterwards the gel was transferred to developing solution (see Appendix A1.24) for between a few seconds and 2-3 minutes until the bands could be seen and then the gel was scanned. The gel

was transferred back to developing solution to allow further development of bands and then scanned. Finally, the gel was transferred to stop solution (see Appendix A1.25) for one hour or kept overnight followed by several washes. This was done to further identify the bands of interest (according to size) using the mass spectrophotometric facility in the department.

Chapter 3

The effects of loss of MED16, MED2 and MED14 mediator subunits of *Arabidopsis* on stress gene regulation and stress tolerance

3.1 Introduction

The Mediator transcriptional coactivator complex is a large multi-protein complex, which was first discovered in yeast (*Saccharomyces cerevisiae*) and which plays an important role in transcription initiation, by connecting sequence-specific transcriptional regulators (transcription factors; TFs) to RNA Polymerase II (Pol II) (Kuras and Struhl, 1999, Struhl, 1996, Yudkovsky et al., 2000). The Mediator complex in yeast comprises 25 protein subunits, which can be divided into four sub domains named the head, middle, tail, and kinase domains (Asturias et al., 1999). Later, the mediator complex was identified in *Drosophila melanogaster* and in humans indicating that the mediator complex is conserved amongst eukaryotes. The presence of the Mediator complex in plants had been suggested based on sequence homology between some plant proteins and known mediator proteins from other species (Autran et al., 2002, Boube et al., 2002b), however, the level of homology was so low that firm conclusions were never drawn until the complex was successfully purified from plants several years ago (Backstrom et al., 2007). The plant mediator complex consists of an estimated 34 subunits (Mathur et al., 2011). Backstrom et al. (2007) found that homologues for most head and middle subunits of yeast Mediator can be found in Arabidopsis but very low homology exists between the yeast and Arabidopsis subunits in the tail domain. Bourbon (2008) was able to

identify evolutionarily conserved signature sequence motifs (SSMs) across the mediator subunit proteins of all eukaryotes, and thereby identified the genes encoding plant mediator subunits, despite this low sequence homology. He suggested that mediator subunits MED2, MED3 and MED5 are located in the tail domain as well the confirmed tail subunits MED14, MED15 and MED16. Further it was suggested that the yeast subunits, MED2, MED3 and MED5, correspond to the metazoan-specific MED29, MED27 and MED24 and the plant specific subunits MED32, MED27 and MED33a/b, that were identified in Arabidopsis (Bourbon, 2008). A mutation in the MED16 subunit of yeast showed the loss of function of other subunits in the tail domain, suggesting that mediator subunits interact with each other (Li et al., 1995, Galdieri et al., 2012) and control gene specific transcriptional regulation.

MED16 in plants was first identified as SFR6 (SENSITIVE TO FREEZING-6). The Arabidopsis *sfr6* loss-of-function mutant was identified on the basis of its failure to increase freezing tolerance through the process of cold acclimation (Warren et al., 1996). Later work revealed that the SFR6/MED16 protein is essential for the activation of some cold- and desiccation-inducible gene expression and that the freezing sensitivity in *sfr6* is due to the failure to fully express cold-regulated genes controlled by the CBF/DREB1 (C-repeat binding factor/drought-responsive element binding factor 1) transcription factors (Yamaguchi-shinozaki and Shinozaki, 1994, Liu et al., 1998) and consequent failure to accumulate the proteins encoded by these genes (Boyce et al., 2003, Knight et al., 2009, Knight et al., 1999). In addition to this important role, SFR6 also plays a role in protection of plants against UV damage and biotrophic bacterial pathogen attack, starvation responses and iron uptake (Wathugala et al., 2012, Hemsley et al., 2014, Zhang et al., 2014). Furthermore other

two known tail subunits, MED 14 and MED15 have been shown to be important in plant immune responses in Arabidopsis (Canet et al., 2012, Zhang et al., 2012, Zhang et al., 2013).

Structural data on the composition of the plant mediator complex is not available. However, assuming the structure of plant mediator is similar to yeast mediator (Bourbon, 2008), we might predict a close physical interaction between MED14 with SFR6/MED16 and might predict that MED2 is part of a tail subunit triad (Zhang et al., 2004a) that is attached to the main body of mediator via SFR6/MED16. Hemsley et al. (2014) recently found that loss of function of MED2 and MED14 disrupts low temperature-induced gene expression in a manner similar to that caused by loss of function of SFR6/MED16. Considering all these facts I focussed in this study on examining the levels of stress tolerance associated with lack of MED2 and MED14 subunits in freezing stress compared to lack of SFR6/MED16. Furthermore, I studied UV-, starvation- and drought stress-induced gene expression and tolerance of these conditions in both mutants to observe whether they were affected similarly to *sfr6* mutants, and to correlate loss of stress-inducible expression with reduced stress tolerance.

The hypothesis of this chapter is:

SFR6/MED16 shares similar roles with MED2 and MED14 in response to abiotic stress and the defect in cold-, UV-, drought- and starvation-induced gene expression correlates with reduced tolerance.

This was studied by using stress gene expression and stress tolerance experiments using *med2-1 and med14-2* mutants (Hemsley et al., 2014) and comparing these with *sfr6-1* and wild type. Cold, UV and drought stresses were used to test the responses

of *med2* and *med14* to compare with *sfr6-1* as very clear impaired responses were previously identified in s*fr6-1*(Knight et al., 2009, Knight et al., 1999, Warren et al., 1996). The objective of this chapter to study whether these reductions in gene expression under cold-, UV-, drought- and starvation- induced stresses correlate with altered stress tolerance.

3.2 Results

3.2.1 Measurement of low temperature induced damage in *med16, med2* and *med14* mutants

The *sfr6/med16 mutant* is well known for its impaired transcriptional responses to cold (Knight et al., 2009, Knight et al., 1999), especially expression of the CBF-controlled *COR* genes such as *KIN2* and *GOLS3,* (Fowler and Thomashow, 2002, Knight et al., 1999, Taji et al., 2002) the promoters of which contain at least one copy of the CRT (C-repeat) element (Yamaguchi-shinozaki and Shinozaki, 1994). This failure to up regulate these genes normally in response to cold acclimation leads to a failure to tolerate freezing temperatures. In yeast MED2 and MED14 subunits are predicted to be physically close to MED16 (based on a combination genetic and protein interaction data; (Guglielmi et al., 2004) and it is thought that their arrangement may be similar in the Arabidopsis Mediator complex. Therefore, the hypothesis was made that MED2 and MED14 might share the same role as SFR6/MED16 in the response to cold stress. Our lab demonstrated reduced levels of *KIN2* and *GOLS3* expression in *med2-1* and *med14-2* in response to cold, similar to those previously observed in *sfr6-1 (*Hemsley et al., 2014). Hence, I continued the

work from this point to further investigate whether this reduction in the level of cold-responsive gene expression might correlate with altered levels of freezing tolerance.

3.2.1.1 Freezing sensitivity of *med16, med2* and *med14*

Warren et al. (1996) identified the *sfr6-1/med16* mutant of Arabidopsis on the basis of its failure to survive freezing temperatures even after being exposed to cold acclimation. This freezing sensitivity correlates with failure to express *COR* genes Knight 1999); genes that have been reported in previous studies to be associated with cold acclimation-induced freezing tolerance (Fowler and Thomashow, 2002, Knight et al., 1999, Taji et al., 2002).

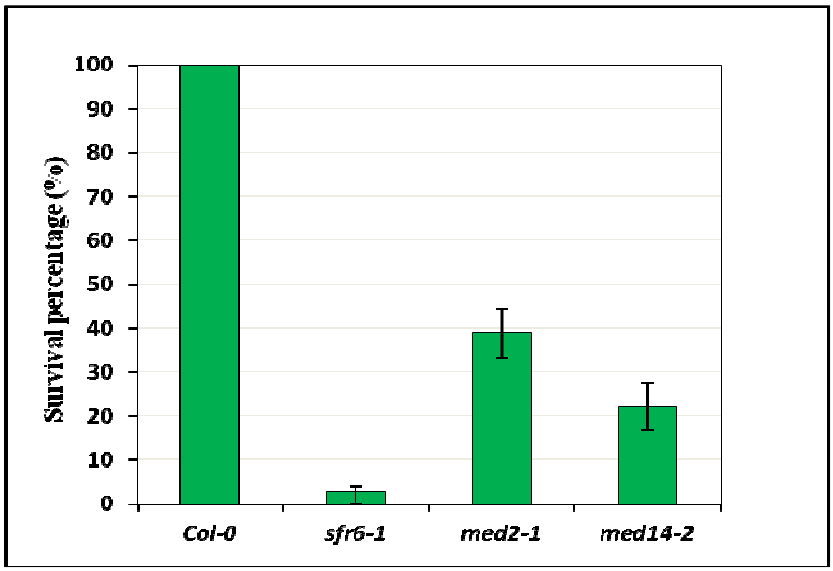

Figure 3.1: Level of freezing tolerance in *med* mutants

The average of three survival percentages from three separate biological experiments (replicates) is shown in the above histogram. The number of plants surviving 7 days after treatment at -7.5^{0}C was recorded. All error bars shown are standard error (±SE) calculated from arcsine transformed values as appropriate for proportional data and indicate the level of variation between biological replicate experiments. Non-overlapping error bars indicate means are significantly different (P = 0.001).

The freezing assay in my study was performed using *sfr6, med2* and *med14* mutants compared to wild type. Five-week-old plants grown under short days (12:12 light:dark cycle) were cold acclimated for 2-weeks at 5°C before subjecting to freezing temperatures (-7.5°C) for 24 h (see Materials and methods section 2.16.2.1). Plants were returned to normal growth conditions and monitored for 7 d. Three separate biological replicate experiments were conducted on three different occasions and each replicate experiment consisted of 12 plants from each plant type arranged randomly on the same shelf of the freezing chamber. Plants' recovery from freezing damage was measured by the number of plants surviving/remaining green seven days after freezing treatment and data are shown in Figure 3.1. Plants were photographed at different stages in the assay and finally plants were scored as having survived if green tissues were visible after 7 days, or if the shoot apex was green.

The survival rate of cold-acclimated Col-0 wild type plants was 100% whereas it was observed that loss of function mutants of both MED2 and MED14 (like *sfr6*) showed reduced rates of survival after freezing. However, the *med2-1* mutant was least severely affected, with nearly 40% survival. The *med14-2* mutant showed 22.2% survival and the *sfr6-1* mutant was the most severely affected mutant, exhibiting 2.8% survival in this freezing tolerance study (Figure 3.1). Interestingly this tolerance result was consistent with the *COR* gene expression pattern *i.e KIN2* and *GOLS3* as reported in Hemsley et al. (2014), where expression was not severely affected in *sfr6-1* and least affected in *med2-1*. Figure 3.2 demonstrates the physical appearance of 5-week-old wild type and mutant plants following 2-weeks acclimation at 5^0C, plants frozen at -7.5^0C for 24h after 2-weeks acclimation and 7-days after freezing at -7.5^0C. No physical difference was observed among mutants

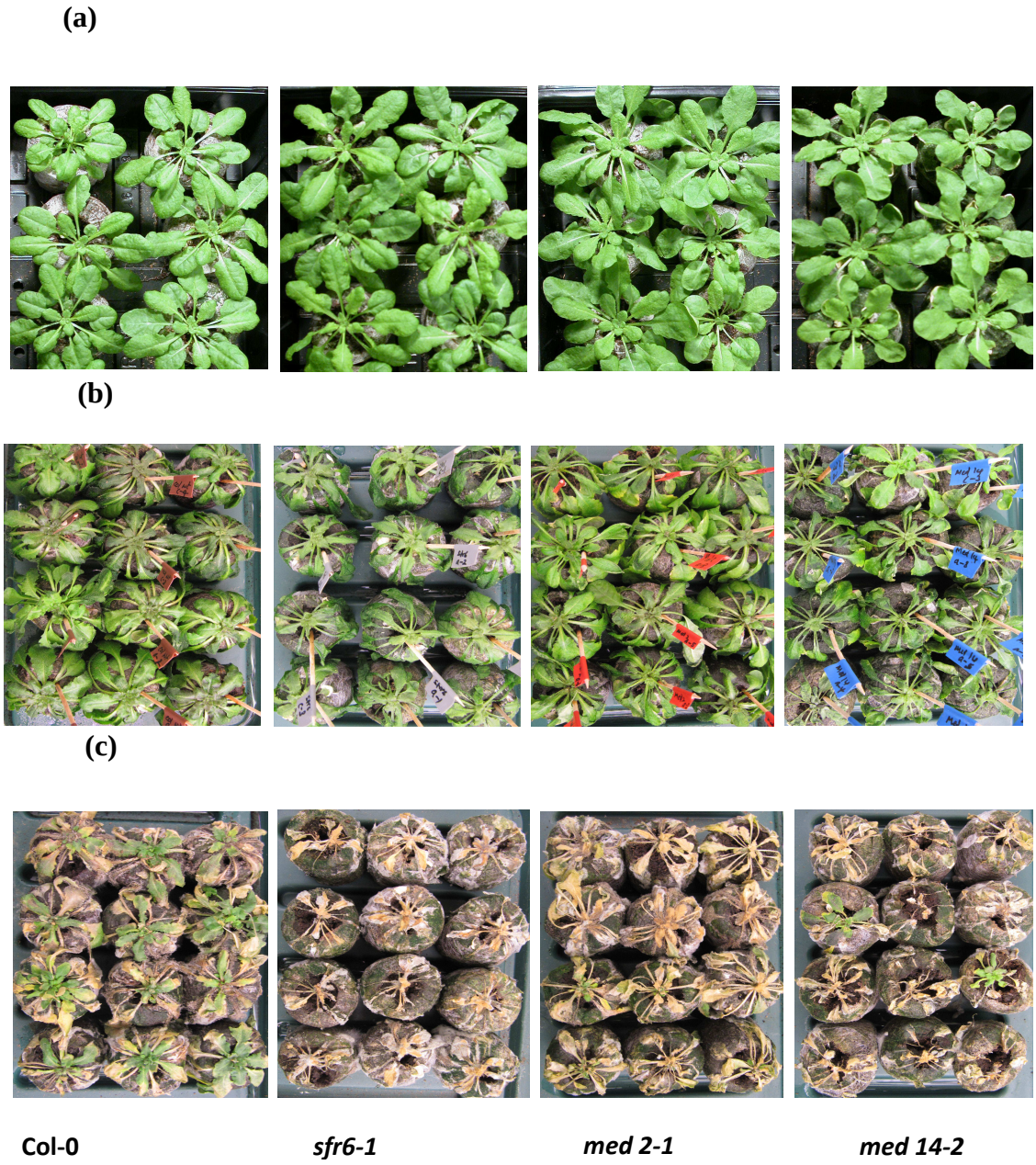

Figure 3.2: Sensitivity of *med* mutants to freezing temperatures

Results of the second freezing tolerance assay are presented here. The row (a) shows 5-week-old plants acclimated at 5^0C for 2 weeks but not frozen. The row (b) shows 5-week-old plants acclimated at 5^0C for 2 weeks and frozen at -7.5^0C for 24h. The bottom row (c) shows the plants 7 days after freezing at -7.5^0C.

compared with wild type (Col-0) after 2-weeks acclimation, however, *sfr6-1* mutants exhibited severe freezing damage after 24h at -7.5^{0}C compared with *med14-2* mutant (Figure 3.1). The *med2-1* mutant was the least affected mutant and its physical appearance was on a par with Col-0. All the Col-0 plants had survived 7 days after freezing in all three replicate experiments conducted and the lowest number of surviving plants was always found amongst the *sfr6-1* mutant plants. The second lowest number of plants remaining green after freezing was observed in *med14-2* (Figure 3.1).

3.2.1.2 Photosynthetic efficiency of wild type and Mediator subunit plants before and after freezing

In each freezing tolerance assay photosynthetic efficiency was measured for each type of plant at key stages of the assay. Fv/Fm (the ratio of variable to maximal fluorescence) is used as a reliable indicator of maximum photochemical quantum efficiency (Genty et al., 1989, Kitajima and Butler, 1975) in photosynthetic plants. Changes in chlorophyll fluorescence emission in photosystem II is a good indicator of plant stress under different environmental conditions such as temperature (Jensen et al., 1997, Larcher et al., 1998, SchÄFer et al., 1997), light (Heber et al., 2000, Demmig and Björkman, 1987, Gauslaa and Solhaug, 2000, Krause, 1988) and water availability (Bilger et al., 1989, Jensen and Feige, 1991, Lange et al., 1989, Scheidegger et al., 1997, Csintalan et al., 1999, Jensen et al., 1999). This parameter was measured in dark-adapted samples (see section 2.16.2.1), calculated from *Fo*, the fluorescence emission when the reaction centres in Photosystem 11 are fully open (Mathis and Paillotin, 1981), and *F*m, the maximum fluorescence emission when all

photosystems are closed following exposure to a source of saturation light (Lazár, 1999). The difference between maximum fluorescence and minimum fluorescence is *Fv (Fv=Fm-Fo)*, or variable fluorescence. *Fv/Fm* is a normalised ratio calculated by dividing variable fluorescence by maximum fluorescence. Therefore *Fv/Fm* is a ratio that represents the maximum potential quantum efficiency of photosystem II if all capable reaction centres were open.

Fv/Fm values either before acclimating or after acclimating did not vary between plant types and all plants showed similar values ranging between 0.87-0.90 (See Figure 3.3); values typical of healthy plants. Conversely, the *Fv/Fm* ratio of 3 days after freezing treatments was different between plant types and the lowest values were exhibited by *sfr6-1* and *med14-2* mutants, although values were not significantly different from each other ($p > 0.01$). *Fv/Fm* values in Col-0 and *med2-1* were very similar and did not differ significantly.

The health of the plants as indicated by chlorophyll florescence measurements was recorded at three different stages of the freezing assay to observe the level of damage in each plant type and is shown in Figure 3.4. At locations where photosynthetic function was optimal the colour is depicted as green on the pseudocolour scale whereas plant parts that show a stress response are coloured yellow and red for moderate and highly stressed areas respectively (Mathis and Paillotin, 1981, Lazár, 1999).

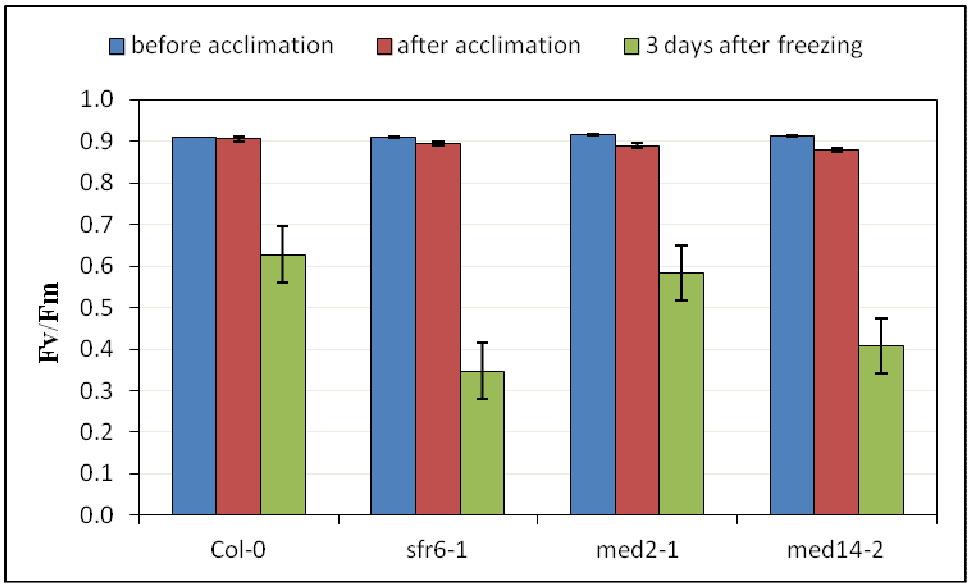

Figure 3.3: Photosynthetic efficiency (*Fv/Fm*) at different stages of the freezing tolerance assay

The histogram shows the average *Fv/Fm* ratio from three different experiments that were specific to different stages in the freezing assay. In each experiment 12 plants/each type were used. Blue bars represent the *Fv/Fm* value in 5-week-old plants before acclimating. Red bars show the *Fv/Fm* value just after 2-weeks of cold acclimation at 5^0C. Green bars signify the ratio between *Fv* and *Fm*, 3-d after plants were frozen at -7.5^0C. Non-overlapping error bars indicate means that are significantly different ($P < 0.01$).

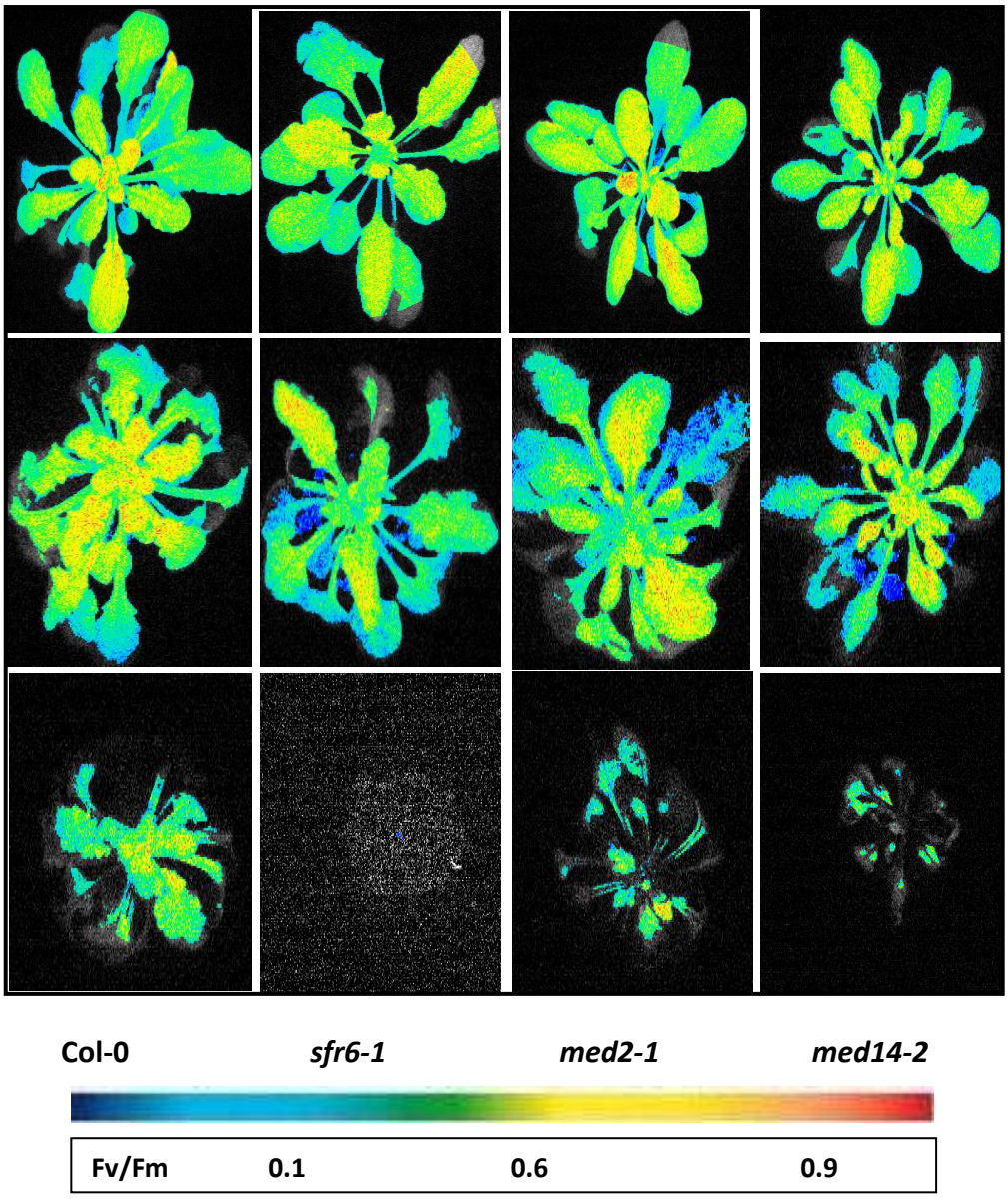

Figure 3.4: Sensitivity of *med* mutants to low temperatures, assessed by measuring chlorophyll fluorescence

A representative picture of each plant type selected from the second freezing tolerance assay is presented here. Fv/Fm values are represented on a pseudo colour scale where the highest ratios (in the range of 0.8-0.9) are depicted by orange and red, ratios in the range of 0.6-0.7 by yellow and green and the lowest ratios by blue. Areas of leaf tissue that are not visible on this image (black) are those that produced no signal at all and correspond to dead tissue. The top row shows 5-week-old plants before acclimating. The middle row shows plants after 2-weeks acclimation at 5^0C. The bottom row shows plants at -7.5^0C. Plants were imaged at same intensity of chlorophyll fluorescence at 754 exposures in each case.

It is clear that all four types of plants were non-stressed or moderately stressed before acclimating at 5°C; the whole leaf area was visible in green/yellow pseudocolour and showed reduction of the area of tissue giving a value in the range of 0.6-0.7 and the highest reduction was found in *sfr6-1*, whilst no such difference between frozen and non-frozen plants was observed in Col-0. Lack of any pseudocolour representation of the leaf tissue in the image corresponds to death of the tissue, resulting in no signal. Three days after freezing treatment, nearly 70% of leaf tissues in Col-0 plants appeared on the image as green/yellow/red, explaining the reason for the highest percentage of survival after freezing being seen in this genetic background. Interestingly no green/yellow/red (higher ratios) leaf area was observed in the images of the *sfr6-1* mutant but blue/black in the image, an observation made in all three biological replicates. In *med14-2*, in *med2-1* plants less green/yellow/red tissues with more blue/black tissues were observed compared to Col-0 in the image.

3.2.1.3 Measuring freezing damage in *med16, med2* and *med14* mutants by assessment of electrolyte leakage levels

The leakage of electrolytes from frozen tissues has been commonly used to quantify freezing injury and it is a sensitive indicator of loss of integrity by the plasmalemma (Calkins and Swanson, 1990, Warren et al., 1996). Twenty-seven-day-old soil-grown plants were acclimated for 2 weeks and leaf samples were taken to quantify the percentage loss of electrolytes after leaves were subjected to temperatures of between 0 and -12°C (see materials and method 2.15.2). Three separate experiments were conducted and in each experiment three leaves were used per replicate tube, with three tubes per genotype/temperature.

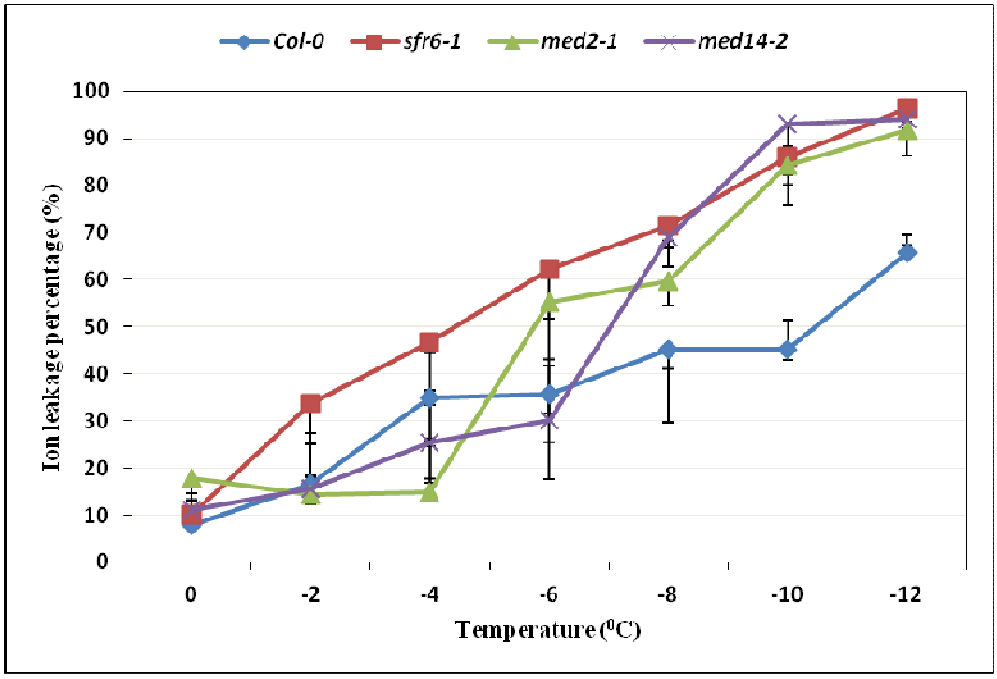

Figure 3.5: Electrolyte leakage in *med* mutants compared with wild type Arabidopsis responding to freezing temperatures

Plants were grown for 27 d before cold acclimating at 5°C for 2 weeks. The graph represents data from three different experiments and data point represents the average of data from the three biological replicate experiments; each experiment used three leaves of each genotype per replicate tube, with three technical replicate tubes per genotype/temperature. Values represent the percentage loss of electrolytes after leaves were subjected to temperatures of between 0 and -12°C.

Electrolyte leakage assays revealed that three mutants, *sfr6-1*, *med2-1* and *med14-2* were more sensitive to freezing than wild type, particularly at lower freezing temperatures (Figure 3.5). The *sfr6-1* mutant was confirmed as exhibiting the highest sensitivity, showing the highest levels of electrolyte leakage across the whole range of temperatures (0 to -12^0C) tested in this study. The level of sensitivity of *med2-1* and *med14-2* mutants at the least severe freezing temperatures (0 to -6^0C) was on a par with Col-0. Interestingly percentage of ion leakage in Col-0 was higher compared to *med2-1* and *med14-2* mutants at -4^0C temperature. However, all three mutants

were significantly more sensitive to low freezing temperatures than wild type ($p<0.01$). Natural logarithm transformed percentage of leakage data were analysed using a one-way ANOVA at each temperature point and error bars represent SE. Data points with non-overlapping error bars are significantly different ($p< 0.01$).

In summary, electrolyte leakage results were consistent with previously reported *COR* gene expression (Hemsley et al., 2014), survival rate and maximum potential quantum efficiency of photosystem II (*Fv/Fm*) as well as with the physical appearance of the whole plants after freezing. Consequently, all of these data support the hypothesis that SFR6/MED16 shares its role in cold acclimation and freezing tolerance through activation of *COR* gene expression with two other predicted Mediator tail subunits, MED2 and MED14.

3.2.2 Response of Mediator subunit mutants to UV stress

Since 1996, when it was discovered that SFR6 is important in cold acclimation and the gain of subsequent freezing tolerance (Warren et al., 1996), it was later revealed that SFR6 was vital for full expression of *COR* genes under both low temperatures and drought conditions (Boyce et al., 2003, Knight et al., 1999). Knight et al. (2008) reported that *sfr6* mutants demonstrate altered functioning of the circadian clock and delayed flowering, most likely as a result of mis-regulation of circadian clock-controlled genes that contain an evening element (EE) in their promoter. These observations suggested a wider role for SFR6 as a regulator of gene transcription, beyond its effect on the response to low temperature. Wathugala et al. (2012) discovered that three genes *PR1*, *EDS5* and *CASPASE8*, which are highly up-regulated by UV-C radiation in wild type plants, showed a significantly reduced level of expression in three *sfr6* mutant alleles. Furthermore they reported that SFR6 is

required only for the induction of specific genes in response to UV-C; this was deduced by showing that two other UV-C inducible genes *OXI1* and *TCH3* (Narusaka et al., 2003) were up-regulated in all *sfr6* mutant alleles to levels as high as seen in wild type. This finding was in agreement with similar observations indicating that SFR6 regulates only specific low temperature-induced gene regulons; those controlled *via* the CRT/DRE *cis* element (Boyce et al., 2003, Knight et al., 1999). Furthermore, Wathugala et al. (2012) reported that the reduced levels of expression seen in *sfr6* mutants under UV-C correlated with reduced UV-C tolerance, with significantly lower rates of survival in *sfr6* mutants compared to wild type even at low levels of UV-C irradiation.

Therefore it was decided to test whether *med2 and med14* mutants were likely to be impaired in the activation of UV-C- responsive gene expression leading to UV stress tolerance, as reported for *sfr6/med16*.

3.2.2.1 Expression of stress-responsive genes after UV-C exposure

Seeds were sown on horizontal MS agar plates. Seven-day-old seedlings were irradiated with 5 KJm^{-2} of UV-C, (wavelength 254 nm) by removing the petri plate lids and placing in a UV cross-linker set to deliver the designated level of energy. Lids were removed from the control plates during the time taken to administer the treatments. Immediately after irradiation all plates including control plates were resealed with micropore tape and returned to the growth chamber and samples were taken 24 h after treatment. (See materials and methods 2.15.1.2). This time point was selected as peak expression time point for *PR1* according to the published data on gene expression assays (Wathugala et al., 2012). Measurements of gene expression were performed using qRT-PCR and *PR1* (Nawrath et al., 2002) gene expression was

measured and normalised to expression of At4G26410, a gene with stable expression levels that are not altered by UV treatments (Genevestigator; https://www.genevestigator.com). Relative expression levels were calculated using the ΔΔCT method (Livak and Schmittgen, 2001), and the error bars in each biological replicate histogram represent RQ_{MIN} and RQ_{MAX} and constitute the acceptable error level for a 95% confidence level according to Student's t test. Data presented in this experiment and all subsequent gene expression experiments reported in this thesis, show separate data for each of the three biological repeat experiments and the average of three biological replicate experiments in separate histogram. Fold differences in induction of stress–responsive genes often vary between repeat experiments (biological replicates) in whole seedlings, however, consistent qualitative differences are observed (This issue is explored further in the discussion).

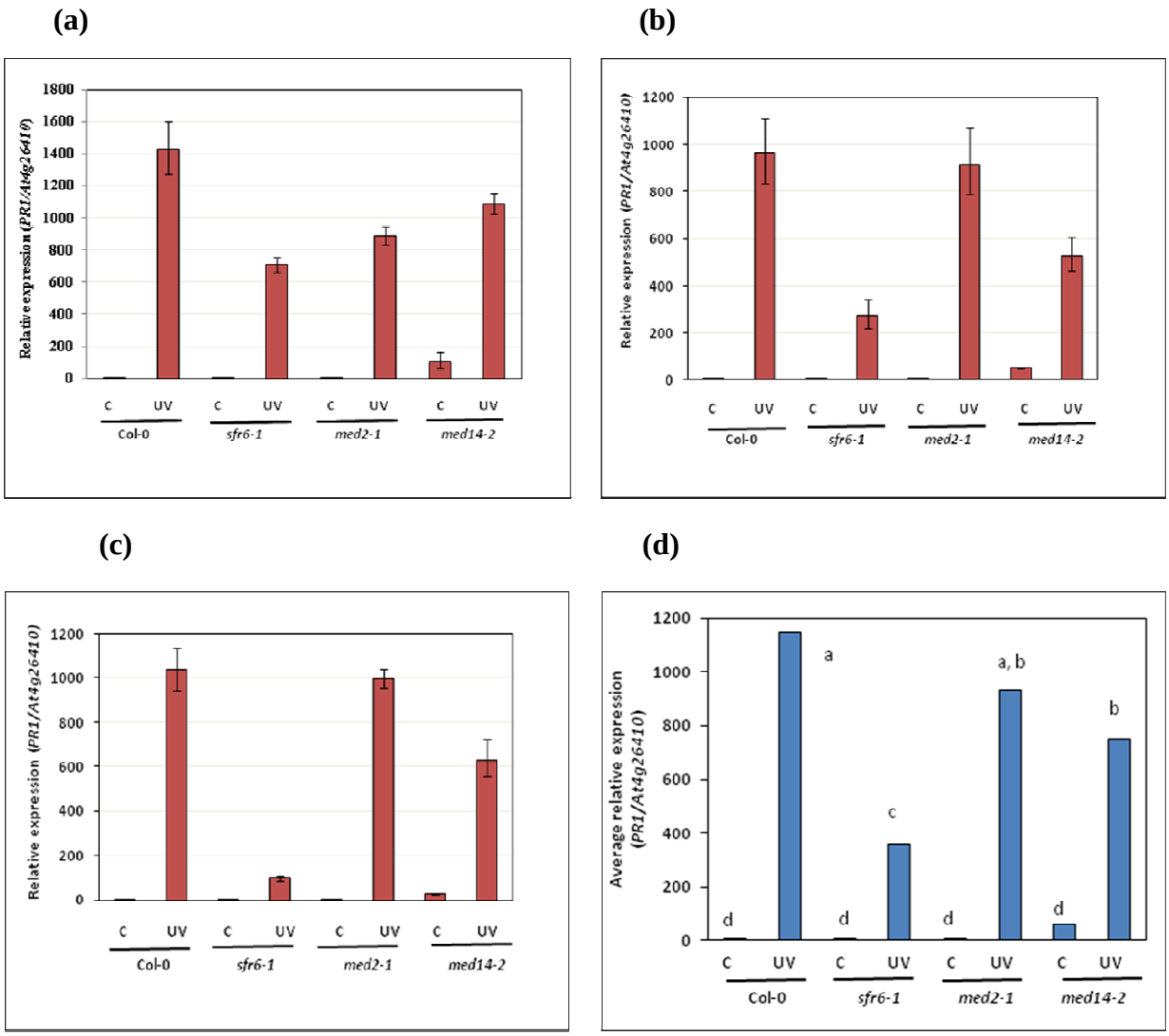

Figure 3.6: Expression of *PR1* in response to 5 kJm^{-2} UV-C exposure

PR1 (*Pathogenesis Related-1*) expression in three *med* mutants was compared with expression in Col-0. Seven-day-old seedlings were exposed to 5 kJm^{-2} UV-C irradiation (UV) or control treatment (C) and seedlings were harvested 24 h after exposure. The first three histograms (a, b and c- with red bars) represent the three independent biological replicates and the fourth histogram (d, with blue bars) represents the average of the above three independent biological replicates. Relative expression represents the fold difference value compared with Col-0 control sample (1). Error bars indicate the level of variation between technical replicates within one biological replicate experiment. Mean average data (in graph d) were analysed using a one-way ANOVA (α=0.05) and pairwise comparisons were made using the Tukey method. Means that do not share a letter are significantly different ($P < 0.001$).

UV-inducible *PR1* expression in three independent biological replicate experiments (Figure 3.6 a, b and c) and the average of the above three independent biological replicates is presented in Figure 3.6 d. High levels of consistency in *PR1* gene expression levels were not observed in three *med* mutants but the lowest *PR1* expression level was detected in *sfr6-1* in all three instances. The second lowest levels of expression were observed in *med14-2* in two instances out of three. *med2-1* was the least affected *med* mutant at 5 kJm^{-2} of UV-C and showed similar levels of *PR1* gene expression to those seen in Col-0 in two out of three experiments conducted (Figure 3.6 a and b). The average values of three biological replicates (Figure 3.6d) show that Col-0 and *med2-1* mutant did not show a significant difference (α=0.05) in *PR1* expression when compared with one another whereas *sfr6-1* and *med14-2* were significantly different in *PR1* expression compared to Col-0. Furthermore, expression in *sfr6-1* was significantly lower to that of *med14-2* and *sfr6-1*showed the lowest average relative expression levels (at α=0.05) with 5 kJm^{-2} UV-C irradiation.

As the next step to see whether the *med2-1* mutant was completely unaffected in its ability to respond to UV-C or just less affected than other two *med* mutants it was decided to study the effect of a higher level of UV-C irradiation on *PR1* gene expression in the mutants. Therefore seven-day-old seedlings were irradiated with 10 kJm^{-2} of UV-C, (wavelength 254 nm) as stated above. In contrast to *PR1* gene expression at 5 kJm^{-2} irradiation, reduced and more consistent *PR1* expression levels were observed in the *med2-1* mutant compared with wild type when treated at 10 kJm^{-2}; the gene expression data from three independent biological replicate experiments are presented in Figure 3.7 a, b and c. The average gene expression level of the above three independent biological replicates is shown in Figure 3.7 d.

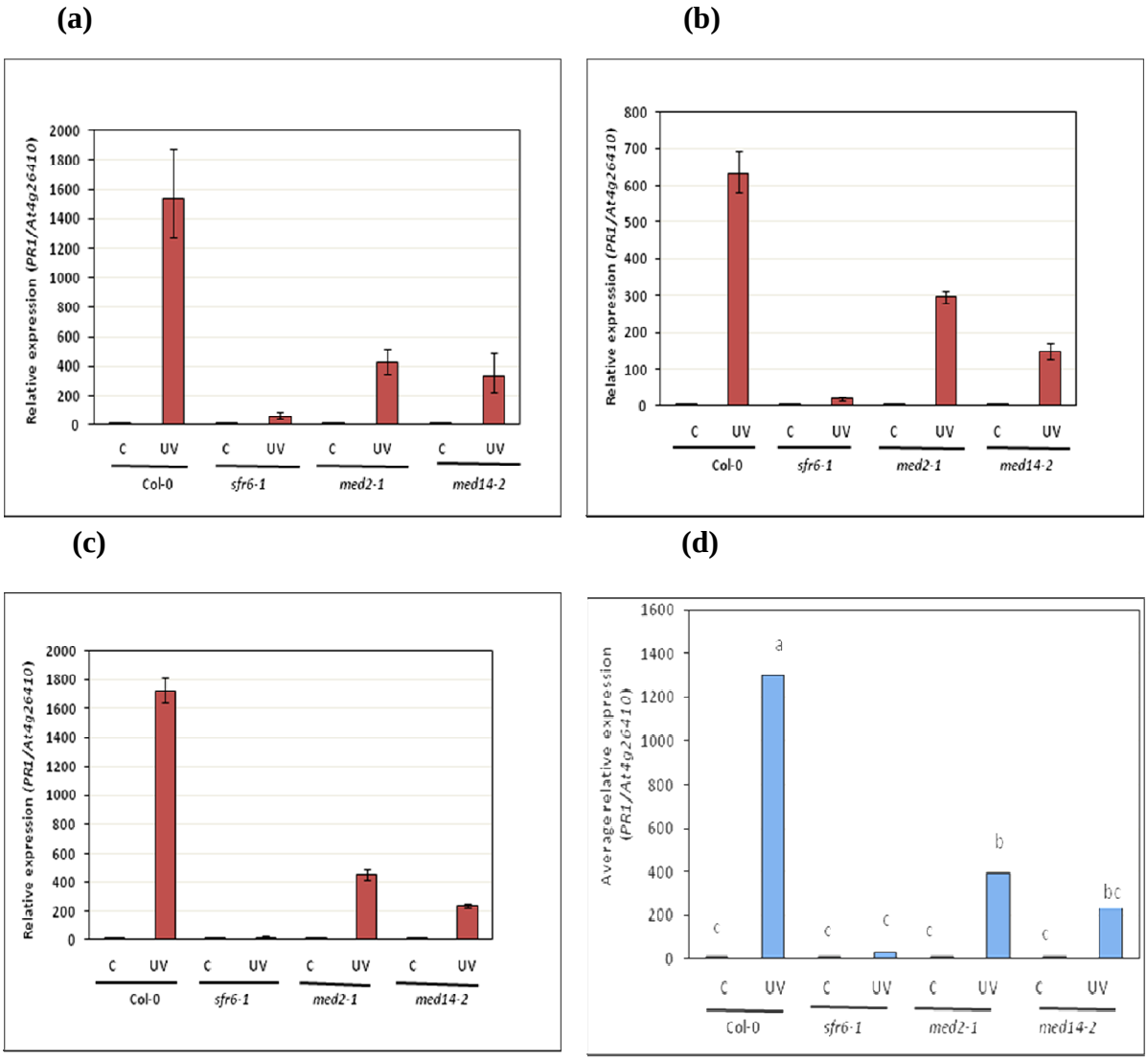

Figure 3.7: Expression of *PR1* in response to 10 kJm^{-2} UV-C exposure

PR1 (*Pathogenesis Related-1*) gene expression in three *med* mutants was compared with Col-0. Seven-day-old seedlings were exposed to 10 kJm^{-2} UV-C irradiation (UV) or control treatment (C) and seedling were harvested 24 h after exposure. The first three histograms (a, b and c- with red bars) represent the three independent biological replicates and the fourth histogram (d, with blue bars) represents the average of the above three independent biological replicates. Relative expression represents the fold value compared with Col-0 control sample. Error bars indicate the level of variation between technical replicates within one biological replicate experiment. Mean average data (in graph d) were analysed using a one-way ANOVA (α=0.05) and pairwise comparisons were made using the Tukey method. Means that do not share a letter are significantly different ($P < 0.001$).

These average data clearly show that *PR1* gene expression in *med2-1* was significantly reduced compared to Col-0. *sfr6-1* demonstrated the least expression of *PR1* , as seen in the previous experiments using 5kJm^{-2} etc. and no significant difference of several hundred folds when compared to *med2-1* and Col-0 (Figure 3.7d).

Interestingly there was no significant difference between expression levels in *med2-1* and *med14-2* at this higher level of (10 kJm^{-2}) of irradiance even though a significant difference in *PR1* gene expression was seen between the two mutants at 5 kJm^{-2} (Figure 3.6 d). Finally all these data show that *PR1* gene expression in the *med14* mutant is highly impaired in response to UV-C while the *med2* mutant was less affected, and data support the hypothesis that MED2 and MED14 share the role of MED16/SFR6 in the transcriptional response to UV-C.

3.2.2.2 Sensitivity of *sfr6*/*med16, med2* and *med14* after UV exposure

Wathugala et al. (2012) reported that seedlings of the *sfr6-1* mutant showed severe damage after exposure to UV-C irradiation and a great reduction in survival rate compared to wild type. Furthermore they suggested that reduced levels of UV-C induced gene expression in *sfr6* mutants resulted in reduced UV-C tolerance.

The UV tolerance assay was carried out using 7 day-old-seedlings irradiated with 5 or 10 kJm^{-2} of UV-C in a UV cross linker (as used for the gene expression analysis described above) with the plate lids off, while control plates were exposed to air for same duration as in UV treatments. Immediately after treatments, all plates were resealed and returned to the growth chamber after being wrapped in aluminium foil to inhibit blue light repair pathway (see materials and methods 2.16.2.2). The number of surviving seedlings with growing apex was recorded 10 days after treatment.

At the lower level of UV-C exposure (5 kJm^{-2}) all three *med* mutants showed a reduced survival rate compared to wild type but differences were not significant ($P>0.05$) (Figure 3.8). At the higher level of UV-C exposure (10 kJm^{-2}) all *med* mutants showed a significant reduction of survival compared to Col-0, however, amongst *med* mutants no significant differences could be observed (Figure 3.8). Figure 3.9 shows the appearance of untreated *med* mutant seedlings and Col-0, to provide a comparison of how seedling growth and health was affected by UV-C (see figure 3.10 and 3.11, which represent the appearance of seedlings after 10 d of 5 kJm^{-2} and 10 kJm^{-2} of UV-C treatments respectively).

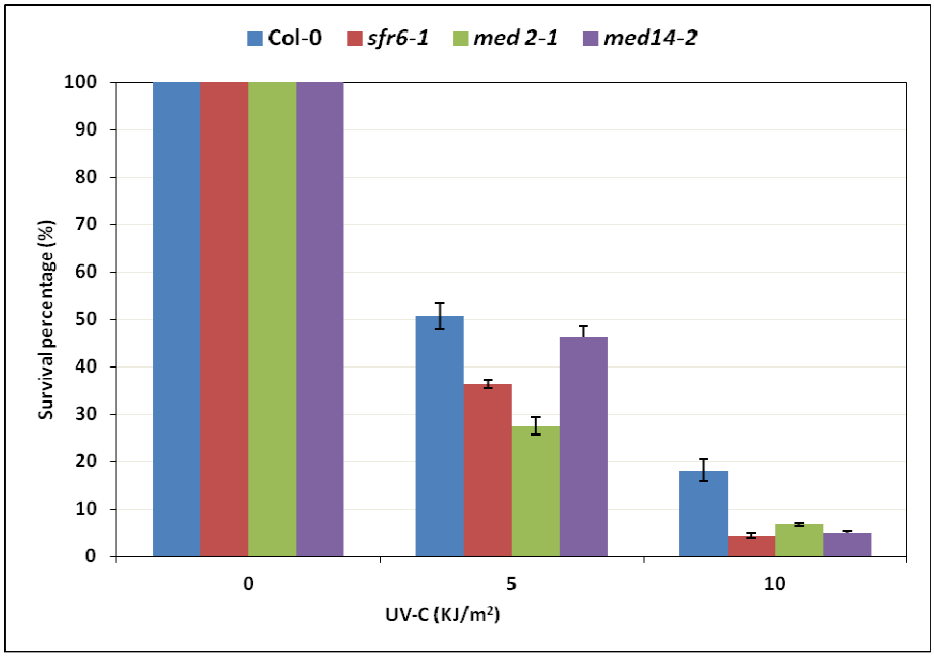

Figure 3.8: Level of UV-C tolerance in *med* mutants

The average of three survival percentages from three separate biological repeat experiments (replicates) is shown in the histogram. The number of plants surviving (remaining green) 7-days after UV-C treatment at 5 kJm^{-2} and 10 kJm^{-2} was used to calculate the percentage survival. Error bars show standard error values (±SE) calculated from arcsine transformed values as appropriate for proportional data and indicate the level of variation between biological replicate experiments. Non-overlapping error bars indicate means that are significantly different ($P < 0.001$).

The tolerance data suggest that all *med* mutants showed reduced level of tolerance of UV-C irradiation and damage was more severe after higher levels of UV-C exposure. In agreement with the impaired *PR1* gene expression observed, *med* mutants demonstrated reduced tolerance compared to Col-0 and in both gene expression and tolerance data are more significant at high dosage of UV-C. Therefore these data signify that the impaired gene expression in *med2* and *med14* correlates with reduced tolerance under UV-C and demonstrate a role for MED2 and MED14, like MED16 in the response to UV-C.

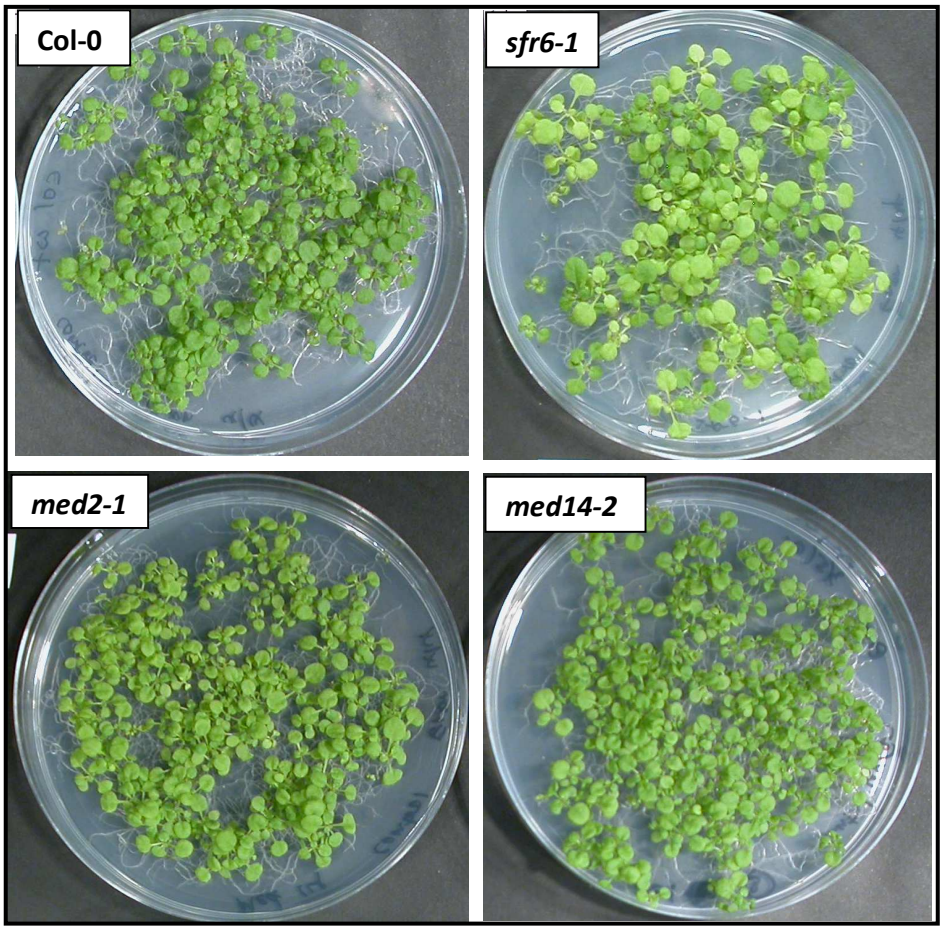

Figure 3.9: Appearance of *med* mutants in normal growth conditions

Non treated control plates of the UV tolerance assay are presented here. Seven-day-old seedlings were exposed to the air during the time taken for the UV exposure and all plates were resealed and returned to the Percival growth chamber at 20±1^{o}C set for long day (16:8 h light: dark) after wrapped in foil for 24 h. The number of surviving seedlings with green meristems was recorded 10 days post treatments and photographed.

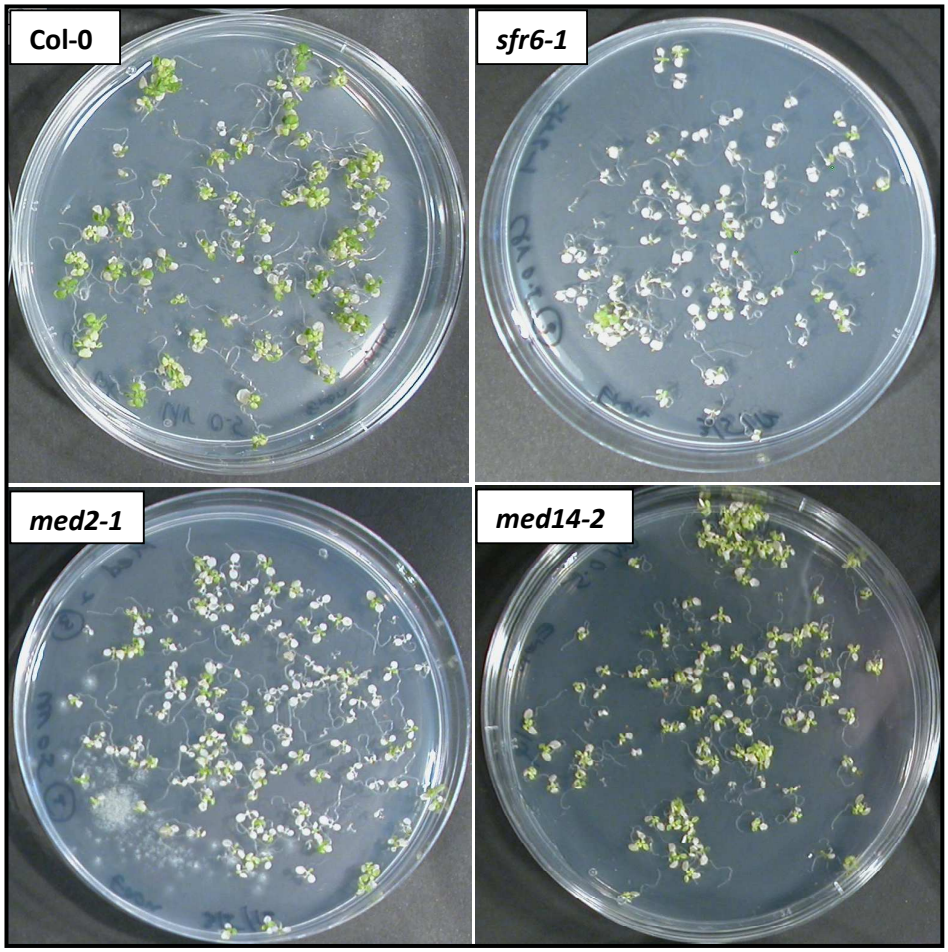

Figure 3.10: Sensitivity of *med* mutants to 5 kJm^{-2} of UV-C exposure

Representative pictures of UV tolerance assays are presented here. Seven-day-old seedlings were irradiated at 5 kJm^{-2} and all plates were resealed and returned to the growth chamber at 20±1^{o}C set for long days (16:8 h light: dark). Plates were wrapped in aluminium foil for 24 h before being unwrapped to avoid activation of the blue light repair pathway. The number of surviving seedlings with green meristems was recorded 10 d post treatment and photographed.

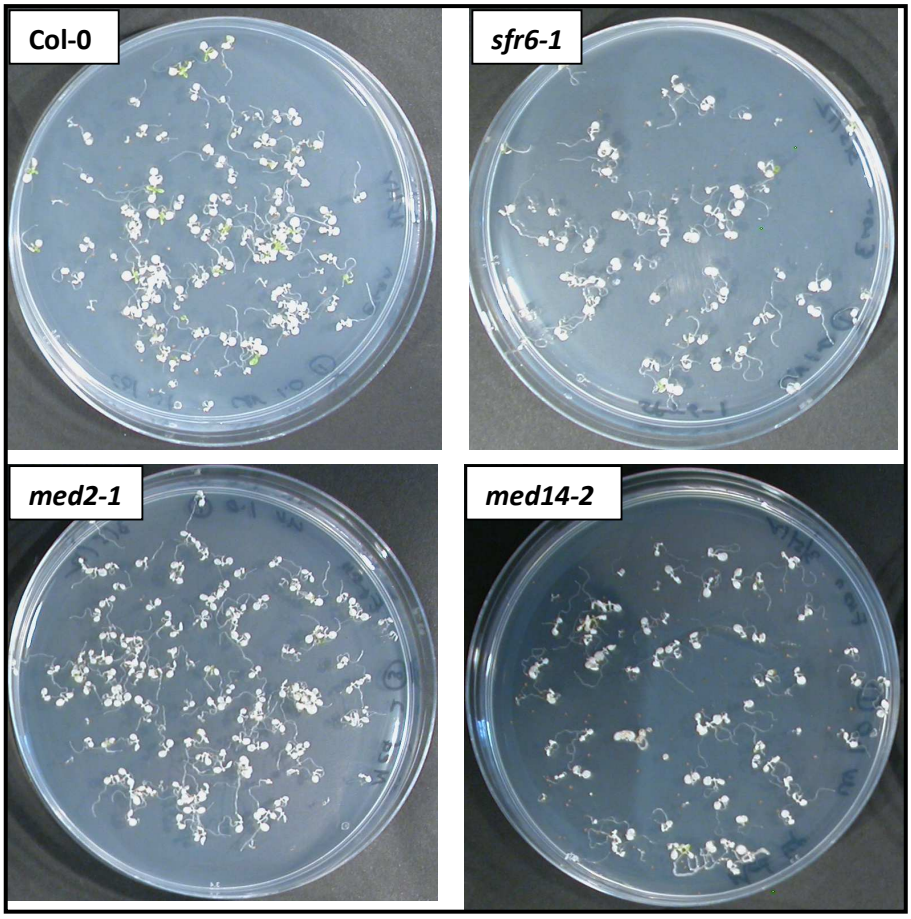

Figure 3.11: Sensitivity of *med* mutants at 10 kJm^{-2} of UV-C exposure

Representative pictures of UV tolerance assays are presented here. Seven-day-old seedlings were irradiated at 10 kJm^{-2} and all plates were resealed and returned to the growth chamber at 20±1^{o}C set for long days (16:8 h light: dark). Plates were wrapped in aluminium foil for 24 h before being unwrapped to inhibit blue light repair pathway. The number of surviving seedlings with green meristems was recorded 10 days post treatment and photographed.

3.2.3 Response of Mediator subunit mutants to drought stress

A reduced transcriptional response to drought stress stimuli has been observed previously in *sfr6* mutants (Knight et al., 1999, Boyce et al., 2003). Osmotic stress (mimic by the addition of mannitol) and the application of ABA (levels of which are elevated during exposure to drought; (Lang et al., 1994) both elicited a much lower level of *COR* gene expression in *sfr6* mutants compared to wild type (Boyce et al., 2003, Knight et al., 1999). Similar expression patterns were obtained with three genes; *KIN1 COR15a* and *LTI78*. The *LTI78*, *KIN1*, and *COR15a* genes are known to be expressed in response to drought signals (Kurkela and Borg-Franck, 1992, Mantyla et al., 1995) as well as in cold. Both cold and drought signalling pathways leading to expression of these genes use many of the same components (Ishitani et al., 1997) and activate the expression of CRT/DRE containing genes (Liu et al., 1998, Boyce et al., 2003).

AtP5CS2 (*P5CSB*) and *AtP5CS1* (*P5CSA*) are two Arabidopsis genes that both encode Δ1-pyrroline-5-carboxylate synthetase (Strizhov et al., 1997), the key enzyme involved in the synthesis of proline (Savouré et al., 1995), a compatible solute that accumulates in response to water stress and to low temperature (Savouré et al., 1997). *AtP5CS2* contains a CRT/DRE motif in its promoter, whereas the *AtP5CS1* gene does not contain this element (Knight et al., 1999). Cold inducibility of *AtP5CS1* as well as *CBF1*, *CBF2*, and *CBF3*, which also lack CRT/DRE motifs (Gilmour et al., 1998) was similar in wild-type and *sfr6* mutants (Knight et al., 1999). COR genes containing the CRT/DRE motif in their promoter are controlled by CBF (DREB1) or DREB2 transcription factors binding to the motif in response to cold or drought respectively (Liu et al., 1998, Yamaguchi-shinozaki and Shinozaki, 1994).

The above data suggested that gene expression deficiency of *sfr6* was limited to genes containing CRT/DRE elements in cold and drought. Microarray analysis has since confirmed this to be the case for cold (Hemsley et al., 2014).

DRE/CRT *cis*-acting elements play a role in ABA- independent gene expression under drought stress (Yamaguchi-Shinozaki and Shinozaki, 2005). The other major regulatory pathway that controls drought-inducible gene expression is ABA-dependent and occurs via the ABRE (ABA-responsive element) *cis*-acting elements (Yamaguchi-Shinozaki and Shinozaki, 2005).

The objective of the experiments described below was to investigate the transcriptional responses and tolerance of mediator mutants, *med*2 and *med14* compared to *med16/sfr6* and Col-0 to drought conditions.

3.2.3.1 Expression of stress-responsive gene under desiccation

Desiccation/drought-responsive gene expression experiments were carried out using 7-day-old seedlings grown on MS medium on petri dishes and subjected to water loss by opening the lids, thereby exposing the seedlings to loss of humidity. Plates were left open in the growth chamber for 6 h during the light cycle with no humidity control while keeping the control plates closed in the same chamber (See section 2.15.1.4). Expression of the desiccation-inducible gene *KIN2* was analysed using qRT-PCR and normalized to expression of *PEX 4* gene, an endogenous control gene (Wathugala et al., 2011). Fold values were calculated using the ΔΔCT method, and the error bars in each biological replicate represent RQ_{MIN} and RQ_{MAX} and constitute the acceptable error level for a 95% confidence level according to Student's t test.

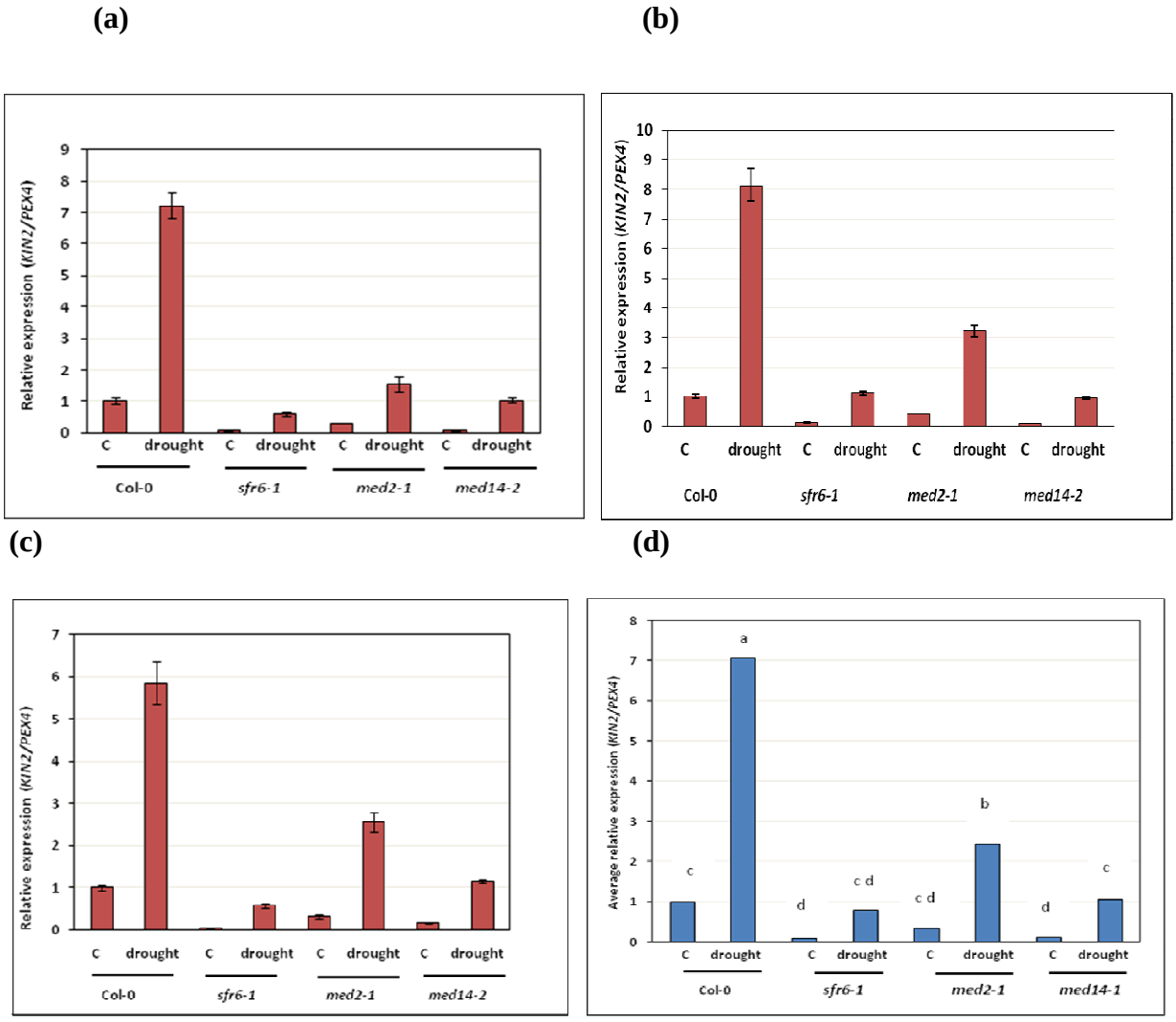

Figure 3.12: Desiccation-induced *KIN2* gene expression in *med* mutants

KIN2 expression in response to desiccation was measured in three *med* subunit mutants compared with Col-0. Seven-day-old seedlings were exposed to growth conditions in the Percival growth chamber by opening the lids for 6 h while keeping the control plates closed under same conditions. The first three histograms (a, b and c- with red bars) represent the gene expression data of three independent biological replicates. Relative expression represents the fold value compared with Col-0 control sample. Error bars indicate the level of variation between technical replicates within one biological replicate experiment. The fourth chart (blue bars; d) represents the average of the above three independent biological replicates. Mean average data (in graph d) were analysed using a one-way ANOVA (α=0.05) and pair wise comparisons were made using the Tukey method. Means that do not share a letter are significantly different ($P < 0.001$).

Desiccation-induced *KIN2* expression was compared between wild type Arabidopsis plants and *sfr6, med2* and *med14* mutants in three independent biological replicate experiments (Figure 3.12 a, b and c). A very consistent pattern of *KIN2* gene expression under drought stress was observed, with *med2-1* the least affected *med* mutant in all three instances compared to Col-0 and *med14-2* was the second in all three instances. The average values of relative expression of *KIN2* in three independent biological replicates is presented in Figure 3.12 d and the lowest (Figure 3.12 a, b and c). *sfr6-1* showed the lowest *KIN2* expression in all three experiments.

The average data were analysed using a one-way ANOVA (α=0.05) and pairwise comparisons were done using the Tukey method. Means that do not share a letter are significantly different ($P < 0.000$). Average gene expression data from three individual experiments confirm that *KIN2* expression in response to desiccation was significantly different in *med2-1* and *med14-2*, however, no significant difference could be observed between *med14-2* and *med16/sfr6-1* (Figure 3.12 d). Results of this study demonstrated that expression of *KIN2*, a gene induced under desiccating conditions as well as in cold conditions showed impaired expression in all *med* mutants tested in this study compared to Col-0 (Figure 3.12).

3.2.3.2 Drought tolerance of *sfr6*/*med16, med2* and *med14* mutants

After observing consistently reduced desiccation-induced gene expression patterns in mediator mutants, the next logical step was to study whether these changes had an effect on drought tolerance. Therefore drought tolerance assays were performed using sseedlings grown on peat plugs maintained in short day conditions for 25 d post-germination. Plants were subjected to water withdrawal for 14 days (after which approximately 50% of wild type plants showed a wilting appearance) and then re-

watered. The number of plants surviving and exhibiting re-growth was assessed after a further 10 days (see materials and methods 2.16.2.3). Average data from three separate biological replicate experiments are presented in Figure 3.13.

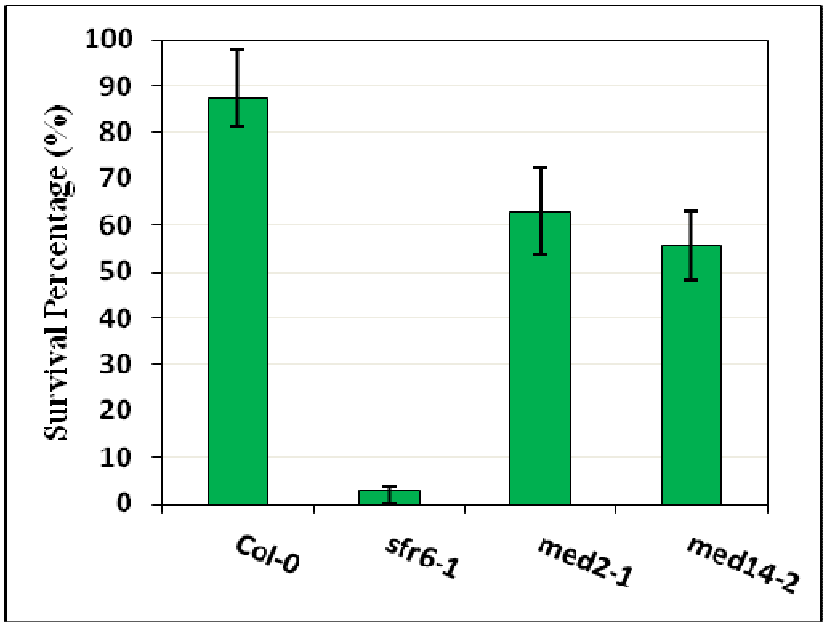

Figure 3.13: Level of drought tolerance in mediator mutants

The average of three survival percentages from three separate biological experiments (replicates) with 15 plants per experiment is shown in the above of histogram. Twenty five-day-old plants were subjected to water withdrawal for 14 days, re-watered and the number of plants surviving on the twelfth day after re-watering was recorded. Error bars represent standard error (±SE) calculated from arcsine transformed values as appropriate for proportional data and indicate the level of variation between biological replicate experiments. Non-overlapping error bars represent means that are significantly different from one another ($P < 0.001$).

These data demonstrate reduced tolerance in all three *med* mutants and it is significantly different ($P<0.001$) compared to Col-0. Average tolerance data suggests that there was no significant difference between the tolerance of *med2-1* and *med14-2* but tolerance of these two mutants were significantly different compared to *sfr6-1*

(Figure 3.13). Although the general appearance of the most of the plants are good, more number of dead plants could be seen in *med2-1* and *med14-2* compared to wild type and all the dead plants in *sfr6-1* (Figure 3.14).

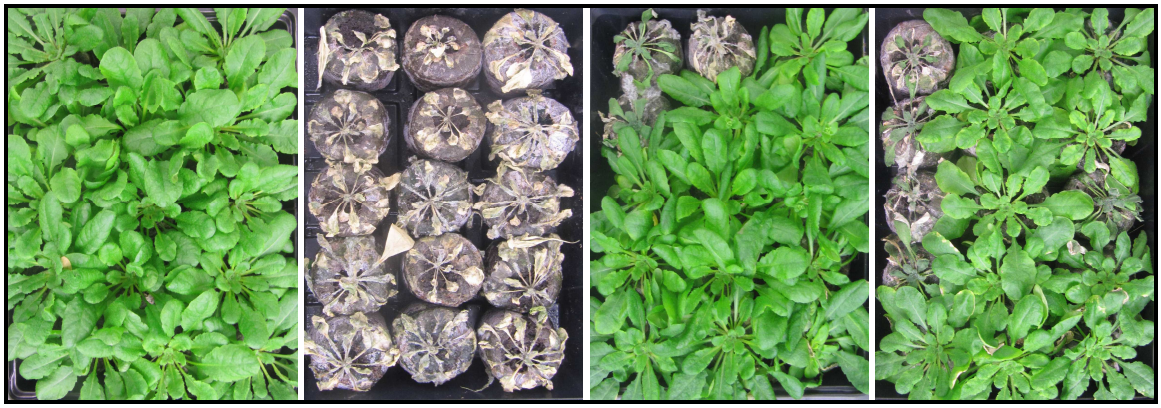

Col-0 ***sfr6-1*** ***med2-1*** ***med14-2***

Figure 3.14: Sensitivity of *med* mutants under drought conditions

A representative picture of each plant type selected from the second drought tolerance assay is presented here. Twenty-five-day-old plants grown on peat plugs were subjected to withdrawal of water for 14 days (after which approximately 50% of wild type plants showed a wilting appearance) and then re-watered. The number of plants surviving and exhibiting re-growth was assessed after a further 10 days and plants photographed.

Upon critical analysis of data I could draw the same conclusion that reduced gene expression under drought stress is correlated with reduced tolerance and three mediator subunits play an important role in drought-inducible gene expression but interestingly MED2 and MED14 do not appear to have a major role in drought tolerance.

3.3 Summary

Experiments conducted in this chapter were designed to study the transcriptional responses of *med2* and *med14* compared to *med16*/*sfr6* and Col-0 under UV and drought conditions as well as their ability to tolerate freezing, UV and drought stress conditions.

Average *PR1* gene expression under UV-C induction was tested and results revealed that at 5kJm^{-2}of UV-C exposure *med2-1* was not badly affected but at 10kJm^{-2} *PR1* expression of this mutant affected significantly. The *med14-2* mutant was significantly affected at both levels of UV-C exposure and impaired levels of *PR1* gene expression at 10kJm^{-2} exposure were similar to the level of *sfr6-1* mutant.

Drought inducible average *KIN2* expression in *med2-1* and *med14-2* were reduced significantly compared to Col-0 and expression levels in *med14-2* and *sfr6-1* were not significantly different.

Freezing tolerance data reported using electrolyte leakage assay and percentage of survival under freezing were demonstrated that all three med mutants were severely affected compared to Col-0. Among *med* mutants *sfr6-1* was highly sensitive to freezing conditions while *med2-1* was the least affected mutant. The med*14-2* mutant demonstrated the moderate sensitivity under freezing conditions among med mutants tested under this study. Tolerance under high dosage (10kJm^{-2}) of UV-C exposure was highly reduced in all three *med* mutants compared to wild type although tolerance data at 5kJm^{-2} not shown similar pattern as in *PR1* gene expression data. Results of drought tolerance assays revealed that both *med2-1* and *med14-2* mutants demonstrated the reduced tolerance compared to Col-0 but not up to the level of *sfr6-1*.

Comparing the gene expression and tolerance data shown in this chapter a clear relationship emerges between reduced levels of tolerance and impaired gene expression under cold and UV but not under drought.. Further these results indicate that MED2 and MED14 share the same role as MED16/SFR6 in gene regulation under cold, drought, and UV stresses. Moreover the tolerance data presented here provide evidence that reduced levels of gene expression in the three mediator subunit mutants is correlated with reduced levels of tolerance under each stress condition. The degree to which tolerance levels reflect deficiencies in gene expression varied, with large changes in drought-inducible *COR* gene expression in *med2* and *med14* mutants having relatively small effects on desiccation tolerance.

Chapter 4

An attempt to identify different domains in SFR6/MED16 that are required for transcriptional responses under specific abiotic stresses

4.1 Introduction

SFR6 was discovered as a protein required for acquisition of freezing tolerance (Knight et al., 1999, Warren et al., 1996) and later was identified as MED16, a tail subunit of the plant mediator complex (Bäckström et al., 2007). Impaired transcriptional responses in *sfr6-1* lead to freezing sensitivity due to mis-regulation of *COR* gene expression (Knight et al., 2009, Knight et al., 1999). Apart from being required for low temperature tolerance and gene expression, SFR6/MED16 is important in drought gene expression (Knight et al., 1999). Further regulatory effects of SFR6/MED16 were observed by Wathugala et al. (2012) and Zhang et al. (2012) in plant defence systems and they found altered expression of pathogen associated genes activated by both salicylic acid and jasmonic acid pathways in *sfr6* mutants. Recently, altered transcriptional regulation in iron homeostasis was reported in *sfr6* mutants part of the photoperiodic regulatory pathway and controls circadian clock gene expressions. Hemsley et al. (2014) reported that SFR6 is important in the regulation of dark-inducible genes and that the *sfr6-1* mutant is impaired in transcriptional regulation of *DIN6*. These findings supported that the SFR6 protein is important in a wide array of stress gene regulation.

SFR6 is a comparatively large protein and the predicted size is 1268 amino acids in length with a molecular mass of 137 kDa (Knight et al., 2009). Therefore the hypothesis was proposed that different domains/regions of the SFR6 protein might be

responsible for the activation of genes responsible for the plant response to each stress such as cold, UV, drought and starvation Alternatively, it may be that the entire protein is required for response to all of these conditions. Thus considering the broad range of stress- and developmental-related functions the aims I tested in this chapter are;

(a) To identify the domain/ region(s) of SFR6/MED16 that are necessary for its targeting to the nucleus, an essential property of a protein that is involved in transcription.

(b) To identify different domain/regions of the SFR6 protein responsible for the activation of genes responsible for each stress such as cold, UV, drought and starvation by studying which of the SFR6/MED16 (domains can complement the functions of SFR6 protein in an *sfr6* mutant).

4.2 Results

4.2.1 Generation of different truncations of SFR6/MED16 of Arabidopsis

Full length *AtSFR6* cDNA (3.753 kbp) synthesised from RNA collected from wild type Arabidopsis tissue was used as starting material in this study to create different truncations of SFR6/MED16. To select the different domains, I studied the SFR6 sequence of different plant species and particularly the sequence signature motifs (SSM) that are conserved between all eukaryotic species studied (Bourbon, 2008). Protein motifs of SFR6/MED16 that were predicted to be involved in protein-protein or protein-DNA interactions were considered and disruptions to the structure of the protein (especially α-helices and β-sheets) was avoided in generation of truncated versions. After this had been taken into account, truncations were designed to represent approximately the first two thirds of the protein, lacking the C terminus (SF14,879aa; 96.7kDa) , two truncations representing the middle part (SF25,654aa; 71.9kDa and SF24, 532aa; 58.5kDa), one representing the C-terminal two thirds (SF36, 616aa; 67.7kDa) and a truncation that lacks the figure-terminal Zinc Finger (ZnF) motif of the protein (SF15, 1001aa; 110.1kDa). The full length version of SFR6/MED16 (SF16, 1269aa; 139.6kDa) was also constructed (SF16) (Figure 4.1).

After selecting the positions of the six different truncations (as shown in figure 4.1) the coding sequences for these were amplified from full length *AtSFR6* cDNA (See section 2.4.1). These amplified truncated fragments were purified and then cloned into Gateway Entry vector (p-ENTR D-TOPO) (see section 2.5.1) (see Appendix A3.1). Correct orientation of the fragments in the entry vector was tested using primers specific for the 35S promoter and the beginning of each construct (see Appendix A2.1 for primer sequences). For further confirmation that sequences were

correct along the full length of each truncated fragment, amplified fragments were sequenced using different primers designed for the SFR6 (see section 2.7) coding sequence. After confirming the correct sequence of each truncation, each sequence was sub-cloned downstream of the *CaMV* 35S promoter of the Binary Gateway destination vector *pB7WG2* (Karimi et al., 2002) (see Appendix A3.3) for stable overexpression in Arabidopsis (see Appendix A3.5-A3.10) or into the *pK7WGF2* (see Appendix A3.11) vector (Karimi et al., 2002) for transient expression of GFP-tagged versions of these proteins in tobacco plants (see section 2.5.2).

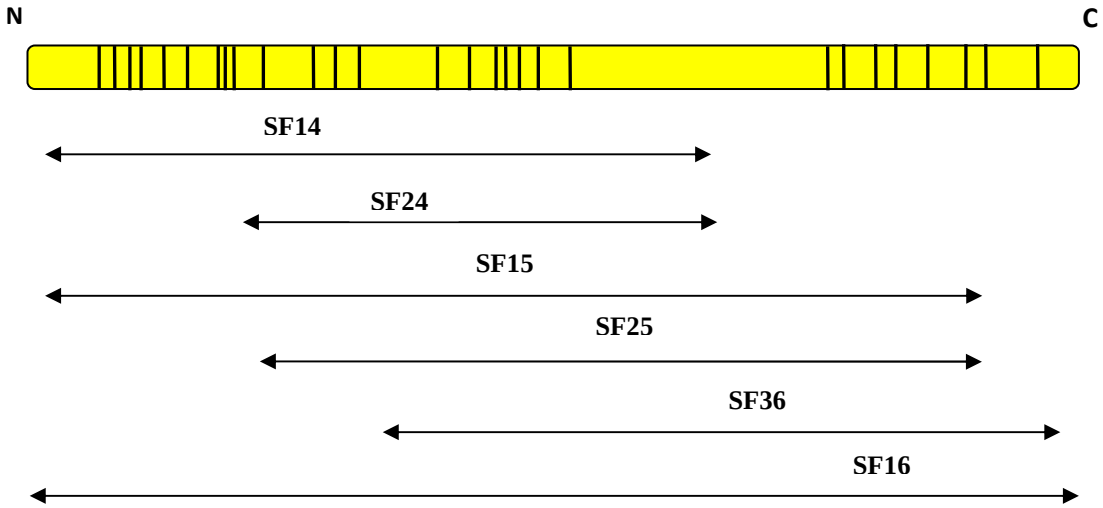

Figure 4.1(a): Schematic representation of different truncations of SFR6/MED16 created in this study

Vertical lines on the SFR6/MED16 represent the SSMs (Sequence Signature Motifs)(Bourbon, 2008). Positions of the aa represents six different truncations of SFR6/MED16 1-1269aa (1269):SF16; 1-1004aa (1004): SF15; 1-879aa (879): SF14; 347-879aa (532): SF24; 347-1001aa (654): SF25; 653-1296aa (616):SF36

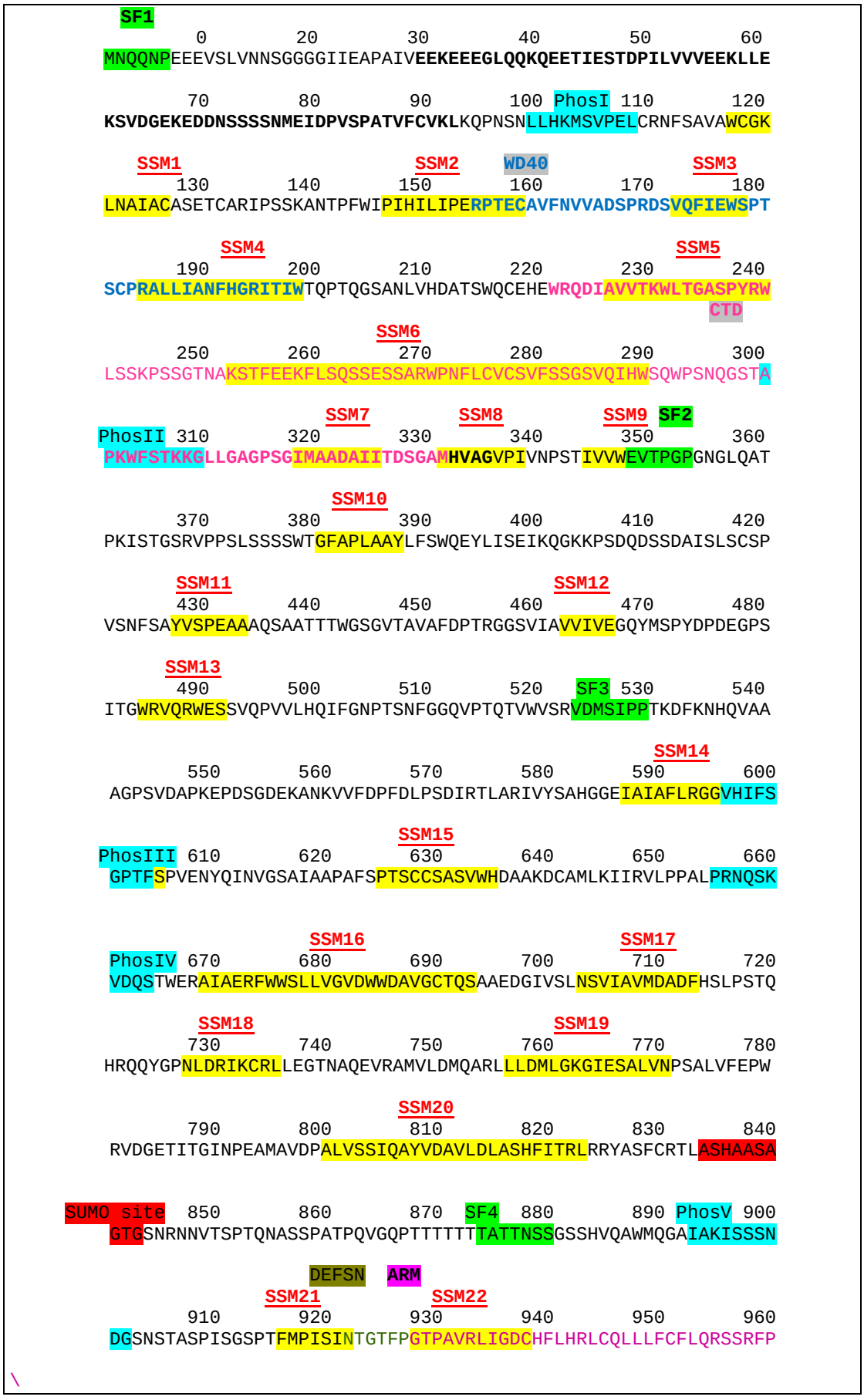
SF1
0 20 30 40 50 60
MNQQNPEEEVSLVNNSGGGGIIEAPAIVEEKEEEGLQQKQEETIESTDPILVVVEEKLLE
70 80 90 100 PhosI 110 120
KSVDGEKEDDNSSSSNMEIDPVSPATVFCVKLKQPNSNLLHKMSVPELCRNFSAVAWCGK
SSM1 SSM2 WD40 SSM3
130 140 150 160 170 180
LNAIACASETCARIPSSKANTPFWIPIHILIPERPTECAVFNVVADSPRDSVQFIEWSPT
SSM4 SSM5
190 200 210 220 230 240
SCPRALLIANFHGRITIWTQPTQGSANLVHDATSWQCEHEWRQDIAVVTKWLTGASPYRW
CTD
SSM6
250 260 270 280 290 300
LSSKPSSGTNAKSTFEEKFLSQSSESSARWPNFLCVCSVFSSGSVQIHWSQWPSNQGSTA
SSM7 SSM8 SSM9 SF2
PhosII 310 320 330 340 350 360
PKWFSTKKGLLGAGPSGIMAADAIITDSGAMHVAGVPIVNPSTIVVWEVTPGPGNGLQAT
SSM10
370 380 390 400 410 420
PKISTGSRVPPSLSSSSWTGFAPLAAYLFSWQEYLISEIKQGKKPSDQDSSDAISLSCSP
SSM11 SSM12
430 440 450 460 470 480
VSNFSAYVSPEAAAQSAATTTWGSGVTAVAFDPTRGGSVIAVVIVEGQYMSPYDPDEGPS
SSM13
490 500 510 520 SF3 530 540
ITGWRVQRWESSVQPVVLHQIFGNPTSNFGGQVPTQTVWVSRVDMSIPPTKDFKNHQVAA
SSM14
550 560 570 580 590 600
AGPSVDAPKEPDSGDEKANKVVFDPFDLPSDIRTLARIVYSAHGGEIAIAFLRGGVHIFS
SSM15
PhosIII 610 620 630 640 650 660
GPTFSPVENYQINVGSAIAAPAFSPTSCCSASVWHDAAKDCAMLKIIRVLPPALPRNQSK
SSM16 SSM17
PhosIV 670 680 690 700 710 720
VDQSTWERAIAERFWWSLLVGVDWWDAVGCTQSAAEDGIVSLNSVIAVMDADFHSLPSTQ
SSM18 SSM19
730 740 750 760 770 780
HRQQYGPNLDRIKCRLLEGTNAQEVRAMVLDMQARLLLDMLGKGIESALVNPSALVFEPW
SSM20
790 800 810 820 830 840
RVDGETITGINPEAMAVDPALVSSIQAYVDAVLDLASHFITRLRRYASFCRTLASHAASA
SUMO site 850 860 870 SF4 880 890 PhosV 900
GTGSNRNNVTSPTQNASSPATPQVGQPTTTTTTTATTNSSGSSHVQAWMQGAIAKISSSN
DEFSN ARM
SSM21 SSM22
910 920 930 940 950 960
DGSNSTASPISGSPTFMPISINTGTFPGTPAVRLIGDCHFLHRLCQLLLFCFLQRSSRFP

\

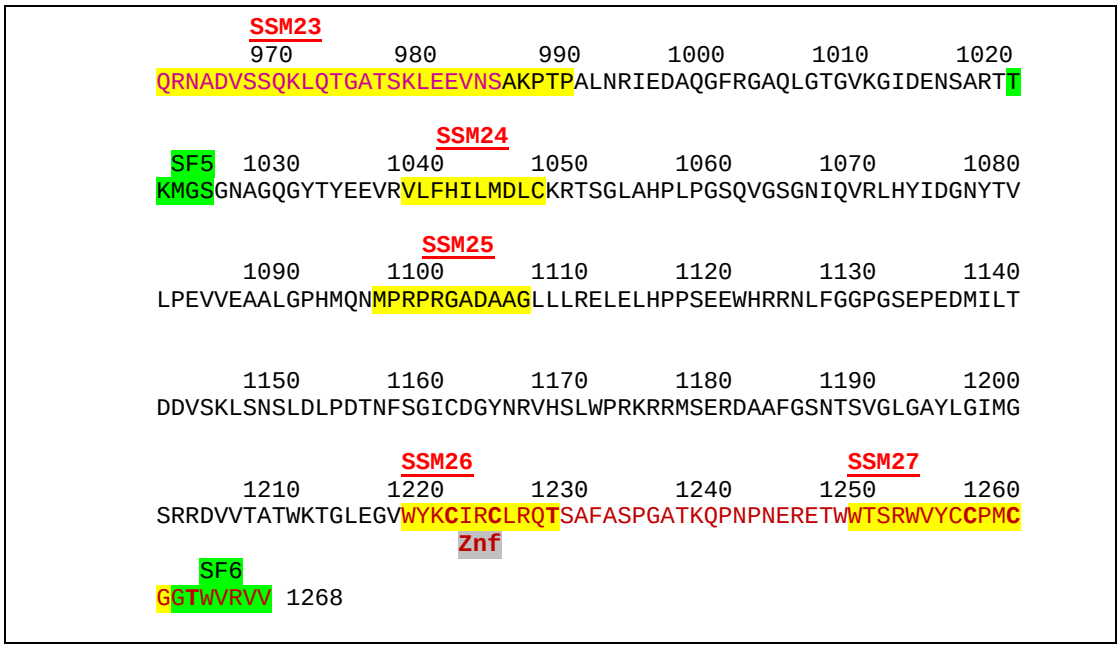

Figure 4.1(b): Sequence Signature Motifs (SSM), Simple Modular Architecture Research Tool domains (SMART) and other special features in SFR6 protein sequence. SF1-6 shows the position of the beginning of each SF constructs; PhosI-V shows the position of predicted phosphorylating sites; SSM1-27 shows the identified SSM domains; WD40 CTD ARM are specific protein binding sites; DEFSN shows the deffencing domain SUMO site shows the SUMOlating domain in SFR6; Znf shows the zinc finger domain in SFR6

4.2.1.1 Generation of GFP-tagged versions of SFR6/MED16 truncated forms

An in-frame fusion of truncated versions of SFR6/MED16 with N-terminal GFP were cloned as described in section 2.5.1 and 2.5.2 in to pK7WGF2 (see appendix A3.12-A3.17). Each in *pK7WGF2* was tested for correct orientation of the insert in the destination vector. This was followed by restriction digestion to confirm the correct size was and further confirmed by PCR with specific primers designed to the 35S promoter and to each insert (see Appendix A2.1 for primer sequences). One positive line for each construct was sequenced to confirm the presence of whole sequence of the truncated fragment of SFR6/MED16. After that each construct in

pK7WGF2 destination vector was transformed in to *Agrobacterium tumefaciens* strain GV3101 and used for tobacco infiltration (see section 2.11.2) or DNA was used for direct transformation by biolistic transformation in leek cells (see section 2.11.3) to study the ability of each truncation of SFR6/MED16 to localise to the nucleus that explain and to express each protein of correct predicted size.

4.2.2 Examination of the ability of the truncated fragments of SFR6/MED16 to target to the nucleus

The following experiments were designed to identify the domain of SFR6/MED16 that is responsible for targeting the protein to the nucleus. Six different fusions of SFR6/MED16 truncations with GFP (described in section 4.2.1) were tested for their ability to localise to the nucleus. Transient expression of the fusions in tobacco plants was carried out using infiltration and biolistic transformation technique was performed in leek cells as described in section 4.2.1.1. GFP fluorescence was observed using a confocal laser scanning microscope (see section 2.14.5).

As an exploratory experiment GFP tagged SF- constructs were delivered to leek tissue using biolistic transformation. In this method DNA of each construct is coated onto gold particles and delivered via microprojectile bombardment. After 48 h leaf tissues were observed under a confocal microscope to visualise GFP fluorescence in cells. GFP- tagged GUS protein (35S::GUS::GFP) was used as a cytosolic control in this experiment along with six different SF constructs. Results of two experiments revealed that all constructs were targeted to the nucleus (although the levels of fluorescence observed differed between the truncations). However, I observed damage to the tissues due to the delivery method and poor reproducibility of results

in biolistic transformation. Therefore, nuclear targeting experiments were continued using transient expression in tobacco plants using infiltration technique.

Transient expression of GFP tagged proteins in tobacco was conducted in three different experiments and all six constructs were observed to be localised to the nucleus. Figure 4.2 shows GFP fluorescence in the nucleus for all five truncations and full length SFR6 compared with GFP tagged GUS protein (35S::GUS::GFP), the cytosolic control for this experiment, which showed mostly cytosolic localisation. Although all fusion proteins were localised to the nucleus, the level of expression of GFP fluorescence in cells was different for each fusion. Therefore mean fluorescence levels (unit as grey values) in the Region of Interests (ROI) within the nucleus and cytoplasm was analysed and fluorescence ratio between nucleus (ROI nucleus) and cytoplasm (ROI cytoplasm) was compared between fusions. Figure 4.3 represents the average ratio of mean fluorescence in the nucleus and cytoplasm (ROI nucleus/ ROI cytoplasm) from three different experiments conducted separately. Advanced fluorescence Lite of Leica application suite was used to calculate fluorescence expressed in nucleus and cytoplasm of the cells.

The average ratio of fluorescence expression in nucleus and cytoplasm varied between different fusions and the highest expression ratio was reported in leaves expressing 35S::SF16, encoding the full length SFR6 protein, which has been shown previously to be nuclear targeted (Figure 4.2)(Knight et al., 2009). The second highest ratio was reported in leaves expressing SF36, which lacks the N terminal one third of the SFR6 protein. The other four constructs showed lower average ratios of fluorescence expression compared to SF16 and SF36 but higher than the 35S::GFP::GUS, the cytosolic control used in this experiment.

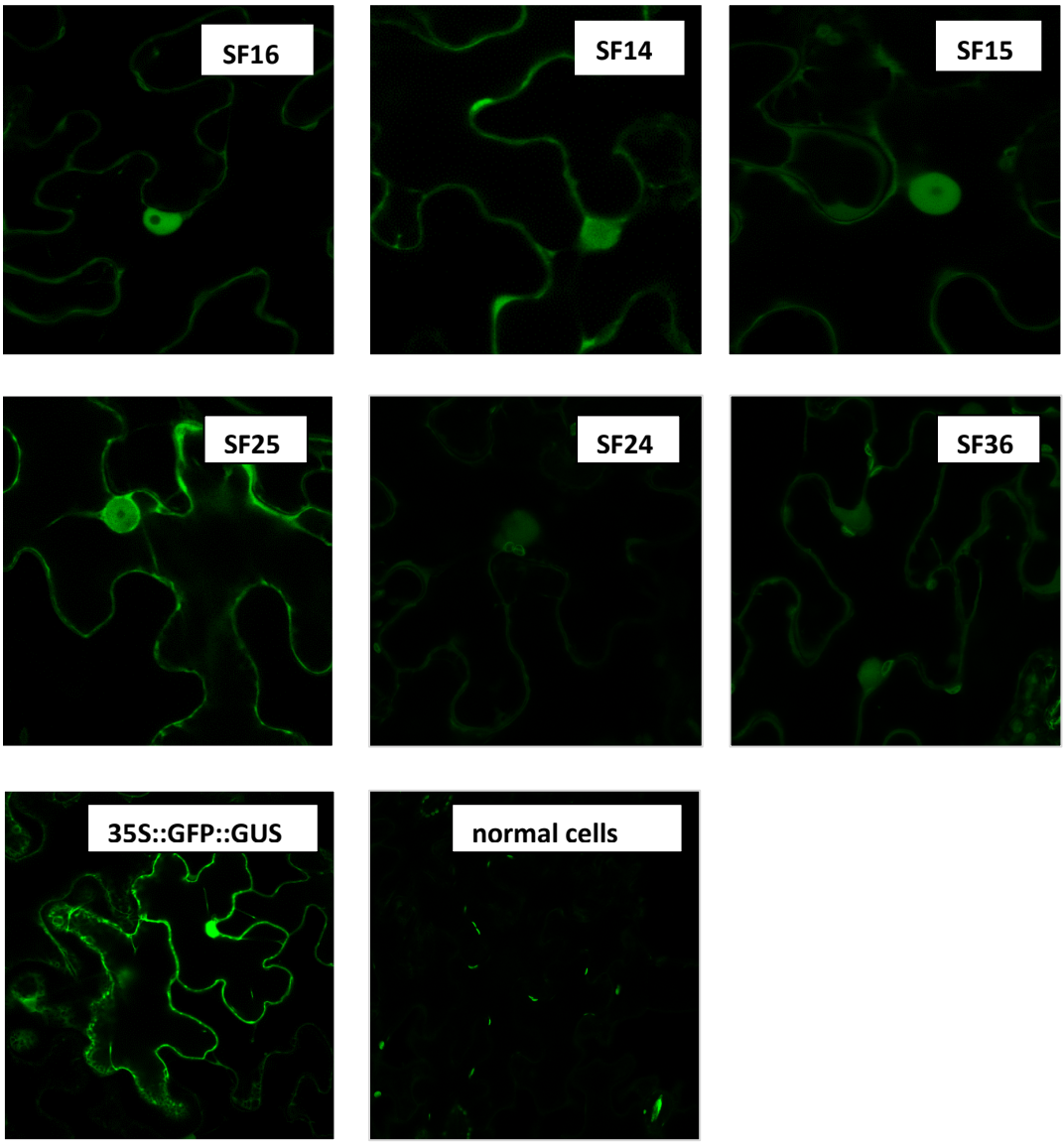

Figure 4.2: Sub-cellular localization of SF- constructs tagged with GFP in untransformed wild type tobacco

Six truncations of SFR6/MED16 with N-terminal tagged GFP under control of 35S promoter were expressed in tobacco plants using the Agrobacterium infiltration technique. After 48 h leaf samples were observed under a confocal microscope and compared with cytosolic control of GUS fused to GFP, under the control of the 35S promoter. Images were taken with identical parameters to allow comparison between different truncations of SFR6/MED16.

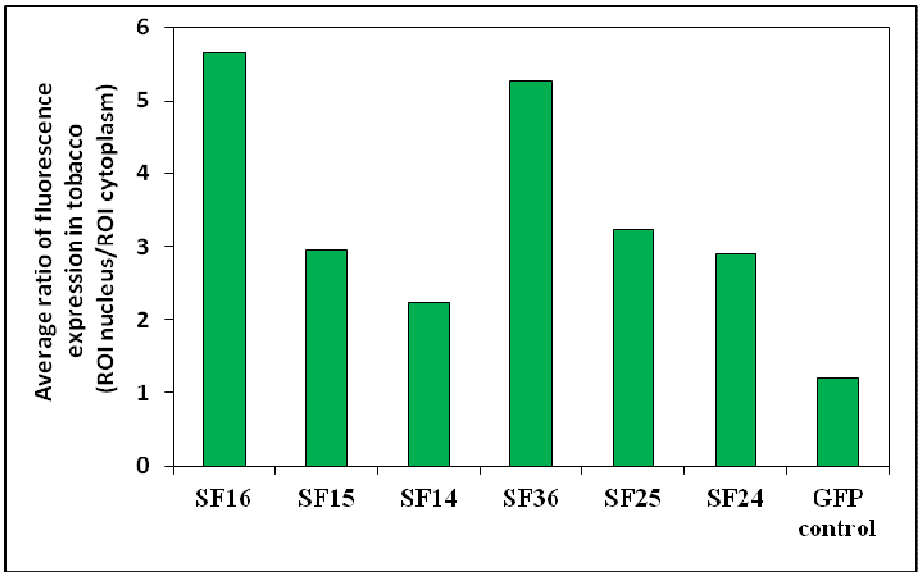

Figure 4.3: Average ratio of fluorescence in nucleus and cytoplasm in tobacco leaf cells

Constitutive overexpression of six truncations/full length of SFR6/MED16 tagged with GFP was acheived in tobacco plants using infiltration and after 48 h leaf samples were observed under confocal microscope. Amount of florescence expressed in nucleus and cytoplasm was calculated using Leica Application Suite and fluorescence ratio between nucleus and cytoplasm was compared with cytosolic control of GUS attached to GFP under control of 35S promoter.

This provides evidence that C-terminus of the SFR6 protein is more important compared to the N-terminus for directing of proteins to the nucleus.

Though the average ratio of fluorescence in nucleus and cytoplasm in nuclear targeting experiments suggests that C-terminus of the SFR6 is important I searched for potential nuclear localisation signals (NLS) within the SFR6 protein using NUCPred program (https://www.sbc.su.se/~maccallr/nucpred/). The amino acid sequence of GFP tagged full length SFR6 protein was used for analysis. The program predicted that the strongest nuclear localisation motif is located towards the end of C-

terminus of the protein at the location of 1172-1184 aa of SFR6/MED16 (Figure 4.4). However, I observed all truncated fragments were targeted the nucleus including truncations such as SF15, SF14, SF25 and SF24 which lack the above positions of the aa in C-terminus of the protein as well as SF16 and SF36 that consists above aa positions. This is contradictory to the predicted nuclear localization signal using NUCPred program that indicated the nuclear localizing signal is in the C-terminus of the protein. The reason might be another factor apart from NLS that helps protein to go to the nucleus, possibly these truncated fragments could pass through the nuclear membranes through the process of diffusion. However Young-Hee Cho et al. (2012) reported that protein approximately 84.5 kD in size localized the nucleus even without nuclear export signal. Further they described the impossibility of diffusion of such a big protein to the nucleus and proposed the ability of certain proteins to leave the cytoplasm and enter the nucleus under certain conditions.

```
   1  MVSKGEELFTGVVPILVELDGDVNGHKFSVSGEGEGDATYGKLTLKFICT   50
  51  TGKLPVPWPTLVTTLTYGVQCFSRYPDHMKQHDFFKSAMPEGYVQERTIF  100
 101  FKDDGNYKTRAEVKFEGDTLVNRIELKGIDFKEDGNILGHKLEYNYNSHN  150
 151  VYIMADKQKNGIKVNFKIRHNIEDGSVQLADHYQQNTPIGDGPVLLPDNH  200
 201  YLSTQSALSKDPNEKRDHMVLLEFVTAAGITLGMDELYKDITSLYKKAGS  250
 251  AAAPFTMNQQNPEEEVSLVNNSGGGGIIEAPAIVEEKEEEGLQQKQEETI  300
 301  ESTDPILVVVEEKLLEKSVDGEKEDDNSSSSNMEIDPVSPATVFCVKLKQ  350
 351  PNSNLLHKMSVPELCRNFSAVAWCGKLNAIACASETCARIPSSKANTPFW  400
 401  IPIHILIPERPTECAVFNVVADSPRDSVQFIEWSPTSCPRALLIANFHGR  450
 451  ITIWTQPTQGSANLVHDATSWQCEHEWRQDIAVVTKWLTGASPYRWLSSK  500
 501  PSSGTNAKSTFEEKFLSQSSESSARWPNFLCVCSVFSSGSVQIHWSQWPS  550
 551  NQGSTAPKWFSTKKGLLGAGPSGIMAADAIITDSGAMHVAGVPIVNPSTI  600
 601  VVWEVTPGPGNGLQATPKISTGSRVPPSLSSSSWTGFAPLAAYLFSWQEY  650
 651  LISEIKQGKKPSDQDSSDAISLSCSPVSNFSAYVSPEAAAQSAATTTWGS  700
 701  GVTAVAFDPTRGGSVIAVVIVEGQYMSPYDPDEGPSITGWRVQRWESSVQ  750
 751  PVVLHQIFGNPTSNFGGQVPTQTVWVSRVDMSIPPTKDFKNHQVAAAGPS  800
 801  VDAPKEPDSGDEKANKVVFDPFDLPSDIRTLARIVYSAHGGEIAIAFLRG  850
 851  GVHIFSGPTFSPVENYQINVGSAIAAPAFSPTSCCSASVWHDAAKDCAML  900
 901  KIIRVLPPALPRNQSKVDQSTWERAIAERFWWSLLVGVDWWDAVGCTQSA  950
 951  AEDGIVSLNSVIAVMDADFHSLPSTQHRQQYGPNLDRIKCRLLEGTNAQE 1000
1001  VRAMVLDMQARLLLDMLGKGIESALVNPSALVFEPWRVDGETITGINPEA 1050
1051  MAVDPALVSSIQAYVDAVLDLASHFITRLRRYASFCRTLASHAASAGTGS 1100
1101  NRNNVTSPTQNASSPATPQVGQPTTTTTTTATTNSSGSSHVQAWMQGAIA 1150
1151  KISSSNDGSNSTASPISGSPTFMPISINTGTFPGTPAVRLIGDCHFLHRL 1200
1201  CQLLLFCFLQRSSRFPQRNADVSSQKLQTGATSKLEEVNSAKPTPALNRI 1250
1251  EDAQGFRGAQLGTGVKGIDENSARTTKMGSGNAGQGYTYEEVRVLFHILM 1300
1301  DLCKRTSGLAHPLPGSQVGSGNIQVRLHYIDGNYTVLPEVVEAALGPHMQ 1350
1351  NMPRPRGADAAGLLLRELELHPPSEEWHRRNLFGGPGSEPEDMILTDDVS 1400
1401  KLSNSLDLPDTNFSGICDGYNRVHSLWPRKRRMSERDAAFGSNTSVGLGA 1450
1451  YLGIMGSRRDVVTATWKTGLEGVWYKCIRCLRQTSAFASPGATKQPNPNE 1500
1501  RETWWTSRWVYCCPMCGGTWVRVV                            1524
```

negative **positive**

(none-nuclear) (nuclear)

Figure 4.4: Nuclear localisation signal analysed using NUCPred program

Positively and negatively influencing subsequences are coloured according to the above colour scale where red colour represents the highest possibility to localise to the nucleus and blue colour shows no targeting of the nucleus. Red/orange coloured underline protein sequence is the predicted nuclear localizing sequence (NLS) for SFR6 protein tagged with GFP. Following positions of the aa represents the six different types of SFR6/MED16 truncations tagged with GFP. 1-239aa:GFP; 240-256aa; linkage between GFP and truncations between SFR6/MED16(transgene); 257-1524 aa:SF16; 257-1257aa: SF15; 257-1135aa: SF14; 604-1135aa: SF24; 604-1257aa: SF25; 910-1524aa: SF36.

Before embarking on experiments to examine nuclear localisation of all the truncated fragments of SFR6, I analysed the expression SF proteins in plants using transient

expression of each -SF protein in tobacco using infiltration (see section 2.11.2) to gain evidence that the sequence was in frame and expressed a protein of the correct size. After that western blotting was performed to identify whether proteins are expressed in plants and I found all of the six GFP-tagged SF proteins were expressed in tobacco plants and produced proteins of the expected size for fusions with GFP (figure 4.5).

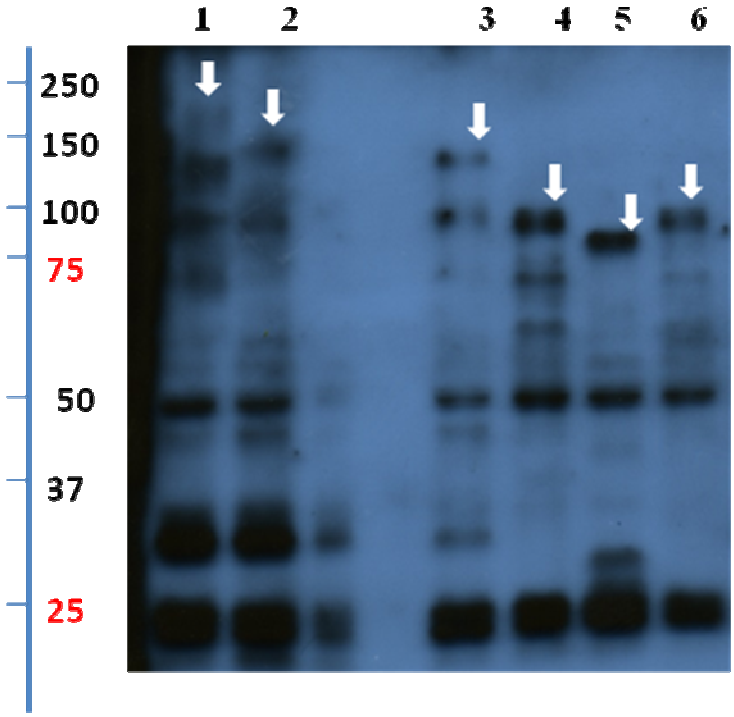

Figure 4.5: Level of protein expression of –SF truncated fragments of SFR6

Total proteins extracted from tobacco leaves infiltrated with *Agrobacterium tumefaciens* expressing SF constructs tagged with GFP were loaded on an SDS gel @ 10mg/ml and transferred to PVDF membranes and incubated with α-GFP primary antibodies at 1:5000 dilution with 10ml of 5% milk (w/v) solution. After incubation of the membrane with α-rabbit goat secondary antibody proteins were visualised using a chemiluminescent detection method. As a loading control an SDS gel with the same samples at the same concentration was stained with Coomassie blue to detect proteins and scanned. White coloured arrows indicate the correct size of bands in each lane. This experiment was conducted three times and same results were reproduced. Lane 1 to 6 represents GFP::SF16 (167kDa), GFP::SF15 (138 kDa), GFP::SF14 (124.5kDa), GFP::SF36 (95.3 kDa), GFP::SF24 (86 kDa) and GFP::SF25 (99.6 kDa) respectively.

4.2.3 Generation of stable lines expressing different truncations of SFR6/MED16 in Arabidopsis

After transformation of each construct in to *pB7WG2*, correct orientation of the fragments in the destination vector was tested using primers designed for the 35S promoter region of the vector with an internal primer designed for each construct, followed by restriction digestion. Thereafter each construct in the *pB7WG2* destination vector was transformed in to *Agrobacterium tumefaciens* strain C58C1. This *Agrobacterium* strain was used to transform both Col-0 and *sfr6* plants using floral dip method (Clough and Bent, 1998) (see section 2.10.1). Successfully transformed plants (T_1) were selected on soil using the Basta herbicide **(**see section 2.10.1.4) as the Basta resistant marker was in the destination vector. Following this selection, Basta resistant T_1 individual plants were transferred to peat plugs and T_1 plants were tested for the presence of the transgene using genomic DNA and the

(a)

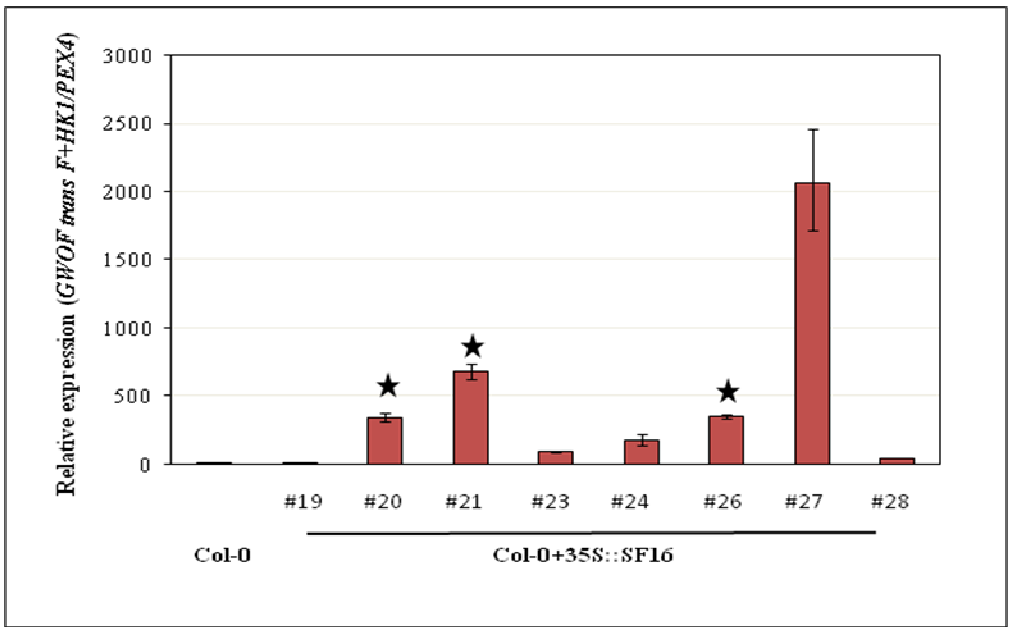

(*Figure continues to the following page*)

(b)

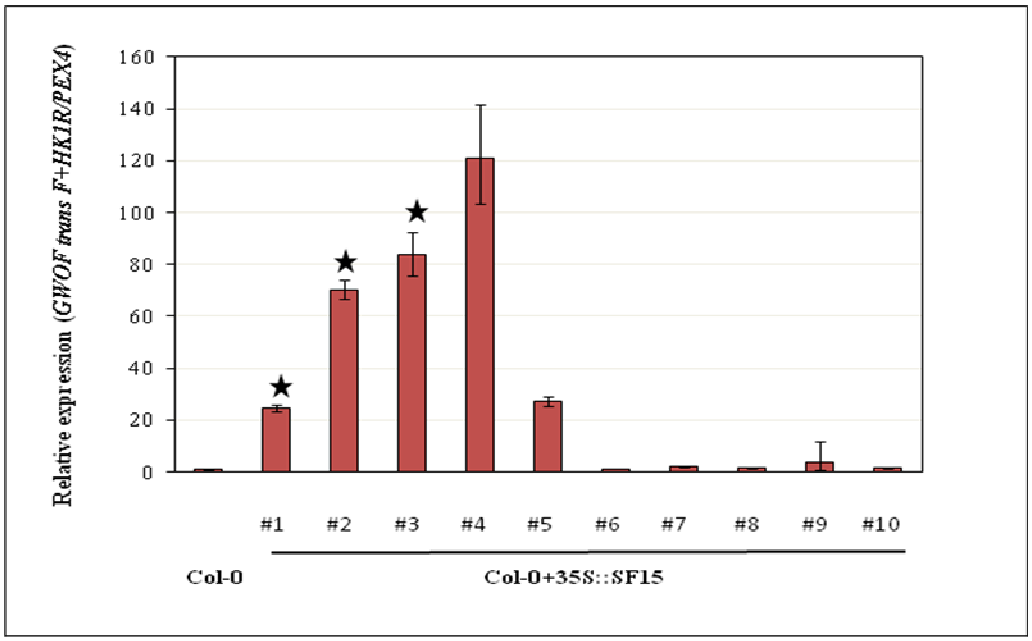

(c)

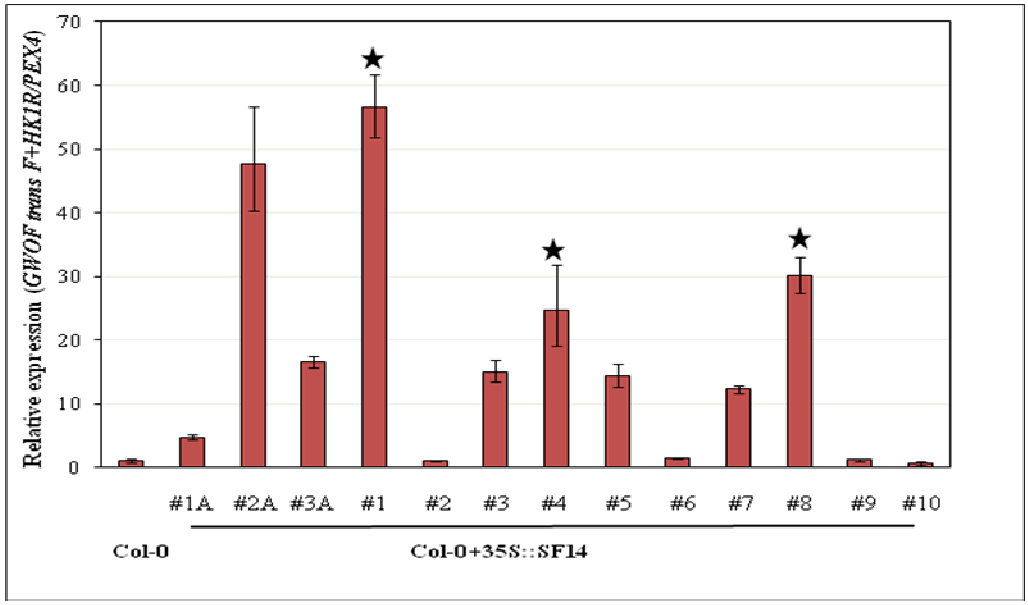

(*Figure continues to the following page*)

(d)

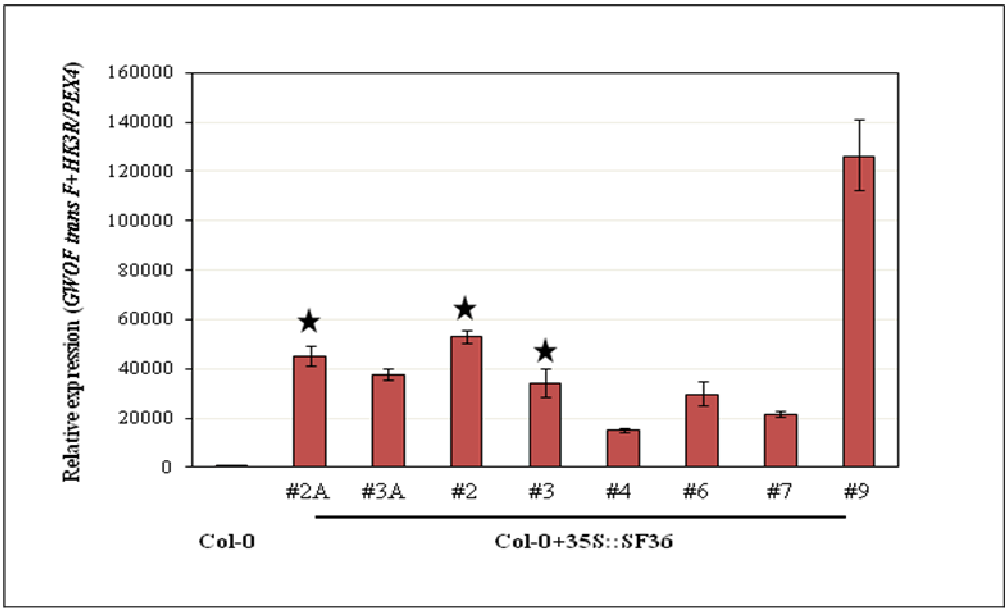

Figure 4.6: Level of expression of SF- constructs in Col-0 background in T_1 generation

Expression levels of -SF16, -SF15, -SF14 and -SF36 in different transformed lines in Col-0 background were compared with Col-0 in histogram a, b, c and d respectively in T_1 plants. Seven-day-old seedlings grown on MS agar plates were used. *GWOF trans* (GateWay Open Frame) Forward primer designed for the 35S promoter region was used with the reverse primer designed for the beginning of each truncation of SFR6/MED16. Expression is shown after normalisation to *PEX4*. Fold values were calculated using the ΔΔCT method, and the error bars in each biological replicates represent RQ_{MIN} and RQ_{MAX} and constitute the acceptable error level for a 95% confidence level according to Student's t test. Error bars indicate the level of variation between technical replicates within one biological replicate experiment. ★ symbol in the graph represents the different lines from each construct selected for crossing with *sfr6-1*.

level of expression of each transgene was analysed by qRT-PCR (Figure 4.2). The transgene was sequenced from the gDNA of tranformants to confirm the presence of correct truncations in plants.

Successfully transformed lines expressing each truncation were obtained in Col-0 background but no successfully transformed lines were obtained in the *sfr6-1* background. The level of transgene expression was measured using primers designed to the vector and the beginning of each truncation (see Appendix A2.1 for primer sequence). However, in the Col-0 background, only 35S::SF16, 35S::SF15, 35S::SF14 and 35S::SF36 transformants were obtained (Figure 4.6) and no plants expressing 35S::SF25 or 35S::SF24 were recovered (Figure 4.7). As no expression of 35S::SF25 and 35S::SF24 was observed in the Col-0 background, no further work continued in Arabidopsis plants with these two truncated fragments.

As direct transformation of *sfr6-1* with the constructs was not successful, selected lines of 35S::SF16, 35S::SF15, 35S::SF14 and 35S::SF36 in Col-0 background were crossed with *sfr6-1* plants to obtain construct in the *sfr6-1* mutant background.

(a)

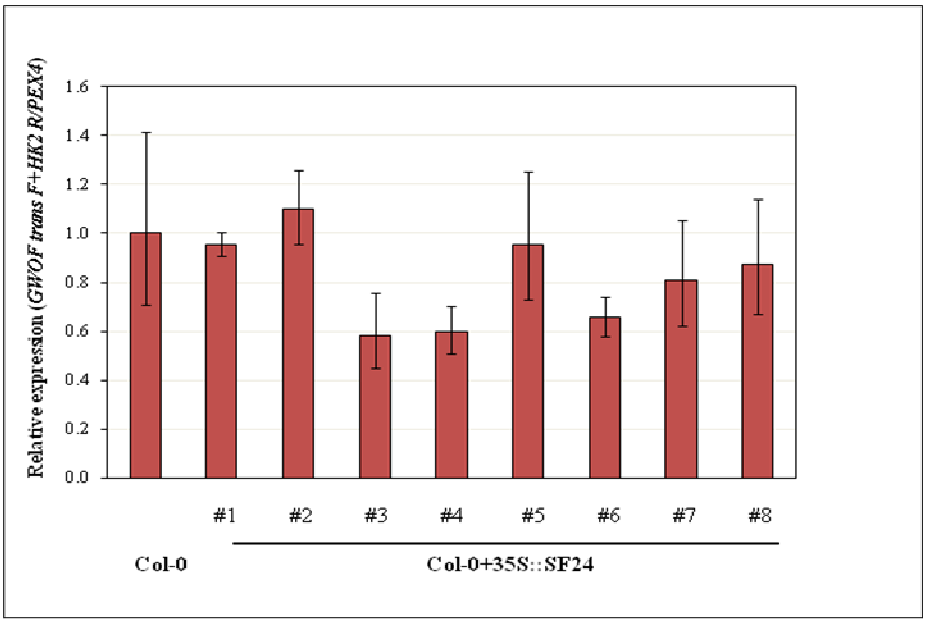

(*Figure continues to the following page*)

(b)

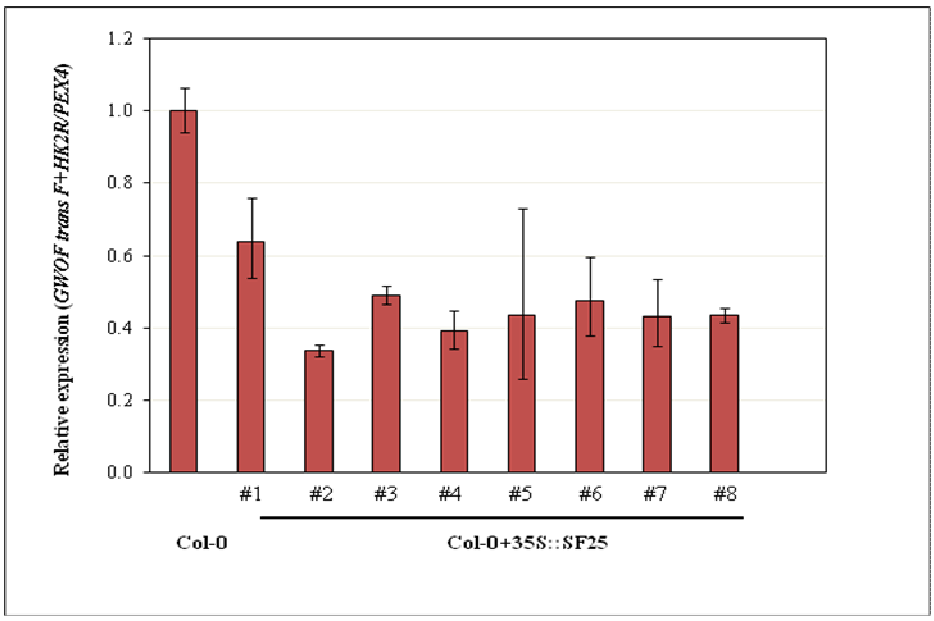

Figure 4.7: Level of expression of SF24 and SF25 constructs in Col-0 background in T_1 generation

Expression levels of -SF24 and -SF25 in different lines in Col-0 background were compared with Col-0 background respectively in histogram a and b in T_1 plants. Seven-day-old seedlings grown on MS agar plates were used. A forward primer designed for the 35S promoter region was used with the reverse primer designed for the beginning of each truncation of SFR6/MED16. Expression is shown after normalisation to *PEX4*. Fold change in expression values were calculated using the ΔΔCT method, and the error bars in each biological replicates represent RQ_{MIN} and RQ_{MAX} and constitute the acceptable error level for a 95% confidence level according to Student's t test. Error bars indicate the level of variation between technical replicates within one biological replicate experiment.

After crossing above expressing lines in wild type background with *sfr6-1* plants, F_1 seeds were collected separately and grown up to obtain F_1 plants and screened for the presence of transgene. Above positive F1 plant lines were continued to obtain F2 seeds. Then F2 plants were tested for the presence of the transgene and the expression levels of each construct (Figure 4.8). Except line #2.2 of *sfr6-*

1+35S::SF15 all other lines were expressing the construct (Figure 4.8 a). Among those expressing lines in F_2 plants further screened to obtain homozygous lines for sfr6-1 mutation using sequencing facility in the department (DBS, Durham University). For that using specially designed primers were amplified a region around the SNP was amplified which could then be sequenced (See Appendix A2.1 for primer sequence). Selected homozygous lines of *sfr6-1* consisted with each construct were used to get F_3 seeds to continue complementation experiments under each stress condition.

(a)

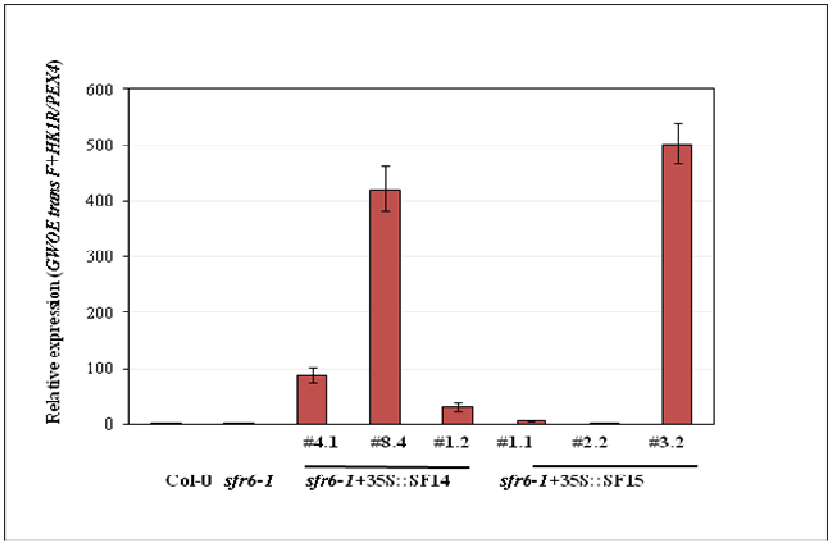

(b)

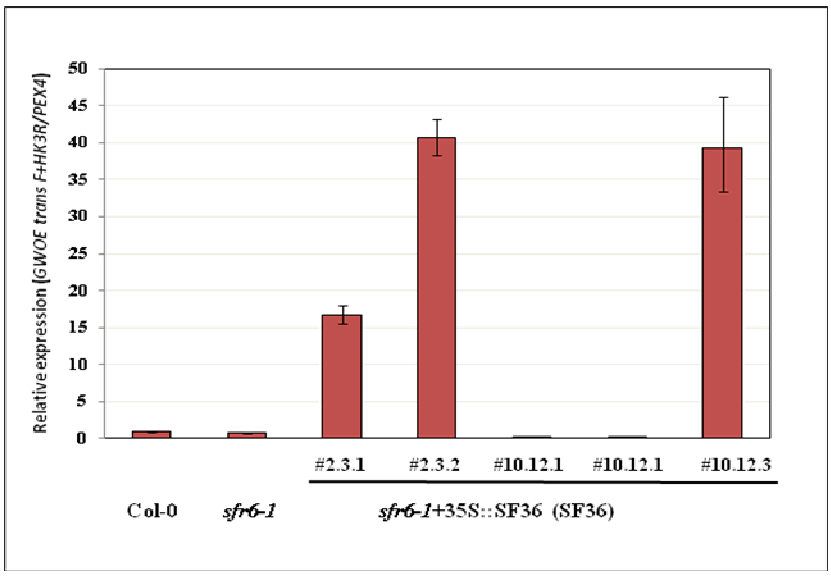

(*Figure continues to the following page*)

(c)

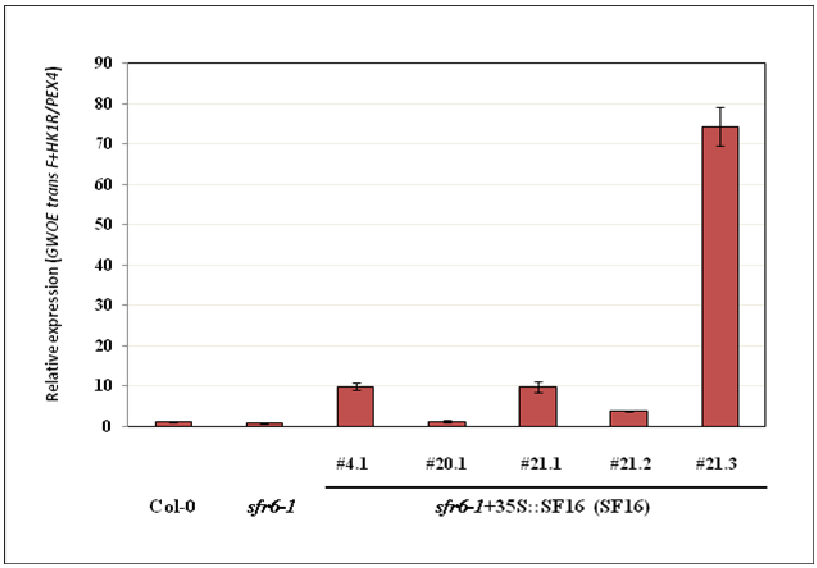

Figure 4.8: Level of expression of SF constructs in *sfr6-1* background in F_2 generation

Expression levels of SF14/SF15,SF16 and SF36 in different lines in *sfr6-1* background were compared with Col-0 and *sfr6-1* mutant respectively in histogram a and b in F_1 plants. Seven-day-old seedlings grown on MS agar plates were used. Forward primer designed for the 35S promoter region was used with the reverse primer designed for the beginning of each domain of SFR6/MED16. Expression is shown after normalisation to *PEX4*. Fold values were calculated using the ΔΔCT method, and the error bars in each biological replicates represent RQ_{MIN} and RQ_{MAX} and constitute the acceptable error level for a 95% confidence level according to Student's t test. Error bars indicate the level of variation between technical replicates within one biological replicate experiment.

Five homozygous lines of *sfr6-1*+35S::SF14 and *sfr6-1*+35S::SF15 were selected using allelic discrimination method (see section 2.10.3) followed by sequencing for complementation experiments while homozygous lines were selected from *sfr6-1*+35S::SF36 and *sfr6-1*+35S::SF16 new transgenic plant lines checking that the chromatograms of the sequenced amplicons showed only the mutant version of the sequence at the site of the sfr6-1 SNP the EMS mutation.

4.2.4 Use of over-expressing SF domains in Col-0 background under cold stress conditions

Beginning of the formation of transgenic plants representing different domains of SFR6/MED16, I made all domains expressing in Col-0 through the floral dipping method (See section 2.10). The expression levels of each domain over-expressing in Col-0 are presented in Figure 4.6 and 4.7. Expression of *KIN2* gene under cold stress condition was tested using the transgenic lines over-expressing SF16, SF15, SF14 and SF36 in Col -0 compared to wild type plants treated 6h at 5^{o}C. Results of this experiment revealed that any enhanced *KIN2* gene expression under cold conditions of each domain overexpressing in wild type background (See Appendix A4.1 for gene expression results).

4.2.5 Complementation experiments using -SF domains in *sfr6* mutant background under different abiotic stress conditions

To study whether different domains/regions of the SFR6 protein are responsible for the activation of genes responding to each stress, I conducted complementation experiments with homozygous lines of *sfr6-1* expressing each truncation (or full length SFR6) under cold, starvation and UV stress conditions. Five homozygous (for sfr6-1 mutation) lines of *sfr6-1*+35S::SF14 and *sfr6-1*+35S::SF15 and four lines of *sfr6-1*+35S::SF36 and six lines of *sfr6-1*+35S::SF16 were tested in the F_3 generation. The above lines were compared with wild type and *sfr6-1* mutant and with three lines of *sfr6-1* mutant complemented with AtSFR6 genomic DNA (*sfr6-1*+35S::gSFR6) (Wathugala et al., 2011) as the best available control to test stress gene complementation experiments.

I here first present the results of complementation of stress gene expression experiments with *sfr6-1*+35S::SF14 and *sfr6-1*+35S::SF15 compared with wild type and *sfr6-1*, three lines of *sfr6-1* mutant complemented with AtSFR6 and *sfr6-1*+35S::GUS (GUS, as control for the presence of SFR6). The same set of stress gene experiments were conducted subsequently with the lines expressing the two other constructs *i.e sfr6-1*+35S::SF36 and *sfr6-1*+35S::SF16 with same controls as described above. This is due to the time difference taken to obtain F_3 homozygous seeds of each transgenic line. The perfect control for all of these experiments would have been *sfr6-1*+35S::SF16, which is the complementation of full length of AtSFR6 (cDNA) (see Figure 4.1) which was created in a similar way to three other constructs tested in stable plant expression.

Prior to the start of stress gene expression experiments, the level of *SFR6* transcript expression was tested in all lines compared to wild type, *sfr6-1* mutant and other controls mentioned above. Seven-day-old seedlings of F_3 transgenic plants including all truncated versions of SFR6/MED16 were used to test the level of expression of SFR6 with primers designed to recognise the 10^{th} and 11^{th} exon in the cDNA of SFR6 (SFR6 mid forward and reverse primers, see Appendix A2.1 for primer sequence) designed for the part of the *SFR6* gene that was present in all truncations Levels of *SFR6* expression in all five lines of *sfr6-1*+35S::SF14 and *sfr6-1*+35S::SF15 were higher (ten fold higher except in one line) than in wild type and similar results were obtained for all three lines of *sfr6-1* mutant complemented with AtSFR6 (*sfr6-1*+35S::gSFR6) (Figure 4.9).

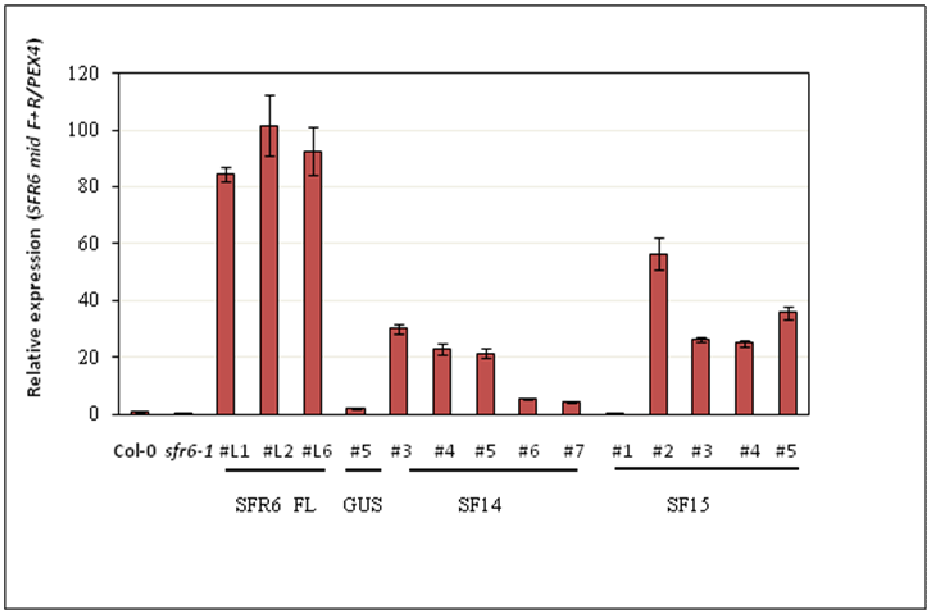

Figure 4.9: Level of expression of *SFR6* in selected lines of SF14 and SF15 in *sfr6-1* background in F_3 generation

Expression levels of *SFR6* in different lines of 35S::SF14 (SF14) and 35S::SF15 (SF15) in *sfr6-1* background were compared with Col-0, *sfr6-1*, three lines of *sfr6-1* mutant complemented with AtSFR6 (SFR6 FL) and *sfr6-1*+35S::GUS (GUS, as control for the presence of SFR6). Seven-day-old seedlings grown on MS agar plates were used. Primers were designed for the 10th and 11th exon in the cDNA of SFR6/MED16 and expression is shown after normalisation to *PEX4*. Fold values were calculated using the ΔΔCT method, and the error bars in each biological replicates represent RQ_{MIN} and RQ_{MAX} and constitute the acceptable error level for a 95% confidence level according to Student's t test. Error bars indicate the level of variation between technical replicates within one biological replicate experiment.

The level of *SFR6* expression in *sfr6-1* appeared similar to the level in Col-0 (Figure 4.9); the primers used in this analysis was designed for the middle part of SFR6 gene downstream of the point mutation in the *sfr6-1* mutant (see Appendix A2.2 for the point mutation and Appendix A.2.1 for primer sequence) .The lack of difference in *SFR6* expression levels between wild type and *sfr6-1* was not unexpected as the transcript was likely to be produced normally despite the single base change that

resulted in the premature stop codon. This primer combination enabled testing of the transcript levels of all truncated versions of SFR6 in the *sfr6-1* mutant background with one set of primers due to the common position of primers in all truncations for accurate comparison. Line #6 and #7 of *sfr6-1*+35S::SF14 showed lowest expression of *SFR6* and the other three lines were moderate expressers of *SFR6* compared to three different lines of controls of *sfr6-1*+35S::SFR6. Line #1 of *sfr6-1*+35S::SF15 is the lowest expresser and #2 is the highest expresser of *SFR6* of *sfr6-1*+35S::SF15 while #3, #4 and #5 are moderate expressers of *SFR6*. The other control, *sfr6-1*+35S::GUS was used to show no effect of vector on gene expression and had showed similar levels of *SFR6* expression compared to wild type and *sfr6-1* (Figure 4.9). Plant lines exhibiting different levels of *SFR6* gene expression were tested for stress gene complementation.

In *sfr6-1*+35S::SF16 (SF16) and *sfr6-1*+35S::SF36 (SF36), the presence of the transgene specifically (i.e. excluding the contribution of the native *SFR6* transcript) and expression levels of each construct were tested in the F_3 generation (Figure 4.10). Levels of transgene expression in six lines of *sfr6-1*+35S::SF16 are presented in figure 4.10 (a) and all lines expressed relatively low levels of transgene compared to the levels observed in other constructs except B2. Out of four lines of *sfr6-1*+35S::SF36 two lines did not express the transgene (B2 and B24) at all and line #B7 and #B25 were used for the rest of the gene expression experiments.

(a) **(b)**

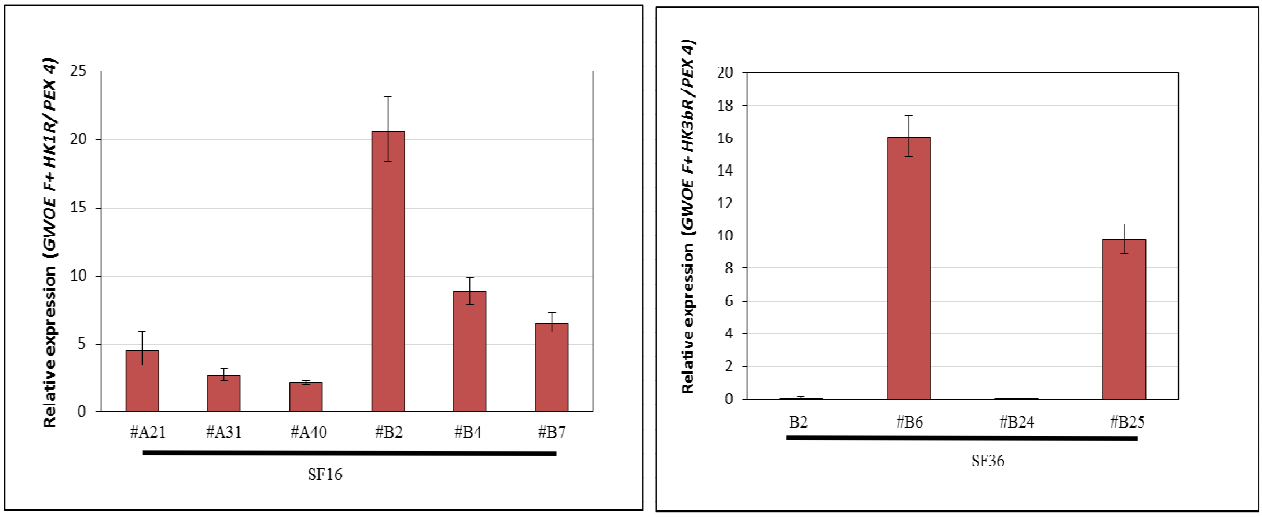

Figure 4.10: Level of expression of SF16 and SF36 constructs in *sfr6-1* background in F_3 generation

Expression levels of SF16 and SF36 in different lines of 35S::SF16 (SF16) and 35S::SF3 (SF36) in *sfr6-1* background in F_3 are presented in histogram a and b respectively. Seven-day-old seedlings grown on MS agar plates were used. A forward primer designed for the 35S promoter region was used with a reverse primer designed for the beginning of each truncation of SFR6/MED16. Expression is shown after normalisation to *PEX4*. Fold values were calculated using the ΔΔCT method, and the error bars in each biological replicates represent RQ_{MIN} and RQ_{MAX} and constitute the acceptable error level for a 95% confidence level according to Student's t test. Error bars indicate the level of variation between technical replicates within one biological replicate experiment.

After testing the level of transgene expression in *sfr6-1*+35S::SF16 (SF16) and *sfr6-1*+35S::SF36 (SF36), the level of *SFR6* expression (native and transgene transcript) in the same lines was compared to that of Col-0 and *sfr6-1* (Figure 4.11). Expression levels of *SFR6* in all transgenic lines were low compared with the apparent levels of transcript indicated using the GW primer (see Appendix A2.1) (figure 4.10). This is hard to understand the inconsistence of expressions. It is difficult to conclude that these lines are expressing at all. However they may be expressing to a low level that

is similar to what is seen in the wild type and level of *SFR6* expression in #A21, #A31 and #B25 is low compared to other three lines.

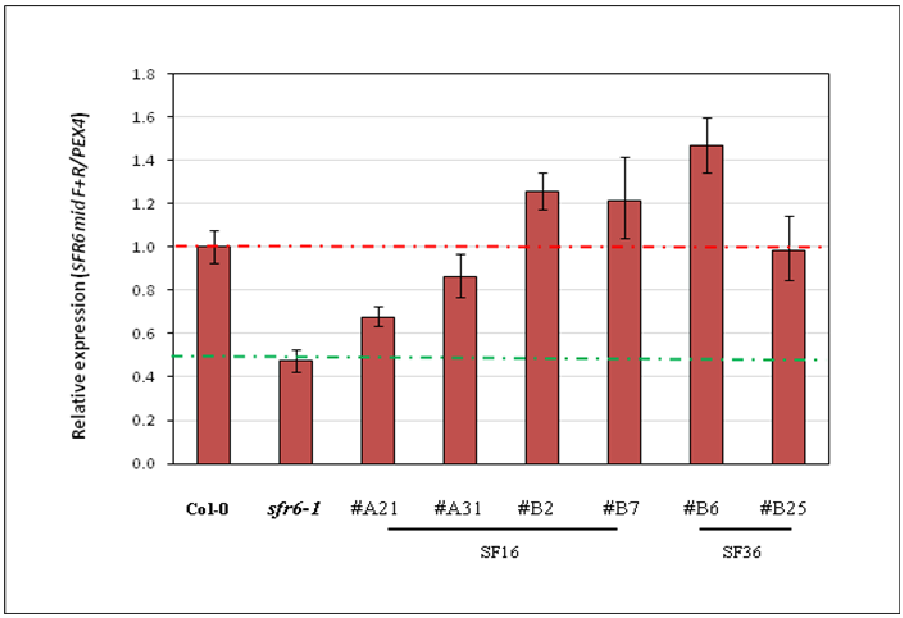

Figure 4.11 Level of expression of *SFR6* in selected lines of SF16 and SF36 in *sfr6-1* background in F_3 generation

Expression levels of *SFR6* in different lines of 35S::SF16 (SF16) and 35S::SF36 (SF36) in *sfr6-1* background were compared with Col-0 and *sfr6-1*. Seven-day-old seedlings grown on MS agar plates were used. Primers were designed for the 10th and 11th exon in the cDNA of SFR6/MED16 and expression is shown after normalisation to *PEX4*. Fold values were calculated using the ΔΔCT method, and the error bars in each biological replicates represent RQ_{MIN} and RQ_{MAX} and constitute the acceptable error level for a 95% confidence level according to Student's t test. Error bars indicate the level of variation between technical replicates within one biological replicate experiment. Red and green dashed lines represent the level of *SFR6* expression in Col-0 and *sfr6-1* respectively.

F_3 seeds were used to continue complementation experiments under each stress condition. Five homozygous lines of *sfr6-1*+35S::SF14 and *sfr6-1*+35S::SF15 were selected for complementation experiments while two and four lines were selected

from *sfr6-1*+35S::SF36 and *sfr6-1*+35S::SF16 respectively from above described plant lines (See Appendix A2.4 for the chromatograms of each homozygous lines of *sfr6-1).* All plant lines were sequenced for identification of the region containing the EMS point mutation to make sure that no copy of the wild type alleles was present in the genomic DNA. Further I did not use the genotyping assay because of the complications that could be introduced with an unknown number of copies of the transgene that would be recognised as wild type.

4.2.5.1 Complementation of visible phenotype of SF transgenic lines

The *sfr6-1* shows pale green colour compared to Col-0 during early stages of seedlings with bigger cotyledons (Knight et al., 2009). Therefore all lines homozygous for the *sfr6-1* mutation and that overexpressed SF16, SF15, SF14 and SF36 truncations were tested for their ability to complement the visible pale leaf and cotyledon phenotype. Fourteen day-old seedlings grown on MS medium from each line of –SF truncated versions were studied to determine the level of green colour restored in each line. Percentage of green colour restoration was calculated by scoring individual seedlings as yellow or green. In *sfr6-1*+35S::SF14 (SF14) four lines out of five remained pale yellow colour and line SF14#7 showed restoration of green colour in approximately 60% of the studied seedling population. In *sfr6-1*+35S::SF15 (SF15), line #1 showed 90% of green colour restoration while other four lines remained approximately 60% of green colour restoration in the studied seedling population. Out of two lines of *sfr6-1*+35S::SF36 (SF36) line #B6 showed approximately 90% of green colour restoration while #B25 showed approximately 45% of green colour restoration in the studied seedling population. In *sfr6-1*+35S::SF16 (SF16) line #B7 showed nearly 90% of green colour restoration and #A21 showed approximately 80% of green colour restoration. The other two lines of

SF16 remained similar colour as in *sfr6-1*. Four different lines of *sfr6-1*+35S::SF16 (SF16) were supposed to be the perfect control of this experiment and expected to be fully complemented, yet this is the first indication that in atleast some of the lines was not successful. Wathugala et al. (2011) reported the fully restoration of green colour in complemented lines of genomic SFR6 (full length) and the difference compared to present study is the completed lines created using cDNA of SFR6.

(a)

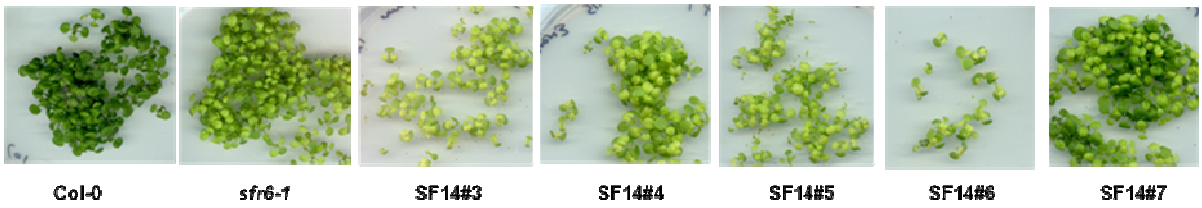

(b)

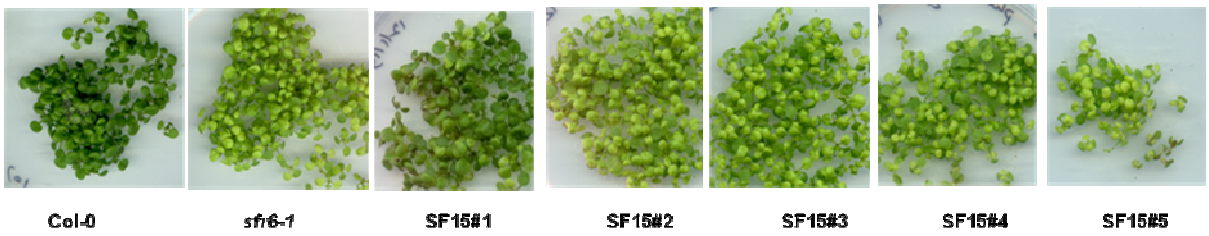

(c)

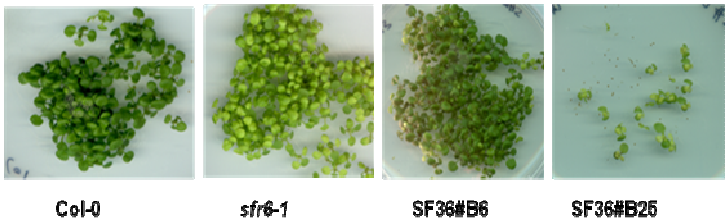

(d)

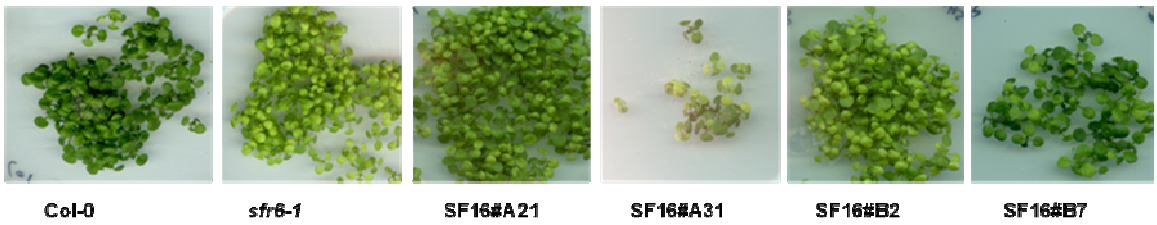

Figure 4.12 Level of green colour restoration in different lines of -SF truncations in *sfr6-1* background in F_3 generation

Fourteen-day-old seedlings grown on MS medium from lines homozygous for *sfr6-1* mutation and over-expressing SF16, SF15, SF14 and SF36 truncations were tested for their ability to restore the visible green leaf and cotyledon phenotype. The number of seedlings in green colour similar to the Col-0 was counted and approximate percentage of green colour restoration was calculated by scoring individual seedlings as yellow or green.

4.2.5.2 Complementation of flowering time phenotype of SF transgenic lines

The *sfr6-1* mutant shows late flowering (Knight et al., 2008) compared to Col-0 and I studied time taken to flower in different lines complemented with truncations of SFR6. Five-week-old plants representing different lines of SF constructs were grown on soil and compared with Col-0 and *sfr6-1* plants (Figure 4.13). In *sfr6-1*+35S::SF14 (SF14) line #7 showed complementation of flowering time phenotype but the other four lines showed late flowering (Figure 4.13 a). Line #1 in *sfr6-1*+35S::SF15 (SF15) showed a similar flowering time phenotype as in Col-0 while #2, #3 and #4 showed early flowering compared to *sfr6-1* but not a complete complementation of flowering time phenotype. Line #4 in *sfr6-1*+35S::SF15 (SF15) showed a similar flowering time phenotype as in *sfr6-1* (Figure 4.13 b). Line #A21 in *sfr6-1*+35S::SF16 (SF16) showed complementation of flowering time phenotype while #B2 showed flowering time phenotype similar to *sfr6-1*. Line #A31 and B#7 showed early flowering compared to *sfr6-1* but not up to the level as fully complementation (Figure 4.13 c). Out of two lines in *sfr6-1*+35S::SF36 (SF36) line #B6 showed complementation of flowering time phenotype while #B25 showed similar flowering time phenotype as in *sfr6-1*(Figure 4.13 d). Same representative plants from Col-0 and *sfr6-1* were used to compare the flowering time phenotype of different lines of SF transgenic plants as described in figure 4.13.

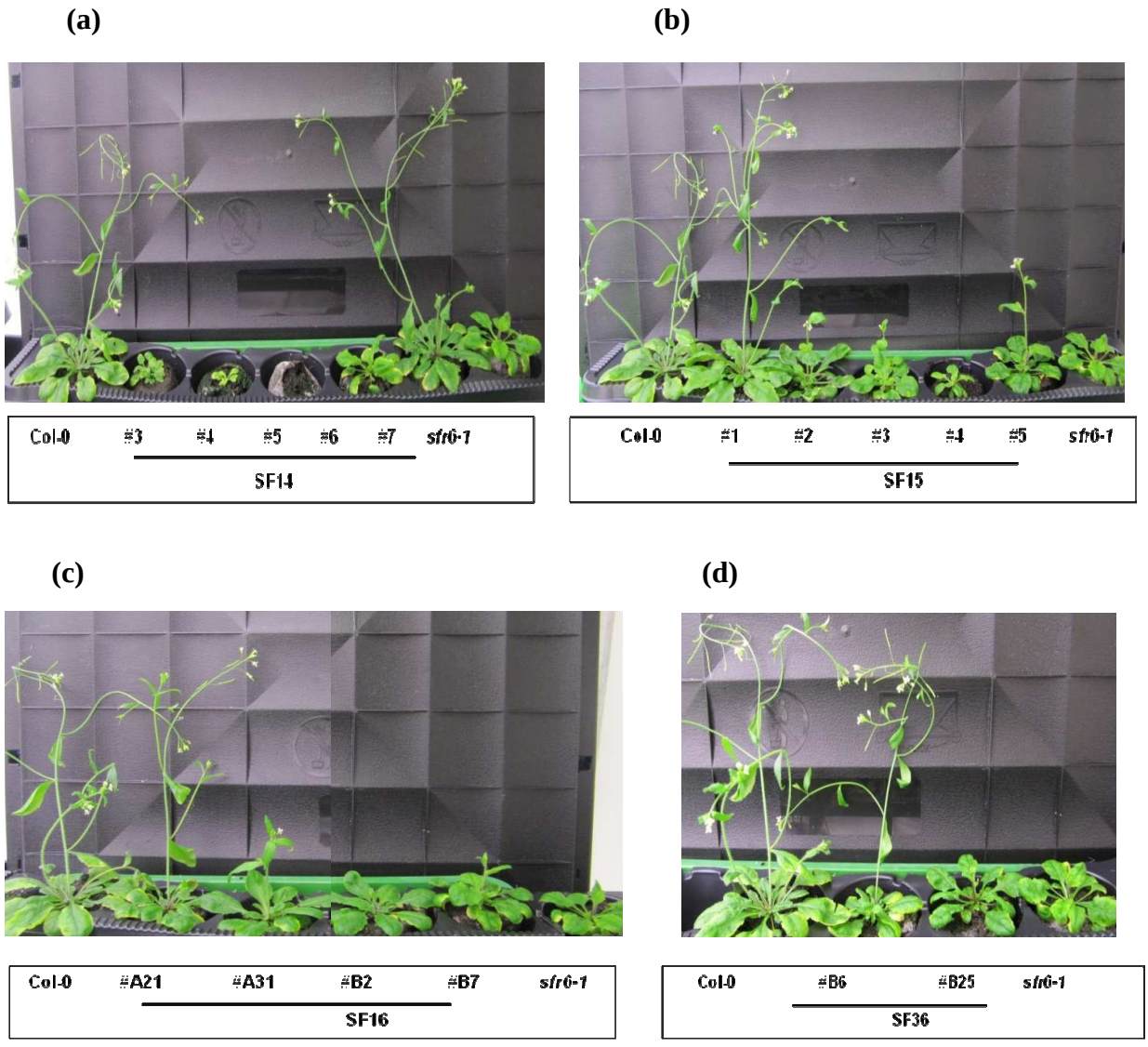

Figure 4.13 Restoration of flowering time phenotype in different lines of SF truncations in *sfr6-1* background in F_3 generation

Five-weeks-old seedlings grown on soil were used to study the ability of lines homozygous for the *sfr6-1* mutation and overexpressing SF16, SF15, SF14 and SF36 truncations to restore the flowering time phenotype of Col-0. Same Col-0 and *sfr6-1* plants were used to compare different lines of SF transgenic plants.

4.2.5.3 Analysis of the ability of SF truncations to complement the cold gene expression phenotype

Experiments were carried out using seven-day-old seedlings grown on MS media on petri dishes and treated at 5°C for 6 h in SANYO growth chamber. Control plates were kept at 20°C (ambient temperature) (see 2.15.1.1). Expression of the cold-inducible gene *KIN2* was analysed using qRT-PCR. Cold-inducible *KIN2* expression in *sfr6*-1+35S::SF14 (SF14) and *sfr6*-1+35S::SF15 (SF15) was compared with Col-0, *sfr6-1*, *sfr6*- 1+35S::SFR6 (SFR6 FL) and *sfr6*-1+35S::GUS (GUS) in three independent biological replicate experiments (Figure 4.14 a, b and c). An increased level of *KIN2* gene expression in full length SFR6 complemented lines (*sfr6*- 1+35S::SFR6/SFR6 FL) was observed compared to Col-0 and a consistent level of gene expression in three biological replicate experiments was seen.

(a)

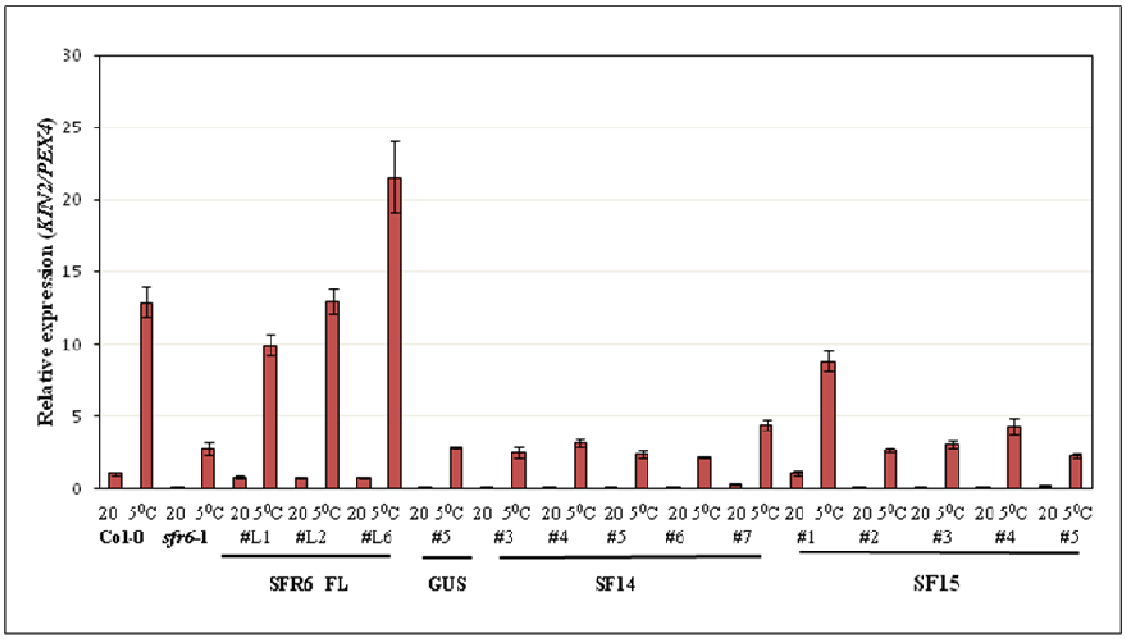

(*Figure continues to the following page*)

(b)

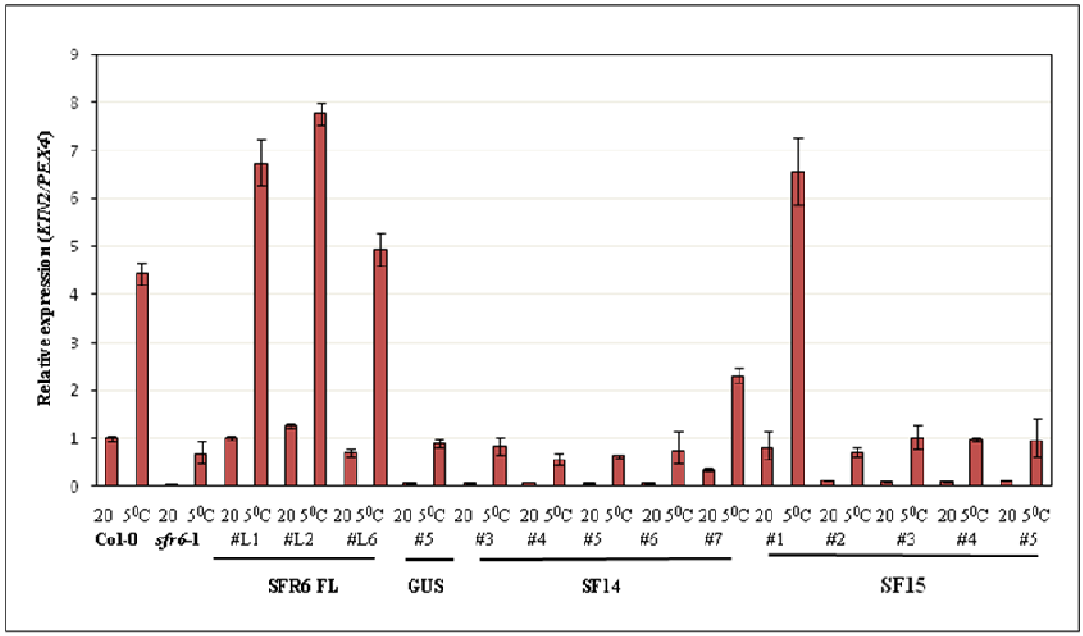

(c)

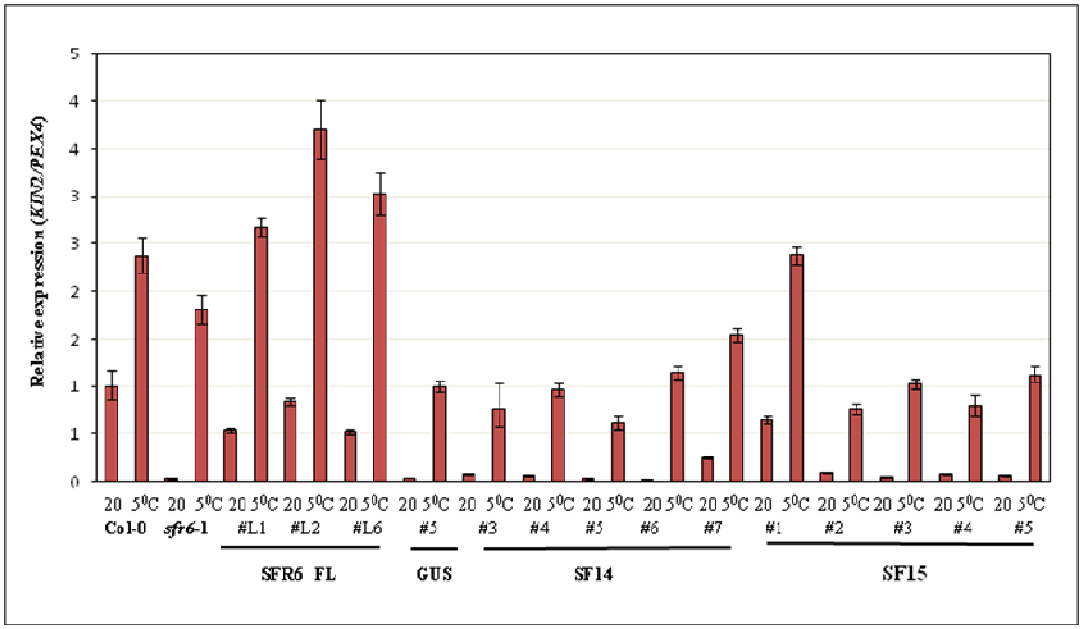

(*Figure continues to the following page*)

(d)

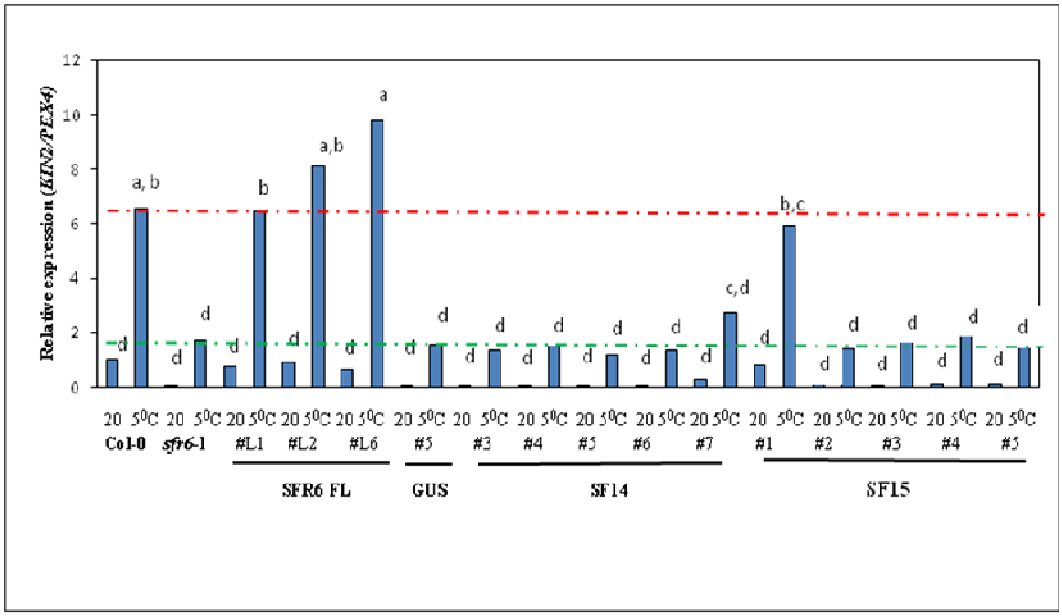

Figure 4.14: Complementation of cold-induced *KIN2* expression in SF14 and SF15 transgenic lines

KIN2 expression in seven-day-old seedlings in response to cold treatment was measured in *sfr6*-1+35S::SF14 (SF14) and *sfr6*-1+35S::SF15 (SF15) transgenic lines compared with Col-0, *sfr6*-1, three different lines of *sfr6*- 1+35S::SFR6 (SFR6 FL) and *sfr6*-1+35S::GUS (GUS). The first three histograms (a, b and c- with red bars) represent the gene expression data of three independent biological replicates. Expression is shown after normalisation to *PEX4* in all graphs. Relative expression in the graphs represents the fold value compared with Col-0 control sample and calculated using the ΔΔCT method and the error bars in each biological replicate represent RQ_{MIN} and RQ_{MAX} and constitute the acceptable error level for a 95% confidence level according to Student's t test The fourth chart (blue bars; d) represents the average of the above three independent biological replicates. Mean average data (in graph d) were analysed using a one-way ANOVA (α=0.05) and pair wise comparisons were made using the Tukey method. Means that do not share a letter are significantly different. *KIN2* expression in Col-0 and *sfr6-1* represents in red and green dotted lines respectively.

Similar patterns of *KIN2* gene expression in -SF14 and -SF15 transgenic lines were observed in three replicate experiments and many lines showed a comparable level of

KIN2 gene expression as seen in *sfr6-1* mutant except in SF14#7 and SF15#1, indicating that complementation may have been partially successful in these two lines but was not in the others. This change in *KIN2* expression is clear in Figure 4.14 d, which shows the average gene expression data from three biological replicate experiments. The level of average *KIN2* expression in SF15#1 was not significantly different compared to Col-0 and three lines of SFR6 FL ($p<0.001$) while SF14#7 showed significantly different levels of *KIN2* expression (Figure 4.14d). Interestingly SF14#7 and SF15#1 showed the lowest levels of *SFR6* expression, as shown in figure 4.9.

Cold gene expression experiments with *sfr6*-1+35S::SF36 (SF36) and *sfr6*-1+35S::SF16 (SF16) were conducted as described above and expression of the cold-inducible gene *KIN2* was compared with that of Col-0, *sfr6-1*, *sfr6*- 1+35S::SFR6 (SFR6 FL) and *sfr6*-1+35S::GUS (GUS) in three independent biological replicate experiments (Figure 4.15 a, b and c).

(a)

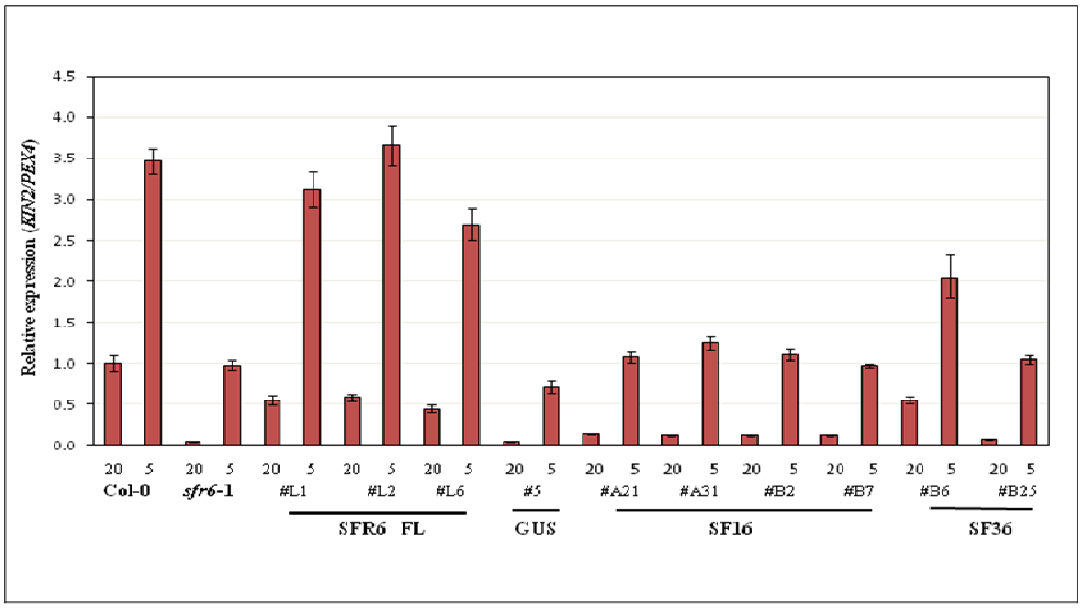

(*Figure continues to the following page*)

(b)

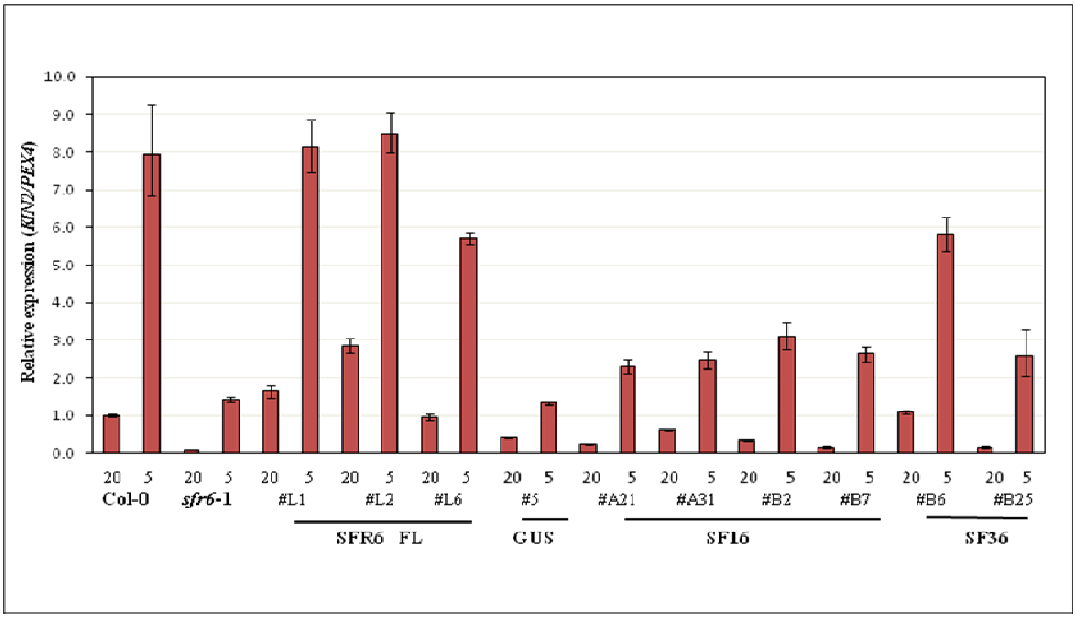

(c)

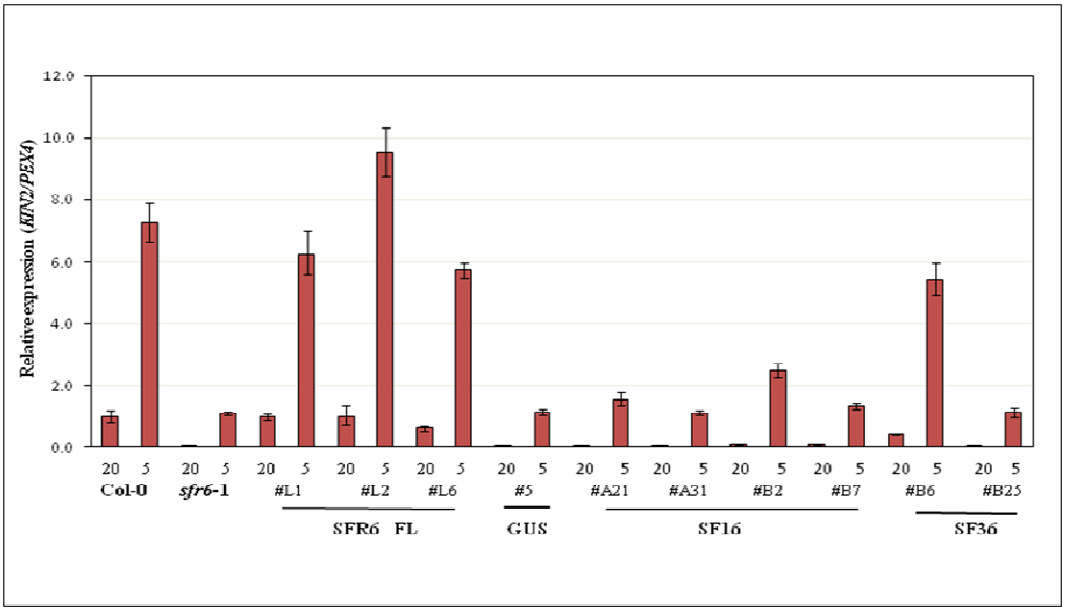

(*Figure continues to the following page*)

(d)

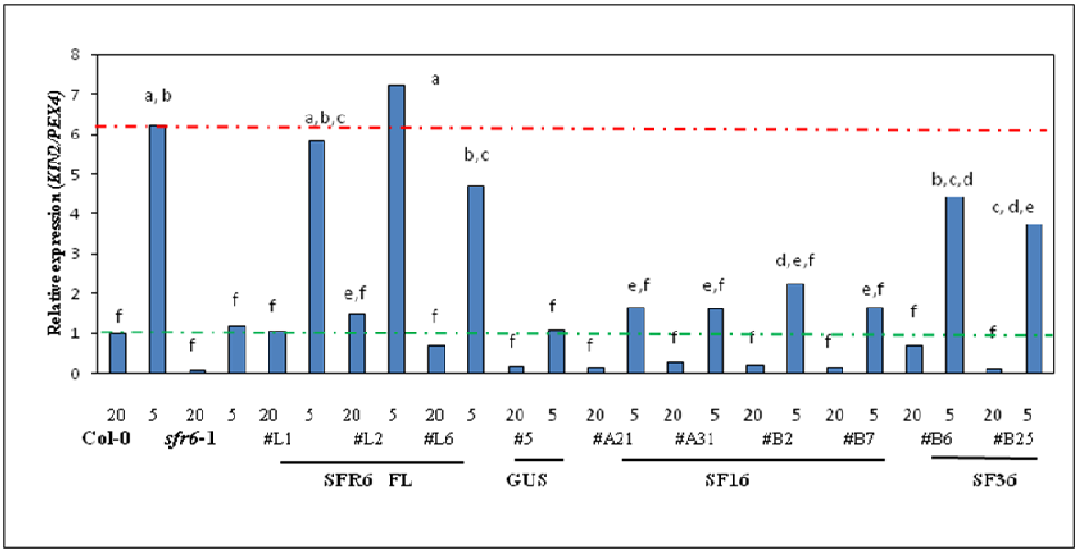

Figure 4.15: Complementation of cold-induced *KIN2* expression in SF36 and SF16 transgenic lines

KIN2 expression in seven-day-old seedlings in response to cold treatment was measured in *sfr6*-1+35S::SF36 (SF36) and *sfr6*-1+35S::SF16 (SF16) transgenic lines compared with Col-0, *sfr6*-1, three different lines of *sfr6*- 1+35S::SFR6 (SFR6 FL) and *sfr6*-1+35S::GUS (GUS). The first three histograms (a, b and c- with red bars) represent the gene expression data of three independent biological replicates. Expression is shown after normalisation to *PEX4* in all graphs. Relative expression in the graphs represents the fold value compared with Col-0 control sample and calculated using the ΔΔCT method and the error bars in each biological replicate represent RQ_{MIN} and RQ_{MAX} and constitute the acceptable error level for a 95% confidence level according to Student's t test. The fourth chart (blue bars; d) represents the average of the above three independent biological replicates. Mean average data (in graph d) were analysed using a one-way ANOVA (α=0.05) and pair wise comparisons were made using the Tukey method. Means that do not share a letter are significantly different. *KIN2* expression in Col-0 and *sfr6-1* represents in red and green dotted lines respectively. In X-axis number 20 and 5 represents the ambient and cold temperatures respectively.

Greater levels of *KIN2* gene expression in full length of SFR6 complemented lines in *sfr6-1* (*sfr6*- 1+35S::SFR6/SFR6 FL) were observed compared to Col-0 and levels of

gene expression were consistent between three biological replicate experiments. These three complemented lines were created using genomic DNA. Full length of SFR6 complemented lines created in this project (SF16) was from cDNA. In contrast, *KIN2* gene expression in these lines was not complemented but the level of expression was slightly higher than *KIN2* expression in *sfr6-1*. A similar trend was observed in all three biological replicate experiments of all four lines of SF16 truncated fragments (Figure 4.11 a, b and c). This is very difficult to explain why the complementation failed. I could be explained reason is simply that the lines were not expressing SFR6 or not to a high enough level or the feature of transgene as it was created from cDNA as two possible causes.

Line #B6 out of two complemented lines of SF36 (*sfr6*-1+35S::SF36) showed a higher level of *KIN2* expression compared to #B25 line. However, an average of three biological replicates (Figure 4.15d) showed that *KIN2* expression in #B6 and #B25 was not significantly different ($p<0.001$) to the expression levels in #L1 and #L6, which are the completed lines of full length of genomic SFR6 lines in *sfr6-1* (*sfr6*-1+35S::SFR6/SFR6 FL). Further the level of *SFR6* and SF36 expression was higher in SF36#B6 compared to SF36#B25 (Figure 4.10 and 4.11 respectively.

4.2.5.4 Analysis of the ability of SF truncations to complement the dark gene expression phenotype

Experiments were carried out using seven-day-old seedlings grown on 0.5x MS media on petri dishes and subjected to 6 h dark conditions by wrapping individual plates in two layers of aluminium foil, during the light cycle in the Percival growth chamber. Control plates remained unwrapped in the chamber under normal light conditions (see 2.15.1.3). Expression of the dark-inducible gene *DIN6* was analysed using qRT-PCR.

Dark-inducible *DIN6* expression in 1+35S::SF14 (SF14) and *sfr6*-1+35S::SF15 (SF15) was compared with Col-0, *sfr6-1*, *sfr6*- 1+35S::SFR6 (SFR6 FL) and *sfr6*-1+35S::GUS (GUS) in three independent biological replicate experiments (Figure 4.16 a, b and c). An enhanced level of *DIN6* gene expression was demonstrated in full length of SFR6 complemented lines in *sfr6-1* (*sfr6*- 1+35S::SFR6/SFR6 FL), and these levels were similar to the levels of expression in Col-0.

DIN6 expression in all transgenic lines of SF14 reported consistent transcriptional pattern in three replicates and #3 and #7 showed a higher level of *DIN6* expression in each experiment. However, average gene expression data from three biological replicate experiments (Figure 4.16 d) revealed that increased levels of *DIN6* expression in #3 and #7 of SF14 were significantly different to the level of *DIN6* expressed in either Col-0 or three lines of SFR6 FL ($p<0.001$). The other three lines of SF14 showed similar level of *DIN6* expression as seen in *sfr6-1* mutant. Conversely SF14#3, the highest expresser of *DIN6*, is the highest expresser of *SFR6* while second highest *DIN6* expresser (SF14#7) was the lowest expresser of SFR6 (Figure 4.9).

(a)

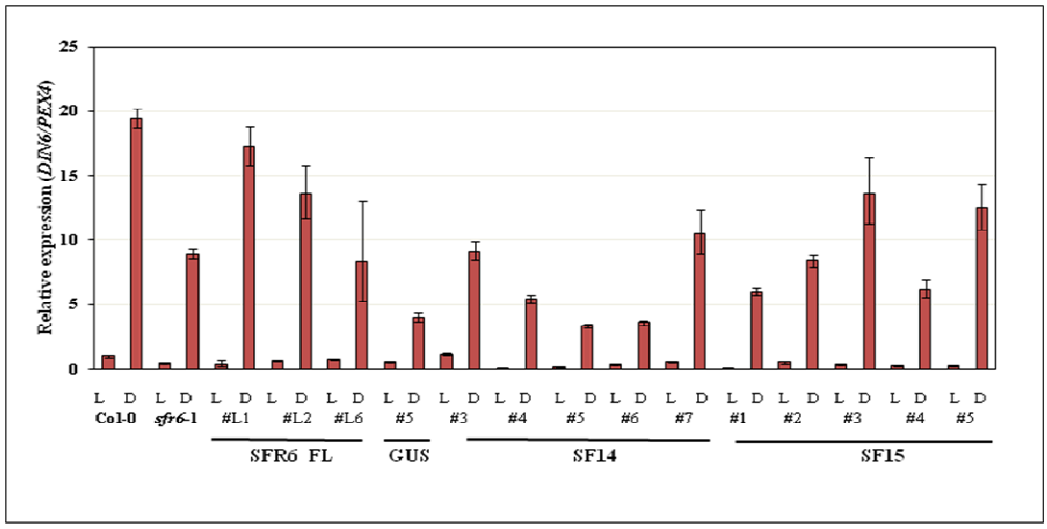

(*Figure continues to the following page*)

(b)

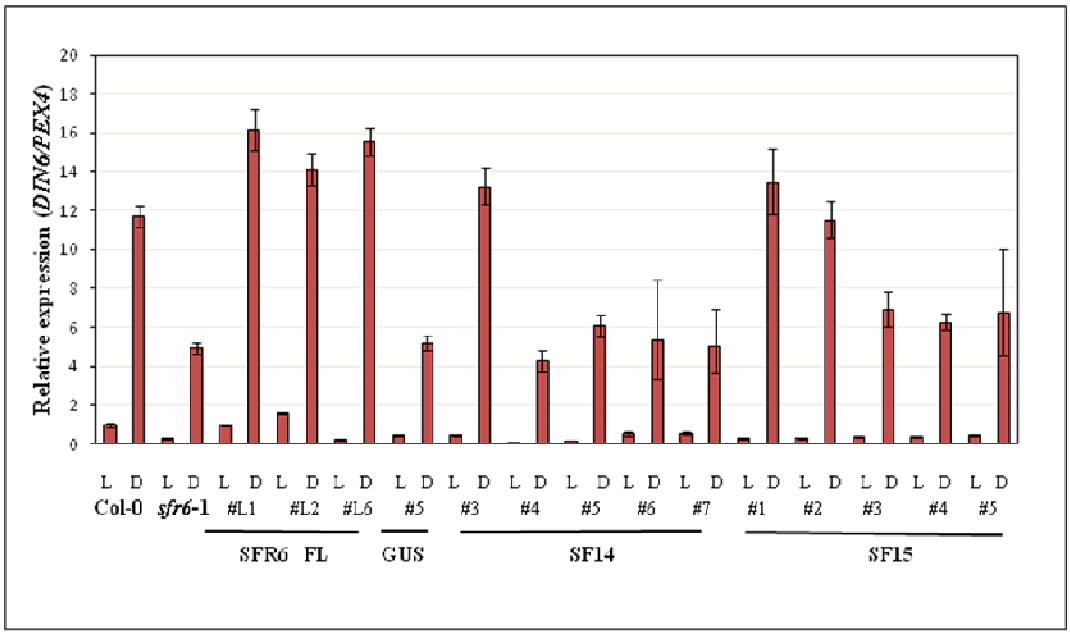

(c)

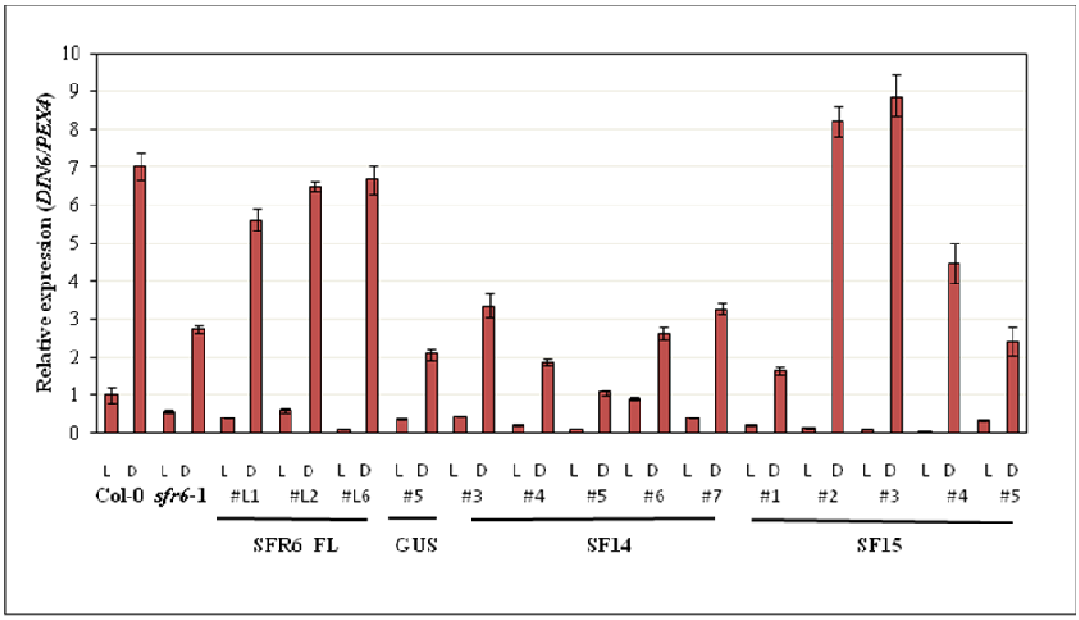

(*Figure continues to the following page*)

(d)

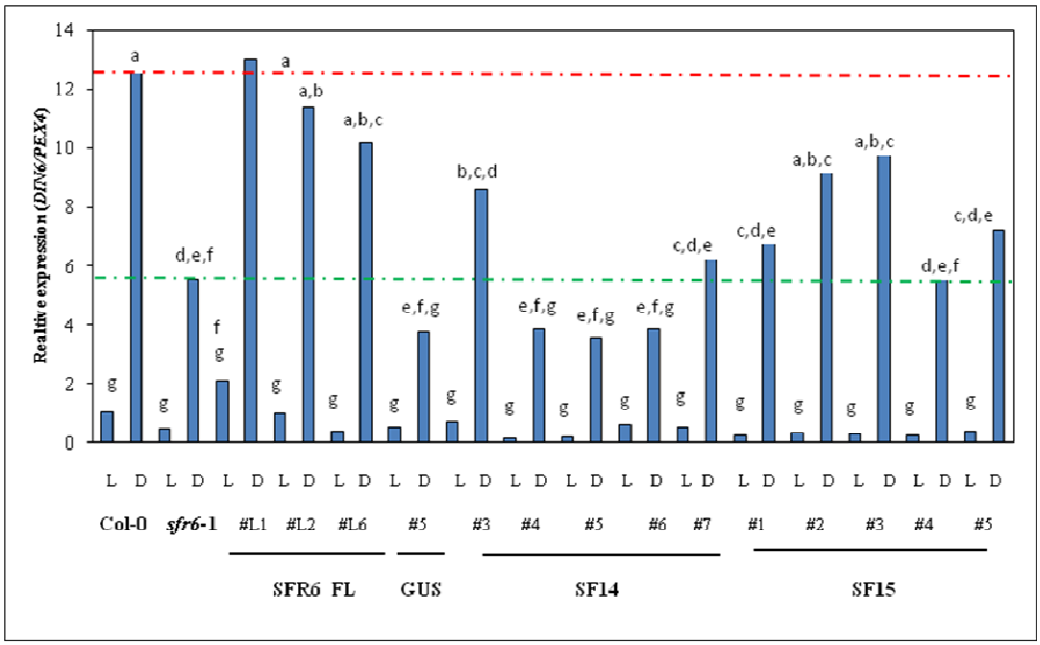

Figure 4.16: Complementation of dark-induced *DIN6* expression in SF14 and SF15 transgenic lines

Seven-day-old seedlings of *sfr6*-1+35S::SF14 (SF14) and *sfr6*-1+35S::SF15 (SF15) transgenic lines were compared with Col-0, *sfr6*-1, three different lines of *sfr6*- 1+35S::SFR6 (SFR6 FL) and *sfr6*-1+35S::GUS (GUS) were used for the experiment. Seedlings wrapped for 6 h in a double layer of aluminium foil (dark; D) or left unwrapped (Light; L) were used to measure dark inducible *DIN6* gene expression. The first three histograms (a, b and c- with red bars) represent the gene expression data of three independent biological replicates. Expression is shown after normalisation to *PEX4* in all graphs. Relative expression in the graphs represents the fold value compared with Col-0 control sample and calculated using the ΔΔCT method and the error bars in each biological replicate represent RQ_{MIN} and RQ_{MAX} and constitute the acceptable error level for a 95% confidence level according to Student's t test. The fourth chart (blue bars; d) represents the average of the above three independent biological replicates. Mean average data (in graph d) were analysed using a one-way ANOVA (α=0.05) and pair wise comparisons were made using the Tukey method. Means that do not share a letter are significantly different. *DIN6* expression in Col-0 and *sfr6-1* represents in red and green dotted lines respectively.

Compared to SF14 transgenic lines, SF15 showed varying expression levels of *DIN6* under dark conditions among five different lines in three different biological replicates. However, average gene expression data from three biological replicate experiments revealed that SF15#2 and SF15#3 exhibited the highest levels of *DIN6* expression and that these were significantly similar to the level of *DIN6* expressed in Col-0 and three lines of SFR6 FL ($p<0.001$) (Figure 4.16d). Interestingly, *SFR6* expression was lower in SF15#2 than in any of the other SF15 lines.SF15 lines while a moderate level of *SFR6* expression in SF15#3 was detected (Figure 4.9). Although the average trend is increased level of *DIN6* gene expression in SF15#1 and SF15#5 compared with untransformed *sfr6-1*, the level of expression was significantly different compared to Col-0 and three lines of SFR6 FL ($p<0.001$) while SF15#4 showed a similar level of *DIN6* expression as in *sfr6-1* mutant.

(a)

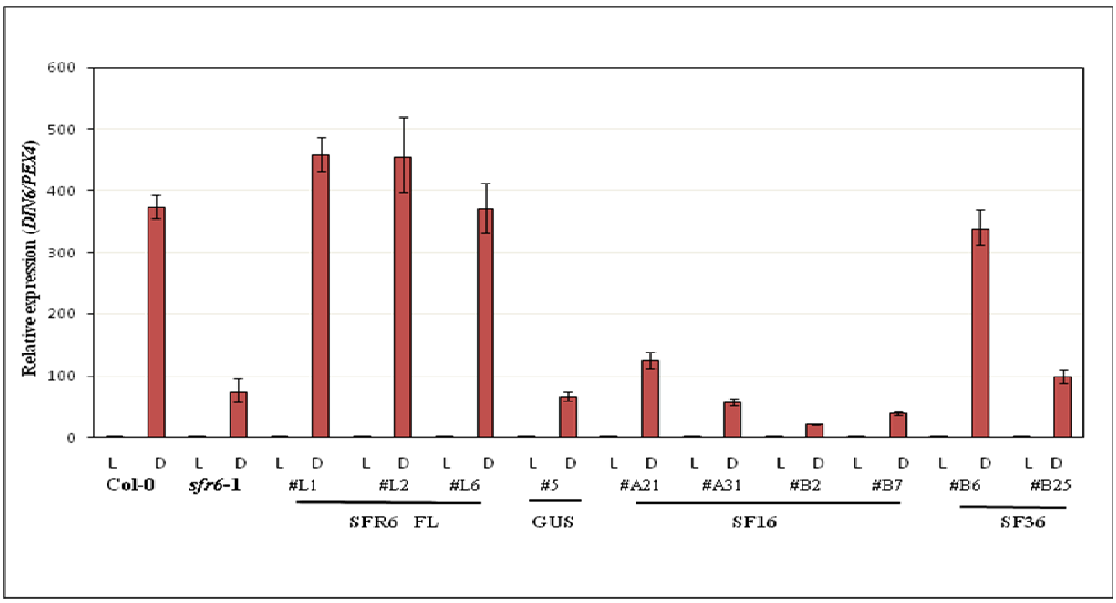

(*Figure continues to the following page*)

(b)

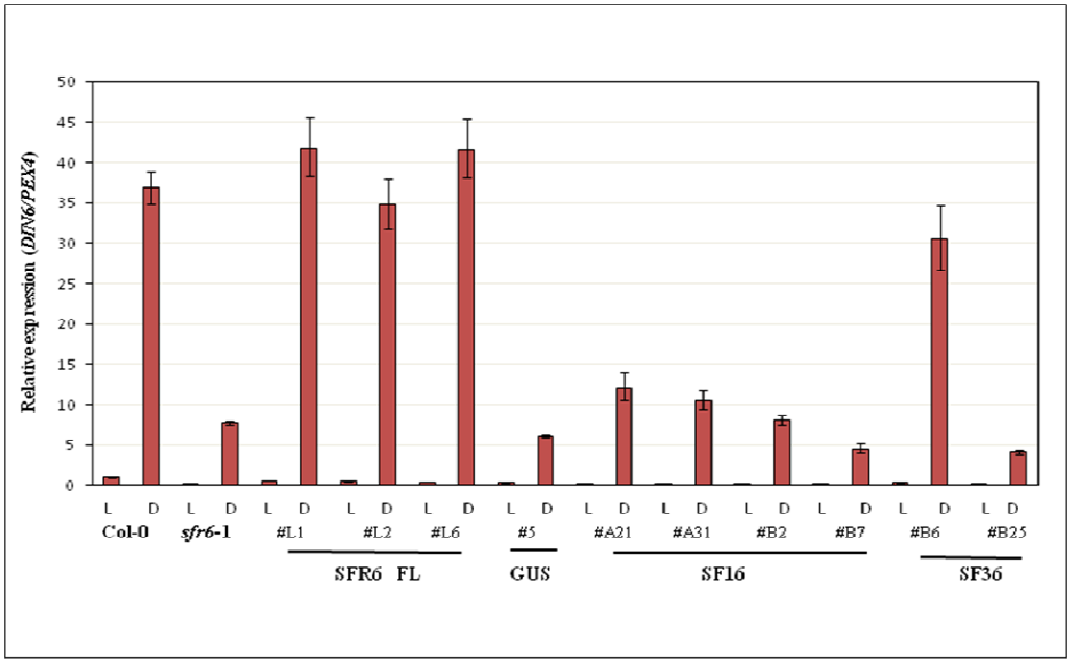

(c)

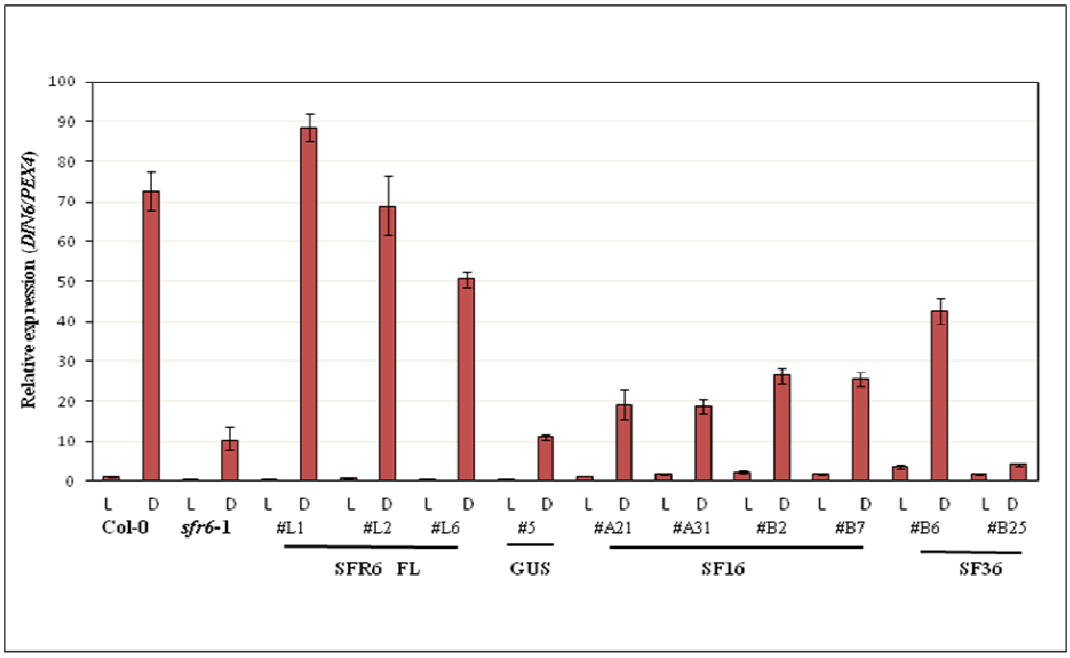

(*Figure continues to the following page*)

(d)

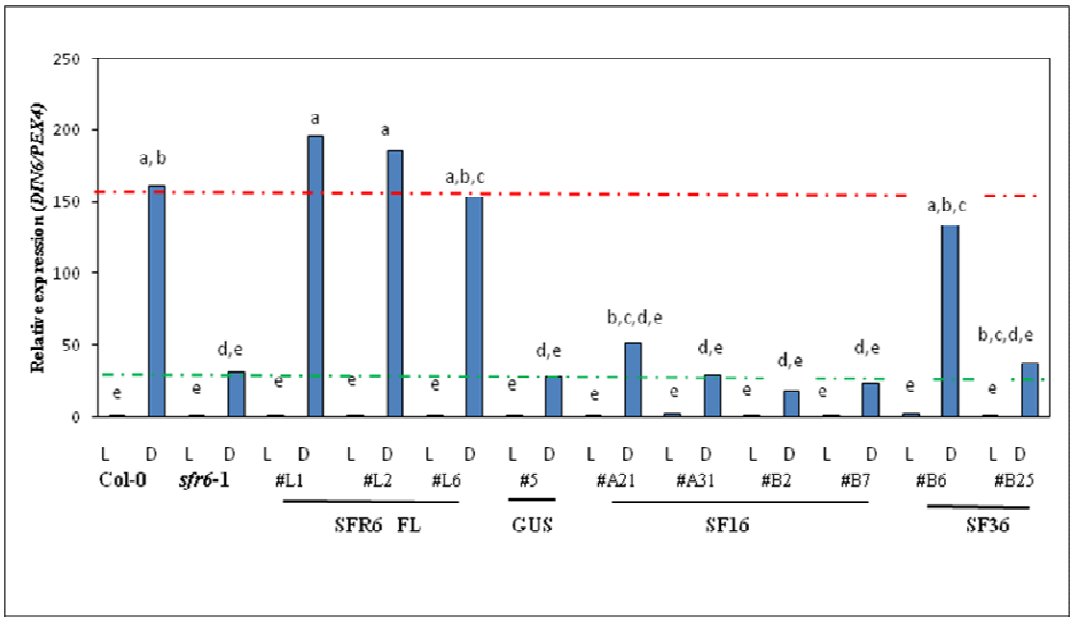

Figure 4.17: Complementation of dark-induced *DIN6* expression in SF36 and SF16 transgenic lines

Seven-day-old seedlings of *sfr6*-1+35S::SF36 (SF36) and *sfr6*-1+35S::SF16 (SF16) transgenic lines compared with Col-0, *sfr6*-1, three different lines of *sfr6*- 1+35S::SFR6 (SFR6 FL) and *sfr6*-1+35S::GUS (GUS) were used for the experiment. Seedlings wrapped for 6 h in a double layer of aluminium foil (dark; D) or left unwrapped (Light; L) were used to measure dark inducible *DIN6* gene expression. The first three histograms (a, b and c- with red bars) represent the gene expression data of three independent biological replicates.Expression is shown after normalisation to *PEX4* in all graphs. Relative expression in the graphs represents the fold value compared with Col-0 control sample and calculated using the ΔΔCT method and the error bars in each biological replicate represent RQ_{MIN} and RQ_{MAX} and constitute the acceptable error level for a 95% confidence level according to Student's t test The fourth chart (blue bars; d) represents the average of the above three independent biological replicates. Mean average data (in graph d) were analysed using a one-way ANOVA (α=0.05) and pair wise comparisons were made using the Tukey method. Means that do not share a letter are significantly different. *DIN6* expression in Col-0 and *sfr6-1* represents in red and green dotted lines respectively.

Dark-induced *DIN6* gene expression in *sfr6*-1+35S::SF36 (SF36) and *sfr6*-1+35S::SF16 (SF16) was compared with Col-0, *sfr6-1*, *sfr6*- 1+35S::SFR6 (SFR6 FL) and *sfr6*-1+35S::GUS (GUS) in three independent biological replicate experiments (Figure 4.17 a, b and c).

Increased levels of *DIN6* gene expression in full length genomic *SFR6* complemented lines in *sfr6-1* (*sfr6*- 1+35S::SFR6/SFR6 FL) was observed in all three biological replicate experiments compared to Col-0. These full length genomic SFR6 complemented lines were compared with four lines of SF16, the cDNA complemented lines. *DIN6* gene expression in these lines was not complemented but level of *DIN6* expression was higher in SF16#A21 than in *sfr6-1* (Figure 4.17 d). Line #B6, one line out of two lines of SF36, showed higher level of *DIN6* expression compared to the other line and that level of expression was not significantly different to the level of *DIN6* expression in three lines of full length genomic *SFR6* complemented lines as well as Col-0 ($p<0.129$). However, average expression of *DIN6* in #B25 was similar to the level of expression in *sfr6-1*.

4.2.5.5 Analysis of the ability of SF truncations to complement of the UV gene expression phenotype

Seven-day-old seedlings grown on MS media on petri dishes were irradiated with 5 KJm^{-2} of UV-C, (wavelength 254 nm) as described before. Lids were removed from the control plates during the time taken to administer the treatments. Immediately after irradiation, all plates with lids on were returned to the growth chamber and samples were taken 24 h after treatment (See 2.15.1.2). Expression of the UV-inducible *PR1* gene was measured using RT-PCR.

UV-inducible *PR1* expression in *sfr6-1*+35S::SF14 (SF14) and *sfr6*-1+35S::SF15 (SF15) was compared with Col-0, *sfr6-1*, *sfr6*- 1+35S::SFR6 (SFR6 FL) and *sfr6*-1+35S::GUS (GUS) in three independent biological replicate experiments (Figure 4.18 a, b and c). Though the relative expression levels of *PR1* was highly variable between biological replicates, increased or similar levels of *PR1* gene expression in full length of SFR6 complemented lines in *sfr6-1* (*sfr6*-1+35S::SFR6/SFR6 FL) were seen compared to Col-0 in all three biological replicate experiments.

An irregular pattern of *PR1* gene expression in different lines of SF14 was observed in three biological replicate experiments (Figure 4.18 a, b and c) and average gene expression data from three biological replicate experiments (Figure 4.18 d) revealed that the increased levels of *PR1* expression in #4, #5 and #7 of SF14 compared with those in *sfr6-1* were not significantly different compared to *sfr6-1* ($p<0.474$).

(a)

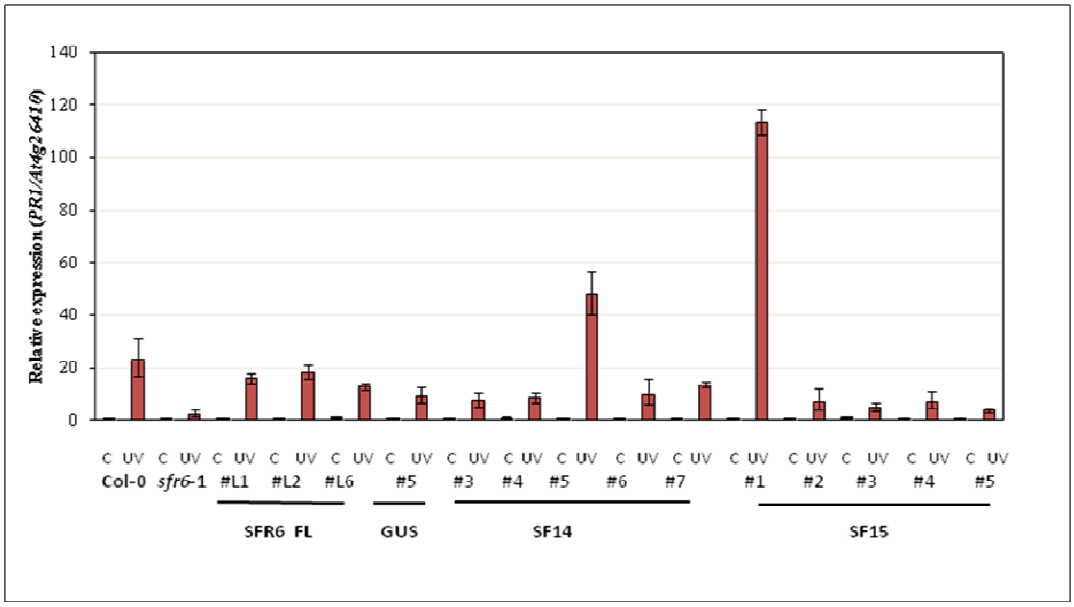

(*Figure continues to the following page*)

(b)

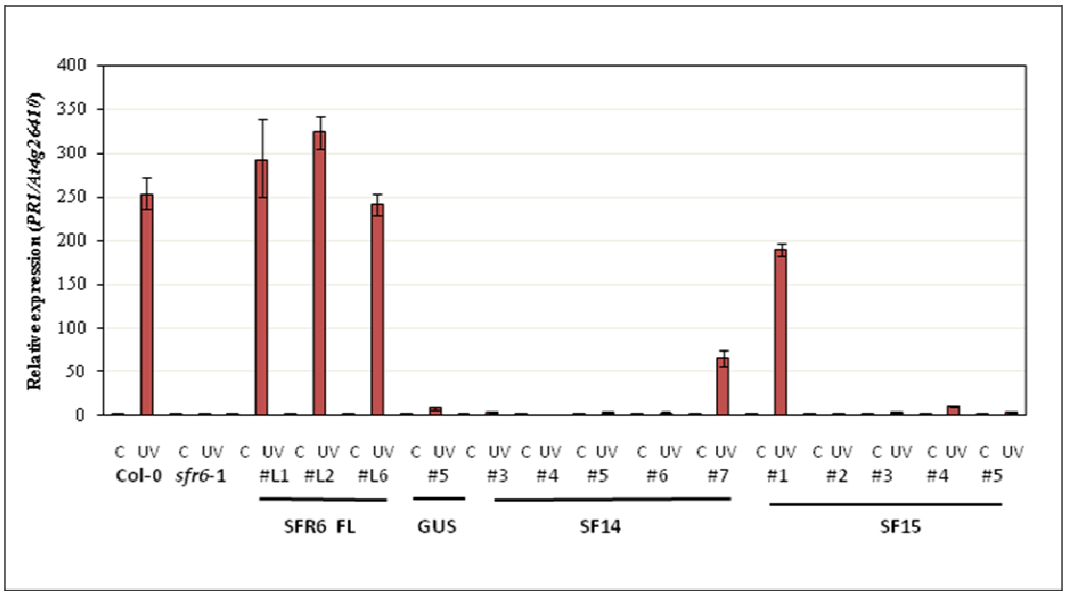

(c)

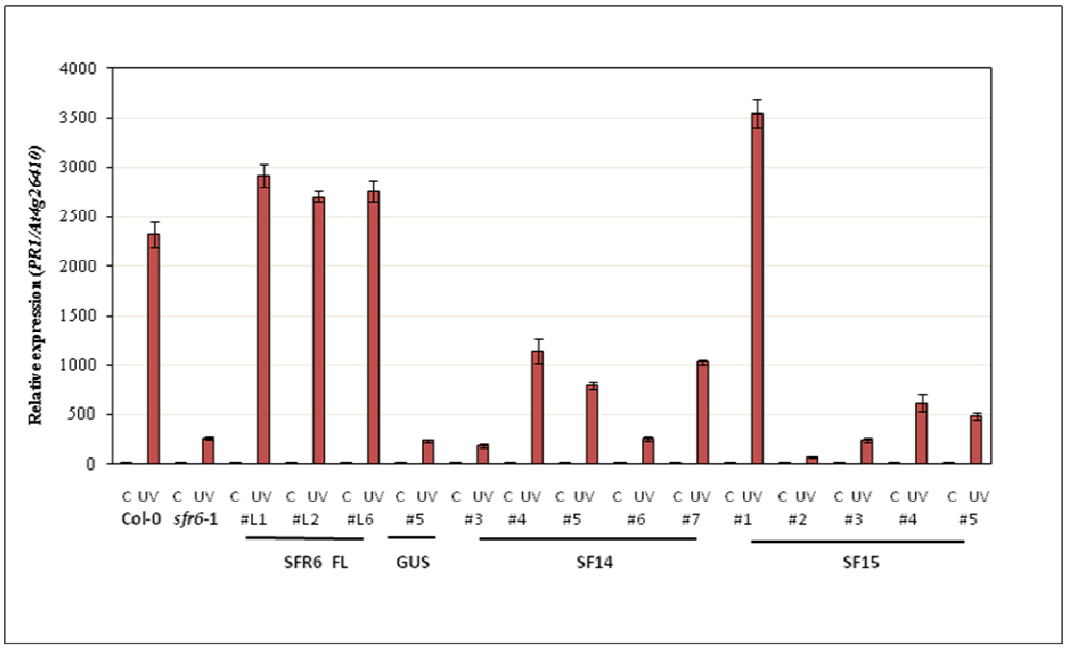

(Figure continues to the following page)

(d)

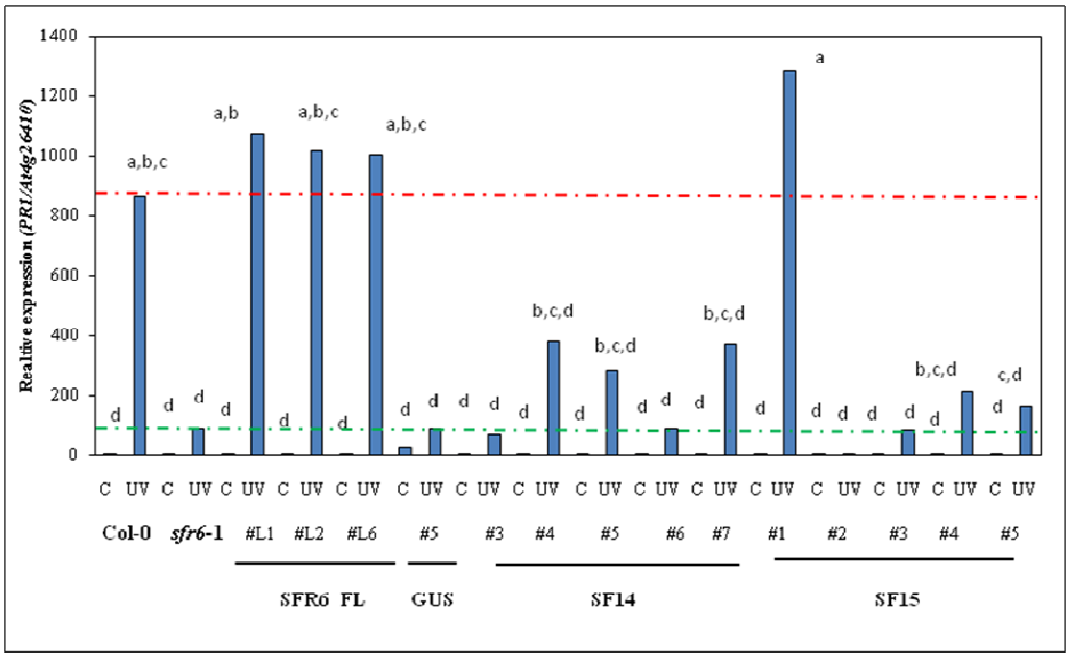

Figure 4.18: Complementation of UV-induced *PR1* expression in SF14 and SF15 transgenic lines

PR1 expression in seven-day-old seedlings in response to 5kJm^{-2} of UV exposure was measured in *sfr6*-1+35S::SF14 (SF14) and *sfr6*-1+35S::SF15 (SF15) transgenic lines compared with Col-0, *sfr6*-1, three different lines of *sfr6*- 1+35S::SFR6 (SFR6 FL) and *sfr6*-1+35S::GUS (GUS). The first three histograms (a, b and c- with red bars) represent the gene expression data of three independent biological replicates. Expression is shown after normalisation to *At4g2640* in all graphs. Relative expression in the graphs represents the fold value compared with Col-0 control sample and calculated using the ΔΔCT method and the error bars in each biological replicate represent RQ_{MIN} and RQ_{MAX} and constitute the acceptable error level for a 95% confidence level according to Student's t test The fourth chart (blue bars; d) represents the average of the above three independent biological replicates. Mean average data (in graph d) were analysed using a one-way ANOVA (α=0.05) and pair wise comparisons were made using the Tukey method. Means that do not share a letter are significantly different. *PR1* expression in Col-0 and *sfr6-1* represents in red and green dotted lines respectively.

Consistently higher levels of *PR1* gene expression in SF15#1 were observed in all biological replicates and average gene expression data from three biological replicate experiments (Figure 4.18 d) demonstrated that increased levels of *PR1* expression in SF15#1 were not significantly different to the level of *PR1* observed in Col-0 and three lines of full length of SFR6 complemented lines in *sfr6-1* (SFR6 FL). On the other hand, the remaining four lines of SF15 did not show a significant increase in *PR1* gene expression compared to the *sfr6-1* mutant ($p<0.474$) (Figure 4.18 d).

UV gene expression experiments with *sfr6*-1+35S::SF36 (SF36) and *sfr6*-1+35S::SF16 (SF16) were conducted as describe above and expression of the UV-inducible gene *PR1* was compared with Col-0, *sfr6-1*, *sfr6*- 1+35S::SFR6 (SFR6 FL) and *sfr6*-1+35S::GUS (GUS) in three independent biological replicate experiments (Figure 4.19 a, b and c). Though the expression

(a)

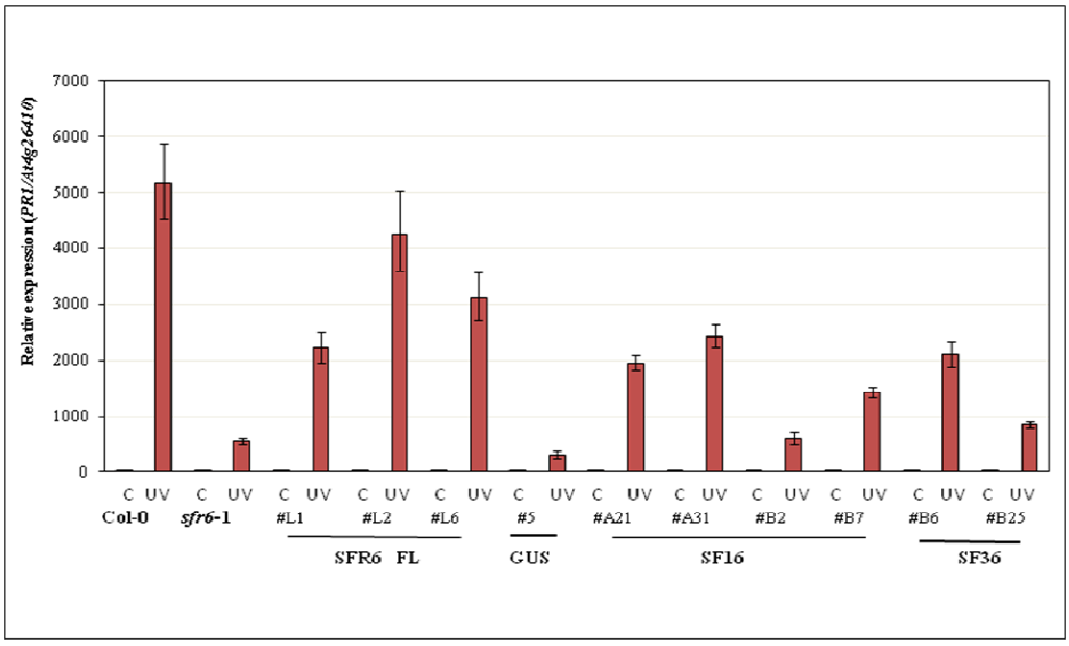

(*Figure continues to the following page*)

(b)

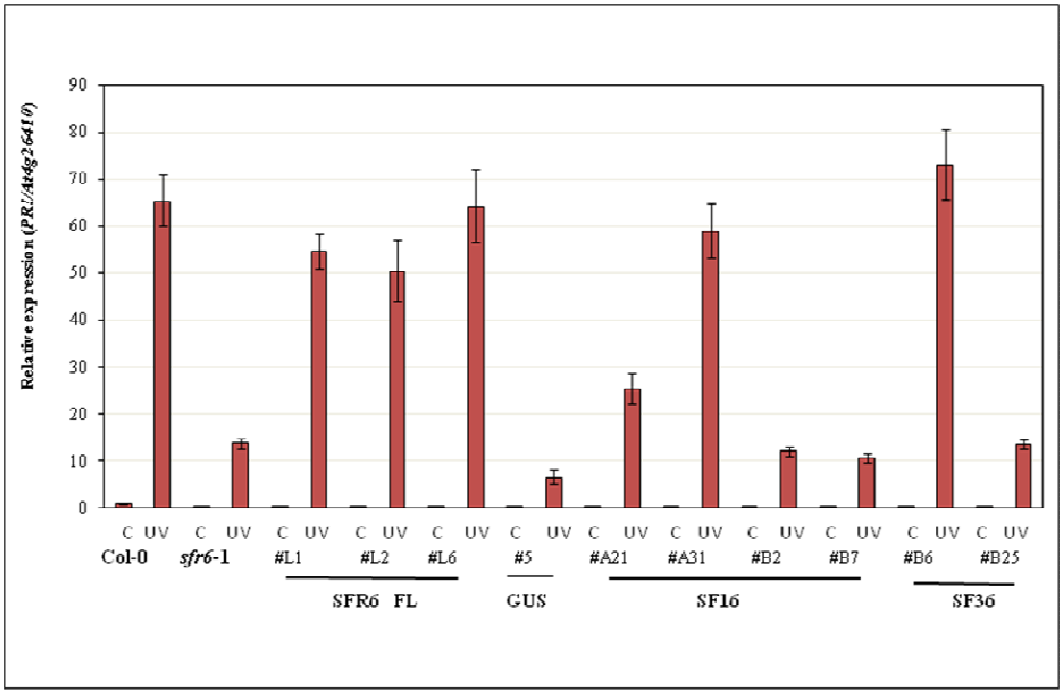

(c)

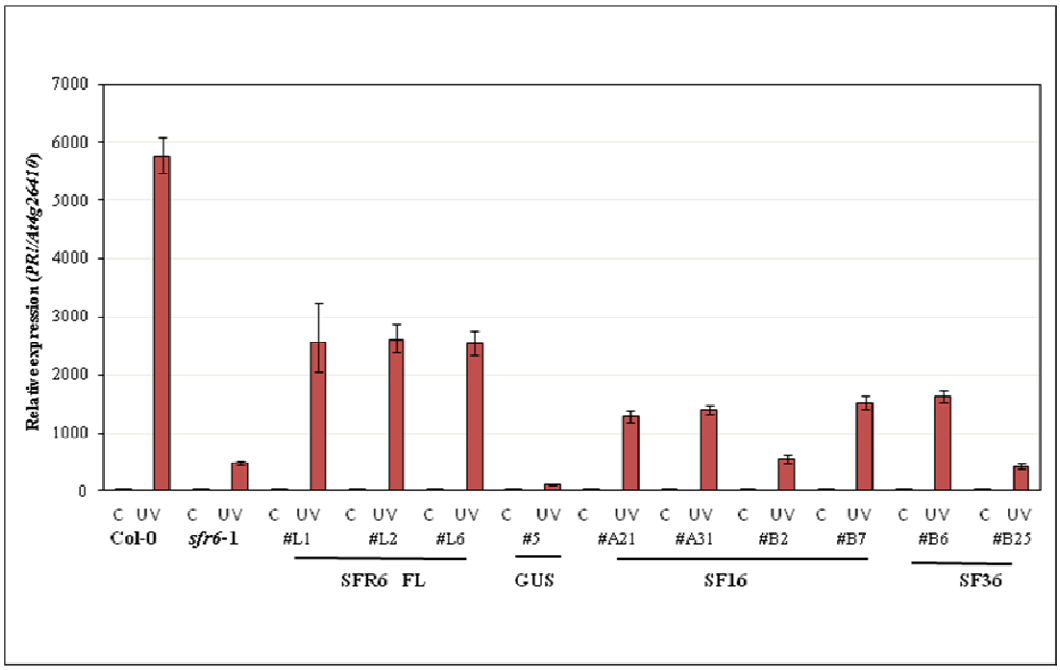

(*Figure continues to the following page*)

(d)

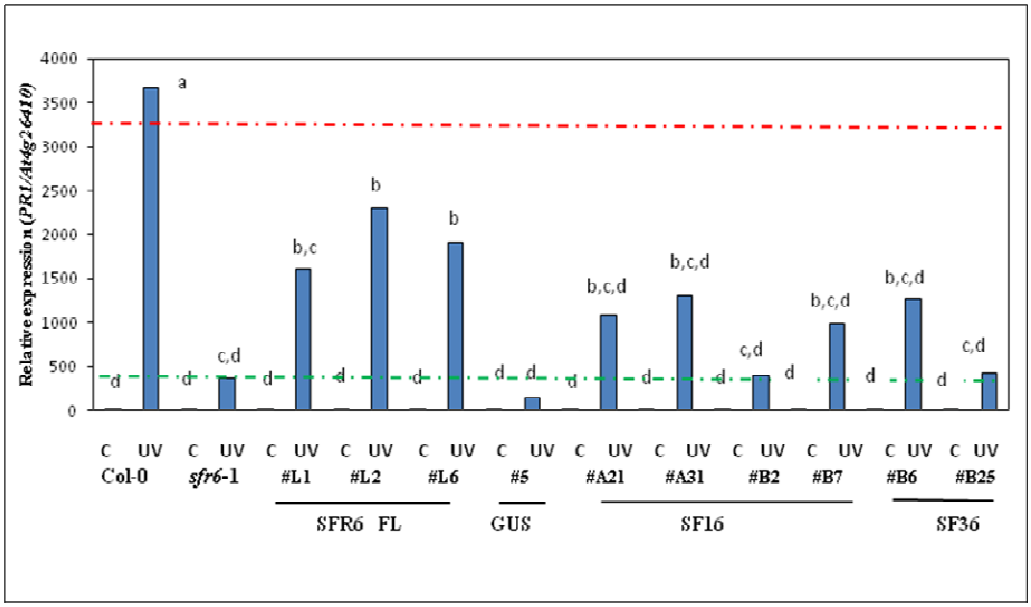

Figure 4.19: Complementation of UV-induced *PR1* expression in SF36 and SF16 transgenic lines

PR1 expression in seven-day-old seedlings in response to 5kJm^{-2} of UV exposure was measured in *sfr6*-1+35S::SF36 (SF36) and *sfr6*-1+35S::SF16 (SF16) transgenic lines compared with Col-0, *sfr6*-1, three different lines of *sfr6*- 1+35S::SFR6 (SFR6 FL) and *sfr6*-1+35S::GUS (GUS). The first three histograms (a, b and c- with red bars) represent the gene expression data of three independent biological replicates. Expression is shown after normalisation to *At4g2640* in all graphs. Relative expression in the graphs represents the fold value compared with Col-0 control sample and calculated using the ΔΔCT method and the error bars in each biological replicate represent RQ_{MIN} and RQ_{MAX} and constitute the acceptable error level for a 95% confidence level according to Student's t test The fourth chart (blue bars; d) represents the average of the above three independent biological replicates. Mean average data (in graph d) were analysed using a one-way ANOVA (α=0.05) and pair wise comparisons were made using the Tukey method. Means that do not share a letter are significantly different. *PR1* expression in Col-0 and *sfr6-1* represents in red and green dotted lines respectively.

levels of *PR1* were slightly different in different biological experiments, average expression data of three lines of SF16 *i.e* #A21, #A31 and #B7 and #B6 of SF36

showed increased levels of *PR1* expression compared to *sfr6-1*. However, levels of *PR1* expression of the above lines were not highly significantly different either to three lines of full length genomic SFR6 complemented lines (SFR6 FL #L1, #L2 and #L3) or *sfr6-1*(Figure 4.19d).

Table 4.1: Summary of the results of complementation experiment of SF truncations

Original F2 line	**Rel level of transgene expression in F_2**	**Individual line**	**Level of total SFR6 expression in F3**	**Level of SF transgene expression in F3**	**Visible appearance**	**Flowe-ring**	**Cold *KIN2***	**Dark *DIN 3***	**UV *PR 1***
4.1	**. med**	**SF14 #3**	**Medium**		**X**	**X**	**X**	**X**	**X**
4.1		**SF14#4**	**Medium**		**X**	**X**	**X**	**X**	**PC**
8.4	**. high**	**SF14#5**	**Medium**		**X**	**X**	**X**	**X**	**PC**
8.4		**SF14#6**	**Low**		**X**	**X**	**X**	**X**	**X**
8.4		**SF14#7**	**Low**		**PC**	**Y**	**PC**	**PC**	**PC**
1.1	. low	SF15#1	Low		Y	Y	Y	**PC**	Y
3.2	. high	SF15#2	High		PC	PC	X	Y	X
3.2		SF15#3	Medium		PC	PC	X	Y	X
3.2		SF15#4	Medium		PC	X	X	X	**PC**
3.2		SF15#5	Medium		PC	PC	X	**PC**	**PC**
10.12.3	**. high**	**SF36#B6**	**barely higher than Wt**	**Rel. high**	**Y**	**Y**	**Y**	**Y**	**PC**
10.12.3		**SF36#B25**	**No higher than Wt**	**Rel. high**	**PC**	**X**	**PC**	**PC**	**X**
4.1 (med)	. med	SF16#A21	No higher than Wt	Rel. low	Y	Y	X	**PC**	PC
4.1 (med)		SF16#A31	No higher than Wt	Rel. low	X	PC	X	X	PC
21.1 (high)	. med	SF16#B2	No higher than Wt	Rel. high	X	X	X	X	X
21.1 (high)		SF16#B7	No higher than Wt	Rel. med	Y	PC	X	X	PC

Abbreviations used in the table as follows; X= not complemented, PC= partially complemented, Y=fully complemented (or closed to fully); Rel. low/high means compared with other transgenic but not wild type control used. Level of SF transgene expression of SF14 and SF15 in F3 did not tested as no problem was observed in the level of expressions in SFR6 in F3 generation.

4.3 Summary

All experiments conducted in this chapter were designed to study the complementation effects of different truncated fragments of SFR6 under cold, dark and UV stress conditions. This was to identify whether any part of the SFR6 protein (domain/region) had a specific role in activating expression in response to one specific signal but not to other stress. Several lines from each truncated fragment of SFR6 were tested comparing to Col-0, *sfr6-1* and three lines of full length genomic SFR6 complemented lines (SFR6 FL #L1, #L2 and #L3). Experiments conducted for the identification of the truncated fragments of SFR6/MED16 that targeted the nucleus revealed that all six truncated fragments representing different region of SFR6 are targeted the nucleus. However, the predicted nuclear localisation signal using NUCPred program is located towards the C-terminus of the SFR6 protein. Even though all SFR6 truncations are targeted to the nucleus, the average ratio of fluorescence in nucleus and cytoplasm in tobacco leaf cells demonstrated that SF16 (full length of SFR6) and SF36 exhibited the highest ratio (i.e. were more apportioned to the nucleus) whereas the other four truncations showed lower ratios compared to above mentioned two truncations.

Complementation of visual phenotype of SF transgenic lines demonstrated that several lines were able to restore green colour phenotype of Col-0 in varying degree. SF15#1, SF36#B6 and SF16#B7 lines were able to restore the green colour phenotype of Col-0 approximately 90%, SF16#A21 nearly up to 80% and SF14#7 about 60%. Further all those lines showed restoration of flowering time phenotype i.e early flowering as in Col-0 except in #B7 in SF16 though it demonstrated high level

of green colour restoration phenotype. Despite these visual indications that the SF16 construct might give partial complementation, the stress assays below indicated they were not complemented at all.

Complementation of stress gene expression experiments conducted under cold, dark and UV stresses demonstrated that some lines in different SF truncated fragments showed varying degrees of complementation of stress gene expression compared to *sfr6-1*. SF15#1 demonstrated 100% complementation of cold and UV responsive gene expression but not dark responsive gene expression. So that this indicates of the necessity of missing part of this protein in these transgenic lines is required for dark responses.

In SF15 line #1 and #5 showed slightly higher level of dark inducible gene expression compared to *sfr6-1* but in #2 and #3 showed fully complementation. In SF14 truncations all lines showed similar or slightly higher level of cold and dark inducible gene expression compared to *sfr6-1*. However, UV inducible gene expression studies showed that three lines (#4, #5 and #7) out of five in SF14 demonstrated approximately 50% of complementation (partial complementation). In SF36 line #B6 demonstrated the fully complementation of cold inducible gene expression where #B25 showed partial complementation. Complementation of nearly 100% of dark inducible and 50% of UV inducible gene expression was observed in SF36# B6 but partial complementation of dark and similar level of UV inducible gene expression as in *sfr6-1* was observed in SF36# B25. Cold and dark inducible gene expression in all lines of SF16 was slightly higher than *sfr6-1* but no complementation effect could be observed in all the lines except #A21 which showed partial complementation under dark conditions. However, in UV gene expression experiments, nearly 50% of complementation effect in #A21, #A31 and #B7. Even

though #A21 of SF16 showed restoration of flowering time phenotype as well as #B7 of SF16 showed higher level of green colour restoration, none of them able to demonstrate stress gene complementation in this study.

Chapter 5

The effects of KIN10, a putative interactor of MED16, on transcriptional regulation and stress tolerance in Arabidopsis

5.1 Introduction

SnRK1 (Sucrose non fermenting1 (Snf1) related protein kinase1) is a member of a family of plant protein kinases that resemble yeast Snf1 and animal AMPK kinases (Adenosine Monophosphate-activated Protein kinases), enzymes that are important in transcriptional, metabolic and developmental regulation in response to energy depletion stress (Baena-Gonzalez, 2010, Baena-Gonzalez and Sheen, 2008). SNF1/AMPK/SnRK1 are known to be regulated by several upstream kinases through phosphorylation of a conserved threonine residue in the T-loop (Hardie, 2007, Hedbacker and Carlson, 2008, Shen et al., 2009). The SnRK1 enzyme consists of three subunits; alpha, beta and gamma, which form a heterotrimeric complex. Two isoforms of the catalytic alpha subunit exist in plants, KIN10 and KIN11; KIN12 is likely to be a pseudogene (Ghillebert et al., 2011). Transcriptional regulation by KIN10 in response to darkness, sugar deprivation and other stress is mediated via direct targets genes of KIN10 such as genes involved in major catabolic pathways, including cell wall, starch, sucrose, amino acid, lipid, and protein degradation that provide alternative sources of energy and metabolites as well as a large number of genes encoding putative transcription factors (TFs); histones and histone deacetylases are highly activated or repressed by KIN10 (Baena-Gonzalez et al., 2007, Contento et al., 2004, Thimm et al., 2004, Baena-Gonzalez and Sheen, 2008).

KIN10/KIN11 trigger transcriptional activation and repression of more than 1000 genes under energy stress conditions such as high/low sucrose, low glucose concentrations or dark conditions, (which limit photosynthesis), and cause changes in the expression (Baena-Gonzalez et al., 2007, Baena-Gonzalez and Sheen, 2008), allowing plants to re-establish homeostasis by suppressing energy-consuming processes (Baena-Gonzalez et al., 2007). In addition to the well-known roles of SnRK1 in phosphorylation and in modulating the activities of enzymes important for carbon and nitrogen metabolism (Halford et al., 2003, Hardie et al., 1998, Sugden et al., 1999), much research work has reported that activation of KIN10/KIN11 in energy stress conditions ultimately affects growth and development of plants by targeting many regulatory factors and downstream signalling pathways that are normally activated by ABA (Baena-Gonzalez, 2010, Baena-Gonzalez et al., 2007, Lovas et al., 2003, Lu et al., 2007, Thelander et al., 2004, Zhang et al., 2001, Jossier et al., 2009, Rodrigues et al., 2013).

Lee et al. (2009) reported that SnRK1 activity in young rice seedlings caused enhanced tolerance of flooding (hypoxia) and Young-Hee Cho et al. (2012) reported similar effects in Arabidopsis plants expressing rice SnRK1, with plants showing improved tolerance under submergence conditions. Lovas et al. (2003) observed increased sensitivity to salt stress in potato plants in which repression of StubGAL83 (a regulatory β subunit of SnRK1) had been achieved using antisense, as well as delayed tuberisation and increased number of tubers per plant. Baena-Gonzalez et al. (2007) revealed that KIN10 overexpression caused enhanced starvation tolerance, life span extension, altered plant morphology and timing of development in Arabidopsis. Furthermore they reported that dark-induced (*DIN*) genes are affected

by KIN10 under different stress conditions and particularly repressed by sugars and light and they demonstrated this effect using transgenic plants overexpressing KIN10. Moreover, Baena-Gonzalez et al. (2007) reported that *DIN1* and *DIN6* were affected by KIN10 under stress conditions such as, submergence/flooding conditions as well as in the presence of DCMU (3-(3,4–dichlorophenyl)-1,1-dimethylurea) which interrupts the photosynthetic electron transport chain in photosynthesis and thus blocks the plants ability to convert light energy to chemical energy in addition to effects under starvation conditions.

A yeast-2-hybrid screen conducted in our laboratory identified KIN10 as a putative interactor of full length SFR6/MED16 (Hemsley and Knight, unpublished) and work from our laboratory has shown that *DIN6* gene expression is impaired in *sfr6* mutants (Hemsley et al., 2014). In the light of evidence of interactions between KIN10 and SFR6/MED16 and the fact that these two proteins affect expression of some of the same stress-responsive genes (e.g. the *DIN* genes), study of the effects of KIN10 on transcriptional activation of stress genes is of particular relevance to study of SFR6/MED16. Upon considering this situation, this chapter attempts to answer the following questions:

(1) Does KIN10 control the expression of the same set of stress-inducible genes as SFR6/MED16 or a subset of these?
(2) Do KIN10 and SFR6/MED16 act on the same pathway leading to expression of stress genes?
(3) With which part of SFR6/MED16 does KIN10 interact?

5.2 Results

5.2.1 Measurement of stress inducible-transcription in loss of function mutants of KIN10

To test the first hypothesis, whether KIN10 and SFR6 control the expression of same set of stress inducible genes, loss of function mutants of KIN10 were employed. All experiments described in this chapter were designed for the investigation of whether dark-inducible and other stress gene expression was similarly impaired in both *sfr6* and *kin10* mutants. The main focus was on the stress conditions cold, UV, and drought due to the reason that impaired gene expression in response to these conditions has been reported for *sfr6/med16* mutants (Boyce et al., 2003, Knight et al., 2009, Knight et al., 1999, Wathugala et al., 2012). In addition the transcriptional response to conditions including darkness, inhibition of photosynthesis (using DCMU) (Baena-Gonzalez et al., 2007) and ABA stimuli, known to require KIN10, was tested in *sfr6-1* mutants.

The *Akin10* mutant (SALK_127939 line from the SIGnAL T-DNA collection (Fragoso et al., 2009)) was used to test the effect of loss of KIN10 on *DIN6* transcription in seven-day-old seedlings subjected to 6 h darkness during the normal light period. The effect on *DIN6* gene expression was not consistent in repeat experiments with the above *kin10-1* mutant. This may have been due to a conditional aspect of the insertional mutation; the T-DNA insertion in this mutant is in 3' untranslated region of the *KIN10*, and it is possible KIN10 transcript levels are not always reduced under all experimental conditions.

Therefore, an alternative T-DNA insertion line was obtained from the Gabi-Kat collection (web site http://www\.gabi-kat.de/) (GK line ID 579E09) (the homozygous line a kind gift from Markus Teige, University of Vienna, Department of Biochemistry, Austria). In this mutant the insertion is in the last exon of the gene. All data presented in this chapter are derived using this mutant (*kin10-2*, GK579E09) including data using KIN10 complemented lines and a newly generated *sfr6kin10* double mutant.

5.2.1.1 Expression of dark inducible genes

Light is an essential source of energy for plant development and metabolism and it affects gene expression by altering metabolic flow in plants (Fujiki et al., 2001, Tuteja and Sopory, 2008). Therefore identification of different conditions that modify the metabolic status via adopting photosynthetically unfavourable light conditions is an important approach to understand transcriptional responses of plants considering it as a potential stress condition.

5.2.1.1.1 Expression of *DIN6* in response to dark conditions

It has been reported previously that transient overexpression of KIN10 in protoplasts can elevate the expression of some stress-responsive genes (Baena-Gonzalez et al., 2007). However, necessity of KIN10 for expression has not been demonstrated, All dark stress gene experiments described in this chapter were carried out using seven-day-old seedlings grown on 0.5X MS media on petri dishes (except where stated otherwise) and subjected to 6 h darkness by wrapping individual plates in two layers of aluminium foil, during the light cycle in the Percival growth chamber. Control plates remained unwrapped in the chamber under normal light conditions (see 2.12.3).

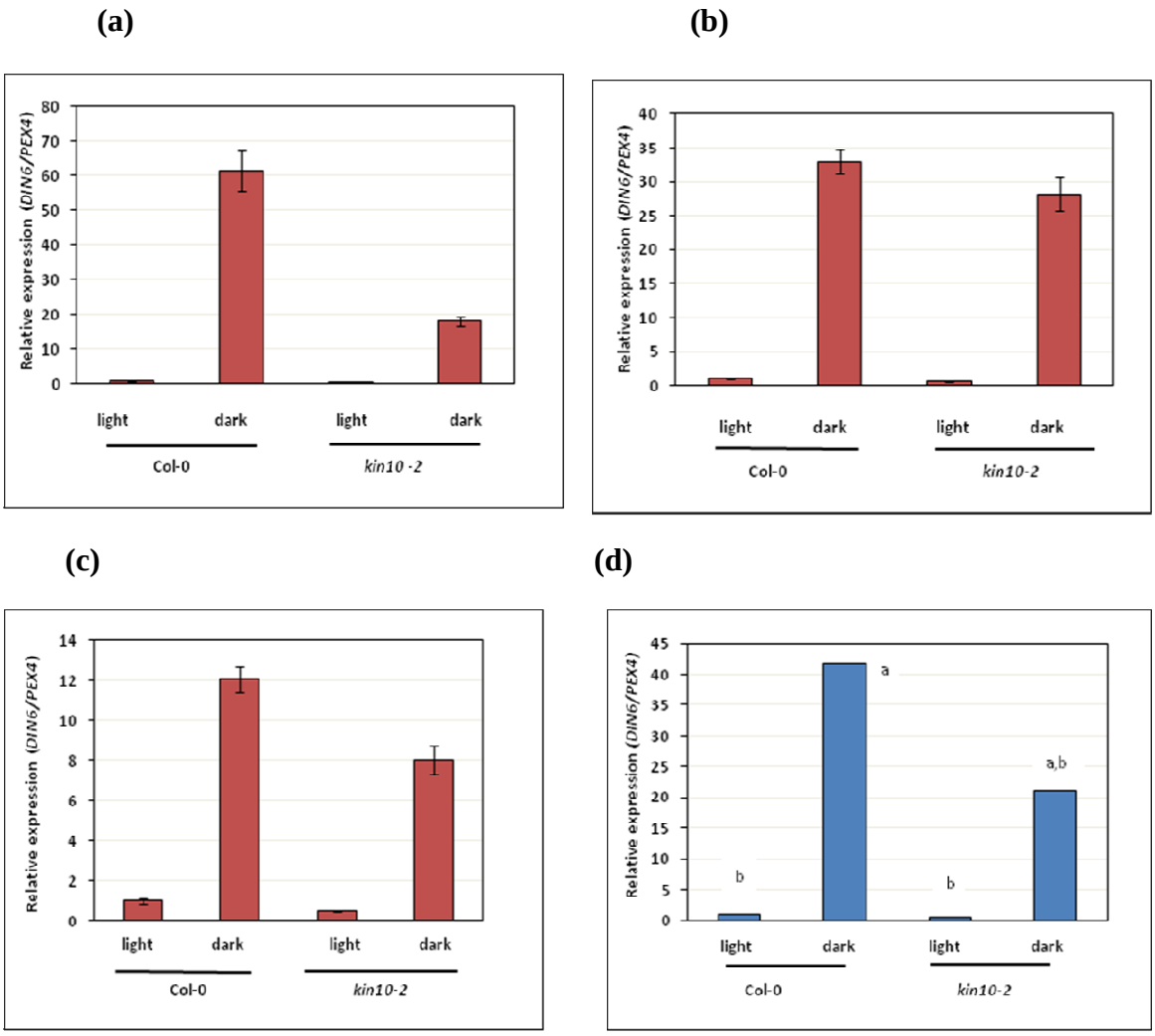

Figure 5.1: Dark-induced stress gene expression of *kin10*-2 and Col-0

DIN6 expression in response to dark conditions was measured in *kin10-2* mutants compared with Col-0. Seven-day-old seedlings were subjected to 6 h dark conditions by wrapping in aluminium foil (dark) or leaving them unwrapped (light). In this figure and all of the gene expression figures in this chapter, the first three histograms (a, b and c- with red bars) represent the gene expression data from three independent biological replicates. The error bars in each biological replicate represent RQ_{MIN} and RQ_{MAX} and constitute the acceptable error level for a 95% confidence level according to Student's t test and indicate the level of variation between technical replicates within one biological replicate experiment. The fourth chart (blue bars; d) represents the average of the above three independent biological replicates. Mean average data (in graph d) were analysed using a one-way ANOVA (α=0.05) and pair wise comparisons were made using the Tukey method. Means that do not share a letter are significantly different.

Expression of the dark-inducible gene *DIN6* was analysed in this and all experiments described subsequently by using qRT-PCR and normalised to expression of *PEX4* gene an endogenous control gene (Wathugala et al. (2011). "Relative expression" in these and all subsequent graphs presented in this chapter represents the fold difference in expression level compared with the Col-0 control sample and was calculated using the ΔΔCT method (Livak and Schmittgen, 2001). Dark-inducible *DIN6* expression in *kin10*-2 was compared with wild type Arabidopsis plants in three independent biological replicate experiments (Figure 5.1 a, b and c). Reduced levels of *DIN6* gene expression under dark stress were observed in all three biological replicate experiments; however, the degree of reduction in expression was different in each instance. Although a reduction in relative expression was seen in all three replicates, the average gene expression in dark was not significantly different in *kin10*-2 (Figure 5.1d) compared to wild type ($p<0.023$).

5.2.1.1.2 Expression of *DIN6* in response to DCMU

In addition to the dark stimulus, Fujiki et al. (2001) reported that application of the herbicide DCMU (3-(3,4–dichlorophenyl)-1,1-dimethylurea) can also induce the expression of *DIN* genes, by interrupting the photosynthetic electron transport chain in photosynthesis and thus blocking the plant's ability to convert light energy to chemical energy. As fold increases in *DIN6* expression in response to dark to loss of KIN10 were variable, I examined the effect of DCMU on *DIN6* gene expression to ascertain whether this form of stimulus would be more reproducible than darkness.

To test effects of DCMU on *DIN6* expression in *kin10-2*, seven-day-old seedlings were floated (15-20 seedlings per treatment) on 5 ml of 20 μM DCMU contained in transparent six-well plates or 5 ml of sterile water (control) in the Percival growth

chamber for 6 h (see 2.12.5). Expression of *DIN6* was analysed using qRT-PCR as described above.

DIN6 expression in *kin10-2* was compared with wild type Arabidopsis plants in three independent biological replicate experiments (Figure 5.2 a, b and c). A highly reduced level of *DIN6* gene expression in *kin10-2* was observed in one individual replicate experiments out of three and in second and third replicate experiments higher level of *DIN6* expression were observed. Average gene expression data from three individual experiments showed that the level of *DIN6* expression was reduced in *kin10-2* but this level of expression was not significantly different from that seen in Col-0 ($p<0.561$) (Figure 5.2 d). Though I expected improvement, DCMU did not improve the reproducibility of the response compared to the response under dark conditions.

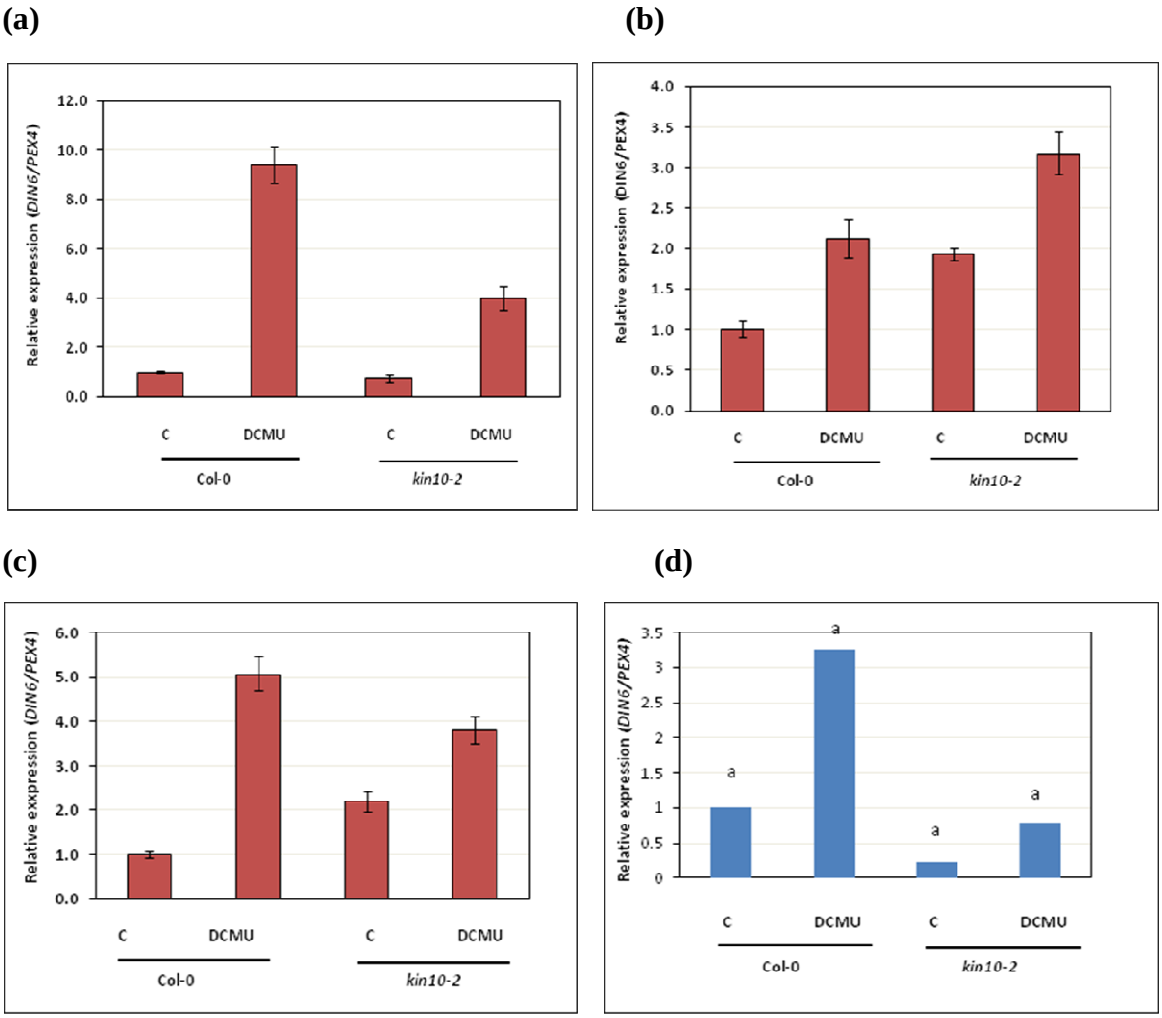

Figure 5.2: *DIN6* expression in response to DCMU

DIN6 expression in response to DCMU treatment was measured in *kin10-2* compared with Col-0. Seven-day-old seedlings were floated on 20 μM of DCMU (DCMU) or sterile water (C) for 6 h in the Percival growth chamber.The first three histograms (a, b and c- with red bars) represent the gene expression data of three independent biological replicates after normalisation to *PEX4*; error bars represent technical variability. The fourth chart (blue bars; d) represents the average of the above three independent biological replicates. Mean average data (in graph d) were analysed using a one-way ANOVA (α=0.05) and pairwise comparisons were made using the Tukey method. Means that do not share a letter are significantly different.

5.2.1.2 Expression of cold and drought-responsive genes

Cold- and drought-inducible gene expression is strongly impaired in *sfr6* mutants (Boyce et al., 2003, Knight et al., 2009, Knight et al., 1999). So the possibility that KIN10 also shared in this regulation was tested in the experiments described next.

5.2.1.2.1 Cold-induced *KIN2* expression

Seven-day-old seedlings grown on 0.5X MS media on petri dishes in the Percival growth chamber were treated at 5^{o}C for 6 h in a SANYO growth chamber while control plates were kept at 20^{o}C (ambient temperature; amb) (see 2.12.1). Expression of the cold-inducible gene *KIN2* was analysed using qRT-PCR as described above and normalised to expression of *PEX4*.

Cold-inducible *KIN2* expression in *kin10*-2 was compared with wild type Arabidopsis plants in three independent biological replicate experiments (Figure 5.3 a, b and c). Consistent levels of *KIN2* gene expression in *kin10*-2 in response to cold were not observed across the three individual replicate experiments. However average gene expression data from three individual experiments showed a reduced level of *KIN2* in the mutant compared with wild type although the expression level was not significantly different ($p<0.551$) (Figure 5.3d). Data were analysed using one-way ANOVA ($\alpha=0.05$) and pairwise comparisons were made using the Tukey method.

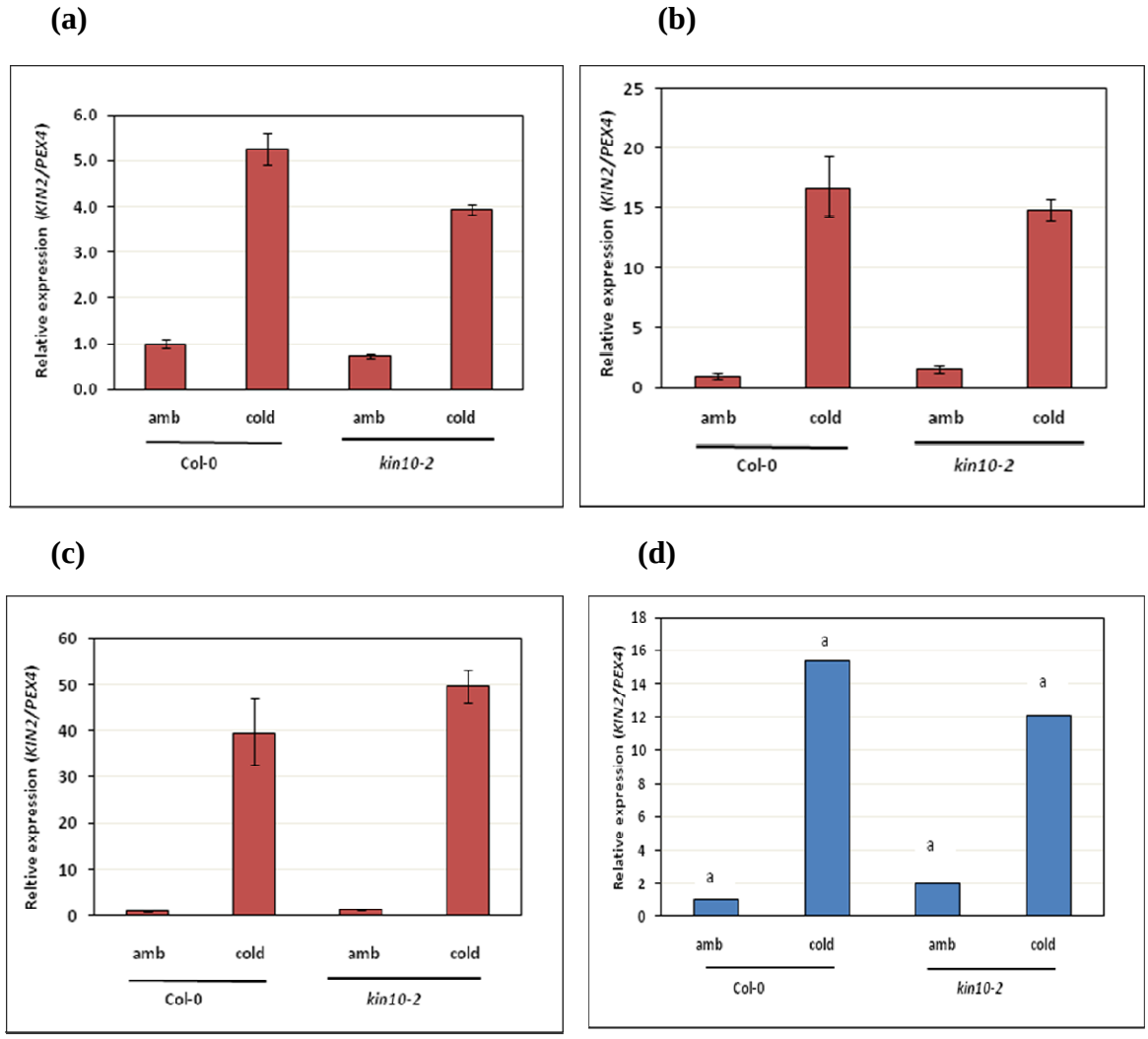

Figure 5.3: Cold-induced *KIN2* expression in *kin10*-2 and Col-0

KIN2 expression in response to cold was measured in *kin10*-2 compared with Col-0. Seven-day-old seedlings grown on 0.5X MS media on petri dishes were treated at 5^{o}C for 6 h (cold) while control plates were kept at 20^{o}C (amb).The first three histograms (a, b and c- with red bars) represent the gene expression data of three independent biological replicates. Expression is shown after normalisation to *PEX4* in all graphs. The fourth chart (blue bars; d) represents the average of the above three independent biological replicates. Mean average data (in graph d) were analysed using a one-way ANOVA (α=0.05) and pairwise comparisons were made using the Tukey method. Means that do not share a letter are significantly different.

5.2.1.2.2 Expression of desiccation-responsive genes

Water withdrawal experiments were conducted to study desiccation-induced gene expression. Seven-day-old seedlings grown on 0.5X MS media on petri dishes were subjected to water withdrawal by opening the lids, thereby exposing the seedlings to dehydration when returned to the Percival growth chamber. Plates were left open in the growth chamber for 6 h during the light cycle with no humidity control while keeping the control plates closed under the same conditions (see 2.12.4). The desiccation/drought-inducible genes *KIN2, LTI65* and *P5CS1* were selected for study; *KIN2* is a *COR* gene that contains the CRT/DRE *cis*-acting element (Baker et al., 1994) in their promoters and are thus targets of the CBF1/DREB1B transcription factors (Stockinger et al., 1997, Liu et al., 1998). *P5CS1* is known to be expressed in response to water stress and low temperature and encodes D1-pyrroline-5-carboxylate synthetase (Strizhov et al., 1997), the rate-limiting enzyme in the proline synthesis pathway (Savouré et al., 1995). *LTI65* and *P5CS1* do not contain a CRT/DRE element in its' promoter.

Expression of these desiccation/drought-inducible genes was analysed using qRT-PCR and normalised to expression of *PEX 4*, an endogenous control gene. Relative expression represents the fold value compared with the Col-0 control sample and calculated using the ΔΔCT method as described before. Desiccation-inducible *KIN2* expression in *kin10-2* was compared with wild type Arabidopsis plants in three independent biological replicate experiments (Figure 5.4 a, b and c). Consistently low levels of *KIN2* gene expression in *kin10-2* compared with wild type were observed in all three individual replicate experiments. Average gene expression data from three individual experiments shows that the reduction in *KIN2* expression in *kin10-2* was highly significant compared to Col-0 ($p<0.001$) (Figure 5.4 d).

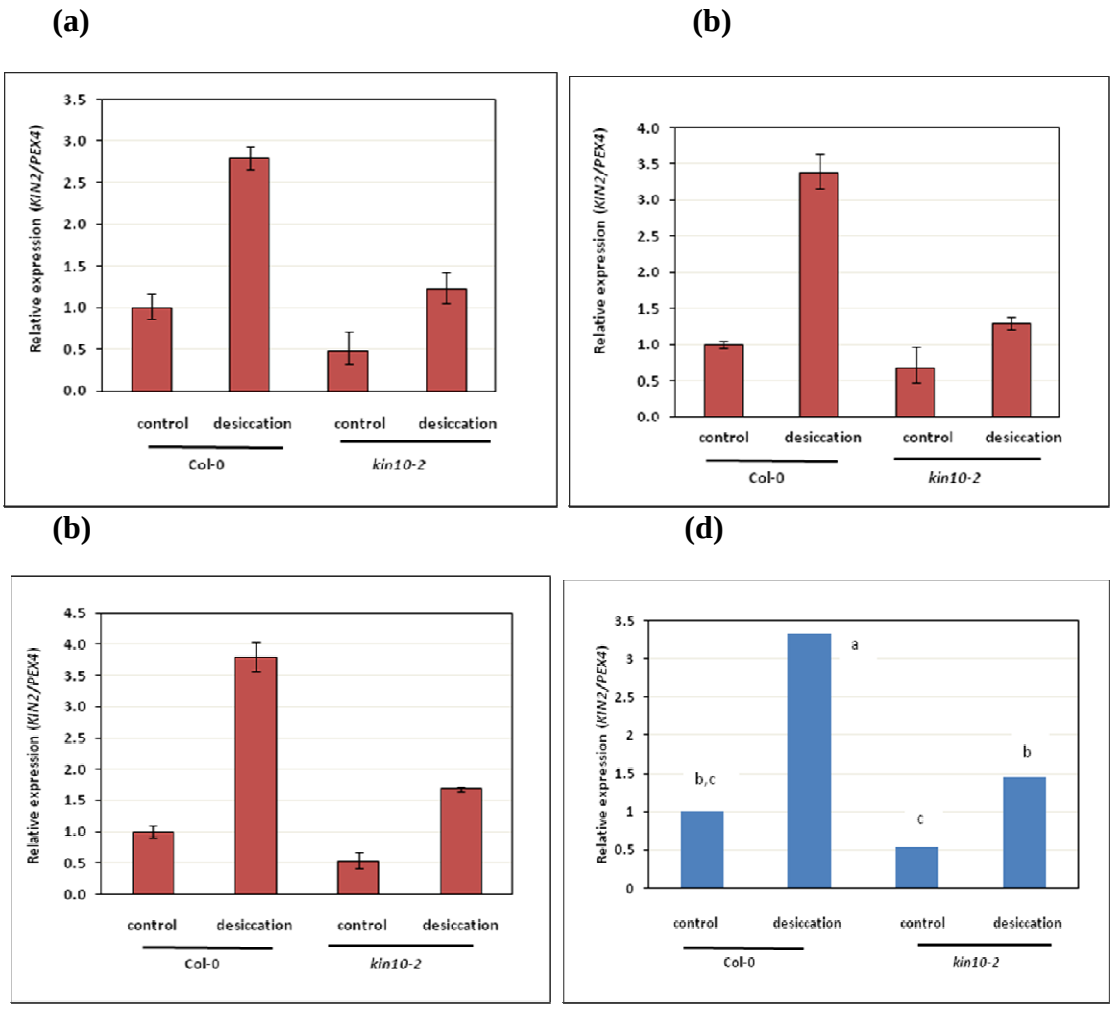

Figure 5.4: Desiccation-induced *KIN2* gene expression of *kin10*-2 and Col-0

KIN2 expression in response to desiccation stress was measured in *kin10-2* compared with Col-0. Seven-day-old seedlings grown on 0.5X MS media on petri dishes were subjected to water withdrawal by opening the lids for 6 h (desiccation) while control plates kept closed (control).The first three histograms (a, b and c- with red bars) represent the gene expression data of three independent biological replicates. Expression is shown after normalisation to *PEX4* in all graphs. The fourth chart (blue bars; d) represents the average of the above three independent biological replicates. Mean average data (in graph d) were analysed using a one-way ANOVA (α=0.05) and pair wise comparisons were made using the Tukey method. Means that do not share a letter are significantly different.

Desiccation/drought-inducible *LTI65* expression in *kin10-2* was compared with wild type Arabidopsis plants in the same RNA samples as above (Figure 5.5 a, b and c). In

each instance reduced expression of *LIT65* in *kin10-2* was observed. Unlike in desiccation-induced *KIN2* expression, the average gene expression data from three individual experiments revealed that the reduction in the level of *LTI65* expression in *kin10-2* was not significant compared to Col-0 ($p<0.155$) (Figure 5.5d).

Gene expression data from the third desiccation- inducible gene, *P5CS1* showed impaired expression in *kin10-2* compared to wild type in the three independent biological replicate experiments (Figure 5.6 a, b and c). Similar to desiccation-induced *KIN2* expression, the average gene expression of *P5CS1* in three individual experiments showed that the reduced level of *P5CS1* expression in *kin10-2* was highly significant compared to Col-0 ($p<0.001$) (Figure 5.6 d). Gene expression data were analysed using a one-way ANOVA ($\alpha=0.05$) and pair wise comparisons were made using Tukey method.

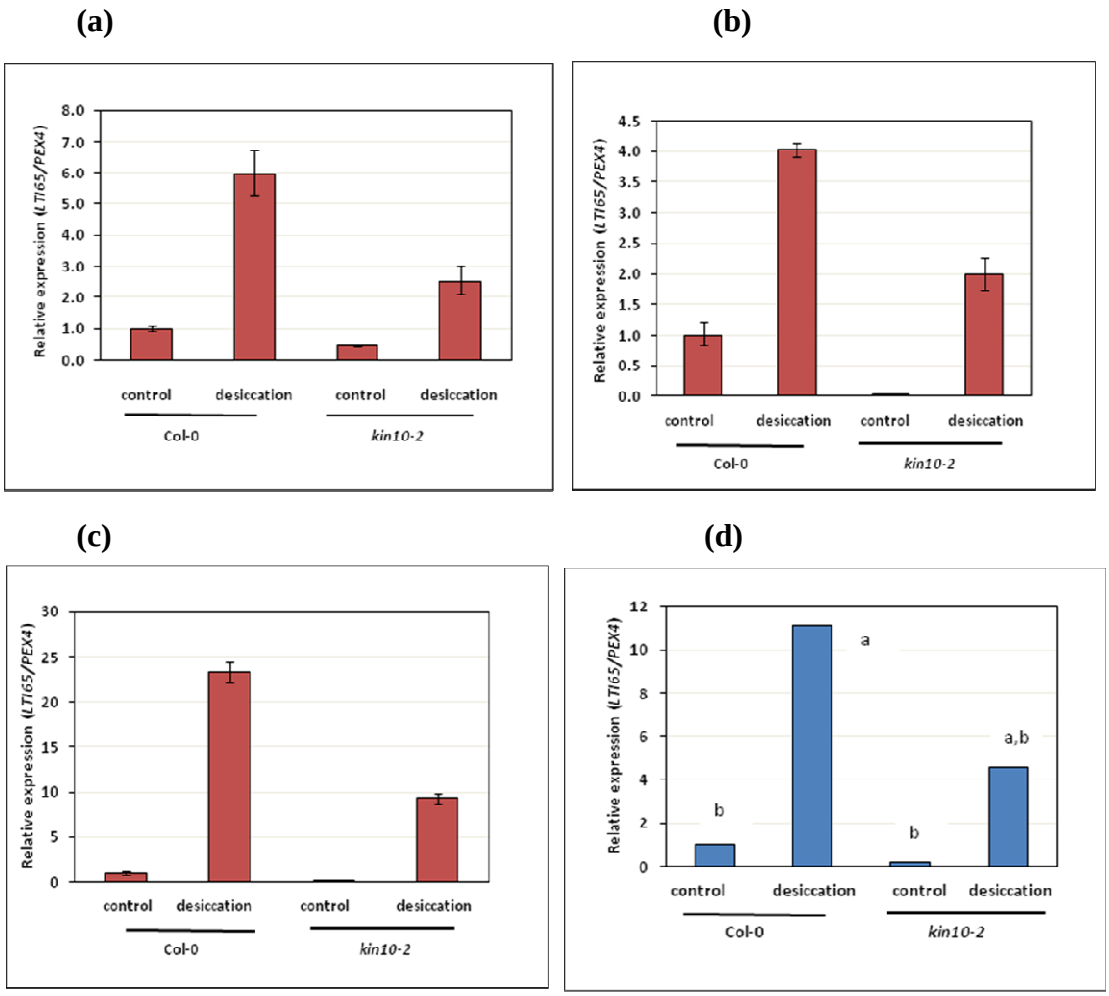

Figure 5.5: Desiccation-induced *LTI65* gene expression in *kin10-2* and Col-0

LTI65 expression in response to desiccation was measured in *kin10-2* mutants compared with Col-0. Seven-day-old seedlings were grown on 0.5X MS media on petri dishes and subjected to water withdrawal by opening the lids for 6h (desiccation) while control plates kept closed (control). The first three histograms (a, b and c- with red bars) represent the gene expression data of three independent biological replicates. Expression is shown after normalisation to *PEX4* in all graphs. The fourth chart (blue bars; d) represents the average of the above three independent biological replicates. Mean average data (in graph d) were analysed using a one-way ANOVA (α=0.05) and pair wise comparisons were made using the Tukey method. Means that do not share a letter are significantly different.

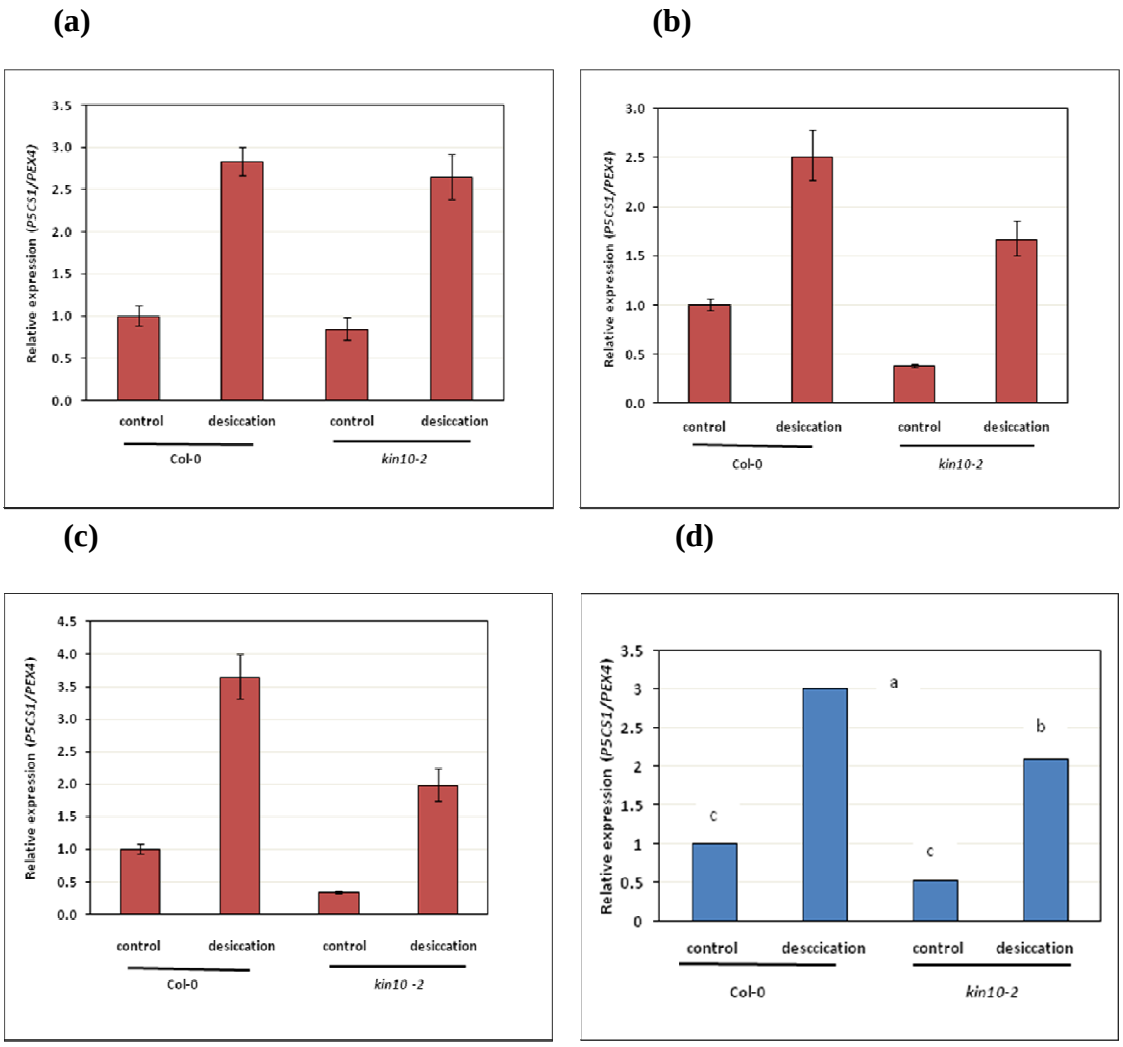

Figure 5.6: Desiccation-induced *P5CS1* gene expression in *kin10-2* and Col-0

P5CS1 gene expression in response to desiccation was measured in *kin10-2* compared with Col-0. Seven-day-old seedlings grown on 0.5X MS media on petri dishes were subjected to water withdrawal by opening the lids for 6 h (desiccation) while control plates were kept closed (control).The first three histograms (a, b and c- with red bars) represent the gene expression data of three independent biological replicates. Expression is shown after normalisation to *PEX4* in all graphs. The fourth chart (blue bars; d) represents the average of the above three independent biological replicates. Mean average data (in graph d) were analysed using a one-way ANOVA (α=0.05) and pair wise comparisons were made using the Tukey method. Means that do not share a letter are significantly different.

5.2.1.2.3 Expression of *COR* genes in response to ABA

The transcriptional response to ABA is impaired in *sfr6* mutants (Boyce et al., 2003, Knight et al., 1999) therefore a possible role for KIN10 in the control of gene expression in response to ABA was investigated. The above gene shown to be mis-regulated in *kin10-2* mutant in response to desiccation which have ABRE in their promoter. Therefore KIN10 might require for ABA mediated gene expression. Seven-day-old seedlings were floated (15-20 seedlings per treatment) in 5 ml of 100 μM ABA or 0.1% ethanol as control in transparent six-well plates for 6 h in the Percival growth chamber (see 2.12.6). Expression of *KIN2* and *P5CS1* was analysed using qRT-PCR and normalised to expression of *PEX4*. Relative expression represents the fold value compared with the Col-0 control sample and calculated as described in the first gene expression results.

KIN2 expression was compared between *kin10-2* and wild type Arabidopsis plants in two independent biological replicate experiments (Figure 5.7 a and b). ABA-induced *KIN2* expression in *kin10-2* in both instances was similar to that of Col-0 and the average difference was not significant ($p<0.07$) between the two plant types (Figure 5.7 d). As the results of two replicate experiments were both very consistent and showed no difference between wild type and mutant, the experiment was not repeated a third time. *P5CS1* gene expression was also tested in the same samples and a similar level of expression observed in *kin10-2* and wild type (Figure 5.8 a and b). Average *P5CS1* gene expression (Figure 5.8c) was not significant between the two plant types ($p<0.10$). Data were analysed using a one-way ANOVA ($\alpha=0.05$) and pairwise comparisons were made using the Tukey method.

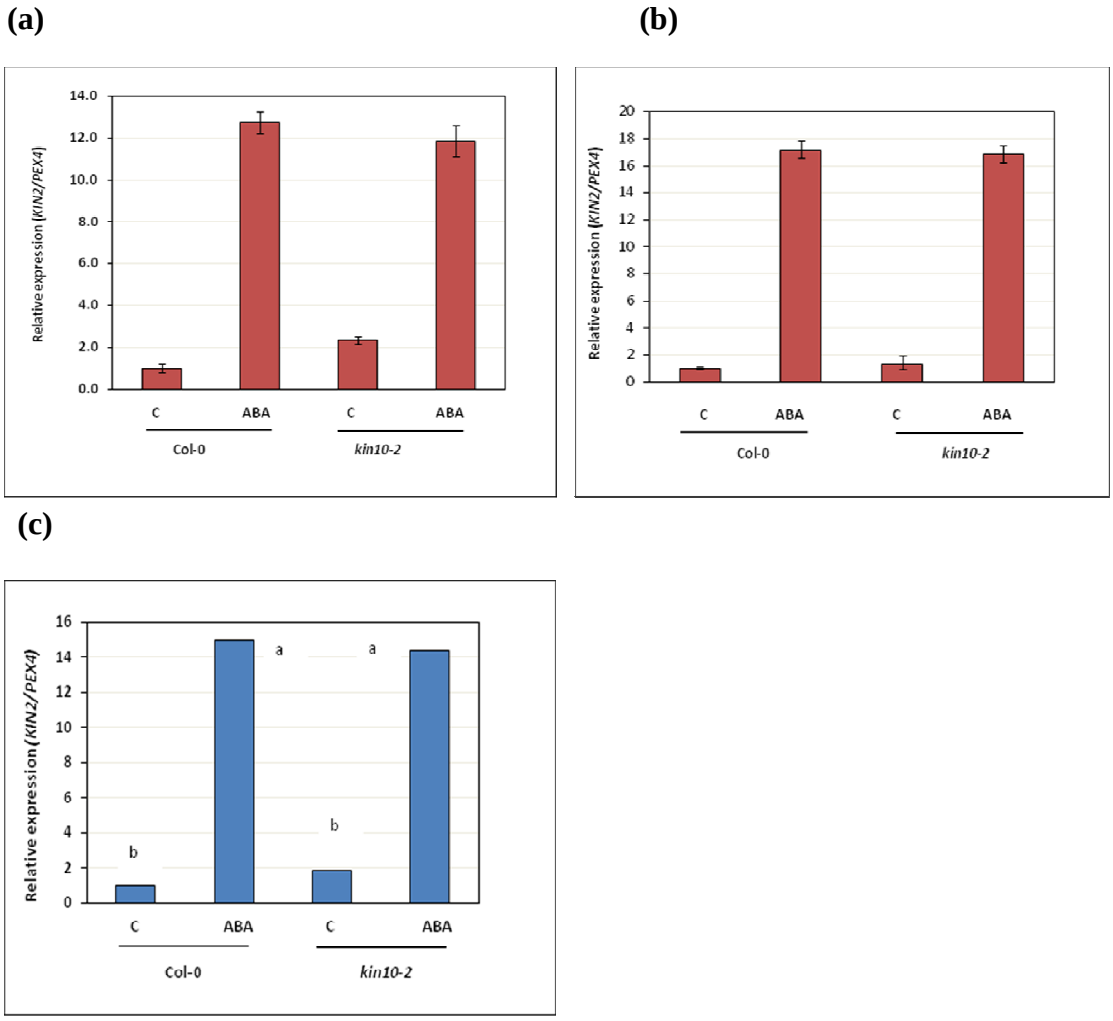

Figure 5.7: *KIN2* expression in response to ABA

KIN2 expression in response to ABA treatment was measured in *kin10-2* mutant compared with Col-0. Seven-day-old seedlings grown on 0.5X MS agar plates were floated on 100 µM of ABA (ABA) or 0.1% ethanol (control) for 6 h in the Percival growth chamber. The first two histograms (a and b with red bars) represent the gene expression data of two independent biological replicates. Expression is shown after normalisation to *PEX4* in all graphs. The third chart (blue bars; c) represents the average of the above two independent biological replicates. Mean average data (in graph c) were analysed using a one-way ANOVA (α=0.05) and pairwise comparisons were made using the Tukey method. Means that do not share a letter are significantly different.

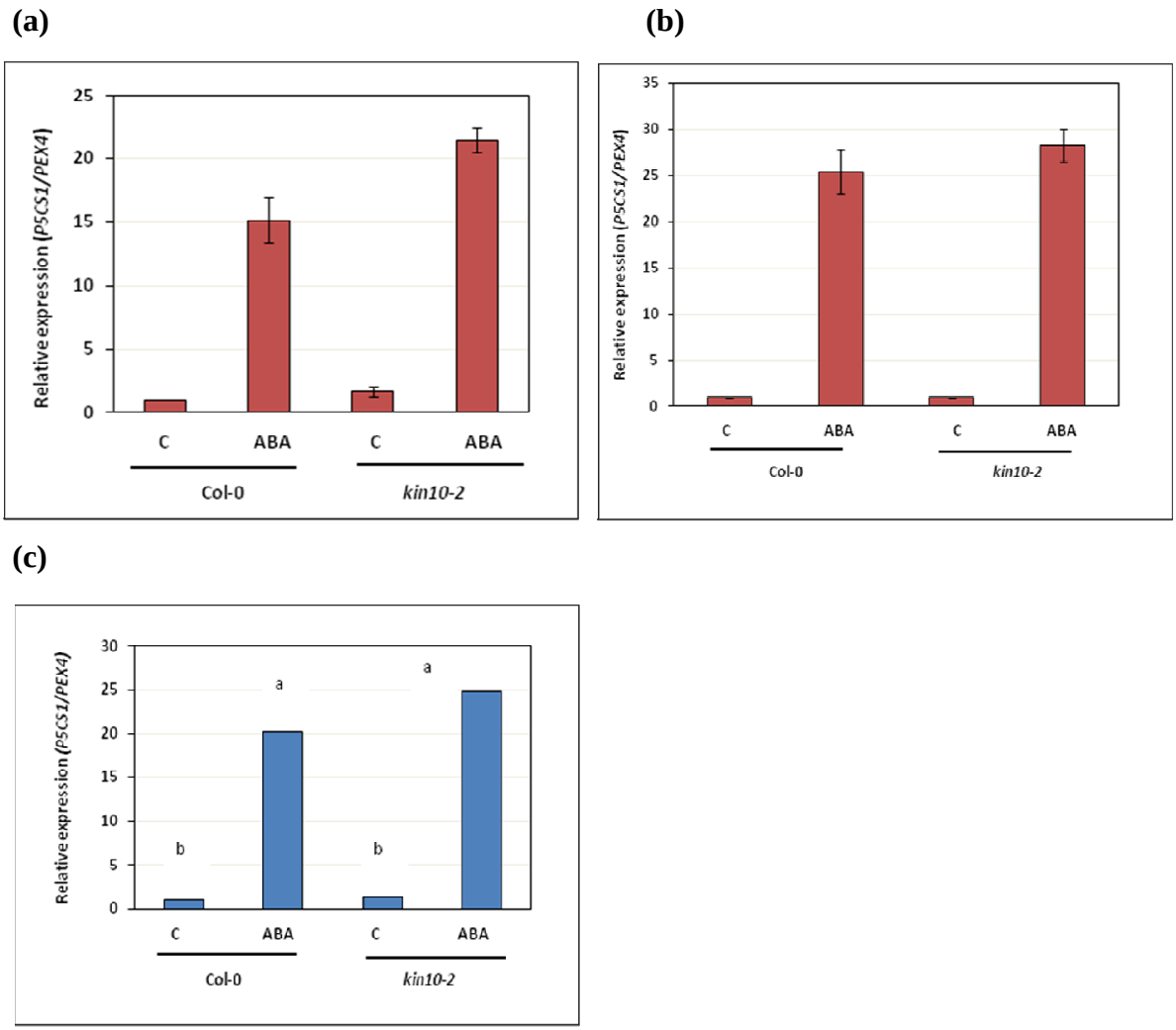

Figure 5.8: *P5CS1* expression in response to ABA

P5CS1 expression in response to ABA treatment was measured in *kin10-2* compared with Col-0. Seven-day-old seedlings grown on 0.5X MS agar plates were floated on 100 µM of ABA (ABA) or 0.1% ethanol (control) for 6 h in the Percival growth chamber. The first two histograms (a and b with red bars) represent the gene expression data of two independent biological replicates. Expression is shown after normalisation to *PEX4* in all graphs. The third chart (blue bars; c) represents the average of the above two independent biological replicates. Mean average data (in graph c) were analysed using a one-way ANOVA (α=0.05) and pair wise comparisons were made using the Tukey method. Means that do not share a letter are significantly different.

5.2.1.3 Expression of UV-C responsive *PR1* gene

A number of genes inducible under UV-C have been shown to require SFR6 for their full expression (Wathugala et al., 2012), therefore the possible role of KIN10 in the regulation of such genes was tested, Seven-day-old seedlings grown on 0.5X MS media on petri dishes were irradiated with 5 kJm^{-2} of UV-C, (wavelength 254 nm) by removing the petri plate lids and placing in a UV cross-linker set to deliver the designated level of energy. Lids were removed from the control plates during the time taken to administer the treatments. Immediately after irradiation, lids were replaced and all plates returned to the growth chamber and samples were taken 24 h after treatment (See 2.12.2). This time point was selected as the peak expression time point for *PR1* (Nawrath et al., 2002). Measurements of gene expression were performed using qRT-PCR and *PR1* gene expression was measured and normalised to expression of At4G26410, a gene with stable expression levels that are not altered by UV treatments (Wathugala et al., 2012). Relative expression represents the fold value compared with the Col-0 control sample and calculated using the ΔΔCT method as described earlier.

UV-inducible *PR1* expression in *kin10-2* was compared with wild type Arabidopsis plants in three independent biological replicate experiments (Figure 5.9 a, b and c) and data revealed that *PR1* gene expression was higher in *kin10-2* in all three instances compared to wild type plants. However, the average gene expression data from three individual experiments showed that the increased level of *PR1* expression in *kin10-2* was not significant compared to Col-0 ($p<0.148$) (Figure 5.9 d). Data were analysed using a one-way ANOVA ($\alpha=0.05$) and pairwise comparisons were made using the Tukey method.

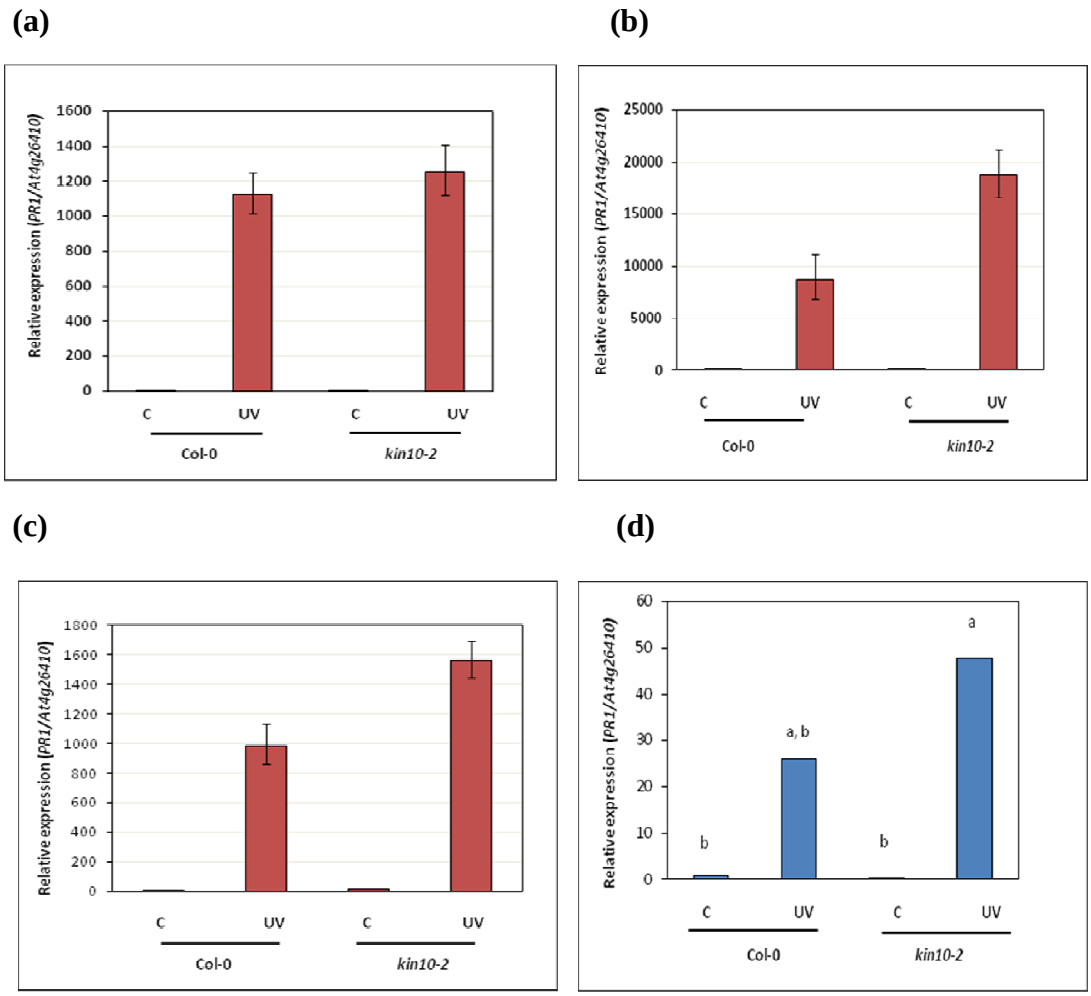

Figure 5.9: UV-induced gene expression in *kin10-2* and Col-0

PR1 expression in response to UV exposure was measured in *kin10-2* compared with Col-0. Seven-day-old seedlings grown on 0.5X MS media on petri dishes and subjected to 5 kJm^{-2} of UV-C (UV) while control plates kept open to air (control) during the time of treatments. The first three histograms (a, b and c- with red bars) represent the gene expression data of three independent biological replicates. Expression is shown after normalisation to *At4g26410* in all graphs. The fourth chart (blue bars; d) represents the average of the above three independent biological replicates. Mean average data (in graph d) were analysed using a one-way ANOVA (α=0.05) and pairwise comparisons were made using the Tukey method. Means that do not share a letter are significantly different.

5.2.2 Complementation of *kin10-2* mutant with wild type *AtKIN10*

To study the effects of KIN10 on stress gene expression, I used only one *kin10* mutant allele in this study due to unavailability of another reliable *kin10* mutant. The other mutant allele originally studied, *Akin10* (*kin10-1*), had shown an apparent conditional phenotype due to the location of the insertion in the mutant and I therefore avoided using it as the second mutant allele in this study. Therefore, to confirm linkage of the observed phenotype with the KIN10 locus, I created KIN10 complemented lines in a *kin10-2* mutant background. *kin10-2* mutant plants were transformed with 35S::HisHA-KIN10 using the floral dip method (see section 2.10.1). A 35S:: HisHA-KIN10 construct was made by Dr. Piers Hemsley by cloning HisHA-KIN10 in to pENTR D-TOPO (see section 2.5.1) and recombining this into pK7WG2 using the Gateway® recombination cloning method (see section 2.5.2).

T_1 plants were screened for the presence of the T-DNA insert in the genomic KIN10 sequence of *kin10-2* and for the presence of the transgene (HisHA-KIN10) (see Appendix A2.3) and lines scoring positive for both of these were grown to the T_2 generation. In the T_2 generation plants were selected that were homozygous for the insertion and scored positively for presence of the transgene. The level of *KIN10* expression was studied in four independent lines that fulfilled these criteria and compared to levels of expression in *kin10-2* `mutant and Col-0. Primers designed for the middle of the *KIN10* transcript, capable of detecting both native and transgenic *KIN10* transcript (see Appendix A2.3) were used to compare the level of *KIN10* expression in *kin10-2* putative complemented lines, *kin10-2* `mutant and Col-0. The four complemented lines expressed *KIN10* (Figure 5.10 a) to a higher level than observed in Col-0 due the use of the 35S promoter. Primers, including a reverse

primer complementary to the 3'UTR of the *KIN10* transcript (downstream of the predicted insertion site) were used to compare the level of native *KIN10* expression in same lines (Figure 5.10 b). Only Col-0 showed detectable *KIN10* expression, (Figure 5.10 b) indicating that all of the putative complemented lines were homozygous for the mutation.

(a) **(b)**

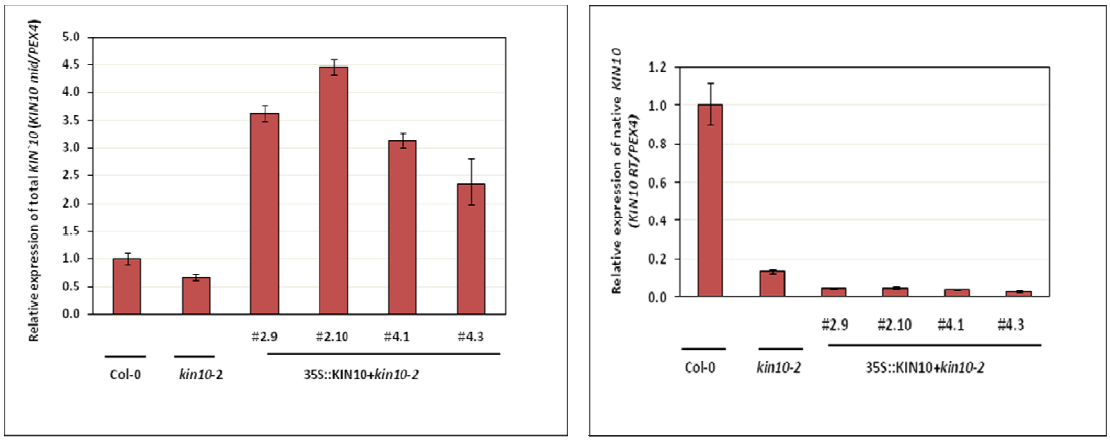

Figure 5.10: *KIN10* expression levels in putative complemented *kin10-2* lines

KIN10 expression in *kin10-2*+35S::HisHA-KIN10 lines were compared with Col-0 and *kin10-2*. Seven-day-old seedlings grown on 0.5X MS agar plates were used. Figure 5.10 (a) represents the level of total *KIN10* expression (detecting both native and transgenic) using primers designed for the middle part of the *KIN10* transcript and primers designed for the untranslated 3' end of the *KIN10* shown in Figure 5.10 (b) shows level of native *KIN10* expression in four complemented lines of *kin10-2*, *kin10-2* `mutant and Col-0. Expression is shown after normalisation to *PEX4*. Relative expression represents the fold value compared with Col-0 control sample and calculated using the ΔΔCT method. Error bars indicate the level of variation between technical replicates within one biological replicate experiment.

5.2.2.1 Protein expression in KIN10 complemented lines

Levels of *KIN10* transcript expression were confirmed in KIN10 complemented lines (Figure 5.10) and KIN10 protein expression in these lines was assayed as described

in section 2.16. Immuno-blot analysis (see section 2.16.5) was conducted using AKIN10 Rabbit polyclonal (primary antibody). Membranes were observed after incubation with a goat anti-rabbit secondary antibody conjugated to HRP to visualize the protein using chemiluminescence (see section 2.16.6) method.

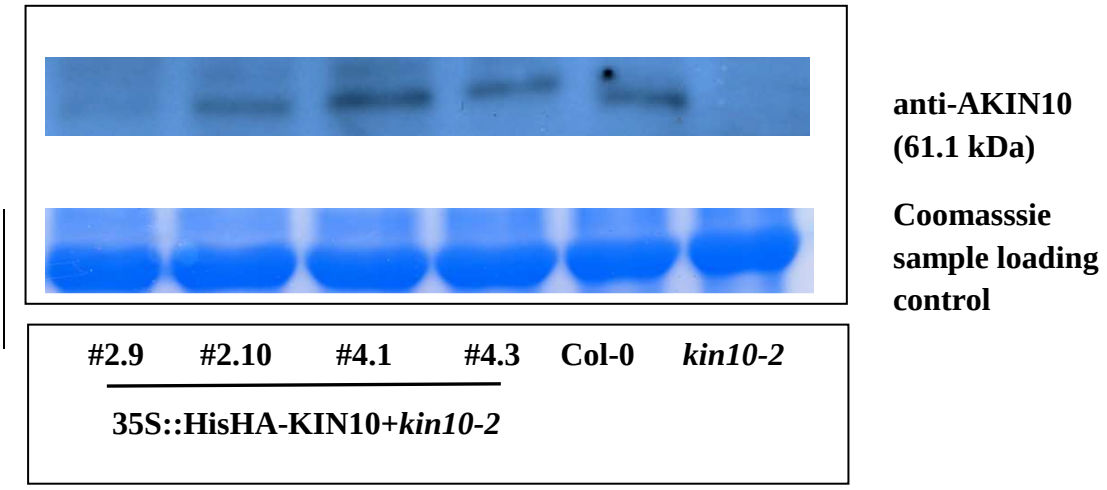

Figure 5.11: Level of KIN10 protein expression in complemented lines

Seven-day-old seedlings (20-25 seedlings) were used to extract protein and 30µl of total lysate (2mg/ml) was loaded onto an SDS gel. The membrane was incubated with AKIN10 rabbit polyclonal primary antibody at 4^0C overnight followed by 2 h secondary antibody binding with goat anti-rabbit HRP, both at 1:2000 dilution in 5% milk solution. Proteins were visualized using chemiluminescence and the membrane was observed under a Photon Counting camera using Photek Image32 software.

KIN10 protein expression in the four putative complemented lines (*kin10-2* + 35S::HisHA-KIN10) compared with Col-0 and *kin10-2* (Figure 5.11). No KIN10 expression was observed in the *kin10-2* knockout line whereas all four complemented *kin10-2* lines expressed KIN10 to levels that were similar to wild type but varied between lines. Line #2.9 demonstrated the lowest level of expression, lower than Col-0 and the highest level of expression was observed in line #4.1.

These data did not correlate closely with *KIN10* transcript expression (Figure 5.10), however, all four lines of *kin10-2* complementations clearly expressed KIN10 protein, unlike *kin10-2* mutants.

5.2.2.2 Dark-induced gene expression in KIN10 complemented lines

Experiments were carried out using seven-day-old seedlings grown on 0.5x MS media on petri dishes and subjected to 6 h in dark conditions by wrapping individual plates in two layers of aluminium foil within the light cycle in the Percival growth chamber. Control plates were kept under the same conditions in the Percival by exposing to light conditions (see 2.12.3). Expression of the dark-inducible gene *DIN6* was analysed using qRT-PCR and normalised to expression of *PEX4*. Relative expression represents the fold value compared with Col-0 control sample and calculated using the ΔΔCT method as described early in this chapter.

Dark-inducible *DIN6* expression in four confirmed KIN10 complemented lines was compared with wild type, and *kin10-2* mutants in three independent biological replicate experiments (Figure 5.12 a, b and c). Increased levels of *DIN6* gene expression under dark stress were observed in all four complemented lines compared to *kin10-2* in three biological replicate experiments and *DIN6* expression in complemented lines was similar to the level of *DIN6* expression in wild type plants. The average values of relative expression of *DIN6* in three independent biological replicates is presented in Figure 5.12 d and data were analysed using a one-way ANOVA (α=0.05) and pairwise comparisons were performed using the Tukey method. Average gene expression data from three individual experiments confirm that *DIN6* expression in dark was significantly high in three out of four

complemented lines compared to *kin10-2* (Figure 5.12 d) but not significantly different compared to wild type (P<0.020).

Therefore this shows the DIN6 phenotype of *kin10*-2 mutants could be restored to wildtype levels by complementation with the KIN10 gene. This proves the phenotype observed in the mutant can actually be attributed to the KIN10 gene.

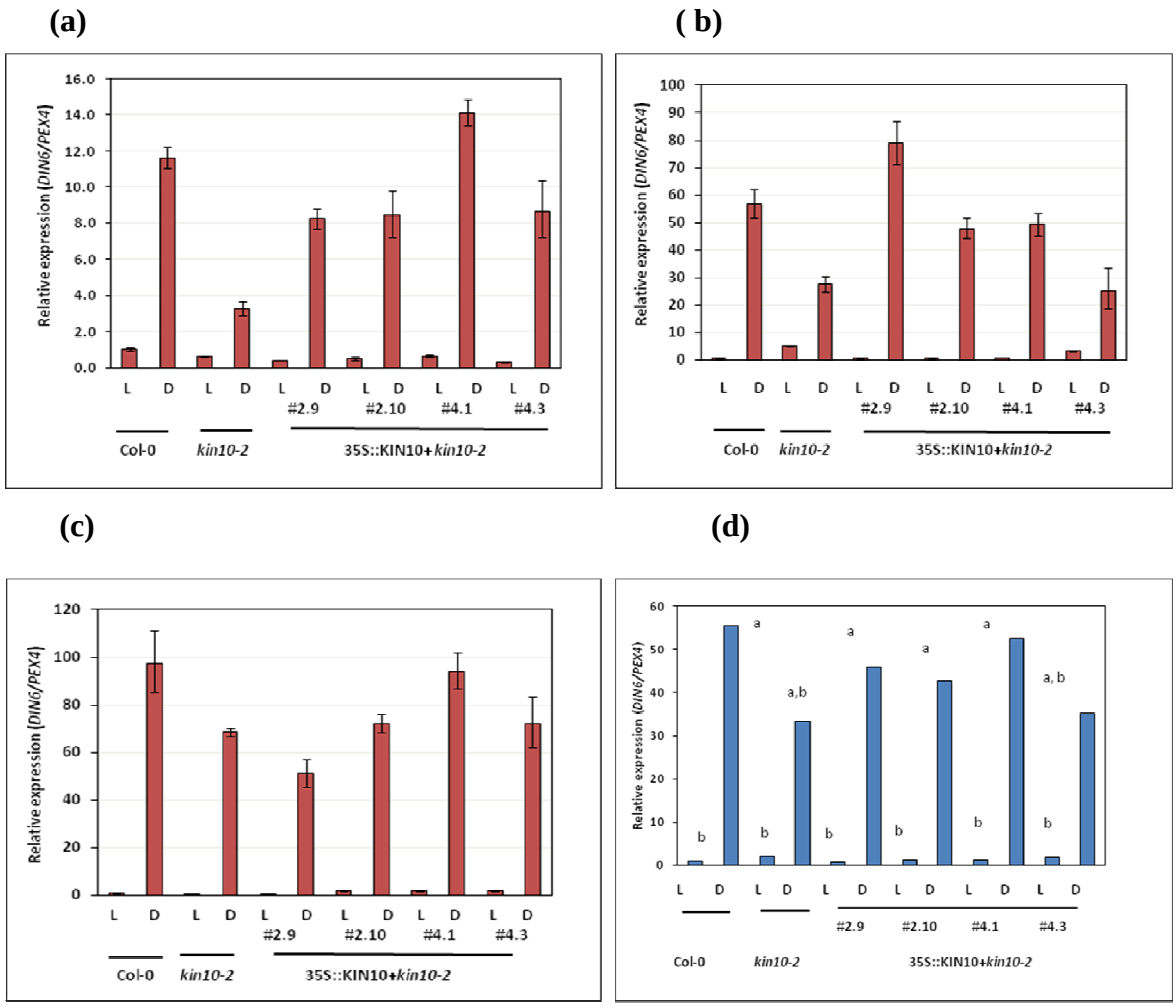

Figure 5.12: Dark-induced stress gene expression in *kin10-2* complemented lines

DIN6 expression in response to darkness was measured in KIN10 complemented lines compared with Col-0 and *kin10-2*. Seven-day-old seedlings grown on 0.5x MS media on petri dishes were subjected to 6 h dark conditions (D) by wrapping in two layers of aluminium foil and control plates (L) were kept unwrapped in the growth chamber. The first three histograms (a, b and c- with red bars) represent the gene expression data of three

independent biological replicates. Error bars indicate the level of variation between technical replicates within one biological replicate experiment. The fourth chart (blue bars; d) represents the average of the above three independent biological replicates. Mean average data (in graph d) were analysed using a one-way ANOVA (α=0.05) and pairwise comparisons were made using the Tukey method. Means that do not share a letter are significantly different.

5.2.2.3 Desiccation-induced gene expression in KIN10 complemented lines

Water withdrawal experiments were conducted to study desiccation-induced gene expression using seven-day-old seedlings grown on 0.5x MS media on petri dishes and subjected to water withdrawal by opening the lids, thereby exposing the seedlings to growth conditions in the Percival chamber. Desiccation-treated plates were left open in the growth chamber for 6 h during the light cycle with no humidity control while keeping the control plates closed under the same conditions (see 2.12.4).

Expression of *KIN2* in response to desiccation was analysed using qRT-PCR and normalised to expression of *PEX 4* gene. Relative expression represents the fold value compared with Col-0 control sample and calculated using the ΔΔCT method, as described earlier. Desiccation-inducible *KIN2* expression in four KIN10 complement lines was compared with wild type and *kin10-2* mutants of Arabidopsis plants in three independent biological replicate experiments (Figure 5.13 a, b and c). Higher levels of *KIN2* gene expression in all four lines of *kin10-2*+35S::HisHA-KIN10 were observed compared to *kin10-2* in all three individual replicate experiments and those levels were even higher than those seen in Col-0. Even though there was an apparent difference in *KIN2* expression between Col-0 and *kin10-2* it was not significant (Figure 5.13 d).

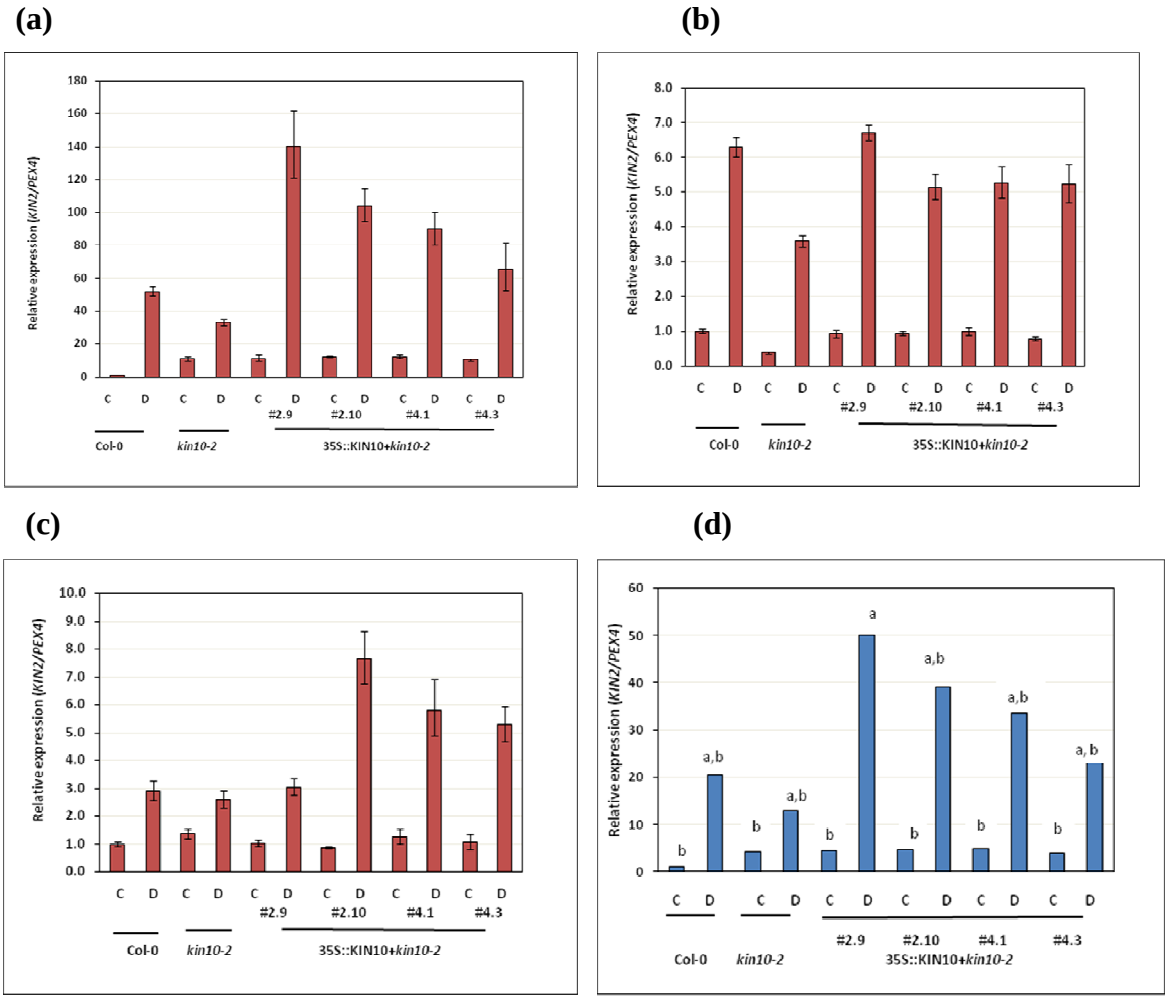

Figure 5.13: Desiccation-induced *KIN2* gene expression in *kin10-2* complemented lines

KIN2 expression in response to desiccation was measured in KIN10 complemented lines compared with Col-0 and *kin10-2*. Seven-day-old seedlings were grown on 0.5x MS medium on petri dishes were subjected to 6 h water withdrawal/desiccation (D) by opening the lids and control plates (C) were kept unopened in the growth chamber. The first three histograms (a, b and c- with red bars) represent the gene expression data of three independent biological replicates. Expression is shown after normalisation to *PEX4* in all graphs. The fourth chart (blue bars; d) represents the average of the above three independent biological replicates. Mean average data (in graph d) were analysed using a one-way ANOVA (α=0.05) and pair wise comparisons were made using the Tukey method. Means that do not share a letter are significantly different.

Similarly, the average gene expression of *KIN2* in four complemented lines was not highly significant compared to either Col-0 or *kin10-2* mutant ($p<0.693$) (Figure 5.13d). Data were analysed using a one-way ANOVA ($\alpha=0.05$) and pairwise comparisons were performed using the Tukey method. However the trend was that complementation appeared to restore KIN2 expression to wild type levels.

In summary, these experiments showed that KIN10 was required for full expression of genes in response to some stress conditions such as desiccation and dark, but not all, of the conditions that require SFR6 particularly under cold and UV stress conditions. The experiments also indicated that the effects of loss of KIN10 were not as severe as those attributable to loss of SFR6.

5.2.3 Epistatic analysis using a *sfr6-1kin10-2* double mutant

The above experiments established that loss of KIN10 results in middle version of some of the same transcriptional defects associated with loss of SFR6. The following experiments were designed to test whether one mutation was epistatic to the other, by examining whether the effect of combining both mutation in one plant was additive.

5.2.3 1 Selection of double mutant lines of *sfr6-1kin10-2*

To test the second hypothesis proposed in this chapter, that KIN10 and SFR6 act in the same pathway leading to stress gene expression, I produced a *sfr6*-1*kin10-2* double mutant to be used in epistatic analysis.

The homozygous *sfr6-1* mutant was crossed with *kin10-2* (the pollen donor*)* and the F_1 generation was tested for the presence of the T-DNA insertion in *KIN10* (see Appendix A2.3 for primers). Three successful crosses were used to obtain F_2 seeds

and this generation was tested for the absence of native genomic KIN10 and the presence of the T-DNA insertion using the same set of primers described above (i.e. confirmation of homozygosity for the insertion). Finally, F_3 plant lines fulfilling the above requirements were screened to obtain lines homozygous for the *sfr6-1* mutation. Plants were genotyped using a TaqMan allelic discrimination assay to identify the SNP associated with *sfr6-1* (see Appendix A2.3) using Applied Biosystems 7300 machine (see section 2.10.3).

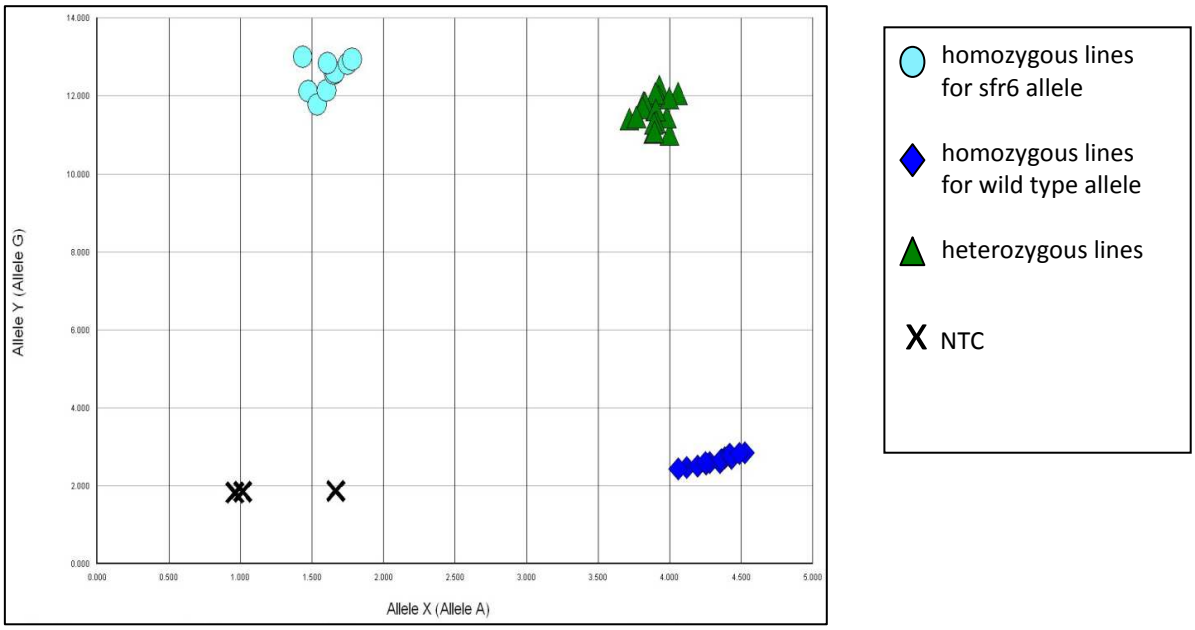

Figure 5.14: Results of allelic discrimination assay of *sfr6-1kin10-2* double mutant lines

Genomic DNA was extracted from leaves of three-week-old plants. Three technical replicates were used for each sample. Water was used as non-template control (NTC) along with two positive controls of Col-0 and *sfr6-1* mutant. The graph represents data corresponding to the selection of two lines that were identified as homozygous for *sfr6-1*. The allelic discrimination plot clearly indicates the homozygotes for each allele, blue circles for allele Y (*sfr6*), diamond shapes for allele X (wild type) and the heterozygotes (green triangles) for the presence of both alleles.

Results of the allelic discrimination assay used to select two homozygous lines for the *sfr6-1* mutation from a single original cross are presented in Figure 5.14. The same procedure was followed to select a third homozygous line but using different lines originating from a separate original cross. The allelic discrimination plot clearly indicated (Figure 5.14) that homozygotes for allele Y (*sfr6*) in blue circles and homozygotes for allele X (wild type) in blue diamond shapes. Further heterozygote lines displaying both allele forms are indicated by green coloured triangles.

5.2.3.2 Dark-inducible gene expression in *sfr6-1kin10-2* double mutant lines

In this experiment I attempted to investigate whether the addition of the *kin10-2* mutation would further diminish the level of dark-inducible gene expression in the *sfr6-1* background. For this, dark gene expression experiments were carried out using seven-day-old seedlings grown on 0.5X MS media on petri dishes and subjected to 6 h dark conditions by wrapping individual plates in two layers of aluminium foil during the light cycle in the Percival chamber. Control plates were kept under the same conditions in the chamber by exposing to light (see 2.12.3).

Expression of *DIN6* in response to darkness was analysed using qRT-PCR and normalised to expression of *PEX 4*. Relative expression represents the fold value compared with Col-0 control sample and calculated using the ΔΔCT method, and the error bars in each biological replicate represent RQ_{MIN} and RQ_{MAX} and constitute the acceptable error level for a 95% confidence level according to Student's t test. *DIN6* expression was compared in three lines of *sfr6 kin10-2* the double mutant, wild type and the two single mutants of Arabidopsis plants in three independent biological replicate experiments (Figure 5.15 a, b and c). *DIN6* gene expression in *sfr6 kin10-2* double mutants was lower than observed in wild type and this was observed in all

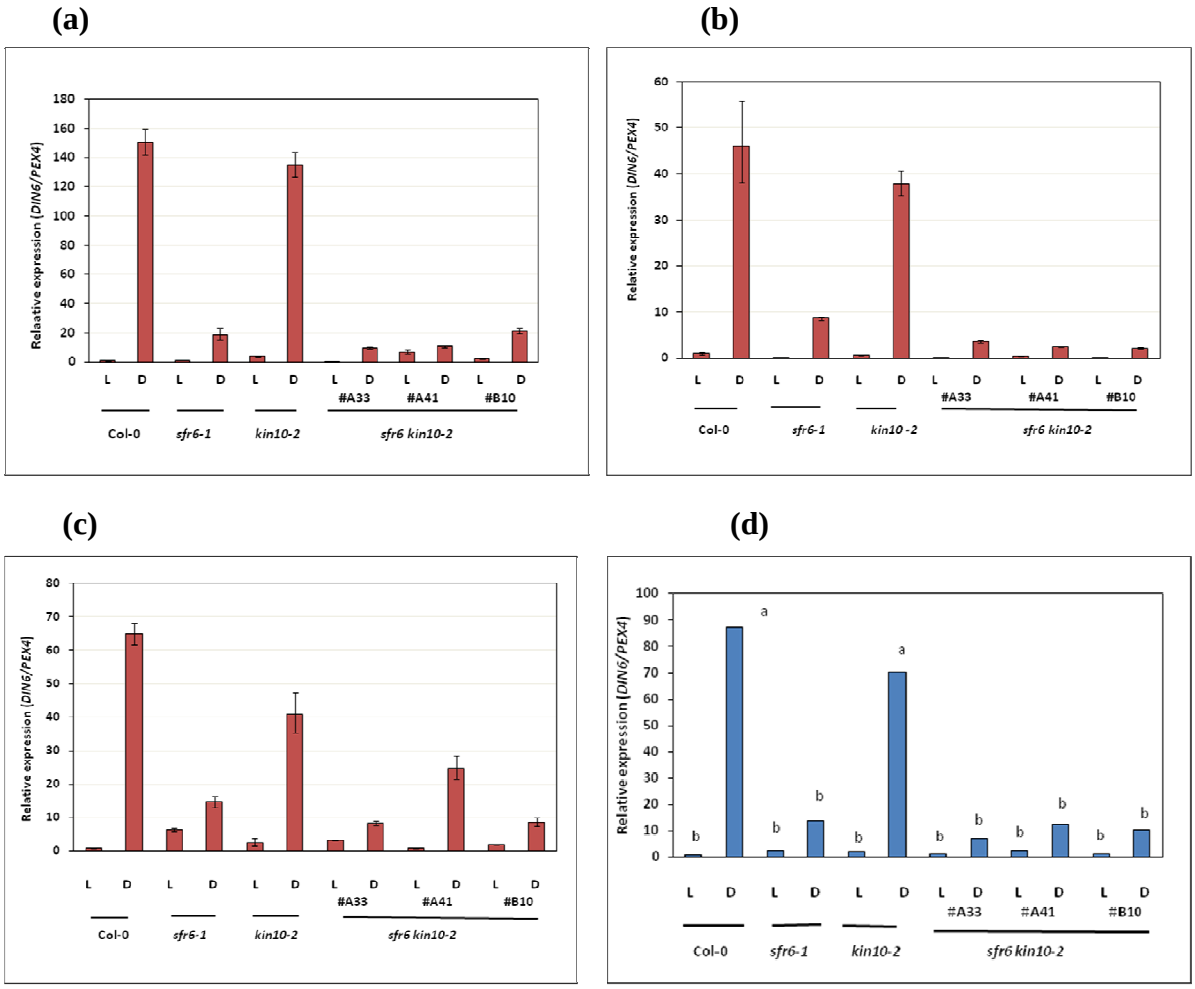

Figure 5.15: Dark-induced stress gene expression in *sfr6-1kin10-2* lines

DIN6 expression in response to darkness was measured in three lines of *sfr6kin10-2* compared with Col-0, *sfr6* and *kin10-2*. Seven-day-old seedlings were grown on 0.5X MS medium on petri dishes and subjected to 6 h dark conditions (D) by wrapping in aluminium foil. Control plates (L) were kept under the same conditions in the Percival by exposing to the light conditions. The first three histograms (a, b and c- with red bars) represent the gene expression data of three independent biological replicates. Error bars indicate the level of variation between technical replicates within one biological replicate experiment. The fourth chart (blue bars; d) represents the average of the above three independent biological replicates. Mean average data (in graph d) were analysed using a one-way ANOVA (α=0.05) and pair wise comparisons were made using the Tukey method. Means that do not share a letter are significantly different.

three biological replicate experiments. Average gene expression data from three individual experiments showed significant differences between ($p<0.001$) all three lines of *sfr6kin10-2* compared with *kin10-2* and wild type but no significant difference compared with the *sfr6-1* mutant (Figure 5.15 d). Data were analysed using a one-way ANOVA ($\alpha=0.05$) and pairwise comparisons were performed using the Tukey method.

5.2.3.3 Desiccation-induced gene expression in *sfr6-1kin10-2* double mutant lines

This experiment was designed to investigate whether addition of the *kin10-2* mutation would increase the effect of the *sfr6-1* mutation on desiccation-induced gene expression. Experiments were carried out using seven-day-old seedlings grown on 0.5X MS medium on petri dishes and subjected to water loss by opening the lids thereby exposing the seedlings to growth conditions in the Percival growth chamber. Plates were left open in the growth chamber for 6 h during the light cycle with no humidity control while keeping the control plates closed under the same conditions (see 2.12.4).

Expression of the drought-inducible *KIN2* gene was analysed using qRT-PCR and normalised to expression of *PEX4* gene. Relative expression was calculated as explained above. Desiccation-inducible *KIN2* expression in three lines of *sfr6-1kin10-2* was compared with wild type, *sfr6-1* and *kin10-2* mutants of Arabidopsis plants in three independent biological replicate experiments (Figure 5.16 a, b and c). Greatly reduced levels of *KIN2* gene expression in three lines of *sfr6-1kin10-2* were observed in all three individual replicate experiments compared to *kin10-2* but levels were similar to those observed in *sfr6-1*. Further average gene expression data from three individual experiments was highly significant between ($p<0.001$) all three lines of

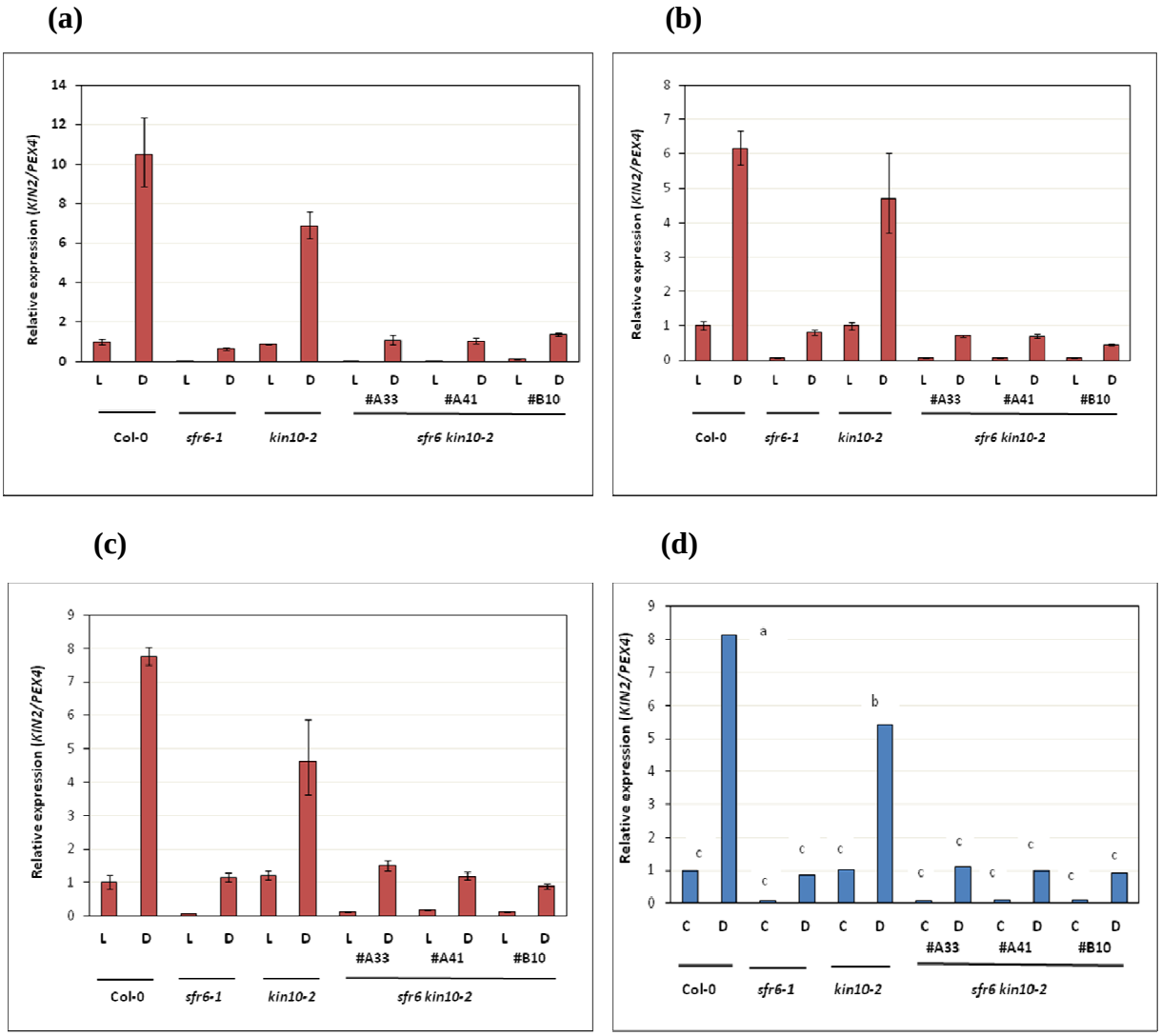

Figure 5.16: Desiccation-induced *KIN2* gene expression in *sfr6-1kin10-2*

KIN2 expression in response to desiccation was measured in three lines of *sfr6-1kin10-2* double mutant compared with Col-0, *sfr6* and *kin10-2*. Seven-day-old seedlings were grown on 0.5X MS medium on petri dishes were subjected to 6 h water withdrawal/desiccation (D) by opening the lids and control plates (C) were kept unopened in the growth chamber. The first three histograms (a, b and c- with red bars) represent the gene expression data of three independent biological replicates. Expression is shown after normalisation to *PEX4* in all graphs. The fourth chart (blue bars; d) represents the average of the above three independent biological replicates. Mean average data (in graph d) were analysed using a one-way ANOVA (α=0.05) and pair wise comparisons were made using the Tukey method. Means that do not share a letter are significantly different.

sfr6-1kin10-2 compared with *kin10-2* and wild type however not significant compared with the *sfr6-1* mutant (Figure 5.16 d). Data were analysed using a one-way ANOVA (α=0.05) and pairwise comparisons were performed using the Tukey method.

5.2.3.4 Response of *sfr6-1kin10-2* double mutants to drought stress

Level of desiccation/drought-induced gene expression, *KIN2* were reduced in all three lines of the *sfr6-1kin10-2* double mutant, but were not lower than those seen in the single *sfr6-1* mutant. Reduced levels of desiccation–induced *KIN2* gene expression are strongly correlated with reduced levels of drought tolerance (reported in chapter 3 in section 3.2.31). The purpose of this experiment was to check the effect of double mutation is not additive *i.e* drought tolerance in the double mutant, showed a similar pattern to that observed in the single *sfr6-1* mutant as seen in *KIN2* gene expression.

Therefore, a drought tolerance assay was conducted with wild type, single mutants of *sfr6-1* and *kin10-2* and three lines of *sfr6-1kin10-2* double mutants. Drought tolerance assays were performed using seedlings grown on peat plugs and maintained in short days for 25 d post-germination. Plants were subjected to water withdrawal for 14 days (after which approximately 50% of wild type plants showed a wilting appearance) and then re-watered. The number of plants surviving out of ten plants used in each experiment and exhibiting re-growth with green meristems was assessed after a further 10 days (see materials and methods 2.15.4). Average data from three separate biological replicate experiments is presented in Figure 5.17.

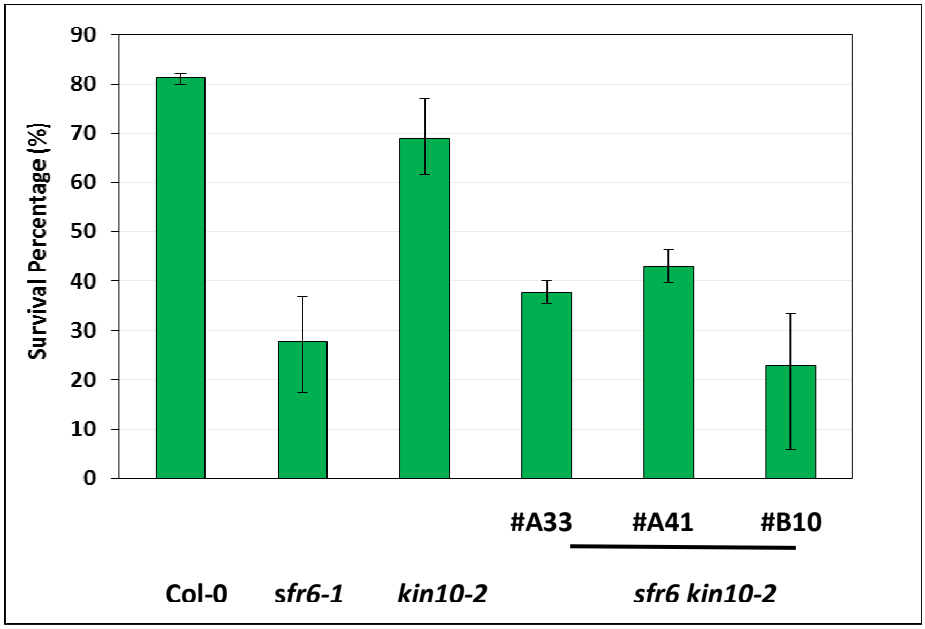

Figure 5.17: Level of drought tolerance in *sfr6-1kin10-2* mutants

The average of three survival percentages from three separate biological experiments (replicates) conducted with ten plants in each experiment is shown in the above histogram.Twenty five day-old plants were subjected to water withdrawal for 14 days, re-watered and the number of plants surviving on the twelfth day after re-watering was recorded. Error bars shown represent standard error (±SE) calculated from arcsine transformed values as appropriate for proportional data and indicate the level of variation between biological replicate experiments. Non-overlapping error bars denote means that are significantly different ($P < 0.001$).

These data demonstrate the reduced tolerance in all three lines of *sfr6-1kin10-2* mutants and it is significantly different ($\alpha=0.05$) compared to Col-0 and *kin10-2* mutant. Average tolerance data shows no significant difference between the three lines of double mutants and to *sfr6-1* (Figure 5.17). This is further supported by the Figure 5.18, a representative picture taken from the second drought tolerance experiment in this study. Perhaps surprisingly, the *kin10-2* single mutant showed no reduction in desiccation tolerance compared to wild type, despite its reduced levels

of desiccation-induced *KIN2* expression. It seems most likely that the reduction in *KIN2* expression observed in *kin10-2* was insufficient to exert a significant effect on tolerance though *kin10-2* shows reduced tolerance compared to wild type. However in neither case (expression or tolerance) were the effects of the two mutations in response to desiccation additive.

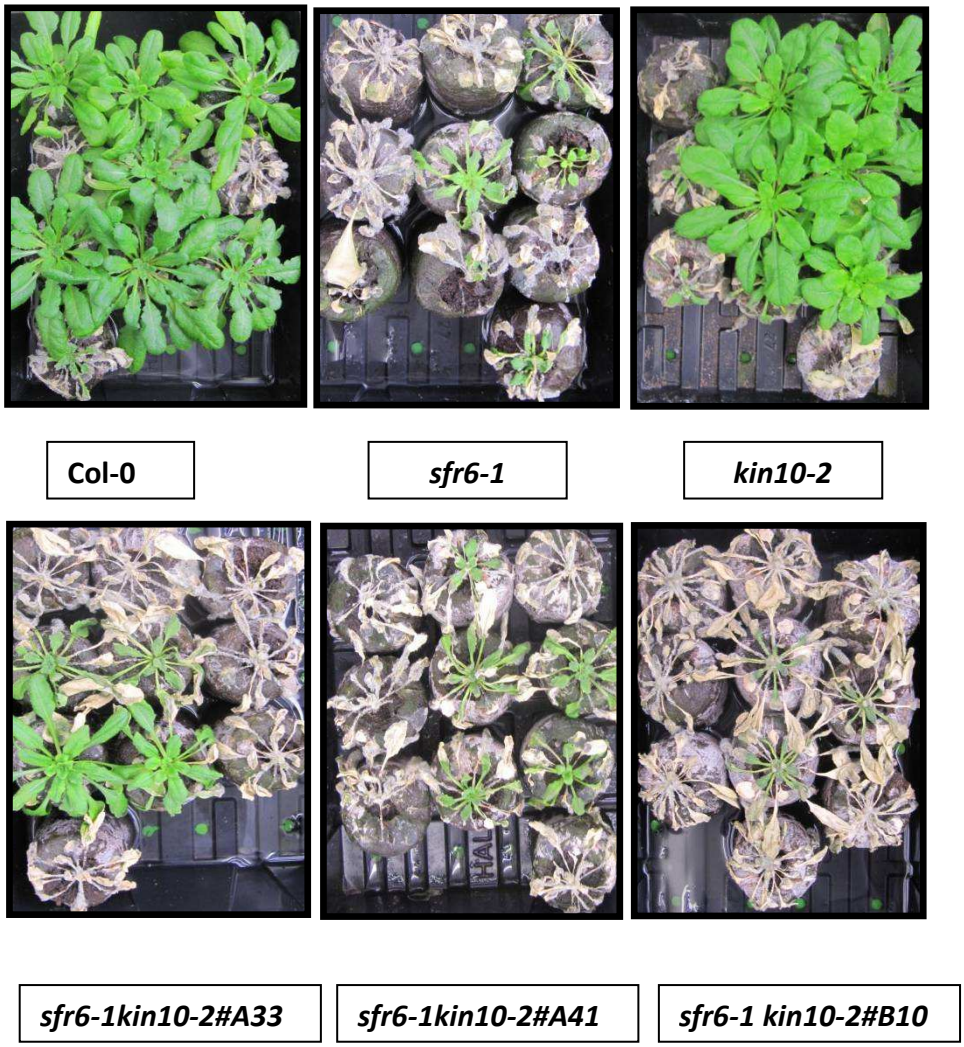

Figure 5.18: Sensitivity of *sfr6-1kin10-2* double mutants to drought conditions

Representative pictures of each plant type selected from the second drought tolerance assay are presented here. Twenty five-day-old plants grown on peat plugs were subjected to withdrawal of water for 14 days (after which approximately 50% of wild type plants showed a wilting appearance) and then re-watered. The number of plants surviving and exhibiting re-growth was assessed after a further 10 days and photographed.

5.2.3.5 Response of *sfr6-1kin10-2* double mutant to dark-induced starvation stress

To study whether the reduced level of gene expression under dark conditions correlates with reduced level of dark-induced starvation tolerance, experiments were conducted using the plant lines described above. Seven-day-old seedlings grown on 0.5×MS agar plates were covered in two layers of foil for 14 days to provide dark conditions whilst keeping control samples unwrapped. All plates were transferred to a Percival growth chamber (see section 2.15.5) and after 14 days of dark plates were unwrapped and returned back to the same conditions in the Percival. Number of plants surviving and exhibiting re-growth was assessed after a 3 days of normal light:dark cycle in the Percival growth chamber. Average data from two separate biological replicate experiments are presented in Figure 5.19.

Average data of these experiments demonstrate that reduced level of starvation tolerance in all three lines of *sfr6-1kin10-2* mutants and it is significantly different (α=0.05) compared to Col-0 and *kin10-2* mutant. Data showed that there was no significant difference between the three lines of double mutants and *sfr6-1* (Figure 5.19). Figure 5.20, a representative picture taken from second starvation tolerance experiment in this study showed the appearance of the plants after recovery from dark-induced starvation. As seen in the previous experiments with regard to desiccation, there was no evidence that the effects of the two mutations were additive.

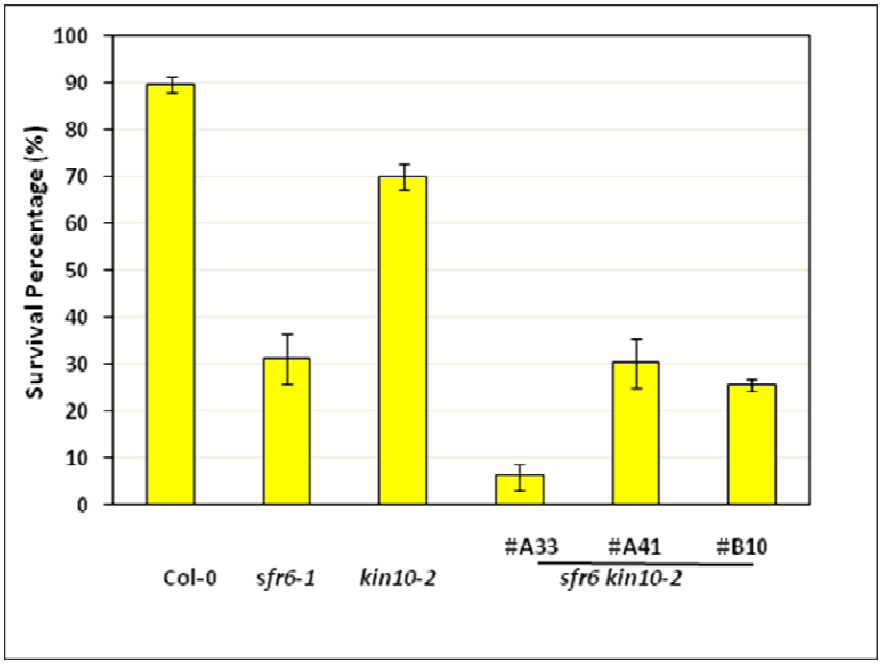

Figure 5.19: Level of dark-induced starvation tolerance in *sfr6-1kin10-2* mutants

The average of survival percentages from two separate biological experiments (replicates) conducted on 0.5×MS agar plates is shown in the above histogram. Seven-day-old seedlings on plates were covered in two layers of foil for 14 days and then plates were unwrapped and returned to the Percival growth chamber and the number of plants surviving and exhibiting re-growth was recorded after 3 days. Error bars shown represent standard error (±SE) calculated from arcsine transformed values as appropriate for proportional data and indicate the level of variation between biological replicate experiments. Non-overlapping error bars denote means that are significantly different ($P < 0.001$).

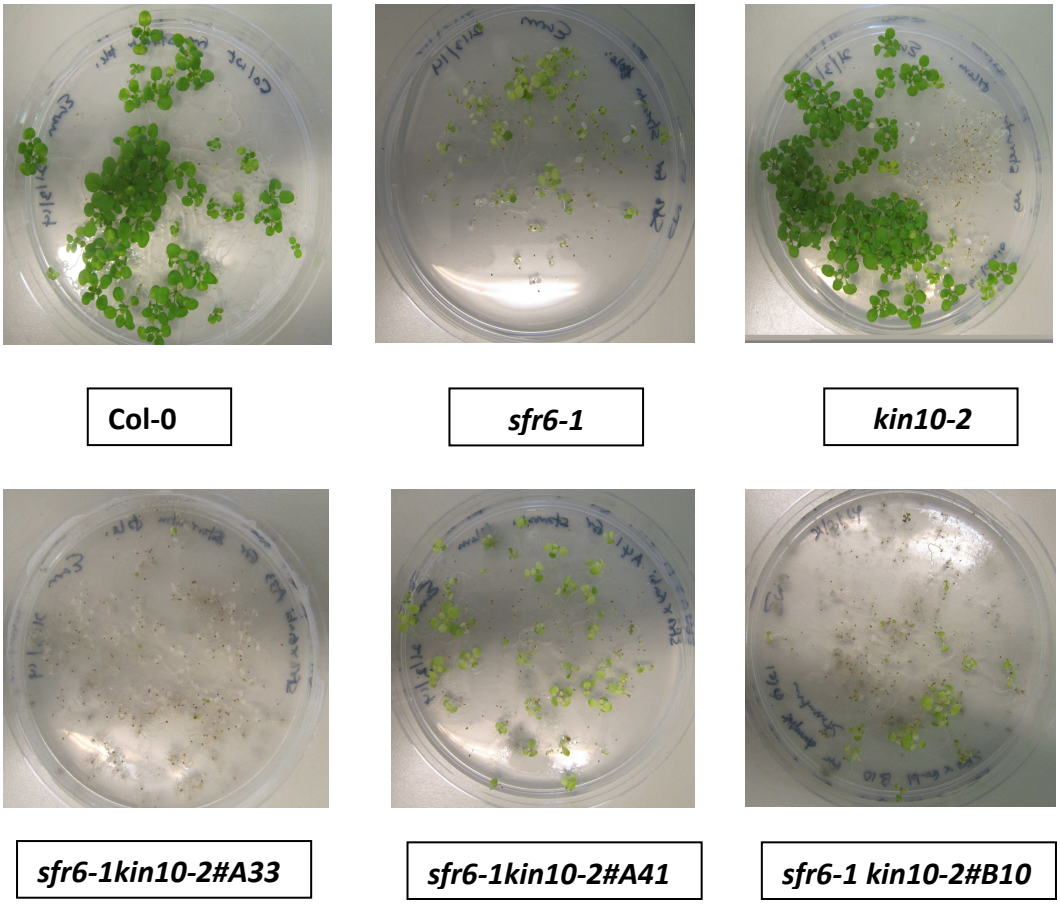

Figure 5.20: Sensitivity of *sfr6-1kin10-2* double mutants under dark-induced starvation conditions

Representative pictures of each plant type selected from the second starvation tolerance assay are presented here. Seven-day-old seedlings grown on 0.5×MS agar plates were covered in two layers of foil for 14 days to provide dark conditions and kept in Percival growth chamber. After 14 days plates were unwrapped and returned back to same conditions in the Percival and number of plants surviving and exhibiting re-growth was assessed after a further 3 days and photographed.

In summary both gene expression and tolerance data under desiccation-induced drought and dark-induced starvation conditions demonstrated that effect of *sfr6-1* and *kin10-2* double mutant were not additive, indicating that both genes were likely to act on the same pathway.

5.2.4 Overexpression of KIN10 in wild type and *sfr6* mutant backgrounds

5.2.4.1 Selection of KIN10 overexpression lines in Col-0 and *sfr6-1* backgrounds

Use of KIN10 overexpressing lines in wild type and *sfr6-1* mutant backgrounds formed the basis of the second approach to test my second hypothesis *i.e* KIN10 and SFR6 acts on the same pathway leading to expression of stress genes. The aim of these experiments was also to test the order in which KIN10 and SFR6 may act on the pathway. Baena-Gonzalez et al. (2007) showed that plants (leaves and mesophyll cells) overexpressing KIN10 exhibit higher level of stress gene expression compared to wild type, especially dark-induced genes like *DIN1* and *DIN6*, specifically in the absence of stress. Therefore it was of interest to study the behaviour of *sfr6-1* mutants overexpressing KIN10 to study whether they would exhibit increased expression of stress genes in the absence of stress. Equal increases in stress gene expression in response to KIN10 overexpression in both backgrounds would signify that SFR6 is not required for this particular function of KIN10. Lack of effect of overexpression of KIN10 in *sfr6-1* mutants would indicate that SFR6 is essential for KIN10 to perform its function.

Col-0 and *sfr6-1* mutant plants were transformed with an N-terminal fusion of KIN10 with His and HA epitope tags (35S::HisHA-KIN10), the same vector used to create KIN10 complemented lines (see sections 2.5.1 and 2.5.2) under the control of the constitutive 35S promoter, using the floral dip method (see section 2.10.1) and kanamycin resistant transformants were selected (see section 2.10.1.4). Putative T_1 transformants were screened for the presence of the transgene (HisHAKIN10) as described in section 5.2.2 and 5.2.3 and seeds collected from lines that scored positive in Col-0 and *sfr6-1* backgrounds. T_2 plants were tested for the expression of *KIN10* using seven-day-old seedlings grown on 0.5X MS medium on petri dishes

with primers designed for the fifth and sixth introns of KIN10 transcript (see Appendix A2.3 for the primers KIN10-mid-RT F/R) to detect both native and transgene KIN10. Results showed that *KIN10* expression was elevated in all putative transformants with a Col-0 background but that none of *sfr6-1* background putative transformants expressed elevated levels of *KIN10* (Figure 5.21 a and b). Repeated attempts were made to assay for the presence of a full length transcript generated from the construct but all confirmed that transcripts from the KIN10 transgene were either not present in the putative transformants (despite showing basta resistance), or were truncated.

Following failure to transform *sfr6-1* plants with 35S::HisHA-KIN10, *sfr6-1* mutant plants were crossed with two independent wild type 35S:: KIN10 transformants created as described above. Col-0 wild type lines #6 and #11 overexpressing HisHA-KIN10 were used to cross with *sfr6-1* mutant plants, as they exhibited the highest and lowest levels of *KIN10* expression respectively amongst the wild type transformants (Figure 5.21a).

(a)

(b)

(a)

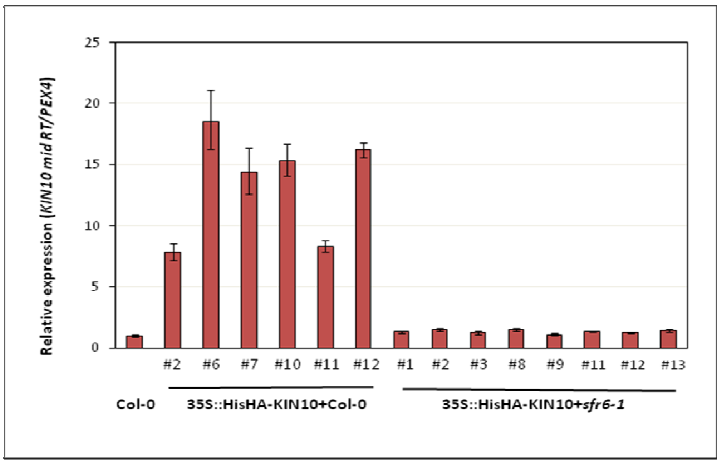

(b)

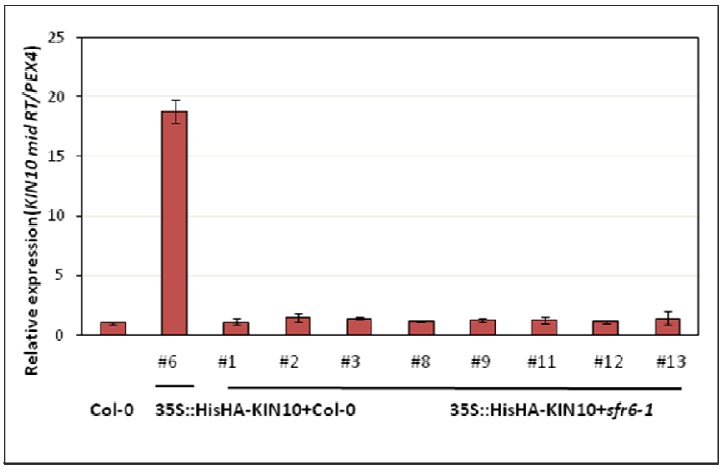

Figure 5.21: *KIN10* expression in wild type and *sfr6-1* mutant plants transformed with 35S::HisHA-KIN10

KIN10 expression in T_2 generation of Col-0 + 35S::HisHA-KIN10and *sfr6-1* + 35S::HisHA-KIN10+*sfr6-1* was compared with expression in untransformed Col-0. Seven-day-old seedlings grown on 0.5X MS agar plates were used. Figure 5.21 (a) represents the level of *KIN10* expression measured using cDNA reverse transcribed by AMV (Avian Myeloblastosis Virus) reverse transcriptase in conjunction with an oligo dT primer. Figure 5.20 (b) represents the level of *KIN10* expression measured using cDNA reverse transcribed with M-MLV (Moloney Murine Leukemia Virus) reverse transcriptase with an oligo dT primer. Expression is shown after normalisation to *PEX4*. Relative expression represents the fold value compared with Col-0 control sample and calculated using the ΔΔCT method, and the error bars in each graph represent RQ_{MIN} and RQ_{MAX} and constitute the acceptable error level for a 95% confidence level according to Student's t test. Error bars indicate the level of variation between technical replicates within one biological replicate experiment.

The F_1 generation of the above crosses were tested for the presence of the transgene using primers specific to both the tag (forward primer) and to the *KIN10* cds (reverse primer. See Appendix A2.3 for the primer sequences) and positive lines were selected for the production of F_2 seeds. F_2 seedlings from the selected lines were tested to obtain lines homozygous for the *sfr6-1* mutation. Plants were genotyped using a TaqMan allelic discrimination assay to identify the SNP associated with *sfr6-1* (see appendix A2.1) using Applied Biosystems 7300 machine (see section 2.10.3).

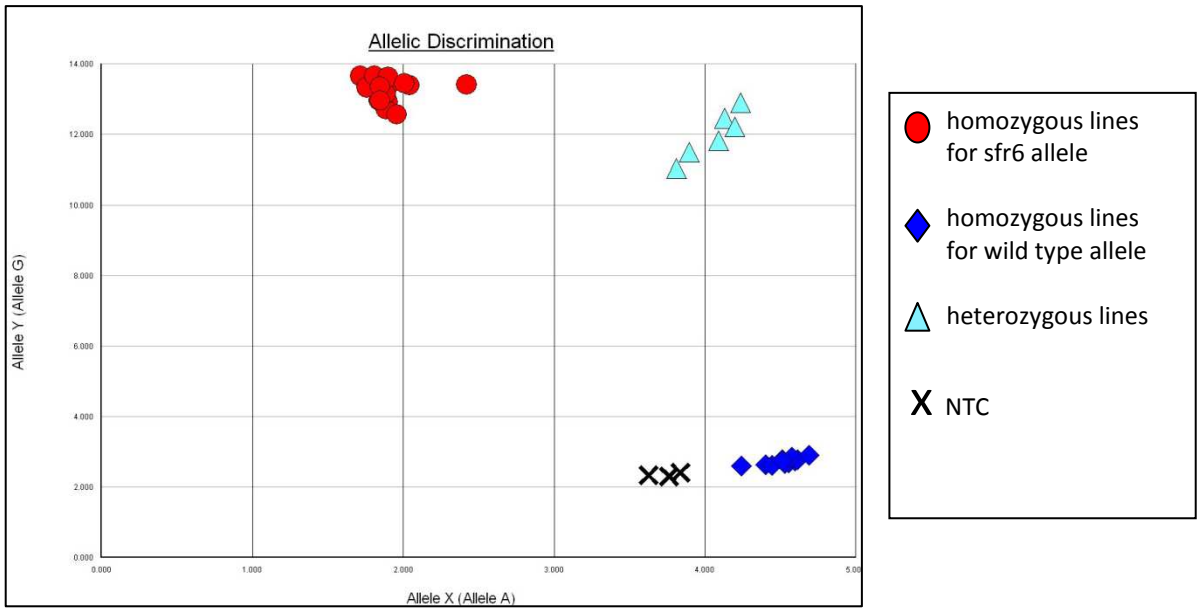

Figure 5.22: Results of Allelic discrimination assay of F_2 segregants from two cross between *sfr6-1* and Col-0 35S::HisHA-KIN10

Genomic DNA was extracted from leaves of three-week-old plants. Three technical replicates were used for each sample. Water was used for no template control (NTC) along with positive and negative (Col wt and *sfr6* mutant) controls. The graph shows data from segregating lines that were identified as homozygous for the *sfr6-1* mutation (red circles), homozygous for the wild type allele (dark blue diamonds) or heterozygous (turquoise triangles). Also shown are known Col-0 and *sfr6-1* homozygous lines for comparison (same symbols).

Results of the allelic discrimination assay were used to select three lines homozygous for the *sfr6-1* mutation; two of which were the progeny of a cross with Col-0 transformant #6 and one the progeny of a cross with #11 (figure 5.21). Three segregating lines that were homozygous for the wild type *SFR6* allele originating from the same two crosses between the line #6 and #11 were also selected.

5.2.4.2 *KIN10* expression levels in 35S::His-HA-KIN10 transformants *in* Col-0 and *sfr6-1* backgrounds

Levels of *KIN10* expression were tested in lines of 35S::HisHA-KIN10 overexpressers of both backgrounds using seven-day-old seedlings of F3/T3 generations. All selected overexpression lines from wild type (Col-0) and *sfr6* background showed a higher level of *KIN10* expression compared to Col-0 (Figure 5.23 a, b and c) untransformed line. Level of *KIN10* expression pattern was consistent among three biological replicates however highest expressers were the lines originated from line #6 overexpressing 35S::HisHA-KIN10 in Col-0 where as lowest expressers were the lines from crosses with #11 overexpressing 35S::HisHA-KIN10 in Col-0 (Figure 5.23a). Relative expression represents the fold value compared with Col-0 control sample and calculated using the ΔΔCT method, and the error bars in each biological replicate represent RQ_{MIN} and RQ_{MAX} and constitute the acceptable error significant difference among Col-0, *sfr6-1* and six other lines of 35S::HisHA-KIN10 overexpression in both Col-0 and *sfr6-1* ($p<0.001$) except line #11 of Col-0+35S::HisHA-KIN10+Col-0 and line #11.2.5 of *sfr6-1*+35S::HisHA-KIN10 (Figure 5.23 d). Data were analysed using a one-way ANOVA ($\alpha=0.05$) and pairwise comparisons were done using Tukey method. All overexpression lines in both wild type and *sfr6* background were overexpressing *KIN10* compared to Col-0 (wild type untransformed).

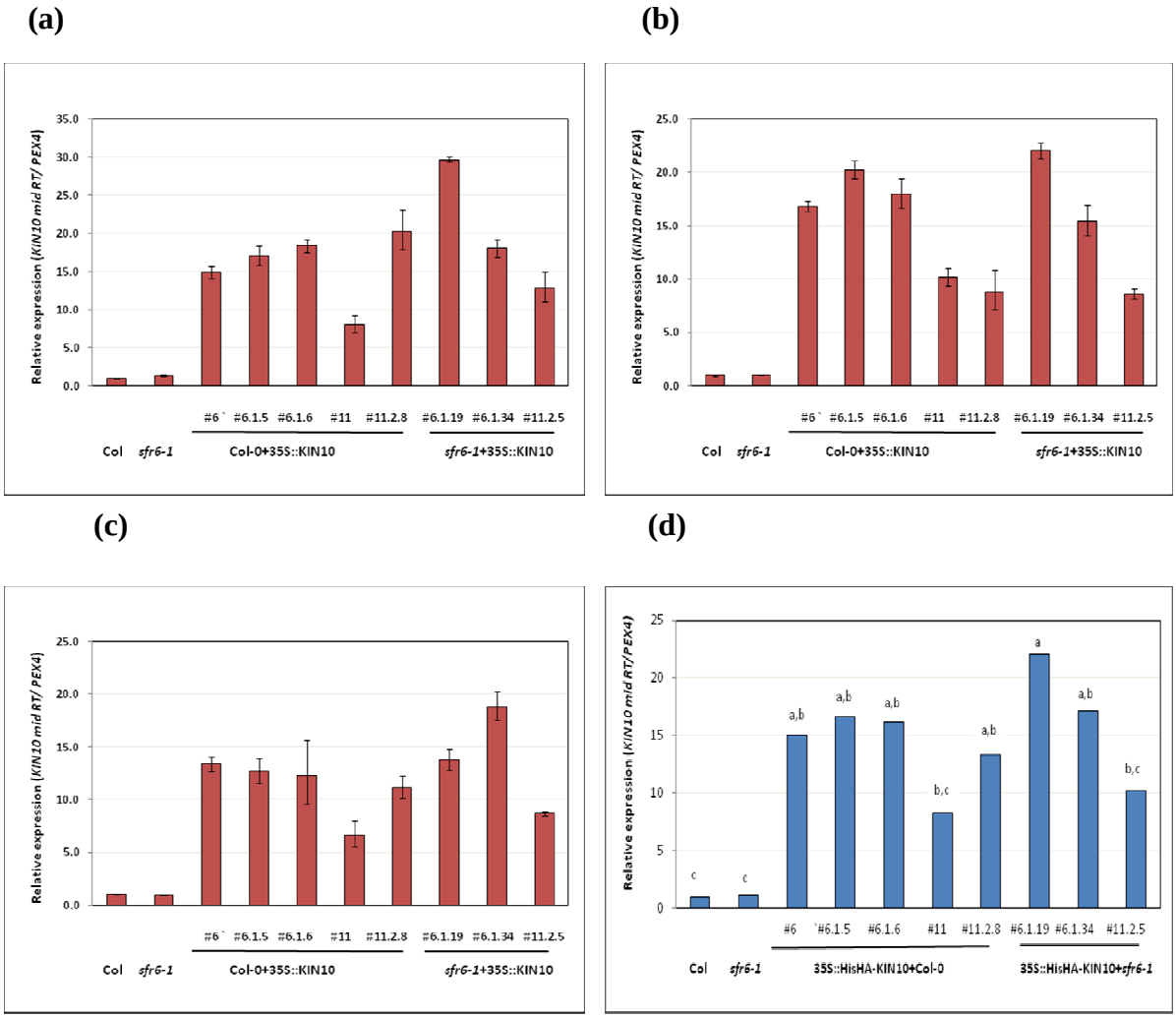

Figure 5.23: *KIN10* overexpression in Col-0 and *sfr6-1* backgrounds

KIN10 expression levels were compared in Col-0 and *sfr6-1* lines overexpressing HisHA-KIN10 and untransformed lines of the same backgrounds. Seven-day-old seedlings grown on 0.5X MS agar plates were used to monitor *KIN10* expression using primers designed to detect both the native *KIN10* transcript and the transcript arising from the overexpression construct. Expression is shown after normalisation to *PEX4*. Relative expression represents the fold value compared with Col-0 control sample and calculated using the ΔΔCT method, and the error bars in each biological replicate represent RQ_{MIN} and RQ_{MAX} and constitute the acceptable error level for a 95% confidence level according to Student's t test. Error bars indicate the level of variation between technical replicates within one biological replicate experiment. The red dashed line represents the level of *KIN10* expression in untransformed Col-0.

5.2.4.3 Protein expression in different KIN10 overexpression lines

Levels of *KIN10* transcript expression were confirmed to be higher in KIN10 overexpresion lines in *sfr6-1* and Col-0 backgrounds compared to untransformed wild type (Col-0) (Figure 5.24). KIN10 protein expression in these lines was assayed as described in section 2.16. Immuno-blot analysis (see section 2.16.5) was conducted using AKIN10 Rabbit polyclonal primary antibody. Membranes were observed after incubation with a goat anti-rabbit antibody conjugated to HRP to visualise the protein using chemiluminescence (see section 2.16.6) method.

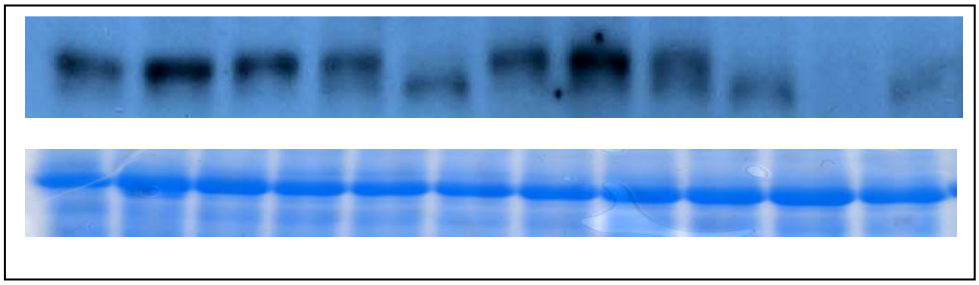

Figure 5.24: Level of KIN10 protein expression in KIN10 overexpression lines

Seven-day-old seedlings (20-25 seedlings) were used to extract protein and 30µl of total lysate (2mg/ml) were used on SDS gel. Membrane was incubated with AKIN10 Rabbit polyclonal primary antibody at 4^0C overnight followed by 2 h secondary antibody binding with Goat anti-Rabbit HRP both were at 1:2000 dilutions in 5% milk solution. Proteins were visualized using chemiluminescence and membrane was observed under a Photon Counting camera using Photek Image32 software. Samples represents the lanes are as follows; Lane 1= #6, lane 2= #6.1.5, lane 3= #6.1.6, lane 4= #11, lane 5= #11.2.8 of 35S::HisHA-KIN10+Col-0 and lane 6= #6.1.19, lane 7= #6.1.34, lane 8= #11.2.5 of 35S::HisHA-KIN10+*sfr6-1*, lane 9= Wt, lane 10= *kin10-2*, lane 11= *sfr6-1*

Lines overexpressing *KIN10* in both wild type and *sfr6-1* backgrounds were tested for overexpression of KIN10 protein compared to *sfr6-1* (Figure 5.24). No KIN10 expression was observed in the *kin10-2* knockout line and weak bands could see in both Col-0 and *sfr6-1*. Strong bands were observed in all other samples compared to Col-0. The highest level of KIN10 expression was in #6.1.34 that overexpressing KIN10 in *sfr6-1* background transformant. Relative levels of KIN10 protein expression in these lines are likely to be higher than in the wild type overexpression lines. However lanes 5 and 9 show a band that is not the same size as the KIN10 band in all the other lanes, so these might not be real KIN10 levels. As lane 9 is wild type KIN10 (not tagged transgenic KIN10) , it is clear that lane 5 might be similar to wild type (not transgenic KIN10) so not a KIN10 over expresser.

5.2.4.4 Dark- and cold-inducible gene expression in wild type and *sfr6-1* KIN10 overexpression lines

Previous published work by Baena-Gonzalez et al. (2007) showed that transient overexpression of KIN10 in protoplasts from mesophyll cells caused elevated levels of *DIN6* and *DIN1* expression specifically in the absence of stress. Therefore experiments described below were designed to study, the effect of KIN10 stable overexpression in seedlings of wild type and in *sfr6-1* mutant background to test second hypothesis proposed in this chapter, that KIN10 and SFR6 act in the same pathway leading to stress gene expression as well as to test whether MED16/SFR6 is required for expression mediated by KIN10.

Equivalent increases in stress gene expression in response to KIN10 overexpression in both backgrounds would suggest that SFR6 is not required for this particular function of KIN10. Lack of effect of overexpression of KIN10 in *sfr6-1* mutants would show that SFR6 is essential for KIN10 to perform its function.

DIN6 gene expression was measured in untreated seven-day-old seedlings overexpressing HisHA.KIN10. Two lines out of five lines of Col-0 overexpressing HisHA-KIN10 exhibited significantly higher levels of *DIN6* gene expression and two lines shown higher levels but not significantly high compared to Col-0 whereas one line showed similar level of expression as in Col-0. In contrast to above all three *sfr6-1* lines overexpressing HisHA-KIN10 showed reduced levels of *DIN6* compared to Col-0, similar to the levels of expression observed in untransformed *sfr6-1*. Average gene expression data across three independent biological repeat experiments showed no significant difference between Col-0, *sfr6-1* and the three *sfr6-1* KIN10 overexpressers but significant differences were observed between four out of the five wild type overexpressing lines and all three overexpressers in the *sfr6-1* background ($p<0.001$) (Figure 5.25 d). Data were analysed using a one-way ANOVA ($\alpha=0.05$) and pairwise comparisons were made using the Tukey method.

Similar results were obtained when the same samples were tested for expression of another dark-responsive gene, *BCAT2*, (Figure 5.26 a, b and c). Significantly increased levels of *BCAT2* expression were observed in one line out of five and other three lines shown increased levels but not significantly high in wild type overexpressing KIN10 compared to untransformed Col-0, however, increases were less pronounced than those seen with *DIN6* (Figure 5.25). Average gene expression data from three individual experiments (Figure 5.26 d) demonstrated that wild type overexpresser line #11.2.8 was the highest expresser of *BCAT2* and the increase in expression level was highly significant compared to Col-0 ($p<0.000$). Data were analysed using a one-way ANOVA ($\alpha=0.05$) and pairwise comparisons were made using the Tukey method.

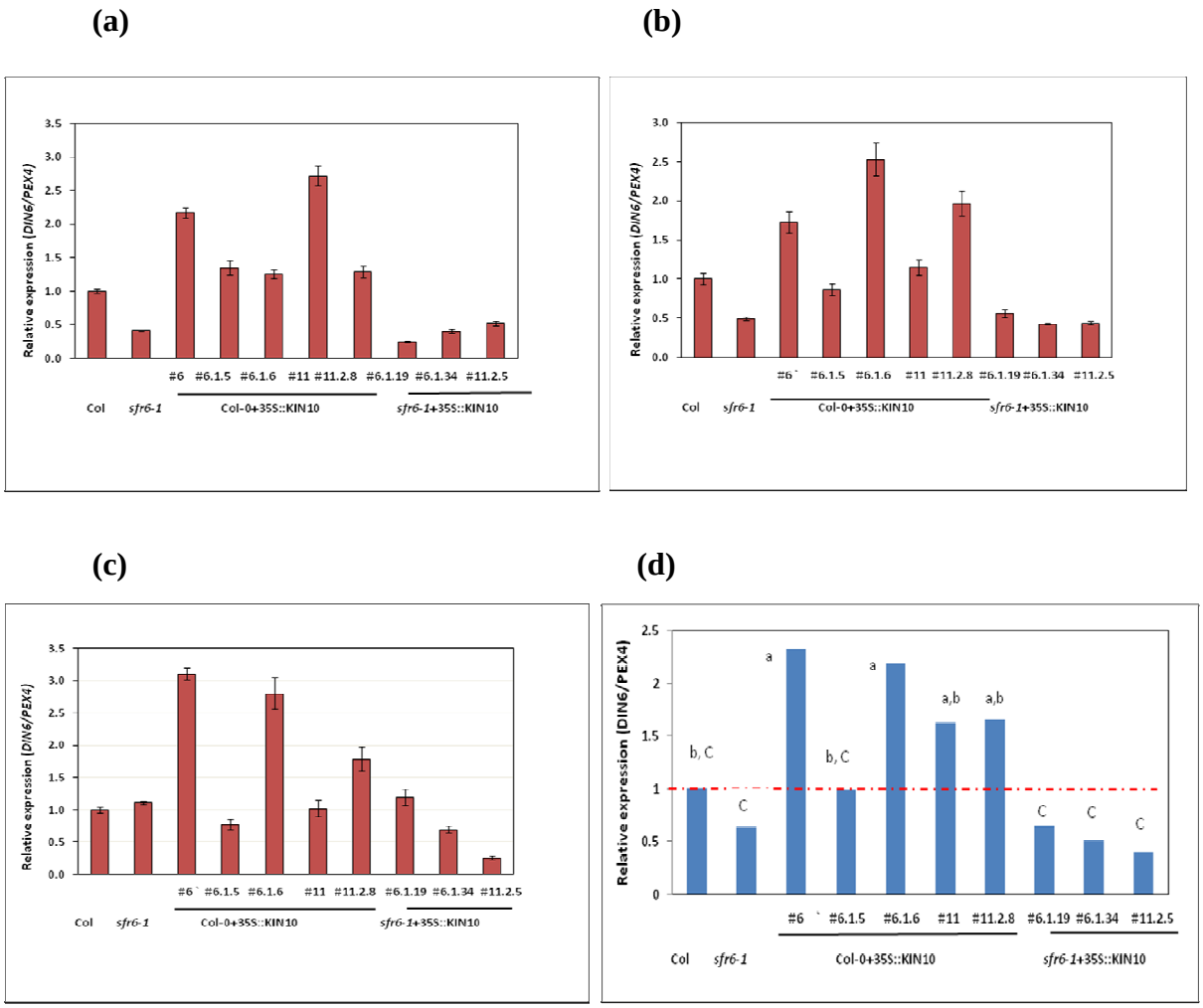

Figure 5.25: *DIN6* gene expression in untreated KIN10 over-expression lines in wild type and *sfr6-1* backgrounds

DIN6 expression in response to light was measured in Col-0 and *sfr6*-1 mutants with and without His-HA overexpression. Seven-day-old seedlings grown on 0.5X MS media on petri dishes were sampled during the light period. The first three histograms (a, b and c- with red bars) represent the gene expression data of three independent biological replicates. Error bars indicate the level of variation between technical replicates within one biological replicate experiment. The fourth chart (blue bars; d) represents the average of the above three independent biological replicates. Mean average data (in graph d) were analysed using a one-way ANOVA (α=0.05) and pairwise comparisons were made using the Tukey method. Means that do not share a letter are significantly different. The red dashed line represents the level of *DIN6* expression in Col-0.

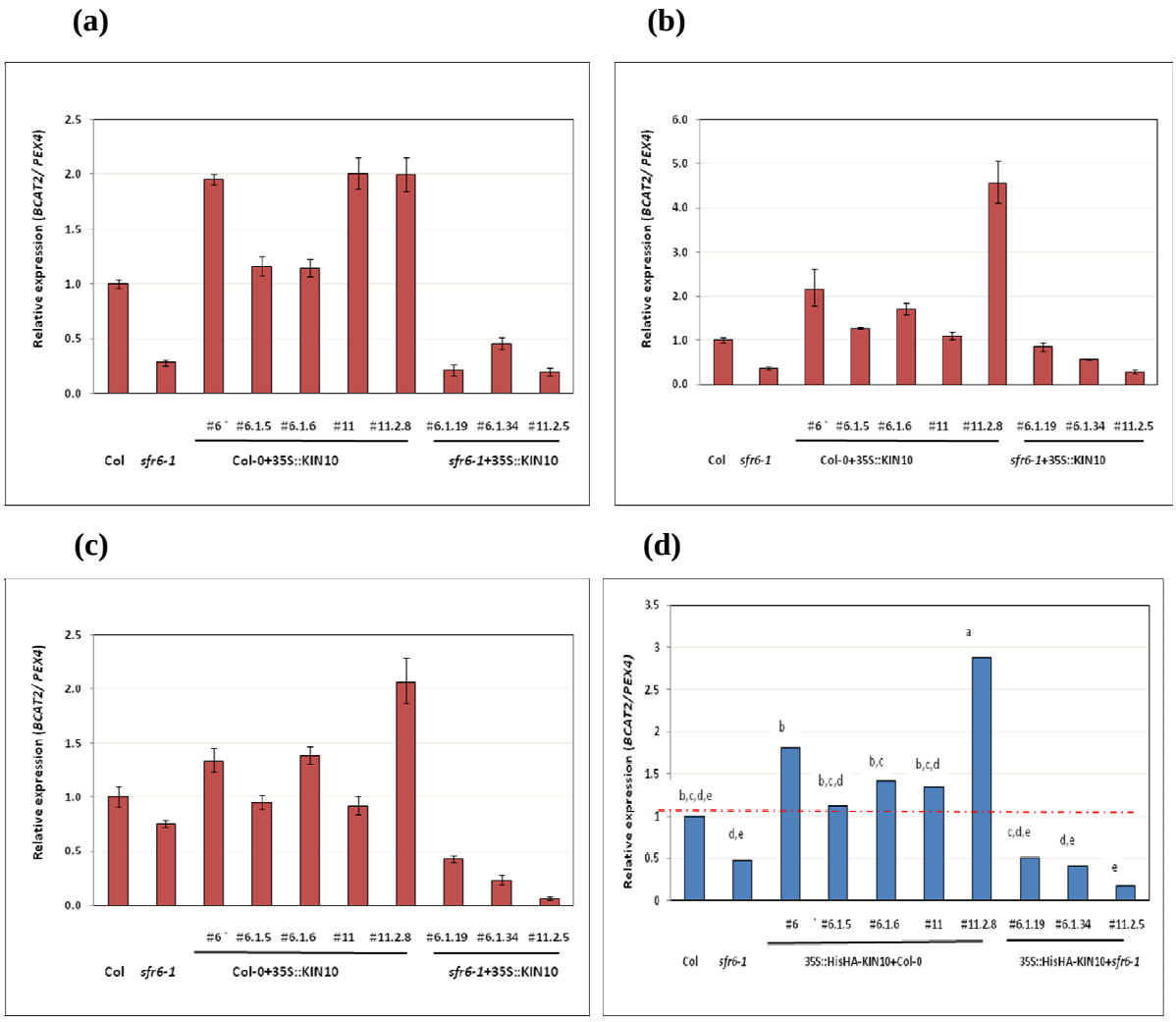

Figure 5.26: *BCAT2* expression in untreated KIN10 over-expression lines in wild type and *sfr6-1* backgrounds

BCAT2 expression in response to light was measured in Col-0 and *sfr6*-1 mutants with and without His-HA overexpression. Seven-day-old seedlings grown on 0.5X MS media on petri dishes were sampled during the light period. The first three histograms (a, b and c- with red bars) represent the gene expression data of three independent biological replicates. Error bars indicate the level of variation between technical replicates within one biological replicate experiment. The fourth chart (blue bars; d) represents the average of the above three independent biological replicates. Mean average data (in graph d) were analysed using a one-way ANOVA (α=0.05) and pairwise comparisons were made using the Tukey method. Means that do not share a letter are significantly different. The red dashed line represents the level of *BCAT2* expression in Col-0.

These data clearly demonstrated that reduced level of *BCAT2* gene expression in plants overexpressing HisHA-KIN10 in *sfr6-1* background compared to wild type (Col-0) overexpression lines, which further agrees with the results obtained with *DIN6* gene expression.

In addition, same light exposed samples were tested for expression of another dark-responsive gene, *KIN2* using seven-day-old seedlings. *KIN2* expression was measured in the five wild type background KIN10 overexpression lines and three *sfr6-1* background overexpressers and compared with Col-0 and *sfr6*-1 in three independent biological replicate experiments (Figure 5.27 a, b and c).

Four lines out of five wild type background KIN10 overexpressers exhibited higher expression of *KIN2* compared to Col-0 (line #11.2.8 is not actually shown the expression of correct size of protein) whereas none of the three overexpression lines in the *sfr6-1* background showed increases in *KIN2* expression above levels seen in untransformed *sfr6-1*. Although a consistent trend was clearly visible across replicate experiments, average data did not show significant differences between Col-0, *sfr6-1*, ($p<0.464$) the three *sfr6-1* KIN10 overexpressers and four of the five wild type overexpression lines, although wild type line #6 did show a significant difference from the others (Figure 5.23d). Data were analysed using a one-way ANOVA ($\alpha=0.05$) and pairwise comparisons were made using the Tukey method.

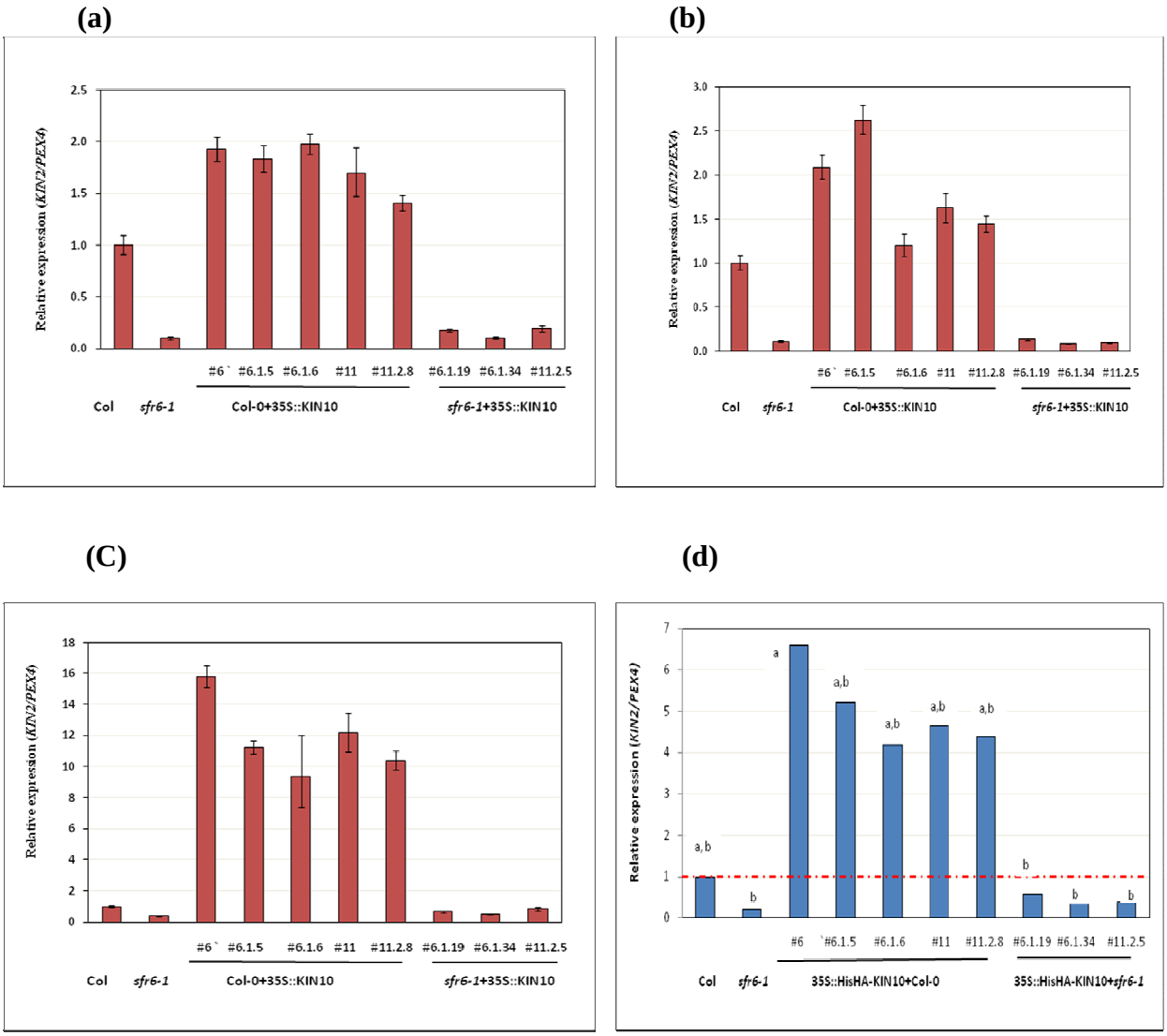

Figure 5.27: *KIN2* gene expression in unstressed KIN10 over-expression lines in wild type and *sfr6-1* backgrounds

KIN2 expression in non cold/drought treated but in response to light was measured in Col-0 and *sfr6*-1 mutants with and without His-HA overexpression. Seven-day-old seedlings grown on 0.5X MS media on petri dishes were sampled during the light period. The first three histograms (a, b and c- with red bars) represent the gene expression data of three independent biological replicates. Error bars indicate the level of variation between technical replicates within one biological replicate experiment. The fourth chart (blue bars; d) represents the average of the above three independent biological replicates. Mean average data (in graph d) were analysed using a one-way ANOVA (α=0.05) and pairwise comparisons were made using the Tukey method. Means that do not share a letter are significantly different. The red dashed line represents the level of *KIN2* expression in Col-0.

By analysing *DIN6*, *BCAT2* and *KIN2* gene expression data, I could see a consistent pattern of gene expression showing that higher level of expression of above three genes in wild type plants overexpressing KIN10 and but not the lines of *sfr6-1* overexpressing KIN10. The effect of *DIN6* expresssion in total seedlings of this study in is in the agreement with the finding of Baena-Gonzalez et al. (2007) who reported that overexpression of KIN10 caused elevated levels of *DIN6* expression in protoplasts of wild type. Increases in *KIN2* expression (Figure 5.27) were large compared to increases in *DIN6* and *BCAT2* in wild type background and the impairment in expression of *KIN2* in *sfr6-1* more pronounced. All these data imply that, this effect was not evident in the *sfr6-1* background, suggesting the necessity of SFR6/MED16 for KIN10 to function in this manner, and indicating that KIN10 may act upstream of SFR6/MED16 in the control of stress gene expression.

5.2.5 Phenotypic study of KIN10 overexpression in Col-0 and *sfr6-1* backgrounds

Baena-Gonzalez et al. (2007) reported that KIN10 overexpression in wild type caused altered inflorescence architecture and delayed flowering and onset of senescence under very long days (20h light/ 4h dark). Therefore flowering phenotype of KIN10 overexpression in wild type as well as in *sfr6-1* background was an interest to see any altered flowering phenotype in *sfr6-1* background. *sfr6-1* mutant plants are known to be late flowering compared to wild type plants (Knight et al., 2008, Knight et al., 1999).

Seven-day old seedlings were planted on single peat plugs and maintained in long day conditions (see section 2.1.4) for 4-weeks. Comparison of the flowering time

(a)

(b)

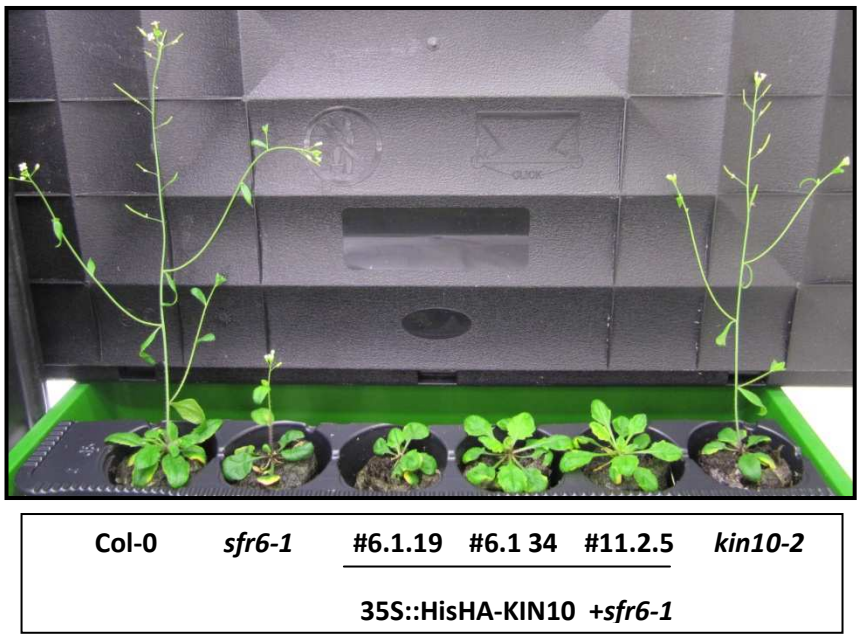

Figure 5.28: Flowering phenotype of KIN10 overexpressing lines

Plants were grown individually on peat plugs and maintained under long day conditions (16h light/8 h dark) at 20^{o}C. The flowering phenotype of five–week-old plants overexpressing KIN10 in wild type and *sfr6*-1 backgrounds was compared with Col-0, *kin10-2* and *sfr6-1* mutants. Same control Col-0 plant is in both photographs and chosen as a representative plants of 15 plants observed in this phenotypic study.

phenotype of KIN10 overexpressers in Col-0 and *sfr6-1* backgrounds was observed using 15 plants of each.

I observed the same altered phenotype in KIN10 overexpressing in wild type background (Figure 5.28 a) as reported previously; plants exhibited a short inflorescence and delayed flowering compared to Col-0 and *kin10-2* evidencing the role of KIN10 in determining plant shape and developmental transition timing (Baena-Gonzalez et al., 2007).

These flowering phenotype data may suggest that KIN10 overexpression in *sfr6-1* background failed to cause phenotypic effects seen in Col-0 overexpressers, adding to evidence of the necessity of SFR6 for activation of different signalling pathways by KIN10. However, given the already severely delayed flowering in *sfr6* mutants (Knight 2008) it is difficult to conclude for certain that KIN10 overexpression does not further delay flowering in this background.

5.2.6 Interaction between KIN10 and truncated fragments of SFR6/MED16

A yeast-2-hybrid screen in our laboratory identified KIN10 as a putative interactor of SFR6/MED16 and confirmed this interaction by Co-immunoprecipitation (Hemsley and Knight, unpublished). To test which domains of SFR6/MED16 interact with KIN10 the ability of truncated fragments of SFR6/MED16 (created in chapter 4) to interact with KIN10 was studied.

Six SF truncations tagged with GFP created in chapter 4 and the 35S::HisHA-KIN10 construct (see section 5.2.2) were transformed into *Agrobacterium tumefaciens* as described in section 2.11.2. Tobacco leaves were co-infiltrated with the two cultures of *Agrobacterium* (as described in section 2.11.2). After 48 h incubation leaf samples were harvested and protein extraction and quantification was carried out as in section

2.17.2 and 2.16.2. Then two SDS gels were prepared using 20 µl of total protein lysate (10 mg/ml) and transferred to membranes as described in sections 2.16.3 to 2.16.4. Two membranes were used in western blotting: one membrane was incubated with a 1:2000 dilution of α-His H8 epitope tag primary antibody and the second membrane was incubated with α-GFP developed in Rabbit (Rb pAb to GFP, Abcam) at 1:5000 dilution. After that secondary antibody binding was carried out with goat anti mouse (IgG HRP conjugate, BioRad) and goat anti Rabbit (IgG peroxidise antibody, Sigma) with α-His and α-GFP membranes respectively at same dilutions used for primary antibody binding and membrane bound proteins were visualized using chemiluminescent detection method as described in section 2.16.6.

Detection of GFP-tagged SF proteins and HisHA-tagged KIN10 is presented in Figure 5.29. In the total protein extract α-GFP detected proteins of different sizes as predicted for the SF truncations tagged with GFP *i.e* GFP-SF16 (167 kDa), GFP-SF15 (138 kDa), GFP-SF14 (124.5 kDa) and GFP-SF36 (95.3 kDa), but a band of the correct size could not be detected for GFP-SF25 (99.6 kDa). This was despite the fact that other bands were present in the total lysate. This experiment was conducted four times and only once I observed the correct size of band for GFP-SF25. The membrane incubated with α-His (Pierce^{TM}6xHis Epitope tag antibody (His H8); Thermo Scientific) detected the HisHA-tagged KIN10. This showed that HisHA.KIN10 was successfully expressed in all of the total lysates in which it was expected (the first five lanes of the membrane from the left), Comparison with size markers confirmed the size of the protein was consistent with the expected size of 61.2 kDa (Figure 5.29).

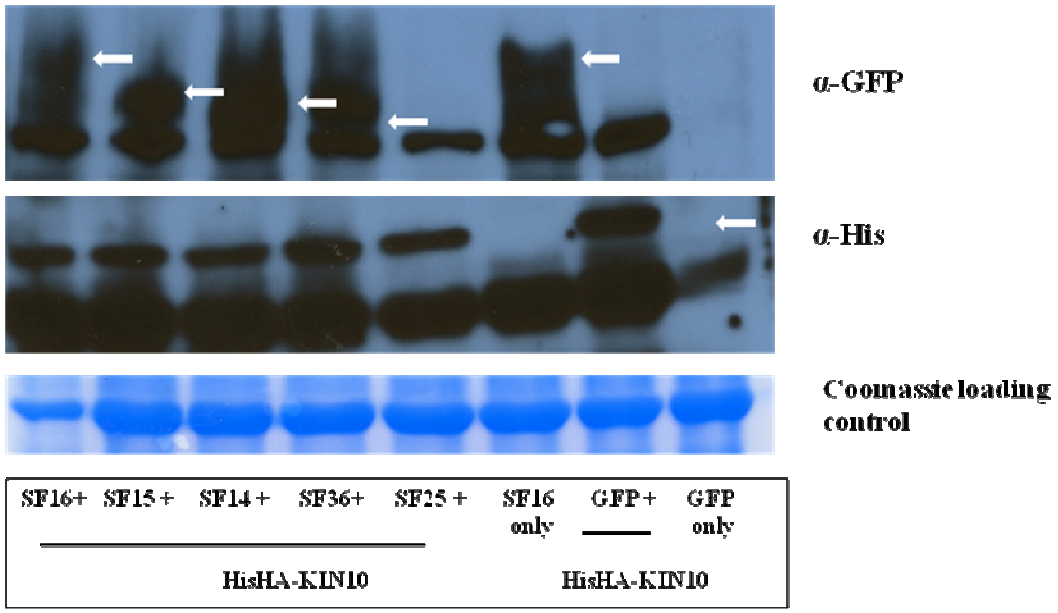

Figure 5.29: Detection of tagged SFR6 and KIN10 in total lysates

Total proteins extracted from tobacco leaves infiltrated with SF constructs tagged With GFP and with 35S::HisHA-KIN10 were loaded on an SDS gel at a concentration of 10 mg/ml and transferred to PVDF membranes and incubated with α-GFP and α-His primary antibodies at 1:5000 and 1:2000 dilutions respectively with 10 ml of 5 % milk (w/v). After incubation of membranes with relevant secondary antibody proteins were visualised using a chemiluminescent detection method. As a loading control an SDS gel with the same samples at same the concentration was stained with Coomassie blue to detect proteins and scanned. White colour arrows indicate the correct size of band in each lane. This experiment was conducted three times and similar results were reproduced.

The last three samples were used as controls in the pull down assay that followed western blotting of the total lysate. The sixth lane was GFP-SF16 (167 kDa) infiltrated in the absence of exogenous KIN10, therefore a band 167 kDa could be detected with α-GFP but no band with α-His was visible (Figure 5.29). The seventh lane was GFP only control with HisHA-KIN10 which showed a band of the correct size for GFP and no band with α-GFP corresponding to the size of any of the

fragments of SFR6 but band for the size of KIN10 (61.2 kDa) protein with α-His. The eighth lane was GFP control with no HisHA-KIN10 and here bands were observed neither with α-GFP nor α-His. The SDS gel was run with same set of samples and loaded with the same amount (20 µl) of total protein lysate at 10 mg/ml. The gel was stained with Coomassie blue to observe and compare quality and amount of proteins with the loading control for the western blot (see Figure 5.29). This western blotting experiment was conducted three times and the same results were reproduced.

After confirming both proteins were detectable as expected expressed in total protein extracts, the same set of samples was used to perform a pull down assay. Two ml of diluted samples at a concentration of 10 mg/ml (as described earlier for the SDS gel) of protein were mixed with 30 µl of GFP-Trap-A beads (50% slurry; Chromotek) and incubated on a roller mixer for 4 hours at 4°C in the cold room. As described in section 2.17.2 beads were washed and mixed with 30 µl of 2x SDS buffer and then stored at -20^{o}C after heating at 95°C for 5 minutes. Two SDS gels were run using 30 µl of GFP trap beads (in 2X SDS buffer) after having been heated at 95°C for 5 minutes (as described in sections from 2.16.3 to 2.16.4.) Then the resultant two membranes were used in western blotting with 10 ml of 5% milk (w/v) solution with the same primary and secondary binding antibodies at similar dilutions as described above under the proteins expression study in total extract. Results of the pull down assay are presented in Figure 5.30.

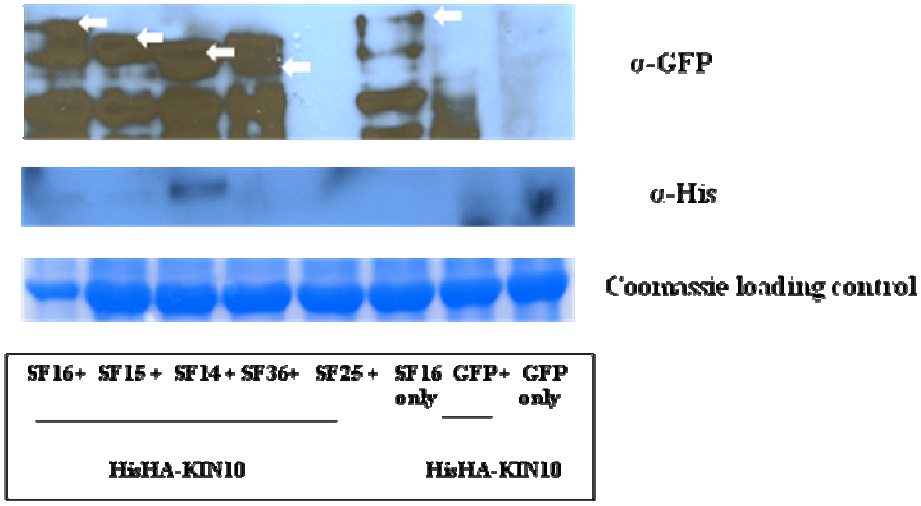

Figure 5.30: Detection of tagged SFR6 and KIN10 in Co-IP pulldowns experiments

Two ml of total proteins (10mg/ml) extracted from Tobacco leaves infiltrated with SF constructs tagged with GFP and 35S::HisHA-KIN10 were pulled down using 30 µl of GFP-Trap-A beads and an SDS gel run using 30 µl of GFP trapped beads. Proteins were transferred to PVDF membranes and incubated with α-GFP and α-His Primary antibodies at 1:5000 and 1:2000 dilutions respectively with 10ml of 5% milk (w/v) solution. After incubation of membranes with the relevant secondary antibody proteins were visualised using a chemiluminescent detection method. As a loading control an SDS gel with the same samples at the same concentration was stained with Coomassie blue to detect proteins and scanned. . White colour arrows indicate the correct size of band in each lane This pulldown experiment was conducted three times and similar results were obtained.

After pull down the GFP tagged full length and truncated SFR6 proteins with GFP-trap beads, western blot with α-GFP detected GFP-SF16 (167 kDa), GFP-SF15 (138 kDa), GFP-SF14 (124.5 kDa) and GFP-SF36 (95.3 kDa) but not GFP-SF25 (99.6 kDa). Neither could a band corresponding to the predicted size of GFP-SF25 be detected in the total lysate (Figure 5.29) and out of four replicate experiments only once the predicted size of GFP-SF25 band was detected. Bands corresponding to the

remaining SF proteins were clearly visible. With α-His antibody KIN10 (61.2 kDa) was detected in pulldowns with SF16, SF15 and SF14. No KIN10 was detected in the pulldown with SF36 or SF25 (Figure 5.30).

The negative controls confirmed that the band identified as KIN10 using α-His was not present in pulldowns originating from leaves that were transformed with full length SF16GFP but not KIN10 (Figure 5.30), demonstrating that full length SFR6 alone could not bind to α-His. The GFP only control with HisHA-KIN10 showed no band with α-GFP. Though a KIN10 band (61.2 kDa) was observed in this lane in the total lysate (Figure 5.29), no KIN10 band was detected after pull down, most likely due to the lack of SFR6. This confirms that GFP alone could not be pulled down by HisHA-KIN10 and that full or partial SFR6 was necessary for pull down to occur. The GFP only control without HisHA-KIN10 (lane 8) confirmed that bands detected by either α-GFP or α-His were not present, indicating that the bands interpreted as being specific to GFP and KIN10 were indeed not non-specific bands. An SDS gel was run with the same set of samples and loaded with the same amount of total protein lysate at 10 mg/ml. The gel was stained with Coomassie blue to observe and compare quality and amount of proteins as a loading control for the western blotting (see Figure 5.30). This pull down/CO-IP experiment was conducted three times and the same results were produced. These data confirm initial reports from our laboratory that full length SFR6 can interact with KIN10. They also provide further information as to the regions of the SFR6 protein likely to participate in this interaction. The failure of SF36 to interact with KIN10 indicates that the N-terminal part of SFR6 is required for the interaction (about 633 amino acids) and the ability of SF14 and SF15 to interact with KIN10 suggests that the C-terminal (about 396 amino acids) amino acids of SFR6 are not required.

5.3 Summary

Results presented in this chapter derived from using the *kin10*-2 mutant show the necessity for KIN10 in the control of a subset of the stress-inducible genes controlled by SFR6/MED16, although the effect of loss of KIN10 was less severe than loss of SFR6/MED16. The well studied *PR1* gene that was severely affected by loss of function of SFR6/MED16 under UV stress was not significantly affected by loss of function of KIN10. A Similar response in *KIN2* expression under cold stress was observed where *KIN2* expression was severely affected by loss of function of SFR6/MED16 (Knight et al., 1999) but no such effect was observed in loss of function mutants of KIN10. Similar Observations were made relating to ABA induced *KIN2* expression where no effect was observed by KIN10. Data obtained under dark/starvation and desiccation/drought stress conditions demonstrated a correlation between reduced gene expression and reduced tolerance in the experiments conducted with *sfr6* and *kin10* mutants.

Epistatic analysis using a double mutant of *sfr6 kin10-2* demonstrated that these two proteins act on the same pathway leading to stress inducible gene expression, particularly under dark and desiccation (drought) stress conditions. Ectopic expression of dark- and cold-/drought-inducible genes could be elicited in wild type plants by stable overexpression of KIN10, however, this was not observed in response to KIN10 overexpression in *sfr6-1* backgrounds. These results indicate that SFR6 is essential for the activation of stress inducible genes by KIN10.

Finally, results from co-immunoprecipitation experiments revealed that regions within the N-terminal part of SFR6/MED16 are essential for interaction with KIN10 and that interaction is unlikely to occur via the C-terminus of the protein (about 396 amino acids).

Chapter 6

Discussion

6.1 Background to the study

Plants are sessile organisms and always being challenged by various stresses including both abiotic and biotic conditions. Highly varying abiotic stress conditions such as extreme temperature, drought, UV and salinity alter metabolism, growth and development of plants and eventually prevent optimum yield potentials of plants particularly food crops being attained (Verslues et al., 2006, Araus et al., 2002, Boyer, 1982). Studying various tolerance and defence mechanisms that evolve in plants to cope with extreme environmental conditions particularly by sensing various signalling pathways is an important attempt to develop stress tolerance in crops as gene expression plays a vital role in determining tolerance for plants. Understanding of all possible stress responses and signalling pathways is the key requirement to underpin plants with improved stress tolerance using a transgenic approach. Introducing novel genes to the genome of agriculturally important crops or altering the expression of existing genes is a key goal in plant molecular biology to obtain plants with improved stress tolerance. Loss of function mutants lacking in tolerance of a stress are an important tool in uncovering components in a stress response (Atkinson and Urwin, 2012, Grativol et al., 2012).

Plant species display varying degrees of tolerance to freezing but can increase their freezing tolerance by being exposed to chilling temperatures, a process known as cold acclimation (Struhl, 1998, Thomashow, 1999). By screening an EMS-mutagenised population of Arabidopsis Warren et al. (1996) isolated the *sfr* mutations, which result in sensitivity to freezing after cold acclimation and studied

mutants homozygous for mutations *sfr2* to *sfr7* for cold-induced gene expression. Later studies revealed that *sfr6* mutants (the focus of this thesis) are unable to cold acclimate due to an inability to express *COR (Cold On Regulated)* genes controlled by CBF/DREB1 transcription factors in response to low, non-freezing temperatures (Knight et al., 2009, Knight et al., 1999). Furthermore *COR* genes are also inducible by dehydration stress and their induction is similarly defective in *sfr6* mutants in response to these conditions also (Boyce et al., 2003, Knight et al., 1999). Under drought stress conditions the DREB2 trans-acting factors, which bind to same CRT/DRE motif as the CBF/DREB1 transcription factors (Stockinger et al., 1997; Liu et al., 1998) are responsible for effecting expression (Liu et al., 1998, Stockinger et al., 1997).

CBF/DREB1 gene expression itself was shown not to be mis-regulated at the transcriptional level in *sfr6* mutants (Knight et al., 1999) but SFR6 acts downstream of CBF transcription factors to control expression of *COR* genes through the CRT (C-repeat) motif. In 2009, Knight *et al,* identified *SFR6* as *At4g04920,* encoding a predicted protein of 1268 amino acids in length with molecular mass of 137 kDa. SFR6 was identified as MED16 one of the subunits of the Mediator complex (Bäckström et al., 2007, Bourbon, 2008); a multi-subunit protein complex that is conserved in all eukaryotes and plays an important role in transcription initiation by linking sequence-specific transcriptional regulators to RNA Polymerase II (Pol II). The Mediator complex is grouped into three main domains head, middle and tail as well as an additional detachable kinase domain (Guglielmi et al., 2004) and MED16 was identified as one of the tail subunits, the tail being the part considered most likely to interact with trans-acting factors (Bourbon, 2008, Conaway and Conaway, 2011).

During the past seven years several studies have reported that SFR6/MED16 controls other stress gene regulons in addition to those activated by cold and dehydration conditions as well as controlling circadian gene expression (Boyce et al., 2003, Knight et al., 2009, Knight et al., 2008, Knight et al., 1999, Hemsley et al., 2014). A protective role of SFR6/MED16 in plants against UV damage was reported (Wathugala et al., 2012), consistent with its role as a positive regulator of UV-inducible gene expression. Furthermore they showed that in the UV response, SFR6 acts downstream of transcription factors like ERF5 as similar response under cold with consistent with its role as a mediator subunit. Further they reported both salicylic-acid (SA) and jasmonic-acid (JA) mediated gene transcription is regulated by SFR6/MED16, indicating a role for SFR6 under biotic stress conditions. Zhang et al. (2014) and Yang et al. (2014) reported that SFR6 is involved in iron deficiency responses and modulation of iron uptake through the control of gene expression under iron limited conditions. Furthermore the importance of SFR6 in starvation-induced stress condition was reported (Hemsley et al., 2014). All these data evidence the wide range of stress responses of SFR6/MED16 and therefore the objective of this study was to investigate and increase understanding of SFR6/MED16's multiple roles as part of the Mediator complex and in particular how it works with other proteins that are part of the complex or that may interact with the complex.

6.2 SFR6/MED16 shares some roles with the predicted tail subunits MED2 and MED14 in transcriptional regulation and abiotic stress tolerance

MED16/SFR6 is involved in the regulation of transcriptional responses to a variety of different stresses such as cold, drought, UV and pathogen infection. Though MED16 is involved in many types of gene expression, it is not required for all gene expression under every stress condition (Hemsley et al., 2014). This was evidenced by demonstrating some cold-inducible genes that were expressed even in the absence of SFR6/MED16. In addition, it is also true that more than one subunit may be required for a particular stress response and necessity of MED5, MED14 and MED16 has been reported for the induction of dark-induced gene expression (Hemsley et al. (2014)). By considering the structure of the yeast mediator complex, we would predict a close physical interaction between MED14 and MED16 and might expect MED2 to exist in close proximity to SFR6/MED16, although it should be stressed that the structure of plant mediator has been hypothesised to be similar to that of yeast mediator but it has not yet been proven (Bourbon, 2008, Guglielmi et al., 2004).

To investigate whether other tail subunits of the complex participate in controlling the same regulons as controlled by MED16/SFR6, two of the less studied plant Mediator subunits were chosen for this investigation: MED2 and MED14. Loss of function mutants for these two subunits (described in chapter 3) were used to examine whether MED2 and MED14, have similar roles to those of MED16. Further the tolerance experiments described in chapter 3 were designed to investigate whether any alterations in the transcriptional responses that occurred in MED2 and MED14 associated with reduced tolerance similar to that of SFR6/MED16 in cold, UV and drought stress conditions.

Recent work in our laboratory had shown that loss of function of MED2 and MED14 impairs low temperature-induced expression of a number of *COR* genes that also require SFR6/MED16 (Hemsley et al., 2014). However we do not have any microarray data for MED2 and MED14 to evidence that these mutants failed to express whole *COR* genes but do have evidence of qRT-PCR data of several genes. My first question was to ascertain whether the transcriptional changes seen in MED2 and MED14 under low temperature indeed correlate with changes in tolerance. Therefore freezing tests were important to study the existence of shared role of the above subunits at low temperature. A freezing-sensitive phenotype in *med2* and *med14* mutants would suggest these subunits are likely to control the whole *COR* gene regulon as in SFR6 rather than just a few *COR* genes. Freezing tolerance data indeed correlate with pattern of impaired gene expression in the three mediator subunit mutants (see Chapter 3 section 3.2). In freezing tolerance assays I observed a significant reduction in three *med* mutants in their percentage of survival and further this confirmed by more quantitative analysis of the freezing damage using percentage of electrolyte leakage (Calkins and Swanson, 1990, Warren et al., 1996) in leaf tissues.

Further experiments described in chapter 3 were designed to investigate whether MED2 and MED14 play a similar role to that of SFR6/MED16 in the transcriptional regulation of genes expressed in response to two other abiotic stresses. Results presented in chapter 3 show that loss of function of MED2 and MED14 caused reduced transcriptional responses to UV and drought stresses in addition to the impaired transcriptional responses to cold stress (Hemsley et al. (2014)). Under UV-C exposure both gene expression and tolerance data are highly significant at a high dosage of UV-C. Reduced *PR1* gene expression as well as reduced UV-C tolerance

was observed in all three *med* mutants compared to Col-0 signifying that the impaired gene expression in *med2* and *med14* correlates with reduced tolerance under UV-C.

Reported work related to SFR6/MED16 demonstrated that impaired gene expression is strongly correlated with reduced tolerance of the plants to freezing (Knight et al., 2009, Knight et al., 1999) and UV and pathogen infection (Wathugala et al., 2012, Zhang et al., 2013) but no clear evidence was found to show that correlation between drought-induced gene expression and tolerance occurs under real drought conditions. Therefore in this study I developed a physiologically relevant drought assay that mimics the conditions occurring under natural drought, using water withdrawal from 25 day-old plants to study whether there is a correlation between drought-induced gene expression and tolerance in two other mediator mutants as reported under cold and UV stress conditions in *sfr6-1* mutants. Knight et al. (1999) first reported that drought-induced *COR* gene transcript expression is impaired in *sfr6-1* mutants in response to mannitol treatments. This mannitol-induced osmotic stress treatment is not equivalent to the real drought stimuli that occur in the natural environment and is less physiologically relevant (Claeys and Inzé, 2013, Verslues et al., 2006, Lawlor, 2013). Therefore it was important to develop a method to induce gene expression and to quantify damage caused by drought stress as actually exists in natural conditions.

I examined drought-inducible gene expression in seven day-old seedlings after withdrawal of water for 6 h by exposing agar-grown seedlings to air. In this study I was able to demonstrate impaired drought gene expression in all three *med* mutants under desiccation/water withdrawal that is physiologically similar to a real drought conditions. Similar to cold stress drought tolerance data showed strong correlation with desiccation-induced gene expression in mediator mutants. Therefore tolerance

of three different stress conditions correlated closely with the pattern of impaired gene expression observed under each stress condition.

Drought tolerance data demonstrated that *med2-1* and *med14-2* reported a similar level of tolerance but it was significantly lower to the percentage survival in *sfr6-1*. However, strong *KIN2* gene induction could be seen under desiccation-induced drought conditions in *med2-1* and *med14-2* mutants. A considerable proportion of the genes expressed under cold conditions are also expressed under drought stress but only 10% of drought-inducible genes are induced by cold stress (Shinozaki and Yamaguchi-Shinozaki, 2007). Therefore it is important not to assume that because the *COR* genes require SFR6/MED16, MED14 and MED2 for drought-inducible expression, the vast number of other drought-inducible genes will also require SFR6. This might suggest not only *COR* genes like *KIN2* we tested here are important in drought tolerance but many other genes are important whereas in freezing tolerance it is clear that *COR* genes are very significant and evidenced by strong reduction in both cold gene expression and freezing tolerance (Mahajan and Tuteja, 2005, Chinnusamy et al., 2007). Further, more significant reduction in drought tolerance in *sfr6-1* might be due an additional defect only in *sfr6-1* perhaps failing in other gene expression particularly non CRT/DRE genes responsive to drought conditions. Therefore, drought-inducible genes like *P5CS1* that are not controlled via the CRT/DRE (see section 5.2.1.2.2 described in Chapter 5) might responsible in above described extra effect in *sfr6.*

In accordance with cold and UV stress, findings indicated that the level of drought-induced gene expression is strongly correlated with reduced drought tolerance in *sfr6-1*. Therefore these data evidence that the extent of loss of gene expression in *med2* and *med14* is likely to be similar to the effects seen in *sfr6-1*. Similarly,

starvation tolerance experiments conducted in Chapter 5 demonstrated a strong correlation between reduced dark gene expression (see section 5.2.3.2) and dark-induced starvation tolerance (see section 5.2.3.5) in *sfr6-1* mutants as well.

All three *med* mutants showed reduced tolerance to both dosages of UV-C irradiation applied, however, differences between the mutants and wild type were less obvious in response to lower doses. Also results indicate that MED2 is less important in the response to UV than are MED14 and MED16, a conclusion supported by the relative effects of each mutation upon gene expression. The findings of this study extend the evidence of the role of three different mediator subunits MED16/SFR6, MED2 and MED14 in drought and UV-C induced stress tolerance as well as SFR6/MED16 in starvation tolerance by broadening the responses of Mediator tail subunits.

Although there is a correlation between transcription of the genes tested and tolerance, generally the results indicate that in some cases particularly under drought MED16/SFR6 is more important than MED2 and MED14. So it is likely that SFR6 controls more genes (or more different regulons) than the MED2 and MED14 regulates.

6.2.1 Is there greater overlap between the roles of MED14 and MED16 than MED2 and MED16?

Amongst the three *med* mutants *sfr6-1* was always the most highly affected mutant in terms of gene expression, showing significantly low *PR1* (see section 3.2.2) and *KIN2* (see section 3.2.3) gene expression compared to *med2-1* and Col-0 under UV and drought stress respectively. *med2-1* was less affected compared to other two *med* mutants under each stress but showed significant reduction of *PR1* at high level of

UV-C irradiation and in drought compared to Col-0. Conversely, *med14-2,* like *sfr6,* always showed a significant reduction in gene expression compared to Col-0. However, although I observed a trend of reduced expression indicating *sfr6-1* was the most affected, followed by *med14* and finally *med2*, these differences were not significant in every occurrence across the three *med* mutants (see section 3.2.2 and 3.2.3). Reproducibility of the data is very important for the validation of results. However, dependence on the *P* value to determine the significance of results is not always accurate (Halsey et al., 2015, Mobley et al., 2013) due wide sample-to-sample variability as well as variability among different biological replicates. Therefore, the *P* value gives little information about the probable result of a replication of an experiment. Statistical power of the test greatly affects the capacity to interpret *P* value and unless statistical power is very high, the *P* value exhibits high variability and does not reliably indicate the strength of evidence to reject null hypothesis (Halsey et al., 2015). Further he reported that tests at least with 90% of statistical power has great chance to return similar *P* value in repeat experiments but not less than that. However most scientific studies have less than 80% of statistical power often around 50% and 21% in psychological (Maxwell, 2004) and neuroscience (Button et al., 2013) respectively. Therefore interpreting results totally based on *P* value is misleading and I considered the trend along with *P* value to report results on transcriptional data in these experiments as well as other results reporting in this thesis.

Averaging of gene expression data from three biological replicates was extremely difficult as the relative levels of gene expression varied sometimes thousand folds in one replicate compared to the other biological repeat. For this reason, I have focussed on the transcriptional trends in these experiments. When viewed as a

collective of results, data from this study and others (Hemsley et al., 2014, Canet et al., 2012, Zhang et al., 2013) suggest that *med14-2* shares all of its gene expression phenotypes with *sfr6-1* but that med*2-1* does not exhibit every phenotype shown by *sfr6* mutants. The type of knockout can affect the extent of the deficiency but only the real role of the subunits can cause some outputs to be affected by loss of *med2* and not others.

The type of the knockout is one of the possible reasons to explain the less affected phenotype in *med2-1* compared to *med14-1*. med*14-1* is an insertion into the last exon that might lose the important C-terminal domain (Li et al., 1995) but med*2-1* is an insert into the promoter and further this supported by the report by Hemsley et al. (2014) that *MED2* expression is not completely knocked out, so this might be a reason that mutant never shows a very strong phenotype. Aside from the issues of the severity of *sfr6* and *med2* mutant phenotypes, there clearly are some roles shared by MED2 and SFR6/MED16 and this fact might be explained by the fact that in yeast, the triad of tail subunits comprising Med2p, Med3p and Med15p are linked to the rest of the Mediator complex via Sin4p (MED16) (Kang et al., 2001, Li et al., 1995). If this were the case in plants also, loss of MED16 might be expected to result in loss of MED2, and hence an overlap in phenotype (Robinson et al., 2015).

An overlapping function of SFR6/MED16 with MED14 in defence gene expression was reported by Zhang et al. (2013) and particularly significant was the suppression of salicylic acid-induced defence responses to a virulent strain of the bacterial pathogen *Pseudomonas syringae*. A physical connection between Sin4p (MED16/SFR6) and Rgr1p (MED14) was demonstrated by Li et al. (1995a) where deletion of the C-terminus of Rgr1p caused loss of both Sin4p and the triad, indicating that Rgr1 anchors the mediator tail domain to the rest of the Mediator

complex. *sfr6-1* mutation demonstrated a more severe phenotype than *med14-1* and this could be explained again by the type of knockout of *sfr6-1* which has no protein produced at all but *med14-2* might produce a truncated protein. Furthermore if *med14-1* lacked the C-terminal domain, it might fail to interact with MED16 but still it could attach to mediator complex and be able to do something in relation to those stress that I studied.

MED15, one of the proposed subunit of the Mediator tail triad was shown to be required for regulating SA-induced defence responses. Salicylic acid (SA) is a key component in regulating defence gene expression pathway such as induction of pathogenesis-related genes like *PR1* in response to biotrophic and hemibiotrophic pathogens as well as under UV-C irradiation (Wathugala et al., 2012). In this thesis study impaired UV-C gene expression in *med2-1* suggests that MED2 is also required for SA-induced defence responses, further evidencing that most of the tail subunits in the Mediator complex play a role in SA-induced plant defence.

The different levels of sensitivity of the three *med* mutants under cold, UV and drought suggests that MED2, MED14 and MED16/SFR6 are important in transcriptional regulation under different stress conditions involving the control of a number of different regulons. This concurs with Kidd et al., (2009) who reported that plant mediator controls a range of gene expression responses through multiple subunits and association with specific transcription factors.

Elfving et al. (2011) evidenced that MED25 is required for the regulation of both plant development (flowering time) (Cerdán and Chory, 2003, Ou et al., 2011) and pathogen defence (Kidd et al., 2009). The possible association of MED8 with specific transcription factors was suggested (Kidd et al., 2009) as it demonstrates a

similar role to MED25 in both flowering time and pathogen defence. However, the current prediction is that MED25 is physically closer to MED16 than to MED8 yet despite the fact they probably occupy positions in the complex that are distant from one another, they both share in the control of specific responses to biotrophic pathogens (Kidd et al., 2009, Wathugala et al., 2012). This might due to different transcription factors bind to each subunit but activating the same genes under stress conditions. Interestingly, MED25, recently shown to interact with MED16, does not share a role with MED16 in controlling cold and starvation-responsive transcription (Hemsley et al., 2014). So position and proximity of subunits may not be the most important factor in determining which subunits operate to control the same regulons (Kidd et al., 2009, Wathugala et al., 2012, Zhang et al., 2013).

MED2, MED14 and MED16/SFR6 are predicted to be located in the tail part of the plant mediator complex, based on the yeast mediator interaction map (Guglielmi et al., 2004, Robinson et al., 2015). Findings from this study have shown a similar role for MED2 and MED14 as MED16/SFR6. However some mediator subunits like MED25 and MED8 are not in close to each other and share their effects at the same time MED16 and MED25 predicted to be close to each other but yet not share effects.

Recently it was found that MED25 interacts with MED16 to regulate iron homeostasis (Yang et al., 2014), so it is likely that MED25 is a mediator tail subunit but it was not known when I started this research work. Therefore MED25 was not included in this study as potential tail subunit to further investigate. However the many studies related to MED25 revealed that role of MED25 is vital in both biotic and abiotic stress conditions. Kidd et al. (2009) reported that MED25 (PFT1) acts as key regulator of the jasmonate signalling (JA) pathway and is important to acquire

resistance against leaf infecting necrotrophic fungal pathogens. Chen et al. (2012b) revealed MED25 positively regulates JA signalling while negatively regulating ABA signalling pathways, highlighting the existence of an antagonistic interaction between JA and ABA signalling. This suggests that MED25 is important in fine tuning plant resistance to particular pathogens via regulating ABA signalling apart from JA driven pathogen resistance. Moreover Elfving et al. (2011) revealed that MED25 is important in drought and salt resistance. All these evidences might be consistent with that MED25 being a tail subunit of the mediator complex like MED2 and MED14 that studied in the present study.

Some other subunits across the mediator complex are involved in regulating stress responses, indicating that several subunits irrespective to the position could involve in similar role. The Mediator head subunit MED8 is known to regulate jasmonic acid-dependent defence responses; reduced resistance of the *med8* mutant to leaf infecting necrotrophic pathogens was reported but susceptibility to the root infecting hemibiotrophic fungal pathogen (Kidd et al., 2009, Thatcher et al., 2009). MED21, part of the middle section of the complex has been identified as important in disease resistance against necrotrophic pathogens (Dhawan et al., 2009). MED18 was recently discovered as second head subunit in Mediator that is important for disease symptoms and pathogen growth in plants infected with necrotrophic fungal pathogens but it functions independently of JA signalling (Lai et al., 2014) indicating that it is mechanistically distinct from MED25 and MED8 in plant pathogen tolerance.

Considering all of the evidence available so far regarding the role of different mediator subunits I could summarise that several subunits across the complex representing head, middle and tail domains are important for the tolerance against

pathogen infections but only MED16 and MED25 were known to be important in abiotic stress tolerance to acquire freezing and drought/salt tolerance respectively. However findings of my study indicate that MED2 and MED14 share the same role as MED16/SFR6 in gene regulation under cold, drought, and UV stresses. However, under dark conditions *med2* mutants showed unaffected gene expression compared to other two med mutants Hemsley et al. (2014). This further suggests that these mediator subunits might share their roles under several but not at all stress conditions.

6.3 The role of KIN10 and MED16 in stress-inducible transcription

6.3.1 KIN10 controls the expression of a subset of stress-inducible genes controlled by SFR6/MED16

In chapter 5 experiments were designed to investigate the effect of KIN10 upon transcriptional activation of stress genes. KIN10 was previously identified as a putative interactor of SFR6/MED16 (Hemsley and Knight, unpublished) and *med16* and *kin10* mutants were observed to share impaired dark- inducible *DIN6* expression under starvation conditions (Hemsley et al., 2014, Baena-Gonzalez et al., 2007). Further investigation of shared transcriptional targets of KIN10 and MED16 might support the hypothesis that these two proteins do interact and that this interaction has functional significance in abiotic stress responses.

KIN10 (AKIN10/At3g01090) is one subunit of the SnRK1 kinase enzyme complex, which is important in energy sensing particularly under energy depleting conditions (Baena-Gonzalez, 2010, Baena-Gonzalez and Sheen, 2008) and this catalytic subunit

in Arabidopsis is orthologues of yeast Snf1 and mammalian AMPK act as evolutionarily conserved energy gauges by controlling the reprogramming of transcription in response to seemingly unrelated darkness, sugar and stress conditions (Baena-Gonzalez and Sheen, 2008, Polge and Thomas, 2007, Ghillebert et al., 2011). Upon deprivation of sugar and energy, KIN10 targets a remarkably broad array of genes that orchestrate transcription networks, promote catabolism and suppress anabolism (Baena-Gonzalez et al., 2007, Baena-Gonzalez and Sheen, 2008).

In yeast, SNF1 was identified to be responsive to several stress conditions such as oxidative stress, sodium ion stress, changes in alkaline pH conditions as well as an inhibitor of the respiratory chain (Ghillebert et al., 2011, Hong and Carlson, 2007) .Young et al. (2003) reported that expression of quarter of the yeast genome (2126 genes) is modified during the shift of yeast cells from fermentative to an oxidative (respiratory) metabolism, where SNF1 kinase play a major role (Hardie et al., 1998) by encoding genes mainly involved in transcription, signalling, carbohydrate metabolism and respiration (Young et al., 2003). This activation of gene transcription occurs via the interaction of SNF1 with different members of the transcriptional machinery by direct interaction with RNA polymerase II to modulate its activity, (Kuchin et al., 2000), by phosphorylating histone H3, regulating TATA-binding proteins (TBP) (Shirra et al., 2005, Lo et al., 2005, Lo et al., 2001) or directly phosphorylating GCN5, a histone acetyltransferase that controls transcription of multiple yeast genes (Liu et al., 2005b). Kuchin et al. (2000) revealed that Snf1 interacts with mediator/srb proteins, *i.e* Sin4 (yeast MED16), srb10 (CDK8) and srb11 (CycC) in the Yeast-two-hybrid and co-immunoprecipitate experiments *in vivo*. Recently Ng et al. (2013) demonstrated that in Arabidopsis KIN10 interacts

with another mediator subunit, CDK8 (part of the kinase submodule) the same subunit in yeast and plants which interacts with kinase, using fluorescence complementation assays. This finding indicates the possibility that KIN10 might interact with more than one subunit of mediator complex like in yeast. Miller et al. (2012) reported that number of Mediator subunits is phosphorylated and SNF1 might be the kinase that does this. However above interaction might or might not be a phosphorylation event.

SFR6/MED16 is a tail subunit in the plant Mediator complex and important in transcriptional regulation under different stress conditions and recently I discovered similar transcriptional responses in MED14 other than earlier known regulons (see Chapter 3). Therefore making link that yeast SIN4 interacts with SNF1, MED14 in yeast interacts with SNF1 (Young et al., 2009) and showing similar transcriptional responses as MED16/SFR6 in plants and by being both tail subunits in the mediator I strongly hypothesise the possibility of existing interactions between SFR6 and SnRK1.

As explained earlier there is evidence that KIN10 and SFR6 share role in response to starvation (Baena-Gonzalez et al., 2007, Hemsley et al., 2014) but no experiments had never been done in two loss of function mutants side by side and no attempt made to look closely at other regulons. The effect on *DIN6* expression under limited conditions of photosynthesis and respiration such as dark, DCMU (a herbicide that affects the photosynthetic electron transport chain in photosynthesis) was studied in protoplasts (Baena-Gonzalez et al., 2007) and effects of flooding/ submerged were studied by (Young-Hee Cho et al., 2012). Therefore I focused to investigate stress gene expression in loss of function of mutants of KIN10 under cold, desiccation/drought and UV which are well studied stresses in SFR6/MED16.

Results of the three biological replicates presented in Chapter 5 (see sections 5.1.1.1 5.2.1.2) showed that under cold, desiccation/drought and dark *kin10-2* showed impaired gene expression as in *sfr6-1* but to a lesser and varying degree. Even though the trend showed impaired cold gene expression in *kin10-2*, it was not significantly reduced compared with Col-0 whereas in *sfr6-1* mutants *COR* gene expression is always severely impaired (Boyce et al., 2003, Knight et al., 2009, Knight et al., 1999). Dark-inducible starvation conditions and dark-inducible gene *DIN6* is well-studied as it is targeted by KIN10 (Baena-Gonzalez et al., 2007, Contento et al., 2004), however, interestingly, I observed that desiccation/drought-induced *KIN2* expression was severely affected compared to the level of reduction in *DIN6* expression in the mutant under dark conditions (see sections 5.1.1.1 and 5.2.1.2). I used two other drought-inducible genes *LTI65* and *P5CS1* that do not contain CRT/DRE elements in their promoter (and therefore are not subject to regulation by DREB2) therefore ABRE genes (Yamaguchi-shinozaki and Shinozaki, 1994) and found that *P5CS1* showed a highly significantly reduced level of expression in *kin10-2* and moderately reduced (but not significantly different) level of *LTI65* expression in *kin10-2* in all three replicate experiments. Whilst different levels of significant differences were observed in the expression of different genes it is clear that all of the desiccation/drought-induced genes tested were affected by loss of KIN10, an observation that has not previously been reported.

DIN6 gene expression was examined by (Baena-Gonzalez et al., 2007) in Arabidopsis protoplasts overexpressing KIN10 and detached leaves of plants expressing DIN6-LUC and showed higher induction compared to Col-0 but they did not examine the levels of *DIN6* expression in a KIN10 mutant background. In this

study I used whole plants of a KIN10 loss-of-function mutant but did not observe significant differences in *DIN6* expression between Col-0 and *kin10-2* in average data of three biological replicates though the trend of reduced *DIN6* expression was observed in individual experiment. All experiments were repeated three times to reproduce results to obtain better validation but I found average results of three biological replicates did not give statistically significant results. In many instances the reduced gene expression was clear in each individual experiment though the average values were not statistically significant. Due to high sample variability at each occurrence dependence on the *P* value to determine the significance of results is not always accurate (Halsey et al., 2015, Mobley et al., 2013) as explained early in this chapter. Averaging of gene expression data from three biological replicates was extremely difficult as the relative levels of gene expression varied sometimes thousand folds in one replicate compared to the other biological repeat. Therefore interpreting results totally based on *P* value is misleading and I considered the trend along with *P* value to report results on transcriptional data in these experiments. I used DCMU treatments to study if the level of *DIN6* upregulation would be more consistent between experiments than darkness due to its direct involvement by interrupting the photosynthetic electron transport chain in photosynthesis, However in this study I could not observe consistent data with less reproducibility.

Surprisingly, though UV-C induced *PR1* gene expression was up-regulated in *kin10-2* compared to Col-0 no consistent pattern of gene expression was observed in all three biological replicates with highly different transcriptional regulation observed in control of pathogenesis-related target genes by KIN10. Therefore results indicate that PR1 is not a target of KIN10 though PR1 is a target of SFR6. This is one of the

notable deviations of KIN10 target gene that I observed in these experiments which was totally contradictory to the behaviour of SFR6/MED16 on pathogenesis-related gene expression.

I used only one *kin10* mutant allele in this study as *Akin10*-1 mutant did not produce consistent results in repeat experiments, which might have been due to a conditional aspect of the insertional mutation; therefore KIN10 complemented lines were created in the *kin10-2* mutant background. *DIN6* and *KIN2* gene expression experiments with four complemented lines showed restoration of the wild type gene expression phenotype (see section 5.2.2.1 and 5.2.2.2).

Therefore with the findings of this study I can conclude that KIN10 affects the expression of some of the same target genes as in SFR6/MED16 under different stress conditions and could see similar transcriptional regulation under some but not under all stress conditions. Furthermore, the desiccation/drought gene expression phenotype is more prominent compared to well-studied dark gene expression phenotype so far in the level of whole plant. Summary of the transcriptional responses that MED16/SFR6 and KIN10 regulates under different stress conditions is given in the Figure 6.1.

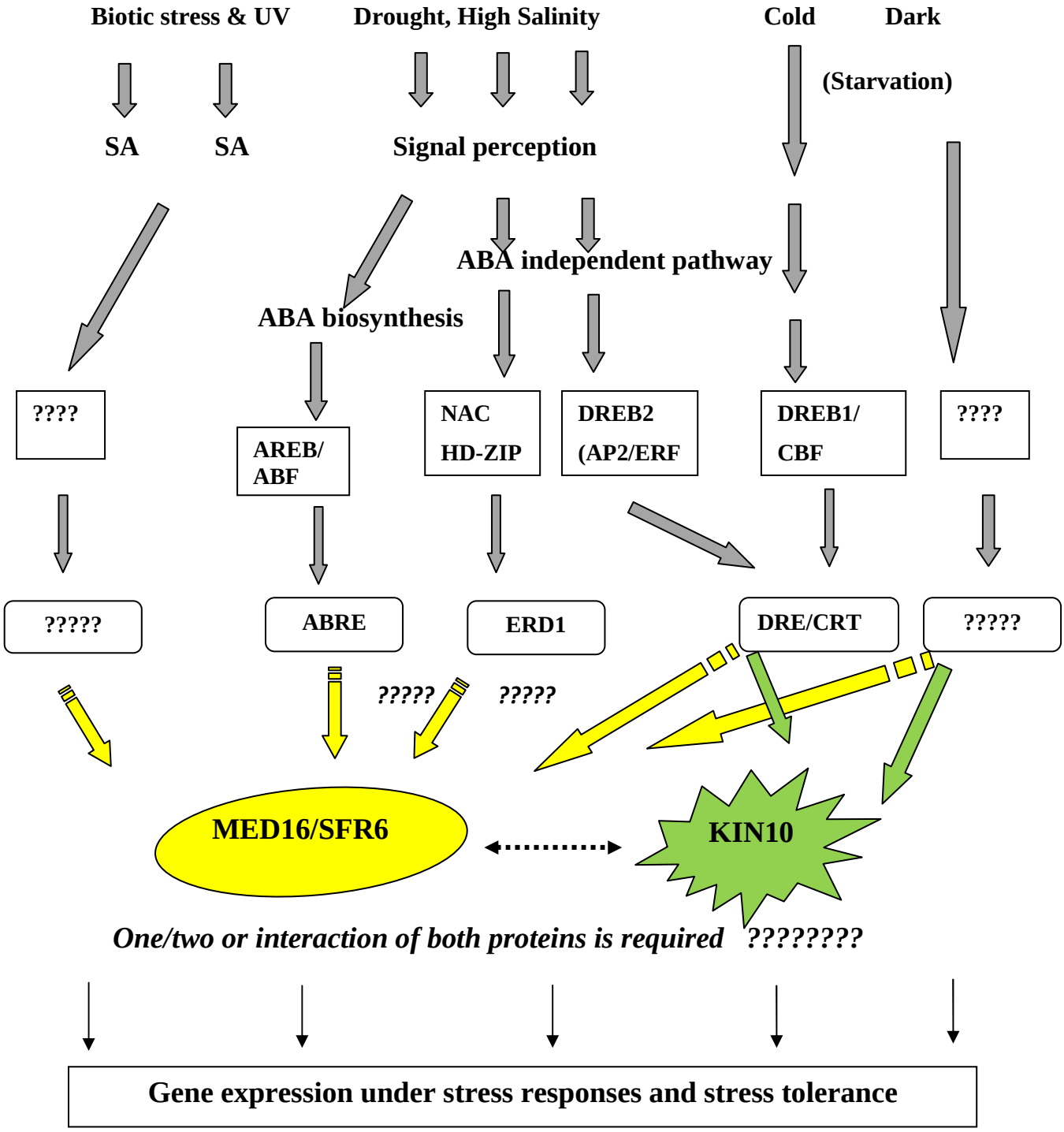

Figure 6.1: Summary of the transcriptional responses under different stress conditions. This diagram shows different stress conditions studied in this research work that require MED16/SFR6 and/or KIN10 in order to elicit changes in gene expression and tolerance. Promoter elements are shown where known. Dotted lines between MED16 and KIN10 represents that they might act together under certain stress conditions. Yellow colour arrows represent the stress conditions where MED16/SFR6 is involved and green colour represent the stress conditions where the involvement of KIN10 is known. Question marks in boxes represent the unknown TF as well as binding elements under certain stress conditions.

6.3.2 Involvement of MED16 domains in interaction with KIN10 and evidence that KIN10 and MED16/SFR6 act on the same pathway to regulate dark and drought gene expression

Observing similar defects in transcriptional regulation in mutants of both SFR6/MED16 and KIN10 together with the fact that some Mediator tail subunits *i.e* Med14 (Rgr1) interact with Snf1 (Young et al., 2009) and Med16 interacts with Snf1 (Kuchin et al., 2000) in yeast assumption was made that plant Mediator tail subunit SFR6/MED16 could interacts with KIN10. The pull down experiments with GFP tagged full length and truncated SFR6 proteins suggested that some of the SFR6 truncations might interact with KIN10. This further agree with the preliminary studies carried out using yeast-two-hybrid in the lab found that KIN10 as an interactor of SFR6 and that interaction was confirmed by Co-IP (Hemsley and Knight unpublished) with full length SFR6. Moreover present study provides further information about the regions that are more likely to interact with KIN10.

The experiments provided evidence that three of the constructs, including full length SFR6, were able to interact with KIN10: SF14, SF15 and SF16 could interact with KIN10 showing the necessity of the N-terminal part of SFR6 to make interactions with KIN10 whereas SF36 was unable to keep that interaction, likely due to lack of 633aa from the N-terminus of the protein. Moreover these results make the argument that the C-terminus (about 396 amino acids) is not important in making interaction with KIN10 although it has Zn figure domain as well as many of plant specific SSM regions towards the C-terminus.

When studying the SFR6-KIN10 interaction the next question that arises is that of which type of interaction that SF truncations might have with KIN10. This could purely be a physical interaction or result of a phosphorylation event. Considering the

SMART (Simple Modular Architecture Research Tool) domains as well as potential phosphorylation sites in SFR6 suggests that five phosphorylation sites and two protein binding domains located in the SFR6 protein (see Figure 6.1). Out of five potential phosphorylation sites, two are located in the domains of 100-110aa and 300-310 aa that are located between SF1 and SF3 region of the truncations whereas the other three are located within the region of SF3-SF4 (600-610aa, 650-670aa and 890-910 aa). Moreover the predicted SUMO site (ASHAASAGTG) is located in the region of 830-850 aa (see Figure 4.1b). Two protein binding domains are located in the regions of SSM5 and SSM22. SF15 and SF16 cover all 5 phosphorylation sites, the SUMO site as well as two protein binding domains, however, SF14, which demonstrated the KIN10 interaction, lacks the 5^{th} phosphorylation site as well as the second protein binding domain that is located within the SSM22. With this evidence I could suggest that 5^{th} phosphorylation site and protein binding domain in SSM22 are less important compared other sites. The SF36 truncation that did not produce interaction with KIN10 in three consecutive experiments includes the last three phosphorylation sites out of five, the SUMO site as well as one of two protein binding domains. This result indicates that first two phosphorylation sites and first protein binding domain are more important over others as I observed same results for the interaction of SF36 with KIN10. However this might not be the sole reason but some other special features within the first 525aa region collectively cause the impact on having interaction between SF truncations that consists of N-terminus of the protein and KIN10.

Previous reports on transcriptional as well as proteomic work in yeast recorded that mediator subunits of MED1, MED2, MED4, MED5, MED6, MED13, MED14 , MED15 and MED17 (Chang et al., 2004, Guidi et al., 2004, Hallberg et al., 2004,

Liu et al., 2004, Miller et al., 2012, Soufi et al., 2009, Albuquerque et al., 2013, Li et al., 2007, Gruhler et al., 2005) are phosphorylated and for some, phosphorylation influenced their function (Chang et al., 2004, Guidi et al., 2004, Hallberg et al., 2004, Liu et al., 2004, Miller et al., 2012). The majority of these phosphorylated subunits are located either in tail or middle subunits in the mediator complex. Therefore, there is a good chance for MED16 to be phosphorylated by KIN10 and might cause activation of different transcriptional responses.

Young-Hee Cho et al. (2012) demonstrated not only Arabidopsis SnRK1 (Bitria´n et al., 2011) but also rice SnRK1 regulates gene activity and induced the activity of the *DIN6* promoter and responded to hypoxia in a manner similar to Arabidopsis. And they speculate that under submergence conditions, (the main stress they studied) the protein kinases associated with target gene chromatin in the protein complexes that recruited specific DNA-binding partners *i.e* transcription factors. Moreover they conducted experiments to validate the Protein Kinase (PKs) function in gene regulation, by using inactive forms of SnRK1s as ATP binding site-mutated PKs (OsSnRK1 and KIN10) and as catalytically inactive PKs (OsSnRK1 and KIN10) in which phosphorylation of all types of SnRK1s was detected but none of the mutant kinases was able to activate the DIN6-LUC reporter, suggesting that intact PK activities of OsSnRK1 and KIN10 are essential for gene regulation. Therefore as *DIN6* is one of the target genes of both SFR6 and KIN10 and I might speculate that same phosphorylation event might happen. Therefore highly conserved protein kinase in plants (SnRK1/KIN10) has high possibility to interact with SFR6 and in this study it further confirms that particular domains are more important when making interactions between KIN10 and SFR6.

Separate set of experiments were carried out to test that KIN10 and MED16/SFR6 act on the same pathway to regulate dark and drought gene expression using double mutant of *sfr6-1* and *kin10-2* and over-expression lines of KIN10 in both Col-0 and *sfr6-1* backgrounds. I created three lines of *sfr6kin10-2* double mutants and only dark and drought gene expression experiments were conducted with double mutant lines as these were the two conditions that showed the most notable differences in stress gene expression between wild type plants and the *kin10-2* single mutant. I observed reduced level of both *DIN6* and *KIN2* expression in 3 lines of double-loss-of-function mutants similar to the level of that in *sfr6-1* mutant which was the severely affected loss-of-function mutant compared to *kin10-2*. Therefore results of these experiments showed that there was no additive effect due to loss of both SFR6 and KIN10, indicating these two proteins act on same pathway to regulate stress gene expression. Furthermore, drought tolerance and dark-induced starvation tolerance results presented in 5.2.3.4 and 5.3.3.4 sections also indicated that double mutants were affected similarly to the *sfr6-1* single mutant. The reduced level of drought tolerance (measured by survival) in *sfr6-1* and double mutant lines was not as pronounced as the reduction in drought/desiccation-induced *KIN2* expression in these lines, indicating that many genes might be involved in control of drought tolerance other than *COR* genes. However, the starvation tolerance phenotype seen in the mutants was more significant than the dark gene expression phenotype.

The second strategy that I used to study whether SFR6 and KIN10 and act on same pathway to regulate stress genes targeted by both SFR6 and KIN10 was use of KIN10 over-expression lines in Col-0 and *sfr6-1* backgrounds. Baena-Gonzalez et al. (2007) showed that protoplasts of wild type plants over-expressing KIN10 exhibit higher levels of stress gene expression compared to wild type (*i.e* dark induced genes

like *DIN3* and *DIN6)* even in the absence of stress. I examined the behaviour of *sfr6-1* mutants which over-expressed KIN10 to study whether they could highly express these stress genes even without the stress. If the expression of stress genes were to be elevated, as in wild type, it would suggest that SFR6 does not help to perform the function of KIN10. If the overexpression of KIN10 has no effect in *sfr6-1* mutants, this might signify that SFR6 is essential for KIN10 to perform its functions and it gives an indication further to the evidence from double loss-of-function mutants described above, that SFR6 and KIN10 act together on same pathway leading to control of stress gene expression.

Four out of five wild type lines overexpressing KIN10 showed higher levels of *DIN6* expression in unstressed plants and all five lines gave high level of *BCAT*2 expression. Conversely, none of three *sfr6* mutant lines overexpressing KIN10 showed elevated levels of *DIN6, BCAT* or *KIN2* compared to their untransformed counterparts in three replicate experiments. Consistent with previously reported results on *KIN2* expression in single and double mutants of KIN10, here KIN10 over-expression lines also showed significantly high levels of *KIN2* expression in untreated plants of wild type lines and highly reduced level of *KIN2* in all three lines of *sfr6-1* mutant lines overexpressing KIN10. Expression levels of all three genes tested in these experiments is evidence that there was no effect of overexpressing KIN10 in *sfr6-1* mutant plants on KIN10 target genes as seen in Col-0 plants, giving a clear indication that for KIN10 to activate target genes, SFR6 is a requirement. Therefore, I demonstrated that SFR6 is important for the activation of target genes by KIN10 and acting both SFR6 and KIN10 in same regulatory pathway to control stress genes specially under dark and drought induced stresses.

Jossier et al. (2009) reported that plants over-expressing SnRK1/KIN10 exhibited a hypersensitive phenotype post-germination when supplemented with ABA but not at the seed germination stage. However, they did not report on the level of ABA-responsive gene expression in the mutant background. In the present study, I tested the gene expression response of *kin10-2* plants supplemented with ABA but was unable to observe differences in the gene expression phenotype compared to Col-0 (see section 5.2.1.2.3). In addition to *DIN6*, *KIN2* gene expression was tested in response to cold, drought/desiccation and ABA and I could see absolutely different expression trends in *kin10-2* mutants compared to wild type. *kin10-2* exhibited significantly reduced *KIN2* gene expression under drought/desiccation, no apparent effect of cold induced *KIN2* and no any effect of ABA induced *KIN2* expression at all. Regulation of KIN10 in ABA responses was reported by Jossier et al. (2009) but I could not observe any effects of KIN10 in response to ABA.

The only plant mediator subunit reported so far that has been shown to interact with KIN10 is CDKE1 (CDK8) in Arabidopsis (Ng et al. (2013). CDK8/CDKE1 is a subunit in mediator kinase module which was earlier known as being implicated in floral organ identity (Wang and Chen, 2004). Gonzalez et al. (2007) revealed interaction of CDK8 with Leunig (a transcription co-repressor interacts with HISTONE DEACETYLASE19) a regulator of JA-dependent defence responses, as well as MED14. Ng et al. (2013) recently demonstrated that CDK8 regulates mitochondrial retrograde signalling (arising due to reactive oxygen species in mitochondria or plastids and altering/modifying nuclear gene expression) in response to H_2O_2 and cold stress. In their screening they identified Regulator of Alternative Oxidase1, a mutant (*rao1*) as restrograde signalling component and later found it was a mutation in the CDK8/CKDE1, one of the mediator subunits. Furthermore, they

demonstrated that KIN10 interacts with RAO1 and is transported to the nucleus. Furthermore, the gene expression profile studied for *rao1* plants under AA treatments (Antimycine A– potent inhibitor of the mitochondrial respiration binds to the quinol reduction site of cytochrome complex) showed significant overlap with expression profile for the *KIN10* gene targets and one of those targets was *DIN6*.

These data provide evidence that KIN10 interacts the Mediator complex and suggest the possibility that, as in yeast, KIN10 and might interact with other different sites in the mediator. Linking that MED14 in yeasts interacts with SNF1 (Young et al., 2009) to plant that KIN10 might interact with MED14 perhaps referring to the fact that KIN10 interact with CDK8 (Ng et al., 2013). Based on the results I reported under this section prove that KIN10 and SFR6 act on the same pathway leading to stress gene expression.

6.3.3 The altered visible phenotype observed in Col-0 by KIN10 overexpression is affected in the *sfr6-1* background

Baena-Gonzalez et al. (2007) reported their attempt to study long term effects of KIN10 at the whole-plant level using transgenic lines overexpressing KIN10 and *kin10* loss-of –function mutants. Observations were made on root growth of above lines and reported that KIN10 over-expression lines displayed some advantages in primary root growth and development under low light and limited energy supply (Baena-Gonzalez et al., 2007). With exogenous energy supply (sucrose) they observed reduced root and shoot growth in KIN10 over-expression lines and suggested KIN10 repression of biosynthetic activities in plants. However KIN10 silenced lines (loss-of–function) exhibited enhanced root and shoot growth by utilizing exogenously supplied sucrose. Furthermore, they observed increased

accumulation of anthocyanin in Col-0 and *kin10* mutants when sucrose levels were increased to 3% but not in KIN10 overexpression lines, suggesting that the repression effects of KIN10 overexpression (Baena-Gonzalez et al., 2007). Furthermore, they reported enhanced starvation tolerance in KIN10 overexpression lines through promotion of plant survival whereas wild type seedlings underwent rapid senescence particularly under no exogenous glucose supply and light limiting conditions where photosynthesis is affected (Baena-Gonzalez et al., 2007). All above data evidence that KIN10 plays a wide role in vegetative and reproductive growth that is important in developmental transition in plants.

Interestingly the same study reported changes in KIN10 overexpression lines grown in soil, especially discovering a new role of KIN10 in determining plant shape and developmental transition in Arabidopsis. KIN10 overexpression lines exhibited altered inflorescence architecture and delayed flowering and onset of senescence under long day conditions (20 h light/ 4 h dark) (Baena-Gonzalez et al., 2007). I studied the flowering phenotype of KIN10 overexpression lines created during this study in both Col-0 and *sfr6-1* backgrounds and made similar observations as those reported by Baena-Gonzalez et al. (2007) in KIN10 overexpression lines of Col-0 (see section 5.2.6). In the current study KIN10 overexpression lines in Col-0 background exhibited significantly short inflorescences and no branching compared to Col-0 and *kin10-1*. The results were consistent with all four lines of KIN10 over-expressers used in the study and I did not observe any defect in vegetative growth of plants.

The flowering phenotype of KIN10 overexpressers in *sfr6-1* was monitored in the present study and I observed different phenotypic characteristics compared to wild type KIN10 over-expressers. None of the plants representing three lines of KIN10

overexpressers in *sfr6-1* background exhibited flowering at the same time point (25 days-old in soil) as seen in Col-0 background. *sfr6-1* is a known mutant that exhibits delayed flowering (Knight et al., 2008) and I observed similar characteristic of untransformed *sfr6-1* in KIN10 overexpressing in *sfr6-1* mutant background. Due to that I could not look for the other effects of overexpression such as effects on root branching, inflorescence etc. though I designed this experiment to test whether KIN10 had any additional effects. The failure to demonstrate at least similar flowering effects as observed in KIN10 over-expressing lines in Col-0 suggests that lack of SFR6 prevents the role of over-expressing KIN10 providing further evidence that the necessity of SFR6 to activate different signalling pathways by KIN10.

6.4 Exploring the function of SFR6/MED16 protein domains

The Mediator complex was first identified and purified from yeast (*Saccharomyces cerevisiae*) (Kim et al., 1994) which is required for reconstitute the activation of RNA polymerase II transcription. Morphological and biochemical studies on yeast mediator suggested that complex is consisted with 25 subunits and grouped in to four modules, name as the head, middle, tail and kinase modules (Guglielmi et al., 2004, Dotson et al., 2000). Studies based on electron microscopy and reconstitution experiments led to identify different subunits under each mediator module/domain. The Mediator complex was biochemically identified in several species across eukaryotes including yeast, mammals, metazoans, insects and worms (Kim et al., 1994, Thompson et al., 1993, Fondell et al., 1996, Sato et al., 2003, Malik and Roeder, 2000, Park et al., 2001, Kwon et al., 1999). Limited homology of Mediator complex have been identified among these eukaryotes and the presence of the

complex in plants was suggested based on these sequence homologies (Autran et al., 2002, Clay and Nelson, 2005, Gonzalez et al., 2007).

Sequence signature motifs (SSM) were identified by (Bourbon, 2008) based on regions previously defined as conserved protein domains from systematic database searches and he stated that only a few residues in most SSMs have remained unchanged during evolution. Therefore this divergence is in keeping with the low conservation of most MED proteins and defined SSMs were distributed throughout the primary sequences of most of the med proteins except in Med15 (Bourbon, 2008). Many of the SSMs were included within the regions delineated as inter subunit interaction domains and some others are involved in functional connections with Pol II or general transcription factors (Bourbon, 2008, Myers et al., 1998, Robinson et al., 2015). Yeast MED16 consists of 27 SSM regions where seven WD repeats are located in the N-terminal half and there is a C-terminal C2-C2 zinc finger (ZF) motif (Bourbon, 2008, Robinson et al., 2015). The WD repeats correspond to distinguishable domains identified in many functionally distinct proteins (See Figure 6.1). Moreover, within the region of the last 295 aa in between the middle and the conserved zinc finger domain of MED16 is consists of plant specific amino acid sequences. Therefore either SSM regions or plant specific region might be responsible for particular functions of MED16 *i.e* TF binding.

6.4.1 Transiently expressed truncated versions of SFR6/MED16 localise to the nucleus

Six different in-frame fusions of truncated versions of SFR6/MED16 with N-terminal GFP were tested for their ability to localise to the nucleus in transiently expressing in tobacco. GFP fluorescence, which was observed using confocal laser

scanning microscope, confirmed that all six constructs were localised to the nucleus (see section 4.2.2). However, the distribution of the expression of GFP fluorescence in cells was different for each fusion when compared with GFP tagged GUS protein (35S::GUS::GFP), the cytosolic control for this experiment, which showed mostly cytosolic localisation. Therefore to compare different fusions, mean fluorescence levels (unit as grey values) in the Region of Interests (ROI) within the nucleus and cytoplasm was analysed and fluorescence ratio between nucleus (ROI nucleus) and cytoplasm (ROI cytoplasm) was compared between fusions. The highest expression ratio was observed in leaves expressing 35S::SF16, encoding the full length SFR6 protein, which has been shown previously to be nuclear targeted (Knight et al., 2009). In leaves expressing SF36 reported the second highest ratio, which lacks the N terminal third of the SFR6 protein where as the other four constructs showed lower average ratios of fluorescence expression compared to SF16 and SF36 but higher than the 35S::GFP::GUS, the cytosolic control used in this experiment. This provides evidence that C-terminus of the SFR6 protein is much essential compared to the N-terminus for directing of proteins to the nucleus.

The potential nuclear localisation signals (NLS) within the SFR6 protein using NUCPred program (https://www.sbc.su.se/~maccallr/nucpred/) with the amino acid sequence of GFP tagged full length SFR6 protein predicted that the strongest nuclear localisation motif is located towards the end of C-terminus of the protein at the location of 1172-1184 aa of SFR6/MED16 (see section 4.2.2). However, I observed all truncated fragments were targeted the nucleus including truncations such as SF15, SF14, SF25 and SF24 which lack of above positions of the a.a. in C-terminus of the protein. This finding is contradictory to the predicted nuclear localisation signal using NUCPred program that indicated the nuclear localising signal is in the C-

terminus of the protein. Therefore it suggests that some other factor might responsible apart from NLS that helps protein to go to the nucleus. Possibly these truncated fragments could pass through the nuclear membranes through the process of diffusion. However Young-Hee Cho et al. (2012) reported that a protein of approximately 84.5 kD in size localised the nucleus even without nuclear import signal.

6.4.2 Role of MED16 domains in defining visible phenotypes; flowering and green colour restoration

Experiments were conducted to study the ability of SF truncations to complement some or all of phenotypes such as visible yellow phenotype of *sfr6-1* and flowering (Knight et al., 2008). Crossing of *sfr6-1* mutants with Col-0 plants that overexpressed SF constructs were used to obtain SF constructs to *sfr6-1* background due to no successful direct transformation of *sfr6-1* mutants with SF constructs. The reason might be the poor flowering ability of *sfr6-1* mutants (Knight et al., 1999) and other associated malfunctions of the mutant.

First, the level of *SFR6* transcript expression in F_3 lines homozygous for the *sfr6-1* mutation was tested in all transgenic lines compared to wild type, *sfr6-1* mutant and three lines of *sfr6-1* mutant complemented with AtSFR6 and *sfr6-1*+35S::GUS (GUS, as control for the presence of SFR6). Levels of total *SFR6* expression (native and transgene) in all five lines of *sfr6-1*expressing either 35S::SF14 or 35S::SF15 were higher (ten-fold higher except in one line) than in wild type (see section 4.2.4). Expression levels of *SFR6* in all lines of *sfr6-1* expressing either 35S::SF16 or 35S::SF36 were low compared to the level of transgene expression for other constructs. Due to the observed low expression of *SFR6* in these lines, the level of

the *SFR6* transgene (rather than total *SFR6*) expression in F_3 plants was analysed for comparison. (As the *sfr6-1* mutant differs only by a SNP normal levels of SFR6 transcript are likely to be observed in mutant plants whereas measurement of the transgene specifically will not detect these transcripts). Transgene expression in F3 appeared higher compared to *SFR6* expression in both these constructs but transgene expression in six lines of *sfr6-1*+35S::SF16 was relatively low compared to the levels observed for other constructs. It is hard to understand the inconsistency of expression in these transformed lines but it seems most probable that there is little or no transgene expression in the SF16 lines (see Table 4.1). However, I can conclude that one of the two methods of measuring transcript is not working properly. Either the SFR6 primers are failing to pick up the transgenic SFR6 or the transgene primers are detecting something that is not the real transgene.

Selected homozygous lines for the *sfr6-1* mutation that overexpressed SF16, SF15, SF14 and SF36 truncations were tested for their ability to complement the visible pale leaf and cotyledon phenotype. This is a prominent phenotypic characteristic of *sfr6-1* that shows pale green colour compared to Col-0 during early stages of seedlings with bigger cotyledons (Knight et al., 2009). Percentage of green colour restoration was calculated by scoring individual seedlings as yellow or green. One line out of five in *sfr6-1*+35S::SF14 (SF14) was restored to a green colour partially but others remained pale in colour. In *sfr6-1*+35S::SF15 (SF15), one line is completely restored to green colour while the other four lines remained partial restoration of green colour (see Table 6.1).

Out of two lines of *sfr6-1*+35S::SF36 (SF36), one showed complete restoration of green colour while other one showed partial restoration. However in *sfr6-1*+35S::SF16 (SF16) only two lines were showed complete restoration of green

colour and other two lines were remained similar colour as in *sfr6-1*. Though I intended to create fully complemented control lines of *sfr6-1*+35S::SF16 (SF16), which would be the perfect control for this experiment, it did not succeed. However, complete restoration of green colour in lines of genomic SFR6 (full length) was reported by Wathugala et al. (2011) and the difference compared to present study is the completed lines created using cDNA of SFR6 in a same vector with different antibiotic resistance (see Table 4.1).

Along with green colour restoration experiments flowering time phenotype of different lines of complemented truncations of SFR6 were studied as *sfr6-1* mutant shows late flowering (Knight et al., 2008) compared to Col-0 (See section 4.2.4.2). In *sfr6-1*+35S::SF14 (SF14) line #7 showed fully complementation of flowering time phenotype but the other four lines showed late flowering where this was consistent with green colour restoration phenotype. Line #1 in *sfr6-1*+35S::SF15 (SF15) showed similar flowering time phenotype as in Col-0 while #2, #3 and #4 showed partial complementation *i.e* early flowering compared to *sfr6-1* but not a complete complementation of flowering time phenotype and these results are in consistent with green colour restoration phenotype of this construct. However line #4 in *sfr6-1*+35S::SF15 (SF15) showed a similar flowering time phenotype as in *sfr6-1* but in contrast it showed partial complementation of visible phenotype. Line #A21 in *sfr6-1*+35S::SF16 (SF16) showed complementation of flowering time phenotype as similar to green colour restoration but in contrast line#B7 not shown complementation of flowering time phenotype though it fully complemented the green colour restoration phenotype (see sections 4.2.4.1 and 4.2.4.2). SF16#B2 remained similar to *sfr6-1* mutant in both flowering time and visual appearance. The

other line, SF16#A31 showed no complementation of visual appearance at all but partial complementation of flowering time phenotype. These varying results of full length complemented SFR6 lines lead to difficulty in understanding the differences amongst lines, perhaps this might due to the differences in level of *SFR6* transgene expression in the four independent lines. Line #B6 of *sfr6-1*+35S::SF36 (SF36) showed full complementation of flowering time phenotype as well as visual phenotype but in #B25 partial complementation of visual but not flowering time phenotype.

By considering all data for complementation of flowering time, at least one line from each truncation of SFR6 was recorded as full complementating the phenotype (Table 4.1). But for the visual appearance (green colour restoration) except no any line in *sfr6-1*+35S::SF14 (SF14) but at least one line from other SFR6 truncations showed full complementation. This suggests that sequence of the common area of the SFR6 protein for all the truncations might responsible for the regulation of flowering time in Arabidopsis. As no full complementation was observed in any of the lines in SF14, in the regulation of visible phenotype, the protein available in missing area of SF14 but present in all other three truncations *i.e* in the area representing the one third of the protein in C-terminus which covers SSM21 and SSM22 might responsible in Arabidopsis.

6.4.3 Role of MED16 domains in Transcriptional activation under cold, drought, dark and UV stress conditions

Stress gene complementation experiments conducted under cold, dark and UV stresses demonstrated that some lines in different SF truncated fragments showed varying degrees of

complementation of stress gene expression compared to *sfr6-1*. Out of the five lines tested for cold, dark and UV stresses, none of the SF14 lines showed full complementation of respective stress gene expression, although one line (SF14 line #7) showed partial complementation of all cold, dark and UV responsive gene expression compared to *sfr6-1*. This is the line showing full complementation of flowering time phenotype and partial complementation of visible appearance. Interestingly this line showed a low level of *SFR6* expression in F3. The lack of full complementation of stress gene expression under any of the stress conditions tested indicates the necessity of one third of the C-terminus of the protein (the section lacking in the SF14 truncation) for stress gene expression. This C-terminus end consists of the putative nuclear targeting signal, Zn finger domain as well as eight SSM regions out of 28 defined by Bourbon (2008). Therefore some or all of these unique features of SFR6 might responsible for stress inducible gene expression.

SF15 is the truncation which lacks zinc figure domain of SFR6 protein. SF15#1 demonstrated fully complementation of cold and UV responsive gene expression but partial complementation of dark-responsive gene expression. *SFR6* gene expression of the above line was the lowest compared to other four lines. In SF15 line #2 and #3 showed nearly full complementation of dark inducible *DIN6* gene expression but neither showed partial complementation of other stress-inducible gene expression. Line #5 in SF15 showed partial complementation of dark and UV inducible gene expression while #4 of SF15 possessed partial complementation of UV gene expression only.

When the complementation of stress inducible gene expression in SF15 is summarised, at least one or maximally two lines showed fully complementation of stress inducible gene expression. These lines show varying levels of *SFR6* expression ranging low to high and no consistent pattern observed (see Table 4.1). Moreover this indicates that the SF15 truncation has ability to fully complement stress

inducible gene expression though it lacks of Zn finger domain as well as last four SSM regions in its structure.

Out of two lines of SF36 tested, one (#B6) showed full complementation of cold- and dark-inducible gene expression but only partial complementation of UV-inducible gene expression. Line #B25 showed partial complementation of cold and dark gene expression but no UV-inducible gene expression (see Table 4.1). Levels of *SFR6* expression in the F3 generation of #B25 were lower than in #B6 and this might be the reason for not observing a complementation effect on stress-inducible gene expression in this line. Furthermore #B6 demonstrates full complementation of flowering time as well as visible phenotype apart from above stress gene complementation thereby shown the importance of this truncation in many of the characteristics studied. SF36 is the truncation which lacks one third of the protein from the N-terminus as well as nearly 11 SSM regions. However this truncation is consists of both zinc finger and nuclear targeting signal.

Most of the lines that showed the full complementation exhibited a low level of *SFR6* expression Therefore I would argue that ability of complementation is connected to their level of SFR6 expression. The ones that express less might be the ones that “work” well. I could suggest that neither very high level nor very low level of expression might affect the actual expression of genes that responsible for the better functioning of the plants. This could be a valid reason that very high expression of transgenes or expression of multiple copies (which can happen with basta resistance and floral dip method) can cause expression to be switched off (silenced).

SF16 is the full length of SFR6 protein that would be expected to achieve full complementation of *sfr6-1*. Unfortunately none of the lines showed full

complementation of stress inducible gene expression (see Table 6.1). One of the main reasons that I could understand is the level of *SFR6* gene expression in all these lines was not higher than in untransformed Col-0 though they were appeared to express considerable levels of transgene in F3 generation. Unlike under the control of native promoter, all lines were under the control of 35S promoter that constitutively overexpressed each truncation and therefore it should express higher levels of transgene than recorded in each transgenic line. This might be a reason that none of SF16 lines showed the complementation or too high a level of expression occurred with this method (35S) might cause a dominant negative phenotype.

As it should express the same level at all the time under the control of 35S promoter, if the level of transgene expression was not sufficient to complement stress gene expression, it would be questionable how they managed to complement flowering time and green colour phenotype. Another possible explanation is that the lines shown green was not actually due to restoration but it might be wild type plants. However, this argument can simply be ignored as no normal *KIN2* expression was observed in those lines; they exhibited low levels of *KIN2* expression typical of the mutant. Finally I can suggest that though it is hard to believe, it is theoretically possible that a mutated version of the SFR6 transcript is present in these lines and this encodes a protein that can help with the green colour (or basically iron uptake) and flowering time but not any of the other functions in stress gene expression such as cold, dark and UV.

The other possible reason for not showing complementation effect in SF16 is due to a mistake that could have taken place while creating the SF16 construct. However I have fully sequenced the construct and performed all possible screening to ensure there were no errors but it is a possibility that there were errors that were not picked

up by sequencing. However, data evidence that transcript for SFR6 appears to be there but this does not do any role therefore it might be a faulty one.

Contradictory to the above argument I can suggest that, more likely that in these particular segregating lines the transgene is not present or it is present but doesn't produce transcript. All transgenic lines were sequenced to confirm they are homozygous *sfr6* but not heterozygotes so that I could avoid suggesting this possibility as a reason for showing the complementation effects. Although I did not compare wild type SF16 lines and *sfr6* SF16 lines side by side, wild type SF16 lines seemed to show very high *SFR6* expression (hundred folds) but the *sfr6* lines were much lower . This supports the idea that something happened wrong in the generations in between. The two main things that could go wrong are that the wrong segregants were identified in the F_3 generation or that the gene was silenced. This also suggests that there may be nothing at all wrong with the construct as it expressed well in wild type.

Wathugala et al. (2012) reported that full length lines of genomic *SFR6* shown full complementation of cold inducible gene expression. The differences between above genomic SFR6 complemented lines with SF16 is that SF16 was created with cDNA in a basta resistance vector background instead of kanamycin resistant background in genomic version. This kanamycin selection might less prone to multiple insertions of the transgene than in basta selection. If, as I suggest above, there is a dominant negative effect in SF16 transgenic lines due to overexpression of transgene we must question why it does not happen with the genomic full length complemented lines created by Wathugala et al. (2012).

Kim et al. (2004) reported the use of protein truncations of MED16 in *Drosophila* to study interactions with protein activators. In the above study MED16 was expressed

as three overlapping fragments covering 1-333aa, 175-524aa and 377-818aa and used to study their interactions with activator proteins, which were analysed systematically by GST pull-down assays. They found that only one of them interacted with the activator protein. Therefore this study is little similar to the study that I have attempted and agree that some truncations are able to work but not all. Furthermore transcription factors need to be bound to the truncated fragments of SFR6 in order to activate stress responsive gene expression. Therefore depending on the availability of transcription factor binding sites/domains in the truncations of SFR6, the ability of stress gene expression might be changed. One of the mediator subunits, MED25, was shown to be interact with many transcription factors (Çevik et al., 2012, Blomberg et al., 2012, Ou et al., 2011, Chen et al., 2012b) in control of different transcriptional regulons and Çevik et al. (2012) reported about twelve different transcription factors that interact with MED25. Therefore there might be a possibility that all the transcription factor binding sites are in the same region or perhaps in different regions and that might cause the differences of truncations in complementation experiments.

When summarise the data regarding the regions that important in stress gene regulation as detailed in Table 4.1. I can state that SF15 is important in all stress-induced gene expression *i.e* under cold, dark and UV conditions where as SF36 is important in cold and dark-induced gene expression but not under UV-induced stress conditions as atleast one line from above two truncations were able to demonstrate full complementation of genes responsible under each stress condition. Either SF16 or SF14 were not able to show full complementation of stress-inducible genes under cold, dark or UV stress conditions (Table 4.1). Therefore I can speculate that the region covers by SF15 might consist of most of the unique binding sites or it might

be necessary for the proteins to fold in a way that it can bind the transcription factors. Further this region is consists of 23 SSM regions out of 27 SSM regions as suggested by Bourbon (2008). Moreover I can suggest that last four SSM regions might not the unique sites for transcription factor binding or protein folding sites that facilitate transcription factors to bind.

Chapter 7

Conclusions and Future Work

7.1 Major findings of this research project

Major findings of this study can be summarised as stated below:

1. MED2 and MED14 subunits are required for cold acclimation that leads to acquire freezing tolerance in a similar way as seen in SFR6/MED16.

2. SFR6/MED16 shares roles under drought and UV-C in both transcriptional regulation as well as abiotic tress tolerance with the predicted tail subunits MED2 and MED14 in addition to earlier studied cold and starvation induced stress conditions.

3. KIN10 controls the expression of a subset of stress-inducible genes controlled by SFR6/MED16, particularly drought- and starvation-induced genes but not under all stress conditions. Furthermore, the desiccation/drought gene expression phenotype is more dominant compared to well-studied dark gene expression phenotype in the level of whole plant.

4. KIN10 and MED16/SFR6 act on the same pathway to regulate dark and drought gene expression.

5. Transiently expressed six truncated versions of SFR6/MED16 have ability to localize the nucleus irrespective to the presence of nuclear localisation signal as predicted by

the NUCPred programme but nuclear localisation signal might be locate in the middle part of the protein that common to all the truncations.

6. SFR6 truncation which lack of zinc finger domain *i.e* SF15 truncation did not result in any loss of ability to transcribe genes in response to cold, dark and UV-C induced stress gene expression, flowering time as well as visible phenotype. However, no full complementation of stress gene expression in SF14 truncations indicates the necessity of one third of the C-terminus end of the protein for stress gene expression.

7. The truncation which lacks one third of the protein from the N-terminus *i.e* SF36 truncation tested shown full complementation of cold and dark inducible gene expression but partial complementation of UV inducible gene expression.

8. SFR6/MED16 domains of SF14; lacks one third of the C-terminus end of the protein, SF1; lacks zinc finger domain and SF16; full length interacts with KIN10 indicating the important role of N-terminus end of SFR6 protein in this interactions.

7.2 Future Work

1. Further studies on confirmation of interactions between SFR6 truncations and KIN10

In this current study only Co-immuno precipitation experiments were conducted to identify the domains that interact with KIN10 and yeast two-hybrid experiments or any other relevant method need to be carried out to further confirm the interactions between SFR6 domains and KIN10.

2. Microarray analyses are need to identify all the other genes that areupregulated under dark and drought conditions

Conducting microarray analysis by comparing samples from dark and drought treated *sfr6-1* and *kin10-2* mutants will help to study the extent of sharing roles of SFR6 and KIN10 as well as lead to identification of transcription factors that involved in drought and dark conditions through SFR6.

3. Further characterization of functions of full length complemented lines of SFR6

It is necessary to reanalyse the level of expression of *SFR6* in same lines or other existing lines that were not used in the analysis. If any successful lines which express good levels of *SFR6* can be used in stress gene complementation experiments.

Bibliography

Abe, H., Urao, T., Ito, T., Seki, M., Shinozaki, K. & Yamaguchi-Shinozaki, K. 2003. Arabidopsis AtMYC2 (bHLH) and AtMYB2 (MYB) Function as Transcriptional Activators in Abscisic Acid Signaling. *The Plant Cell Online,* 15**,** 63-78.

Abe, H., Yamaguchi-Shinozaki, K., Urao, T., Iwasaki, T., Hosokawa, D. & Shinozaki, K. 1997. Role of arabidopsis MYC and MYB homologs in drought- and abscisic acid-regulated gene expression. *The Plant Cell Online,* 9**,** 1859-68.

Agarwal, M., Hao, Y., Kapoor, A., Dong, C.H., Fujii, H., Zheng, X. & Zhu, J.K. 2006. A R2R3 type MYB transcription factor is involved in the cold regulation of CBF genes and in acquired freezing tolerance. *Journal of Biological Chemistry,* 281**,** 37636-37645.

Albuquerque, C. P., Wang, G., Lee, N. S., Kolodner, R. D., Putnam, C. D. & Zhou, H. 2013. Distinct SUMO ligases cooperate with Esc2 and Slx5 to suppress duplication-mediated genome rearrangements. *PLoS Genet,* 9**,** e1003670.

Andersson, U., Filipsson, K., Abbott, C. R., Woods, A., Smith, K., Bloom, S. R., Carling, D. & Small, C. J. 2004. AMP-activated protein kinase plays a role in the control of food intake. *Journal of Biological Chemistry,* 279**,** 12005-12008.

Apel, K. & Hirt, H. 2004. Reactive oxygen species: metabolism, oxidative stress, and signal transduction. *Annu. Rev. Plant Biol.,* 55**,** 373-399.

Araus, J., Slafer, G., Reynolds, M. & Royo, C. 2002. Plant breeding and drought in C3 cereals: what should we breed for? *Annals of Botany,* 89**,** 925-940.

Aroca, R. 2012. Plant responses to drought stress. *From Morphological to Molecular Features.* Springer.

Ashton, F. M. 1981. *Mode of Action of Herbicides* Wiley.

Asturias, F. J., Jiang, Y. W., Myers, L. C., Gustafsson, C. M. & Kornberg, R. D. 1999. Conserved structures of mediator and RNA polymerase II holoenzyme. *Science,* 283**,** 985-987.

Atkinson, N. J. & Urwin, P. E. 2012. The interaction of plant biotic and abiotic stresses: from genes to the field. *Journal of Experimental Botany,* 63**,** 3523-3543.

Autran, D., Jonak, C., Belcram, K., Beemster, G. T., Kronenberger, J., Grandjean, O., Inzé, D. & Traas, J. 2002. Cell numbers and leaf development in Arabidopsis: a functional analysis of the STRUWWELPETER gene. *EMBO J,* 21**,** 6036-6049.

Avonce, N., Leyman, B., Mascorro-Gallardo, J. O., Van Dijck, P., Thevelein, J. M. & Iturriaga, G. 2004. The Arabidopsis trehalose-6-P synthase AtTPS1 gene is a regulator of glucose, abscisic acid, and stress signaling. *Plant Physiology,* 136**,** 3649-3659.

Avruch, J., Hara, K., Lin, Y., Liu, M., Long, X., Ortiz-Vega, S. & Yonezawa, K. 2006. Insulin and amino-acid regulation of mTOR signaling and kinase activity through the Rheb GTPase. *Oncogene,* 25**,** 6361-6372.

Backstrom, S., Elfving, N., Nilsson, R., Wingsle, G. & Bjorklund, S. 2007. Purification of a plant mediator from Arabidopsis thaliana identifies PFT1 as the Med25 subunit. *Molecular Cell,* 26**,** 717-729.

Baena-Gonzalez, E. 2010. Energy signaling in the regulation of gene expression during stress. *Mol Plant,* 3**,** 300-13.

Baena-Gonzalez, E., Rolland, F., Thevelein, J. M. & Sheen, J. 2007. A central integrator of transcription networks in plant stress and energy signalling. *Nature,* 448**,** 938-U10.

Baena-Gonzalez, E. & Sheen, J. 2008. Convergent energy and stress signaling. *Trends Plant Sci,* 13**,** 474-482.

Baker, S., Wilhelm, K. & Thomashow, M. 1994. The 5′region of Arabidopsis thaliana cor15a has cis-acting elements that confer cold-, drought- and ABA-regulated gene expression. *Plant Molecular Biology,* 24**,** 701-713.

Bassham, D. C. 2009. Function and regulation of macroautophagy in plants. *Biochimica et Biophysica Acta (BBA)-Molecular Cell Research,* 1793**,** 1397-1403.

Bieza, K. & Lois, R. 2001. An Arabidopsis Mutant Tolerant to Lethal Ultraviolet-B Levels Shows Constitutively Elevated Accumulation of Flavonoids and Other Phenolics. *Plant Physiology,* 126**,** 1105-1115.

Bilger, W., Rimke, S., Schreiber, U. & Lange, O. 1989. Inhibition of energy-transfer to photosystem II in lichens by dehydration: different properties of reversibility with green and blue-green phycobionts. *Journal of Plant Physiology,* 134**,** 261-268.

Bläsing, O. E., Gibon, Y., Günther, M., Höhne, M., Morcuende, R., Osuna, D., Thimm, O., Usadel, B., Scheible, W.-R. & Stitt, M. 2005. Sugars and circadian regulation make major contributions to the global regulation of diurnal gene expression in Arabidopsis. *The Plant Cell Online,* 17**,** 3257-3281.

Blomberg, J., Aguilar, X., Brännström, K., Rautio, L., Olofsson, A., Wittung-Stafshede, P. & Björklund, S. 2012. Interactions between DNA, transcriptional regulator Dreb2a and the Med25 mediator subunit from Arabidopsis thaliana involve conformational changes. *Nucleic Acids Research,* 40**,** 5938-5950.

Boube, M., Joulia, L., Cribbs, D. L. & Bourbon, H. M. 2002. Evidence for a mediator of RNA polymerase II transcriptional regulation conserved from yeast to man. *Cell,* 110**,** 143-151.

Bouly, J. P., Gissot, L., Lessard, P., Kreis, M. & Thomas, M. 1999. Arabidopsis thaliana proteins related to the yeast SIP and SNF4 interact with AKINalpha1, an SNF1-like protein kinase. *Plant J,* 18**,** 541-50.

Bourbon, H.M. 2008. Comparative genomics supports a deep evolutionary origin for the large, four-module transcriptional mediator complex. *Nucleic Acids Research,* 36**,** 3993-4008.

Bowler, C., Montagu, M. V. & Inze, C. 1992. Superoxide Dismutase and Stress Tolerance. *Annual Review of Plant Physiology and Plant Molecular Biology,* 43**,** 83-116.

Boyce, J. M., Knight, H., Deyholos, M., Openshaw, M. R., Galbraith, D. W., Warren, G. & Knight, M. R. 2003. The sfr6 mutant of Arabidopsis is defective in transcriptional activation via CBF/DREB1 and DREB2 and shows sensitivity to osmotic stress. *The Plant Journal,* 34**,** 395-406.

Boyer, J. S. 1982. Plant productivity and environment. *Science,* 218**,** 443-448.

Britt, A. B. 1996. DNA DAMAGE AND REPAIR IN PLANTS. *Annual Review of Plant Physiology and Plant Molecular Biology,* 47, 75-100.

Buchanan-Wollaston, V., Page, T., Harrison, E., Breeze, E., Lim, P. O., Nam, H. G., Lin, J. F., Wu, S. H., Swidzinski, J. & Ishizaki, K. 2005. Comparative transcriptome analysis reveals significant differences in gene expression and signalling pathways between developmental and dark/starvation-induced senescence in Arabidopsis. *The Plant Journal,* 42**,** 567-585.

Button, K. S., Ioannidis, J. P., Mokrysz, C., Nosek, B. A., Flint, J., Robinson, E. S. & Munafò, M. R. 2013. Power failure: why small sample size undermines the reliability of neuroscience. *Nature Reviews Neuroscience,* 14**,** 365-376.

Caldwell, M., Ballaré, C., Bornman, J. & Flint, S. 2003. Bj örn, LO, Teramura, AH, Kulandaivelu, G., Tevini, M., 2003. Terrestrial ecosystems, increased solar ultraviolet radiation and interactions with other climatic change factors. *Photochem. Photobiol. Sci,* 2**,** 29-38.

Caldwell, M. M., Bornman, J., Ballaré, C., Flint, S. D. & Kulandaivelu, G. 2007. Terrestrial ecosystems, increased solar ultraviolet radiation, and interactions with other climate change factors. *Photochemical & Photobiological Sciences,* 6**,** 252-266.

Calkins, J. B. & Swanson, B. T. 1990. The distinction between living and dead plant tissue viability tests in cold hardiness research. *Cryobiology,* 27**,** 194-211.

Camp, W. V., Willekens, H., Bowler, C., Montagu, M. V., Inze, D., Reupold-Popp, P., Sandermann, H. & Langebartels, C. 1994. Elevated Levels of Superoxide Dismutase Protect Transgenic Plants Against Ozone Damage. *Nat Biotech,* 12**,** 165-168.

Canet, J. V., Dobón, A. & Tornero, P. 2012. Non-recognition-of-BTH4, an Arabidopsis mediator subunit homolog, is necessary for development and response to salicylic acid. *The Plant Cell Online,* 24**,** 4220-4235.

Carling, D., Aguan, K., Woods, A., Verhoeven, A., Beri, R. K., Brennan, C. H., Sidebottom, C., Davison, M. D. & Scott, J. 1994. Mammalian AMP-activated protein kinase is homologous to yeast and plant protein kinases involved in the regulation of carbon metabolism. *Journal of Biological Chemistry,* 269**,** 11442-11448.

Carlson, M., Osmond, B. C. & Botstein, D. 1981. Mutants of yeast defective in sucrose utilization. *Genetics* 98**,** 25–40.

Carlsten, J. O., Zhu, X. & Gustafsson, C. M. 2013. The multitalented Mediator complex. *Trends in Biochemical Sciences,* 38**,** 531-537.

Celenza, J. L. & Carlson, M. 1984. Structure and expression of the SNF1 gene of Saccharomyces cerevisiae. *Mol Cell Biol,* 4**,** 54-60.

Celenza, J. L. & Carlson, M. 1986. A yeast gene that is essential for release from glucose repression encodes a protein kinase. *Science,* 233**,** 1175-80.

Cerdán, P. D. & Chory, J. 2003. Regulation of flowering time by light quality. *Nature,* 423**,** 881-885.

Çevik, V., Kidd, B. N., Zhang, P., Hill, C., Kiddle, S., Denby, K. J., Holub, E. B., Cahill, D. M., Manners, J. M. & Schenk, P. M. 2012. MEDIATOR25 acts as an integrative hub for the regulation of jasmonate-responsive gene expression in Arabidopsis. *Plant Physiology,* 160**,** 541-555.

Chang, Y.-W., Howard, S. C. & Herman, P. K. 2004. The Ras/PKA signaling pathway directly targets the Srb9 protein, a component of the general RNA polymerase II transcription apparatus. *Molecular cell,* 15**,** 107-116.

Chen, L., Song, Y., Li, S., Zhang, L., Zou, C. & Yu, D. 2012a. The role of WRKY transcription factors in plant abiotic stresses. *Biochimica et Biophysica Acta (BBA) - Gene Regulatory Mechanisms,* 1819**,** 120-128.

Chen, R., Jiang, H., Li, L., Zhai, Q., Qi, L., Zhou, W., Liu, X., Li, H., Zheng, W. & Sun, J. 2012b. The Arabidopsis mediator subunit MED25 differentially regulates jasmonate and abscisic acid signaling through interacting with the MYC2 and ABI5 transcription factors. *The Plant Cell Online,* 24**,** 2898-2916.

Chen, Y., Ji, F., Xie, H. & Liang, J. 2006. Overexpression of the regulator of G-protein signalling protein enhances ABA-mediated inhibition of root elongation and drought tolerance in Arabidopsis. *Journal of Experimental Botany,* 57**,** 2101-2110.

Chinnusamy, V., Ohta, M., Kanrar, S., Lee, B.H., Hong, X., Agarwal, M. & Zhu, J.K. 2003. ICE1: a regulator of cold-induced transcriptome and freezing tolerance in Arabidopsis. *Genes & Development,* 17**,** 1043-1054.

Chinnusamy, V., Zhu, J. & Zhu, J.K. 2007. Cold stress regulation of gene expression in plants. *Trends in plant science,* 12**,** 444-451.

Cho, J.I., Ryoo, N., Eom, J.S., Lee, D.-W., Kim, H.B., Jeong, S.W., Lee, Y.H., Kwon, Y.K., Cho, M.H. & Bhoo, S. H. 2009. Role of the rice hexokinases OsHXK5 and OsHXK6 as glucose sensors. *Plant Physiology,* 149**,** 745-759.

Cho, Y.H. & Yoo, S.D. 2011. Signaling role of fructose mediated by FINS1/FBP in Arabidopsis thaliana. *PLoS genetics,* 7**,** e1001263.

Cho, Y.H., Yoo, S.D. & Sheen, J. 2006. Regulatory functions of nuclear hexokinase1 complex in glucose signaling. *Cell,* 127**,** 579-589.

Choi, H.I., Hong, J.H., Ha, J.O., Kang, J.Y. & Kim, S. Y. 2000. ABFs, a family of ABA-responsive element binding factors. *Journal of Biological Chemistry,* 275**,** 1723-1730.

Claeys, H. & Inzé, D. 2013. The agony of choice: how plants balance growth and survival under water-limiting conditions. *Plant Physiology,* 162**,** 1768-1779.

Clay, N. K. & Nelson, T. 2005. The recessive epigenetic swellmap mutation affects the expression of two step II splicing factors required for the transcription of the cell proliferation gene STRUWWELPETER and for the timing of cell cycle arrest in the Arabidopsis leaf. *The Plant Cell Online,* 17**,** 1994-2008.

Clough, S. J. & Bent, A. F. 1998. Floral dip: a simplified method forAgrobacterium-mediated transformation ofArabidopsis thaliana. *The Plant Journal,* 16**,** 735-743.

Collins, N. C., Tardieu, F. & Tuberosa, R. 2008. Quantitative Trait Loci and Crop Performance under Abiotic Stress: Where Do We Stand? *Plant Physiology,* 147**,** 469-486.

Conaway, R. C. & Conaway, J. W. 2011. Origins and activity of the Mediator complex. *Seminars in Cell & Developmental Biology,* 22**,** 729-734.

Contento, A. L., Kim, S.J. & Bassham, D. C. 2004. Transcriptome profiling of the response of Arabidopsis suspension culture cells to Suc starvation. *Plant Physiology,* 135**,** 2330-2347.

Cook, D., Fowler, S., Fiehn, O. & Thomashow, M. F. 2004. A prominent role for the CBF cold response pathway in configuring the low-temperature metabolome of Arabidopsis. *Proceedings of the National Academy of Sciences of the United States of America,* 101**,** 15243-15248.

Creed, D. 1984. The photophysics and photochemistry of the near-uv absorbing amino acids–i. Tryptophan and its simple derivatives. *Photochemistry and photobiology,* 39**,** 537-562.

Crowe, J. H., Crowe, L. M., Carpenter, J. F., Rudolph, A., Wistrom, C. A., Spargo, B. & Anchordoguy, T. 1988. Interactions of sugars with membranes. *Biochimica et Biophysica Acta (BBA)-Reviews on Biomembranes,* 947**,** 367-384.

Csintalan, Z., Proctor, M. C. & Tuba, Z. 1999. Chlorophyll fluorescence during drying and rehydration in the mosses Rhytidiadelphus loreus (Hedw.) Warnst., Anomodon viticulosus (Hedw.) Hook. & Tayl. and Grimmia pulvinata (Hedw.) Sm. *Annals of Botany,* 84**,** 235-244.

Da Silva Xavier, G., Leclerc, I., Salt, I. P., Doiron, B., Hardie, D. G., Kahn, A. & Rutter, G. A. 2000. Role of AMP-activated protein kinase in the regulation by glucose of islet beta cell gene expression. *Proc Natl Acad Sci U S A,* 97**,** 4023-8.

Da Silva Xavier, G., Leclerc, I., Varadi, A., Tsuboi, T., Moule, S. K. & Rutter, G. A. 2003. Role for AMP-activated protein kinase in glucose-stimulated insulin secretion and preproinsulin gene expression. *Biochemical Journal,* 371**,** 761-74.

Dai, Q., Yan, B., Huang, S., Liu, X., Peng, S., Miranda, M. L. L., Chavez, A. Q., Vergara, B. S. & Olszyk, D. M. 1997. Response of oxidative stress defense

systems in rice (Oryza sativa) leaves with supplemental UV-B radiation. *Physiologia Plantarum,* 101**,** 301-308.

Davies, S. P., Hawley, S. A., Woods, A., Carling, D., Haystead, T. A. & Hardie, D. G. 1994. Purification of the AMP-activated protein kinase on ATP-gamma-sepharose and analysis of its subunit structure. *Eur J Biochem,* 223**,** 351-7.

Davis, J. A., Takagi, Y., Kornberg, R. D. & Asturias, F. J. 2002. Structure of the yeast RNA polymerase II holoenzyme: Mediator conformation and polymerase interaction. *Molecular cell,* 10**,** 409-415.

Defronzo, R. A., Bonadonna, R. C. & Ferrannini, E. 1992. Pathogenesis of NIDDM. A balanced overview. *Diabetes Care,* 15**,** 318-68.

Demmig, B. & Björkman, O. 1987. Comparison of the effect of excessive light on chlorophyll fluorescence (77K) and photon yield of O2 evolution in leaves of higher plants. *Planta,* 171**,** 171-184.

Deprost, D., Yao, L., Sormani, R., Moreau, M., Leterreux, G., Nicolaï, M., Bedu, M., Robaglia, C. & Meyer, C. 2007. The Arabidopsis TOR kinase links plant growth, yield, stress resistance and mRNA translation. *EMBO Rep,* 8**,** 864-870.

Devine, M., Duke, S. O. & Fedtke, C. 1992. *Physiology of herbicide action,* PTR Prentice Hall.

Dhawan, R., Luo, H., Foerster, A. M., Abuqamar, S., Du, H.-N., Briggs, S. D., Scheid, O. M. & Mengiste, T. 2009. HISTONE MONOUBIQUITINATION1 interacts with a subunit of the mediator complex and regulates defense against necrotrophic fungal pathogens in Arabidopsis. *The Plant Cell Online,* 21**,** 1000-1019.

Ding, N., Zhou, H., Esteve, P.O., Chin, H. G., Kim, S., Xu, X., Joseph, S. M., Friez, M. J., Schwartz, C. E. & Pradhan, S. 2008. Mediator links epigenetic silencing of neuronal gene expression with x-linked mental retardation. *Molecular cell,* 31**,** 347-359.

Dong, C.H., Hu, X., Tang, W., Zheng, X., Kim, Y. S., Lee, B.H. & Zhu, J.K. 2006. A putative Arabidopsis nucleoporin, AtNUP160, is critical for RNA export and required for plant tolerance to cold stress. *Mol Cell Biol,* 26**,** 9533-9543.

Dotson, M. R., Yuan, C. X., Roeder, R. G., Myers, L. C., Gustafsson, C. M., Jiang, Y. W., Li, Y., Kornberg, R. D. & Asturias, F. J. 2000. Structural organization of yeast and mammalian mediator complexes. *Proceedings of the National Academy of Sciences,* 97**,** 14307-14310.

Dubouzet, J. G., Sakuma, Y., Ito, Y., Kasuga, M., Dubouzet, E. G., Miura, S., Seki, M., Shinozaki, K. & Yamaguchi-Shinozaki, K. 2003. OsDREB genes in rice, Oryza sativa L., encode transcription activators that function in drought-, high-salt-and cold-responsive gene expression. *The Plant Journal,* 33**,** 751-763.

Edwards, K., Johnstone, C. & Thompson, C. 1991. A simple and rapid method for the preparation of plant genomic DNA for PCR analysis. *Nucleic Acids Research,* 19**,** 1349.

Ehlert, A., Weltmeier, F., Wang, X., Mayer, C. S., Smeekens, S., Vicente-Carbajosa, J. & Dröge-Laser, W. 2006. Two-hybrid protein–protein interaction analysis in Arabidopsis protoplasts: establishment of a heterodimerization map of group C and group S bZIP transcription factors. *The Plant Journal,* 46**,** 890-900.

Elfving, N., Davoine, C., Benlloch, R., Blomberg, J., Brännström, K., Müller, D., Nilsson, A., Ulfstedt, M., Ronne, H. & Wingsle, G. 2011. The Arabidopsis thaliana Med25 mediator subunit integrates environmental cues to control plant development. *Proceedings of the National Academy of Sciences,* 108**,** 8245-8250.

Farooq, M., Wahid, A., Kobayashi, N., Fujita, D. & Basra, S. 2009. Plant drought stress: effects, mechanisms and management. *Sustainable Agriculture*. Springer.

Fondell, J. D., Ge, H. & Roeder, R. G. 1996. Ligand induction of a transcriptionally active thyroid hormone receptor coactivator complex. *Proceedings of the National Academy of Sciences,* 93**,** 8329-8333.

Fowler, S. & Thomashow, M. F. 2002. Arabidopsis transcriptome profiling indicates that multiple regulatory pathways are activated during cold acclimation in addition to the CBF cold response pathway. *The Plant Cell Online,* 14**,** 1675-1690.

Fragoso, S., Espíndola, L., Páez-Valencia, J., Gamboa, A., Camacho, Y., Martínez-Barajas, E. & Coello, P. 2009. SnRK1 isoforms AKIN10 and AKIN11 are differentially regulated in Arabidopsis plants under phosphate starvation. *Plant Physiology,* 149**,** 1906-1916.

Frohnmeyer, H. & Staiger, D. 2003. Ultraviolet-B Radiation-Mediated Responses in Plants. Balancing Damage and Protection. *Plant Physiology,* 133**,** 1420-1428.

Fujiki, Y., Yoshikawa, Y., Sato, T., Inada, N., Ito, M., Nishida, I. & Watanabe, A. 2001. Dark-inducible genes from Arabidopsisthaliana are associated with leaf senescence and repressed by sugars. *Physiologia Plantarum,* 111**,** 345-352.

Fujita, M., Fujita, Y., Maruyama, K., Seki, M., Hiratsu, K., Ohme-Takagi, M., Tran, L.-S. P., Yamaguchi-Shinozaki, K. & Shinozaki, K. 2004. A dehydration-induced NAC protein, RD26, is involved in a novel ABA-dependent stress-signaling pathway. *The Plant Journal,* 39**,** 863-876.

Fujita, Y., Fujita, M., Satoh, R., Maruyama, K., Parvez, M. M., Seki, M., Hiratsu, K., Ohme-Takagi, M., Shinozaki, K. & Yamaguchi-Shinozaki, K. 2005. AREB1 is a transcription activator of novel ABRE-dependent ABA signaling that enhances drought stress tolerance in Arabidopsis. *Plant Cell,* 17**,** 3470-3488.

Furihata, T., Maruyama, K., Fujita, Y., Umezawa, T., Yoshida, R., Shinozaki, K. & Yamaguchi-Shinozaki, K. 2006. Abscisic acid-dependent multisite phosphorylation regulates the activity of a transcription activator AREB1. *Proceedings of the National Academy of Sciences of the United States of America,* 103**,** 1988-1993.

Galdieri, L., Desai, P. & Vancura, A. 2012. Facilitated assembly of the preinitiation complex by separated tail and head/middle modules of the mediator. *Journal of molecular biology,* 415**,** 464-474.

Gauslaa, Y. & Solhaug, K. A. 2000. High-light-intensity damage to the foliose lichen Lobaria pulmonaria within natural forest: the applicability of chlorophyll fluorescence methods. *The Lichenologist,* 32**,** 271-289.

Geisler, M., Kleczkowski, L. A. & Karpinski, S. 2006. A universal algorithm for genome-wide in silicio identification of biologically significant gene promoter putative cis-regulatory-elements; identification of new elements for reactive oxygen species and sucrose signaling in Arabidopsis. *The Plant Journal,* 45**,** 384-398.

Genty, B., Briantais, J.M. & Baker, N. R. 1989. The relationship between the quantum yield of photosynthetic electron transport and quenching of chlorophyll fluorescence. *Biochimica et Biophysica Acta (BBA)-General Subjects,* 990**,** 87-92.

Ghillebert, R., Swinnen, E., Wen, J., Vandesteene, L., Ramon, M., Norga, K., Rolland, F. & Winderickx, J. 2011. The AMPK/SNF1/SnRK1 fuel gauge and energy regulator: structure, function and regulation. *FEBS J,* 278**,** 3978-90.

Gibson, S. I. 2005. Control of plant development and gene expression by sugar signaling. *Current Opinion in Plant Biology,* 8**,** 93-102.

Gill, S. S. & Tuteja, N. 2010. Reactive oxygen species and antioxidant machinery in abiotic stress tolerance in crop plants. *Plant Physiology and Biochemistry,* 48**,** 909-930.

Gillmor, C. S., Park, M. Y., Smith, M. R., Pepitone, R., Kerstetter, R. A. & Poethig, R. S. 2010. The MED12-MED13 module of Mediator regulates the timing of embryo patterning in Arabidopsis. *Development,* 137**,** 113-122.

Gilmour, S. J., Sebolt, A. M., Salazar, M. P., Everard, J. D. & Thomashow, M. F. 2000. Overexpression of the Arabidopsis CBF3transcriptional activator mimics multiple biochemical changes associated with cold acclimation. *Plant Physiology,* 124**,** 1854-1865.

Gilmour, S. J., Zarka, D. G., Stockinger, E. J., Salazar, M. P., Houghton, J. M. & Thomashow, M. F. 1998. Low temperature regulation of theArabidopsisCBF family of AP2 transcriptional activators as an early step in cold-inducedCORgene expression. *The Plant Journal,* 16**,** 433-442.

Gissot, L., Polge, C., Bouly, J. P., Lemaitre, T., Kreis, M. & Thomas, M. 2004. AKIN beta 3, a plant specific SnRK1 protein, is lacking domains present in yeast and mammals non-catalytic beta-subunits. *Plant Molecular Biology,* 56**,** 747-759.

Gissot, L., Polge, C., Jossier, M., Girin, T., Bouly, J. P., Kreis, M. & Thomas, M. 2006. AKIN beta gamma contributes to SnRK1 heterotrimeric complexes and interacts with two proteins implicated in plant pathogen resistance through its KIS/GBD sequence. *Plant Physiology,* 142**,** 931-944.

Godfray, H. C. J., Beddington, J. R., Crute, I. R., Haddad, L., Lawrence, D., Muir, J. F., Pretty, J., Robinson, S., Thomas, S. M. & Toulmin, C. 2010. Food security: the challenge of feeding 9 billion people. *Science,* 327**,** 812-818.

Gong, Z., Lee, H., Xiong, L., Jagendorf, A., Stevenson, B. & Zhu, J.-K. 2002. RNA helicase-like protein as an early regulator of transcription factors for plant chilling and freezing tolerance. *Proceedings of the National Academy of Sciences,* 99**,** 11507-11512.

Gonzalez, D., Bowen, A. J., Carroll, T. S. & Conlan, R. S. 2007. The transcription corepressor LEUNIG interacts with the histone deacetylase HDA19 and mediator components MED14 (SWP) and CDK8 (HEN3) to repress transcription. *Mol Cell Biol,* 27**,** 5306-5315.

Gonzali, S., Loreti, E., Solfanelli, C., Novi, G., Alpi, A. & Perata, P. 2006. Identification of sugar-modulated genes and evidence for in vivo sugar sensing in Arabidopsis. *Journal of Plant Research,* 119**,** 115-123.

Grativol, C., Hemerly, A. S. & Ferreira, P. C. G. 2012. Genetic and epigenetic regulation of stress responses in natural plant populations. *Biochimica et Biophysica Acta (BBA) - Gene Regulatory Mechanisms,* 1819**,** 176-185.

Green, R. & Fluhr, R. 1995. UV-B-Induced PR-1 Accumulation Is Mediated by Active Oxygen Species. *The Plant Cell Online,* 7**,** 203-212.

Grossweiner, L. I. 1984. Photochemistry of proteins: a review. *Current eye research,* 3**,** 137-144.

Gruhler, A., Olsen, J. V., Mohammed, S., Mortensen, P., Færgeman, N. J., Mann, M. & Jensen, O. N. 2005. Quantitative phosphoproteomics applied to the yeast pheromone signaling pathway. *Molecular & Cellular Proteomics,* 4**,** 310-327.

Guglielmi, B., Van Berkum, N. L., Klapholz, B., Bijma, T., Boube, M., Boschiero, C., Bourbon, H.M., Holstege, F. C. & Werner, M. 2004. A high resolution protein interaction map of the yeast Mediator complex. *Nucleic Acids Research,* 32**,** 5379-5391.

Guidi, B. W., Bjornsdottir, G., Hopkins, D. C., Lacomis, L., Erdjument-Bromage, H., Tempst, P. & Myers, L. C. 2004. Mutual targeting of mediator and the TFIIH kinase Kin28. *Journal of Biological Chemistry,* 279**,** 29114-29120.

Guy, C., Haskell, D. & Li, Q.B. 1998. Association of proteins with the stress 70 molecular chaperones at low temperature: evidence for the existence of cold labile proteins in spinach. *Cryobiology,* 36**,** 301-314.

Halford, N. G., Bouly, J. P. & Thomas, M. 2000. SNF1-related protein kinases (SnRKs) - Regulators at the heart of the control of carbon metabolism and partitioning. *Advances in Botanical Research Incorporating Advances in Plant Pathology, Vol 32,* 32**,** 405-434.

Halford, N. G., Hey, S., Jhurreea, D., Laurie, S., Mckibbin, R. S., Paul, M. & Zhang, Y. H. 2003. Metabolic signalling and carbon partitioning: role of Snf1-related (SnRK1) protein kinase. *Journal of Experimental Botany,* 54**,** 467-475.

Halford, N. G. & Hey, S. J. 2009. Snf1-related protein kinases (SnRKs) act within an intricate network that links metabolic and stress signalling in plants. *Biochemical Journal,* 419**,** 247-259.

Hallberg, M., Polozkov, G. V., Hu, G.Z., Beve, J., Gustafsson, C. M., Ronne, H. & Björklund, S. 2004. Site-specific Srb10-dependent phosphorylation of the yeast Mediator subunit Med2 regulates gene expression from the 2-μm plasmid. *Proceedings of the National Academy of Sciences of the United States of America,* 101**,** 3370-3375.

Halliwell, B. 2006. Oxidative stress and neurodegeneration: where are we now? *Journal of Neurochemistry,* 97**,** 1634-1658.

Halsey, L. G., Curran-Everett, D., Vowler, S. L. & Drummond, G. B. 2015. The fickle P value generates irreproducible results. *Nature methods,* 12**,** 179-185.

Han, S. J., Lee, Y. C., Gim, B. S., Ryu, G.-H., Park, S. J., Lane, W. S. & Kim, Y.J. 1999. Activator-specific requirement of yeast mediator proteins for RNA polymerase II transcriptional activation. *Mol Cell Biol,* 19**,** 979-988.

Hanson, J., Hanssen, M., Wiese, A., Hendriks, M. M. & Smeekens, S. 2008. The sucrose regulated transcription factor bZIP11 affects amino acid metabolism by regulating the expression of ASPARAGINE SYNTHETASE1 and PROLINE DEHYDROGENASE2. *The Plant Journal,* 53**,** 935-949.

Hanson, J. & Smeekens, S. 2009. Sugar perception and signaling—an update. *Current Opinion in Plant Biology,* 12**,** 562-567.

Hao, L. H., Wang, H., Sunter, G. & Bisaro, D. M. 2003. Geminivirus AL2 and L2 proteins interact with and inactivate SNF1 kinase. *Plant Cell,* 15**,** 1034-1048.

Hardie, D. G. 2004. The AMP-activated protein kinase pathway - new players upstream and downstream. *Journal of Cell Science,* 117**,** 5479-5487.

Hardie, D. G. 2007. AMP-activated/SNF1 protein kinases: conserved guardians of cellular energy. *Nat Rev Mol Cell Biol,* 8**,** 774-85.

Hardie, D. G., Carling, D. & Carlson, M. 1998. The AMP-activated/SNF1 protein kinase subfamily: metabolic sensors of the eukaryotic cell? *Annu. Rev. Biochem.,* 67**,** 821–855.

Harrington, G. N. & Bush, D. R. 2003. The bifunctional role of hexokinase in metabolism and glucose signaling. *The Plant Cell Online,* 15**,** 2493-2496.

Hasanuzzaman, M., Hossain, M. A. & Fujita, M. 2011a. Nitric oxide modulates antioxidant defense and the methylglyoxal detoxification system and reduces salinity-induced damage of wheat seedlings. *Plant Biotechnology Reports,* 5**,** 353-365.

Hasanuzzaman, M., Hossain, M. A. & Fujita, M. 2011b. Selenium-induced up-regulation of the antioxidant defense and methylglyoxal detoxification system reduces salinity-induced damage in rapeseed seedlings. *Biological trace element research,* 143**,** 1704-1721.

Hawley, S. A., Boudeau, J., Reid, J. L., Mustard, K. J., Udd, L., Makela, T. P., Alessi, D. R. & Hardie, D. G. 2003. Complexes between the LKB1 tumor suppressor, STRAD alpha/beta and MO25 alpha/beta are upstream kinases in the AMP-activated protein kinase cascade. *J Biol,* 2**,** 28.

Hawley, S. A., Pan, D. A., Mustard, K. J., Ross, L., Bain, J., Edelman, A. M., Frenguelli, B. G. & Hardie, D. G. 2005. Calmodulin-dependent protein kinase kinase-beta is an alternative upstream kinase for AMP-activated protein kinase. *Cell Metab,* 2**,** 9-19.

Heber, U., Bilger, W., Bligny, R. & Lange, O. L. 2000. Phototolerance of lichens, mosses and higher plants in an alpine environment: analysis of photoreactions. *Planta,* 211**,** 770-780.

Hedbacker, K. & Carlson, M. 2006. Regulation of the nucleocytoplasmic distribution of Snf1-Gal83 protein kinase. *Eukaryotic Cell,* 5**,** 1950-1956.

Hedbacker, K. & Carlson, M. 2008. SNF1/AMPK pathways in yeast. *Frontiers in Bioscience-Landmark,* 13**,** 2408-2420.

Hemsley, P. A., Hurst, C. H., Kaliyadasa, E., Lamb, R., Knight, M. R., De Cothi, E. A., Steele, J. F. & Knight, H. 2014. The Arabidopsis Mediator Complex Subunits MED16, MED14, and MED2 Regulate Mediator and RNA Polymerase II Recruitment to CBF-Responsive Cold-Regulated Genes. *The Plant Cell Online,* 26**,** 465-484.

Hidema, J. & Kumagai, T. 2006. Sensitivity of Rice to Ultraviolet-B Radiation. *Annals of Botany,* 97**,** 933-942.

Hippeli, S. & Elstner, E. F. 1996. Mechanisms of oxygen activation during plant stress: Biochemical effects of air pollutants. *Journal of Plant Physiology,* 148**,** 249-257.

Hirt, H. & Shinozaki, K. 2004. *Plant responses to abiotic stress,* Springer.

Hollósy, F. 2002. Effects of ultraviolet radiation on plant cells. *Micron,* 33**,** 179-197.

Holsters, M., De Waele, D., Depicker, A., Messens, E., Van Montagu, M. & Schell, J. 1978. Transfection and transformation of Agrobacterium tumefaciens. *Molecular and General Genetics MGG,* 163**,** 181-187.

Holsters, M., Silva, B., Van Vliet, F., Genetello, C., De Block, M., Dhaese, P., Depicker, A., Inzé, D., Engler, G. & Villarroel, R. 1980. The functional organization of the nopaline A. tumefaciens plasmid pTiC58. *Plasmid,* 3**,** 212-230.

Hong, S.-P. & Carlson, M. 2007. Regulation of snf1 protein kinase in response to environmental stress. *Journal of Biological Chemistry,* 282**,** 16838-16845.

Hong, S. P., Leiper, F. C., Woods, A., Carling, D. & Carlson, M. 2003. Activation of yeast Snf1 and mammalian AMP-activated protein kinase by upstream kinases. *Proceedings of the National Academy of Sciences of the United States of America,* 100**,** 8839-8843.

Hudson, E. R., Pan, D. A., James, J., Lucocq, J. M., Hawley, S. A., Green, K. A., Baba, O., Terashima, T. & Hardie, D. G. 2003. A novel domain in AMP-activated protein kinase causes glycogen storage bodies similar to those seen in hereditary cardiac arrhythmias. *Current Biology,* 13**,** 861-866.

Hurley, R. L., Anderson, K. A., Franzone, J. M., Kemp, B. E., Means, A. R. & Witters, L. A. 2005. The $Ca^{2+/}$calmodulin-dependent protein kinase kinases are AMP-activated protein kinase kinases. *Journal of Biological Chemistry,* 280**,** 29060-29066.

Imura, Y., Kobayashi, Y., Yamamoto, S., Furutani, M., Tasaka, M., Abe, M. & Araki, T. 2012. CRYPTIC PRECOCIOUS/MED12 is a novel flowering regulator with multiple target steps in Arabidopsis. *Plant and Cell Physiology,* 53**,** 287-303.

Iseli, T. J., Walter, M., Van Denderen, B. J. W., Katsis, F., Witters, L. A., Kemp, B. E., Michell, B. J. & Stapleton, D. 2005. AMP-activated protein kinase beta subunit tethers alpha and gamma Subunits via its C-terminal sequence (186-270). *Journal of Biological Chemistry,* 280**,** 13395-13400.

Ishitani, M., Xiong, L., Stevenson, B. & Zhu, J.K. 1997. Genetic analysis of osmotic and cold stress signal transduction in Arabidopsis: interactions and convergence of abscisic acid-dependent and abscisic acid-independent pathways. *The Plant Cell,* 9**,** 1935-1949.

Ito, J., Sono, T., Tasaka, M. & Furutani, M. 2011. MACCHI-BOU 2 is required for early embryo patterning and cotyledon organogenesis in Arabidopsis. *Plant and Cell Physiology,* 52**,** 539-552.

Ito, T., Chiba, T., Ozawa, R., Yoshida, M., Hattori, M. & Sakaki, Y. 2001. A comprehensive two-hybrid analysis to explore the yeast protein interactome. *Proceedings of the National Academy of Sciences,* 98**,** 4569-4574.

Ito, Y., Katsura, K., Maruyama, K., Taji, T., Kobayashi, M., Seki, M., Shinozaki, K. & Yamaguchi-Shinozaki, K. 2006. Functional analysis of rice DREB1/CBF-type transcription factors involved in cold-responsive gene expression in transgenic rice. *Plant and Cell Physiology,* 47**,** 141-153.

Jaglo-Ottosen, K. R., Gilmour, S. J., Zarka, D. G., Schabenberger, O. & Thomashow, M. F. 1998. Arabidopsis CBF1 Overexpression Induces COR Genes and Enhances Freezing Tolerance. *Science,* 280**,** 104-106.

Jaglo, K. R., Kleff, S., Amundsen, K. L., Zhang, X., Haake, V., Zhang, J. Z., Deits, T. & Thomashow, M. F. 2001. Components of the Arabidopsis C-repeat/dehydration-responsive element binding factor cold-response pathway are conserved inbrassica napus and other plant species. *Plant Physiology,* 127**,** 910-917.

Jang, J.C. & Sheen, J. 1994. Sugar sensing in higher plants. *The Plant Cell Online,* 6**,** 1665-1679.

Jarvis, P. 1976. The interpretation of the variations in leaf water potential and stomatal conductance found in canopies in the field. *Philosophical Transactions of the Royal Society of London B: Biological Sciences,* 273**,** 593-610.

Jenkins, G. I. 2009. Signal Transduction in Responses to UV-B Radiation. *Annu Rev Plant Biol,* 60**,** 407-431.

Jenks, M. A. & Hasegawa, P. M. 2008. *Plant abiotic stress,* John Wiley & Sons.

Jensen, M., Chakir, S. & Feige, G. 1999. Osmotic and atmospheric dehydration effects in the lichens Hypogymnia physodes, Lobaria pulmonaria, and Peltigera aphthosa: an in vivo study of the chlorophyll fluorescence induction. *Photosynthetica,* 37**,** 393-404.

Jensen, M. & Feige, G. 1991. Quantum efficiency and chlorophyll fluorescence in the lichens Hypogymnia psysodes and Parmelia sulcata. *Symbiosis*.

Jensen, M., Feige, G. & Kuffer, M. 1997. The effect of short-time heating on wet Lobaria pulmonaria: a chlorophyll fluorescence study. *Bibliotheca Lichenologica,* 67**,** 247-254.

Jiang, N. & Taylor, J. S. 1993. In vivo evidence that UV-induced C .fwdarw. T mutations at dipyrimidine sites could result from the replicative bypass of cis-syn cyclobutane dimers or their deamination products. *Biochemistry,* 32**,** 472-481.

Jiang, R. & Carlson, M. 1997. The Snf1 protein kinase and its activating subunit, Snf4, interact with distinct domains of the Sip1/Sip2/Gal83 component in the kinase complex. *Mol Cell Biol,* 17**,** 2099-106.

Jordan, B. R. 1996. The effects of UV-B radiation on plants: a molecular perspective. *In:* CALLOW, J. (ed.) *Advances in Botanical Research.* Academic Press, Boca Raton, FL.

Jordan, B. R., James, P. E. & Mackerness, S. A. H. 1998. Factors Affecting UV-B-Induced Changes in Arabidopsis thaliana L. Gene Expression: the Role of Development, Protective Pigments and the Chloroplast Signal. *Plant and Cell Physiology,* 39**,** 769-778.

Jossier, M., Bouly, J. P., Meimoun, P., Arjmand, A., Lessard, P., Hawley, S., Grahame Hardie, D. & Thomas, M. 2009. SnRK1 (SNF1-related kinase 1) has a central role in sugar and ABA signalling in Arabidopsis thaliana. *The Plant Journal,* 59**,** 316-328.

Kang, C. H., Feng, Y., Vikram, M., Jeong, I. S., Lee, J. R., Bahk, J. D., Yun, D.J., Lee, S. Y. & Koiwa, H. 2009. Arabidopsis thaliana PRP40s are RNA polymerase II C-terminal domain-associating proteins. *Archives of Biochemistry and Biophysics,* 484**,** 30-38.

Kang, J. S., Kim, S. H., Hwang, M. S., Han, S. J., Lee, Y. C. & Kim, Y.J. 2001. The structural and functional organization of the yeast mediator complex. *Journal of Biological Chemistry,* 276**,** 42003-42010.

Kang, J. Y., Choi, H. I., Im, M. Y. & Kim, S. Y. 2002. Arabidopsis basic leucine zipper proteins that mediate stress-responsive abscisic acid signaling. *Plant Cell,* 14**,** 343-357.

Karimi, M., Inzé, D. & Depicker, A. 2002. GATEWAY™ vectors for Agrobacterium mediated plant transformation. *Trends Plant Sci,* 7**,** 193-195.

Karuppanapandian, T., Moon, J. C., Kim, C., Manoharan, K. & Kim, W. 2011a. Reactive oxygen species in plants: their generation, signal transduction, and scavenging mechanisms. *Australian Journal of Crop Science,* 5**,** 709-725.

Karuppanapandian, T., Wang, H. W., Prabakaran, N., Jeyalakshmi, K., Kwon, M., Manoharan, K. & Kim, W. 2011b. 2,4-dichlorophenoxyacetic acid-induced leaf senescence in mung bean (Vigna radiata L. Wilczek) and senescence inhibition by co-treatment with silver nanoparticles. *Plant Physiology and Biochemistry,* 49**,** 168-177.

Kasuga, M., Liu, Q., Miura, S., Yamaguchi-Shinozaki, K. & Shinozaki, K. 1999. Improving plant drought, salt, and freezing tolerance by gene transfer of a single stress-inducible transcription factor. *Nature biotechnology,* 17**,** 287-291.

Katterman, F. 1990. *Environmental injury to plants*, San Diego, etc.: Academic Press.

Kazgan, N., Williams, T., Forsberg, L. J. & Brenman, J. E. 2010. Identification of a nuclear export signal in the catalytic subunit of AMP-activated protein kinase. *Molecular biology of the cell,* 21**,** 3433-3442.

Khoroshilova, E. V., Repeyev, Y. A. & Nikogosyan, D. N. 1990. UV protolysis of aromatic amino acids and related dipeptides and tripeptides. *Journal of Photochemistry and Photobiology B: Biology,* 7**,** 159-172.

Kidd, B. N., Cahill, D. M., Manners, J. M., Schenk, P. M. & Kazan, K. Diverse roles of the Mediator complex in plants. Seminars in Cell & Developmental Biology, 2011. Elsevier, 741-748.

Kidd, B. N., Edgar, C. I., Kumar, K. K., Aitken, E. A., Schenk, P. M., Manners, J. M. & Kazan, K. 2009. The mediator complex subunit PFT1 is a key regulator of jasmonate-dependent defense in Arabidopsis. *The Plant Cell Online,* 21**,** 2237-2252.

Kilian, J., Whitehead, D., Horak, J., Wanke, D., Weinl, S., Batistic, O., D'angelo, C., Bornberg-Bauer, E., Kudla, J. & Harter, K. 2007. The AtGenExpress global stress expression data set: protocols, evaluation and model data analysis of UV-B light, drought and cold stress responses. *The Plant Journal,* 50**,** 347-363.

Kim, M., Lim, J.-H., Ahn, C. S., Park, K., Kim, G. T., Kim, W. T. & Pai, H.S. 2006. Mitochondria-associated hexokinases play a role in the control of programmed cell death in Nicotiana benthamiana. *The Plant Cell Online,* 18**,** 2341-2355.

Kim, T. W., Kwon, Y.-J., Kim, J. M., Song, Y.-H., Kim, S. N. & Kim, Y.J. 2004. MED16 and MED23 of Mediator are coactivators of lipopolysaccharide-and heat-shock-induced transcriptional activators. *Proceedings of the National Academy of Sciences of the United States of America,* 101**,** 12153-12158.

Kim, Y.J., Björklund, S., Li, Y., Sayre, M. H. & Kornberg, R. D. 1994. A multiprotein mediator of transcriptional activation and its interaction with the C-terminal repeat domain of RNA polymerase II. *Cell,* 77**,** 599-608.

Kim, Y. J., Zheng, B., Yu, Y., Won, S. Y., Mo, B. & Chen, X. 2011. The role of Mediator in small and long noncoding RNA production in Arabidopsis thaliana. *EMBO J,* 30**,** 814-822.

Kitajima, M. & Butler, W. 1975. Excitation spectra for photosystem I and photosystem II in chloroplasts and the spectral characteristics of the distribution of quanta between the two photosystems. *Biochimica et Biophysica Acta (BBA)-Bioenergetics,* 408**,** 297-305.

Kleinow, T., Bhalerao, R., Breuer, F., Umeda, M., Salchert, K. & Koncz, C. 2000. Functional identification of an Arabidopsis Snf4 ortholog by screening for heterologous multicopy suppressors of snf4 deficiency in yeast. *Plant Journal,* 23**,** 115-122.

Knight, H., Mugford, S. G., Ülker, B., Gao, D., Thorlby, G. & Knight, M. R. 2009. Identification of SFR6, a key component in cold acclimation acting post-translationally on CBF function. *The Plant Journal,* 58**,** 97-108.

Knight, H., Thomson, A. J. & Mcwatters, H. G. 2008. Sensitive to freezing6 integrates cellular and environmental inputs to the plant circadian clock. *Plant Physiology,* 148**,** 293-303.

Knight, H., Trewavas, A. J. & Knight, M. R. 1996. Cold calcium signaling in Arabidopsis involves two cellular pools and a change in calcium signature after acclimation. *The Plant Cell,* 8**,** 489-503.

Knight, H., Veale, E. L., Warren, G. J. & Knight, M. R. 1999. The sfr6 mutation in Arabidopsis suppresses low-temperature induction of genes dependent on the CRT/DRE sequence motif. *The Plant Cell Online,* 11**,** 875-886.

Knight, M. R., Campbell, A. K., Smith, S. M. & Trewavas, A. J. 1991. Transgenic plant aequorin reports the effects of touch and cold-shock and elicitors on cytoplasmic calcium.

Knight, M. R. & Knight, H. 2012. Low-temperature perception leading to gene expression and cold tolerance in higher plants. *New Phytologist,* 195**,** 737-751.

Koch, K. 1996. Carbohydrate-modulated gene expression in plants. *Annu Rev Plant Biol,* 47**,** 509-540.

Koch, K. 2004. Sucrose metabolism: regulatory mechanisms and pivotal roles in sugar sensing and plant development. *Current Opinion in Plant Biology,* 7**,** 235-246.

Kong, L. J. & Hanley-Bowdoin, L. 2002. A geminivirus replication protein interacts with a protein kinase and a motor protein that display different expression patterns during plant development and infection. *Plant Cell,* 14**,** 1817-32.

Kornberg, R. D. 1999. Eukaryotic transcriptional control. *Trends in Biochemical Sciences,* 24**,** M46-M49.

Kramer, G. F., Norman, H. A., Krizek, D. T. & Mirecki, R. M. 1991. Influence of UV-B radiation on polyamines, lipid peroxidation and membrane lipids in cucumber. *Phytochemistry,* 30**,** 2101-2108.

Krause, G. H. 1988. Photoinhibition of photosynthesis. An evaluation of damaging and protective mechanisms. *Physiologia Plantarum,* 74**,** 566-574.

Kreps, J. A., Wu, Y., Chang, H.S., Zhu, T., Wang, X. & Harper, J. F. 2002. Transcriptome changes for Arabidopsis in response to salt, osmotic, and cold stress. *Plant Physiology,* 130**,** 2129-2141.

Krichevsky, A., Zaltsman, A., Kozlovsky, S. V., Tian, G.W. & Citovsky, V. 2009. Regulation of Root Elongation by Histone Acetylation in< i> Arabidopsis</i>. *Journal of molecular biology,* 385**,** 45-50.

Kuchin, S., Treich, I. & Carlson, M. 2000. A regulatory shortcut between the Snf1 protein kinase and RNA polymerase II holoenzyme. *Proceedings of the National Academy of Sciences,* 97**,** 7916-7920.

Kulik, A., Wawer, I., Krzywinska, E., Bucholc, M. & Dobrowolska, G. 2011. SnRK2 protein kinases--key regulators of plant response to abiotic stresses. *OMICS,* 15**,** 859-72.

Kuras, L. & Struhl, K. 1999. Binding of TBP to promoters in vivo is stimulated by activators and requires Pol II holoenzyme. *Nature,* 399**,** 609-613.

Kurkela, S. & Borg-Franck, M. 1992. Structure and expression of kin2, one of two cold-and ABA-induced genes of Arabidopsis thaliana. *Plant Molecular Biology,* 19**,** 689-692.

Kwon, J. Y., Park, J. M., Gim, B. S., Han, S. J., Lee, J. & Kim, Y.J. 1999. Caenorhabditis elegans mediator complexes are required for developmental-specific transcriptional activation. *Proceedings of the National Academy of Sciences,* 96**,** 14990-14995.

Lai, Z., Schluttenhofer, C. M., Bhide, K., Shreve, J., Thimmapuram, J., Lee, S. Y., Yun, D.J. & Mengiste, T. 2014. MED18 interaction with distinct transcription factors regulates multiple plant functions. *Nature communications,* 5.

Lamb, C. & Dixon, R. A. 1997. THE OXIDATIVE BURST IN PLANT DISEASE RESISTANCE. *Annual Review of Plant Physiology and Plant Molecular Biology,* 48**,** 251-275.

Lang, V., Mantyla, E., Welin, B., Sundberg, B. & Palva, E. T. 1994. Alterations in water status, endogenous abscisic acid content, and expression of rab18 gene during the development of freezing tolerance in Arabidopsis thaliana. *Plant Physiology,* 104**,** 1341-1349.

Lange, O., Bilger, W., Rimke, S. & Schreiber, U. 1989. Chlorophyll Fluorescence of Lichens Containing Green and Blue-Green Algae During Hydration by Water Vapor Uptake and by Addition of Liquid Water*. *Botanica Acta,* 102**,** 306-313.

Larcher, W., Wagner, J. & Lütz, C. 1998. The effect of heat on photosynthesis, dark respiration and cellular ultrastructure of the arctic-alpine psychrophyte Ranunculus glacialis. *Photosynthetica,* 34**,** 219-232.

Lavergne, J. 1982. Mode of action of 3-(3, 4-dichlorophenyl)-1, 1-dimethylurea. Evidence that the inhibitor competes with plastoquinone for binding to a common site on the acceptor side of photosystem II. *Biochimica et Biophysica Acta (BBA)-Bioenergetics,* 682**,** 345-353.

Lawlor, D. W. 2013. Genetic engineering to improve plant performance under drought: physiological evaluation of achievements, limitations, and possibilities. *Journal of Experimental Botany,* 64**,** 83-108.

Lazár, D. 1999. Chlorophyll a fluorescence induction. *Biochimica et Biophysica Acta (BBA)-Bioenergetics,* 1412**,** 1-28.

Lee, K. W., Chen, P. W., Lu, C. A., Chen, S., Ho, T. H. D. & Yu, S. M. 2009. Coordinated Responses to Oxygen and Sugar Deficiency Allow Rice Seedlings to Tolerate Flooding. *Science Signaling,* 2.

Lee, T. I., Wyrick, J. J., Koh, S. S., Jennings, E. G., Gadbois, E. L. & Young, R. A. 1998. Interplay of positive and negative regulators in transcription initiation by RNA polymerase II holoenzyme. *Mol Cell Biol,* 18**,** 4455-4462.

Lee, Y. 1992. Biochemistry of carbohydrate-protein interaction. *The FASEB Journal,* 6**,** 3193-3200.

Lee, Y. C., Park, J. M., Min, S., Han, S. J. & Kim, Y.J. 1999. An activator binding module of yeast RNA polymerase II holoenzyme. *Mol Cell Biol,* 19**,** 2967-2976.

Leshem, Y., Seri, L. & Levine, A. 2007. Induction of phosphatidylinositol 3-kinase-mediated endocytosis by salt stress leads to intracellular production of reactive oxygen species and salt tolerance. *The Plant Journal,* 51**,** 185-197.

Levitt, J. 1980. *Water, radiation, salt, and other stresses*, Elsevier.

Li, X., Gerber, S. A., Rudner, A. D., Beausoleil, S. A., Haas, W., Villen, J., Elias, J. E. & Gygi, S. P. 2007. Large-scale phosphorylation analysis of α-factor-arrested Saccharomyces cerevisiae. *Journal of proteome research,* 6**,** 1190-1197.

Li, Y., Bjorklund, S., Jiang, Y. W., Kim, Y.J., Lane, W. S., Stillman, D. J. & Kornberg, R. D. 1995. Yeast global transcriptional regulators Sin4 and Rgr1 are components of mediator complex/RNA polymerase II holoenzyme. *Proceedings of the National Academy of Sciences,* 92**,** 10864-10868.

Li, Y., Lee, K. K., Walsh, S., Smith, C., Hadingham, S., Sorefan, K., Cawley, G. & Bevan, M. W. 2006. Establishing glucose-and ABA-regulated transcription networks in Arabidopsis by microarray analysis and promoter classification using a Relevance Vector Machine. *Genome Research,* 16**,** 414-427.

Lin, C., Guo, W. W., Everson, E. & Thomashow, M. F. 1990. Cold Acclimation in Arabidopsis and Wheat A Response Associated with Expression of Related Genes EncodingBoiling-Stable'Polypeptides. *Plant Physiology,* 94**,** 1078-1083.

Lindemose, S., O'Shea, C., Jensen, M. & Skriver, K. 2013. Structure, Function and Networks of Transcription Factors Involved in Abiotic Stress Responses. *International Journal of Molecular Sciences,* 14**,** 5842-5878.

Liu, Q., Kasuga, M., Sakuma, Y., Abe, H., Miura, S., Yamaguchi-Shinozaki, K. & Shinozaki, K. 1998. Two Transcription Factors, DREB1 and DREB2, with an EREBP/AP2 DNA Binding Domain Separate Two Cellular Signal Transduction Pathways in Drought- and Low-Temperature-Responsive Gene Expression, Respectively, in Arabidopsis. *The Plant Cell Online,* 10**,** 1391-1406.

Liu, Y., Kung, C., Fishburn, J., Ansari, A. Z., Shokat, K. M. & Hahn, S. 2004. Two cyclin-dependent kinases promote RNA polymerase II transcription and formation of the scaffold complex. *Mol Cell Biol,* 24**,** 1721-1735.

Liu, Y., Schiff, M., Czymmek, K., Tallóczy, Z., Levine, B. & Dinesh-Kumar, S. 2005a. Autophagy regulates programmed cell death during the plant innate immune response. *Cell,* 121**,** 567-577.

Liu, Y., Xu, X., Singh-Rodriguez, S., Zhao, Y. & Kuo, M.H. 2005b. Histone H3 Ser10 phosphorylation-independent function of Snf1 and Reg1 proteins rescues a gcn5− mutant in HIS3 expression. *Molecular and cellular biology,* 25**,** 10566-10579.

Livak, K. J. & Schmittgen, T. D. 2001. Analysis of relative gene expression data using real-time quantitative PCR and the 2− ΔΔCT method. *methods,* 25**,** 402-408.

Lizcano, J. M., Goransson, O., Toth, R., Deak, M., Morrice, N. A., Boudeau, J., Hawley, S. A., Udd, L., Makela, T. P., Hardie, D. G. & Alessi, D. R. 2004. LKB1 is a master kinase that activates 13 kinases of the AMPK subfamily, including MARK/PAR-1. *Embo Journal,* 23**,** 833-843.

Llorente, F., López-Cobollo, R. M., Catalá, R., Martínez-Zapater, J. M. & Salinas, J. 2002. A novel cold-inducible gene from Arabidopsis, RCI3, encodes a peroxidase that constitutes a component for stress tolerance. *The Plant Journal,* 32**,** 13-24.

Lo, W.-S., Duggan, L., Tolga, N., Belotserkovskya, R., Lane, W. S., Shiekhattar, R. & Berger, S. L. 2001. Snf1--a histone kinase that works in concert with the histone acetyltransferase Gcn5 to regulate transcription. *Science,* 293**,** 1142-1146.

Lo, W. S., Gamache, E. R., Henry, K. W., Yang, D., Pillus, L. & Berger, S. L. 2005. Histone H3 phosphorylation can promote TBP recruitment through distinct promoter-specific mechanisms. *The EMBO journal,* 24**,** 997-1008.

Logemann, E. & Hahlbrock, K. 2002. Crosstalk among stress responses in plants: pathogen defense overrides UV protection through an inversely regulated ACE/ACE type of light-responsive gene promoter unit. *Proceedings of the National Academy of Sciences,* 99**,** 2428-2432.

Long, J. C. & Jenkins, G. I. 1998. Involvement of Plasma Membrane Redox Activity and Calcium Homeostasis in the UV-B and UV-A/Blue Light Induction of Gene Expression in Arabidopsis. *The Plant Cell Online,* 10**,** 2077-2086.

Loreti, E., De Bellis, L., Alpi, A. & Perata, P. 2001. Why and how do plant cells sense sugars? *Annals of Botany,* 88**,** 803-812.

Lovas, A., Bimbo, A., Szabo, L. & Banfalvi, Z. 2003. Antisense repression of StubGAL83 affects root and tuber development in potato. *Plant Journal,* 33**,** 139-147.

Lu, C. A., Lin, C. C., Lee, K. W., Chen, J. L., Huang, L. F., Ho, S. L., Liu, H. J., Hsing, Y. I. & Yu, S. M. 2007. The SnRK1A protein kinase plays a key role in sugar signaling during germination and seedling growth of rice. *Plant Cell,* 19**,** 2484-2499.

Lumbreras, V., Alba, M. M., Kleinow, T., Koncz, C. & Pages, M. 2001. Domain fusion between SNF1-related kinase subunits during plant evolution. *EMBO Rep,* 2**,** 55-60.

Lyons, J. 2012. *Low temperature stress in crop plants: the role of the membrane*, Elsevier.

Ma, S. & Bohnert, H. J. 2007. Integration of Arabidopsis thaliana stress-related transcript profiles, promoter structures, and cell-specific expression. *Genome biology,* 8**,** R49.

Mackerness, S. a.-H., Thomas, B. & Jordan, B. R. 1997. The effect of supplementary ultraviolet-B radiation on mRNA transcripts, translation and stability of chloroplast proteins and pigment formation in Pisum sativum L. *Journal of Experimental Botany,* 48**,** 729-738.

Mackerness, S. a. H., John, C. F., Jordan, B. & Thomas, B. 2001. Early signaling components in ultraviolet-B responses: distinct roles for different reactive oxygen species and nitric oxide. *FEBS Lett,* 489**,** 237-242.

Mackerness, S. a. H. & Jordan, B. R. 1999. Changes in gene expression in response to ultraviolet B-induced Stress. *In:* PESSARAKLI, M. (ed.) *Handbook of Plant and Crop Stress.* 2 ed. New York: Marcel Dekker.

Mackerness, S. a. H., Surplus, S. L., Blake, P., John, C. F., Buchanan-Wollaston, V., Jordan, B. R. & Thomas, B. 1999. Ultraviolet-B-induced stress and changes in gene expression in Arabidopsis thaliana: role of signalling pathways controlled by jasmonic acid, ethylene and reactive oxygen species. *Plant, Cell & Environment,* 22**,** 1413-1423.

Mackerness, S. H. 2000. Plant responses to ultraviolet-B (UV-B: 280–320 nm) stress: What are the key regulators? *Plant Growth Regulation,* 32**,** 27-39.

Mahajan, S. & Tuteja, N. 2005. Cold, salinity and drought stresses: an overview. *Archives of Biochemistry and Biophysics,* 444**,** 139-158.

Malik, S. & Roeder, R. G. 2000. Transcriptional regulation through Mediator-like coactivators in yeast and metazoan cells. *Trends in Biochemical Sciences,* 25**,** 277-283.

Maniatis, T., Fritsch, E. F. & Sambrook, J. 1982. *Molecular cloning: a laboratory manual,* Cold Spring Harbor Laboratory Cold Spring Harbor, NY.

Mantyla, E., Lang, V. & Palva, E. T. 1995. Role of abscisic acid in drought-induced freezing tolerance, cold acclimation, and accumulation of LT178 and RAB18 proteins in Arabidopsis thaliana. *Plant Physiology,* 107**,** 141-148.

Mathis, P. & Paillotin, G. 1981. Primary processes of photosynthesis. *The biochemistry of plants,* 8**,** 97-161.

Mathur, S., Vyas, S., Kapoor, S. & Tyagi, A. K. 2011. The Mediator complex in plants: structure, phylogeny, and expression profiling of representative genes in a dicot (Arabidopsis) and a monocot (rice) during reproduction and abiotic stress. *Plant Physiology,* 157**,** 1609-1627.

Maxwell, S. E. 2004. The persistence of underpowered studies in psychological research: causes, consequences, and remedies. *Psychological methods,* 9**,** 147.

Mazza, C. A., Boccalandro, H. E., Giordano, C. V., Battista, D., Scopel, A. L. & Ballaré, C. L. 2000. Functional Significance and Induction by Solar Radiation of Ultraviolet-Absorbing Sunscreens in Field-Grown Soybean Crops. *Plant Physiology,* 122**,** 117-126.

Mckown, R., Kuroki, G. & Warren, G. 1996. Cold responses of Arabidopsis mutants impaired in freezing tolerance. *Journal of Experimental Botany,* 47**,** 1919-1925.

Menand, B., Meyer, C. & Robaglia, C. 2004. Plant growth and the TOR pathway. *TOR.* Springer.

Milla, M. a. R., Maurer, A., Huete, A. R. & Gustafson, J. P. 2003. Glutathione peroxidase genes in Arabidopsis are ubiquitous and regulated by abiotic stresses through diverse signaling pathways. *The Plant Journal,* 36**,** 602-615.

Miller, C., Matic, I., Maier, K. C., Schwalb, B., Roether, S., Strässer, K., Tresch, A., Mann, M. & Cramer, P. 2012. Mediator phosphorylation prevents stress response transcription during non-stress conditions. *Journal of Biological Chemistry,* 287**,** 44017-44026.

Minokoshi, Y., Shiuchi, T., Lee, S., Suzuki, A. & Okamoto, S. 2008a. Role of hypothalamic AMP-kinase in food intake regulation. *Nutrition,* 24**,** 786-790.

Minokoshi, Y., Shiuchi, T., Suzuki, A. & Okamoto, S. 2008b. Regulatory role of AMP-kinase in the paraventricular hypothalamus in food preference. *Neuroscience Research,* 61**,** S26-S26.

Mirza Hasanuzzaman, Nahar, K. & Fujita, M. 2013. Abiotic Stress - Plant Responses and Applications in Agriculture. *In:* (ED.), D. K. V. (ed.) *Extreme Temperature Responses, Oxidative Stress and Antioxidant Defense in Plants.* InTech, DOI: 10.5772/54833.

Mitchelhill, K. I., Stapleton, D., Gao, G., House, C., Michell, B., Katsis, F., Witters, L. A. & Kemp, B. E. 1994. Mammalian AMP-activated protein kinase shares structural and functional homology with the catalytic domain of yeast Snf1 protein kinase. *J Biol Chem,* 269**,** 2361-4.

Mittler, R. 2002. Oxidative stress, antioxidants and stress tolerance. *Trends Plant Sci,* 7**,** 405-410.

Mittler, R., Kim, Y., Song, L., Coutu, J., Coutu, A., Ciftci-Yilmaz, S., Lee, H., Stevenson, B. & Zhu, J.-K. 2006. Gain- and loss-of-function mutations in Zat10 enhance the tolerance of plants to abiotic stress. *FEBS Lett,* 580**,** 6537-6542.

Mittler, R., Vanderauwera, S., Gollery, M. & Van Breusegem, F. 2004. Reactive oxygen gene network of plants. *Trends Plant Sci,* 9**,** 490-498.

Mobley, A., Linder, S. K., Braeuer, R., Ellis, L. M. & Zwelling, L. 2013. A survey on data reproducibility in cancer research provides insights into our limited ability to translate findings from the laboratory to the clinic. *Plos One,* 8**,** e63221.

Moller, I. M., Jensen, P. E. & Hansson, A. 2007. Oxidative modifications to cellular components in plants. *Annu Rev Plant Biol,* 58**,** 459-481.

Moore, B., Zhou, L., Rolland, F., Hall, Q., Cheng, W.-H., Liu, Y.X., Hwang, I., Jones, T. & Sheen, J. 2003. Role of the Arabidopsis glucose sensor HXK1 in nutrient, light, and hormonal signaling. *Science,* 300**,** 332-336.

Morkunas, I., Borek, S., Formela, M. & Ratajczak, L. 2012. Plant responses to sugar starvation. *Carbohydrates–comprehensive studies on glycobiology and glycotechnology. New York NY: InTech***,** 409-438.

Müller, J., Wiemken, A. & Aeschbacher, R. 1999. Trehalose metabolism in sugar sensing and plant development. *Plant Science,* 147**,** 37-47.

Murashige, T. & Skoog, F. 1962. A revised medium for rapid growth and bio assays with tobacco tissue cultures. *Physiologia Plantarum,* 15**,** 473-497.

Myers, L. C., Gustafsson, C. M., Bushnell, D. A., Lui, M., Erdjument-Bromage, H., Tempst, P. & Kornberg, R. D. 1998. The Med proteins of yeast and their function through the RNA polymerase II carboxy-terminal domain. *Genes & Development,* 12**,** 45-54.

Nakashima, K., Tran, L.S. P., Van Nguyen, D., Fujita, M., Maruyama, K., Todaka, D., Ito, Y., Hayashi, N., Shinozaki, K. & Yamaguchi-Shinozaki, K. 2007. Functional analysis of a NAC-type transcription factor OsNAC6 involved in abiotic and biotic stress-responsive gene expression in rice. *The Plant Journal,* 51**,** 617-630.

Narusaka, Y., Narusaka, M., Seki, M., Ishida, J., Nakashima, M., Kamiya, A., Enju, A., Sakurai, T., Satoh, M. & Kobayashi, M. 2003. The cDNA microarray analysis using an Arabidopsis pad3 mutant reveals the expression profiles and classification of genes induced by Alternaria brassicicola attack. *Plant and Cell Physiology,* 44**,** 377-387.

Nath, N., Mccartney, R. R. & Schmidt, M. C. 2003. Yeast Pak1 kinase associates with and activates Snf1. *Mol Cell Biol,* 23**,** 3909-3917.

Nawrath, C., Heck, S., Parinthawong, N. & Métraux, J.P. 2002. EDS5, an essential component of salicylic acid–dependent signaling for disease resistance in Arabidopsis, is a member of the MATE transporter family. *The Plant Cell Online,* 14**,** 275-286.

Newton, P. C., Carran, R. A., Edwards, G. R. & Niklaus, P. A. 2006. *Agroecosystems in a changing climate*, CRC Press.

Ng, S., Giraud, E., Duncan, O., Law, S. R., Wang, Y., Xu, L., Narsai, R., Carrie, C., Walker, H. & Day, D. A. 2013. Cyclin-dependent kinase E1 (CDKE1) provides a cellular switch in plants between growth and stress responses. *Journal of Biological Chemistry,* 288**,** 3449-3459.

Noctor, G. & Foyer, C. H. 1998. Ascorbate and glutathione: Keeping active oxygen under control. *Annual Review of Plant Physiology and Plant Molecular Biology,* 49**,** 249-279.

Novillo, F., Alonso, J. M., Ecker, J. R. & Salinas, J. 2004. CBF2/DREB1C is a negative regulator of CBF1/DREB1B and CBF3/DREB1A expression and plays a central role in stress tolerance in Arabidopsis. *Proceedings of the National Academy of Sciences of the United States of America,* 101**,** 3985-3990.

Novillo, F., Medina, J. & Salinas, J. 2007. Arabidopsis CBF1 and CBF3 have a different function than CBF2 in cold acclimation and define different gene classes in the CBF regulon. *Proceedings of the National Academy of Sciences,* 104**,** 21002-21007.

Örvar, B. L., Sangwan, V., Omann, F. & Dhindsa, R. S. 2000. Early steps in cold sensing by plant cells: the role of actin cytoskeleton and membrane fluidity. *The Plant Journal,* 23**,** 785-794.

Osuna, D., Usadel, B., Morcuende, R., Gibon, Y., Bläsing, O. E., Höhne, M., Günter, M., Kamlage, B., Trethewey, R. & Scheible, W. R. 2007. Temporal responses of transcripts, enzyme activities and metabolites after adding sucrose to carbon-deprived Arabidopsis seedlings. *The Plant Journal,* 49**,** 463-491.

Ou, B., Yin, K.Q., Liu, S.N., Yang, Y., Gu, T., Hui, J. M. W., Zhang, L., Miao, J., Kondou, Y. & Matsui, M. 2011. A high-throughput screening system for Arabidopsis transcription factors and its application to Med25-dependent transcriptional regulation. *Mol Plant,* 4**,** 546-555.

Palenchar, P. M., Kouranov, A., Lejay, L. V. & Coruzzi, G. M. 2004. Genome-wide patterns of carbon and nitrogen regulation of gene expression validate the combined carbon and nitrogen (CN)-signaling hypothesis in plants. *Genome Biol,* 5**,** R91.

Panagopoulos, I., Bornman, J. F. & Björn, L. O. 1990. Effects of ultraviolet radiation and visible light on growth, fluorescence induction, ultraweak luminescence and peroxidase activity in sugar beet plants. *Journal of Photochemistry and Photobiology B: Biology,* 8**,** 73-87.

Park, J. M., Gim, B. S., Kim, J. M., Yoon, J. H., Kim, H.S., Kang, J.G. & Kim, Y.J. 2001. Drosophila Mediator Complex Is Broadly Utilized by Diverse Gene-Specific Transcription Factors at Different Types of Core Promoters. *Mol Cell Biol,* 21**,** 2312-2323.

Park, J. M., Kim, H.-S., Han, S. J., Hwang, M.S., Lee, Y. C. & Kim, Y.J. 2000. In vivo requirement of activator-specific binding targets of mediator. *Mol Cell Biol,* 20**,** 8709-8719.

Paul, M. J., Primavesi, L. F., Jhurreea, D. & Zhang, Y. 2008. Trehalose metabolism and signaling. *Annu. Rev. Plant Biol.,* 59**,** 417-441.

Pellegrineschi, A., Reynolds, M., Pacheco, M., Brito, R. M., Almeraya, R., Yamaguchi-Shinozaki, K. & Hoisington, D. 2004. Stress-induced expression in wheat of the Arabidopsis thaliana DREB1A gene delays water stress symptoms under greenhouse conditions. *Genome,* 47**,** 493-500.

Polekhina, G., Gupta, A., Michell, B. J., Van Denderen, B., Murthy, S., Feil, S. C., Jennings, I. G., Campbell, D. J., Witters, L. A., Parker, M. W., Kemp, B. E. & Stapleton, D. 2003. AMPK beta subunit targets metabolic stress sensing to glycogen. *Current Biology,* 13**,** 867-871.

Polge, C. & Thomas, M. 2007. SNF1/AMPK/SnRK1 kinases, global regulators at the heart of energy control? *Trends Plant Sci,* 12**,** 20-8.

Potters, G., Pasternak, T. P., Guisez, Y., Palme, K. J. & Jansen, M. a. K. 2007. Stress-induced morphogenic responses: growing out of trouble? *Trends Plant Sci,* 12**,** 98-105.

Prasad, T. K. 1996. Mechanisms of chilling-induced oxidative stress injury and tolerance in developing maize seedlings: changes in antioxidant system, oxidation of proteins and lipids, and protease activities. *The Plant Journal,* 10**,** 1017-1026.

Price, J., Laxmi, A., Martin, S. K. S. & Jang, J.C. 2004. Global transcription profiling reveals multiple sugar signal transduction mechanisms in Arabidopsis. *The Plant Cell Online,* 16**,** 2128-2150.

Prinsze, C., Dubbelman, T. & Van Steveninck, J. 1990. Protein damage, induced by small amounts of photodynamically generated singlet oxygen or hydroxyl radicals. *Biochimica et Biophysica Acta (BBA)-Protein Structure and Molecular Enzymology,* 1038**,** 152-157.

Rabbani, M. A., Maruyama, K., Abe, H., Khan, M. A., Katsura, K., Ito, Y., Yoshiwara, K., Seki, M., Shinozaki, K. & Yamaguchi-Shinozaki, K. 2003. Monitoring expression profiles of rice genes under cold, drought, and high-salinity stresses and abscisic acid application using cDNA microarray and RNA gel-blot analyses. *Plant Physiology,* 133**,** 1755-1767.

Rahmani, F., Hummel, M., Schuurmans, J., Wiese-Klinkenberg, A., Smeekens, S. & Hanson, J. 2009. Sucrose control of translation mediated by an upstream open reading frame-encoded peptide. *Plant Physiology,* 150**,** 1356-1367.

Ramon, M. & Rolland, F. 2007. Plant development: introducing trehalose metabolism. *Trends Plant Sci,* 12**,** 185-188.

Ramon, M., Rolland, F. & Sheen, J. 2008. Sugar sensing and signaling. *The Arabidopsis Book*.

Rehem, B. C., Bertolde, F. Z. & De Almeida, A.A.F. 2011. Regulation of Gene Expression in Response to Abiotic Stress in Plants. *Edited by Paula Bubulya***,** 13.

Reiling, J. & Sabatini, D. 2006. Stress and mTORture signaling. *Oncogene,* 25**,** 6373-6383.

Reymond, P. & Farmer, E. E. 1998. Jasmonate and salicylate as global signals for defense gene expression. *Current Opinion in Plant Biology,* 1**,** 404-411.

Robberecht, R. 1989. Environmental photobiology. *The science of photobiology*. Springer.

Robinson, P. J., Trnka, M. J., Pellarin, R., Greenberg, C. H., Bushnell, D. A., Davis, R., Burlingame, A. L., Sali, A. & Kornberg, R. D. 2015. Molecular architecture of the yeast Mediator complex. *eLife***,** e08719.

Robinson, S. J. & Parkin, I. A. 2008. Differential SAGE analysis in Arabidopsis uncovers increased transcriptome complexity in response to low temperature. *BMC Genomics,* 9**,** 434.

Rodrigues, A., Adamo, M., Crozet, P., Margalha, L., Confraria, A., Martinho, C., Elias, A., Rabissi, A., Lumbreras, V. & González-Guzmán, M. 2013. ABI1 and PP2CA phosphatases are negative regulators of Snf1-related protein kinase1 signaling in Arabidopsis. *The Plant Cell Online,* 25**,** 3871-3884.

Rolland, F., Baena-Gonzalez, E. & Sheen, J. 2006. Sugar sensing and signaling in plants: conserved and novel mechanisms. *Annu. Rev. Plant Biol.,* 57**,** 675-709.

Rolland, F., Moore, B. & Sheen, J. 2002. Sugar sensing and signaling in plants. *Plant Cell,* 14**,** S185-S205.

Russell, J. & Zomerdijk, J. C. The RNA polymerase I transcription machinery. Biochemical Society symposium, 2006. Europe PMC Funders, 203.

Sakamoto, H., Maruyama, K., Sakuma, Y., Meshi, T., Iwabuchi, M., Shinozaki, K. & Yamaguchi-Shinozaki, K. 2004. Arabidopsis Cys2/His2-type zinc-finger proteins function as transcription repressors under drought, cold, and high-salinity stress conditions. *Plant Physiology,* 136**,** 2734-2746.

Sakuma, Y., Maruyama, K., Osakabe, Y., Qin, F., Seki, M., Shinozaki, K. & Yamaguchi-Shinozaki, K. 2006. Functional Analysis of an Arabidopsis Transcription Factor, DREB2A, Involved in Drought-Responsive Gene Expression. *The Plant Cell Online,* 18**,** 1292-1309.

Sancar, A. & Sancar, G. B. 1988. DNA repair enzymes. *Annual review of biochemistry,* 57**,** 29-67.

Sanford, J. C. 1988. The biolistic process. *Trends in Biotechnology,* 6**,** 299-302.

Sato, S., Tomomori-Sato, C., Banks, C. A., Sorokina, I., Parmely, T. J., Kong, S. E., Jin, J., Cai, Y., Lane, W. S. & Brower, C. S. 2003. Identification of mammalian Mediator subunits with similarities to yeast Mediator subunits Srb5, Srb6, Med11, and Rox3. *Journal of Biological Chemistry,* 278**,** 15123-15127.

Sato, Y., Masuta, Y., Saito, K., Murayama, S. & Ozawa, K. 2011. Enhanced chilling tolerance at the booting stage in rice by transgenic overexpression of the ascorbate peroxidase gene,OsAPXa. *Plant Cell Reports* 30**,** 399-406.

Savouré, A., Hua, X.-J., Bertauche, N., Van Montagu, M. & Verbruggen, N. 1997. Abscisic acid-independent and abscisic acid-dependent regulation of proline biosynthesis following cold and osmotic stresses in Arabidopsis thaliana. *Molecular and General Genetics MGG,* 254**,** 104-109.

Savouré, A., Jaoua, S., Hua, X.-J., Ardiles, W., Van Montagu, M. & Verbruggen, N. 1995. Isolation, characterization, and chromosomal location of a gene encoding the Δ 1-pyrroline-5-carboxylate synthetase in Arabidopsis thaliana. *FEBS Lett,* 372**,** 13-19.

Schäfer, E., Kunkel, T. & Frohnmeyer, H. 1997. Signal transduction in the photocontrol of chalcone synthase gene expression*. *Plant, Cell & Environment,* 20**,** 722-727.

Scheidegger, C., Frey, B. & Schroeter, B. 1997. Cellular water uptake, translocation and PSII activation during rehydration of desiccated Lobaria pulmonaria and Nephroma bellum. *Bibliotheca Lichenologica,* 67**,** 105-118.

Schluepmann, H., Van Dijken, A., Aghdasi, M., Wobbes, B., Paul, M. & Smeekens, S. 2004. Trehalose mediated growth inhibition of Arabidopsis seedlings is due to trehalose-6-phosphate accumulation. *Plant Physiology,* 135**,** 879-890.

Schuller, H.J. 2003. Transcriptional control of nonfermentative metabolism in the yeast Saccharomyces cerevisiae. . *Curr. Genet. ,* 43, 139–160.

Seki, M., Ishida, J., Narusaka, M., Fujita, M., Nanjo, T., Umezawa, T., Kamiya, A., Nakajima, M., Enju, A. & Sakurai, T. 2002a. Monitoring the expression pattern of around 7,000 Arabidopsis genes under ABA treatments using a full-length cDNA microarray. *Functional & integrative genomics,* 2**,** 282-291.

Seki, M., Narusaka, M., Abe, H., Kasuga, M., Yamaguchi-Shinozaki, K., Carninci, P., Hayashizaki, Y. & Shinozaki, K. 2001. Monitoring the expression pattern of 1300 Arabidopsis genes under drought and cold stresses by using a full-length cDNA microarray. *The Plant Cell Online,* 13**,** 61-72.

Seki, M., Narusaka, M., Ishida, J., Nanjo, T., Fujita, M., Oono, Y., Kamiya, A., Nakajima, M., Enju, A. & Sakurai, T. 2002b. Monitoring the expression profiles of 7000 Arabidopsis genes under drought, cold and high-salinity stresses using a full-length cDNA microarray. *The Plant Journal,* 31**,** 279-292.

Sharma, P., Jha, A. B., Dubey, R. S. & Pessarakli, M. 2012. Reactive Oxygen Species, Oxidative Damage, and Antioxidative Defense Mechanism in Plants under Stressful Conditions. *Journal of Botany,* 2012**,** 26.

Sheen, J., Zhou, L. & Jang, J.C. 1999. Sugars as signaling molecules. *Current Opinion in Plant Biology,* 2**,** 410-418.

Shen, W. & Hanley-Bowdoin, L. 2006. Geminivirus infection up-regulates the expression of two Arabidopsis protein kinases related to yeast SNF1-and mammalian AMPK-activating kinases. *Plant Physiology,* 142**,** 1642-1655.

Shen, W., Reyes, M. I. & Hanley-Bowdoin, L. 2009. Arabidopsis Protein Kinases GRIK1 and GRIK2 Specifically Activate SnRK1 by Phosphorylating Its Activation Loop. *Plant Physiology,* 150**,** 996-1005.

Shinkle, J. R., Atkins, A. K., Humphrey, E. E., Rodgers, C. W., Wheeler, S. L. & Barnes, P. W. 2004. Growth and morphological responses to different UV wavebands in cucumber (Cucumis sativum) and other dicotyledonous seedlings. *Physiologia Plantarum,* 120**,** 240-248.

Shinozaki, K. & Yamaguchi-Shinozaki, K. 2000. Molecular responses to dehydration and low temperature: differences and cross-talk between two stress signaling pathways. *Current Opinion in Plant Biology,* 3**,** 217-223.

Shinozaki, K. & Yamaguchi-Shinozaki, K. 2007. Gene networks involved in drought stress response and tolerance. *Journal of Experimental Botany,* 58**,** 221-227.

Shinozaki, K., Yamaguchi-Shinozaki, K. & Seki, M. 2003. Regulatory network of gene expression in the drought and cold stress responses. *Curr Opin Plant Biol,* 6**,** 410-7.

Shinwari, Z. K., Nakashima, K., Miura, S., Kasuga, M., Seki, M., Yamaguchi-Shinozaki, K. & Shinozaki, K. 1998. AnArabidopsisGene Family Encoding DRE/CRT Binding Proteins Involved in Low-Temperature-Responsive Gene Expression. *Biochem Biophys Res Commun,* 250**,** 161-170.

Shirra, M. K., Rogers, S. E., Alexander, D. E. & Arndt, K. M. 2005. The Snf1 protein kinase and Sit4 protein phosphatase have opposing functions in regulating TATA-binding protein association with the Saccharomyces cerevisiae INO1 promoter. *Genetics,* 169**,** 1957-1972.

Simpson, S. D., Nakashima, K., Narusaka, Y., Seki, M., Shinozaki, K. & Yamaguchi-Shinozaki, K. 2003. Two different novel cis-acting elements of erd1, a clpA homologous Arabidopsis gene function in induction by dehydration stress and dark-induced senescence. *The Plant Journal,* 33**,** 259-270.

Sinha, A. K., Hofmann, M. G., Römer, U., Köckenberger, W., Elling, L. & Roitsch, T. 2002. Metabolizable and non-metabolizable sugars activate different signal transduction pathways in tomato. *Plant Physiology,* 128**,** 1480-1489.

Slocombe, S. P., Laurie, S., Bertini, L., Beaudoin, F., Dickinson, J. R. & Halford, N. G. 2002. Identification of SnIP1, a novel protein that interacts with SNF1-related protein kinase (SnRK1). *Plant Molecular Biology,* 49**,** 31-44.

Smeekens, S. 2000. Sugar-induced signal transduction in plants. *Annu Rev Plant Biol,* 51**,** 49-81.

Smeekens, S., Ma, J., Hanson, J. & Rolland, F. 2010. Sugar signals and molecular networks controlling plant growth. *Current Opinion in Plant Biology,* 13**,** 273-278.

Smith, K. C. 1992. Spontaneous mutagenesis: Experimental, genetic and other factors. *Mutation Research/Reviews in Genetic Toxicology,* 277**,** 139-162.

Solanke, A. U. & Sharma, A. K. 2008. Signal transduction during cold stress in plants. *Physiology and Molecular Biology of Plants* 14**,** 69-79.

Soufi, B., Kelstrup, C. D., Stoehr, G., Fröhlich, F., Walther, T. C. & Olsen, J. V. 2009. Global analysis of the yeast osmotic stress response by quantitative proteomics. *Molecular bioSystems,* 5**,** 1337-1346.

Stapleton, A. E. & Walbot, V. 1994. Flavonoids Can Protect Maize DNA from the Induction of Ultraviolet Radiation Damage. *Plant Physiology,* 105**,** 881-889.

Steinberg, G. R. & Kemp, B. E. 2009. AMPK in Health and Disease. *Physiological Reviews,* 89**,** 1025-1078.

Steponkus, P., Uemura, M. & Webb, M. 1993. A contrast of the cryostability of the plasma membrane of winter rye and spring oat-two species that widely differ in their freezing tolerance and plasma membrane lipid composition. *Advances in low-temperature biology,* 2**,** 211-312.

Steponkus, P. & Webb, M. 1992. Freeze-induced dehydration and membrane destabilization in plants. *Water and Life.* Springer.

Stockinger, E. J., Gilmour, S. J. & Thomashow, M. F. 1997. Arabidopsis thaliana CBF1 encodes an AP2 domain-containing transcriptional activator that binds to the C-repeat/DRE, a cis-acting DNA regulatory element that stimulates transcription in response to low temperature and water deficit. *Proceedings of the National Academy of Sciences,* 94**,** 1035-1040.

Stratmann, J. 2003. Ultraviolet-B radiation co-opts defense signaling pathways. *Trends in Plant Science,* 8**,** 526-533.

Strizhov, N., Ábrahám, E., Ökrész, L., Blickling, S., Zilberstein, A., Schell, J., Koncz, C. & Szabados, L. 1997. Differential expression of two P5CS genes controlling proline accumulation during salt-stress requires ABA and is regulated by ABA1, ABI1 and AXR2 in Arabidopsis. *The Plant Journal,* 12**,** 557-569.

Struhl, K. 1996. Chromatin structure and RNA polymerase II connection: implications for transcription. *Cell,* 84**,** 179-182.

Struhl, K. 1998. Histone acetylation and transcriptional regulatory mechanisms. *Genes & Development,* 12**,** 599-606.

Sugden, C., Crawford, R. M., Halford, N. G. & Hardie, D. G. 1999. Regulation of spinach SNF1-related (SnRK1) kinases by protein kinases and phosphatases is associated with phosphorylation of the T loop and is regulated by 5′-AMP. *The Plant Journal,* 19**,** 433-439.

Suter, M., Riek, U., Tuerk, R., Schlattner, U., Wallimann, T. & Neumann, D. 2006. Dissecting the role of 5′-AMP for allosteric stimulation, activation, and deactivation of AMP-activated protein kinase. *Journal of Biological Chemistry,* 281**,** 32207-32216.

Sutherland, C. M., Hawley, S. A., Mccartney, R. R., Leech, A., Stark, M. J. R., Schmidt, M. C. & Hardie, D. G. 2003. Elm1p is one of three upstream kinases for the Saccharomyces cerevisiae SNF1 complex. *Current Biology,* 13**,** 1299-1305.

Suzuki, N. & Mittler, R. 2006. Reactive oxygen species and temperature stresses: A delicate balance between signaling and destruction. *Physiologia Plantarum,* 126**,** 45-51.

Swindell, W. R. 2006. The association among gene expression responses to nine abiotic stress treatments in Arabidopsis thaliana. *Genetics,* 174**,** 1811-1824.

Taji, T., Ohsumi, C., Iuchi, S., Seki, M., Kasuga, M., Kobayashi, M., Yamaguchi-Shinozaki, K. & Shinozaki, K. 2002. Important roles of drought-and cold-inducible genes for galactinol synthase in stress tolerance in Arabidopsis thaliana. *The Plant Journal,* 29**,** 417-426.

Takagi, Y., Calero, G., Komori, H., Brown, J. A., Ehrensberger, A. H., Hudmon, A., Asturias, F. & Kornberg, R. D. 2006. Head module control of mediator interactions. *Molecular cell,* 23**,** 355-364.

Thatcher, L. F., Manners, J. M. & Kazan, K. 2009. Fusarium oxysporum hijacks COI1-mediated jasmonate signaling to promote disease development in Arabidopsis. *The Plant Journal,* 58**,** 927-939.

Thelander, M., Olsson, T. & Ronne, H. 2004. Snf1-related protein kinase 1 is needed for growth in a normal day-night light cycle. *Embo Journal,* 23**,** 1900-1910.

Thimm, O., Bläsing, O., Gibon, Y., Nagel, A., Meyer, S., Krüger, P., Selbig, J., Müller, L. A., Rhee, S. Y. & Stitt, M. 2004. mapman: a user-driven tool to display genomics data sets onto diagrams of metabolic pathways and other biological processes. *The Plant Journal,* 37**,** 914-939.

Thomashow, M. F. 1998. Role of cold-responsive genes in plant freezing tolerance. *Plant Physiology,* 118**,** 1-8.

Thomashow, M. F. 1999. Plant cold acclimation: freezing tolerance genes and regulatory mechanisms. *Annual review of plant biology,* 50**,** 571-599.

Thomashow, M. F. 2001. So what's new in the field of plant cold acclimation? Lots! *Plant Physiology,* 125**,** 89-93.

Thompson, C. M., Koleske, A. J., Chao, D. M. & Young, R. A. 1993. A multisubunit complex associated with the RNA polymerase II CTD and TATA-binding protein in yeast. *Cell,* 73**,** 1361-1375.

Tollervey, D., Lehtonen, H., Jansen, R., Kern, H. & Hurt, E. C. 1993. Temperature-sensitive mutations demonstrate roles for yeast fibrillarin in pre-rRNA processing, pre-rRNA methylation, and ribosome assembly. *Cell,* 72**,** 443-457.

Toroser, D., Plaut, Z. & Huber, S. C. 2000. Regulation of a Plant SNF1-Related Protein Kinase by Glucose-6-Phosphate. *Plant Physiology,* 123**,** 403-412.

Tran, L.S. P., Nakashima, K., Sakuma, Y., Simpson, S. D., Fujita, Y., Maruyama, K., Fujita, M., Seki, M., Shinozaki, K. & Yamaguchi-Shinozaki, K. 2004. Isolation and Functional Analysis of Arabidopsis Stress-Inducible NAC Transcription Factors That Bind to a Drought-Responsive cis-Element in the early responsive to dehydration stress 1 Promoter. *The Plant Cell Online,* 16**,** 2481-2498.

Tuteja, N., Gill, S. S. & Tuteja, R. 2012. *Improving crop productivity in sustainable agriculture,* John Wiley & Sons.

Tuteja, N. & Sopory, S. K. 2008. Chemical signaling under abiotic stress environment in plants. *Plant signaling & behavior,* 3**,** 525-536.

Udvardi, M. K., Kakar, K., Wandrey, M., Montanari, O., Murray, J., Andriankaja, A., Zhang, J. Y., Benedito, V., Hofer, J. M. I., Chueng, F. & Town, C. D. 2007. Legume transcription factors: Global regulators of plant development and response to the environment. *Plant Physiology,* 144**,** 538-549.

Uemura, M. & Steponkus, P. L. 1997. Effect of Cold Acclimation on Membrane Lipid Composition and Freeze-Induced Membrane Destablization. *Plant cold hardiness.* Springer.

Uemura, M., Warren, G. & Steponkus, P. L. 2003. Freezing sensitivity in the sfr4 mutant of Arabidopsis is due to low sugar content and is manifested by loss of osmotic responsiveness. *Plant Physiology,* 131**,** 1800-1807.

Uetz, P., Giot, L., Cagney, G., Mansfield, T. A., Judson, R. S., Knight, J. R., Lockshon, D., Narayan, V., Srinivasan, M. & Pochart, P. 2000. A comprehensive analysis of protein–protein interactions in Saccharomyces cerevisiae. *Nature,* 403**,** 623-627.

Ulm, R. & Nagy, F. 2005. Signalling and gene regulation in response to ultraviolet light. *Current Opinion in Plant Biology,* 8**,** 477-482.

Umezawa, T., Yoshida, R., Maruyama, K., Yamaguchi-Shinozaki, K. & Shinozaki, K. 2004. SRK2C, a SNF1-related protein kinase 2, improves drought tolerance by controlling stress-responsive gene expression in Arabidopsis thaliana. *Proceedings of the National Academy of Sciences of the United States of America,* 101**,** 17306-17311.

Uno, Y., Furihata, T., Abe, H., Yoshida, R., Shinozaki, K. & Yamaguchi-Shinozaki, K. 2000. Arabidopsis basic leucine zipper transcription factors involved in an abscisic acid-dependent signal transduction pathway under drought and high-salinity conditions. *Proceedings of the National Academy of Sciences,* 97**,** 11632-11637.

Usadel, B., Bläsing, O. E., Gibon, Y., Retzlaff, K., Höhne, M., Günther, M. & Stitt, M. 2008. Global transcript levels respond to small changes of the carbon status during progressive exhaustion of carbohydrates in Arabidopsis rosettes. *Plant Physiology,* 146**,** 1834-1861.

Venu, R.C., Sreerekha, M., Madhav, M. S., Nobuta, K., Mohan, K. M., Chen, S., Jia, Y., Meyers, B. C. & Wang, G.L. 2013. Deep transcriptome sequencing reveals the expression of key functional and regulatory genes involved in the abiotic stress signaling pathways in rice. *Journal of plant biology,* 56**,** 216-231.

Verslues, P. E., Agarwal, M., Katiyar-Agarwal, S., Zhu, J. & Zhu, J. K. 2006. Methods and concepts in quantifying resistance to drought, salt and freezing, abiotic stresses that affect plant water status. *The Plant Journal,* 45**,** 523-539.

Vincent, O., Townley, R., Kuchin, S. & Carlson, M. 2001. Subcellular localization of the Snf1 kinase is regulated by specific beta subunits and a novel glucose signaling mechanism. *Genes & Development,* 15**,** 1104-1114.

Vogel, J. T., Zarka, D. G., Van Buskirk, H. A., Fowler, S. G. & Thomashow, M. F. 2005. Roles of the CBF2 and ZAT12 transcription factors in configuring the low temperature transcriptome of Arabidopsis. *The Plant Journal,* 41**,** 195-211.

Wade, H. K., Bibikova, T. N., Valentine, W. J. & Jenkins, G. I. 2001. Interactions within a network of phytochrome, cryptochrome and UV-B phototransduction pathways regulate chalcone synthase gene expression in Arabidopsis leaf tissue. *The Plant Journal,* 25**,** 675-685.

Wang, W. & Chen, X. 2004. HUA ENHANCER3 reveals a role for a cyclin-dependent protein kinase in the specification of floral organ identity in Arabidopsis. *Development,* 131**,** 3147-3156.

Wang, W., Vinocur, B. & Altman, A. 2003. Plant responses to drought, salinity and extreme temperatures: towards genetic engineering for stress tolerance. *Planta,* 218**,** 1-14.

Warren, G., Mckown, R., Marin, A. & Teutonico, R. 1996. Isolation of mutations affecting the development of freezing tolerance in Arabidopsis thaliana (L) Heynh. *Plant Physiology,* 111**,** 1011-1019.

Wathugala, D. L., Hemsley, P. A., Moffat, C. S., Cremelie, P., Knight, M. R. & Knight, H. 2012. The Mediator subunit SFR6/MED16 controls defence gene expression mediated by salicylic acid and jasmonate responsive pathways. *New Phytologist,* 195**,** 217-230.

Wathugala, D. L., Richards, S. A., Knight, H. & Knight, M. R. 2011. OsSFR6 is a functional rice orthologue of SENSITIVE TO FREEZING-6 and can act as a regulator of COR gene expression, osmotic stress and freezing tolerance in Arabidopsis. *New Phytologist,* 191**,** 984-995.

Welters, P., Takegawa, K., Emr, S. D. & Chrispeels, M. J. 1994. AtVPS34, a phosphatidylinositol 3-kinase of Arabidopsis thaliana, is an essential protein with homology to a calcium-dependent lipid binding domain. *Proceedings of the National Academy of Sciences,* 91**,** 11398-11402.

Weltmeier, F., Rahmani, F., Ehlert, A., Dietrich, K., Schütze, K., Wang, X., Chaban, C., Hanson, J., Teige, M. & Harter, K. 2009. Expression patterns within the Arabidopsis C/S1 bZIP transcription factor network: availability of heterodimerization partners controls gene expression during stress response and development. *Plant Molecular Biology,* 69**,** 107-119.

Wery, J., Silim, S. N., Knights, E. J., Malhotra, R. S. & Cousin, R. 1993. Screening techniques and sources of tolerance to extremes of moisture and air temperature in cool season food legumes. *Euphytica,* 73**,** 73-83.

White, R. J. 2004. RNA polymerase III transcription and cancer. *Oncogene,* 23**,** 3208-3216.

Wiese, A., Elzinga, N., Wobbes, B. & Smeekens, S. 2005. Sucrose-induced translational repression of plant bZIP-type transcription factors. *Biochem Soc Trans,* 33**,** 272-275.

Wingler, A. & Roitsch, T. 2008. Metabolic regulation of leaf senescence: interactions of sugar signalling with biotic and abiotic stress responses. *Plant Biology,* 10**,** 50-62.

Wojtaszek, P. 1997. Oxidative burst: an early plant response to pathogen infection. *Biochem. J.,* 322**,** 681-692.

Woods, A., Dickerson, K., Heath, R., Hong, S. P., Momcilovic, M., Johnstone, S. R., Carlson, M. & Carling, D. 2005. Ca2+/calmodulin-dependent protein kinase kinase-beta acts upstream of AMP-activated protein kinase in mammalian cells. *Cell Metab,* 2**,** 21-33.

Woods, A., Johnstone, S. R., Dickerson, K., Leiper, F. C., Fryer, L. G., Neumann, D., Schlattner, U., Wallimann, T., Carlson, M. & Carling, D. 2003a. LKB1 is the upstream kinase in the AMP-activated protein kinase cascade. *Curr Biol,* 13**,** 2004-8.

Woods, A., Vertommen, D., Neumann, D., Turk, R., Bayliss, J., Schlattner, U., Wallimann, T., Carling, D. & Rider, M. H. 2003b. Identification of phosphorylation sites in AMP-activated protein kinase (AMPK) for upstream AMPK kinases and study of their roles by site-directed mutagenesis. *J Biol Chem,* 278**,** 28434-42.

Wu, Y., Deng, Z., Lai, J., Zhang, Y., Yang, C., Yin, B., Zhao, Q., Zhang, L., Li, Y. & Yang, C. 2009. Dual function of Arabidopsis ATAF1 in abiotic and biotic stress responses. *Cell research,* 19**,** 1279-1290.

Xiao, W., Sheen, J. & Jang, J.C. 2000. The role of hexokinase in plant sugar signal transduction and growth and development. *Plant Molecular Biology,* 44**,** 451-461.

Xu, R. & Li, Y. 2011. Control of final organ size by Mediator complex subunit 25 in Arabidopsis thaliana. *Development,* 138**,** 4545-4554.

Xu, S., Li, J., Zhang, X., Wei, H. & Cui, L. 2006. Effects of heat acclimation pretreatment on changes of membrane lipid peroxidation, antioxidant metabolites, and ultrastructure of chloroplasts in two cool-season turfgrass species under heat stress. *Environmental and Experimental Botany,* 56**,** 274-285.

Yamaguchi-Shinozaki, K. & Shinozaki, K. 1994. A Novel Cis-Acting Element in an Arabidopsis Gene Is Involved in Responsiveness to Drought, Low-Temperature, or High-Salt Stress. *Plant Cell,* 6**,** 251-264.

Yamaguchi-Shinozaki, K. & Shinozaki, K. 2005. Organization of< i> cis</i>-acting regulatory elements in osmotic-and cold-stress-responsive promoters. *Trends Plant Sci,* 10**,** 88-94.

Yang, Y., Ou, B., Zhang, J., Si, W., Gu, H., Qin, G. & Qu, L. J. 2014. The Arabidopsis Mediator subunit MED16 regulates iron homeostasis by associating with EIN3/EIL1 through subunit MED25. *The Plant Journal,* 77**,** 838-851.

Yordanov, I., Velikova, V. & Tsonev, T. 2000. Plant responses to drought, acclimation, and stress tolerance. *Photosynthetica,* 38**,** 171-186.

Young-Hee Cho, Jung-Woo Hong, Eun-Chul Kim & Yoo, S.D. 2012. Regulatory Functions of SnRK1 in Stress-Responsive Gene Expression and in Plant Growth and Development. *Plant Physiology* 158**,** 1955–1964.

Young, E. T., Dombek, K. M., Tachibana, C. & Ideker, T. 2003. Multiple pathways are co-regulated by the protein kinase Snf1 and the transcription factors Adr1 and Cat8. *Journal of Biological Chemistry,* 278**,** 26146-26158.

Young, E. T., Yen, K., Dombek, K. M., Law, G. L., Chang, E. & Arms, E. 2009. Snf1-independent, glucose-resistant transcription of Adr1-dependent genes in a mediator mutant of Saccharomyces cerevisiae. *Molecular microbiology,* 74**,** 364-383.

Yu, S.M. 1999. Cellular and genetic responses of plants to sugar starvation. *Plant Physiology,* 121**,** 687-693.

Yudkovsky, N., Ranish, J. A. & Hahn, S. 2000. A transcription reinitiation intermediate that is stabilized by activator. *Nature,* 408**,** 225-229.

Zarka, D. G., Vogel, J. T., Cook, D. & Thomashow, M. F. 2003. Cold induction of Arabidopsis CBF genes involves multiple ICE (inducer of CBF expression) promoter elements and a cold-regulatory circuit that is desensitized by low temperature. *Plant Physiology,* 133**,** 910-918.

Zhang, F., Sumibcay, L., Hinnebusch, A. G. & Swanson, M. J. 2004a. A triad of subunits from the Gal11/tail domain of Srb mediator is an in vivo target of transcriptional activator Gcn4p. *Mol Cell Biol,* 24**,** 6871-6886.

Zhang, X., Fowler, S. G., Cheng, H., Lou, Y., Rhee, S. Y., Stockinger, E. J. & Thomashow, M. F. 2004b. Freezing-sensitive tomato has a functional CBF cold response pathway, but a CBF regulon that differs from that of freezing-tolerant Arabidopsis. *The Plant Journal,* 39**,** 905-919.

Zhang, X., Wang, C., Zhang, Y., Sun, Y. & Mou, Z. 2012. The Arabidopsis mediator complex subunit16 positively regulates salicylate-mediated systemic acquired resistance and jasmonate/ethylene-induced defense pathways. *The Plant Cell Online,* 24**,** 4294-4309.

Zhang, X., Yao, J., Zhang, Y., Sun, Y. & Mou, Z. 2013. The Arabidopsis Mediator complex subunits MED14/SWP and MED16/SFR6/IEN1 differentially regulate defense gene expression in plant immune responses. *The Plant Journal,* 75**,** 484-497.

Zhang, Y., Primavesi, L. F., Jhurreea, D., Andralojc, P. J., Mitchell, R. A., Powers, S. J., Schluepmann, H., Delatte, T., Wingler, A. & Paul, M. J. 2009. Inhibition of SNF1-related protein kinase1 activity and regulation of metabolic pathways by trehalose-6-phosphate. *Plant Physiology,* 149**,** 1860-1871.

Zhang, Y., Wu, H., Wang, N., Fan, H., Chen, C., Cui, Y., Liu, H. & Ling, H. Q. 2014. Mediator subunit 16 functions in the regulation of iron uptake gene expression in Arabidopsis. *New Phytologist*.

Zhang, Y. H., Shewry, P. R., Jones, H., Barcelo, P., Lazzeri, P. A. & Halford, N. G. 2001. Expression of antisense SnRK1 protein kinase sequence causes abnormal pollen development and male sterility in transgenic barley. *Plant Journal,* 28**,** 431-441.

Zhu, J.K. 2002. Salt and drought stress signal transduction in plants. *Annu Rev Plant Biol,* 53**,** 247.

Zhu, X., Zhang, Y., Bjornsdottir, G., Liu, Z., Quan, A., Costanzo, M., López, M. D., Westholm, J. O., Ronne, H. & Boone, C. 2011. Histone modifications influence mediator interactions with chromatin. *Nucleic Acids Research,* 39**,** 8342-8354.

Appendix 1

Media and Solutions

A1.1 10x TBE buffer

9.3 g EDTA

55 g Boric acid

108 g Tris base

Dissolved in 1 L of distilled water

A1.2 10 x Blue DNA sample loading buffer

0.025 g Xylene cyanol

0.025 g Bromophenol blue

1.25 ml 10 % SDS

1.25 ml Glycerol

Dissolve in 6.25 ml of distilled water

A1.3 1xTE buffer

Add the following to 990 ml distilled water

400 µl 0.25 M EDTA

10 ml 1M Tris-HCl (pH 8.0)

A1.4 Edwards' extraction buffer

1 ml 1M Tris-HCl (pH 7.5)

0.25 ml 0.5 M EDTA (pH 8.0)

1.5 ml 1 M NaCl

0.25 ml 10 % SDS

Add 2.25 ml to make up to 5 ml

A1.5 STET buffer

4.0 g Sucrose

2.5 ml of Triton X-100

200 µl of 0.25 M EDTA

2.5 ml of 1 M Tris-HCl

50 µl of 20 % Sodium Azide

Dissolved in 50 ml of water

A1.6 TER buffer

Add RNAse A to 1×TE to a concentration of 10 µg/ml

A1.7 Protein extraction buffer

150 mM Tris-HCl pH 7.5

150 mM NaCl

10% Glycerol

10 mM EDTA

1 mM Sodium molybdate

1 mM NaF

Freshly add 10 mM DTT; 0.5% (w/v) PVPP; 1% (v/v) protease inhibitor cocktail (Sigma); 1% (v/v) NP-40

A1.8 2x SDS gel loading buffer

0.125 M Tris-HCl pH 6.8

4% SDS

10% β-Mercaptoethanol

20% Glycerol

20 mg Bromophenol blue

A1.9 Resolving/Separating Buffer

1.5 M Tris-HCl pH 8.8

0.384% SDS

A1.10 Resolving/Separating gel (one gel)

3.33 ml of 30% Acrylamide

2.6 ml of Resolving buffer

4.1 ml distilled water

100 µl 10% Ammonium persulphate (APS)

10 µl of TEMED

A1.11 Stacking Buffer

0.5 M Tris-HCl pH 6.8

0.4% SDS

A1.12 Stacking Gel

0.65 ml of 30% Acrylamide

1.25 ml of Stacking buffer

3 ml distilled water

25 µl 10% Ammonium persulphate (APS)

5 µl of TEMED

A1.13 10x SDS Running buffer

0.25 M Tris-HCl

1.92 M Glycine

1% SDS

1 L distilled water

A1.14 Cold Transfer Buffer (2 L)

10 mM $NaHCO_3$

3 mM Na_2CO_3

A1.15 20% Methanol based transfer buffer (1 L)

3 g Tris base

14.5 g Glycine

200 ml Methanol

0.3 ml Conc. HCL

1 L distilled water

A1.16 20x TBS Buffer pH 6.8 (1L)

48.4 g Tris-HCl

175.4 g NaCl

1 L distilled water

A1.17 TBS-T Buffer

1 L of TBS buffer with 1 ml of Tween-20

A1.18 ECL Solution I (Enhanced Chemiluminescent I)

1 ml Luminol (3-Aminophthal hydrazide)

0.44 ml Coumaric acid

10 ml of 1M Tris-HCl (pH 8.5)

volume up to 100 ml with distilled water

A1.19 ECL Solution II (Enhanced Chemiluminescent II)

64 µl of 30% H_2O_2

10 ml of 1M Tris-HCl (pH 8.5)

volume up to 100 ml with distilled water and wrapped in Al foil before stored at 4^oC

A1.20 Stripping Solution

15 g Glycine

1 g SDS

10 ml Tween-20

Adjust pH up to 2.2 and volume up to 1L

A1.21 Fixative solution

40% Methanol

10% Acetic acid

50% distilled water

A1.22 Hypo- Solution

0.5 g Sodium thiosulphate

17 g Sodium Acetate

75 ml Methanol

Volume up to 250 ml in distilled water

A1.23 Silver Staining Solution

0.625 g Silver nitrate in 250 ml of water

A1.24 Developing Solution

Dissolve 6.25 g Na_2CO_3 in 250 ml of distilled water and add 100 µl of 37% formaldehyde just before use.

A1.25 Stop Solution

3.65 g EDTA in 250 ml of distilled water

Appendix 2

Oligonucleotides (Primers)

A2.1 Oligonucleotides used for the study

Primer Name	Primer Sequence (5' to 3')	Description
HK1	CACCATGAATCAGCAAAACCC	Used to create SFR6 truncation with beginning of the protein (SF1)
HK2	CACCATGGAGGTGACCCCTGGCCCTGGA	Used to create SFR6 truncation beginning with SF2
HK3	CACCATGCTTCCGCGTAACCAATCAAAGG	Used to create SFR6 truncation beginning with SF3
HK4	CTAGGAGTTTGTCGTAGCAGTAG	Reverse primer used to create SF14 truncation
HK5	CTACCCGGAATCCCTGGGCGTCC	Reverse primer used to create SF15 truncation
HK6	CTATACAACACGGACCCACGTTCC	Reverse primer used to create SF16 truncation
HK1R	CTGTAGCCGGACTCACAGG	Used to amplify SF14, SF15 and SF16 to detect transgene in PCR with pB7WG2-F
HK2R	GCAGACTGAGCTGCAGCCTC	Used to amplify SF24 and SF25 to detect transgene in PCR with pB7WG2-F
HK3 Rev	TGCGGGTGCAGCAATTGC	Used to amplify SF36 to detect transgene in PCR with pB7WG2-F
HK1 Rev.RT	CGATGATTCCTCCACCACCGC	Used to quantify level of expression of SF14, SF15 and SF16 transgenes with GWOE trans -F primer
HK2 Rev.RT	GGTGGCACACGACTGCCTG	Used to quantify level of expression of SF24 and SF25 transgenes with GWOE trans -F primer
HK3 Rev.RT	CATCCCACCAATCAAC	Used to quantify level of expression of SF36 transgenes with GWOE trans -F primer
GWOE trans -F	GCAGGCTCCGCGGCCGCCCC	Used to quantify level of expression of SF transgenes with above three forward primers
pB7WG2- F	GAAACCTCCTCGGATTCCAT	Used to detect transgenes of SF1-6 in genomic DNA extracted from plants
BASTA -F	GAAGTCCAGCTGCCAGAAAC	To detect basta resistance marker in transgenic lines of SF1-6 in genomic DNA extracted from plants
BASTA -R	TCGAGGGGATCTACCATGAG	
HisHA forward	CACCATCACCATTACCCATACG	To detect tag used in creating the

		overexpressing lines of KIN10
Kin10 Rev b	GCCCGAAATTACCTCTGGAGCGG	Used to detect transgene of KIN10 with HisHA forward primer
KIN10 mid F	GAAGATAAAGGGAGGGATATACA	Used to quantify transcript of *KIN10* from the middle part of the protein
KIN10 mid R	TCGTTTCATGGGGTCAACT	
KIN10 PCR F (new)	CTTACCGACTGTCTTCCAG	Used to detect wild type KIN10 transcript
Kin10 end Rev	TCAGAGGACTCGGAGCTGAGC	
AK10-GABIa	CCAGCATAATAGAGAACGAAGC	Used to detect of KIN10
AK10-GABIb	GTCCGGTTTAGTATTCAGAGG	Used to detect G*abi* inset in *kin10-2* mutant background
O8409 LB	ATATTGACCATCATACTCATTGC	
KIN10-Rt-FOR	TGCAGAGAGTACAAGGTCCTCA	Used to quantify transcript of *KIN10* from the end of the protein
KIN10-Rt-Rev (new)	GATTATTCTTGAAGAGGTCCGG	
LTI65-RT-For	CACGGCGCACCAGTGTATGAATCC	Used to quantify transcript of *LTI65*
LTI65-RT-Rev	GGCTCAATGGGTTTGGTGTGG	
P5CS1 Rt For (new)	CGTCGTTAAGGTTGGGACAGCAG	Used to quantify transcript of *P5CS1*
P5CS1 Rt Rev (new)	CCATCCGAGTTTAATTCCGC	
KIN2-F	CAACAGGCGGGAAAGAGTAT	Used to quantify transcript of *KIN2*
KIN2-R	CAACAACAAGTACGATGAGTACGA	
PR1-F	CATCCTGCATATGATGCTCCT	Used to quantify transcript of *PR1*
PR1-R	TCGTGGGAATTATGTGAACG	
At4g26410 F	CTCGTTCCCTCCGTGAAAAT	Used as endogenous control to quantify transcript of *PR1*
At4g26410 R	TGAAGAAAGCATTCTCATAGGTCTT	
DIN6 -F	GGCCAAGAGAGTTCGTGTTC	Used to quantify transcript of *DIN6*
DIN6-R	AGACGTTGATGGGCCAAGTA	
PEX-F	TCATAGCATTGATGGCTCATCCT	Used as endogenous control to quantify transcript of many genes except *PR1* in this study
PEX-R	ACCCTCTCACATCACCAGATCTTAG	
SFR6- mid F	AAGCCCAATCAGTGGTTCAC	Used to quantify transcript of *SFR6* from the middle part of the protein
SFR6- mid R	AGACCGCTGGAGAAAACAGA	
BCAT2 F	CGCAAAACTCTGGTTCTACCTC	Used to quantify transcript of *BCAT2*

BCAT2 R	GATGCAGCTTGTGCGTTGTA	

Applied Biosystems probe identifier SNP492-SNP1 (TaqMan probe) was used for genotyping for single nucleotide polymorphism (SNP) genotyping assay of *sfr6-1*

For primer: CGTATGATCCAGATGAAGGTCCTT

Rev primer GCAGTACAACAGGTTGAACACTTGA

Reporter sequence 1 CACGG CTGGAGAGTA (wild type version linked to VIC reporter dye)

Reporter sequence 2 CACAGGCTGAAGAGTA (mutant version with base substitution at SNP, linked to reporter dye FAM)

A2.2 Map of the primers used for SFR6 sequence (AT4G04920.1)


ATCACAGGCTGGAGAGTACAGCGCTGGGAATCAAGTGTTCAACCTGTTGTACTGCATCAGATATTTGG
AAACCCAACTTCAAATTTTGGAGGACAGGTCCCCACGCAAACTGTCTGGGTATCCAGAGTGGATATGA
GCATACCACCTACTAAAGATTTTAAGAATCATCAAGTAGCTGCAGCAGGACCAAGTGTGGATGCACCA
AAGGAGCCTGATTCTGGTGATGAGAAGGCTAACAAGGTTGTATTTGATCCTTTTGATTTGCCAAGTGA
TATTCGGA
CACTTGCACGGATTGTCTATTCTGCTCATGGTGGTGAAATTGCGATTGCTTTTCTTCGTGGTGGAGTT
CATATCTTTTCTGGTCCAACTTTTTCACCTGTTGAAAACTATCAAATAAATGTTGGATCTGCAATTGC
TGCACCCGCATTTTCACCAACAAGCTGTTGTTCGGCTTCTGTATGGCATGATGCTGCTAAGGACTGCG
CAATGT
HK3b-F
TGAAAATCATCCGTGTTCTTCCTCCTGCTCTTCCGCGTAACCAATCAAAGGTTGATCAATCAACATGG
GAGCGGGCGATCGCTGAGAGgtatgtaatctctggtatatattttctagcttgtctgcttgcaaagga
acttatattgtgacttgagatatgaatctgcattctttcttaacagATTCTGGTGGAGTCTTTTGGTC
GGAGTT
HK3b Rev.RT
GATTGGTGGGATGCAGTTGGCTGCACACAGAGTGCTGCAGAGGATGGGATAGgtatactttagtgcta
agtttcttgatttaagtgttatttaatatctgcagttggatttttttgggtctttagttgtggaacaa
ccactggaattagttttgcttagaaatatgacagtttgtattttagtttgggaataagttctagtttt
taaaggctgagtgtcattcaaagaacctttttctctgtttttctattttgcttttatactaaggtttga
atgatagaaactttgaatgatagtggttcaaatattatattgtattgtttgaataatatactgcttaa
agcattggatgatgtatttctttttatgattacagTTTCATTGAACAGCGTGATTGCTGTCATGGATG
CTGATTTTCACT
HK3b-R
CCCTTCCTTCAACACAGCACAGACAACAATATGGCCCTgtatgtttttactcaacccgaatccaactc
attatctttttccttttttaaatgtctgaactgtttgcgttgcggtaccgtttattatgtctttgcaaa
atatttatatatatatatatttttttttctggttttataatgtaaagcttctctattccatgagca
tgcaga
acctattttgtgttgttcttttatcggactataagatagtgtagctttctctaatttaaaaaaagaaa
gaaaaaaggaacaaacttcatctgactttagattatttgagtagccaatatacaatgcatctgattga
ctgattctaagacgctgaacaaaatcttggcagtctattgccccccttgagattcttcgtgttttttt
gctttttttccttttttggttggttgcgcttttttggtaaagaacttgtatttttatggtttacagAACCT
AGATAGGATCAAATGTCGGTTACTTGAAGGAACCAATGCTCAAGAGGTTCGTGCCATGGTTTTAGATA
TGCAAGCAAGGTTGTTGTTGGACATGCTTGGAAAAGGTATTGAATCAGCTCTTGTGAATCCTTCGGCG
TTGGTTTTTGAGCCATGGCGAGTAGATGGGGAGACAATAACAGGCATCAATCCGGAGGCAATGGCTGT
TGATCCTGCTCTTGTTTCCAGTATTCAGgtatcttgatgccttcaaatctgaggataaagttgtaggt
tttctttgatgaaagatgaaaattcaggctcaaaccctgggaacggttcatgcagtgttttcatttaa
agagtagttgctctttgctgatatatcttagtttttacttttaataatcagccaacacatgctgtatt
agatttggttatttagcacagcttaagacattttagatcatattgtgacattgcatattctatcatgg
atctcatatcattgtatatgaaacagaccatatcactatccttttacaagtttggtttcctgttgcag
atttttctgtactctaattccttttccgcttcatttacagGCTTATGTGGATGCTGTTCTTGATCTTG
CTTCTCATTTCATCACACGTTTAAGGCGTTATGCGAGTTTTTGTCGGACTCTTGCAAGCCATGCTGCT
TCTGCTGGAACTGGCAGTAATCGCAACAATGTTACCAGTCCCACACAAAATGCATCATCTCCTGCAAC
ACCTCAGGgtcagtatactattgattttgtcatacctaatttactccagcatgacaacaagggctttg
aatggtacatagcgacaaaaaatttcattcccttgtcattcggtgatgatacgaagcacttgtttggt
cctagatttattgaatatgagatgagtttcttaagtctagatattcttcatctctgtgaactatagcg
tattgtccagctctttttccacgtagattatgggagatacaactggttatatttgttgttgggcttg
gcatctctcttgtaggggtgcaattgggggatatttcaactcttttatgtacagTTTTTCCTGACAAG
TCACTGTATCTTGCAGTAGGTCAACCTACTACTACTACTA
HK4-R
CTACTACTGCTACGACAAACTCCAGCGGAAGCTCACATGTGCAAGCTTGGATGCAGGGGGCCATAGCG
AAAATTAGTAGCTCGAATGATGGATCCAACTCTACTGCAAGCCCAATCAGTGGTTCACCTACCTTCAT
GCCAATAAGCATCAATACAGGAACATTTCCAGGAACACCTGCTGTTCGGCTCATTGGGGATTGTCATT
TCCTTCATCGGTTATGCCAGCTGTTGCTCTTCTGTTTTCTCCAGCGGTCTTCACGATTTCCACAGCGA
AATGCTGATGTTAGTTCACAAAAACTTCAAACGGGGGCTACCAGCAAATTGGAAGAAGTCAACTCTGC
TAAACCAACC
HK5-R

CCTGCCTTGAACAGGATAGAGGACGCCCAGGGATTCCGGGGTGCCCAGTTGGGTACTGGAGTGAAAGG
GATTGATGAAAATTCTGCTCGTACAACAAAGATGGGTTCTGGGAATGCCGGTCAAGGATATACTTATG

AGGAGgttggcacctatattcctgtgtcctctttattttgatacaattatctgtggaacccttttgtt
gttacctcaagaatagaggcttaggcttaatctggtcaatatgggtaagaataatgggaacccttggt
aggttggggaaaaatatgatagactttgtagattttgaaacgaagaaagcaatgccatctttgatggt
acaataatct
agaaaatttcttataatgactggatactttctgatcttccagGTGAGAGTTCTTTTCCATATACTAAT
GGATCTCTGCAAGCGAACATCTGGTCTTGCGCATCCCTTACCTGGCTCTCAGGTAGGTAGTGGAAACA
TTCAAGTTCGACTGCATTATATTGATGGAAATTACACTGTGTTACCCGAGGTGGTAGAAGCGGCTCTT
GGACCACATATGCAGgtaatctgtgtttatagtaaagtagtgaaactatttttttcaattgttcttgtt
agtgatatttggtcaagtacattatgaaataatatcttgtgatctatattctcataagataatttgtt
gtaaaaactg
aattaacagAACATGCCTCGCCCAAGAGGAGCTGATGCTGCTGGTCTTCTACTTCGGGAGTTAGAGCT
TCATCCGCCTTCCGAAGAATGGCATAGAAGAAATTTATTTGGTGGTCCCGGGTCAGAGCCTGAGGATA
TGATCTTGACAGACGATGTTTCCAAGCTGAGTAATTCCTTAGATCTGCCTGATACAAACTTTTCCGGA
ATATGTGATGGATACAACAGAGTCCATAGTCTTTGGCCAAGAAAACGCAGGATGTCTGAAAGAGATGC
AGCTTTTGGTTCAAATACTTCTGTGGGTTTGGGTGCATATCTTGGGATCATGGGTTCTCGTAGGGATG
TTGTGACCGCGACATGGAAAACTGGTCTTGAAGGAGTTTGGTACAAGgttggttacgctcatacattt
cccttaacatttctttattgttgtaatgtgataaagaagtaaaaagttcttctgtcacaccttagtaa
catgattgactttcttattgcagTGCATAAGATGCCTAAGGCAGACATCTGCATTTGCTTCACCAGGT
GCCACTAAGCAGCCAAATCCGAATGAACGAGAAACCTGGTGGACAAGTCGTTGGGTTTATTGCTGCCC
CATGTGTGGTGGAACGTG
HK6-R ←
GGTCCGTGTTGTATAGgcgaacaaatgaacttcccatctactatattggtattggatcgaatagccag
aaaatcagtgattttgaggagcaaagagtgcaaaccaaacacacttctgcaagtttattctgttactt
ctaatccttattcccggactggtgtgatctaacccctgtccaatatggaaatcttgaatggaactggg
agggagacagtgtctgcaaagattcaagacacggtgtagtgaaacaggtcttggtgtatagcgattta
ttagacttatggtctatagagtttacttcttgtggaatgtaaaactctttcaggctgcaacatcattt
tttaaatttctttaaagggctgtaacctttaacttaagtggtgtagtaaagactctagaagtcatggt
ggtgatgatgtaagggcccattggtaaagaccgttatggactttgaccgtagaaattttggttgtaga
gaatttgactataaagattttaagtttaaaaactttggccatgattggtaactaaaaagtaaaaactt
tagaaactgtt

Yellow colour highlighted areas denote primers used for DNA amplification and green colour highlighted areas denoted the primers used for real-time analysis. Arrows indicate the primer orientation. Orange text colour in uppercase represents the introns of the SFR6 nucleotide and blue colour text in lower case represents exons of SFR6 nucleotide.

A2.3 Map of the primers used for KIN10 (AT3G01090.2)

actttttcagctcagaaaatttgggacttttttttgctgcatttttttggttccgaattttctcctcc
gccttttttaatttttggtaagtttcgatatctctcaattttcttatttcggaaataaaaaaaattct
cgccctttttgcaaatcaatggattgatcttgaaatcgtcatttctgaatcgggtacgagagatccagt

aatcctctgcgattgaattattattagggttcatattccgaattggggatagtctgaaaattgctatt
ttaagctctcttcttagtgttggttggtttattctggataataaaagggatcctaattctcgctaaat
tctcATGTTCAAACGAGTAGATGAGTTTAATTTAGTTTCTTCAACGATCGATCACAGAATCTTCAAAA
GTgtaaaaattacttgctttttgttcctattactctttgcagtttgttttgtgtgttgtgtactagt
agatctaatatctctctctttttttgtagAGAATGGATGGATCAGGCACAGGCAGTAGAAGTGGGG
TAGAATCGATTCTACCAAATTACAAGCTTGGGAGAACTCTTGGTATTGGTTCCTTTGGTAGGGTGAAG
ATAGCTGAGCATGCATTGACAGGACATAAGGTTGCTATCAAGATCCTCAATCGTCGCAAAATCAAGAA
CATGGAGATGGAGGAGAAAGgtacaagttttgttttgtgtatccattccaccttagttgtgacttcac
ggtactcttggaatatataaatatatagcttctttttcgtcttccttcctttgaacttatttggtctt
tgatgcagTGAGGAGAGAGATCAAAATCTTGAGACTATTTATGCATCCTCACATCATCCGTCTCTATG
AGGTTATAGAGACTCCCACAGATATTTATCTTGTCATGGAGTATGTGAACTCTGGTGAGCTATTTGAC
TATATTGTTGAGAAGGGTAGATTGCAGGAGGATGAGGCGAGGAACTTTTTTCAGCAGgtatgttttta
ttttattttatcaacatgtaactttccaagcaaccattcgattttatattatatttgagagttaagaa
ttagctacttggctttgatgtagATAATATCAGGAGTGGAATACTGCCATCGAAACATGGTGGTTCAC
AGAGACCTCAAGCCTGAAAACTTGCTTTTGGACTCTAAATGCAATGTAAAGATTGCTGATTTTGGCCT
GAGCAACATAATGCGAGATGGTCATTTTTTGAAGAC

Kin10 Rev b

AAGTTGTGGAAGTCCAAATTATG**CCGCTCCAGAG**gtaagtgcttcagccctcaggtatctgaggaata
ct

Kin10 Rev b ←

ataattaggcttgtttcaaatgataggttatagtcgagatctataaattgtttcag**GTAATTTCGGGC**
AAGTTATATGCTGGCCCTGAAGTAGATGTCTGGAGCTGTGGTGTGATACTCTACGCTCTTCTCTGTGG
GACG

→ **Kin10 mid F**

CTTCCATTTGATGATGAAAACATTCCCAACCTTTTTAA**GAAGATAAAG**gtacattctattactcctcc
tctttcgtctatttgaactaatgcttgaatttttatttttattttcgtatcacccttcgactgtaac
cttt

Kin10 mid F

ttttttctcttttcgtcctatag**GGAGGGATATACA**CATTACCTAGCCATTTATCTCCTGGTGCTAG
AG

Kin10 mid R ←

ATTTGATCCCCCGGATGCTTGT**AGTTGACCCCATGAAACGA**GTAACCATCCCTGAGATCCGGCAACAC
CCTTGGTTCCAAGCTCATCTTCCGAGGTATTTAGCTGTTCCTCCTCCAGATACTGTGCAACAGGCAAA
AAAGgtaagcctaacgtatctactcttattttcattagagaaatctctattcccatttttcgataaag
gcgtaaaagcgctgtcttcatttgtagATTGACGAGGAGATTCTCCAAGAAGTTATCAATATGGGATT
TGACAGAAACCACCTCATCGAATCGCTCCGCAACCGAACCCAGAATGATgtatgtgtttcccacccac
ttgttctttt

→ **KIN10 PCR F**

(new)

gctgtttctttcatttcaaagattaaaaaaaattccatcaaaagatcttaaatactgtatt**cttaccg**
actgtcttccagGGCACTGTGACGTACTATCTGATACTGGACAATCGTTTCCGTGCCTCTAGTGGTTA
TCTCGGGGCTGAGTTTCAAGAGACCATGgttagtctttttgtccttttcgactttagcaaaagatct
ttgacgtaatgcttcattgtttgatttaatcagGAAGGTACTCCCCGTATGCATCCAGCAGAAAGCGT
TGCTTCACCTGTTAGCCATCGGCTTCCAGGACTGATGGAATATCAAGGAGTTGGCTTGAGATCTCAAT
ACCCTGTTGAGAGAAAATGGGCTCTTGGACTTCAGgttttgatattttctgtatttatggtataaaga
cttcagcttttgatatatatgtgattaatattgtaacaatttgatcgcacagTCTCGGGCTCATCCCC
GTGAAATAATGACGGAAGTCCTGAAAGCCCTGCAAGATTTGAATGTATGTTGGAAGAAGATAGGGCAC
TACAACATGAAGTGCAGATGGGTTCCTAACAGCAGCGCAGATGGTATGCTCAGTAACTCGATGCACGA
TAACAACTACTTTGGAGA

→ **AK10-GABIa(AKIN10 F)**

CGAGT**CCAGCATAATAGAGAACGAAGCA**GCTGTTAAGTCGCCCAATGTTGTCAAGTTTGAAATTCAGg
taaatcctcttctccacttcatgatacatatcggtttcccgtacgacattgtttctgatgtgtgattt
cgagtgaaagaaagctttgtgtattagtgtccatggccatttttgtaactgaattagaactagagtga
atcttc
atgaatctaactatcaatcaatattttctgggcttgatgacgtttgttattgttgatggtgaaacagT
TG

→ **KIN10-Rt-For**

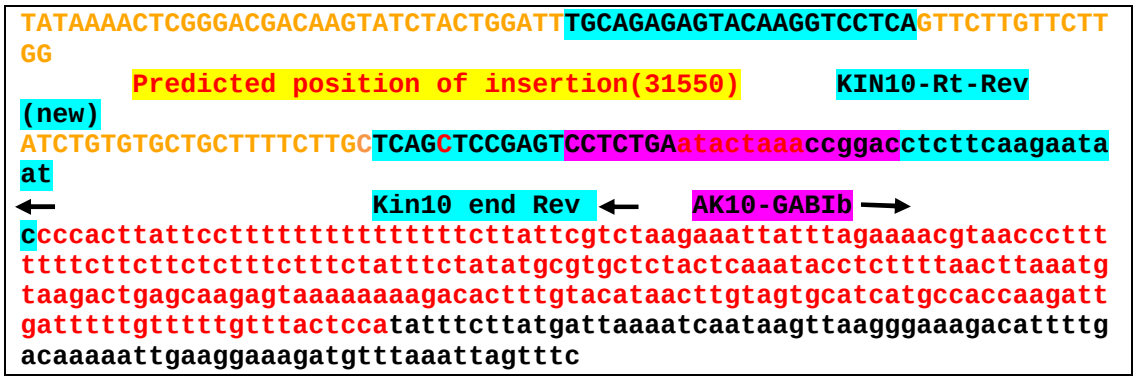

Blue and purple colour highlighted areas denote primers used for DNA amplification and real-time analysis. Arrows indicate the primer orientation. Orange text colour in uppercase represents the introns of the KIN10 nucleotide and blue colour text in lower case represents exons of KIN10 nucleotide.

A2.4 Chromatograms of homozygous lines of *sfr6-1*

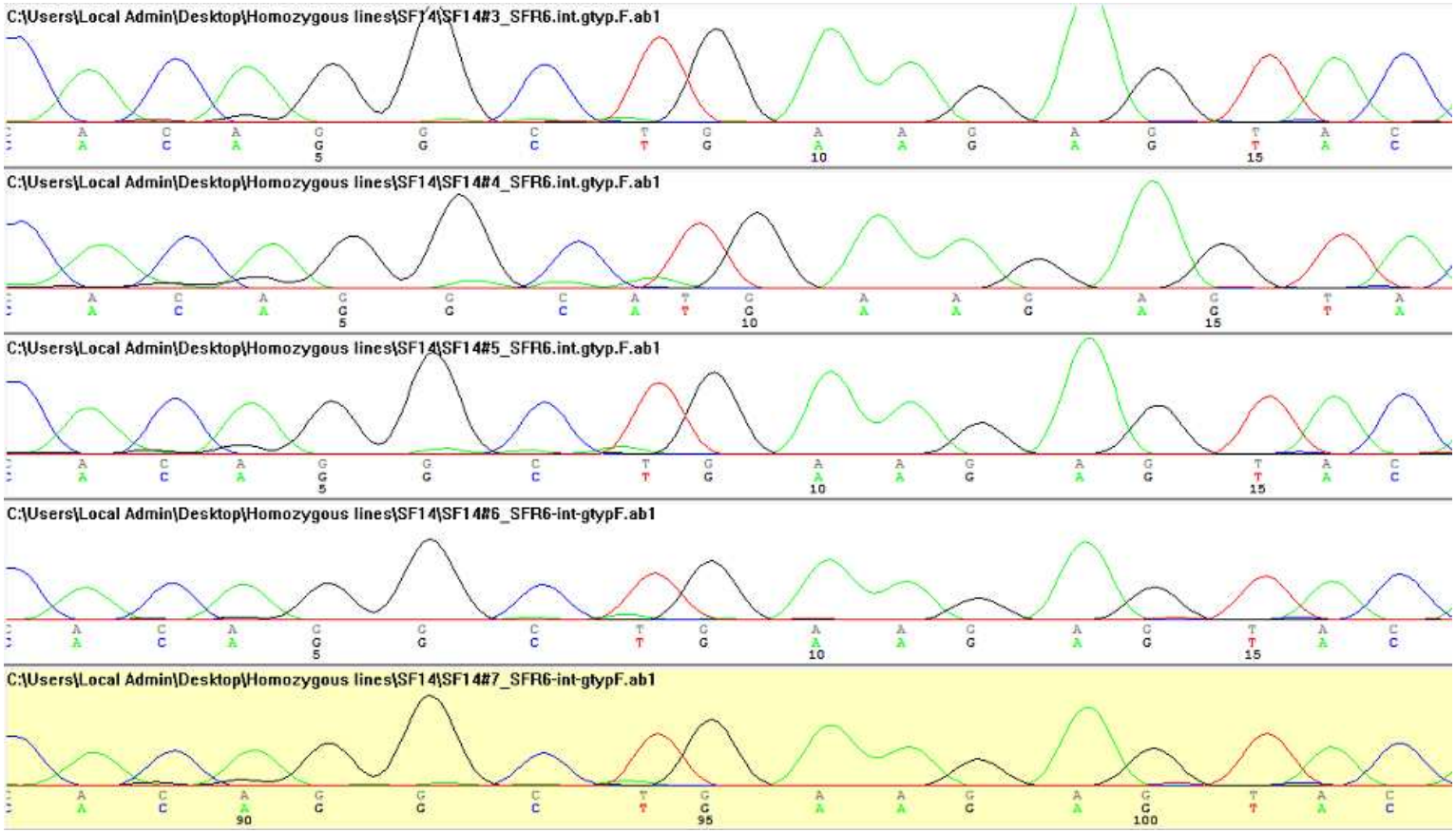

(a) Chromatograms for five homozygous lines of transgenic plants of *sfr6-1*+35S::SF14 (SF14) : SF14#3, SF14#4, SF14#5, SF14#6 and SF14#7 in the above digram represents SF14#1, SF14#2, SF14#3, SF14#4 and SF14#5 respectively in this study.

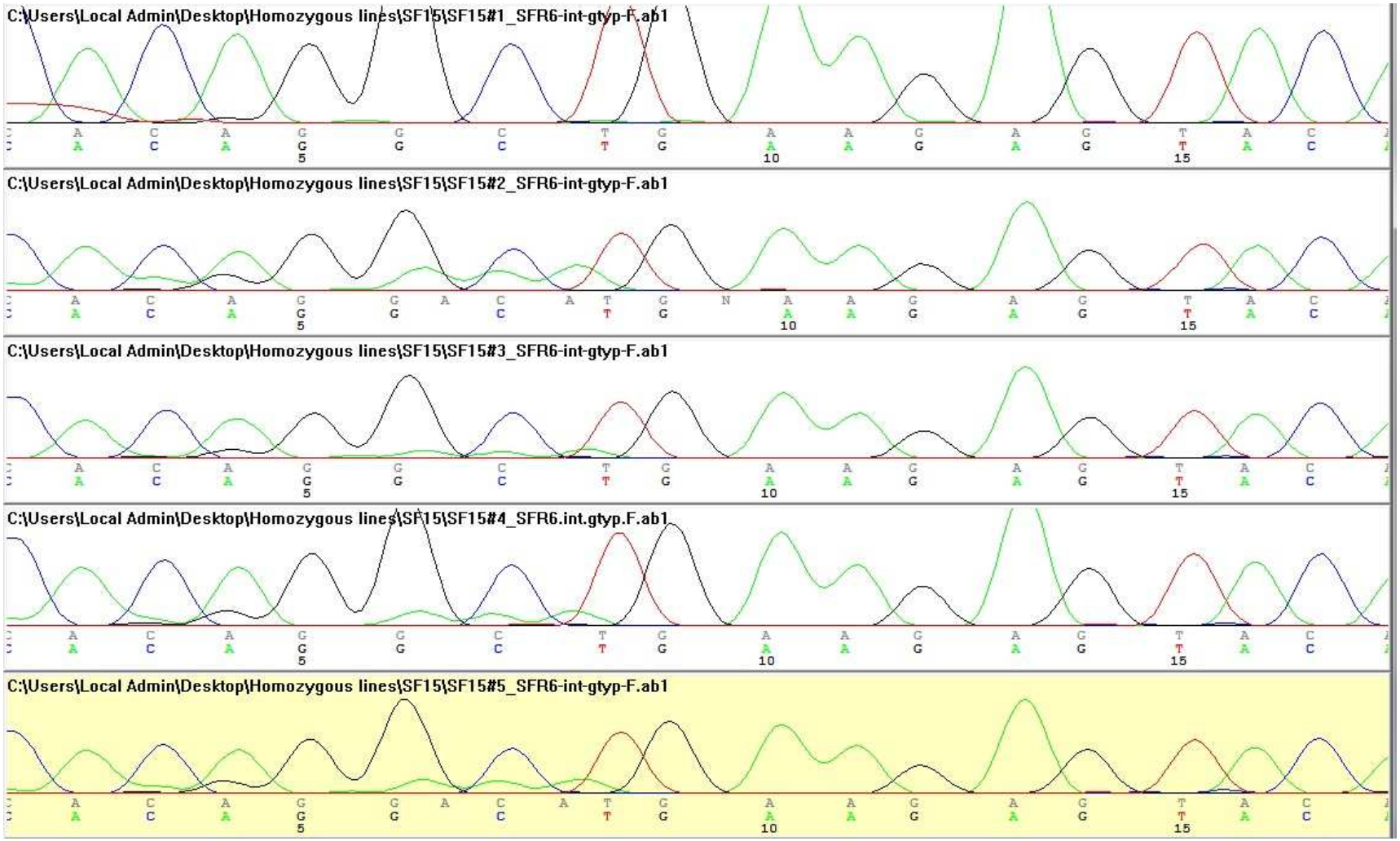

(b) Chromatograms for five homozygous lines of transgenic plants of *sfr6-1*+35S::SF15 (SF15)

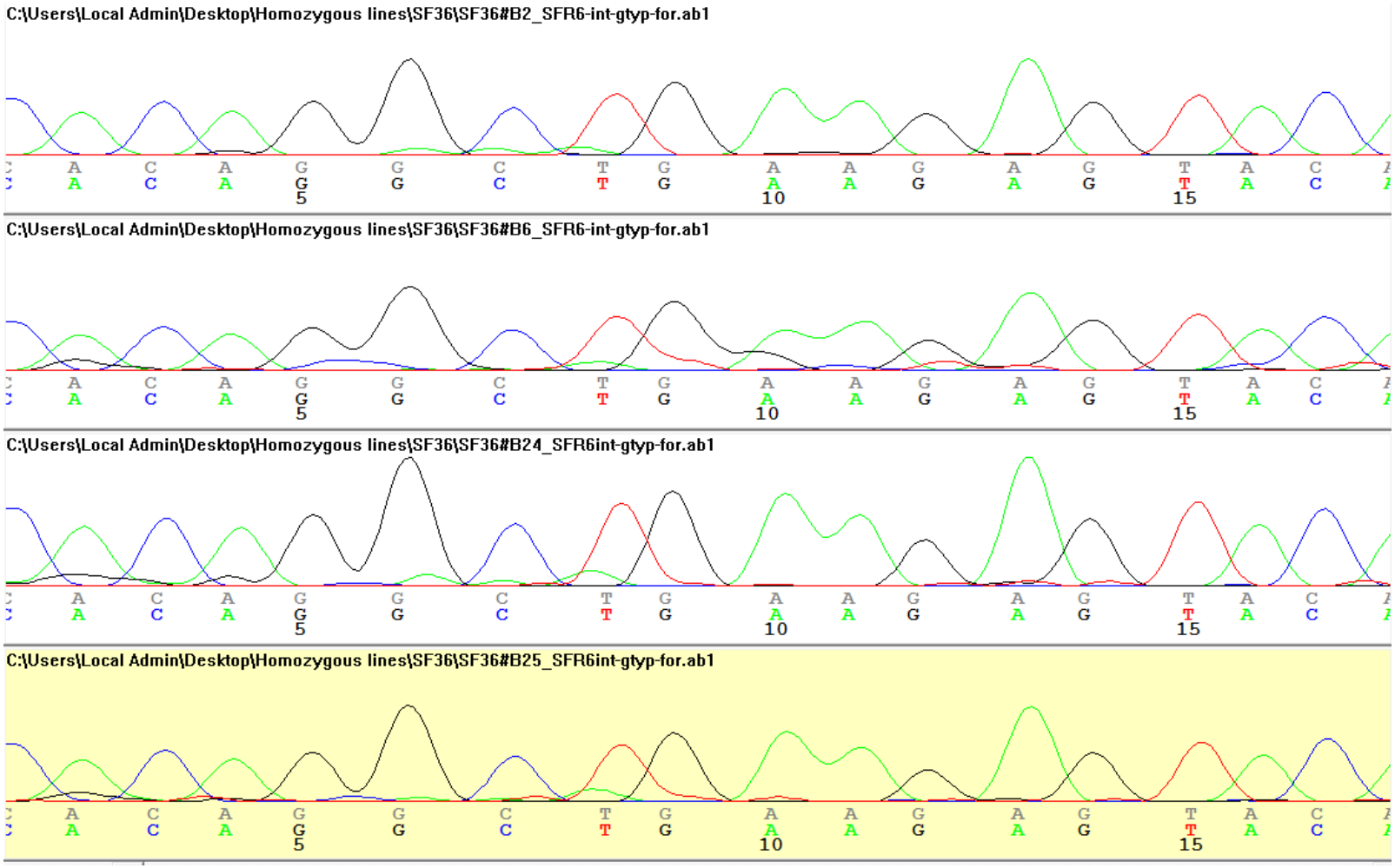

(c) Chromatograms for four homozygous lines of transgenic plants of *sfr6-1*+35S::SF36 (SF36)

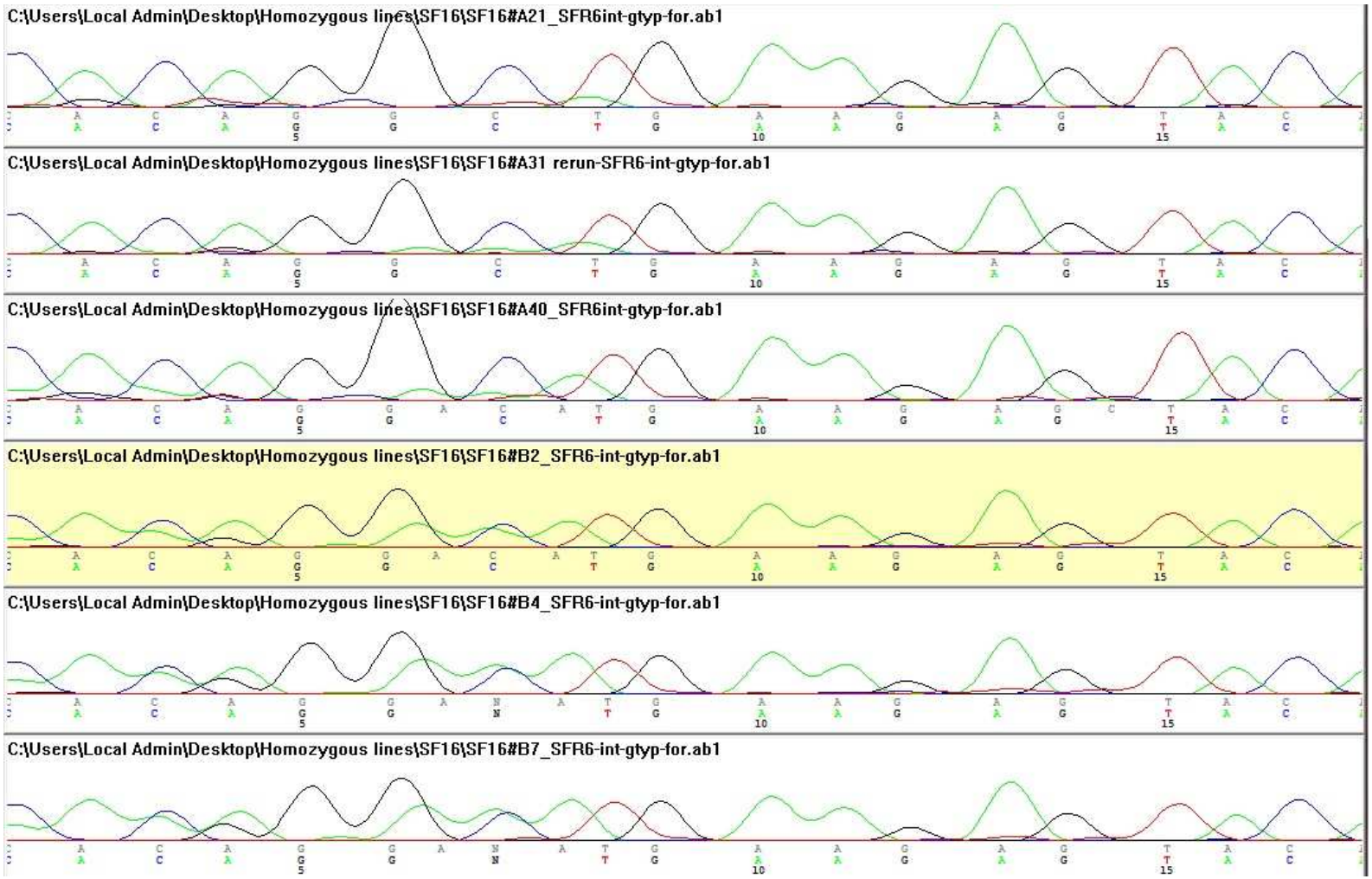

(d) Chromatograms for six homozygous lines of transgenic plants of *sfr6-1*+35S::SF16 (SF16)

Appendix 3

Plasmid Vectors

A3.1: Detailed vector diagram of pENTR-D-TOPO entry vector annotated with specific features using SnapGene R 2.6.2

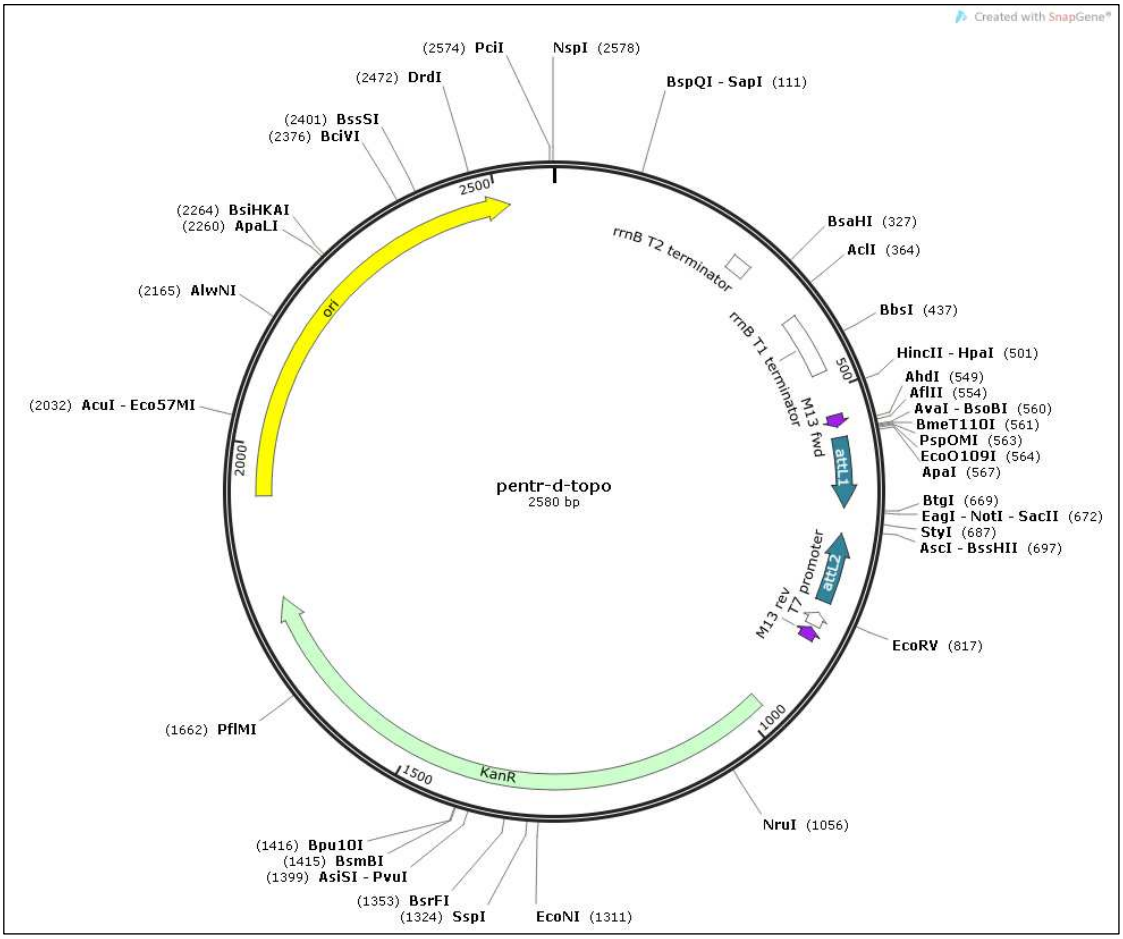

A3.2: Detailed vector diagram of pK7WG2 stable plant expressing destination vector annotated with specific features using SnapGene R 2.6.2

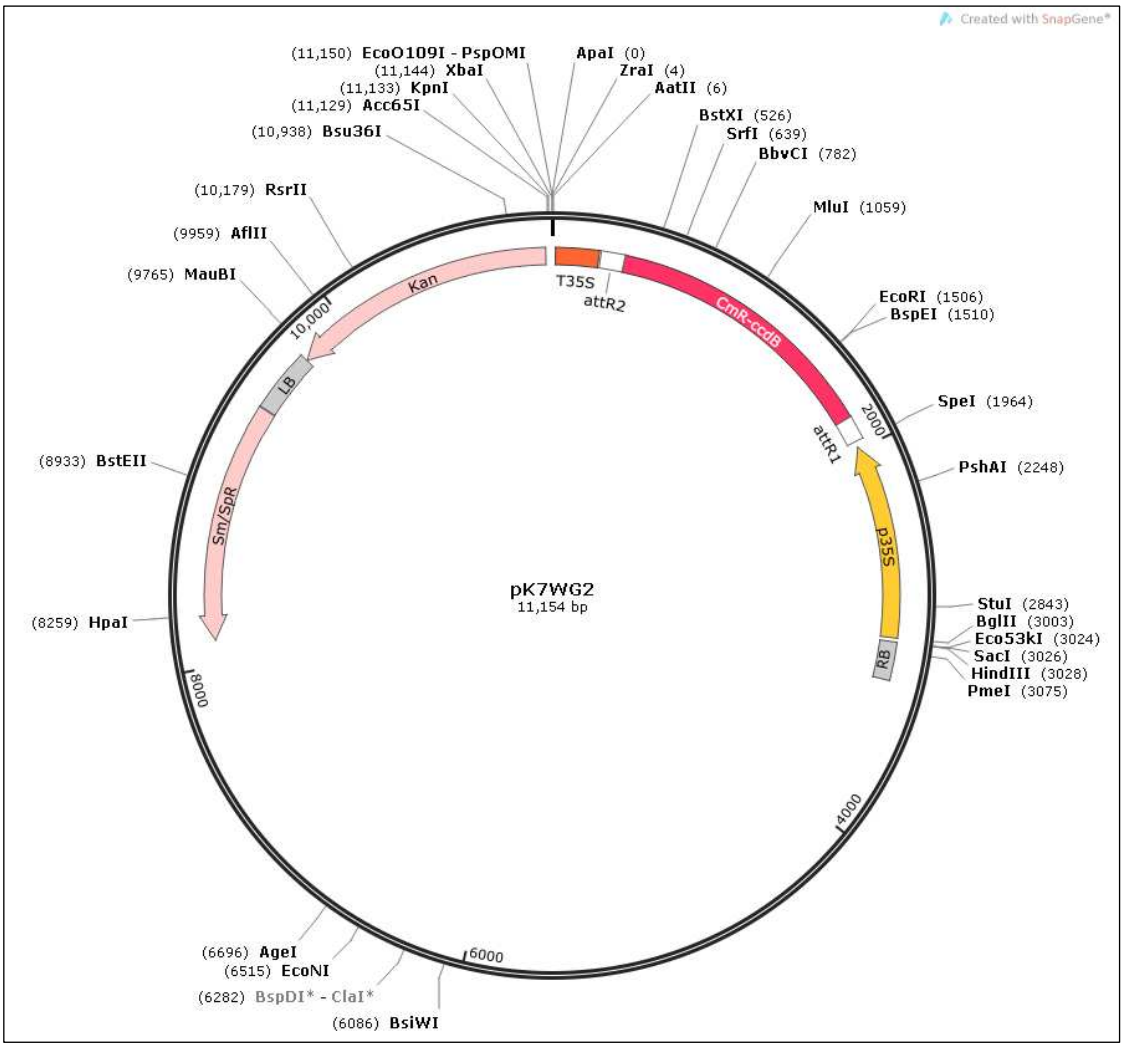

A3.3: Detailed vector diagram of pB7WG2 stable plant expressing destination vector annotated with specific features using SnapGene R 2.6.2

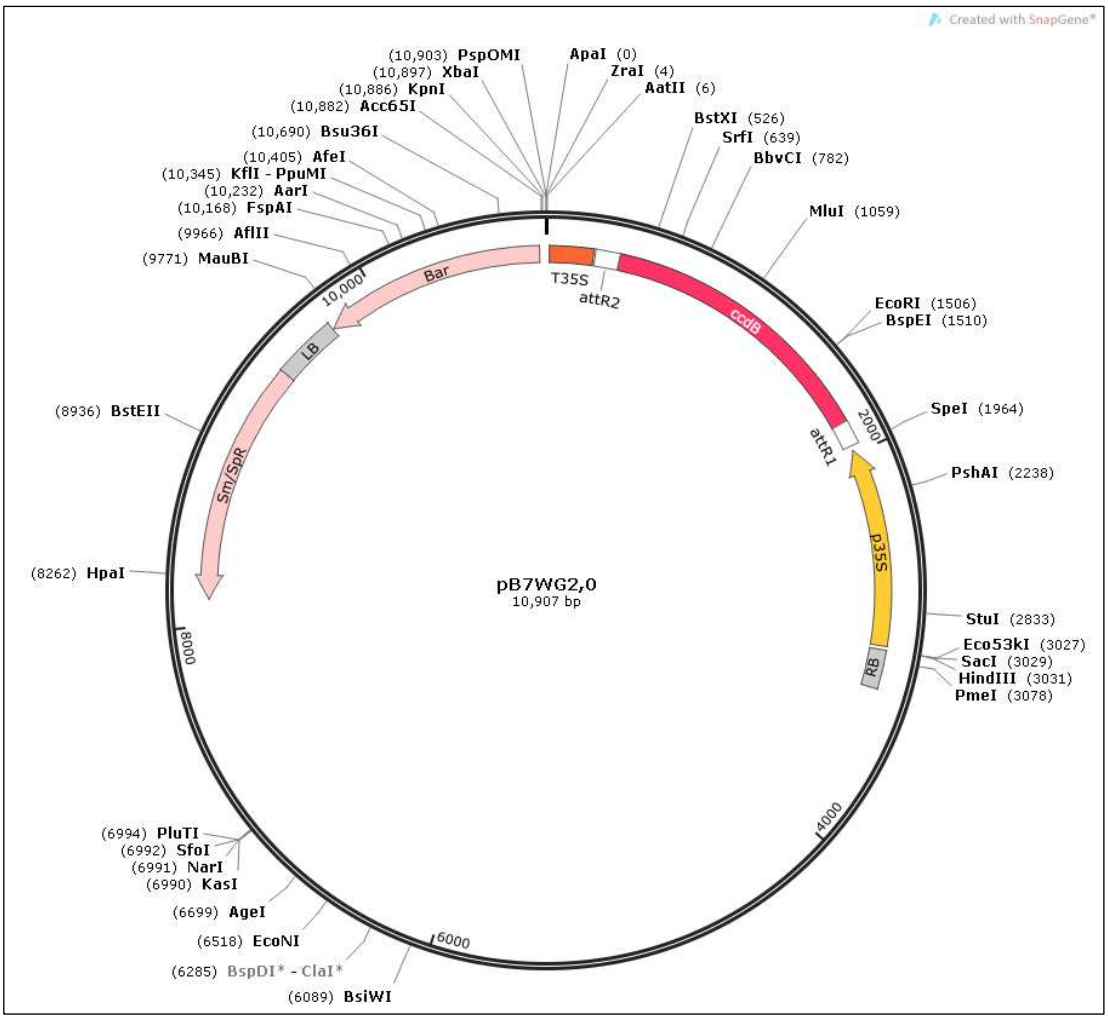

A3.4: Schematic representation of cloning of SF construct to the stable plant expression vector pB7WG2 *via* pENTR-D-TOPO entry vector SnapGene R 2.6.2

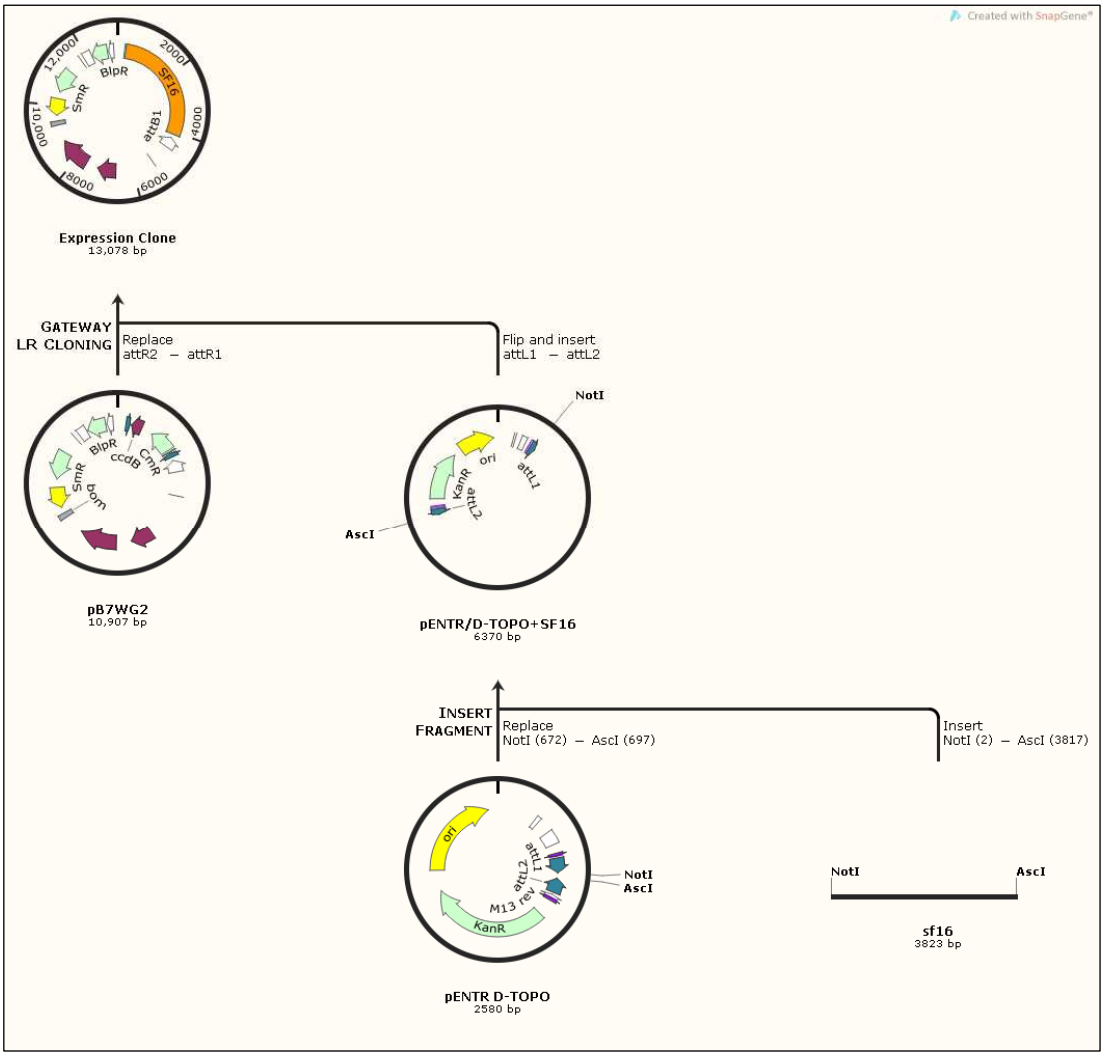

A3.5: Detailed vector diagram of SF16 construct in pB7WG2 stable plant expressing destination vector annotated with specific features using SnapGene R 2.6.2

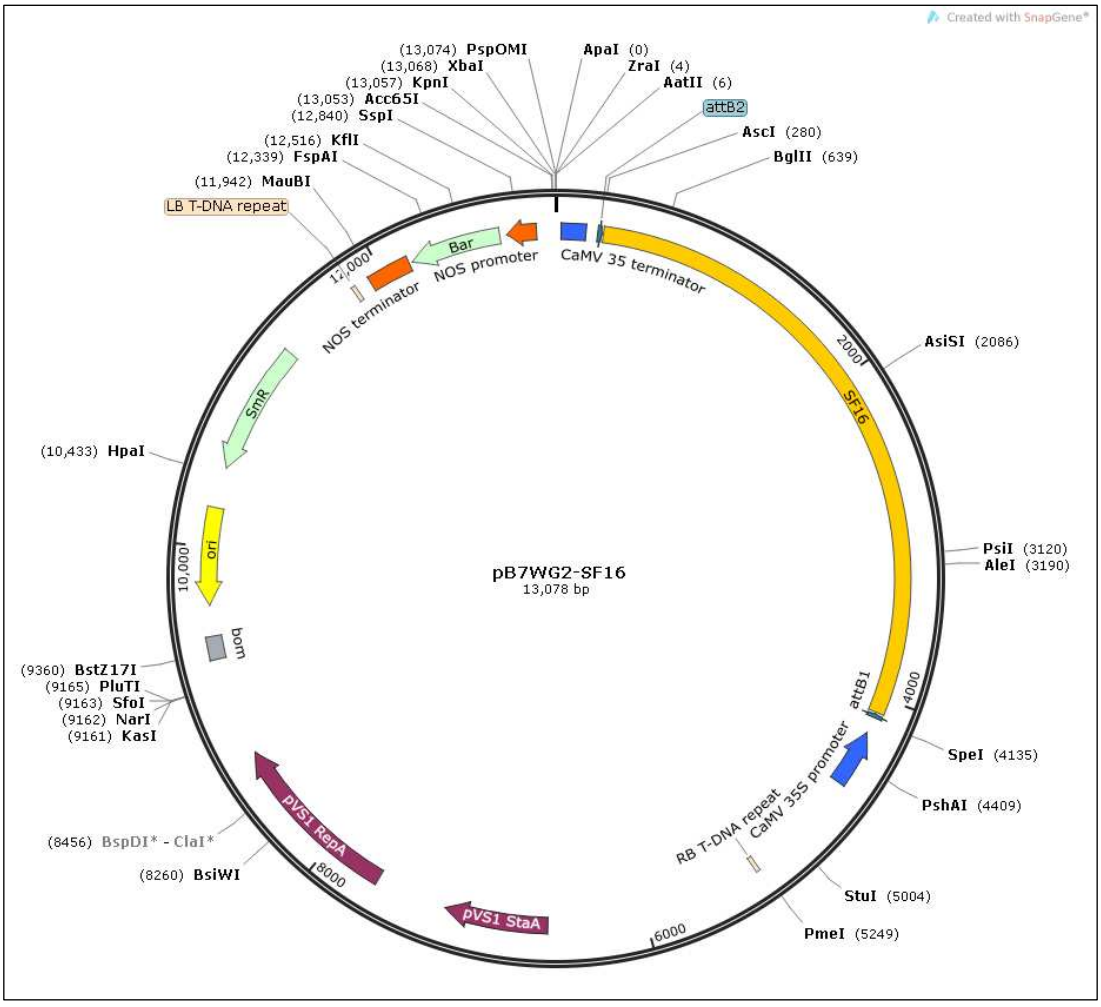

A3.6: Detailed vector diagram of SF15 construct in pB7WG2 stable plant expressing destination vector annotated with specific features using SnapGene R 2.6.2

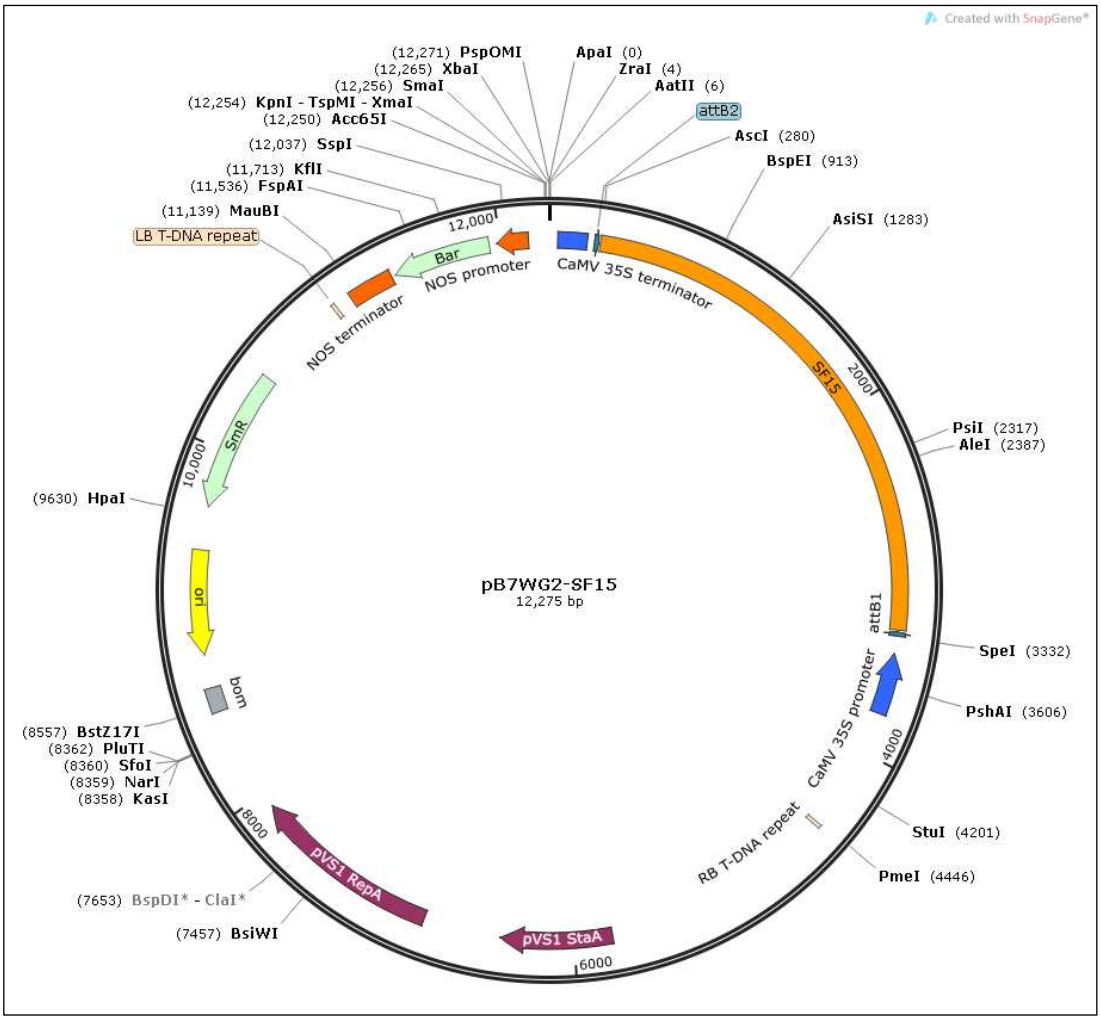

A3.7: Detailed vector diagram of SF14 construct in pB7WG2 stable plant expressing destination vector annotated with specific features using SnapGene R 2.6.2

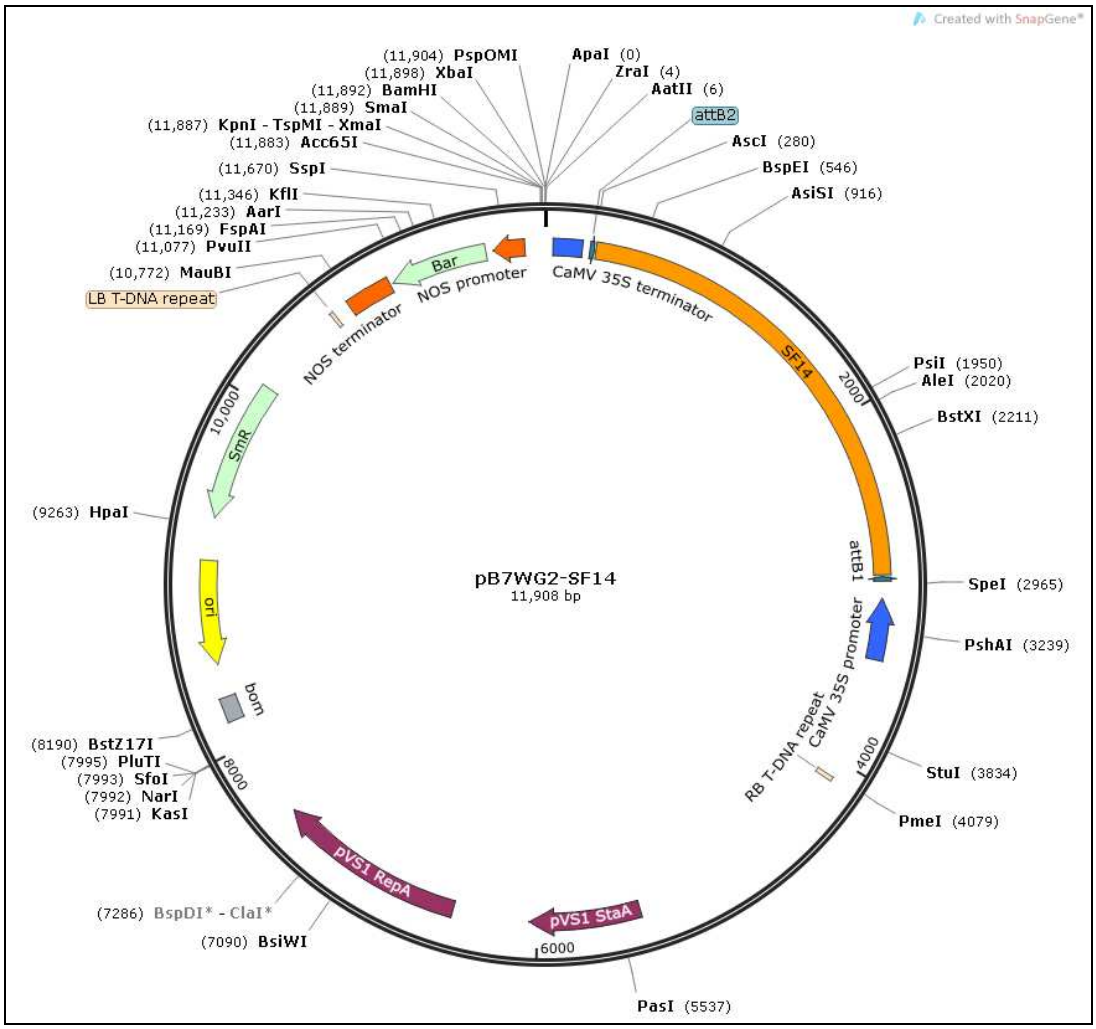

A3.8: Detailed vector diagram of SF36 construct in pB7WG2 stable plant expressing destination vector annotated with specific features using SnapGene R 2.6.2

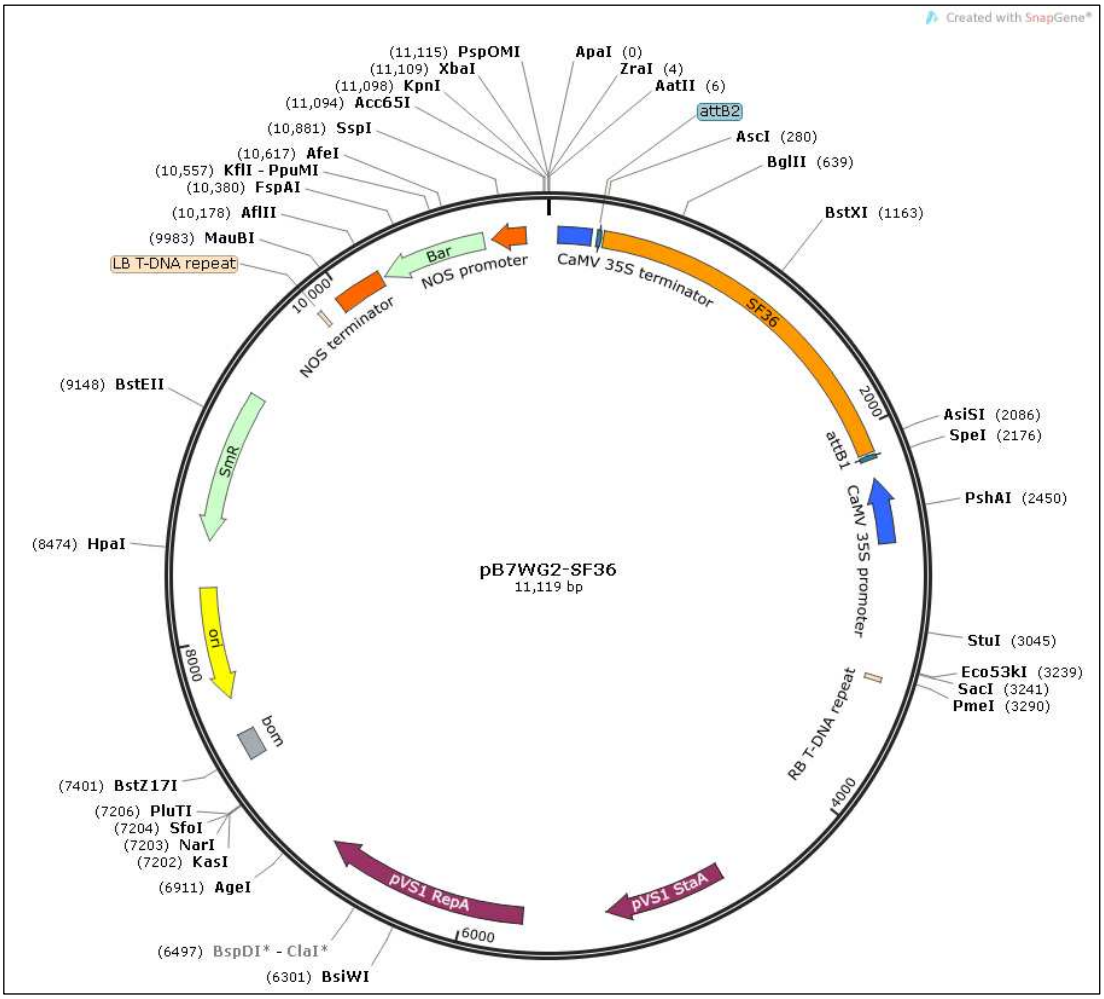

A3.9: Detailed vector diagram of SF25 construct in pB7WG2 stable plant expressing destination vector annotated with specific features using SnapGene R 2.6.2

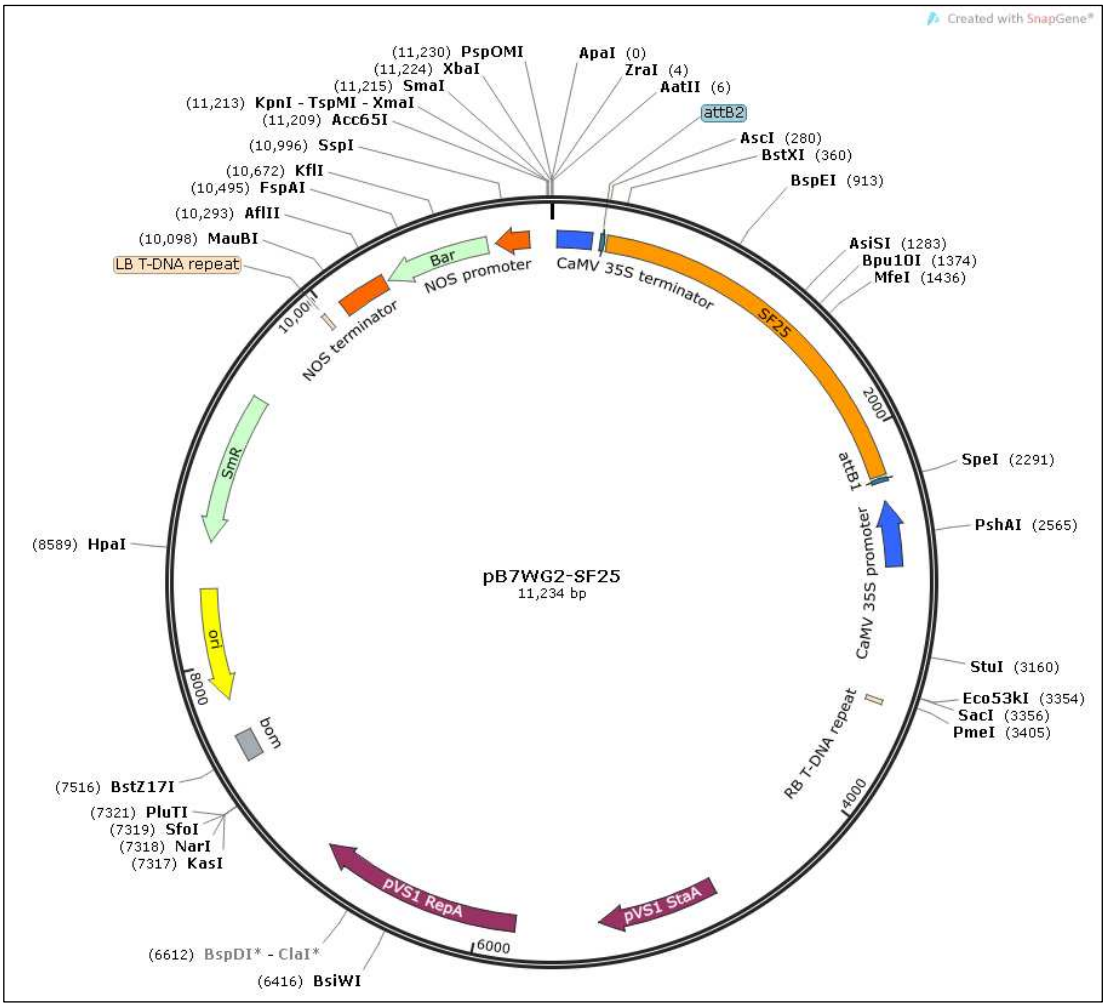

A3.10: Detailed vector diagram of SF24 construct in pB7WG2 stable plant expressing destination vector annotated with specific features using SnapGene R 2.6.2

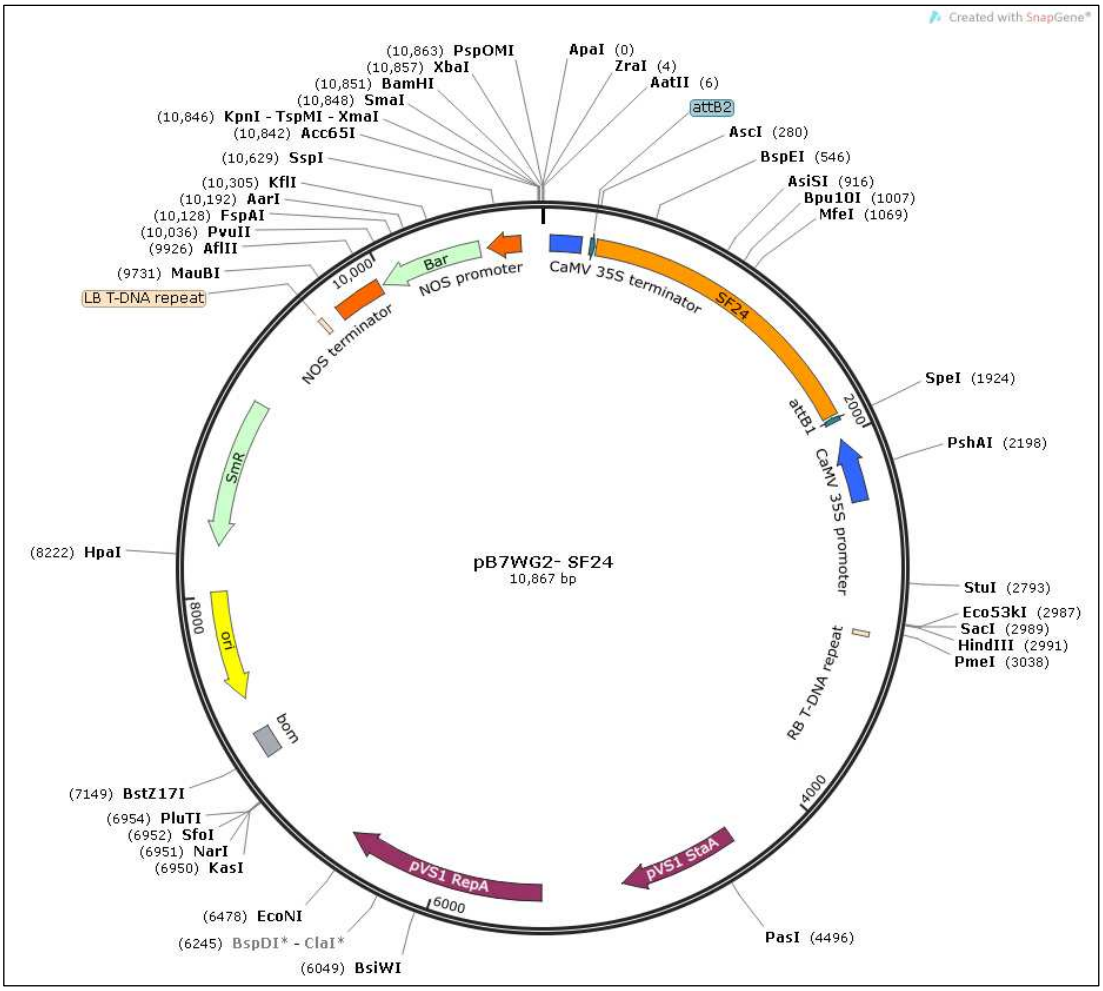

A3.11 Detailed vector: diagram of pK7WGF2 GFP-expressing destination vector annotated with specific features using SnapGene R 2.6.2

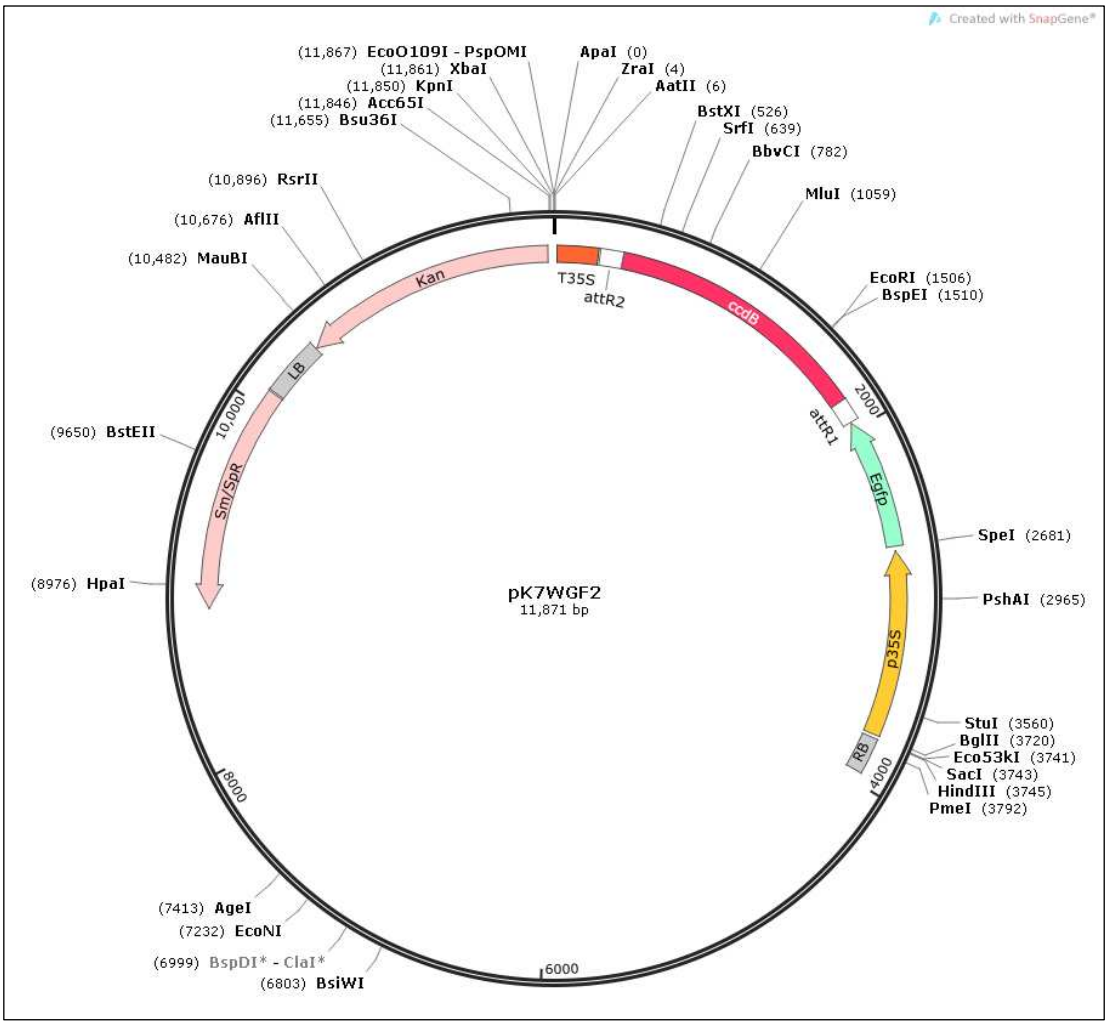

A3.12: Detailed vector diagram of SF16 construct in pK7WGF2 GFP-expressing destination vector annotated with specific features using SnapGene R 2.6.2

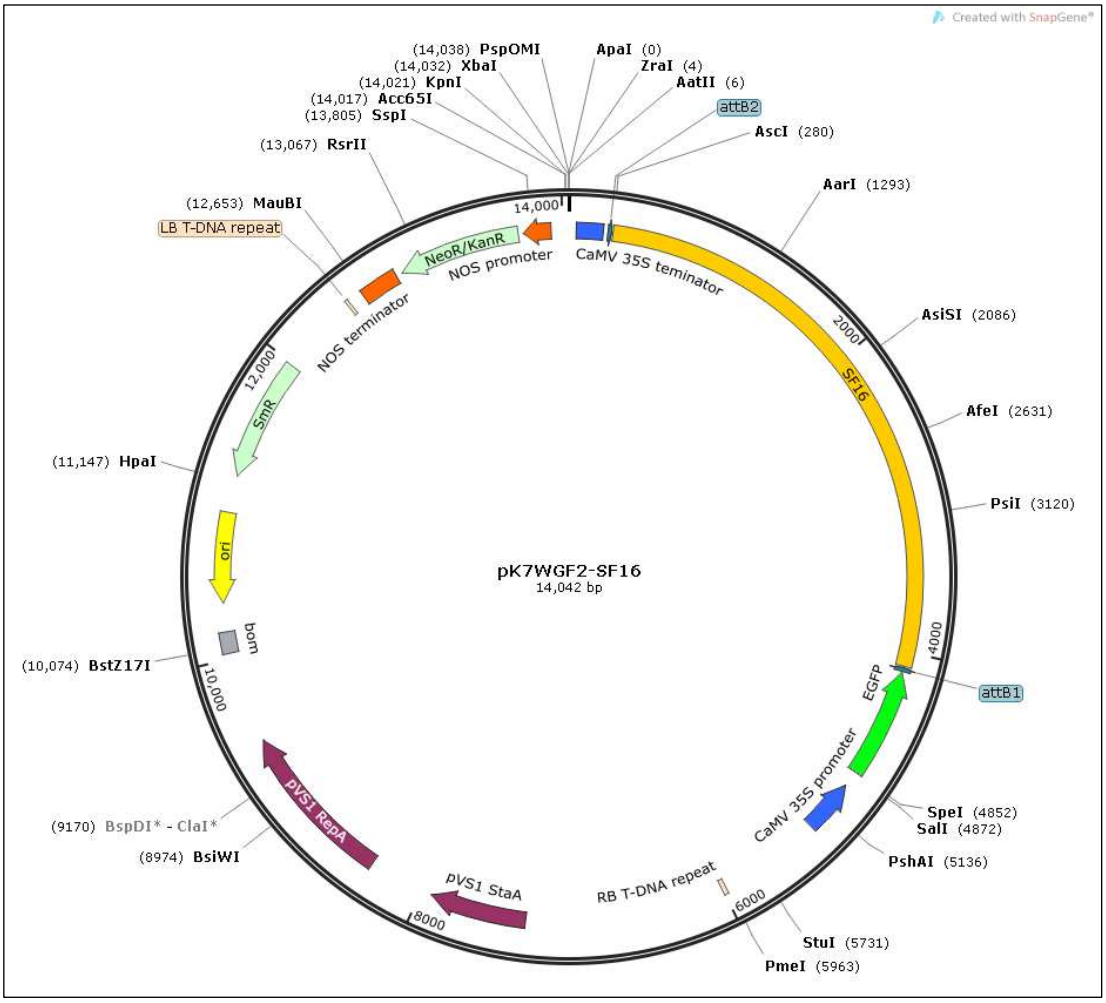

A3.13: Detailed vector diagram of SF15 construct in pK7WGF2 GFP-expressing destination vector annotated with specific features using SnapGene R 2.6.2

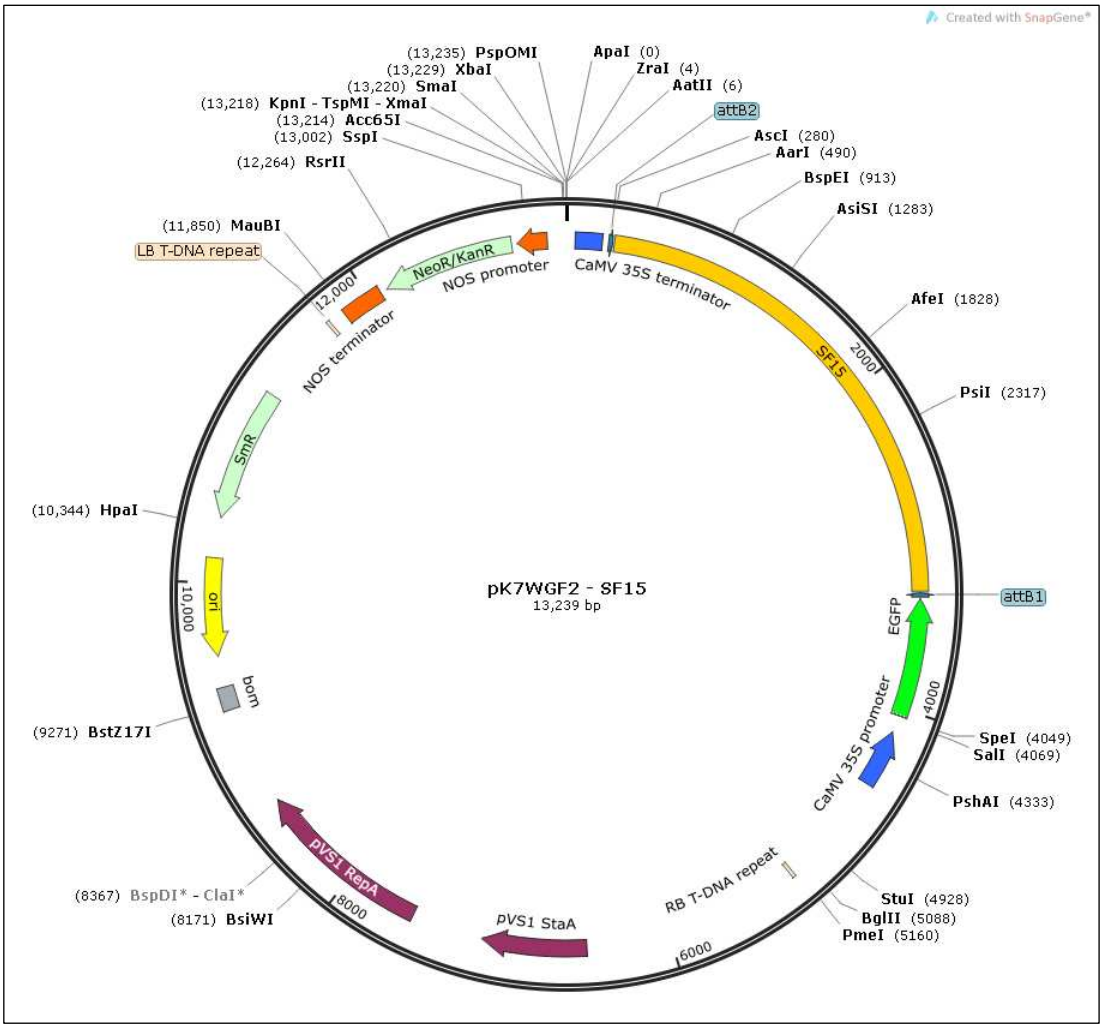

A3.14: Detailed vector diagram of SF14 construct in pK7WGF2 GFP-expressing destination vector annotated with specific features using SnapGene R 2.6.2

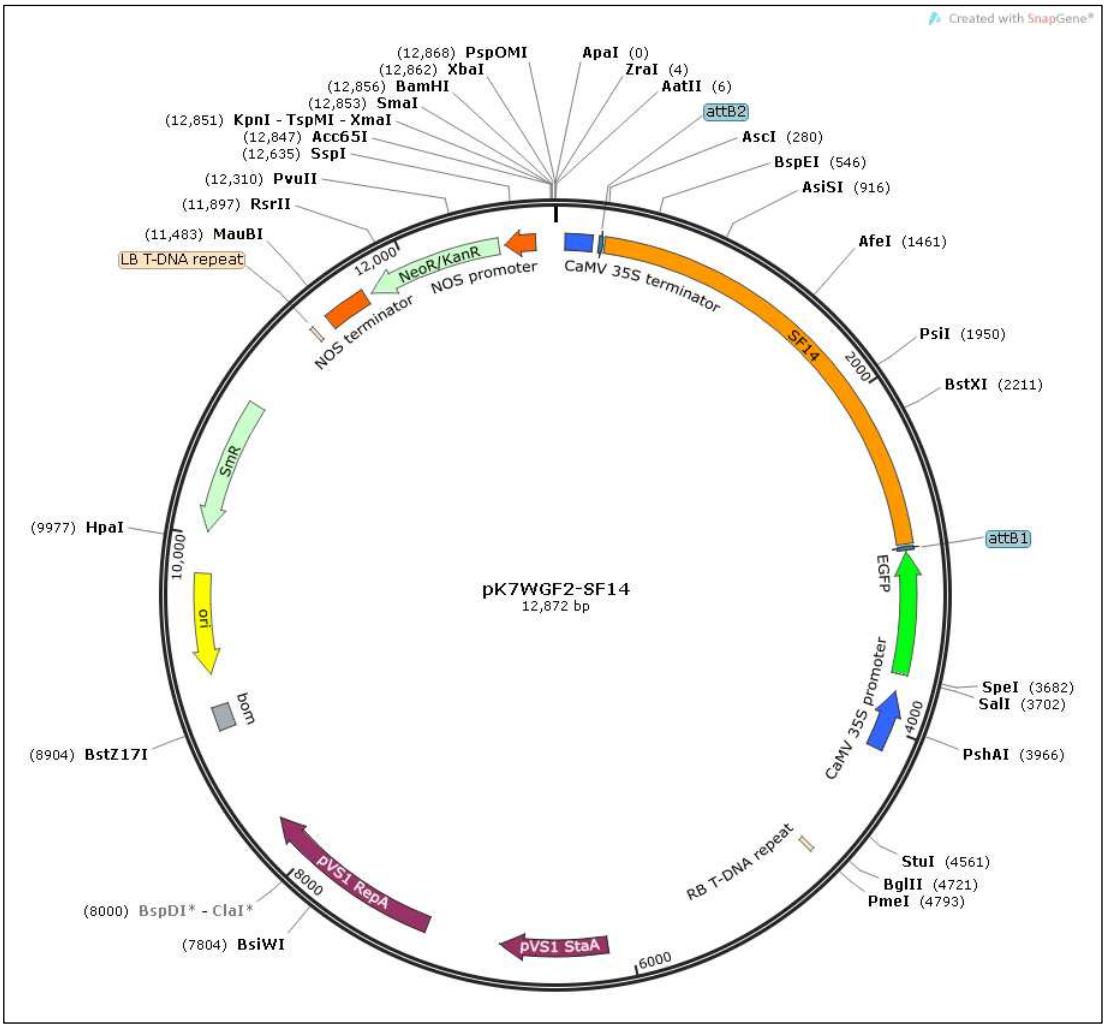

A3.15: Detailed vector diagram of SF36 construct in pK7WGF2 GFP-expressing destination vector annotated with specific features using SnapGene R 2.6.2

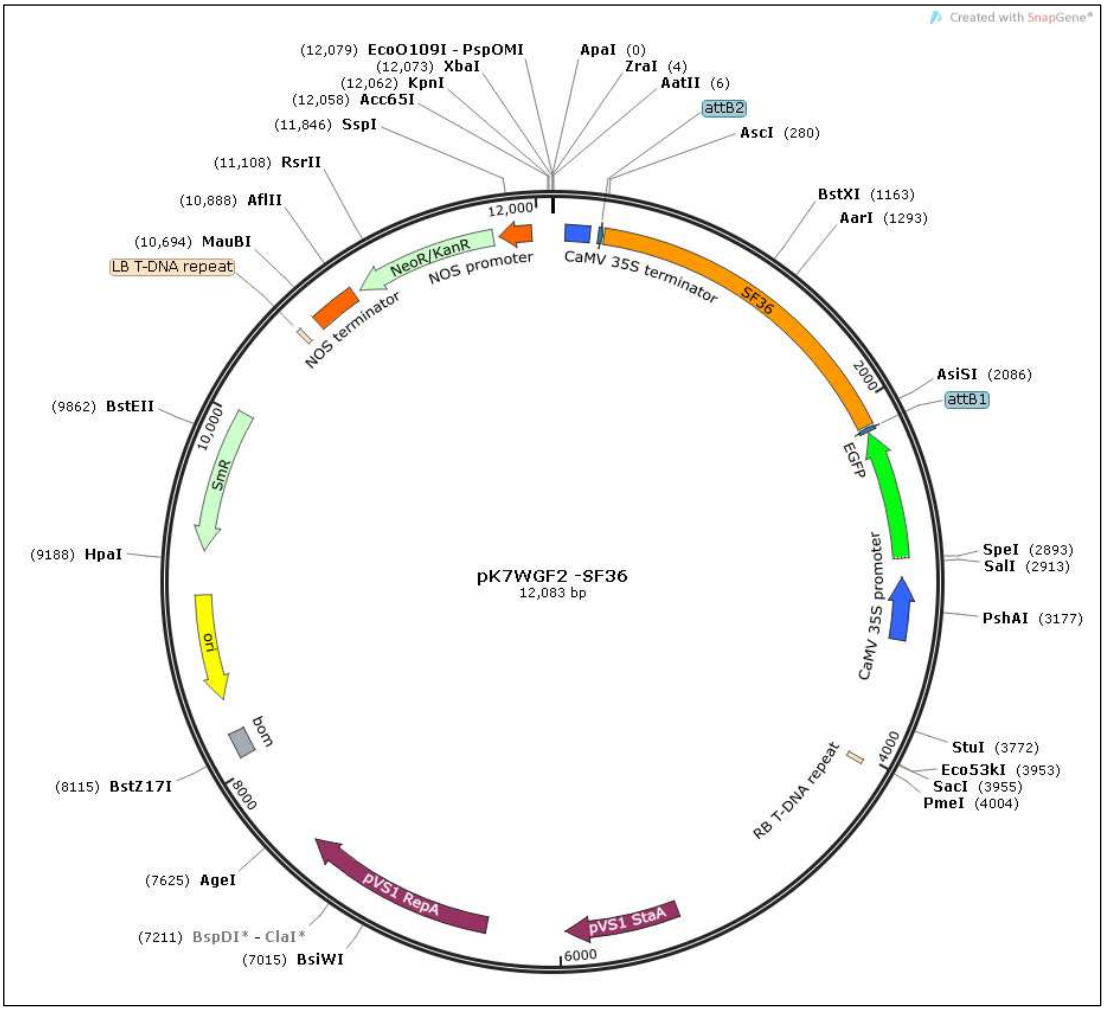

A3.16: Detailed vector diagram of SF25 construct in pK7WGF2 GFP-expressing destination vector annotated with specific features using SnapGene R 2.6.2.

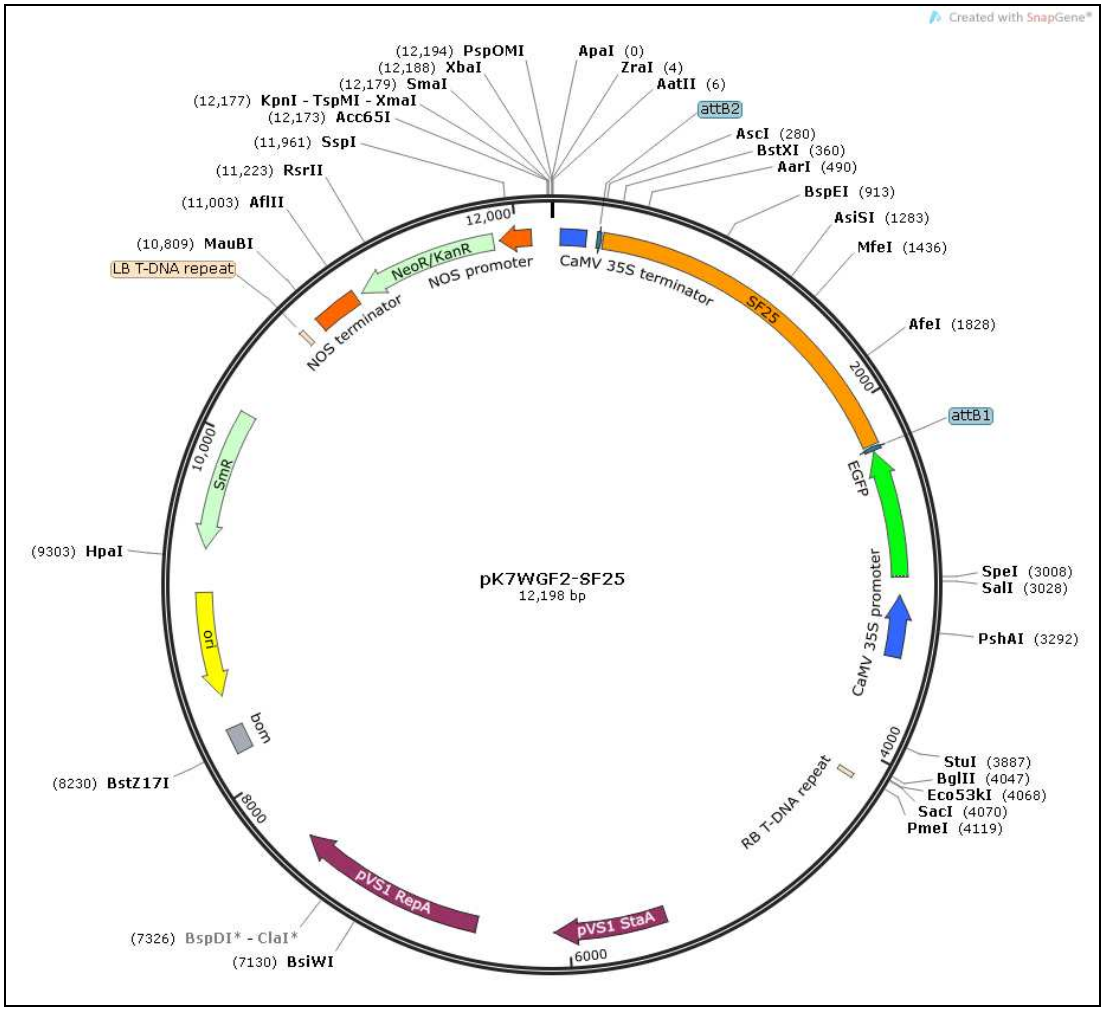

A3.17: Detailed vector diagram of SF24construct in pK7WGF2 GFP-expressing destination vector annotated with specific features using SnapGene R 2.6.2

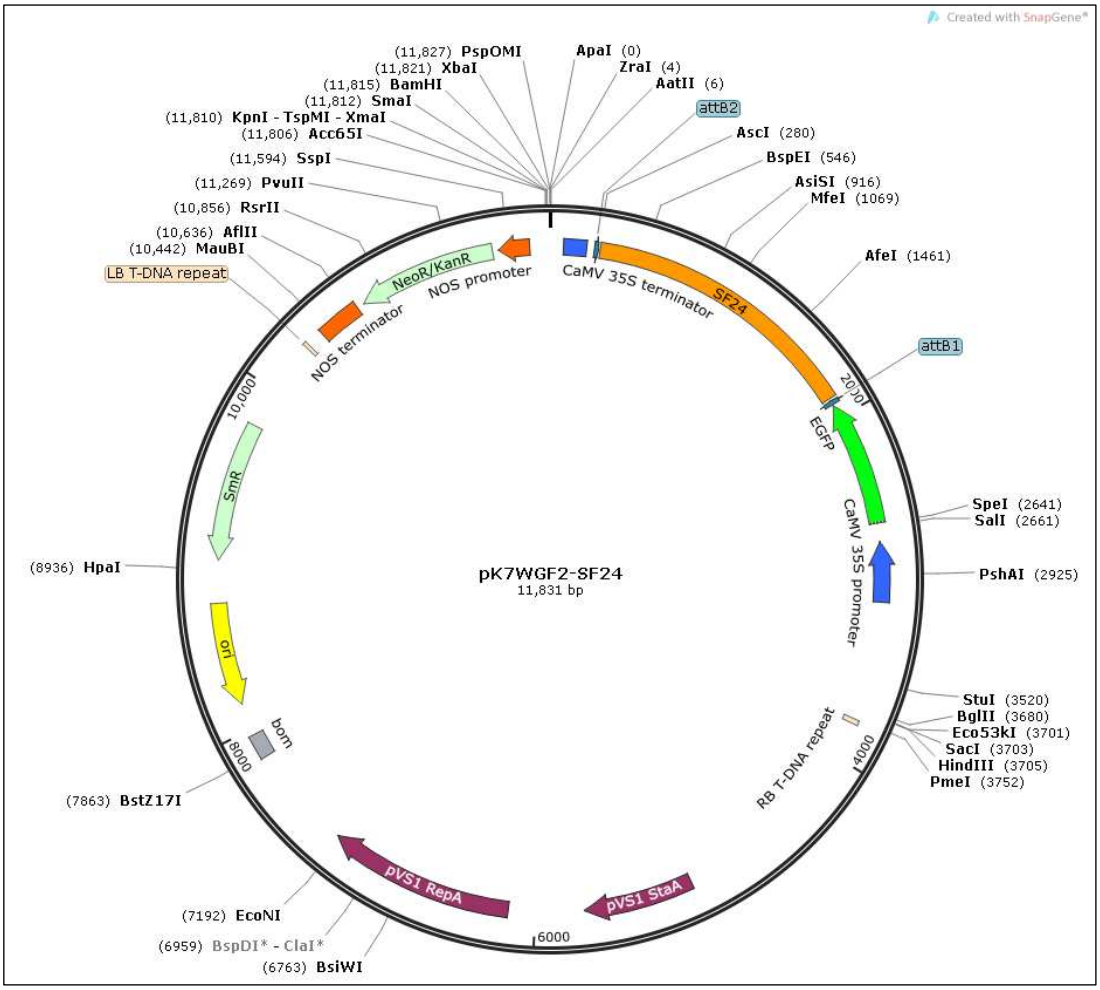

Appendix 4

Supplementary gene expression data

A4.1: Wild type cold gene expression

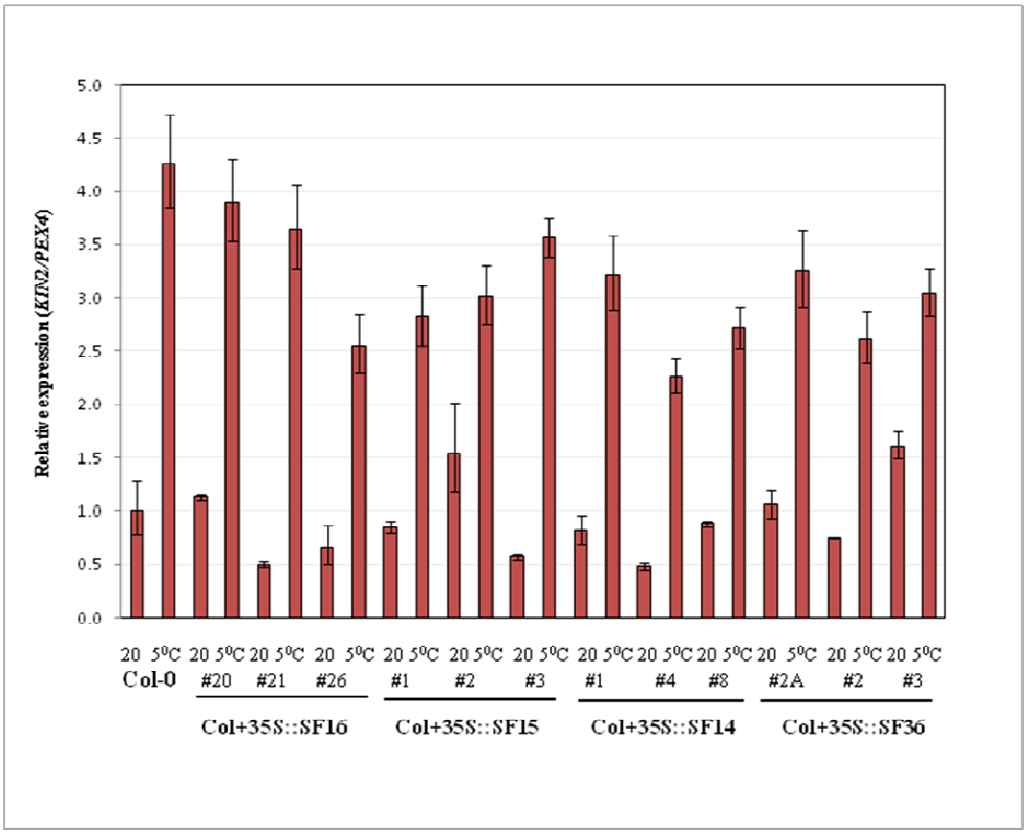

Figure A4.1: Cold-induced *KIN2* expression in SF16, SF15, SF14 and SF36 truncations overexpressing in Col-0 transgenic lines

KIN2 expression in seven-day-old seedlings in response to cold treatment was measured in Col-0+35S::SF16 (SF16), Col-0-1+35S::SF15 (SF15), Col-0+35S::SF14 (SF14) and Col-0+35S::SF36 (SF36) transgenic lines compared with Col-0. Expression is shown after normalisation to *PEX4* in all graphs. Fold values were calculated using the ΔΔCT method, and the error bars in each biological replicates represent RQ_{MIN} and RQ_{MAX} and constitute the acceptable error level for a 95% confidence level according to Student's t test. Error bars indicate the level of variation between technical replicates within one biological replicate experiment.